ЖУРНАЛ
ЭКСПЕРИМЕНТАЛЬНОЙ И ТЕОРЕТИЧЕСКОЙ
ФИЗИКИ
АКАДЕМИЯ НАУК СССР

SOVIET PHYSICS

JETP

Volume 36 (9) NUMBER 6

A Translation

of the

Journal of Experimental and Theoretical Physics

of the

Academy of Sciences of the USSR

Volume 36

DECEMBER, 1959

Published by the

AMERICAN INSTITUTE OF PHYSICS
INCORPORATED

SOVIET PHYSICS
JETP

A translation of the Journal of Experimental and Theoretical Physics of the USSR.

A publication of the

AMERICAN INSTITUTE OF PHYSICS

Governing Board

RALPH A. SAWYER, *Chairman*

Members:

WALTER S. BAIRD
JESSE W. BEAMS
RAYMOND T. BIRGE
R. H. BOLT
HARVEY BROOKS
J. W. BUCHTA
J. H. DILLON
VERNET E. EATON
HERBERT A. ERF
IRVINE C. GARDNER
S. A. GOUDSMIT
WINSTON E. KOCK
R. BRUCE LINDSAY
WALTER C. MICHELS
G. E. PAKE
R. RONALD PALMER
JOSEPH B. PLATT
RALPH A. SAWYER
H. D. SMYTH
JOHN STRONG
GEORGE E. UHLENBECK

Administrative Staff

ELMER HUTCHISSON
Director

HENRY A. BARTON
Associate Director

WALLACE WATERFALL
Secretary and Treasurer

THEODORE VORBURGER
Advertising Manager

RUTH F. BRYANS
Publication Manager

ALICE MASTRO
Circulation Manager

KATHRYN SETZE
Assistant Treasurer

EUGENE H. KONE
Director of Public Relations

EDWARD P. TOBER
Manager, Production and Distribution

W. C. KELLY
Director of Education Projects

EMILY WOLF
Office Manager

American Institute of Physics Advisory Board on Russian Translations

ROBERT T. BEYER, *Chairman*
J. GEORGE ADASHKO, FREEMAN DYSON, DWIGHT GRAY, MORTON HAMERMESH, HAROLD F. WEAVER

Editor of SOVIET PHYSICS—JETP

J. GEORGE ADASHKO, 25 WEST 81ST ST., NEW YORK 24, NEW YORK

SOVIET PHYSICS—JETP is a monthly journal published by the American Institute of Physics and contains a complete translation of the JOURNAL OF EXPERIMENTAL AND THEORETICAL PHYSICS of the U.S.S.R. Academy of Sciences.

This translating and publishing project was undertaken by the institute in the conviction that dissemination of the results of researches everywhere in the world is invaluable to the advancement of science. The NATIONAL SCIENCE FOUNDATION of the United States has encouraged the project initially and is supporting it in large part by a grant.

The American Institute of Physics and its translators propose to translate faithfully all the material appearing in the original articles. The views expressed in the translations are therefore those of the original authors, and not those of the translators nor of the American Institute of Physics.

Volume 1 of SOVIET PHYSICS—JETP corresponds to Russian Volume 28 (1955). Two volumes are published annually, each of six issues. Each volume contains the translation of one volume of the JOURNAL OF EXPERIMENTAL AND THEORETICAL PHYSICS.

Beginning with Vol. 9 (36), the transliteration of the names of Russian authors follows British Standard 2979, which is being adopted in 1959 by a large number of scientific journals in the United States. The Library of Congress transliteration is followed in the earlier volumes.

Subscription Prices

Per Year (12 issues)

General:

United States and Canada	$75.00
Elsewhere	79.00

Libraries of non-profit degree-granting Institutions:

United States and Canada	$35.00
Elsewhere	39.00
Back Numbers	$ 8.00

Subscriptions should be addressed to the American Institute of Physics, 335 East 45th Street, New York 17, New York.

SOVIET PHYSICS, JETP is published monthly by the American Institute of Physics, Inc. Second Class postage paid at Ann Arbor, Michigan.

Copyright by American Institute of Physics 1959

SOVIET PHYSICS

JETP

A translation of the Journal of Experimental and Theoretical Physics of the USSR.

SOVIET PHYSICS JETP VOL. 36(9), NO. 6, pp.1151-1426 DECEMBER, 1959

MOMENTUM SPECTRUM OF PARTICLES OF THE HARD COMPONENT OF COSMIC RAYS AT AN ALTITUDE OF 9 KM

L. T. BARADZEĬ, M. V. SOLOV'EV, Z. I. TULINOVA, and L. I. FILATOVA

Nuclear Physics Institute, Moscow State University

Submitted to JETP editor December 12, 1958

J. Exptl. Theoret. Phys. (U.S.S.R.) **38**, 1617-1620 (June, 1959)

The momentum spectrum of particles of the hard component of cosmic rays was measured at an altitude of 9 km, with the aid of a cloud chamber placed in a magnetic field, in the range $0.3 \times 10^9 - 6 \times 10^9$ ev/c. The particles were also grouped according to the charge. It was found that the $(1-5) \times 10^9$ ev/c protons comprise $(50 \pm 10)\%$ of the total number of particles.

MEASUREMENTS of the momentum spectrum of particles of the hard component of cosmic rays at an altitude of 9000 m were carried out, using a cloud chamber in a magnetic field.

A schematic representation of the setup is given in Fig. 1. The apparatus was operated by 5-fold coincidences $C_1C_2C_3C_4C_5$, so that the particles had to pass through an absorber of lead 9 cm thick, placed between the counter trays C_4 and C_5. The side counters a (in the projection b, Fig. 1) were connected in anticoincidence. The topography of the magnetic field in the gap is given in Fig. 2. The average value of the magnetic field amounted to 9090 oe. Deviation of the intensity value within the volume of the chamber from the average was not greater than 3%.

During the fourteen hours of operation of the array, approximately 700 cloud chamber photographs were taken. A total of 445 tracks was selected for measurements of the trajectories of

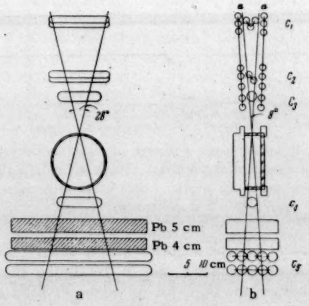

FIG. 1. Diagram of the array.

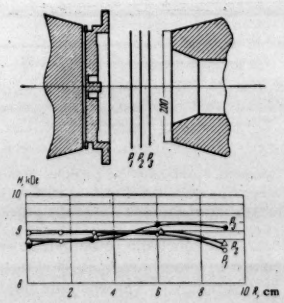

FIG. 2. Topography of the magnetic field in the gap.

particles which passed within the acceptance angle of the array, were not accompanied by other particles, and had a length of 15 to 17 cm. The curvature of the tracks was measured with an IG-22 optical compensator. The error of measurement for the tracks of the specified length was not greater than ± 0.02 m^{-1}. The value of the apparent curvature of tracks in the chamber was determined from check photographs obtained with the electromagnet shut off. Check photographs were alternated with the photographs of actual events. The curvature of tracks was measured on approximately 100 control photographs. The distribution of apparent curvatures obtained coincides with the normal distribution for the value of the standard deviation $\Delta(1/R) = 0.03$ m^{-1} and the systematical curvature $(1/R)_{syst} = (-0.013 \pm 0.003)$ m^{-1}.

Since the tracks used for constructing the momentum spectrum formed angles smaller than 4° with the plane of the chamber, the inaccuracy in the value of the particle momentum due to a conical projection of the track in photographing was not greater than 1%.

Thus, the foregoing value of $\Delta(1/R)$ for check tracks can be taken as the standard error of the measurements of the curvature of a track. For the intensity of magnetic field used, the value of the maximum detectable momentum amounted to $\sim 9 \times 10^9$ ev/c.

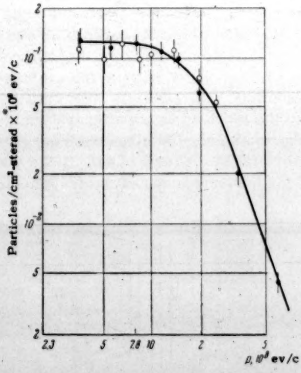

FIG. 3. Momentum spectrum of the particles of the hard component of cosmic rays at the altitude of 9000 m (black and light points – data of two different series of measurements).

The momentum spectrum of the particles of the hard component of cosmic rays at 9000 m is shown in Fig. 3 (black points). The absolute intensity of the spectrum corresponds to the integral intensity of the hard component equal to 3.0 ± 0.15 particles -cm^{-2}-min^{-1}-sterad^{-1}. This value is in good agreement with the data of other experiments.[1] In the momentum range $(2 \text{ to } 6) \times 10^9$ ev/c, the spectrum can be represented by a power function with an exponent of 2.8 ± 0.5. If the particles of the hard component were μ mesons, then the minimum momentum of particles in the chamber determined by ionization losses in the filter should amount to 2.3×10^8 ev/c. The minimum momentum of particles recorded by the array was found to be equal to $(2.5 \pm 0.1) \times 10^8$ ev/c.

If the above method is used for chamber triggering, the intensity of particles with small momentum may be underestimated as a result of their being blown away by the field of the electromagnet. The calculation showed that the number of particles with momentum 3.5×10^8 ev/c is 10% too low because of such an effect. Accordingly, the first point in the spectrum was corrected by this amount. For the next point of the spectrum, the correction because of this is negligible.

In the range of small curvatures, the shape of the spectrum is distorted because of the error in the measurements of the curvature. To estimate the magnitude of these distortions, the change of the shape of the experimentally-found spectrum was calculated for varying values of the track curvatures for a specified error. Results of the calculation for measurements of curvatures with standard deviations of 0.03 m^{-1} (dotted line) and 0.15 m^{-1} (dot-dash line) are given in Fig. 4. In

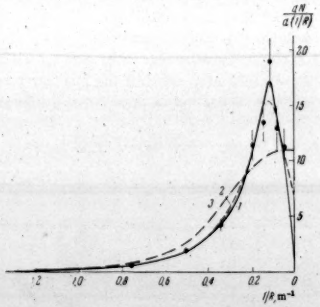

FIG. 4. Solid curve – spectrum of curvatures obtained in the experiment; dot and dot-dash curves – data of calculations for measurements of curvatures with standard deviations equal to 0.3 m^{-1} and 0.15 m^{-1} respectively.

the calculation, the distribution of errors was assumed to be Gaussian. From the figure shown, one can conclude that, for an error of 0.03 m^{-1} for curvatures > 0.04 m^{-1} (momentum $\sim 7 \times 10^9$ ev/c) one can neglect the distortion of the spec-

trum, considering the statistical accuracy obtained.

Data on the momentum spectrum of penetrating particles of cosmic radiation were also obtained in a series of experiments devoted to the study of nuclear-active particles. The position of the counters triggering the chamber was, in this case, such that the effect of "blowing away" the particles with small momentum was absent. In this series of measurements, a thin beryllium plate was placed in the chamber, as a result of which the error in the measurement of the momentum was increased to 0.15 m^{-1}. The light points in Fig. 3 represent data obtained in this series of experiments. The intensities are corrected according to calculated data of Fig. 4. The data of both experiments are consistent.

The momentum spectrum of negatively-charged particles (curve 1) which, according to present ideas, are μ mesons, is shown in Fig. 5. Particles with momentum $< 2.3 \times 10^8$ ev/c are absent.

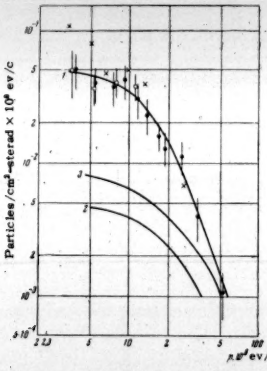

FIG. 5. Spectrum of negatively charged particles (curve 1) at the altitude of 9 km: ○, ● – data of two series of measurements, × – from the data of references 2 and 3. Curve 2 – spectrum of μ mesons at sea level, arriving from the altitude of 9 km. Curve 3 – spectrum of μ^- mesons at sea level according to references 5 and 6.

As has been stated above, this momentum is the minimum value for μ mesons passing through the lead absorber. For comparison, data are given on the spectrum of μ mesons obtained by Anderson et al.[3] The spectra are normalized for the number of particles with momentum between 1×10^9 and 3×10^9 ev/c. The reason for the observed discrepancy in the momentum range of $\sim 5 \times 10^8$ ev/c is evidently the inaccurate method of taking into account the number of electrons which were recorded by the setup of Anderson.[3]

Using the value given by Sands[4] for the probability that a μ meson with momentum p at an altitude h_1 reaches the altitude h_2, one can obtain the spectrum of μ^- mesons arriving from the altitude of 9 km at sea level (curve 2, Fig. 5). Comparing this spectrum with the experimentally-observed spectrum of μ^- mesons at sea level[5,6] (curve 3, Fig. 5), one can conclude that, in the momentum range from 5×10^8 to 3×10^9 ev/c, about 60% of μ mesons reaching sea-level are produced at altitudes greater than 9 km.

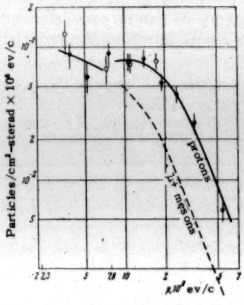

FIG. 6. Spectrum of positively charged particles at 9 km altitude; ●, ○ – data of two series of measurements.

The momentum spectrum of positively-charged particles is shown in Fig. 6. Since, for the passage through the lead absorber, protons should have a momentum $> 7.8 \times 10^8$ ev/c, the particles with smaller momenta are μ^+ mesons. The ratio of the number of positive to negative μ mesons in the momentum range from 3 to 7×10^8 ev/c amounts to 1.7 ± 0.4.

For momenta larger than 7.8×10^8 ev/c, the measured spectrum of positive particles contained both μ^+ mesons and protons. The fraction of protons among the positive particles can be determined if the value of the positive excess $k = \mu^+/\mu^-$ is known. Direct measurements of k for the momentum range under consideration at the altitude of 9 km are not available. Data obtained at sea level and at mountain altitudes show that the value of the positive excess does not depend strongly both on momentum and on altitude, and lies between 1.2 and 1.3 (reference 7). It was stated above that more than half of the μ mesons are produced above 9 km. The value of the positive excess cannot therefore greatly exceed the values at sea level and at mountain altitudes. For the extreme as-

sumption that, for μ mesons produced below 9 km, the value of the positive excess is zero, we can conclude that, at the altitude of 9 km, the value of the positive excess amounts to 1.4. Therefore, the value of the positive excess changes little with variation of altitude up to 9 km.

If we assume a value $k = 1.25$ for the momentum range above 10^9 ev/c, we can determine the intensity of μ^+ mesons for this momentum range (dotted curves). Then, in the momentum range from 1 to 5×10^9 ev/c, protons amount to $(50 \pm 10)\%$ of the total number of penetrating particles. It should be mentioned that, in the momentum range $(2 \text{ to } 5) \times 10^9$ ev/c, the spectra of negative and positive particles can be represented by power functions with identical exponents, within the limits of error.

In conclusion, the authors take the opportunity to express their gratitude to Yu. A. Smorodin for devoted guidance and discussion of results.

[1] S. N. Vernov and A. N. Charakhch'yan, Dokl. Akad. Nauk SSSR **91**, 478 (1953).

[2] R. V. Adams and C. D. Anderson, Revs. Modern Phys. **20**, 334 (1948).

[3] Adams, Anderson, and Cowan, Revs. Modern Phys. **21**, 72 (1949).

[4] M. Sands, Phys. Rev. **77**, 180 (1950).

[5] W. L. Whittemore and R. P. Shutt, Phys. Rev. **86**, 940 (1952).

[6] Glaser, Hamermesh, and Safonov, Phys. Rev. **80**, 625 (1950).

[7] B. G. Owen and J. G. Wilson, Proc. Phys. Soc. **A64**, 417 (1951).

Translated by H. Kasha
340

SPECTROSCOPIC INVESTIGATION OF AN INTENSE PULSED DISCHARGE IN HYDROGEN. III
DETERMINATION OF THE PARAMETERS OF A HIGH-TEMPERATURE PLASMA

S. Yu. LUK'YANOV and V. I. SINITSYN

Submitted to JETP editor December 16, 1958

J. Exptl. Theoret. Phys. (U.S.S.R.) **36**, 1621-1624 (June, 1959)

The results of a spectroscopic measurement of the parameters of a high-temperature plasma are presented. It is shown that at the time of maximum compression the density of charged particles along the axis of the discharge is 35 — 40 times greater than the original density of neutral atoms. The ionic temperature reaches one or two million degrees.

IN the present paper we report the results of an investigation on a test sample consisting of approximately $^3/_4$ of a liter of high-temperature plasma formed by an intense discharge in hydrogen at the instant of maximum compression. The discharge was produced in a straight cylindrical chamber connected to a pulsed circuit. The circuit and the construction of the apparatus have been described in the literature.[1] We list the circuit parameters: $C = 86\,\mu f$; $V_0 = 35$ kv; $J_{max} = 460$ kiloamp; $dJ/dt = 1.5 \times 10^{11}$ amp/sec (at $t = 0$).

The chief interest of physicists who have been concerned with studying such discharges has been the second compression stage of the pinch, at which time hard radiation is observed.[2,3] The present communication is devoted primarily to the results of a spectroscopic investigation of the first compression stage.

The electronic temperature T_e was estimated from the energy distribution in the continuous plasma spectrum; the absolute intensity of the continuum was used to determine the density of charged particles. As is well known, the spectral densities of the bremsstrahlung and recombination radiation of a hydrogen plasma can be given in the form:

$$I_b(\nu, T_e) = \alpha_1 n^2 T^{-1/2} \exp(-h\nu/T_e) L, \quad (1)$$

$$I_r(\nu, T_e) = \alpha_2 n^2 T^{-3/2} \exp[-h(\nu - \nu_i)/T_e] m^{-3}. \quad (2)$$

Here $n = n_i = n_e$ is the density of charged particles, T_e is the electronic temperature, m is the principle quantum number of the level to which recombination occurs, $h\nu_i$ is the energy of this level, α_1 and α_2 are combinations of constants, L is a correction factor introduced in making quantitative measurements (when $T_e \gg h\nu$ this factor increases logarithmically with increasing temperature[4]). The distribution of the total energy $I_b + I_r$ recorded at low temperatures is determined by the factor $\exp(-h\nu/T_e)$. If this distribution is measured in relative units the slope of the line $\ln(I/I_0) = \varphi(h\nu)$ plotted along the experimental points gives T_e at a given instant of time. Unfortunately, at high electronic temperatures this method is effective only if the measurements are carried out over a wide spectral region. Measurements carried out in the visible and near ultraviolet regions provide only a rough estimate of T_e.

It should be noted, however, that even a very approximate knowledge of the electronic temperature in a high-temperature region does not prevent a relatively accurate determination of the density of charged particles from the intensity of the continuum. As a numerical calculation will show, the quantity that depends on the electronic temperature in $I_b + I_r$ varies very slowly in the visible region if $T_e > 10$ ev. For example it is found that a change of T_e by a factor 30 (from 10 ev to 300 ev) corresponds to a change of 20% in n. Thus, from the intensity of the continuum one can obtain a fairly reliable estimate of n. Obviously the dimensions of the radiating volume of the plasma must be known.

The intensity of the continuous spectrum required for estimating T_e and the measurement of n were made by a photoelectric method. In order to obtain reliable collimation of the light from an isolated radiating volume a monochrometer with an FEU-12 photomultiplier was located at a considerable distance from the discharge chamber (up to 20 m). The apparatus was calibrated with a tungsten filament. The size of the

Line	λ, A	Transitions	Excitation energy, *ev	Line	λ, A	Transitions	Excitation energy, *ev
N V	4945	$6^3G - 7^3H$	90.56	N V	4619.4	$3^3S - 3^3P$	58.98
N V	4943	$6^3F - 7^3G$	90.56	N IV	4057.80	$3^1P - 3^1D$	52.98
N II	4621.39	$3^3_2P - 3^3_2P$	21.06	N IV	3484.90	$3^3S - 3^3P$	50.11
N II	4607.15	" "	21.06	N IV	3482.98	" "	50.11
				N IV	3478.69	" "	50.11

*The excitation energy is computed from the ground state of the corresponding ion.

radiating volume was determined from streak photographs of a luminescent diameter of the discharge channel. Only a narrow spectral region was used for the pictures. These spectral streak photographs are made by combining a monochrometer with a photochronograph.

The ionic temperature was determined from the Doppler broadening of the N IV 3479 (3^3S-3^3P) line by introducing a small amount of nitrogen into the discharge. The observations were carried out along the discharge axis. The broadening of the N IV 3479 line due to the quadratic Stark effect was apparently small. Although the numerical values of the Stark constants for the case considered here are not known to the author the experiments carried out at different hydrogen densities indicate that the effect is small. To within 3% the experimental profile of the line coincides with a Gaussian curve. The Zeeman splitting is apparently less than 0.05 A, and this value lies within the limits of the experimental accuracy. The measurements were carried out by means of the so-called spectral sweep method[1] using an ISP-28 spectrograph with quartz objectives. We may note that the nitrogen "thermometer" on the N IV 3479 line was also used to measure the ionic temperature of a plasma in reference 5.

As has been noted earlier[1] in experiments carried out with a mixture of 95% H_2 + 5% N_2, at maximum compression one observes lines due to highly ionized nitrogen in addition to the continuum. The most intense observed nitrogen lines are listed in the table.

An estimate of the lower limit for T_e, made on the basis of an analysis of the energy distribution in the continuous spectrum, yields $T_e > 10$ ev.

The cross section of the pinch, determined from a photograph with sweep transverse to the discharge axis and from photoelectric observations along the discharge axis at the time of maximum compression, indicate values of 35 – 40 mm. As an illustration, Fig. 1 shows spectral sweep photographs of the discharge.

The density of charged particles for $p_0 = 0.05$ mm Hg reaches $n = 1.2 \times 10^{17}$ cm^{-3}; assuming 100% ionization this figure corresponds to a density along the chamber axis which is 35 times greater than the initial value (in the calculations the value $T_e = 100$ ev is taken). It is interesting to note that the experimental data are in good agreement with the theoretical estimates (cf. for example reference 6). In Fig. 2 is shown the density of charged particles ($n \approx \sqrt{I}$) as a function of pressure. It is apparent that up to a pressure of $p_0 \approx 0.2$ mm Hg the experimental points lie on a straight line. This result may be taken as direct proof that the parameters characterize a hydrogen

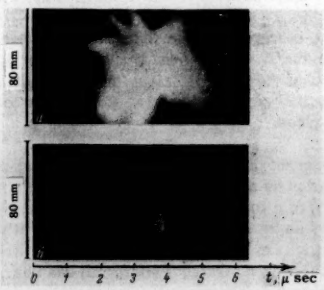

FIG. 1. Streak photograph of the discharge channel with spectrally resolved light at a pressure $p_0 = 0.1$ mm Hg: a) for the spectral region in the vicinity of H_α ($\Delta\lambda = 100$ A); b) in the region $\lambda = 6400$ A ($\Delta\lambda = 100$ A, continuum). The pictures were taken through a side window with which it was possible to view a portion of the discharge 8 cm in size.

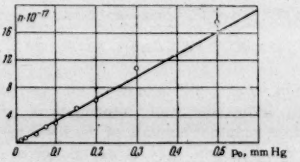

FIG. 2. The density of charged particles ($n \sim \sqrt{I}$) measured at the time of maximum compression as a function of initial pressure in the chamber.

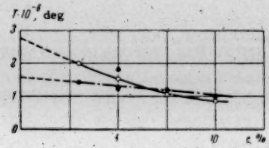

FIG. 3. Ionic temperature measured from the Doppler broadening of the N IV 3479 line at maximum compression of a discharge in deuterium as a function of the concentration of nitrogen impurity: ○) $p_0 = 0.05$ mm Hg and the resolution time $\Delta\tau = 1.3$ microseconds; ●) $p_0 = 0.1$ mm Hg, $\Delta\tau = 0.9$ microseconds; ▲) discharge in hydrogen (H_2) $p_0 = 0.05$ mm Hg, $\Delta\tau = 1.3$ microseconds. (In the reduction to the same $\Delta\tau$ the curves are displaced vertically).

discharge which is free from impurities. It is possible that at high initial pressures the role of free-bound transitions becomes more important.

The ionic temperature determined from the Doppler width of the N IV 3479 line is 1.2×10^6 °K (for $p_0 = 0.05$ mm Hg). It should be noted that the quantity T_i may be too high if at the first contraction of the pinch most of the particles participate in the directed motion along the axis. On the other hand, the value of T_i can be too low for two reasons: first, even a small admixture of nitrogen causes a large increase in the mass of the gas and this reduces the kinetic energy of the contracting plasma. The second effect is purely instrumental in nature. The resolution time of the spectral sweep is somewhat greater than the time during which the maximum temperature exists in the pinch. Hence the experimental curve is the result of the superposition of instantaneous contours (corresponding to somewhat lower temperatures) and its width is smaller. In Fig. 3, as an example, it is shown that by extrapolating the values of T_i obtained from experiments with impurities it is possible to determine the ionic temperature under "pure conditions". In principle such extrapolation methods allow us to circumvent the numerous difficulties involved in any exact determination of T_i.

[1] S. Yu. Luk'yanov and V. I. Sinitsyn, J. Exptl. Theoret. Phys. (U.S.S.R.) **34**, 849 (1958), Soviet Phys. JETP **7**, 587 (1958).

[2] Artsimovich, et al., Атомная энергия (Atomic Energy) **3**, 84 (1956).

[3] S. Yu. Luk'yanov and I. M. Podgornyĭ, Атомная энергия (Atomic Energy) **3**, 97 (1956).

[4] V. I. Kogan and A. B. Migdal, Физика плазмы и проблемы управляемых термоядерных реакций (Plasma Physics and the Problem of a Controlled Thermonuclear Reaction), Izd-vo Akad. Nauk SSSR, Vol. 1, p. 172, 1958.

[5] P. C. Thonemann, et al., Nature **181**, 217 (1958).

[6] Braginskiĭ, Gel'fand, and Fedorenko, Физика плазмы и проблемы управляемых термоядерных реакций (Plasma Physics and the Problem of a Controlled Thermonuclear Reaction), Izd-vo Akad. Nauk SSSR, Vol. 4, p. 201, 1958.

Translated by H. Lashinsky
341

INVESTIGATION OF THE INITIAL STAGES OF PLASTIC DEFORMATION OF ROCK SALT CRYSTALS

R. I. GARBER and L. M. POLYAKOV

Physico-Technical Institute, Academy of Sciences, Ukrainian S.S.R.

Submitted to JETP editor December 20, 1958

J. Exptl. Theoret. Phys. (U.S.S.R.) **36**, 1625-1630 (June, 1959)

Plastic deformation processes in rock salt, involving the formation of elementary displacements that constitute a special deformations stage, are investigated. Further deformation results in single slip bands. The activation energy required for the annealing of the residual stresses of the elementary displacements is half that of the slipping bands. An additional attenuation of light has been detected near the traces of the elementary displacements. It is proposed to attribute this to the influence of systems of line inhomogeneities differently oriented on both sides of each trace. It is established that certain traces of elementary displacements contract after removal of the load, similar to the case of elastic twins of sodium saltpeter. It is established that the trace of the elementary displacement on the lateral surface of the crystal has a smooth profile, extending over a distance of approximately 1500 A. The smooth form of the profile is well explained by the influence of surface-tension forces, which are in thermodynamic equilibrium with the additional residual stresses.

SLIPPING in plastic deformation is usually described as simple shear, shear with bending of the glide planes, twinning over irrational planes, displacement, and multiplication of the dislocations. However, the large number of observed phenomena makes it impossible to describe this complicated process with any one mechanism alone. For a detailed analysis it is best to subdivide the entire process into individual stages, as was done in the investigation of mechanical twinning.[1,2]

The stages of the process are best established in accordance with the type of the deformation elements and the magnitude of the stress at which they appear. In the deformation of rock-salt crystals, we can distinguish the following stages (σ is the normal stress in g/mm^2):

Elastic deformation	$\sigma < 70$
Elementary shear	$\sigma \approx 70$
Single slip band	$\sigma \approx 100$
Stacks of slip bands	$\sigma > 100$
Isotropic scattering of light (Tyndall cone)	$\sigma > 120$
Asterism	$\sigma > 600$
Failure	$\sigma > 2000$

In the present paper we consider the initial stages of deformation, which terminate in formation of a single slip band. The first stage is elastic deformation. It is characterized by homogeneous distribution of the strains in a homogeneous stressed state, and by the absence of other changes of shape, dimensions, or physical properties of the specimens. In elastically-deformed specimens we can observe, under crossed polarizing prisms, homogeneous transmission of light, the intensity of which increases with increasing stress. The initial illumination is restored after removal of the load. When an elastically-stressed specimen is rotated, the illumination is restored every 90°. For well annealed rock-salt crystals without imperfections, cut along the (100) cleavage planes, these stages correspond to a compression or tension stress $\sigma < 60-70$ g/mm^2. Changes in photo-conductivity and color at lower stresses, described in references 3 and 4, must be attributed to uneven distribution of stresses over the volume of the specimen. The yield point as determined by this method cannot be connected directly with any element of deformation, and characterizes merely the presence of local overstresses in the specimen. Elementary shears occur in annealed specimens that have no defects, under slow smooth loading. In experiments with a rigid loading device, shears of this type appear at a deformation rate up to 0.5% per minute. At a higher rate of deformation, this stage does not appear.

The appearance of elementary shear in a specimen is manifest by a characteristic clear strain pattern in polarized light, which is retained in a somewhat modified form (the illuminated portions become noticeably darker) also after the load is removed from the specimen. The appearance of

intersecting elementary shears changes radically the picture of the stress distribution. Stresses of opposite sign cancel each other, while those of equal sign add together. The elementary shears, as a rule, originate on the surface; as the stress increases, the region of shear penetrates deeper into the specimen and gradually grows through the entire specimen. The shear appears on a surface defect, capable of causing the necessary stress concentration. Stepanov[5] has shown that the shear can be localized by producing a scratch several microns deep on the surface of the specimen. It is characteristic, that annealing at 600°C for six hours does not eliminate the effects of the scratch.

FIG. 1. Crystal with incomplete traces of elementary shear along the (110) plane, which break off inside the specimen. Polarization microscope, crossed prisms. Compression stress along the (010) axis – 70 g/mm² (× 25).

Figure 1 shows a photograph of a rock-salt crystal in transmitted light, under crossed polarization prisms, after several traces of the elementary shear have been produced in it. Some of the traces do not pass through the entire specimen. A small increase in stress in the specimen results in new traces and a certain elongation of those already existing. Electron-microscope photographs of the cleavage surface perpendicular to the slip planes show curving and other distortion of the tapering trace of the elementary shear near its vertex (Fig. 2). The increase in the resistance to further spread of the shear can be attributed to redistribution of the stresses. The traces of the elementary

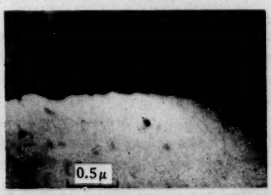

FIG. 2. Distortions that lead to the tapering of the trace of the elementary shear. Electron microscope, lacquer replica contrasted with chromium (× 25,000).

shear have a higher illumination on the surface of the specimen, corresponding to higher values of the stress remaining after removal of the load. It is in these places that the shears, which penetrate into the crystal where the stresses are considerably lower, originate. As the stress increases to $\sigma \approx 100$ g/mm², the elementary shear develops into a single slip band (Fig. 3).

FIG. 3. Transformation of elementary shear traces, 2 into single slip bands, 1 (so called "pencil lines"), after the shear is increased. Crossed prisms (× 25).

If the lateral surfaces of the specimen are coated with warm water prior to loading, the elementary shears may occur inside the specimen in the form of short lines, which are brightest in the middle. The water dissolves and "cures" the surface imperfections. As a result, the weakest places are the imperfection regions inside the specimens. As the stress is increased, the trace of such a shear spreads also to the lateral faces of the specimen. Sometimes the traces of the shear pass through the vertices of the two-faced angles of the pores, which are bounded along the cleavage and serve to concentrate the stresses.

The elementary shears are sensitive to variable stresses. If a specimen with traces of elementary shears is loaded (10–15) times and the stress is raised to approximately 70 g/mm², slip bands are formed in the region of the elementary shears. In an investigation of reverse slip in rock salt[6] it was noted that certain slip bands were partially shortened after unloading. This phenomenon, similar to elastic twinning, was observed in calcite, sodium saltpeter, and antimony; it was also observed during slip in elementary shear production. To observe this phenomenon it is necessary to employ a rigid loading device to produce the strain at a rate up to 0.5% per minute, and to remove the load immediately after loading. The vertical shear traces of Fig. 4 are shortened after unloading, while the horizontal traces can serve as reference lines.

The crystallographic orientation of the elementary shears is determined not only by the fact that

FIG. 4. Shortening of two longitudinally incomplete traces after unloading and formation of tapered elementary shear traces. Crossed prisms (×25).

the maximum tangential stress occurs in the {(110)} planes in compression along the edge of the cube. In specimens variously oriented with respect to the crystallographic axes, the elementary shear traces are always located in the planes of the rhombic dodecahedron {(110)}. If the specimen axis is oriented along the [110] direction then the greatest shear stresses are in the (100) plane and are directed along the edge of the cube. However, in this case too, the elementary shears occur in the plane of the rhombic dodecahedron, the normal to which $[0\bar{1}\bar{1}]$ makes an angle of 60° with the axis of the compression forces, and the shear stress is one-half or one-third the shear stress in the (010) plane along the [100] direction. As can be seen, the law of tangential stresses is obeyed also in the formation of elementary shears.

The difference between the elementary shear stage and the later stages of the deformation is also disclosed by an investigation of the residual stresses during the annealing process. Samples of rock salt were deformed until elementary shears ($\sigma_0 \approx 70$ g/mm^2) were formed or until slip bands and packets of slip bands were formed ($\sigma_0 \approx 120$, 250, and 500 g/mm^2), and were then annealed at 350–750°C. The time interval τ needed to eliminate the residual birefringence in the specimen was determined during the annealing. The experimental data were used to plot curves of ln τ (1/T) (Fig. 5). The linearity of these curves is the reason for believing that the removal of the distortions that remain after deformation is an activation process.

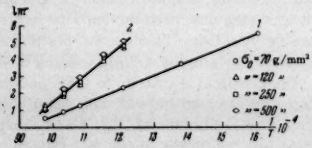

FIG. 5. Logarithm of the relaxation time of the residual stresses as a function of the reciprocal of the absolute annealing temperature and of the maximum stress during deformation, σ_0. 1) elementary shears, 2) later stages of deformation.

All the experimental points of Fig. 5 fall on two straight lines with different slopes. The points on line 1 correspond to annealing of crystals with elementary shear traces, while those on line 2 pertain to subsequent stages of deformation. If the activation energy of strain relief is determined from the slope of the ln τ (1/T) lines, we obtain for line 1, corresponding to elementary shears, $E_1 = 14$ kcal/g-mole, and for line 2, pertaining to slip bands and packets of slip bands, $E_2 = 30$ kcal/g-mole. The obtained results lead us to believe that to remove the residual stresses in the former case it is enough to have a diffusion displacement of the molecules in the slip plane, while in the latter case volume migration is essential.

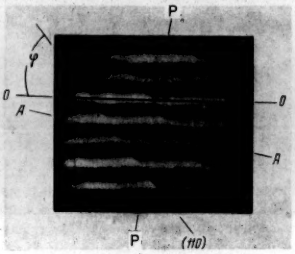

FIG. 6. Curving of compensator interference fringes on the elementary shear traces. The residual stresses on both sides of the elementary shear traces are of equal magnitude and opposite sign. Crossed polarization prisms. A quartz wedge – compensator – is installed in the focal plane of the eyepiece. A–A) analyzer, P–P) polarizer, O–O) hairline on the compensator.

Figure 6 is a photograph of a specimen with two elementary shears taken in transmitted monochromatic light under crossed polarization prisms and a compensator in the form of a quartz wedge, located between the prisms and made coincident with the image of the crystal. The interference fringes are displaced symmetrically from the normal position, which has been fixed with the aid of the hairline O—O. Consequently, on each elementary shear trace the residual stresses are approximately equal in absolute magnitude and opposite in sign. The normal stresses are determined in this case from the known formula[10]

$$\sigma = a \sin \varphi / ALd, \qquad (1)$$

where A is the distance between neighboring interference fringes, a the displacement of the interference fringe in the stressed portion, φ the angle between the shear trace and the edge of the quartz wedge, L the corresponding piezo-optical con-

stant of rock salt, and d the thickness of the specimen along the beam. The residual stresses calculated from (1) are approximately equal to the average stresses in the specimen during the production of elementary shears ($\sigma \approx 66$ g/mm^2).

On the whole, the picture agrees with the scheme proposed by Obreimov and Shubnikov.[7] However, if the density of the image of a crystal with elementary shears, obtained under crossed polarization prisms, is measured along a straight line perpendicular to the shear traces, a clearly asymmetrical curve is obtained. The latter is in clear contradiction with the conclusions made on the basis of Fig. 6, where it is assumed that the illumination in Fig. 1 is determined only by birefringence due to residual stresses. This contradiction appears also in observing the variation in the illumination on both sides of the shear trace upon rotation of the crystal relative to the beam. By placing the crystal between crossed polarization prisms, it is easy to verify that the illumination on either side of the elementary shear trace changes from maximum to minimum as the table with the crystal is rotated 90° relative to the beam. The initial distribution of the illumination is restored only when the specimen is rotated 180°. Were the illumination produced only by birefringence, it would be restored in crossed prisms by rotating the table 90°, i.e., four times per revolution. The contradiction can be resolved by assuming that the birefringence is accompanied by additional scattering, reflection, or absorption, leading to the attenuation of the light of definite polarization at definite crystal positions. Such an effect can be expected from a system of scratches, cracks, or groups of dislocations. It must be assumed that these imperfections are differently oriented on the two sides of the shear trace, since the minimum illumination on one side of the trace corresponds to the maximum illumination on the other side. The orientations of the imperfections may, for example, coincide with the planes of the cube.

An investigation of the illumination near the trace upon rotation of the crystal has in fact disclosed additional attenuation of the light, possibly as a result of diffraction by the system of scratched irregularities of the type indicated above.

In a previously published paper by one of the authors and Kovalev,[8] it was shown that electron-microscope photographs of deformed rock salt show systems of cracks oriented along the cube planes in the slip-band packets.

Interesting information on deformation can be obtained by studying the shape of the lateral surface of the specimen at the place where the elementary shears emerge. A sample of rock salt was deformed until elementary shears were formed, and a collodion replica of the cleavage plane parallel to the lateral surface was made and contrasted by a molecular beam of chromium, directed at a small angle to the surface. The replica was then viewed in an electron microscope (Fig. 7). The density of

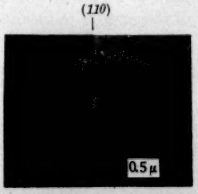

FIG. 7. Emergence of elementary shear trace on the (100) plane. Lacquer replica contrasted with chromium, at an angle of 12° to the direction (010). (× 25,000)

the negative of the electron-microscope print was measured along a line perpendicular to the slip trace. Using the microphotogram and knowing the contrasting condition, it is possible to plot the profile of the lateral surface of the specimen by the procedure described in reference 9. The height of the profile in section x is

$$h_x = \cot\theta \left[\int_0^x \frac{\ln (D_0 / D_x)}{\ln (D_0 / D_h)}\, dx - x \right], \qquad (2)$$

where θ is the angle between the contrasting direction and the normal to the surface of the replica ($0 < \theta < 90°$), D_0 the density of the electron-diffraction negative in the portions of the print not covered by chromium, D_x the density in section x, D_h the density in the horizontal sections located far away from the curved portion of the surface of the replica. In the derivation of Eq. (2) it was assumed that the distance from the source of the contrasting molecular beam to the print is much greater than the dimensions of the print, and that absorption and scattering of the electrons occurs only in the chromium contrasting layer.

The profile of the lateral surface of the specimen (Fig. 8) has a smooth shape at the place of

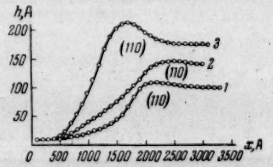

FIG. 8. Relief of the cleavage surface along the (100) plane of crystals with elementary shear traces: 1) $\sigma = 66$, 2) $\sigma = 80$, 3) $\sigma = 95$ g/mm^2.

emergence of the elementary shear. The lateral surface is concave on one side of the shear trace and convex on the other. The small steps, usually employed to represent schematically the emergence of dislocations and similar phenomena in describing pure shear, are obtained at later stages of the deformation.

The shape of the obtained profile makes it possible to state that the shear has oaused one portion of the crystal to become displaced relative to the other. The major part of the step is smoothed by the concave part of the profile. Adjacent to this section is a convex bead, the height of which is approximately one-tenth that of the step. The causes of the appearance of such a bead are still not clear. It is possible that the residual stresses cause elastic bulging of the region of the crystal adjacent to the shear trace. This recalls to some extent the elastic deformation of the surface near a forming elastic twin, as described in reference 1. Such a formation was recently called the accommodation region.[10]

If the smoothness of the concave portion of the profile is due to surface-tension forces, stresses τ should occur inside the deformed region ABC (Fig. 9) and in its direct vicinity. The average density of elastic energy is

$$\bar{E} = \bar{\tau}^2 / 2G, \tag{3}$$

where G is the shear modulus. The condition of stability of the profile can be written by equating the elastic energy in the deformed volume ABC to the surface energy difference connected with the change in the area of the lateral surface in the region of the shear (see Fig. 9). We have

$$\alpha_{(110)} \widehat{AB} + \bar{E} S_{ABC} \geqslant \alpha_{(100)} \overline{AC} + \alpha_{(110)} \overline{BC}. \tag{4}$$

(S_{ABC} is the area of the triangle ABC). Inasmuch as the curvature of arc AB is small, we can put

$$\widehat{AB} = \overline{AB}. \tag{5}$$

The tangent of γ — the slope of the surface for the elementary shears—ranges from 0.03 to 0.12, while the height h of the profile is from 10^{-6} to 2.5×10^{-6} cm. Inserting these values into (4), (3), and (5), we determine the magnitude of the critical tangential stresses under which the profile still remains smooth

$$\bar{\tau}_c \geqslant \left[\frac{4G\,(\alpha_{(100)} + V\overline{2}\,\alpha_{(110)})\,\gamma}{(1+\gamma)\,h} \right]^{1/2}. \tag{6}$$

Putting $\alpha_{(100)} = 500$ erg/cm^2, $\alpha_{(110)} = 1250$ erg/cm^2, and $G = 1.26 \times 10^{11}$ dyne/cm^2 we obtain an average value $\bar{\tau}_c \gtrsim 10^{10}$ dyne/cm^2 for h = 250 A and $\gamma = 0.12$.

Equating the theoretical strength of the crystal with the local stresses at the emergence of the elementary shear, as calculated by Eq. (6), we note that in practice the profile remains curved until the crystal fails in the region of emergence of the shear.

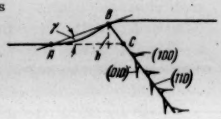

FIG. 9. Arrangement of elementary shear trace of distortions on the cleavage surface (100), and of the systems of scratches which possibly lead to the observed attenuation of light on one side of the trace under crossed prisms of a polarization microscope.

Observations in polarized light show that the trace is much brighter at the place of emergence on the lateral surface. This can be attributed to the stresses due to curving of the surface. If the radius of curvature of the convex portion of the profile is denoted by R, the magnitude of the stresses, $\tau = \alpha/R = 6.2 \times 10^6$ dyne/cm^2, is indeed approximately equal to the residual stresses near the elementary shear trace. It is seen from this that the increased brightness can be explained by superposition of stresses due to curvature of the surface on the residual stresses that arise during the formation of the elementary shear.

The resolving power of the method used here is different along the x axis and the h axis (see Fig. 8). It amounts to 100 A along the x axis, and therefore one of the results is the conclusion that in the elementary shear the plastic deformation is localized in a layer not more than 10^{-6} cm thick parallel to the shear trace.

In conclusion the authors express their gratitude to V. K. Sklyarov and I. M. Fishman for their help in performing these experiments.

[1] R. I. Garber, J. Exptl. Theoret. Phys. (U.S.S.R.) **17**, 47 (1947).

[2] Garber, Gindin, and Polyakov, Paper delivered at International Conference on the Mechanical Properties of Crystals, Leningrad, May 1958.

[3] M. N. Podaschevsky, Z. Physik, **91**, 97 (1934).

[4] A. Smekal, Z. Metallkunde **26**, 220 (1934).

[5] A. V. Stepanov, Dokl. Akad. Nauk SSSR **15**, 539 (1937).

[6] R. I. Garber, Dokl. Akad. Nauk SSSR **63**, 235 (1948).

[7] I. V. Obreimov and L. V. Shubnikov, Ж. Российского физ.-хим. о-ва, (J. of Russian Phys.-Chem. Soc.) **58**, 817 (1926).

[8] R. I. Garber and A. I. Kovalev, Dokl. Akad. Nauk SSSR **86**, 901 (1952).

[9] Garber, Gindin, and Shubin, J. Exptl. Theoret. Phys. (U.S.S.R.) **36**, 376 (1959), Soviet Phys. JETP **9**, 260 (1959).

[10] V. I. Startsev and V. M. Kosevich, Dokl. Akad. Nauk SSSR **101**, 861 (1955).

Translated by J. G. Adashko
342

INTERACTION BETWEEN 660-Mev PROTONS AND ATOMIC NUCLEI AND THE NUCLEAR INTERNAL MOMENTUM DISTRIBUTION OF NUCLEONS

L. S. AZHGIREĬ, I. K. VZOROV, V. P. ZRELOV, M. G. MESHCHERYAKOV, B. S. NEGANOV, R. M. RYNDIN, and A. F. SHABUDIN

Joint Institute for Nuclear Research

Submitted to JETP December 20, 1958

J. Exptl. Theoret. Phys. (U.S.S.R.) **36**, 1631-1649 (June, 1959)

We investigated the angular distributions and (by magnetic analysis) the energy spectra of secondary particles (mainly protons with energies $\gtrsim$ 60 Mev) emitted at angles of 7, 12.2, 18, 24, and 30° in reactions between 660-Mev protons and the nuclei of Be, C, Cu, and U. The differential cross sections for the emission of such secondary charged particles increase with decreasing angle. In order of decreasing energy, the various spectral regions of all the investigated elements correspond respectively to diffractional scattering of protons on nuclei (in the small-angle region), single quasi-elastic nucleon collisions, π-meson production on bound nucleons, and intranuclear cascade.

The experimental energy spectra for single quasi-elastic proton-nucleus scattering are compared with the spectra computed in the impulse approximation under various assumptions regarding the momentum distributions of the nucleons in the nuclei. The Be and C data are consistent with a Gaussian nucleon-momentum distribution with a 1/e value at an energy of approximately 20 Mev.

1. INTRODUCTION

INFORMATION on the momentum distributions of nucleons in the ground states of nuclei are gathered from the energy and angular distributions of the products of nuclear reactions induced by high-energy particles. Chew and Goldberger,[1] in their analysis of the data of Hadley and York[2] on the capture of protons from carbon nuclei by 90-Mev neutrons, have shown that the energy and angle distributions of the deuterons correspond to a momentum distribution of the form $\alpha/\pi(\alpha^2+s^2)^2$ with $\alpha^2/2M = 18$ Mev, rather than a distribution corresponding to a model of a Fermi gas made up of non-interacting particles. Selove[3] found, in the case of neutron capture from carbon nuclei by 95 Mev protons, that the experimental data can be satisfactorily explained by approximating the internuclear momentum distribution of the neutrons by means of a sum of two Gaussian distributions of the form $\exp\{-s^2/s_1^2\} + 0.15\exp\{-s^2/s_2^2\}$, where $s^2/2M$ is the energy of the bound neutron, $s_1^2/2M = 7$ and $s_2^2/2M = 50$ Mev. It is essential to assume the presence of a considerable admixture of high-momentum components in the wave function of the ground states of a light nucleus in order to explain qualitatively the direct knock-out of deuterons from nuclei of lithium, beryllium, carbon, and oxygen by 670 Mev protons,[4] as well as to explain the strong smearing on the high-energy side of the spectra of positive and negative pions produced in p + C collisions at the same energy.[5] According to Henley,[6] a Gaussian momentum distribution, corresponding to a mean kinetic energy of 19.3 Mev, agrees best of all with such characteristics of pion production in p + C collisions at 340 Mev (reference 7), as the threshold value of the proton energy, the excitation curve, and the pion energy and angular distributions.

The character of the momentum distribution of the nucleons in the ground state of the nuclei manifests itself most directly in quasi-elastic scattering of fast protons in light nuclei. This process was investigated experimentally at 340 Mev by Cladis, Hess, and Moyer,[8] who found that, within the framework of the impulse approximation, the energy spectra of the protons that are scattered quasi-elastically in carbon and oxygen nuclei satisfy a Gaussian nucleon-momentum distribution, with a value of 1/e at an energy of 16 ± 3 Mev. Subsequently Wilcox and Moyer,[9] by measuring the energy spectrum of the protons in quasi-elastic p-p collisions at 340 Mev, registered by coincidence from both scattered protons, have shown that the Gaussian distribution of the proton momenta inside the beryllium nuclei, with a value 1/e near

20 Mev, gives an acceptable agreement with experiment. Observations of the angular correlations in quasi-elastic p-p collisions at 925 Mev, principally in light nuclei contained in photoemulsions, have led McEwen, Dixon, and Duke[10] to the conclusion that the proton momentum distribution can be approximated by a Gaussian distribution with $1/e$ at 11 ± 3 Mev, but somewhat better agreement with experiment is obtained by the sum of two Gaussian distributions of the form $\exp\{-s^2/s_1^2\} + 0.05 \exp\{-s^2/s_2^2\}$, with $s_1^2/2M = 7$ and $s_2^2/2M = 40$ Mev. Finally, it follows from experiments on the nuclear photoeffect that a Gaussian distribution with $1/e$ at 19 Mev is a good approximation of the momentum distribution of the quasideuteron groups in carbon and oxygen nuclei.[11]

We can thus conclude from the aggregate of data on high energy nuclear reactions of various types that, unlike the Fermi model with its characteristic sharp upper boundary of nucleon momentum distribution, models that use distributions that smear out towards the higher momenta yield acceptable agreement with experiment.

It is the purpose of this article to discuss the principal results of research on the interaction between 660-Mev protons and nuclei of beryllium, carbon, copper, and uranium. The experiments consisted above all of measuring, by the magnetic deflection method, the energy spectra of secondary particles, particularly quasi-elastically scattered protons. Since the condition of applicability of the impulse approximation should be better satisfied with increasing energy of the incident proton, one would expect that the regions of the spectra measured at large angles, corresponding to the higher energies, would contain essentially protons emitted as the result of paired proton-nucleon collisions in the nuclei. The spectra obtained for quasi-elastically scattered protons were compared with the spectra which were calculated with allowance for relativistic kinematics and which satisfied various assumptions regarding the nucleon momentum distributions in the nuclei. In addition, we measured the angular distributions of the secondary charged particles emitted in the investigated collisions.

The experiments were performed with the six-meter synchrocyclotron of the Joint Institute for Nuclear Research.

2. CALCULATION OF THE MOMENTUM DISTRIBUTION IN QUASI-ELASTIC PROTON-NUCLEON SCATTERING

In the case of light nuclei we can assume that a fast incident nucleon is scattered once by an individual nucleon of the nucleus. If the time of collision between two nucleons is much less than the "time of reversal" of the particles in the nucleus, we can assume, in the spirit of the impulse approximation, that the state of the nucleus does not change noticeably during the collision. Furthermore, the role of interaction between the struck nucleon and the remaining nucleons of the nucleus reduces to the "creation" of a momentum distribution at the nucleon that participates in the collision. Therefore collisions between the incident nucleon and the nucleons of the nucleus can be considered as collisions with free particles, the only difference being that the particles of the nucleus move during the time of collision. The amplitude of such "quasi-elastic" collisions with the nucleus is obtained by summing the amplitudes of scattering by the individual nucleons of the nucleus. In the range of large angles, where interference of the waves scattered by the individual nucleons can be neglected, the problem of scattering by the nucleus reduces essentially to the problem of scattering by a classical ensemble of independent particles that have a specified momentum distribution. The distribution function, in turn, is determined by the square of the modulus of the Fourier component of the wave function of the nucleus. We shall consider below the energy distribution of the nucleons, scattered "quasi-elastically" at a specified angle, in the indicated approximation, with allowance for the relativistic kinematics.

The differential cross section $d\sigma_c = \sigma_c(E_c, \cos\vartheta_c)\, d\omega_c$ of elastic collision of two free nucleons in their center of mass system (c.m.s.), and the distribution function $f(\mathbf{s})(d\mathbf{s})$ of the intranuclear particles by momentum, will be assumed known. The momenta of the incident and scattered nucleons will be denoted in the laboratory system by $\mathbf{p}$ and $\mathbf{q}$, while $\mathbf{s}$ will denote the momentum of the intranuclear nucleon. The energy of a particle with momentum $\mathbf{p}$ will be denoted E_p, etc. The corresponding quantities in the c.m.s. will be identified by a subscript "c", while 4-dimensional momenta will be denoted by $\hat{p}$, $\hat{q}$, etc.

To find the number of collisions that lead to a specified momentum $\mathbf{q}$ (more accurately, to momenta concentrated in the element $(d\mathbf{q})$ about the momentum $\mathbf{q}$), we assume that the incident nucleons, like the target nucleons, are distributed in accordance with a certain law. We introduce the distribution functions $f(\mathbf{r}, \mathbf{p}, t)(d\mathbf{r})(d\mathbf{p})$ and $f_n(\mathbf{r}, \mathbf{s}, t)(d\mathbf{r})(d\mathbf{s})$, which determine the probable numbers of the incident particles and the particles

of the nucleus within the volume elements $(d\mathbf{r})(d\mathbf{p})$ and $(d\mathbf{r})(d\mathbf{s})$ in phase space. The functions f and f_n are scalars under the Lorentz transformation.[12] Let us consider collisions of particles with momenta $\mathbf{p}$ and $\mathbf{s}$. Changing over to the system where the particles with momentum $\mathbf{p}$ are at rest, the number of collisions per unit volume per unit time in this system, i.e., per unit 4-dimensional volume, can be written

$$dN = f^0 f_n^0 (dp^0)(ds^0)\, d\sigma v, \qquad (1)$$

where $d\sigma$ is the invariant differential cross section[13] and v is the relative velocity. The superscript 0 denotes that the corresponding quantities are taken in the system where the incident particles are at rest. Since v and $(dp^0)(ds^0)$ are invariant, we express them in terms of the velocities*

$$v = [|\mathbf{v}_p - \mathbf{v}_s|^2 - [\mathbf{v}_p \times \mathbf{v}_s]^2/c^2]^{1/2}[1 - \mathbf{v}_p\mathbf{v}_s/c^2]^{-1},$$

$$(dp^0)(ds^0) = (dp)(ds)(1 - \mathbf{v}_p\mathbf{v}_s/c^2), \qquad (2)$$

where $\mathbf{v}_s = c^2\mathbf{s}/E_s$ and $\mathbf{v}_p = c^2\mathbf{p}/E_p$, and integrate over $(d\mathbf{p})$ and $(d\mathbf{s})$ to obtain an expression for the total number of collisions per unit 4-dimensional volume, required to obtain the specified result:

$$N = \int (dp)(ds) f(\mathbf{r}, \mathbf{p}, t) f_n(\mathbf{r}, \mathbf{s}, t)$$

$$\times [|\mathbf{v}_p - \mathbf{v}_s|^2 - [\mathbf{v}_p \times \mathbf{v}_s]^2/c^2]^{1/2} d\sigma. \qquad (3)$$

If the incident nucleons form a linear monochromatic beam, then $f(\mathbf{r}, \mathbf{p}, t)$ should be chosen in the form

$$f(\mathbf{r}, \mathbf{p}, t) = \frac{\rho^0}{\sqrt{1-\beta_p^2}}\,\delta(\mathbf{p} - \mathbf{p}_0),$$

where ρ^0 is an invariant that represents the density of the incident particle in the rest system. Then†

$$N = \frac{\rho^0}{\sqrt{1-\beta_p^2}} \times \int (ds) f_n(\mathbf{r}, \mathbf{s}, t)[|\mathbf{v}_p - \mathbf{v}_s|^2 - [\mathbf{v}_p \times \mathbf{v}_s]^2/c^2]^{1/2} d\sigma. \qquad (4)$$

The scattering cross section $d\sigma(\mathbf{q}_c)$ in the specified momentum interval $(d\mathbf{q}_c)$ in the c.m.s. can be written

$$d\sigma(\mathbf{q}_c) = \sigma_c \frac{\delta(q_c - p_c)}{p_c^2}(d\mathbf{q}_c)$$

$$= \sigma_c \left|\frac{\partial E_c'}{\partial q_c}\right| \frac{\delta(E_c' - E_c)}{p_c^2}(d\mathbf{q}_c), \qquad (5)$$

where E_c and E_c' are the total energies in the c.m.s. before and after the collision, while $\sigma_c = d\sigma_c/d\omega$. The law of momentum conservation is assumed to hold in (5). Making use of the fact that if the masses of the colliding particles are equal we have $\partial E_c'/\partial q_c = 2c^2 q_c/E_{cq}$, and also making use of the invariance of $(d\mathbf{q}_c)/E_{cq} = (d\mathbf{q})/E_q$ and of the fact that $d\sigma(\mathbf{q}_c) = d\sigma(\mathbf{q})$, we obtain the scattering cross section in the specified momentum interval $(d\mathbf{q})$ in the laboratory system

$$d\sigma(\mathbf{q}) = \sigma_c \frac{2c^2}{p_c}\,\delta(E_c' - E_c)\,\frac{(dq)}{E_q}, \qquad (6)$$

where the quantities pertaining to the center of mass system are assumed to be expressed in terms of the corresponding quantities in the laboratory system.

Inserting (6) into (5), putting $f_n = \rho_n f(\mathbf{s})$ and dividing N by $\rho^0\rho_n^0 v_p$, we obtain the effective cross section for scattering on one of the nucleons of the nucleus.

$$d\sigma_{\text{eff}} = \frac{2Mc^2}{p}\frac{(dq)}{E_q}\int (ds) f(\mathbf{s})[|\mathbf{v}_p - \mathbf{v}_s|^2 - [\mathbf{v}_p \times \mathbf{v}_s]^2/c^2]^{1/2}\sigma_c$$

$$\times \delta(E_c' - E_c)/p_c\sqrt{1-\beta_p^2} = N/\rho^0\rho_n^0 v_p. \qquad (7)$$

In calculating the integral contained in (7), it is convenient to introduce in s-space a polar system of coordinates (s, θ, Φ) with a polar axis in the direction of momentum transfer $\boldsymbol{\kappa} = \mathbf{q} - \mathbf{p}$. Let us first transform a δ-function. Since $E_c = 2E_{cp} = 2(E_p - \mathbf{v}\cdot\mathbf{p})(1 - v^2/c^2)^{-1/2}$, where $\mathbf{v}$ is the velocity of the center of mass of the colliding nucleons (and analogously for E_c'), we get

$$\delta(E_c' - E_c) = \frac{1}{2}\sqrt{1 - v^2/c^2}\,\delta(E_q - \mathbf{vq} - E_p + \mathbf{vp})$$

$$= (1/2c)\,\delta(\hat{\kappa}\hat{P})\sqrt{\hat{P}^2}, \qquad (8)$$

where $\hat{P}$ and $\hat{\kappa}$ are the 4-vectors of total momentum and momentum transfer, and the scalar product of the two vectors $\hat{a}$ and $\hat{b}$ is defined as $\hat{a}\hat{b} = -(a_4 b_4 + \mathbf{ab}) = a_0 b_0 - \mathbf{ab}$. When integrating over the polar angle θ, we make use of the well-known formula

$$\delta(f(\theta)) = \sum_{\theta_0} \delta(\theta - \theta_0)/|\partial f(\theta)/\partial\theta|_{\theta=\theta_0},$$

where the summation is carried out over all roots of equation $f(\theta_0) = 0$. In this case the role of $f(\theta)$ is played by the function $\hat{\kappa}\hat{P} = (E_q - E_p) \times (E_s + E_p)/c^2 - (\mathbf{p} + \mathbf{s})\boldsymbol{\kappa}$. Setting this equal to zero, we find

$$\cos\theta_0 = [(1/c^2)(E_q - E_p)(E_s + E_p) - \mathbf{p}\boldsymbol{\kappa}]/s|\boldsymbol{\kappa}|. \qquad (9)$$

The condition $|\cos\theta_0| \leq 1$ leads, in conjunction

*The connection between $(ds^0)(dp^0)$ and $(dp)(ds)$ follows from the fact that (dp) can be considered as the fourth component of the infinitesimal 4-vector $\mathcal{E} = ((dp)\mathbf{v}_p, ic(dp))$.

†A formula analogous to (4) was obtained earlier by Chernikov.[14]

with (9), to the result that the permissible values of s are bounded from below by a minimum value $s = s_0$:

$$s_0 = \frac{1}{\varkappa^2 - (E_q - E_p)^2/c^2}\left|\varkappa\left\{\frac{E_p(E_q-E_p)}{c^2} - \varkappa\mathbf{p}\right\}\right.$$
$$+ \frac{E_q - E_p}{c}\left\{\left[\frac{E_p(E_q-E_p)}{c^2} - \mathbf{p}\varkappa\right]^2\right.$$
$$\left.\left. - \left[\frac{(E_q-E_p)^2}{c^2} - \varkappa^2\right]M^2c^2\right\}^{1/2}\right|. \quad (10)$$

The square root within the absolute sign is always real, since $\hat{\kappa}$ is either a space-like or a null vector. The derivative $|\partial f(\theta)/\partial\theta|_{\theta=\theta_0}$ has a value $|\partial(\hat{\kappa}\hat{P})/\partial\theta|_{\theta=\theta_0} = \kappa s \sin\theta_0$. Thus

$$\delta(E_c' - E_c) = \frac{1}{2}\frac{\sqrt{\hat{P}^2}}{c}\frac{\delta(\theta-\theta_0)}{\varkappa s\sin\theta_0}. \quad (11)$$

Inserting (11) into (7) and considering that

$$p_c = \sqrt{\frac{(\hat{P}\hat{p})^2 - \hat{P}^2\hat{p}^2}{\hat{p}^2}} = \frac{1}{\sqrt{\hat{P}^2}}\frac{(Mc)^2}{\sqrt{(1-\beta_p^2)(1-\beta_s^2)}}$$
$$\times\frac{1}{c}[|\mathbf{v}_p - \mathbf{v}_s|^2 - [\mathbf{v}_p\times\mathbf{v}_s]^2/c^2]^{1/2} \quad (12)$$

(this equality can be readily obtained by using the general form of the Lorentz transformation and expressing p_c in terms of the laboratory quantities), we obtain after integrating over θ

$$d\sigma_{\text{eff}} = \frac{c^2}{p\varkappa}\frac{(dq)}{E_q}\int_{s_0}^{\infty}\int_0^{2\pi} d\Phi\,\frac{s\,ds f(s)}{E_s}\,\sigma_c(E_c,\cos\vartheta_c)(\hat{P})^2. \quad (13)$$

A summation of all the nucleons of the nucleus yields

$$\frac{d^2\sigma}{d\omega\,dq} = \frac{1}{p|\mathbf{q}-\mathbf{p}|}\frac{q^2}{\sqrt{c^2q^2 + M^2c^4}}$$
$$\times\sum_{i=1}^{A}\int_{s_0(q)}^{\infty}\int_0^{2\pi} d\Phi\,\frac{s\,ds f(s)}{\sqrt{c^2s^2 + M^2c^4}}\,E_c^2\sigma_c^i(E_c,\vartheta_c). \quad (14)$$

The quantities E_c and $\cos\vartheta_c$ are readily expressed in terms of the laboratory system and equal, respectively

$$E_c = c\sqrt{\hat{P}^2} = c[2(M^2c^2 + E_pE_s/c^2 - \mathbf{ps})]^{1/2},$$

$$\cos\vartheta_c = 1$$
$$+ \frac{E_s(E_q-E_p)/c^2 - (\varkappa s) - (E_pE_q/c^2 - \mathbf{pq}) + M^2c^2}{E_sE_p/c^2 - \mathbf{sp} - M^2c^2}$$
$$= 1 + \frac{2[M^2c^2 - (E_pE_q/c^2) + \mathbf{pq}]}{E_c^2/2c^2 - 2M^2c^2}, \quad (15)$$

where

$$\varkappa s = \varkappa s\cos\theta_0, \qquad \mathbf{pq} = pq\cos\vartheta, \qquad \mathbf{p}\varkappa = p\varkappa\cos\theta_1,$$
$$\cos(\widehat{\mathbf{ps}}) = \cos\theta_0\cos\theta_1 + \sin\theta_0\sin\theta_1\cos\Phi.$$

In the nonrelativistic limit

$$s_0 \to q(q - p\cos\vartheta)/|\mathbf{q}-\mathbf{p}|.$$

Assuming that σ_c depends only on the momentum transfer, we obtain an equation similar to that previously derived by Wolff[15]

$$\frac{d^2\sigma}{d\omega\,dq} = \frac{8\pi q^2}{p|\mathbf{q}-\mathbf{p}|}\sum_{i=1}^{A}\sigma_c^i(\mathbf{q}-\mathbf{p})\int_{s_0}^{\infty} sf(s)\,ds. \quad (16)$$

3. THE EXPERIMENT

The energy spectra of the secondary particles emitted in p + Be, p + C, p + Cu, and p + U collisions, were measured in the approximate energy interval from 100 to 700 Mev, at angles of 7, 12.2, 18, 24, and 30°. The magnetic analyzer used was the same as employed in a previous investigation of momentum spectra of the products of the $pp \to np\pi^+$, $pp \to pp\pi^0$, and $pp \to d\pi^+$ reactions (reference 16) and in experiments on the direct knock-out of deuterons from light nuclei by 670-Mev protons.[4] The papers referred to contain detailed information on the analyzer, its placement relative to the primary beam of the protons, the concrete shield of the synchrocyclotron, and the procedure used to process the measurement data and the corrections introduced. In the present experiment, the changeover from one angle of observation to another was made by moving the target R (using the notation of Fig. 1 in reference 16) along the primary proton beam, which passed near the edge of the pole pieces of the analyzer magnet. In all cases, the particles entered and left at right angles to the boundary of

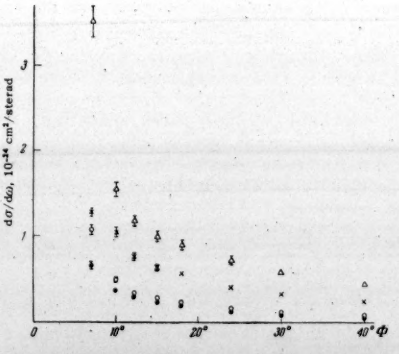

FIG. 1. Angular distribution of secondary charged particles with range > 3.1 g/cm² of tolane, emitted in collisions of 660-Mev protons with Be, C, Cu, and U. The experimental points correspond to: • – beryllium o – carbon, × – copper, Δ – uranium.

TABLE I

Angle of observation Φ, degrees	7	12.2	18	24	30
Distance from target to the edge of the pole piece, cm	410	218	138	94	64
Deflection angle, degrees	18.3	24	29.5	19.5	25.7
Radius of curvature ρ of the central trajectory, cm	360	284.8	222	350	265
Angular divergence of secondary beam in the horizontal plane, degrees	0.10	0.14	0.17	0.20	0.22
Calculated resolution $\Delta H\rho/H\rho$, %	1.9	1.5	1.2	2.6	1.9

the magnetic field. The data of Table I show how changes in the angle of observation affected the distance between the target and the forward edge of the pole, the angle of deflection of the particles in the magnetic field, the radius of curvature of the central trajectory, the angular divergence of the separated beam of secondary particles in the horizontal plane, and the resolution $\Delta H\rho/H\rho$ of the instrument, calculated with allowance for geometrical factors only ($\Delta H\rho$ is the width of the peak at half height).

The energy of the primary protons directly in front of the target was 661 Mev; the mean squared spread in the beam proton energies amounted to approximately 1%. The particles at the analyzer exit were detected by a telescope consisting of four scintillation counters (total thickness 3.1 g/cm^2 of tolane) connected for coincidence. The threshold of proton registration of the telescope was 60 Mev. The registration efficiency for particles in the investigated range of energies was practically 100%. The entire path of the particles in the analyzer, all the way to the telescope, was in vacuum. Targets 2.5 cm high and 1 cm wide were made of chemically pure beryllium, carbon, copper, and uranium and their thicknesses were 3.26, 1.09, 3.45 and 7.62 g/cm^2 respectively.

To find the absolute values of the differential cross sections in the spectrum, $d^2\sigma/d\omega\, dE$, we measured the differential cross sections $d\sigma/d\omega$ for the emission of secondary charged particles in the investigated collisions, within the angle interval from 7 to 40°. In these measurements, made at angles of 24, 30, and 40° with an angular resolution of ±0.8° (the resolution was ±0.4° at smaller angles), the threshold for registration was the same as in the spectrum measurements. From the observed yield of charged particles we calculated the contribution of charged pions, estimated from data on the production of $\pi^{\pm}$ mesons in p + C collisions at 670 Mev,[5] under the assumption that the cross section of the latter process increases as $A^{2/3}$. The contribution of charged pions to the total yield of secondary charged particles did not exceed 7%. The area under the curves of the energy spectra of the secondary particles was normalized to the corresponding experimental values of $d\sigma/d\omega$. Furthermore, the spectra were linearly extrapolated from the last experimental point to the threshold value of the proton-registration energy. The accuracy of this method of estimating $d^2\sigma/d\omega\, dE$ amounts to approximately 20%.

The experimentally-obtained spectrum F(E) is related to the true spectrum G(E) by the following integral equation

$$F(E) = \int_0^{\infty} G(E')\, K(E, E')\, dE', \qquad (17)$$

where K(E, E′) is the experimental curve of the resolution of the instrument. The function K(E, E′) was determined, for each angle of observation, by measuring the form of the peak corresponding to protons from elastic p-p scattering. The peaks were observed under the same conditions as the observations of F(E). The curves obtained for the resolving power fitted best the function

$$K(E, E') = \frac{1}{2a} \exp\{-|E - E'|/a\}, \qquad (18)$$

where E is the energy at the center of the peak of elastic p-p scattering. The solution of Eq. (17) can be written, with sufficient accuracy, in the form

$$G(E) \approx F(E) - a^2 d^2F(E)/dE^2, \qquad (19)$$

since E >> a and since the values of a corresponding to the given angle of observation remain essentially constant over the section of the spectrum occupied by the maximum of the quasi-elastic scattering. Table II gives the values of E, a and $\Delta E/E$, corresponding to the angles under

TABLE II

Angle of observation Φ, degrees	7	12.2	18	24	30
E, Mev	647	621	578	521	455
a, Mev	14.4	9.3	6.3	15.0	10.3
$\Delta E/E$, %	4.7	2.9	1.6	4.4	4.0

Φ, degrees	dσ/dω, 10^{-24} cm²/sterad			
	Be	C	Cu	U
7	0.660±0.033	1.100±0.055	1.168±0.058	3.650±0.182
10	0.376±0.019	0.492±0.015	1.052±0.053	1.554±0.077
12.2	0.298±0.015	0.336±0.017	0.765±0.039	1.180±0.059
15	0.227±0.011	0.276±0.014	0.642±0.032	0.998±0.050
18	0.195±0.010	0.230±0.011	0.556±0.028	0.900±0.045
24	0.125±0.006	0.158±0.008	0.400±0.020	0.716±0.036
30	0.089±0.004	0.114±0.006	0.335±0.017	0.592±0.030
40	0.054±0.003	0.074±0.004	0.228±0.011	0.443±0.022

consideration; here ΔE is the total width at half the height of the peak of elastic p-p scattering. It should be noted that in the region of the maximum of quasi-elastic scattering, measured at an angle of 30°, the magnitude of the correction for the instrumental spectrum errors, $a^2b^2F(E)/dE^2$, amounted to no more than 2 or 3%.

4. EXPERIMENTAL RESULTS

A. Data on angular distribution. The pernucleus values of the differential cross sections for the emission of secondary charged particles, registered under the condition of the present experiments, are listed in Table III as functions of the emission angle Φ in the laboratory system, and are also shown in Fig. 1. The total errors, comprising statistical errors in the measured number of secondary particles and errors in the determined intensity of the primary proton beam, are also indicated.

In the range from 40° to 18°, where diffraction scattering is negligibly small (see below, Figs. 3–7), the values of dσ/dω increase smoothly with diminishing emission angle for all the investigated nuclei. The dependence of dσ/dω on A can be approximated here by a function such as kA^r. The results of such a treatment of the experimental data is shown in Fig. 2. Over the interval from beryllium to copper, the values of dσ/dω increase approximately in the following manner (in units of 10^{-26} cm²/sterad):

$$(d\sigma/d\omega)_{40^\circ} \approx 1.20A^{0.71}, \quad (d\sigma/d\omega)_{30^\circ} \approx 2.12A^{0.67},$$

$$(d\sigma/d\omega)_{24^\circ} \approx 3.62A^{0.58}, \quad (d\sigma/d\omega)_{18^\circ} \approx 6.12A^{0.53}.$$

These results indicate that as the angle decreases, dσ/dω becomes less dependent on A. Judging from the data obtained for uranium, the dependence of dσ/dω on A becomes weaker toward the end of the periodic table. Naturally, it is impossible to use these results to estimate the differential cross sections of the investigated nuclear interactions and to establish their dependence on A, since the average number of secondary particles emitted in each collision

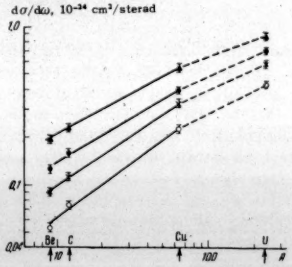

FIG. 2. Differential cross sections for the emission of secondary charged particles with range greater than 3.1 g/cm² of tolane, produced by 660-Mev incident protons, as a function of the mass number. The experimental points correspond to the following angles (laboratory system): ▲ – 18°, ● – 24°, × – 30°, ○ – 40°.

and registered under the conditions of the present experiments is still unknown.

At angles smaller than 18° the differential cross section changes rapidly, and in a manner that is not the same for all investigated nuclei, owing to the considerable contribution of diffraction scattering to the yield of secondary particles.

B. Energy spectra. By measuring the number of secondary particles at the output of the spectrometer as a function of the intensity of the magnetic field we were able, after introducing the necessary corrections and after normalizing the results to unit monitor count, to plot the relative momentum of the secondary particles at equal intervals of Hρ. The transformation from the momentum spectrum to the energy spectrum is made under the assumption that the secondary particles are protons. This assumption calls for a further check in that region of the spectrum which corresponds to the cascade protons, since these still contain a certain relatively small admixture of deuterons, emitted when the secondary nucleons pick up nucleons from the surface of the nucleus.[17] Apparently such an indirect pick up process can also lead to the emission of a small number of fast tritium nuclei. According to the

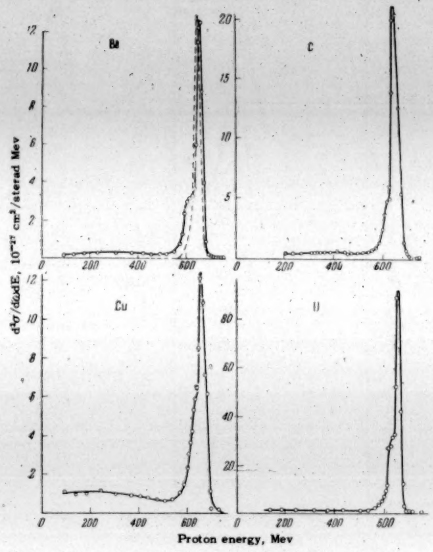

FIG. 3. Energy spectra of secondary charged particles from p + Be, p + C, p + Cu, and p + U collisions at 660 Mev. The dotted lines indicate the resolution curves. The angle of observation is 7°.

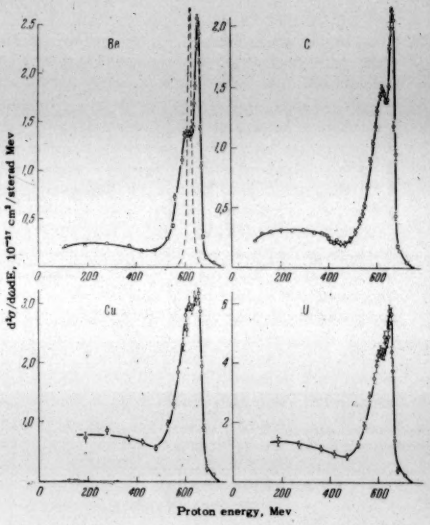

FIG. 4. The same as in Fig. 3. Angle of observation 12.2°.

data of Hess and Moyer,[18] in the bombardment of carbon, copper, and uranium by 300-Mev protons the yields of the secondary protons, deuterons, and tritium nuclei at angles of 26, 40, and 60°, are related approximately as 1000 : 50 : 2, and the energy spectrum of the deuterons, diminishing with energy approximately as E^{-3}, extends almost to 150 Mev. Bearing in mind the relative insensitivity of the intranuclear cascade process to the energy of the incident nucleon, it can be assumed that as the energy is increased from 300 to 670 Mev, the ratio between the yields of the secondary protons, deuterons, and tritium nuclei remains essentially unchanged.

The secondary charged particles observed at small angles may include also deuterons from the reaction $pp \rightarrow d\pi^+$ and $pn \rightarrow d\pi^0$, possibly taking place on bound nucleons. At 660 Mev the contribution of these reactions to the total cross sections of the free pp and np collisions is respectively ~ 7.5 and ~ 4%. One can expect, however, the yield of deuterons from the nuclei to be greatly reduced in view of the fact that the mean free path of the deuterons in nuclear matter is small compared with dimensions of the nucleus.

The energy spectra of secondary protons from p + Be, p + C, p + Cu, and p + U collisions are shown in Figs. 3 — 7 in the form of solid curves, drawn to fit the experimental points; the vertical line at each point denotes the statistical measurement errors. The dotted lines in the same figures show the observed peaks of elastic p-p scattering. The height of these peaks, which represent the resolution curves of the spectrometer, bears no relation to the ordinate scale.

In all the nuclei investigated at 7°, the high-energy portions of the spectrum consist of intense peaks, essentially due to protons that are diffraction-scattered by the nuclei. These peaks are superimposed on the right-side slopes of the maxima of the quasi-elastic proton scattering. The shift of the diffraction-scattering peaks towards energies higher than those of the elastic p-p scattering peaks is due to the different energies of the corresponding recoil nuclei. It can be seen that at 7° the yield of secondary protons with energies E > 500 Mev is due essentially to diffraction scattering. A much smaller contribution to the total yield of secondary protons is made by diffraction scattering at 12.2°, particularly in the case of p + Cu collisions. This property of the spectra at 12.2° is compatible with the known values of the nuclear radii. Thus, if we use the nuclear radii as determined from the cross sec-

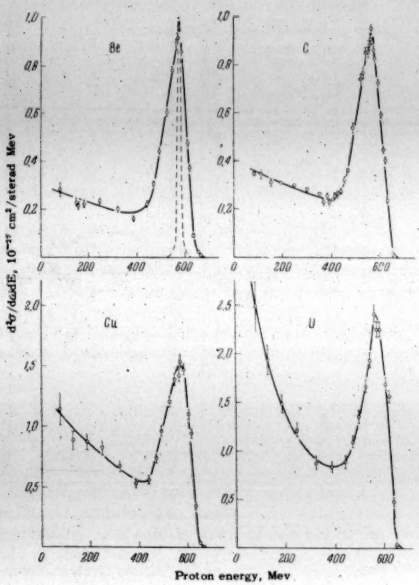

FIG. 5. The same as in Fig. 3. Angle of observation 18°.

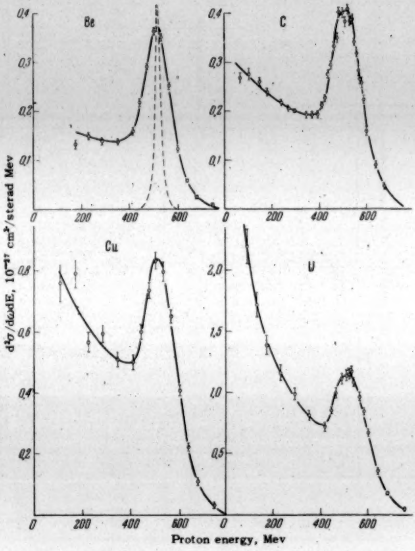

FIG. 6. The same as Fig. 3. Angle of observation 24°.

tions of absorption of 1400-Mev neutrons[19] and 860-Mev[20] and 900-Mev[21] protons, and insert the value $R = 1.26\,A^{1/3} \times 10^{-13}$ cm into the expression for the diffraction-scattering angular distribution

$$d\sigma / d\omega = k^2 (R')^4 \left[J_1\left(2kR' \sin\frac{\theta}{2}\right) \Big/ 2kR' \sin\frac{\theta}{2} \right]^2 \quad (20)$$

(where θ is the scattering angle, $k = 2\pi/\lambda$, λ is the wavelength of the incident proton, R is the radius of the scattering nucleus, $R' = R + 1/k$, and J_1 is the Bessel function of the first kind), we find that near 12.2° there should be a fourth maximum for uranium, while in the case of copper this scattering angle corresponds approximately to the position of the second minimum.

A characteristic feature of the spectra measured at 18° is the absence of typical diffraction peaks and a sharp cutoff of the quasi-elastic scattering maxima near the upper boundary of the energy region that is allowed by the conservation laws. At 24° and 30°, the spectra of all the investigated elements display in the high-energy region pronounced maxima corresponding to single quasi-elastic collisions between the protons and the nucleons in the nuclei. Assuming that the quasi-elastic scattering maxima have a symmetrical form, it is possible to estimate the differential cross section for quasi-elastic scattering by measuring the areas under the curves and comparing their values with the sum $Zd\sigma_{pp}/d\omega + (A-Z)\,d\sigma_{pn}/d\omega$, where $d\sigma_{pp}/d\omega$ and $d\sigma_{pn}/d\omega$ are the corresponding differential cross sections of elastic pp and pn scattering.* It was found that the quasi-elastic scattering in beryllium, carbon, copper, and uranium at 30° amounts to ~60, ~53, ~22, and ~9% of the free scattering, respectively. The important fact is that the proton, after the first collision with one of the nucleons of the nucleus, can be emitted with a noticeable probability even from the heaviest nuclei, without experiencing any other interaction. This fact can be considered as an indication that such nucleon collisions occur predominantly in the surface layer of the nucleus. In connection with this, it must be noted that in the bombardment of aluminum and uranium by 460- and 1840-Mev protons, the calculations of the intranuclear cascades, carried out by Metropolis et al.,[23] predict,

*In these calculations the values of $d\sigma_{pn}/d\omega$ for 670 Mev were assumed equal to the corresponding values of the differential cross sections of elastic np scattering obtained by Kazarinov and Simonov at 580 Mev.[22]

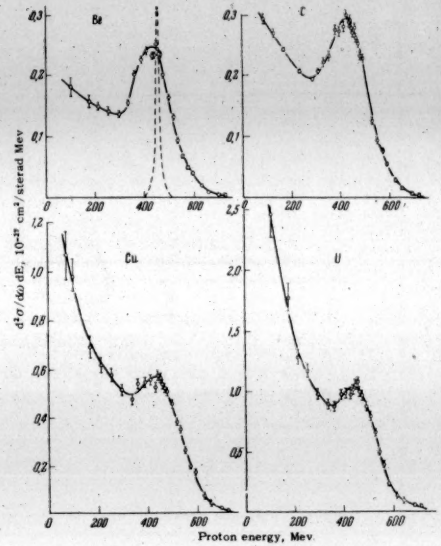

FIG. 7. The same as Fig. 3. Angle of observation 30°.

in the approximation employing a nuclear model with a sharp boundary, a secondary-proton energy spectrum without the maximum due to protons that have experienced only one paired collision. The use of a model of nucleus with diffuse boundary in cascade calculations is expected to increase the relative frequency of proton emission after the first collision, and thus match more accurately the experimental spectrum of the secondary protons.

The strong smearing of the quasi-elastic scattering maxima as compared with the elastic pp-scattering peak is a direct indication of the existence of a momentum distribution of the nucleons in the nuclei. The quasi-elastic scattering maxima are shifted somewhat towards the energies lower than those of the elastic pp scattering peaks. An analogous decrease in the mean proton energy in quasi-elastic scattering was observed also at 340 Mev and was attributed to nucleon collisions in the potential well, to energy losses by excitation of the residual nuclei, and to an increase in the scattering cross sections at relatively small collision energies.[8]

The continuous spectra observed below the quasi-elastic scattering maxima are due to inelastic processes. In the case of p + Be and p + C collisions, the continuous spectra are very similar in form to the spectra of the recoil protons in the reactions $pp \rightarrow np\pi^+$ and $pp \rightarrow pp\pi^0$ (see Figs. 2 and 3 in reference 16). We conclude therefore that when protons of a given energy collide with light nuclei, the continuous spectra of the secondary protons correspond essentially to processes of pion production in single proton-nucleon collisions, and not to an intranuclear cascade process. To the contrary, in the case of p + Cu and p + U collisions the continuous spectra occur essentially as a result of the cascade process. This is proved by the fact that the number of particles in the continuous spectrum increases the more steeply with diminishing energy, the greater the size of the nucleus, and consequently the more intense the development of the cascade process in the nucleus. This feature of continuous spectra becomes more pronounced with increasing angle of observation.

5. COMPARISON OF EXPERIMENTAL AND CALCULATED ENERGY SPECTRA OF QUASI-ELASTIC SCATTERING

For comparison we used spectra of quasi-elastic scattering in beryllium and copper, measured at 30°, since the interference effects should have the least influence in this case. Tests were made on momentum distributions of two types:

a) Gaussian distribution

$$f(s) \sim \exp\{-s^2/s_0^2\}$$

at four values of s_0 corresponding to energies of 16, 18, 20, and 22 Mev;

b) Three-parameter sum of two Gaussian distributions

$$f(s) \sim \exp\{-s^2/s_1^2\} + \alpha \exp\{-s^2/s_2^2\}$$

with $s_1^2/2M = 16$ and $s_2^2/2M = 50$ Mev, and also the similar Selove distribution with $s_1^2/2M = 7$, $s_2^2/2M = 50$ Mev, and $\alpha = 0.15$. The parameter α was chosen to obtain the best agreement between the calculations and the experimental data at the end of the descending branch (towards the higher energies) of the quasi-elastic scattering maximum.

The values of E_c and $\cos\vartheta_c$ calculated from (15) for specified values of s and E_q and the integrals contained in the expression (14) were calculated with the "Ural" electronic computer of the Joint Institute for Nuclear Research. The differential cross sections of the pp and pn scattering, corresponding to each pair of values E_c and $\cos\vartheta_c$, were found from graphs of $d\sigma_{pp}/d\omega$

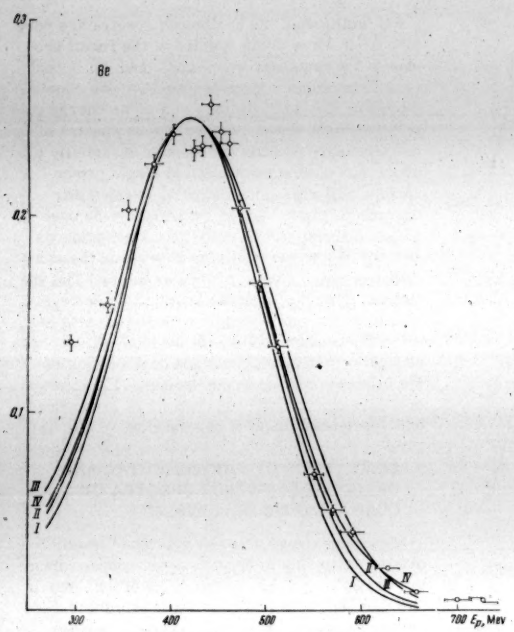

FIG. 8. Energy spectrum of quasi-elastically scattered protons: theoretical curves and experimental data for beryllium at an incident-proton energy of 660 Mev. Angle of observation 30°; I, II, III – Gaussian distribution with values of 1/e at 16, 18, and 22 Mev respectively; IV – sum of two gaussian distributions of the form $\exp\{-s^2/s_1^2\} + \alpha \exp\{-s^2/s_2^2\}$ with $s_1^2/2M = 16$ and $s_2^2/2M = 50$ Mev, $\alpha = 0.06$.

$d\sigma_{pn}/d\omega$, obtained at various energies, plotted for scattering angles in the range $20° \leq \vartheta_c \leq 160°$. Graphical interpolation was used to obtain intermediate values of $d\sigma_{pp}/d\omega$ and $d\sigma_{pn}/d\omega$ from the experimental data on the differential cross sections of pp and pn scattering as gathered by Hess.[24] The values of $d\sigma_{pn}/d\omega$ were estimated in the same manner for energies greater than 580 Mev, using the measured differential cross sections of elastic np scattering at 580 Mev[22] and quasi-elastic pn scattering at 970 Mev.[25]

The final results of the calculations are obtained in the form of a sum of momentum distributions of the emitted protons

$$Zd^2\sigma_{pp}/d\omega\, dq + (A - Z)\, d^2\sigma_{pn}/d\omega\, dq,$$

a sum depending only on q and readily transformed into the energy spectra of protons that have experienced single quasi-elastic collisions. Some of the calculated quasi-elastic scattering energy spectra in beryllium and carbon are shown in Figs. 8 and 9 together with the experimental data. The horizontal lines at the experimental points represent the energy resolution, which has deteriorated from 3.8% at 300 Mev to 4.1% at 660 Mev. Since the calculations do not take into account the presence of the potential well and the effect of excitation of residual nuclei, the theoretical curves had to be shifted towards the lower energies in order to superimpose the theoretical maximum on the quasi-elastic maximum. This shift amounted to approximately 30 Mev for these spectra.

As can be seen from Figs. 8 and 9, at energies less than the energy of maximum quasi-elastic scattering, the theoretical curves lie lower than the experimental points. This discrepancy can be attributed to a superposition of a smeared spectrum of multiple proton scattering in the nuclei on the left branch of the quasi-elastic maximum. The comparison of the theoretical curves with the experimental data was made in the high-energy portion of the spectrum, where the effect of multiple nuclear scattering should be insignificant. The observed spectra agree in first approximation with a Gaussian momentum distribution with 1/e at approximately 20 Mev. It follows therefore that the mean-square value of the nucleon momentum in beryllium and carbon

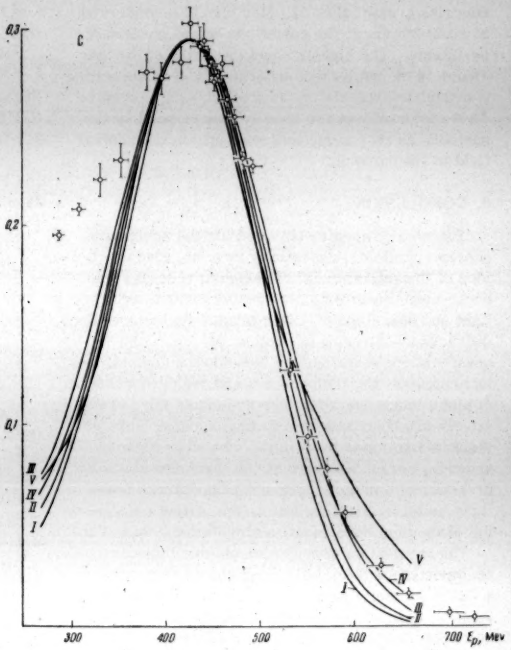

FIG. 9. Same as in Fig. 8 but for carbon. The values used for the sum of the two Gaussian distributions are

$s_1^2/2M = 16$, $s_2^2/2M = 50$ Mev, $\alpha = 0.09$ (*IV*) and $s_1^2/2M = 7$, $s_2^2/2M = 50$ Mev, $\alpha = 0.15$ (*V*)

nuclei corresponds to an energy of approximately 30 Mev. Apparently a somewhat better agreement with experiment at the uppermost edge of the carbon spectrum is given by the three-parameter sum of two Gaussian distributions with $s_1^2/2M = 16$, $s_2^2/2M = 50$ Mev and $\alpha = 0.09$. However, the experimental data are not sufficiently accurate to favor, with any degree of assurance, this distribution over a simple Gaussian distribution. As to the Selove distribution,[3] it contains too many high momenta, and therefore causes the cross sections away from the maximum of quasi-elastic scattering to be too high.

The results obtained are evidence that a theory, based on the concept of two-particle collisions of fast nucleons in the nuclei, can account in general outline for the shape of the high-energy branch of the quasi-elastic maximum. Nevertheless, this circumstance must not be overestimated, since the result of comparison of theory with experiment is determined fully by the shape of the high-energy portion of the spectrum itself, corresponding to collisions of incident protons with high-momentum nucleons, i.e., with nucleons that interact greatly with other particles during the instant of collision. It is clear, however, that the conditions of applicability of the impulse approximation are satisfied worst of all for such collisions. It should be noted in connection with this that the scattering of the protons by tight two-nucleon groups and possibly also by α particles, which exist in nuclei in the form of substructural formations, undoubtedly leads to a certain distortion of the high-energy portion of the quasi-elastic scattering spectrum. On the other hand, the background observed in the region of energies greater than that which the proton can possibly have after the first quasi-elastic scattering may be partially due to the deuterons knocked out from the nuclei by collisions between protons and tight two-nucleon groups.

These remarks do not lessen the importance of the basic fact that an explanation of the observed quasi-elastic scattering spectra calls for distributions that extend to large momenta. Were the nucleons inside the nucleus to have a Fermi momentum distribution with an upper limit corresponding to $E_F \approx 30$ Mev (the degenerate-gas model), no quasi-elastically scattered protons with

energies greater than 525 Mev should be observed at all at 30° under the conditions of the present experiments. The high-momentum states of the nucleons in the nuclei are apparently due to the strong two-nucleon interaction via a short-range potential. These interactions are usually experienced by the nucleons as they move independently in the central field of the nucleus.

6. CONCLUSION

The energy spectra obtained for the secondary charged particles, essentially protons, give an idea of the relative role of various processes that occur upon interaction of 660-Mev protons with light and heavy nuclei. Such processes include diffraction scattering of protons by nuclei and quasi-elastic scattering by individual nucleons, the intranuclear cascade process, and the production of pions in nucleon collisions. Undoubtedly, a relatively small contribution to the secondary-proton yield is also made by collisions between protons and tight two-nucleon groups, as evidenced by the presence of a direct knock-out of deuterons from light nuclei by protons, and by the strong smearing of the pion spectra on the high-energy side.

The momentum distribution obtained for the nucleons in nuclei of beryllium and carbon, namely a Gaussian distribution with $1/e$ at approximately 20 Mev, is in satisfactory agreement with the results obtained at 340 Mev by the Berkeley group.[8,9] Thus, an analysis of the quasi-elastic scattering of protons in light nuclei, over a broad range of collision energies, leads approximately to the same momentum distribution of the nucleons. This fact denotes, apparently, that an analysis of the quasi-elastic scattering in beryllium and carbon nuclei, based on the impulse approximation, is sufficiently well founded. It must be emphasized that at the present measurement accuracy, the spectra of quasi-elastic scattering in beryllium and carbon can be obtained from the same nucleon momentum distribution. As to the spectra of quasi-elastic scattering in copper and uranium, no definite conclusions can be drawn regarding the momentum distribution of the nucleons in heavy nuclei, owing to the strong influence of multiple nuclear scattering in these substances.

The authors thank R. N. Fedorova and I. V. Popova for programming and performance of the calculations, and also S. M. Bilen'kiĭ, N. P. Klepikov, L. M. Soroko, and N. A. Chernikov, for useful discussions.

[1] G. Chew and M. Goldberger, Phys. Rev. **77**, 470 (1950).

[2] J. Hadley and H. York, Phys. Rev. **80**, 345 (1950).

[3] W. Selove, Phys. Rev. **101**, 231 (1956).

[4] Azhgirei, Vzorov, Zrelov, Meshcheryakov, Neganov, and Shabudin, J. Exptl. Theoret. Phys. (U.S.S.R.) **33**, 1185 (1957), Soviet Phys. JETP **6**, 911 (1958).

[5] Azhgirei, Vzorov, Zrelov, Meshcheryakov, and Petrukhin, J. Exptl. Theoret. Phys. (U.S.S.R.) **34**, 1357 (1958), Soviet Phys. JETP **7**, 939 (1958).

[6] E. Henley, Phys. Rev. **85**, 204 (1952).

[7] C. Richman and H. Wilcox, Phys. Rev. **78**, 496 (1950).

[8] Cladis, Hess, and Moyer, Phys. Rev. **87**, 425 (1952).

[9] J. Wilcox and B. Moyer, Phys. Rev. **99**, 875 (1955).

[10] McEwen, Gibson, and Duke, Phil. Mag. **2**, 231 (1957).

[11] Wattenberg, Odian, Stein, Wilson, and Weinstein, Phys. Rev. **104**, 1710 (1956).

[12] S. T. Belyaev and G. I. Budker, Dokl. Akad. Nauk SSSR **107**, 807 (1956), Soviet Phys. Doklady **1**, 218 (1957).

[13] C. Moller, Kgl. Danske Videnskab. Selskab. Mat.-fys. Medd. **23**, 1 (1945).

[14] N. A. Chernikov, Dokl. Akad. Nauk SSSR **114**, 530 (1957), Soviet Phys. Doklady **2**, 248 (1957).

[15] P. Wolff, Phys. Rev. **87**, 434 (1952).

[16] Meshcheryakov, Neganov, Vzorov, Zrelov, and Shabudin, Dokl. Akad. Nauk SSSR **109**, 499 (1956), Soviet Phys. Doklady **1**, 447 (1956).

[17] B. Bransden, Proc. Phys. Soc. **A65**, 738 (1952).

[18] W. Hess and B. Moyer, Phys. Rev. **101**, 337 (1956).

[19] Coor, Hill, Hornyak, Smith, and Snow, Phys. Rev. **98**, 1369 (1955).

[20] Chen, Leavitt, and Shapiro, Phys. Rev. **99**, 857 (1955).

[21] Booth, Ledley, Walker, and White, Proc. Phys. Soc. **A70**, 209 (1957).

[22] Yu. M. Kazarinov and Yu. N. Simonov, J. Exptl. Theoret. Phys. (U.S.S.R.) **31**, 169 (1956), Soviet Phys. JETP **4**, 161 (1957).

[23] Metropolis, Bivins, Storm, Turkevich, Miller, and Friedlander, Phys. Rev. **110**, 185, 204 (1958).

[24] W. Hess, Revs. Modern Phys. **30**, 368 (1958).

[25] Batson, Culwick, Klepp, and Riddiford, see O. Piccioni, Proc. 1958 Ann. Internat. Conf. on High-Energy Physics at CERN, 1958, p. 73.

Translated by J. G. Adashko
343

INVESTIGATION OF GALVANOMAGNETIC PHENOMENA IN CHROMIUM AT LOW TEMPERATURES

E. S. BOROVIK and V. G. VOLOTSKAYA

Physico-Technical Institute, Academy of Sciences, Ukrainian S.S.R.

Submitted to JETP editor December 22, 1958

J. Exptl. Theoret. Phys. (U.S.S.R.) **36**, 1650-1655 (June, 1959)

The Hall effect and magnetoresistance have been studied in chromium in the temperature range 4.2 – 78°K for fields up to 27,000 oe. The electron concentrations and mobilities have been calculated from the data obtained. A preliminary investigation of the properties of zirconium has been carried out.

THERE have been few investigations of galvanomagnetic phenomena in transition metals at high effective fields (i.e., in the region of large magnetoresistance). Magnetoresistance has been studied in molybdenum and tungsten,[1,2] but simultaneous measurements of magnetoresistance and Hall effect at low temperatures have only been made on platinum.[3]

The aim of the present work was to widen the study of transition metals. It is mainly concerned with the properties of chromium, but zirconium has also been investigated in part.

1. SPECIMEN CHARACTERISTICS

The chromium specimen, obtained by vacuum distillation, was needle shaped, ~0.35 mm across and 8 mm long (between the potential leads). As the distillation took place onto a hot plate, the specimen was not annealed further. The zirconium specimen was produced by thermal decomposition of the iodide and further annealing was not carried out. Table I shows the temperature dependence of resistance (in zero field).

TABLE I

T, °K	$(r_{0T}/r_{0.273})\cdot 10^2$	
	Cr	Zr
78	8.04	—
20.4	1.35	3.89
4.2	1.28	3.55
2.4	1.28	—

2. EXPERIMENTAL RESULTS

The galvanomagnetic effects were observed with the magnetic field perpendicular to the direction of current flow in the specimen, which could be rotated about its axis parallel to the current direction.

Judged by the character of the light reflected from it,[4] the chromium specimen appeared to be a single crystal. The anisotropy of magnetoresistance for different parts of the specimen showed that there were apparently small inclusions, with orientations differing from the main one. It seemed that the length axis (the current direction) made a small angle with one of the twofold axes. The anisotropy of magnetoresistance was small, the largest deviation from the mean being less than 4%.

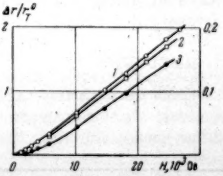

FIG. 1. Magnetoresistance in chromium 1 – at T = 4.2°K; 2 – at T = 20.4°K; 3 – at T = 78°K (the left hand ordinate scale applies to curves 1 and 2, the right hand to curve 3).

For the determinations of the dependence of the galvanomagnetic effects on field strength, the specimen was oriented in the direction corresponding roughly to the mean value of the magnetoresistance. Figure 1 shows the resistance change in a magnetic field. Above 10,000 oe at helium temperatures the resistance varies linearly with field. At 27,000 oe the resistance has increased threefold. The Hall constant is shown in Fig. 2.

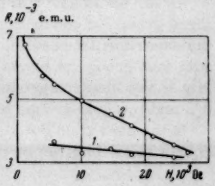

FIG. 2. Hall constant, R, for chromium 1 – T = 78°K; 2 – T = 4.2°K.

At nitrogen temperature it hardly depends on the field. The mean value $R = 3.4 \times 10^{-3}$ e.m.u. is close to the value of 3.6×10^{-3} e.m.u. found by Foner[5] at room temperature. At 4.2° K the Hall constant is very dependent on field.

As has been shown earlier,[6] it is more instructive to use the ratio of the Hall field, E_y, to the field in the current direction, E_x, rather than the Hall constant, in the region of large effective fields. This ratio, E_y/E_x, is plotted in Fig. 3.

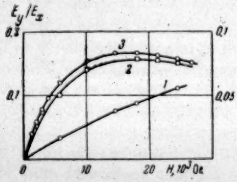

FIG. 3. Dependence of E_y/E_x on the magnetic field for chromium 1 – at T = 78° K; 2 – at T = 20.4° K; 3 – at T = 4.2° K (right hand ordinate scale for curve 1, left hand scale for curves 2 and 3).

It can be seen from curve 3 (Fig. 3) that E_y/E_x has a maximum for a field around 17,000 oe. The maximum value of $E_y/E_x = 0.165$. E_y/E_x decreases in larger fields.

Magnetoresistance measurements on zirconium showed that although the residual resistance of the specimen was of the same order of magnitude as in chromium, the variation of resistance with field was appreciably less. At 4.2° K the resistance increase $\Delta r/r = 0.035$ for a field of 24,600 oe.

3. DISCUSSION

From the experimental data it is seen that, qualitatively, the properties of chromium do not differ appreciably from those of nontransition metals.[6]

The fields used were insufficient to decide definitely on the limiting magnetoresistance law for high fields. From the curves of E_y/E_x, chromium seems to belong to the group of metals for which the Hall field decreases in large fields, while the resistance increases indefinitely, i.e., metals which have equal numbers of holes and electrons.[6] Such a conclusion is not in conflict with the electronic structure of chromium — an element in the fourth group of the periodic table.

As for platinum,[3] a simple model with two or three groups of conduction levels cannot explain the experimental results. An isotropic model with four groups of levels fits the data satisfactorily — two electron groups with densities n_2 and n_4, and two hole groups with densities n_1 and n_3.

In the zero field the electrical conductivity of such a metal is given by the expression

$$\sigma_{0T} = \frac{n_1 e^2 \tau_1}{m_1} + \frac{n_2 e^2 \tau_2}{m_2} + \frac{n_3 e^2 \tau_3}{m_3} + \frac{n_4 e^2 \tau_4}{m_4}. \qquad (1)$$

The effective magnetic field is determined by the dimensionless parameters

$$\varphi_i = eH\tau_i / m_i,$$

where τ_i and m_i are the mean time between collisions and the effective mass of the corresponding groups of conduction levels.

Equations for E_y/E_x and for the magnetoresistance on such a model are given in our paper on platinum[3] [Eqs. (7) and (8)].

Table II shows the values of the various parameters for this model which give the best fit with the experimental data. The carrier concentration per atom, n_i/n_a, the carrier mobility τ_i/m_i at 4.2° K and the effective field, $\varphi_i = eH\tau_i/m_i$ corresponding to H = 25,000 oe and T = 4.2° K, are given for each of the four groups.

TABLE II

Group	1	2	3	4
n_i/n_a	$0.59 \cdot 10^{-2}$	$0.346 \cdot 10^{-2}$	$0.246 \cdot 10^{-1}$	$0.271 \cdot 10^{-1}$
$(\tau_i/m_i)10^{-15}$	10.95	9.87	2.97	1.77
φ_i	4.38	3.95	0.91	0.71

A comparison between the curves calculated from the parameters given in Table II and the experimental data is shown in Fig. 4. The agreement is satisfactory for the field dependence of both the Hall field and the resistivity. Since the anisotropy of magnetoresistance is small, we can conclude that the isotropic model, discussed above, describes the properties of chromium sufficiently closely.

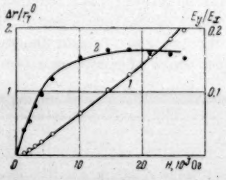

FIG. 4. Comparison between the experimental and calculated values of Hall field and magnetoresistance in chromium. The full curves are calculated values, 1 – for $\Delta r/r$; 2 – for E_y/E_x; the points represent the experimental data.

The small concentration of carriers — a total of only 0.06 per atom — is the most singular property of chromium. Such a small concentration is comparatively rare, and apart from group V elements (Bi, As, Sb) has only been found so far in gallium and beryllium.[6] The mobilities in the carrier groups 1 and 2 are appreciably greater than in groups 3 and 4. This large difference can be

explained if it is assumed that groups 3 and 4 are related to the carriers of the unfilled 3d states, characteristic of transition metals. The carriers of the first two groups, with high mobilities, are connected with the valence electrons. The presence of holes and electrons among the particles of high mobility (groups 1 and 2) can be attributed to overlapping of the 4s and 4p bands. To explain the presence of holes and electrons in the low mobility group one must assume that the d-state is split into separate overlapping bands.

The electronic structure of chromium, like platinum,[3] is thus more complicated than is usually assumed for transition metals.

Since the absolute values of mobility, given in Table II, are determined by the purity of the given specimen, direct comparison with other metals is not possible. For such a comparison, the mobility must be determined in a temperature region where the residual resistance is unimportant. For this purpose the Debye temperature is suitable, and the mobility at this temperature can be calculated from the experimental resistivity-temperature curve from the relation

$$(\tau_i / m_i)_\theta = (\tau_i / m_i)_T \, r_{0T} / r_{0\theta},$$

where $(\tau_i/m_i)_\theta$ is the mobility at the Debye temperature, $r_{0\theta}$ is the resistivity in zero field at the Debye temperature, $(\tau_i/m_i)_T$ and r_{0T} are the same quantities at the temperature of measurement. Such a calculation assumes the same temperature dependence of mobility for all the groups. Table III gives the results of this calculation for chromium (using the data of the present work), platinum,[3] and zinc.[6]

The maximum and minimum values of mobility are given in the table. Comparison of the data in the last column shows that the maximum mobility in chromium is even a little greater than the maximum in the non-transition metal zinc, and four times greater than the maximum in platinum. The mobilities in chromium are, therefore, closer to those of a normal metal. Presumably this is connected with the small carrier concentration. It was noted earlier[6] that the mobility increases in metals with small carrier concentrations.

Because of the small magnetoresistance, only the order of magnitude of the largest mobility in zirconium can be derived from the preliminary results. This turns out to be the same as in platinum.

It is possible to compare the data on carrier concentration with electronic specific heat data on chromium, and obtain values for the effective masses. This comparison can be made in the manner described previously.[6] Strictly speaking, one should consider the contribution of all four carrier groups to the specific heat. However, as the concentration of particles in the first two groups is nearly an order of magnitude smaller and the mobility is several time greater, the contribution of these groups can be neglected.

From the data of Estermann, Friedberg and Goldman[7] the electronic contribution to the heat capacity, $c_V = 3.62 \times 10^{-5} RT$ cal/mole-deg. Using the concentrations shown in Fig. 2, the ratio of the effective mass, m^*, to the free electron mass, m_0, is found to be $m^*/m_0 = 5.3$. This value of m^* is slightly less than the value in platinum[3] and considerably greater than that deduced by Estermann et al.[7] from the concentration derived from the valence ($m^*/m_0 = 2.93$).

CONCLUSIONS

As for platinum,[3] no direct effect of magnetization shows up in chromium. There is some evidence that chromium becomes ordered antiferromagnetically below 475° K.[9] If so, the magnetization at low temperatures must be small and the direct influence of it must be small. One might expect a low-field anomaly connected with the antiferromagnetic domain structure. However, the experimental data give no evidence of such an anomaly.

The characteristic property of chromium revealed in these experiments is the small concentration and high mobility of the conduction elec-

TABLE III

Metal	θ	$T = 4.22°$ K		$T = \theta$	
		$r_{0T} / r_{0.273}$	τ_i / m_i	$r_{0\theta} / r_{0.273}$	τ_i / m_i
Cr	485	$1.28 \cdot 10^{-2}$	$11 \cdot 10^{15}$ $1.8 \cdot 10^{15}$	1.95	$7.2 \cdot 10^{13}$ $1.16 \cdot 10^{13}$
Pt	225°	$6.78 \cdot 10^{-4}$	$20 \cdot 10^{15}$ $1.3 \cdot 10^{15}$	0.81	$1.7 \cdot 10^{13}$ $1.1 \cdot 10^{12}$
Zn	213	$4.7 \cdot 10^{-4}$	$65 \cdot 10^{15}$ $56 \cdot 10^{15}$	0.74	$4.1 \cdot 10^{13}$ $3.5 \cdot 10^{13}$

trons. These properties made possible the attainment of high effective fields, although our specimen had a large residual resistivity. Preliminary measurements on zirconium show that it does not have such anomalous properties.

In conclusion, we would like to express our thanks to B. G. Lazarev for his interest in this work.

[1] A. Foroud and E. Justi, Phys. Z. **40**, 501 (1939).

[2] W. J. de Haas and J. de Nobel, Physica **5**, 449 (1938).

[3] E. S. Borovik and V. G. Volotskaya, Физика металлов и металловедение (Phys. of Metals and Metal Research) **6**, 60 (1958).

[4] Z. S. Yakovleva, J. Exptl. Theoret. Phys. (U.S.S.R.) **3**, 454 (1933).

[5] S. Foner, Phys. Rev. **107**, 1513 (1957).

[6] E. S. Borovik, Izv. Akad. Nauk SSSR, Ser. Fiz. **19**, 429 (1955), Columbia Tech. Transl. p. 383

[7] Estermann, Friedberg, and Goldman, Phys. Rev. **87**, 582 (1952).

[8] I. K. Kikoin, J. Exptl. Theoret. Phys. (U.S.S.R.) **10**, 1242 (1940).

[9] C. G. Shull and M. K. Wilkinson, Revs. Modern Phys. **25**, 100 (1953).

Translated by R. Berman
344

THE REACTION $p + p \rightarrow p + p + \pi^0$ IN THE ENERGY RANGE FROM THRESHOLD TO 665 Mev*

A. F. DUNAĬTSEV and Yu. D. PROKOSHKIN

Joint Institute for Nuclear Research

Submitted to JETP editor December 25, 1958

J. Exptl. Theoret. Phys. (U.S.S.R.) **36**, 1656-1671 (June, 1959)

The angular distributions of π^0 mesons produced in proton-proton collisions have been investigated at 400 – 665 Mev. The distributions were found to be close to isotropic, in agreement with S. Mandel'shtam's phenomenological resonance theory. The total cross sections were measured in the energy range 313 – 665 Mev. At energies above 400 Mev the main contribution to the reaction cross section is made by resonant transitions. At lower proton energies the non-resonant Ss transition becomes significant, its contribution to the total cross section being $0.032\ \eta_m^2 \times 10^{-27}$ cm^2 (where η_m is the maximum π^0-meson momentum in the c.m.s.). A comparison of the measured cross sections of neutral and charged pions with the cross sections calculated from the resonance theory indicates that the transition with the total angular momentum $J = 2$ plays the predominant role.

1. INTRODUCTION

THE production of neutral pions in proton collisions

$$p + p \rightarrow p + p + \pi^0, \qquad \pi^0 \rightarrow 2\gamma \tag{1}$$

occupies a prominent place among the reactions of the type "nucleon plus nucleon → pion." Its distinguishing feature is the rapid increase in the cross section with energy and the relatively small value of the cross section near the threshold, which is a consequence of the forbiddenness of a transition with a final state S for the nucleons and a final state p for the pion relative to the center of mass, a transition that plays a principal role in other meson-production reactions (the Sp transition in the Rosenfeld classification[1]). The first investigations of this reaction[2-8] have shown that in the energy range 340 – 480 Mev its cross section $\sigma_{pp}^{\pi^0}$ increases as η_m^8 (where η_m is the maximum π^0-meson momentum in the c.m.s.), measured in units of meson mass $m_\pi c$), while other reactions are characterized by cross sections that depend on powers of η_m not higher than the fourth. A phenomenological analysis of these data[1,9] has shown that near threshold the reaction (1) is essentially caused by the Pp transition. It has been noted in later papers[6,10,11] that the cross section $\sigma_{pp}^{\pi^0}$ continues to increase rapidly even at 450 – 660 Mev: $\sigma_{pp}^{\pi^0} \sim \eta_m^{4.5}$ according to Soroko[6] and $\sigma_{pp}^{\pi^0} \sim \eta_m^{5.5}$ according to Prokoshkin and Tyapkin.[11] A comparison of the data of Mather and Martinelli[7] or those of Crandall and Moyer[8] with the results of Prokoshkin and Tyapkin[11] shows that at lower energies the cross section varies as η_m^6 and not as η_m^8, from which it has been concluded[11] that the Ss transition plays a substantial role at low energies. Further measurements of the cross section of the reaction (1) at low energies[12] have confirmed this conclusion.

The experimental data obtained in reference 11 were analyzed by Mandel'shtam within the framework of the phenomenological resonance theory.[13] In contrast with the old phenomenological theory[1,9] Mandel'shtam considers the resonant interaction of the pion with the nucleon in the final state of the reaction. It is assumed in his theory that over a wide energy range, where the resonant interaction between the meson and the nucleon is substantial, the matrix elements of the transitions are constant to within factors that consider the meson-nucleon and nucleon-nucleon interaction in the final state. The theory takes into account the interference of nucleon states and "shifted" transitions.[7] The S scattering of the system, when one of the nucleons is in the S state with respect to the meson-nucleon subsystem, for which one possible state $^2P_{3/2}$ is assumed, is described in this case by a single parameter, while

*The results of this investigation were reported at the Fourth Session of the Scientific Council of the Joint Institute for Nuclear Research in May 1958.

the P scattering is described by five parameters. The theory was found to be not critical to relative changes in the parameters of the P scattering, which made it possible to equate some of these parameters to each other and thus reduce the experimentally-determined number of P-scattering parameters from 5 to 2. All three parameters that describe the S and P scattering are determined from the experimental data on the production of charged pions in p-p collisions. The total cross sections of the reaction (1) are calculated in the Mandel'shtam theory without introducing any supplementary free parameters, thus making the comparison of the experimental and theoretical energy dependences of this cross section a good test of the resonance theory. A corresponding comparison with the data of Prokoshkin and Tyapkin,[11] made by Mandel'shtam, has shown an agreement between the experimental and theoretical results.

The angular distribution of π^0 mesons in reaction (1), calculated on the basis of the resonance theory, is close to isotropic at all proton energies. Experiments carried out by various methods in the region near 600 Mev[11,14,15] actually indicate that the angular distribution of the π^0 mesons is isotropic. However, at lower energies (450 – 550 Mev) the measured angular distributions have displayed a tendency towards increased anisotropy.[11] In the range of even lower energies, the angular distribution was analyzed by Moyer and Squire[16] under certain assumptions concerning the character of the π^0-meson spectrum, based on the old phenomenological theory.[1,9] Within the framework of these assumptions, they conclude that the angular distribution of the π^0 mesons is substantially anisotropic at 330 Mev.

The purpose of this work was to investigate the reaction (1) over a wide energy interval. The use of a single procedure gave grounds for hoping to be able to obtain sufficiently accurate data on the variation of the reaction characteristics with the energy. Particular attention was paid to a little-studied characteristic of the reaction – the angular distribution of the π^0 mesons. In investigations of this type it is necessary to take into account the inherent difficulties connected with the fact that the π^0 mesons move at a velocity substantially different from that of light. This causes the angular distribution of the gamma quanta, produced during the decay of the π^0 mesons, to be less anisotropic than the distribution of the π^0 mesons.[17] As the velocity of the π^0 mesons decreases, the anisotropy of the angular distribution of the gamma quanta disappears rapidly. The foregoing is demonstrated in Fig. 1, which illustrates the case when π^0 mesons are distributed proportional to $\frac{1}{3} + b_{\pi^0}\cos^2\vartheta$ in the c.m.s. Here the angular distribution of the gamma quanta is of the form $\frac{1}{3} + b_\gamma \cos^2\vartheta$. The figure shows the value of db_{π^0}/db_γ i.e., the error in the measurement of b_{π^0}, at various energies E_p of the protons that produce the π^0 mesons. It is seen that when E_p decreases this error increases rapidly, consequently increasing the accuracy with which it is necessary to measure the angular distribution of the gamma quanta so as to establish the angular distribution of the π^0 mesons. It is also necessary to take into account the fact that when the proton energy decreases, the more stringent requirements regarding the measurement accuracy are accompanied by an exceedingly rapid reduction in the yield of the gamma quanta from the investigated reaction. This complicates even further the investigation of the angular distributions of the π^0 mesons. In the present investigation we restricted ourselves to a measurement of the angular distributions of gamma quanta in the interval 400 – 665 Mev, where the aforementioned difficulties were not yet too great and the apparatus employed made it possible to determine with sufficient accuracy the angular distribution of the π^0 mesons.

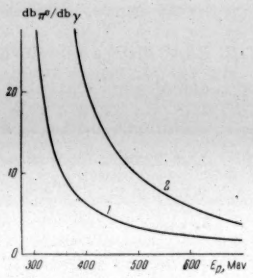

FIG. 1. Dependence of the relative error db_{π^0}/db_γ on the proton energy: 1) For $b_{\pi^0} = 0$; 2 – for $b_{\pi^0} = 1$.

2. MEASUREMENT PROCEDURE

Proton beam. The experiments were performed on the external unpolarized proton beam of the six-meter synchro-cyclotron of the Joint Institute for Nuclear Research. The proton current was measured accurate to 3% with a calibrated helium-filled ionization chamber. Since the cross section of the investigated reaction depends considerably on the proton energy, particularly near threshold, the cross-section measurements must be accompanied by an exact determination of the mean energy of the beam. At small proton energies, on the

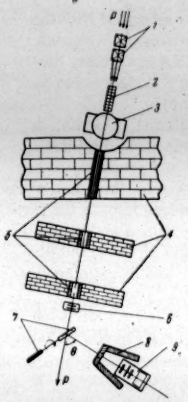

FIG. 2. Arrangement of the apparatus: 1) focusing magnetic lenses, 2) polyethylene absorber, 3) deflecting magnet, 4) shielding walls, 5) steel collimators, 6) ionizing chamber, 7) targets, 8) portion of lead shielding of the gamma telescope, 9) gamma telescope, P – proton beam.

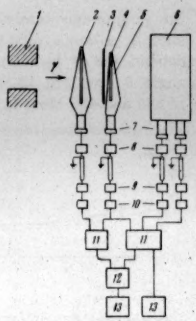

FIG. 4. Diagram of the gamma telescope: 1) lead diaphragm, 2) crystal of anti-coincidence counter, 3) converter, 4) crystal of coincidence counter, 5) foil used to reflect light, 6) radiator of the Cerenkov counter, 7) photomultipliers, 8) shaping stages, 9) cathode follow ups, 10) amplifiers, 11) coincidence circuits, 12) anti-coincidence circuits, 13) scalers.

other hand, it is necessary to measure accurately not only the mean energy, but also the energy spectrum of the beam. The mean energy of the beam was determined in these experiments with accuracy to approximately 1 Mev by the method described in reference 18. The proton energy was reduced by means of polyethylene blocks located in front of the shielding wall (Fig. 2). The energy distributions of the beam protons fits well a Gaussian curve with a dispersion of 2.8 ± 0.3 Mev at maximum proton energy. The dispersion increased with deceleration of the beam, as seen in Fig. 3.

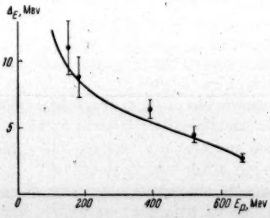

FIG. 3. Dispersion of the beam Δ_E at various proton energies E_p.[18] Solid curve – theoretical dependence of the dispersion on the energy, calculated with allowance for the ionization losses and a "straggling" type of dispersion.

Recording apparatus. Information on the angular distribution of the π^0 mesons and on the value of the total cross section was obtained by registering the gamma quanta from the decay of π^0 mesons, produced in the target by the passage of the proton beam. The gamma quanta were registered with a counter telescope shown schematically in Fig. 4.

The gamma quanta produced in the target were collimated with the aid of a lead diaphragm and fell on the telescope lead converter, where they produced electron-positron pairs. The pairs were registered by a scintillation counter and Cerenkov counter connected for coincidence. Because of the small thickness of the converter (0.5 – 2 mm) and of the scintillators (3 mm) and because of the "broad geometry" of the telescope and the absence of absorbers between the counters, the gamma telescope had a low energy threshold and could register effectively gamma quanta with energies down to 10 Mev. The telescope was made insensitive to either neutrons or charged particles by using a scintillation counter placed in front of the converter and connected for anti-coincidence with the other telescope counters. The counting rate of the telescope placed in the gamma beam was increased 25 fold by placing in it a converter 2 mm thick. Increasing the converter thickness to 5 mm improved this ratio to 40. The telescope could be operated at a relatively large extraneous-radiation background by using coincidence circuits with a time resolution of 10^{-8} sec.

In most of the earlier investigations the efficiency of the gamma telescope was determined by measuring or calculating the sensitivity of the gamma telescope to gamma quanta of various energies, from which the efficiency was found by integrating this energy curve simultaneously with the theoretically-obtained gamma spectra. Consequently the results in these investigations were substantially dependent on the correctness of the theoretical assumptions concerning the gamma spectrum, particularly in those cases[6,16] when the measurements were made with a detector having a high energy threshold. In the present investigation the efficiency was determined experimentally by a method[11] that permitted a determination of

the gamma-quantum yield without making any assumptions concerning their energy spectrum. The dependence of the telescope efficiency w on the angle θ (see Fig. 2), measured at proton energies of 665 and 485 Mev, is shown in Fig. 5. At other

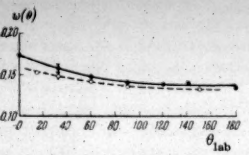

FIG. 5. Efficiency of gamma telescope, w; ● – at E = 665 Mev, ○ – at E = 485 Mev.

energies the dependence $w(\theta)$ has a similar character. As the proton energy decreases, the efficiency decreases and simultaneously, the shape of the $w(\theta)$ curve also changes, because of the reduction in the π^0-meson energy and the velocity of the center-of-mass system. Efficiency measurements made at 665 Mev with graphite, polyethylene, and liquid-hydrogen targets have shown that w is the same for hydrogen and carbon. This result is the consequence of the low energy threshold of the gamma telescope. In spite of the great difference between the gamma spectra at $\theta = 0°$ and $\theta = 180°$ (reference 19) (the mean energies of the spectra are 190 and 75 Mev) the efficiencies $w(0°)$ and $w(180°)$ differ by merely 25%. There is a much smaller difference between the spectra measured for carbon at hydrogen at a single angle,[15,19] and consequently the corresponding efficiencies are also close. As the proton energy decreased, the difference in the efficiency for hydrogen and carbon increased somewhat, but in the investigated energy range this difference still did not influence the results of the measurements, since it was much less than the statistical accuracy of the measured ratio of the gamma yields at different angles. The latter made it possible to use the functions $w(\theta)$, measured for carbon, to find the angular distribution of the gamma quanta from reaction (1) at low proton energies.

Targets. Control experiments. The target used was liquid hydrogen, sealed in a container made of foamed polystyrol. The target was in the form of a cylinder 8 cm in diameter and 25 cm long, so placed that the beam, traveling parallel to the cylinder axis, did not strike the side walls of the target (the beam was 6 cm wide). The conditions for registering the gamma quanta were most favorable in the angle interval $45° < \theta < 145°$. In this case the lead diaphragm, placed in front of the telescope, prevented the gamma radiation from the entrance and exit windows of the target from entering the telescope, and the telescope registered only the gamma radiation from the hydrogen. When the hydrogen was removed from the container, the counting rate of the telescope was decreased to one-tenth at an energy of 660 Mev.

The cross section of reaction (1) was also determined by a differential method, by irradiating targets made of polyethylene and graphite. These targets were approximately $3 g/cm^2$ thick and were chosen such that the beam-energy loss in the target was the same. The polyethylene and graphite targets were placed at an angle of 45° to the proton beam, as shown in Fig. 2, and were introduced into the beam alternately. The targets were changed every 1 – 3 minutes, to eliminate the influence of the change in sensitivity of the registering apparatus on the measurement accuracy. In spite of the fact that ethylene contains only 14% hydrogen, in many cases the difference method yielded a much higher accuracy then the use of liquid hydrogen targets. The reason for this was the difficulty of accurate determination of the effective volume of the liquid-hydrogen target in which the gamma quanta registered by the telescope were produced. Liquid hydrogen was therefore used usually to make accurate relative measurements, while the absolute measurements were made by the differential method.

To obtain a sufficiently high counting rate, the telescope was placed close to the target. This caused the gamma radiation from the various sections of the target to be registered by the telescope with unequal efficiency, and consequently the efficiency of the registration depended on the dimensions of the target. This efficiency, which depends on the dimensions of the target, will be called in the future the form factor of the target. The graphite target was made of light graphite of density 0.9 g/cm^3, and consequently the form factors of the polyethylene and graphite targets differed little. The maximum difference in the form factors for the used targets amounted to 1.5% at $\theta = 90°$, and decreased rapidly with decreasing θ. Since the ratios of the gamma yields from the targets should be measured with accuracy to 1%, great attention was paid to the determination of the form factors of the targets. The form factors were determined experimentally at different angles θ, with accuracy better than 0.5%. Many control experiments, performed with targets of different shapes, have shown good agreement between the measured and calculated form factors. The basic and most laborious control experiment was carried out at a proton energy of 275 Mev. Since this energy is below the threshold of production of π^0 mesons in p-p

TABLE I

θ°	σ'_{pp}, %	θ°	σ'_{pp}, %	θ°	σ'_{pp}, %	θ°	σ'_{pp}, %
E = 665 Mev		E = 665 Mev		E = 560 Mev		E = 485 Mev	
16	14.7±0.8	96	10.8±0.5	16	9.9±0.6	16	5.1±1.0
20	15.4±0.8	120	9.9±0.4	34	9.4±0.9	35	5.3±0.5
33	14.9±0.5	135	9.2±0.8	60	7.5±0.7	60	5.6±0.8
45	14.5±0.8	145	9.4±1.2	90	6.8±0.5	90	4.4±0.7
60	12.7±0.6	160	10.0±1.2	130	6.4±1.0	130	4.0±0.7
75	11.6±0.8			150	6.0±0.7	150	4.5±0.9

collisions, the ratio of the cross sections for hydrogen and carbon measured by the differential method should be zero, if the form factors have been accurately determined. Experiment actually yielded value close to zero:

$$(\sigma^{\gamma}_{pp}/\sigma^{\gamma}_{pC})_{meas} = -0.001 \pm 0.006.$$

3. MEASUREMENT RESULTS

Angular distributions of gamma quanta. In the region of large proton energies, the angular distributions of the gamma quanta were investigated both by the differential method and by the use of liquid hydrogen. In the former case the measurements were performed in two stages: the angular distribution of the gamma quanta produced in collisions between protons and carbon nuclei, $f_{pC}(\vartheta)$ were measured, after which the ratio of the differential cross sections for hydrogen and carbon were found for each angle of observation:

$$\sigma'_{pp} = (d\sigma^{\gamma}_{pp}/d\Omega)/(d\sigma^{\gamma}_{pC}/d\Omega).$$

The angular distribution of the gamma quanta produced on carbon by protons with E = 665 Mev* is shown in Fig. 6. The angular distributions $f^{\gamma}_{pC}(\vartheta)$ at lower energies are similar in form.

The relative cross sections σ'_{pp} were measured by the differential method at energies E = 665, 560, and 485 Mev for a large number of values of θ (see Table I). So detailed an investigation of the function $f^{\gamma}_{pp}(\vartheta)$ was undertaken to verify whether the measurement method employed is accompanied by some noticeable systematic errors. The distribution of the gamma quanta formed in p-p collisions should be symmetrical about $\vartheta = 90°$ in the c.m.s., in view of the indistinguishability of the colliding particles. Any deviation from symmetry in the measured distribution must therefore be considered as an indication of the presence of systematic errors in the procedure.

*Here and below E denotes the effective energy of the beam, determined with allowance for the energy loss in the target and the dispersion of the beam.

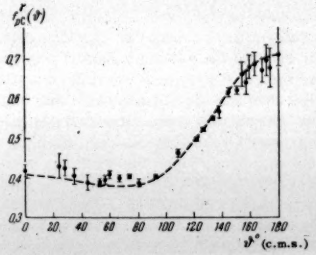

FIG. 6. Angular distribution of gamma quanta produced on carbon by 665 Mev protons. Dotted curve is calculated on the basis of the optical model of the nucleus.[14]

The angular distribution of gamma quanta obtained from the data of Fig. 6 and Table I at E = 665 Mev is shown in Fig. 7. It is represented by the polynomial

$$f^{\gamma}_{pp}(\vartheta) \sim \tfrac{1}{3} + (0.07 \pm 0.02)\cos^2\vartheta.$$

This function, found by the least-squares method and normalized in a suitable manner, is shown dotted in Fig. 7. The angular distribution of the gamma quanta we obtained was found to be symmetrical. If it is approximated by a polynomial that contains, along with the zero and second-order term, also an asymmetric term proportional to $\cos\vartheta$, the contribution of the latter is found to be insignificant: $(0.009 \pm 0.011)\cos\vartheta$. An analysis of the distribution $f^{\gamma}_{pp}(\vartheta)$, measured at E = 665 Mev, shows also that the contribution of the

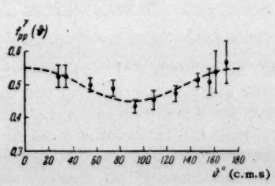

FIG. 7. Angular distribution of gamma quanta from reaction (1) at E = 665 Mev, measured by the differential method. The dotted curve was found by the least-squares method.

cosine powers higher than the second is insignificant: the fraction of gamma quanta distributed in proportion to $\cos^4\vartheta$ amounts to merely (0.015 ± 0.030). The same should also occur at lower proton energies, since the role of the states with large moments diminishes as the reaction threshold is approached. One can therefore assume that in the energy interval $E \lesssim 660$ Mev the gamma quanta from the reaction (1) have the following angular distribution in the c.m.s.

$$f^{\gamma}_{pp}(\vartheta) \sim \tfrac{1}{3} + b_{\gamma}\cos^2\vartheta. \qquad (2)$$

To determine the values of b_γ it is enough to find the ratio of the gamma yields at two angles. Similar measurements were carried out at energies less than 616 Mev, essentially with a liquid-hydrogen target, since the differential method yields accurate values of b_γ only for $E \approx 600$ Mev, as seen from Figs. 7 and 8. The gamma

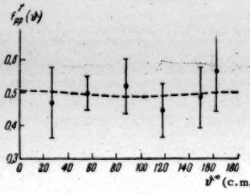

FIG. 8. Angular distribution of gamma quanta from reaction (1) at E = 485 Mev, measured by the differential method. The dotted curve was found by the least-squares method and corresponds to $f^{\gamma}_{pp}(\vartheta) \sim \frac{1}{3} + 0.02\cos^2\vartheta$.

yields were measured at angles $\theta_1 = 55$ to $60°$ and $\theta_2 = 120$ to $125°$. The values of θ_1 and θ_2 varied little with decreasing E. The angles θ_1 and θ_2 were chosen complementary in order to avoid the difficulties connected with the determination of the effective volume of the liquid-hydrogen target. The indicated values of θ_1 and θ_2 are convenient because they correspond to the c.m.s. angles $\vartheta_1 = 90°$ and $\vartheta_2 = 145°$, for which the differential cross sections are connected with the total cross section by the simple relation

$$\sigma^{\pi^0} = \pi\{d\sigma^{\gamma}(\vartheta_1)/d\Omega + d\sigma^{\gamma}(\vartheta_2)/d\Omega\}, \qquad (3)$$

which holds for all values of b_γ. At energies $E > 500$ Mev, the measurements of b_γ were carried out both with the liquid-hydrogen target and the differential method. In the latter case the gamma yields were measured at several angles, including θ_1 and θ_2. The values of b_γ found by the various methods are the same, within the limits of measurement errors. The values obtained for b_γ are listed in Table II.

TABLE II

E, Mev	b_γ	E, Mev	b_γ
665	0.050±0.017	517	0.05±0.06
630	−0.02±0.04	485	0.01±0.04
590	0.06±0.05	440	−0.01±0.06
560	0.02±0.03	400	0.015±0.060

Determination of the angular distribution of the π^0 mesons. The angular distributions of the π^0 mesons can be determined from the measured angular distributions of the gamma quanta. Let us show first how this problem is solved in the case when the π^0 mesons are monoenergetic. Let the π^0 mesons have a velocity β, and let their angular distribution be described in the c.m.s. by the function $V(\cos\vartheta, \varphi)$. The angular distribution of the gamma quanta from the decay of the π^0 mesons, $F(\cos\vartheta, \varphi)$ is determined by the integral equation

$$F(\cos\vartheta, \varphi) = (\xi^2 - 1)\int_{-1}^{1}\int_{0}^{2\pi} V(\cos\vartheta_0, \varphi_0)[\xi - \cos\vartheta\cos\vartheta_0 - \sin\vartheta\sin\vartheta_0\cos(\varphi - \varphi_0)]^{-2} d\cos\vartheta_0 d\varphi_0. \qquad (4)$$

Here $\xi = 1/\beta$. We shall restrict ourselves in the future to the very general case, when the angular distribution of the π^0 mesons is independent of the azimuth angle φ. Then, integrating (4) over φ_0, we get

$$F(\cos\vartheta) = \tfrac{1}{2}(\xi^2 - 1)\int_{-1}^{1} V(\cos\vartheta_0)\, G(\cos\vartheta, \cos\vartheta_0)\, d\cos\vartheta_0. \qquad (5)$$

The kernel of Eq. (5) is symmetrical:

$$G(\cos\vartheta, \cos\vartheta_0) = (\xi - \cos\vartheta\cos\vartheta_0)[(\cos\vartheta + \cos\vartheta_0)^2 - (\xi + 1)(2\cos\vartheta\cos\vartheta_0 - \xi + 1)]^{-3/2}.$$

Formula (5) makes it possible to determine the angular distribution of the π^0 mesons, $V(\cos\vartheta)$, provided the angular distribution of the gamma quanta is known. A solution of this problem can be obtained either by reducing Eq. (5) to a system of linear equations, or by expanding Eq. (5) in eigenfunctions (the eigenfunctions of these equations are Legendre polynomials $P_n(\cos\vartheta)$, which follows from (4) if the "addition theorem" for the Legendre polynomial is used). In the latter case, replacing $F(\cos\vartheta)$ by the series $\Sigma a_n P_n(\cos\vartheta)$, we find

$$V(\cos\vartheta) = \sum_n \frac{a_n}{\alpha_n(\xi)}P_n(\cos\vartheta). \qquad (6)$$

The eigenvalues $\alpha_n(\xi)$ can be readily obtained by using the Neumann formula for the Legendre polynomials

$$\alpha_n(\xi) = (1-\xi^2)\,Q_n'(\xi), \tag{7}$$

where $Q_n'(\xi)$ is the derivative of the Legendre function of the second kind:

$$Q_n(\xi) = P_n(\xi)\tanh^{-1}\frac{1}{\xi} - \sum_{k=0}\frac{2n-4k-1}{(2k+1)(n-k)}P_{n-2k-1}(\xi).$$

The above relations determine the angular distribution of monoenergetic π^0 mesons. This problem becomes more complicated if the π^0 mesons are not monoenergetic. In the most general case, when the distribution function of the π^0 mesons, $U(\cos\vartheta, \xi)$, cannot be separated into angle and energy factors, and it becomes necessary to investigate both the angle and the energy distribution of the gamma quanta in order to determine the distribution $U(\cos\vartheta, \xi)$. In the case when the angular and energy variables can be separated, i.e., when

$$U(\cos\vartheta, \xi) = V(\cos\vartheta)\,R(\xi), \tag{8}$$

the function $V(\cos\vartheta)$ can be determined by finding the average eigenvalues $\overline{\alpha}_n$, which are obtained by averaging the functions (7) over the spectrum $R(\xi)$. To carry out such an averaging in the general case it is necessary to know the spectrum $R(\xi)$. However, if the angular distribution of the gamma quanta differs little from isotropic, it is enough to have only tentative information on the spectrum, which can be obtained from the kinematics of the reaction (1). This last circumstance was used in the present work 4, as seen from Table II, the measured angular distributions of the gamma quanta are close to isotropic. In finding the angular distribution of the π^0 mesons it was assumed that the distribution function could be represented in form (8). As follows from (2) and (6), the angular distribution of the π^0 mesons has the form

$$f_{pp}^{\pi^0}(\vartheta) \sim \frac{1}{3} + b_{\pi^0}\cos^2\vartheta. \tag{9}$$

The values of b_{π^0} for various proton energies are listed in Table III.

TABLE III

E, Mev	b_{π^0}	E, Mev	b_{π^0}
665	0.10±0.03	517	0.13±0.15
630	−0.04±0.08	485	0.02±0.12
590	0.14±0.12	440	−0.03±0.16
560	0.04±0.07	400	$0.07^{+0.40}_{-0.25}$

Total cross sections of reaction (1). At a proton energy E = 660 Mev, we measured the differential cross section for the production of gamma quanta on carbon at $\theta = 33°$. Its value is

$$d\sigma_{pC}^{\gamma}(33°,\ 660\ \text{mev})/d\Omega = (7.6\pm0.4)\cdot10^{-27}\ \text{cm}^2/\text{sterad}$$

and is in good agreement with the cross section measured with the internal beam of the accelerator.[11] Integration of the resultant angular distributions of the gamma quanta, normalized to the aforementioned cross section, gives the value of the total cross section of the reaction (1):

$$\sigma_{pp}^{\pi^0}(660\ \text{Mev}) = (3.22\pm0.17)\cdot10^{-27}\ \text{cm}^2.$$

In experiments with a liquid-hydrogen target we obtain the nearly-equal value

$$(3.4\pm0.4)\cdot10^{-27}\ \text{cm}^2.$$

The dependence of the total cross section of reaction (1) on the proton energy was measured by us in the interval 313 − 665 Mev. The gamma yields were measured at several angles, including the "isotropic" angles[11,17,20] (33 and 96° in the laboratory system at E = 660 Mev), and also at the angles θ_1 and θ_2, which made it possible to determine simply the ratio of the total cross sections at different proton energies. In determining the cross sections by the differential method we used the energy relations for the cross sections of carbon, measured at the "isotropic" angles. One of these is shown in Fig. 9. The relative cross sections σ_{pp}' were determined by the differential method at energies E ≳ 400 Mev (see Table IV). At lower energies, the measurements were carried out only with liquid hydrogen. The relative cross sections σ_{pp}', obtained by comparing the energy relationships of the cross section for the hydrogen (liquid-hydrogen target) in carbon, are

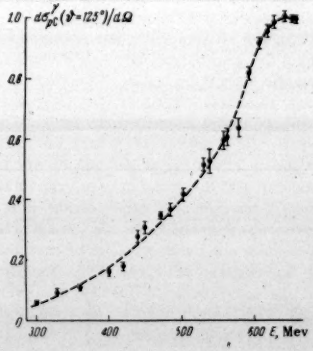

FIG. 9. Dependence of the cross section for production of gamma quanta on carbon on the proton energy (in relative units).

TABLE IV

E, Mev	$\sigma'_{pp}(\theta = 125°)$, %		E, Mev	$\sigma'_{pp}(\theta = 125°)$, %	
	differential method	liquid hydrogen		differential method	liquid hydrogen
660	10.8± 0.6	10.8±0.6	400	1.3±0.4	1.6±0.3
645	—	10.0±0.6	377	—	1.0±0.3
630	9.3 ±0.6	8.7±0.6	360	—	0.9±0.3
610	—	7.6±0.5	350	—	0.7±0.2
590	9.1 ±0.4	7.5±0.6	340[7]	—	0.6±0.1
560	6.8 ±0.5	6.5±0.5	328	—	0.5±0.2
517	5.5 ±0.5	5.0±0.5	313	—	0.3±0.2
485	4.4 ±0.7	3.8±0.4	295	—	<0.3
445	2.9 ±0.5	2.1±0.3			

TABLE V

E, Mev	$\sigma^{\pi^0}_{pp}$		η_m	E, Mev	$\sigma^{\pi^0}_{pp}$		η_m
	Relative units	10^{-27} cm^2			Relative units	10^{-27} cm^2	
665	1.01±0.01	3.24±0.18	1.90	507	0.22±0.01	0.71±0.05	1.38
660	1.00	3.22±0.17	1.89	485	0.139±0.006	0.45±0.03	1.30
652	0.93±0.03	3.00±0.18	1.86	458	0.093±0.008	0.30±0.03	1.19
645	0.91±0.02	2.93±0.17	1.84	445	0.063±0.004	0.20±0.02	1.14
638	0.90±0.03	2.90±0.18	1.82	412	0.039±0.005	0.12±0.02	1.00
630	0.85±0.02	2.74±0.16	1.79	400	0.027±0.004	0.09±0.02	0.95
622	0.81±0.03	2.61±0.17	1.77	374	0.012±0.003	0.04±0.01	0.83
610	0.70±0.02	2.25±0.13	1.73	360	0.009±0.003	0.030±0.008	0.75
597	0.61±0.03	1.96±0.13	1.69	350	0.006±0.002	0.018±0.006	0.70
590	0.57±0.02	1.84±0.13	1.66	328	0.004±0.002	0.014±0.006	0.58
560	0.385±0.013	1.24±0.07	1.56	313	0.002±0.001	0.006±0.004	0.48
531	0.26±0.01	0.84±0.06	1.46	295	<0.001	<0.004	0.32

also given in Table IV. The values σ'_{pp} were normalized in this case to E = 660 Mev. The dependence of the total cross section of reaction (1) on the energy E is given in Table V. The total cross sections listed in the same table were obtained by normalizing the energy dependence of the cross section $\sigma^{\pi^0}_{pp}$ to that measured at E = 660 Mev. To determine the energy dependence of the total cross section we used the data of Fig. 9 and Table IV, and also analogous data obtained by measuring the gamma yields at other angles.

As can be seen from Table V the gamma yield decreases by nearly 500 times with decreasing proton energy in the investigated region. The cross section of reaction (1), measured at 313 Mev, is one-thirtieth the cross section of charged-pion production at the same energy. So small a magnitude of the observed effect makes it necessary to account thoroughly for all the extraneous gamma-radiation sources capable of competing with the investigated reaction. The effect of these sources was analyzed by Moyer and Squire[16] and was found to be insignificant in the investigated region. The greatest danger came in our case from contamination of the proton beam by neutrons knocked out from the polyethylene absorber, used to decelerate the beam. A series of control experiments, in which the slowed-down proton beam was either deflected with a magnet (see 3, Fig. 2), or completely stopped in a polyethylene absorber, has shown that the influence of the neutron admixture is insignificant. An estimate made on the basis of the known neutron yield from the inner target[21] also shows that the contribution due to the neutron admixture is small and amounts to not more than 3% of the cross section measured at E = 313 Mev. The measured gamma-yields can be almost completely attributed to reaction (1) in the investigated energy region. At energies closer to the reaction threshold than in our case, the hard gamma bremsstrahlung of the protons becomes more substantial, and its cross section, according to reference 22, is 10^{-30} cm^2.

4. DISCUSSION

Angular distributions of π^0 mesons. A characteristic feature of the π^0-meson angular distributions obtained in the present investigation is their isotropy over the entire investigated region of proton energies. The angular distributions of references 11 and 16 are more isotropic at low proton energies, as can be seen from Fig. 10. The same diagram shows the energy dependence of the quantity $\delta = 1/(1 + b_{\pi^0})$, which represents the

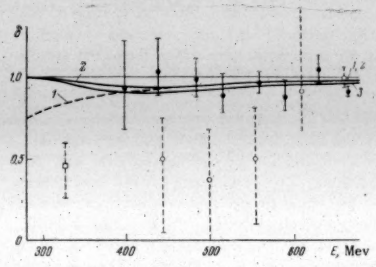

FIG. 10. Angular distributions of π^0 mesons in reaction (1) [the function $\delta(E) = 1/(1 + b_{\pi^0})$ where b_{π^0} is the coefficient in the distribution (9)]. ● – result of the present work, ○ – data of reference 11, □ – data of reference 16. The curves were calculated: 1) under the assumption of (10) without account of the nonresonant Ss transition; 2) the same, but with allowance for the Ss transition, the contribution of which is $0.032\ \eta_m^2 \times 10^{-27}$ cm^2; 3) assuming (11) with allowance for the Ss transition.

fraction of the π^0 mesons isotropically distributed if the angular distribution has the form of Eq. (9) and $b_{\pi^0} \geq 0$. The value of δ at E = 329 Mev has been determined with a detector having a high energy threshold[16] and depends therefore on the correctness of the theoretical assumptions made with respect to the distribution function of the π^0 mesons. On the other hand, the contemporary phenomenological theories[1,9,13] differ greatly in their conclusions concerning the distribution function of the π^0 meson in reaction (1). The experimentally determined values of δ are compared in Fig. 1 with the function $\delta(E)$, calculated by Mandel'shtam (private communication)* on the basis of the theory developed in reference 13. Curve 1 in this diagram is calculated with allowance for only resonant transitions. At large energies δ is close to unity. According to Mandel'shtam, this is due to predominance of P scattering over S scattering, the latter being practically supressed by interference. As the reaction threshold is approached, the anisotropy of the angular distribution of the π^0 mesons produced in resonant transitions increases. However, the contribution due to resonant transitions in this energy range is relatively small. What predominates in this case is the nonresonant Ss transition, which is characterized by an isotropic π^0-meson angular distribution. Therefore the dependence $\delta(E)$, calculated with allowance for the nonresonant Ss transition, is found to be close to unity in the entire investigated energy interval, in agreement with the results of the present work.

The values of δ given in Fig. 10 were determined by us from the experimental values of b_γ, under the assumption that the angle and energy components of the π^0-meson distribution function are independent [see Eq. (8)]. The Mandel'shtam theory, however, predicts that the anisotropy of the angular distribution of the π^0 mesons diminishes with their energy, and the coefficient b_{π^0} may even become negative near the lower boundary of the spectrum (thereby differing from references 1 and 9). Therefore, if δ is calculated from the data of Table II on the basis of spectra taken from the Mandel'shtam theory, they will be located somewhat closer to unity than shown in Fig. 10.

Energy dependence of the cross section of reaction (1). The total cross section measured in

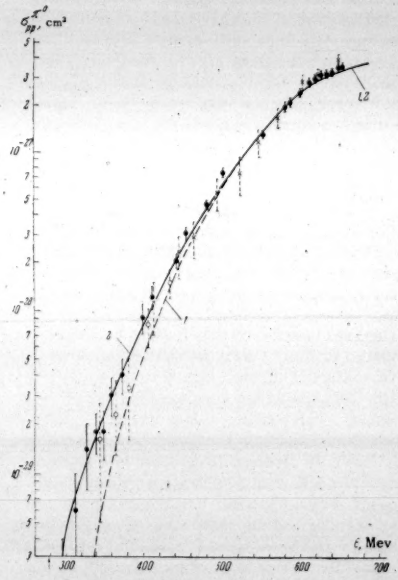

FIG. 11. Total cross sections of reaction (1). ● – results of the present work ■ – from data of the present work and reference 7, × – from data of reference 11, ○ – data of reference 12. The arrow indicates the reaction threshold. 1) resonant curve calculated in reference 13, 2) curve with account of the nonresonant Ss transition, the contribution of which to the total cross section is $0.032\ \eta_m^2 \times 10^{-27}$ cm^2.

*We take this opportunity to thank S. L. Mandel'shtam who graciously communicated to us the results of several of his unpublished calculations.

the present work are shown in Fig. 11. Along with our results, Fig. 11 shows the cross section, determined from our present data on the cross section for carbon and from the data of Mather and Martinelli[7] on the relative cross section σ'_{pp} (see Table IV). The total cross section obtained, $\sigma^{\pi^0}_{pp}$ (340 Mev) = $(0.018 \pm 0.005) \times 10^{-27}$ cm^2, is almost double the cross section [$(0.010 \pm 0.003) \times 10^{-27}$ cm^2] obtained earlier with the results of Mather and Martinelli and those of Crandall and Moyer,[8] and usually cited in earlier papers. This difference is caused by the discrepancy between the cross sections for carbon, measured in the present paper; [$(3.0 \pm 0.4) \times 10^{-27}$ cm^2] and those of reference 8 [$(1.7 \pm 0.4) \times 10^{-27}$ cm^2]. We shall show that the cross section for the production of charged pions on carbon at this energy is $(7.5 \pm 1.0) \times 10^{-27}$ cm^2 (reference 23), from which it follows that $\sigma^{\pi^0}_{pC} = (3.7 \pm 0.5) \times 10^{-27}$ cm^2, if one uses the relation $\sigma^{\pi^+}_{pC} + \sigma^{\pi^-}_{pC} = 2\sigma^{\pi^0}_{pC}$, which follows from the hypothesis that the nuclear forces are independent of the charge, and which is found experimentally to be sufficiently accurate.[24]

As can be seen from Fig. 11, the cross sections measured by us agree, within the limits of experimental error, with the values previously obtained.[11] The cross sections measured at Carnegie[12] are somewhat lower than those of the present paper, possibly owing to the excessive value used in reference 12 for the efficiency of the gamma telescope. The efficiency calculated in that paper at large gamma energies exceeds the maximum value possible, namely $1 - \exp(-\mu d)$ (μ is the coefficient of absorption of gamma quanta in the converter substance and d the thickness of the converter.

The total cross sections obtained by us are compared in Fig. 11 with the theoretical resonance curve of Mandel'shtam. This comparison shows that the behavior of the reaction cross section in the energy region near 600 Mev can be described quite accurately within the framework of a theory that takes only resonant transitions into account. At energies less than 500 Mev a noticeable discrepancy begins to appear between the measured cross sections and the resonance curve, this being explained[13] by the increasing role of non-resonant Ss transition, which is substantial near the reaction threshold. The contribution to the total cross section corresponding to this transition was found by us by comparing the values of the measured cross sections with the resonance curve, and was found to be

$$\sigma_{Ss} = (0.032 \pm 0.007)\,\eta_m^2 \cdot 10^{-27} \text{ cm}^2.$$

Taking into account also the contribution of resonant transitions,[13] the cross section of reaction (1) near the threshold at energies less than 400 Mev can be represented in the form

$$\sigma^{\pi^+}_{pp} = (0.032\eta_m^2 + 0.040\ \eta_m^6 + 0.047\ \eta_m^8) \cdot 10^{-27} \text{ cm}^2.$$

Here the first term is due to nonresonant Ss transition, the second to "shifted" Ss and Sd transitions, and the last one to Pp transitions. The Ps transition, which is also characterized by proportionality to η_m^6, is assumed to be insignificant in Mandel'shtam's theory. In the energy region from 450 to 600 Mev, the cross section of the investigated reaction increases at a constant rate, and varies as $\eta_m^{5.7}$. At still greater energies the increase in the cross sections slows down, in accordance with the Mandel'shtam theory (see Fig. 12).

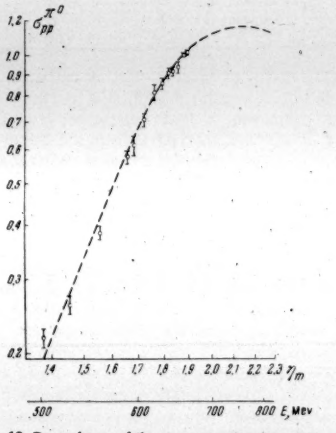

FIG. 12. Dependence of the cross section (in relative units) of reaction (1) on the momentum η_m in the region of the maximum. The experimental data and the theoretical curve, taken from reference 13, are normalized to E = 660 Mev. The errors indicated are those in the relative measurements of the energy dependence of the cross section, and are therefore less than the errors of the absolute measurements of the cross sections, given in Fig. 11.

Comparison of the cross sections for production of neutral and charged pions in proton collisions. The results of the present work and of many other investigations[25] yield information on the ratio $\pi^0/\pi^+ = \sigma^{\pi^0}_{pp}/\sigma^{\pi^+}_{pp,pn}$, where $\sigma^{\pi^+}_{pp,pn}$ is the cross section of the reaction $p + p \rightarrow p + n + \pi^+$, in the final state of which the nucleons are

not bound. At 660 Mev this ratio is

$$\pi^0/\pi^+ = 0.294 \pm 0.015.$$

The ratio π^0/π^+ was calculated by Peaslee[26] for the case when all the transitions are realized through the resonant state ($T = 3/2$, $J = 3/2$), and was found to equal $1/5$. Allowance for the interference of the nucleon states and the differences in the π-meson masses[13] modifies this quantity considerably and brings it closer to the experimental

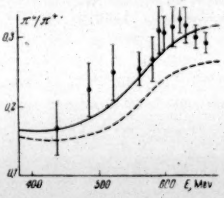

FIG. 13. Ratio of the cross sections of production of π^0 and π^+ mesons by protons at different energies. The solid curve is calculated assuming Eq. (11), while the dotted one corresponds to Eq. (10).

data. The curves shown in Fig. 13 were calculated by Mandel'shtam (private communication) with allowance for the nonresonant Ss transition. The lower curve was calculated under the assumption[13] that the three parameters, which describe P scattering in states with values of total angular momentum $J = 2$, 1, and 0, are equal to each other:

$$|b_{2a}| = |b_{1a}| = |b_{0i}| = b_a, \qquad (10)$$

where b_a is one of the two free parameters of the P scattering in the resonance theory. This assumption was introduced in the theory in a somewhat arbitrary manner. As indicated in Mandel'shtam's private communication, a more correct assumption is

$$|b_{2a}|^2 = 2|b_{1a}|^2 = 2|b_{0i}|^2, \qquad (11)$$

i.e., the production of π^0 mesons is more probable in the state with $J = 2$ than in the states with $J = 1$ and $J = 0$. In the latter case one observes a better agreement between the calculated ratio π^0/π^+ and the experimental data (see Fig. 13). Another circumstance in favor of relation (11) is, as indicated in a private communication by G. Braun, the small magnitude of the radius of the repelling core for the state $^3P_2$, compared with $^3P_1$ and $^3P_0$, thanks to which the production of mesons is less supressed than in the state with $J = 2$ in that with $J = 1$ and $J = 0$.

The quantity π^0/π^+ is thus sufficiently sensitive to the relations between various P-scattering parameters. Other characteristics of reaction (1) are less sensitive to changes in the parameter relations. Thus, the π^0-meson angular distributions calculated for the cases (10) and (11) hardly differ from each other, as can be seen from Fig. 10.

5. CONCLUSIONS

The comparison made in this paper of the experimental data with the Mandel'shtam theory shows that the accuracy with which this theory describes the main properties of the process of π^0-meson production by protons at energies $E < 700$ Mev is quite high. In connection with this, it is of great interest to continue further systematic investigations of this reaction at higher energies, 700 — 1000 Mev, where its cross section, according to theory, passes through a maximum. The data obtained thus far in this energy region[27] are contradictory and cannot therefore be used for comparison with the theory.

In conclusion, we take this opportunity to thank L. I. Lapidus, S. L. Mandel'shtam, L. M. Soroko, and A. A. Tyapkin for discussion of the results of the present work. We are grateful to B. M. Antonov, E. L. Grigor'ev, G. P. Zorin, M. M. Kulyukin, N. A. Mitin, O. V. Savchenko, and I. V. Tsymbulov for help in performing the measurements.

[1] A. Rosenfeld, Phys. Rev. **96**, 139 (1954).
[2] Hales, Hildebrand, Knable, and Moyer, Phys. Rev. **85**, 37 (1952).
[3] Marshall, Marshall, Nedzel, and Warshaw, Phys. Rev. **88**, 632 (1952).
[4] Pontecorvo, Selivanov, and Zhukov, Отчет ОИЯИ (Report, Joint. Inst. for Nuclear Research, Acad. Sci. U.S.S.R.), 1952, p. 81.
[5] Kozodaev, Tyapkin, Bayukov, Markov, Prokoshkin, Izv. Akad. Nauk SSSR, Ser. Fiz. **19**, 589 (1955), Columbia Tech. Transl. p. 529.
[6] L. M. Soroko, J. Exptl. Theoret. Phys. (U.S.S.R.) **30**, 296 (1956), Soviet Phys. JETP **3**, 184 (1956).
[7] J. Mather and E. Martinelli, Phys. Rev. **92**, 749 (1953).
[8] W. Crandall, B. Moyer, Phys. Rev. **92**, 749 (1953).
[9] M. Gell-Mann and K. Watson, Ann. Rev. Nucl. Sci. **4**, 219 (1954).
[10] Tyapkin, Kozodaev, and Prokoshkin, Dokl. Akad. Nauk SSSR **100**, 689 (1955).
[11] Yu. D. Prokoshkin and A. A. Tyapkin, J. Exptl. Theoret. Phys. (U.S.S.R.) **32**, 750 (1957), Soviet Phys. JETP **5**, 618 (1957).
[12] Stallwood, Sutton, Fields, Fox, and Kane, Phys. Rev. **101**, 1716 (1958).
[13] S. Mandelstam, Proc. Roy. Soc. **A244**, 491 (1958).

[14] Yu. Prokoshkin, Proc. CERN Symposium **2**, 385 (1956); cf. data of B. D. Balashov, V. A. Zhukov, B. Pontecorvo, and G. I. Selivanov (p. 393).

[15] Yu. D. Bayukov and A. A. Tyapkin, J. Exptl. Theoret. Phys. (U.S.S.R.) **32**, 953 (1957), Soviet Phys. JETP **5**, 779 (1957).

[16] B. Moyer and R. Squire, Phys. Rev. **107**, 283 (1957).

[17] Yu. D. Prokoshkin, J. Exptl. Theoret. Phys. (U.S.S.R.) **31**, 732 (1956), Soviet Phys. JETP **4**, 618 (1957).

[18] I. M. Vasilevskiĭ and Yu. D. Prokoshkin, Атомная энергия (Atomic Energy), in press.

[19] Bayukov, Kozodaev, and Tyapkin, J. Exptl. Theoret. Phys. (U.S.S.R.) **32**, 667 (1957), Soviet Phys. JETP **5**, 552 (1957).

[20] A. A. Tyapkin, J. Exptl. Theoret. Phys. (U.S.S.R.) **30**, 1150 (1956), Soviet Phys. JETP **3**, 979 (1956).

[21] V. P. Dzhelepov and B. M. Pontecorvo, Атомная энергия (Atomic Energy) **3**, 413 (1957).

[22] A. Ashkin and R. Marshak, Phys. Rev. **76**, 58 (1949). Bjorklund, Crandall, Moyer, and York, Phys. Rev. **77**, 213 (1950).

[23] Richman, Weissbluth, and Wilcox, Phys. Rev. **85**, 161 (1952); Passman, Block, and Havens, Phys. Rev. **88**, 1247 (1952); S. Leonard, Phys. Rev. **93**, 1380 (1954); W. Dudziak, Phys. Rev. **95**, 866 (1954).

[24] Meshkovskiĭ, Pligin, Shalamov, and Shebanov, J. Exptl. Theoret. Phys. (U.S.S.R.) **32**, 1328 (1957), Soviet Phys. JETP **5**, 1085 (1957).

[25] V. S. Neganov and O. V. Savchenko, J. Exptl. Theoret. Phys. (U.S.S.R.) **32**, 1265 (1957), Soviet Phys. JETP **5**, 1033 (1957); Dzhelepov, Moskalev, and Medved', Dokl. Akad. Nauk SSSR **104**, 380 (1955); Paper delivered at Conference on High-Energy Particle Physics, Moscow, 1956. G. M. Meshcheryakov and B. S. Neganov, Dokl. Akad. Nauk SSSR **100**, 677 (1955). Fields, Fox, Kane, Stallwood, and Sutton, Phys. Rev. **109**, 1713 (1958).

[26] D. Peaslee, Phys. Rev. **95**, 1580 (1954).

[27] Hughes, March, Mirhead, and Lock, Proc. CERN Symposium **2**, 344 (1956). Morrison, Fowler, and Garrison, Phys. Rev. **103**, 1472 (1956).

Translated by J. G. Adashko
345

SOVIET PHYSICS JETP VOLUME 36 (9), NUMBER 6 DECEMBER, 1959

MAGNETIC PROPERTIES OF GADOLINIUM OXIDES

K. P. BELOV, M. A. ZAĬTSEVA, and A. V. PED'KO

Moscow State University

Submitted to JETP editor January 5, 1959

J. Exptl. Theoret. Phys. (U.S.S.R.) **36**, 1672-1679 (June, 1959)

Measurements of the temperature dependence of magnetic properties have been made on gadolinium ferrites with garnet and perovskite structures, and also on gadolinium manganite. It has been established that in the garnet ferrite in the neighborhood of the compensation temperature and of the Curie point there occurs an anomalous increase of the coercive force and an extremely small paraprocess. The temperature dependence of the magnetostriction also exhibits an anomalous behavior. The perovskite gadolinium ferrite has a weak ferromagnetism of the hematite type. The magnitude of this ferromagnetism increases after heating of the specimen above the Curie point in a field. Gadolinium manganite has paramagnetic properties; but in the helium temperature range, magnetic hysteresis phenomena are observed.

RECENTLY there has been great interest in the study of the magnetic properties of oxides (ferrites) of the rare earth elements and of yttrium.[1,2] This interest is due to the fact that many of these compounds have antiferromagnetic or ferromagnetic properties. However, knowledge of the magnetic behavior of such materials is still very scanty. The present article presents the results of an investigation of the temperature dependence of the magnetic properties of several oxides of gadolinium, with both garnet and perovskite structures. In our work the specimens used were of quite large dimensions, as compared with those used in other work.[1,2] This enabled us to get more detailed information about the magnetic properties of the gadolinium oxides. Besides magnetization data, we give below data on the coercive force and the magnetostriction.

The specimens were prepared in accordance with standard ceramic practice from oxides of iron, gadolinium, and yttrium. Carefully ground mixtures of the oxides were given a preliminary anneal at 900° C for six hours in air. Then the materials thus obtained were reground, moulded under high pressure, and finally fired at 1300° C for four hours in air. The specimens were rectangular bars of dimensions $60 \times 5 \times 5$ mm.

The methods used for measurement of the magnetic properties were the ballistic, the magnetometric, and the ponderomotive. The magnetostriction was measured by means of wire feelers with the aid of an electrophotooptical amplifier.

1. GADOLINIUM GARNET-FERRITE

The garnet ferrites of the rare-earth elements have the formula $3Me_2O_3 \cdot 5Fe_2O_3$, where Me is one of the rare-earth elements or yttrium. Some of the ions in the garnet lattice may be replaced by other elements. In our experiments we used as such a substituting element yttrium, which has zero atomic magnetic moment. In the garnet ferrite $3Gd_2O_3 \cdot 5Fe_2O_3$, the Gd^{3+} and Fe^{3+} ions have magnetic moments of considerable magnitude; therefore it was of interest to explore the effect of yttrium on the magnetic properties of this ferrite. We prepared a garnet ferrite of composition $3Gd_2O_3 \cdot 4.8Fe_2O_3 \cdot 0.2Y_2O_3$ and made measurements of its saturation magnetization at helium temperatures and of its Curie point; these gave the following values:

$$\sigma_0 = 72.5 \text{ gauss cm}^3/\text{g} = 24\mu_B/\text{mole}, \quad \Theta = 561^\circ \text{ K}.$$

On comparing these values with those obtained by Pauthenet[1] on $3Gd_2O_3 \cdot 5Fe_2O_3$ ($\sigma_0 = 30\ \mu_B$/mole and $\Theta = 570^\circ$ K), we see that the introduction of even a small number of Y ions diminishes σ_0 and Θ very significantly. This is in qualitative agreement with Néel's[3] ideas on the nature of the magnetic properties of the garnet ferrites; these consist briefly of the following.

The crystal lattice of gadolinium garnet-ferrite is cubic; it contains a large number of Fe^{3+} and Gd^{3+} ions distributed among three types of site: d (tetrahedral sites), a (octahedral sites), and c. To explain the magnetic properties of the gar-

net ferrites, Néel[3] suggested that the lattice of these substances should be considered to be made up of three sublattices, formed respectively by the d, a, and c sites. The Fe^{3+} ions are distributed over the lattices containing d and a sites; there are more of the tetrahedral sites d than of the octahedral a. The Gd^{3+} ions are distributed over the third sublattice c. Between the sublattices d and a there is a strong negative exchange interaction, in consequence of which — and because of the excess of tetrahedral d sites — they acquire a ferromagnetic moment. Furthermore, the Fe^{3+} ions on the d and a sublattices act on the Gd^{3+} ions on the c sublattice, in consequence of which there arises a ferrimagnetic coupling here also, though a weaker one than in the case of d and a. The distribution of magnetizations on all three sublattices can be represented schematically as follows:

$$\xrightarrow[Gd^{3+}]{c} \quad \xleftarrow[Fe^{3+}]{d} \quad \underset{Fe^{3+}}{a}\rightarrow .$$

The relative length of each arrow represents the magnitude of the magnetization of the corresponding sublattice. From this scheme it is evident that by substitution of nonmagnetic ions for one or another sublattice of Fe^{3+} and Gd^{3+} ions, the resultant magnetic moment of the ferrite can be changed. From consideration of the scheme presented above, it is evident that the Y^{3+} ions must be distributed on a sites; only then can the resultant magnetic moment of the ferrite decrease. This also leads to diminution of the number of Fe^{3+}-O^{2-}-Fe^{3+} exchange interactions, and hence to a decrease in the magnitude of Θ.

The most interesting peculiarity of the garnet ferrites is this: most of them exhibit a compensation temperature Θ_k; that is, their spontaneous magnetization vanishes not only at the Curie point Θ, but also at a lower temperature Θ_k. At this point there occurs a balancing of the magnetic moments of the sublattices; i.e., here the material becomes antiferromagnetic.

Figure 1 shows the results of measurements of the temperature dependence of the specific magnetization of the garnet ferrite studied, with various magnetic fields applied to the specimen. It is clear that in the neighborhood of −14°C (260°K), there is a compensation point Θ_k. Because of the effect of the magnetic field, however, the compensation is incomplete. In order to determine the exact location of Θ_k, it is necessary to get the curve of spontaneous magnetization, $\sigma_s(T)$. Figure 2 shows such a curve, with coordinates σ_s/σ_0 and T/Θ; the curve was obtained by extrapolating

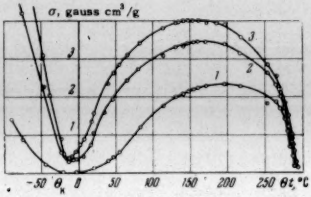

FIG. 1. Dependence of the specific magnetization on temperature at various fields in the garnet ferrite of composition $3Gd_2O_3 \cdot 0.2\ Y_2O_3 \cdot 4.8\ Fe_2O_3$: 1) H = 25.8; 2) H = 129; 3) H = 1550 oe.

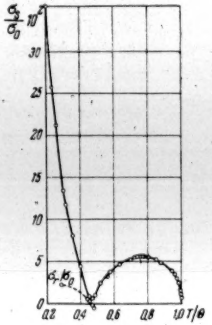

FIG. 2. Temperature dependence of σ_s/σ_0 for the garnet ferrite studied. Dashed curve: temperature dependence of the residual magnetization σ_r/σ_0 in the neighborhood of the compensation point.

the magnetization isotherms $\sigma(H)$ to zero field. The value of σ_0 was determined from the magnetization isotherm taken at 4.3°K. It is evident that at 258°K the spontaneous magnetization is close to zero. The location of Θ_k can be determined still more precisely by finding the temperature dependence of the residual magnetization σ_r. The position of Θ_k is found from the change of sign of the quantity σ_r/σ_0 (cf. Fig. 2). It should be mentioned that here, as in our earlier work[4] on a lithium chromite-ferrite, we apparently do not have complete compensation of the sublattice magnetizations; this is probably connected with the influence of structural inhomogeneities of the garnet-ferrite specimen under study. The presence of incomplete compensation can also be explained by the development of appreciable magnetization upon application of a field even at the compensation point Θ_k (cf. Fig. 1).

A very interesting fact established for our gadolinium garnet is the existence of a maximum on the coercive force vs temperature curve in the neighborhood of Θ_k; there is also an anomalous increase of the coercive force in the Curie point region (cf. Fig. 3). A similar phenomenon had

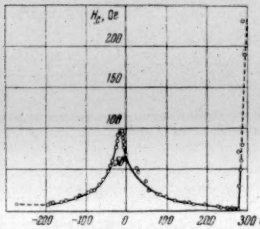

FIG. 3. Dependence of coercive force on temperature in the garnet ferrite $3Gd_2O_3 \cdot 0.2\ Y_2O_3 \cdot 4.8\ Fe_2O_3$.

been observed earlier in our laboratory, for lithium garnet-ferrite, by K. M. Bol'shova and T. A. Elkina. The nature of this increase of H_c is still not altogether clear. It is possible that near the temperatures Θ_k and Θ, there occurs a peculiar magnetic "heterogeneity." Here the main part of the specimen volume is in a nonmagnetic state, but there are individual small sections in which the material is in a ferromagnetic state. This promotes the development of a "single-domain" structure, and consequently the processes of magnetization reversal will occur with greater difficulty; this will lead to an increase of H_c. Formally it is possible to apply here the known relation $H_c \sim K/\sigma_s$, where K is the magnetic anisotropy constant. If K does not decrease with temperature as fast as does σ_s, H_c must increase because of the decrease of σ_s.

We now consider a peculiarity of the paraprocess in gadolinium garnet-ferrite. In this material there is observed an anomalous temperature variation of the paraprocess susceptibility. Whereas in ordinary ferromagnetics and ferrimagnetics it increases monotonically with increase of temperature, reaching a maximum near the Curie point,[5] in gadolinium garnet-ferrite its change with temperature has a more complicated character. As is evident from Fig. 4 (experimental data taken from reference 1), starting from 0°K the paraprocess susceptibility at first increases, reaches a maximum, then on further rise of temperature diminishes; again begins to rise on approach to the Curie point; and after passing it, again suddenly drops. The magnitude of the paraprocess susceptibility is not as large in the temperature interval $\Theta - \Theta_k$ as in the region 0°K to Θ_k; this is anomalous. This peculiar temperature variation of the paraprocess susceptibility in gadolinium garnet-ferrite can be explained on the basis of the following considerations. In our previous researches[5] it has been shown that the paraprocess in a ferromagnetic is larger, the larger the size of the magnetic moments of the atoms that take part in the ferromagnetism, and the smaller the exchange interaction between them. In the case of gadolinium garnet-ferrite, the exchange interaction of sublattice c with sublattices d and a is weaker than that of d and a; the magnetic moment of sublattice c is larger than the resultant moment of sublattices d and a. This leads to the consequence that in gadolinium garnet-ferrite at low temperatures, where the magnetization of the ferrite is basically determined by the magnetic moment of sublattice c, a large paraprocess should be observed, as in fact occurs experimentally. This paraprocess, however, should diminish with rise of temperature, since the magnetic moment of sublattice c is compensated by the resultant moment of sublattices d and a. Above the compensation point, the paraprocess operates through the Fe^{3+} ions, between which there is a larger exchange interaction. Here the paraprocess will be weaker, despite the fact that the ferrite is at a higher temperature. In the region of the Curie point we have the usual susceptibility "splash" characteristic of all ferromagnetics and antiferromagnetics.

The paraprocess model just described is confirmed by our measurements of the magnetostriction of gadolinium garnet-ferrite. Figure 5 gives isotherms of the magnetostriction, measured in the temperature interval −169 to +10°C. It can be seen that at low fields the magnetostriction is negative, at higher fields there develops a positive component of magnetostriction because of the paraprocess. In our ferrite it is especially large at

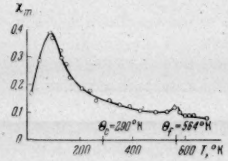

FIG. 4. Dependence of the paraprocess susceptibility on temperature in the garnet ferrite $3Gd_2O_3 \cdot 5Fe_2O_3$.

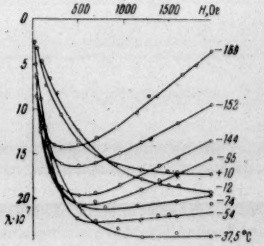

FIG. 5. Dependence of magnetostriction on temperature in the garnet ferrite $3Gd_2O_3 \cdot 0.2\ Y_2O_3 \cdot 4.8\ Fe_2O_3$ (the figures on the curves show the temperature in degrees C).

low temperatures (at −169°C). On approach to the compensation point the paraprocess magnetostriction decreases, since here the paraprocess diminishes in accordance with Fig. 4.

In the neighborhood of the compensation point itself, it was not possible to observe the paraprocess, because here the magnetic fields used were insufficient for attainment of technical saturation of the specimen.

Finally, we present the results of a study of the paraprocess magnetization in gadolinium garnet-ferrite in the immediate vicinity of the Curie point. We have analyzed the magnetization curves in the Curie point region according to the thermodynamic formula $H/\sigma = \alpha + \beta\sigma^2$, where α and β are thermodynamic coefficients.[5] The values of α and β provide a method of determining the temperature behavior of σ_S (from the relation $\sigma_S^2 = -\alpha/\beta$). Figure 6 shows the dependence of

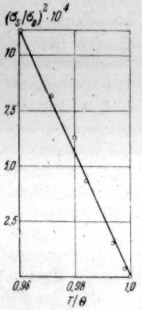

FIG. 6. Dependence of $(\sigma_s/\sigma_0)^2$ on (T/Θ) in garnet ferrite near the Curie point.

$(\sigma_S/\sigma_0)^2$ on T/Θ. It is clear that the equation

$$(\sigma_s/\sigma_0)^2 = \xi(1 - T/\Theta).$$

is satisfied. However, in contrast to other ferrites and ferromagnetics, the calculated value of ξ here is extremely small (cf. table). The table also shows, for comparison, the values for several ferrimagnetics and ferromagnetics.

Material	ξ	b_Θ	σ_0	Θ, °K
$3Gd_2O_3 \cdot 0{,}2Y_2O_3 \cdot 4{,}8Fe_2O_3$	0,04	0,046	72,5	561
Ni	6,95	0,8	55,2	624
20% Cu; 80% Ni	3,44	0,5	35,9	428
35,5% MnO; 15% ZnO; 49,5% Fe_2O_3	0,1—0,7	0,805	152,0	467,5

Figure 7 shows the dependence of the paraprocess magnetization σ on $H^{1/3}$ right at the Curie point. Here the relation $\sigma = b_\Theta H^{1/3}$, derived from thermodynamic theory:[5] is fulfilled; b_Θ describes the inclination of the magnetization curve at the

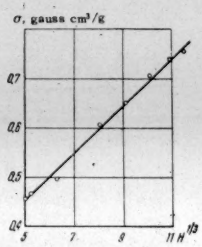

FIG. 7. Dependence of magnetization on $H^{1/3}$ near the Curie point.

Curie point. According to qualitative considerations, the value of b_Θ should be larger, the larger the value of σ_0 in the material under study ($b_\Theta \sim \sigma_0/\sqrt[3]{\Theta}$). However, as is evident from the table, for the garnet ferrite the value of b_Θ is extremely small and not consistent with the high value of σ_0 for this ferrite. The reason for this lies in the fact that the paraprocess at the Curie point is basically determined by sublattices a and d, whose resultant magnetization is small.

2. GADOLINIUM PEROVSKITE-FERRITE

According to earlier investigations,[1,2] the compound $Gd_2O_3 \cdot Fe_2O_3$ (or $GdFeO_3$) is antiferromagnetic with a weak parasitic ferromagnetism. Its magnetic behavior is in many respects similar to that of hematite (αFe_2O_3), and also to that of $CoCO_3$ and $MnCO_3$, which have recently been studied in detail by Borovik-Romanov and coworkers.[6] The similarity consists in the fact that these materials obey the law $\sigma = \sigma_S + \chi H$, where σ_S is a spontaneous magnetization of small magnitude, and where χ is a field-independent susceptibility. Figure 8 gives a series of curves $\sigma(H)$ taken on $Gd_2O_3 \cdot Fe_2O_3$. It is evident that over a wide field interval the isotherms $\sigma(H)$ are straight lines, which cut off on the axis of ordinates a segment equal to σ_S. There is nevertheless a difference in the behavior of $Gd_2O_3 \cdot Fe_2O_3$ as compared with the substances mentioned above. The difference is that in the material studied by us, σ_S is unstable. Heating of the specimen to the Curie point in the presence of a field causes an increase of σ_S.

Figure 9 gives a series of magnetization isotherms taken after heating of the specimen above the Curie point. It is evident that larger values of σ_S are now cut off on the axis of ordinates.

Figure 10 shows the temperature dependence of σ_S at the time of the first and of the second heating of the specimen. It is evident that below 100° the value of σ_S decreases. On the

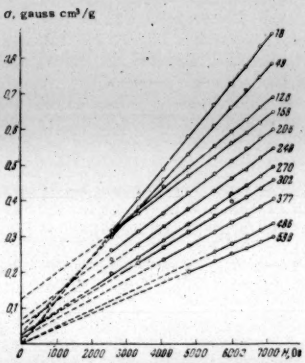

FIG. 8. Dependence of magnetization on field at various temperatures for gadolinium perovskite-ferrite, $Gd_2O_3 \cdot Fe_2O_3$ (the figures on the curves indicate the temperature in degrees C).

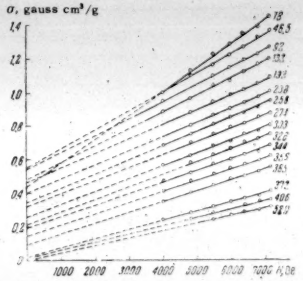

FIG. 9. Same as Fig. 8 after heating above the Curie point in a magnetic field.

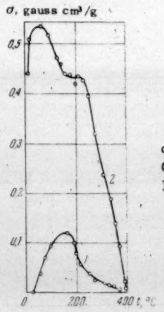

FIG. 10. Temperature dependence of the spontaneous magnetization of $Gd_2O_3 \cdot Fe_2O_3$ in a magnetic field: 1) after first heating; 2) after second.

other hand, our measurements at helium temperatures have shown that at those temperatures σ_s reaches a large value. It must be concluded that the character of the $\sigma_s(T)$ curves in the substance under investigation is very complicated. This is consistent with the results of references 1 and 2.

3. GADOLINIUM PEROVSKITE-MANGANITE

X-ray analysis has shown that the compound $Gd_2O_3 \cdot Mn_2O_3$ has the perovskite structure. Its magnetization curves are of purely paramagnetic character (cf. Fig. 11); however, the values of the

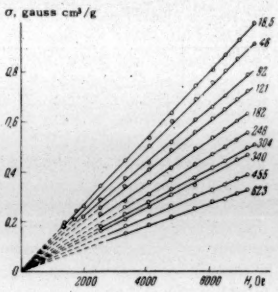

FIG. 11. Dependence of magnetization on field at various temperatures for $Gd_2O_3 \cdot Mn_2O_3$ (the figures on the curves show the temperature in degrees C).

susceptibility are two orders of magnitude larger than in ordinary paramagnetics ($\chi \sim 10^{-4}$). The values of the constants C and Θ also differ from the values for classical paramagnetics. In measurements in the helium temperature range, the function retains its straight-line form. Here, in contrast to the behavior at room temperature, the susceptibility becomes very large; and on decrease of the field, hysteresis occurs. From Fig. 12 it is

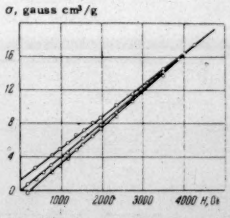

FIG. 12. Magnetic hysteresis in $Gd_2O_3 \cdot Mn_2O_3$ at 4.3°K.

clear that, though the residual magnetization is small, the coercive force reaches 250 oe. From this it was concluded that in this substance, as in $Gd_2O_3 \cdot Fe_2O_3$, parasitic ferromagnetism can be produced by extreme cooling.

We also made an attempt to synthesize the com-

pound $3Gd_2O_3 \cdot 5Mn_2O_3$. It was conjectured that this compound would have the garnet structure. Since instead of Fe^{3+} ions there will be Mn^{3+} ions, it was expected that this compound would be strongly magnetic. The measurements, however, showed that the substance obtained had magnetic properties identical with those of $Fe_2O_3 \cdot Mn_2O_3$. X-ray studies showed that the synthesized material had the perovskite structure; no garnet structure is formed.

[1] R. Pauthenet, Ann. phys. **3**, 424 (1958).

[2] Bozorth, Kramer, and Remeika, Phys. Rev. Letters **1**, 3 (1958); Bozorth, Williams, and Walsh, Izv. Akad. Nauk SSSR, Ser. Fiz., **21**, 1072 (1957), Phys. Rev. **103**, 572 (1956).

[3] L. Néel, Compt. rend. **239**, 8 (1954).

[4] Belov, Bol'shova, Elkina, and Zaĭtseva, Izv. Akad. Nauk SSSR, Ser. Fiz., **22**, 1282 (1958), Columbia Tech. Transl. in press.

[5] K. P. Belov, Usp. Fiz. Nauk **65**, 207 (1958); K. P. Belov and A. N. Goryaga, Физика металлов и металловед. (Phys. of Metals and Metal Research) **2**, 441 (1958).

[6] A. S. Borovik-Romanov and M. P. Orlova, J. Exptl. Theoret. Phys. (U.S.S.R.) **31**, 579 (1956), Soviet Phys. JETP **4**, 531 (1957).

Translated by W. F. Brown, Jr.
346

DEPOLARIZATION OF μ^+ MESONS IN NUCLEAR EMULSION

A. O. VAĬSENBERG, N. V. RABIN, and V. A. SMIRNIT-SKIĬ

Institute of Theoretical and Experimental Physics, Academy of Sciences, U.S.S.R.

Submitted to JETP editor January 7, 1959

J. Exptl. Theoret. Phys. (U.S.S.R.) **36**, 1680-1686 (June, 1959)

Measurements were made of the asymmetry coefficient for π^+-μ^+-e^+ decay in ordinary and diluted NIKFI-R emulsion, and in the same emulsion placed in a strong magnetic field. An analysis of the data obtained and that known from the literature shows that the asymmetry coefficient in NIKFI-R emulsion ($a = -0.077 \pm 0.012$) is substantially less than that in Ilford G-5 emulsion ($a = -0.139 \pm 0.014$). A double dilution of the NIKFI-R emulsion with gelatin sharply increases the asymmetry coefficient ($a = -0.127 \pm 0.028$). The application of a magnetic field restores the polarization in the NIKFI-R emulsion, raising the asymmetry coefficient to a value $a = -0.28 \pm 0.02$ in a field of 17,000 gauss.

1. INTRODUCTION

THE obtaining of exact values for the asymmetry coefficient of a spatial distribution of protons in π^+-μ^+-e^+ decay in nuclear photoemulsions and bubble chambers is of substantial interest for the weak-interaction problem. According to the two-component theory of the neutrino the asymmetry coefficient depends in the following way on the ratio between the vector interaction constant g_V and of the axial vector constant g_A in μ decay:

$$a = \frac{1}{3}\frac{g_V^* g_A + g_A^* g_V}{|g_V|^2 + |g_A|^2}. \quad (1)$$

The magnitude of the asymmetry coefficient has been repeatedly measured in numerous experiments in which the μ^+ meson was stopped in various substances. However, the determination of the quantity a is complicated by the fact that experiments on the depolarization of μ^+ mesons give the quantity $a\xi$, where ξ is the average polarization. The "kinematic" depolarization and the depolarization in matter in the last stages of the retardation and after the stopping of the μ^+ meson exert a substantial influence on the experiment. The "kinematic" depolarization refers to the fact that not only the μ's incident in the collimator direction in the rest system but also the μ's which are moving in other directions after decay emerge from the collimator slit of the accelerator. The polarization losses arising from this cause are 5 — 25%. The depolarization in the last stages of the retardation and after the stopping is apparently connected mainly with the formation of muonium and more complex atomic systems and with the local magnetic fields in the stopping medium. It is reasonable to admit that such a depolarization is absent in metals and in graphite, where muonium is not formed. Therefore, to determine the "pure" asymmetry coefficient one can employ the type of setup described by Lederman et al.[1] and measure the ratio ρ of the asymmetry coefficient in photoemulsion (used as a target) and in graphite, which does not depend on the kinematic depolarization. If the μ mesons are created from π^+ mesons directly stopped in the emulsion, the kinematic depolarization is absent. Therefore, one can get the pure asymmetry coefficient by dividing the asymmetry coefficient a_{em} measured in the emulsion by the quantity ρ. Since ρ can be measured quite exactly, the error in determining a depends on the error in the asymmetry coefficients measured from emulsion or bubble chamber tracks.[2] The values of such measurements are not restricted to this use, however. Since the depolarization of mesons in a substance is closely connected with the existence of muonium atoms and with the effect on them of the internal magnetic fields, it is entirely possible that the study of the asymmetry in π-μ-e decay in various substances has importance for some questions in solid-state physics.

2. THE ASYMMETRY COEFFICIENT IN THE EMULSIONS NIKFI-R AND ILFORD G-5

To study the energy dependence of the asymmetry of decays in nuclear emulsions we had to investigate the integral asymmetry (averaged over the whole spectrum). For example, to be

TABLE I

Angles, in degrees	0—18	18—36	36—54	54—72	72—90	90—108	108—126	126—144	144—162	162—180
NIKFI-R	828	896	856	858	889	900	948	912	969	960
$(\text{NIKFI-R})_{\times 2}$	190	189	206	224	218	241	226	241	247	263

able to examine the asymmetry of a few hundred decay electrons in the initial region of the spectrum, we first chose 9101 π-μ-e decays in NIKFI-R emulsion which had been bombarded in the Joint Institute for Nuclear Research synchrotron under conditions of careful magnetic shielding ($H < 4 \times 10^{-2}$ gauss). These decays satisfied the following criteria: 1) the length of the electron track $l \geq 1$ mm; 2) the source of the π^+-μ-e decay was farther than 100 μ from the surface of the emulsion or the glass.

Such criteria correspond with great accuracy to the considerations of planar correlation given by the formula $(1 + a \cos\theta)\,d\theta$, where a is the asymmetry coefficient and θ is the angle in the plane of the emulsion between the original directions of the μ-meson and positron tracks. The angular distribution of the decays measured is given in Table I (line 2).

The coefficient a can be determined from this table either by the average value of $\cos\theta$, or by the forward-back difference:

$$a/2 = \overline{\cos\vartheta} = \sum n_i \cos\vartheta_i / \sum n_i, \qquad (2)$$

$$a = (\pi/2)\left[\sum_{0-90^\circ} n_i - \sum_{90-180^\circ} n_i\right] \Big/ \sum n_i. \qquad (3)$$

The geometry of our decays was not plane. It is easy to show that the correction coefficient k, which must be divided into the asymmetry coefficient a to take into account the deviation from plane geometry, is equal to

$$k = (\overline{\cos^2\alpha_e} / \overline{\cos\alpha_e})\ (\overline{\cos^2\alpha_\mu} / \overline{\cos\alpha_\mu}), \qquad (4)$$

where the α are the angles of the inclination of the meson and electron tracks to the plane of the emulsion, and $\overline{\cos^2\alpha}$ and $\overline{\cos\alpha}$ are the average values of the second and first powers of the cosines of these angles. Knowing the distribution of the inclination angles for mesons and electrons, it is easy to carry out the corresponding correction. In our case it is close to 5%. According to formulas 1 and 2, after introducing correction 3 we get

$$a = -0.066 \pm 0.018,$$

where the statistical error is $\sqrt{3/N}$, $N = \Sigma n_i$.

Measurements of the asymmetry coefficient for NIKFI-R emulsion were also carried out by Gurevich et al.[4] who got $a = -0.092 \pm 0.018$ by analyzing 8990 decay.

In the recent work of Ivanov and Fesenko[5] the values $a = -0.065 \pm 0.041$ are given. These a values agree rather well, and combining them we get for the asymmetry coefficient in NIKFI-R emulsion

$$a = -0.077 \pm 0.012.$$

The average obtained can be compared with the asymmetry coefficient for Ilford G-5 emulsion in Table II, where all known values of a are given.

TABLE II. Asymmetry coefficient a in photoemulsion

Authors	Meson Source	Emulsions	a
Castagnoli[6]	Cosmic Rays*	Ilford G-5	0.20 ± 0.04
Fowler[7]	" "	"	0.03 ± 0.040
Bøggild[8]	" "	"	0.21 ± 0.04
Bhowmik[9]	" "	"	0.081 ± 0.044
Babayan[10]	" "	"	0.135 ± 0.040
Biswas[11]	Accelerator	"	0.095 ± 0.045
Davis[12]	"	"	0.190 ± 0.060
Friedman[13]	"	"	0.174 ± 0.045
Chadwick[14]	"	"	0.149 ± 0.033
Gurevich[4]	"	NIKFI-R	0.092 ± 0.018
Vaĭsenberg, this work	"	"	0.066 ± 0.018
Ivanov[5]		"	0.065 ± 0.041

*The data of Castagnoli et al. refer in part to cosmic rays and in part to accelerators. The exact distribution of the data on the basis of the information given in their papers is impossible to carry out, but this has little effect on the result of the following averaging (Table III).

It is very difficult to get a unique average from these values. Such a result, apparent "by inspection," is strengthened by the analyses of the table by the usual χ^2 criterion by the binomial expansion for 11 degrees of freedom: for an arbitrary value of a we get $\chi^2 = 25 - 30$, if we consider simultaneously the values of a in the Ilford G-5 and NIKFI-R emulsions. The comparison becomes entirely admissible ($\chi^2 \sim 12$) if it is restricted to the data observed separately for the Ilford G-5 emulsion. The average weighted values for the

asymmetry coefficient for both emulsions are given in Table III.

Looked at in this way, it seems quite credible that μ^+ mesons experience a greater depolarization in NIKFI-R emulsion than in Ilford G-5: the ratio of the depolarization capacities of these two emulsions is close to $(0.139 \pm 0.014)/(0.077 \pm 0.012) = 1.81 \pm 0.33$. This result is difficult to understand, since the density and chemical composition of the two emulsions are almost identical.[15,16]

TABLE III. Average values of the asymmetry coefficient for NIKFI-R and Ilford G-5 emulsions

NIKFI-R	Ilford G-5		
	All data	Cosmic rays	Accelerators
-0.077 ± 0.012	-0.139 ± 0.014	-0.133 ± 0.018	0.148 ± 0.021

3. THE ASYMMETRY COEFFICIENT IN THE DILUTED NIKFI-R EMULSION

The first indication that increasing of the gelatin content of the emulsion leads to an increase in the asymmetry coefficient was given by Chadwick et al., who got for the doubly diluted Ilford G-5 $a_{\times 2} = -0.190 \pm 0.033$, which should be compared with the average value $a = -0.139 \pm 0.014$ (Table III) for ordinary Ilford G-5 emulsion.

In the third line of Table I we give the distribution we got for 2245 π^+-μ-e decays in NIKFI-R emulsion diluted by a double quantity of gelatin (the criterion of the previous choice). With the aid of Eq. (2) or (3) we get from this data $a\,(\text{NIKFI-R})_{\times 2} = -0.136 \pm 0.037$.

An analogous result is obtained in reference 5, where for 2300 π-μ-e decays an asymmetry coefficient for NIKFI-R emulsion with doubled gelatin content was determined to be $a\,(\text{NIKFI-R})_{\times 2} = -0.118 \pm 0.041$. Combining both results, we get

$$a\,(\text{NIKFI-R})_{\times 2} = -0.127 \pm 0.028.$$

Thus the increase in the asymmetry coefficient in doubly-diluted NIKFI-R emulsion, in comparison with ordinary emulsion, is

$$(0.127 \pm 0.028)/(0.077 + 0.012) = 1.65 \pm 0.40.$$

The experiments with diluted emulsions prove conclusively that gelatin is the component of the emulsion in which the polarization of the μ-mesons is conserved to a significant degree. This agrees with the experiments of Lederman et al.[17] which disclosed no significant asymmetry (complete depolarization) in AgBr. Therefore, the difference in the a values for NIKFI-R and Ilford G-5 emulsions, which have almost the same constituents, must indicate different properties of the gelatins: the NIKFI-R gelatin evidently produces depolarization twice as large as the Ilford G-5 emulsion, although the reason for this is not clear.

4. THE ASYMMETRY COEFFICIENT IN A MAGNETIC FIELD

The methods of destroying depolarization acquire a great significance, in connection with the small magnitude of the asymmetry constant of emulsions, for the solution of a series of experimental problems in meson physics. One of these methods is, as has been shown above, the increase in the gelatin content. Another method of removing the depolarization is, as is well known, a strong static magnetic field. Gurevich et al.[4] get an asymmetry coefficient $a = -0.16 \pm 0.04$ for an NIKFI-R emulsion placed in a field of 1000 gauss. Orear[18] and Barkus[19] showed that a magnetic field of about ten kilogauss restored the asymmetry coefficient in an emulsion to the maximum value $a = -(0.24 - 0.26)$, which is characteristic for metals or graphite. We carried out measurements for fields of 2500 and 17,000 gauss. (The measurement technique and method of exposure will be described later.) We obtained the following values of the asymmetry coefficient:

$$a\,(2500) = -0.186 \pm 0.020, \quad a\,(17\,000) = -0.28 \pm 0.02.$$

From these measurements it follows that even in the NIKFI-R emulsion, whose gelatin apparently depolarizes strongly, the magnetic field fully restores the polarization, taking it to the value, close to -0.33, which is required by the theory of the universal Fermi interaction of Feynman and Gell-Mann, in which $|g_V| = |g_A|$. Gurevich and his coworkers came to an analogous result on the basis of their measurements.[21]

5. DISCUSSION OF THE RESULTS

The question of the asymmetry coefficient in emulsion is connected with the distributions of stoppings of μ^+ mesons in gelatin and silver bromide.

$$a_{em} = a_{gel}\, d/(1 + d).$$

We shall begin with the asymmetry coefficient for Ilford G-5 emulsion, $a = -0.139 \pm 0.014$. Assuming that the gelatin in this emulsion has the maximum asymmetry coefficient $a = -0.33$,

we get a lower bound for the magnitude of d. Thus we come to the result that the ratio of the number of stops in gelatin to those in AgBr must be $d \sim 3/4$ or more if the coefficient of asymmetry in gelatin is less than 0.33. This result appears rather unexpected if we consider that the size of d is determined by the ratio of the volumes of gelatin and AgBr, multiplied by the ratio of their stopping powers

$$d = (V_{gel}/V_{AgBr})\,(dE/dx)_{gel}/(dE/dx)_{AgBr}.$$

Actually, for the magnitude of d to be close to 3/4 (or more), it is essential to suppose that the μ meson in the gelatin, which is five times lighter than silver bromide, has the same (or greater) ionization loss per micron of path as it has in AgBr. It is known that at the end of a charged particle path, when charge exchanges and elastic scatterings with the atoms as a whole begin to appear, the stopping power of light substances grows. This question is complicated, and unfortunately there are not enough data existing[21] to judge whether or not similar effects can insure the necessary increase in ionization losses in gelatin. It is entirely possible that the dimensions of the silver bromide crystals influence the distribution of stoppings in gelatin and AgBr. However, the existing data do say that the average size of the grains and their distribution in Ilford G-5 and NIKFI-R emulsions are about the same, so that the different dispersivities of the emulsions can hardly explain the difference in the asymmetry coefficients of Ilford G-5 and NIKFI-R.

A separate measurement of the asymmetry coefficients for gelatin and AgBr could give not only the distribution of stoppings by components but would also permit the investigation of the question of the stopping powers of light and heavy materials at low energies.

The measurements with and without magnetic field on NIKFI-R emulsion showed that, in spite of the strong depolarization in the gelatin of this emulsion, the magnetic field almost completely restores the full polarization of the emulsion. Therefore we can suppose that the mechanism corresponding to depolarization is unique, the same in gelatin as in silver bromide. The strong dependence on the magnetic field and the growth saturation gotten for fields of about ten kilogauss make quite credible the hypothesis that the depolarization mechanism is the formation of muonium. As is well known, muonium is formed with equal probabilities in two quantum states: with antiparallel (singlet) and parallel spins (triplet). The first of these states does not conserve the μ spin direction because of the hyperfine structure interaction. Such a depolarization is removed by a strong magnetic field, which breaks the bond between the meson and electron spins and sets both these spins to precessing around the direction of the H field (Paschen-Back effect). The restoring of polarization in this effect should be proportional to $x^2/(1+x^2)$, where x is the ratio of the applied field H to the field H_0 which is characteristic of the hyperfine structure interaction and which for muonium is $H_0 = 1580$ gauss.

Muonium with spins parallel has a resultant magnetic moment about that of the electron and will be depolarized by the action of even weak internal magnetic fields in the substance. If the applied homogeneous field significantly surpasses in strength the random internal fields, it sends parallel spin muonium into precession about it so that the polarization in the field direction will be conserved. From this it follows that if it is necessary to have fields on the order of several thousand gauss ($H > H_0$) to restore the polarization of muonium with antiparallel spins, then fields on an order exceeding the internal fields are enough to conserve the polarization of triplet muonium. Therefore the curve of the asymmetry coefficient against the increase of the magnetic field may display two components with similar amplitudes: one, increasing with the field by the $x^2/(1+x^2)$ law, and the other whose growth is determined by a parameter characteristic of the strength of the internal fields. To examine such a picture it is important to make measurements with relatively weak fields, where the Paschen-Back effect plays no significant role, i.e., for fields < 500 gauss. This is one of the possible examples of how the study of the changes of the asymmetry coefficient with the field changes can give information on the internal magnetic fields of a substance.

The authors wish to thank A. I. Alikhanov and I. I. Gurevich for their interest in the work and consideration of the results, E. A. Pesotskaya and Z. V. Minervina for their help in working up the data, B. A. Nikol'skiĭ for help in exposing the emulsions in the magnetic field, and D. M. Samoĭlovich, in whose laboratory the emulsion plates were developed.

[1] Garwin, Lederman, and Weinrich, Phys. Rev. **105**, 1415 (1957).

[2] R. A. Swanson, preprint (1958).

[3] A. O. Vaĭsenberg and V. A. Smirnit-skiĭ, Nuclear Physics **5**, 33 (1958).

[4] Gurevich, Kutukova, Mishakova, Nikol'skiĭ, and Surkova, J. Exptl. Theoret. Phys. (U.S.S.R.)

34, 280 (1958), Soviet Phys. JETP **7**, 195 (1958).

[5] Yu. M. Ivanov and A. P. Fesenko, J. Exptl. Theoret. Phys. (U.S.S.R.) **35**, 1297 (1958), Soviet Phys. JETP **8**, 905 (1959).

[6] Castagnoli, Franzinetti, and Manfredini, Nuovo cimento **5**, 684 (1957). Castagnoli, Manfredini, and Merrison, Nuovo cimento **9**, 186 (1958).

[7] Fowler, Freier, Lattes, Ney, and St. Loran, Nuovo cimento **6**, 63 (1957).

[8] Bøggild, Hansen, and Scharff, Nuovo cimento **8**, 1695 (1958).

[9] Bhowmik, Evans, and Prowse, Nuovo cimento **5**, 1663 (1957).

[10] Babayan, Marutyan, Matevosyan, and Sarinyan, J. Exptl. Theoret. Phys. (U.S.S.R.) **35**, 561 (1958), Soviet Phys. JETP **8**, 387 (1959).

[11] Biswas, Ceccarelli, and Grussard, Nuovo cimento **5**, 756 (1957).

[12] Davis, Engler, Gorbel, Hoang, Kaplon, and Klarman, preprint (1958).

[13] J. Friedman and V. Telegdi, Phys. Rev. **106**, 1290 (1957).

[14] Chadwick, Durrani, Eisberg, Jones, Wignall, and Wilkinson, Phil. Mag. **2**, 684 (1957).

[15] НИКФИ, Научно-технический отчет, (Sci. Inst. for Motion Pict. and Photogr. Report) No. 86, M., 1957.

[16] Plinnerton and Waller. International Conference on Nuclear Photography, Strassburg, July 1-6, 1957.

[17] L. M. Lederman, Proceedings of the Rochester Conference, 1957.

[18] Orear, Harris, and Bierman, Phys. Rev. **107**, 322 (1957).

[19] Barkas, Gilles, Heckman, Inman, and Smith, Phys. Rev. **107**, 911 (1957).

[20] S. K. Allison and S. D. Warshaw, Revs. Modern Phys. **25**, 779 (1953).

[21] Ali-Zade, Gurevich, Dobretsov, Nikol'skiĭ, and Surkova, J. Exptl. Theoret. Phys. (U.S.S.R.) **36**, 1327 (1959), Soviet Phys. JETP **9**, 940 (1959).

Translated by W. Ramsay
347

A CASE OF A SHARP INCREASE IN COSMIC-RAY INTENSITY IN THE STRATOSPHERE

N. P. RYMKO, V. F. TULINOV, and A. N. CHARAKHCH'YAN

P. N. Lebedev Physics Institute, Academy of Sciences U.S.S.R.

Submitted to JETP editor January 16, 1959

J. Exptl. Theoret. Phys. (U.S.S.R.) **36**, 1687-1689 (June, 1959)

An increase in the intensity of cosmic radiation was observed in the stratosphere on July 8, 1958 at a latitude of 64° N. At an altitude of 30 km, the intensity was more than twice the normal value. On the other hand, no increase was observed at latitudes of 51° and 41°.

ON July 8, 1958, an anomalously large increase in the intensity of cosmic radiation was observed during measurements in the stratosphere at 64° geomagnetic latitude at the Loparskaya Station (the Northern Scientific Station of the Academy of Sciences U.S.S.R.). The measurements were carried out by means of a single Geiger counter, using the cosmic-ray radio-sonde RK-1 described in reference 1.

Results of measurements carried out on July 8, 1958 are shown in Fig. 1. The statistical accuracy of the data amounts to ~ 2% for pressures greater than 250 g/cm^2, and to 1 — 0.5% for higher altitudes. For a comparison, the average altitude dependence obtained in measurements conducted on July 1, 3, and 7, 1958, is given in the figure.

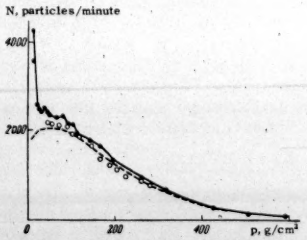

FIG. 1. Number of particles per minute as a function of the atmospheric pressure at the latitude of 64°N: • and ○ — results of measurements on July 8, 1958 during the ascent and descent of the apparatus respectively (time of start: 10 am Moscow time); dotted curve — average value of the number of particles obtained in measurements on July 1, 3 and 7, 1958.

As can be seen from Fig. 1, the greatest increase of the intensity of cosmic radiation was observed at the highest altitude. An especially fast increase in the number of particles occurred at pressures < 20 g/cm^2, which is clearly due to the increased intensity of primary particles of low energies. The range of these particles, judging from the absorption curve is smaller than 15 — 20 g/cm^2.

On July 8, 5 hr 35 min after the first series of measurements, a second series of measurements was carried out in the stratosphere, during which the apparatus attained higher altitudes. However, no increase of intensity was observed in this case. On the contrary, the measured number of particles was lower than the normal by about 10%. Data corresponding to the time when the flare ended can clearly be obtained from the results of the first flight. From the data of Fig. 1 (light points) it can be seen that, during the descent of the apparatus, the measured intensity almost approached the normal at a pressure of ~ 100 g/cm^2, which corresponds to about 12:30 p.m.

Analogous measurements of intensity of cosmic radiation in the stratosphere on July 8 were carried out near Moscow (Dolgoprudnaya Scientific Station of the Physical Institute of the Academy of Sciences U.S.S.R.) and in Simeiz (Crimean Scientific Station of the Physical Institute of the Academy of Sciences). The RK-1 radiosonde sent to the stratosphere at Dolgoprudnaya did not attain large altitudes. However, data up to the altitude of 19 — 20 km at which the measurements were carried out showed that, at the time of the measurements at the Loparskaya Station, the intensity of cosmic rays was 8 or 10% less than normal. The results of measurements made in Simeiz on July 8 coincide with the data obtained on July 4, 3, and 7 at the same place with an accuracy of ±1.5% in the maximum of intensity curve. In the Report on Cosmic Data of the Scientific Institute for the Research of Magnetism, Ionosphere and Propagation of Radio Waves,[2] data on the observation of a very large magnetic storm and ionospheric disturbances are reported for July 8, 1958. Results of measurements of the intensity

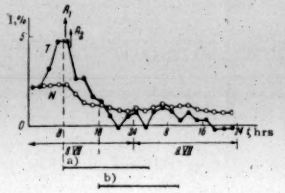

FIG. 2. Intensity of cosmic rays at the surface of the earth (Moscow) on July 8, 1958. ● – for μ meson and ○ – for neutron components (World Time). a) Very large magnetic storm; b) Large ionospheric disturbance.

of cosmic rays on the surface of the earth on July 8 and 9, according to the report are shown in Fig. 2. The y-axis represents the intensity expressed as the percentage of a constant value. The x-axis represents the time of measurement (World Time). Curve T refers to measurements using a cubic telescope, and curve N to measurements of a neutron monitor. Data on the measurement of the neutron monitor (N) for the first hour of measurements on July 8 are normalized to the corresponding data of the cubic telescope (T). The duration of magnetic storms and ionospheric disturbances are also indicated in the figure. A_1 in the figure denotes the time during which the sharpest increase in the number of particles in the atmosphere was recorded at the altitude of ~ 30 km, and A_2 indicates the time when, according to the data taken in the stratosphere, the intensity of the cosmic radiation returned to approximately the normal value.

Attention is drawn to the fact that during a period of about 3 to 9 hours the curves obtained with the telescope indicate an increase in the intensity of cosmic rays on the surface of the earth, while the neutron monitor shows practically a constant value of intensity.

The intensities of cosmic rays at the surface of earth recorded by the cubic telescope and by the neutron monitor correspond to different parts of the energy spectrum of primary particles. The increase in intensity in the measurements of the cubic telescope (μ mesons) corresponds to the increase in the number of cosmic particles with energies mainly $> 10^{10}$ ev. The neutron monitor records the nucleonic component due also to primary particles of lower energies. One should expect, therefore, a stronger deviation of the measurements of the neutron monitor in the same direction as the cubic telescope. Consequently, to make the readings of the various instruments consistent for the period of measurements from 3 to 9 hours, one should evidently draw the following conclusion: together with the increase of the intensity of primary particles in the range of sufficiently high energies ($> 10^{10}$ev), a decrease occurred in the intensity of primary particles in the range of low energies. The latter is in agreement with the data of stratospherical measurements at a latitude of 51° given above.

Hence, from the preliminary analysis of the experimental data in the stratosphere at geomagnetic latitudes of 64, 51, and 41° and also of data obtained at the surface of earth, one can draw the following conclusion on the intensity variation of the primary cosmic radiation on July 8, 1958:

A large increase in the intensity of cosmic radiation in the stratosphere occurred due to primary cosmic particles with energy smaller than 1.5×10^9 ev (for protons). The increase in the number of low-energy primary particles was accompanied by a decrease in the intensity of primary particles of moderate energy ($10^{10} > E > 1.5 \times 10^9$ ev) and an increase in intensity of primary particles of higher energies ($> 10^{10}$ ev).

The authors would like to express their deep gratitude to S. N. Vernov for his interest in the work and discussion of the results, and to A. G. Bednyakov for help in carrying out the measurements.

[1] Vernov, Tulinov, and Charakhch'yan, Dokl. Akad. Nauk SSSR **122**, 788 (1958), Soviet Phys. "Doklady" **3**, 980 (1958).

[2] Космические данные (Cosmic Data) (monthly report), 7 (29), Moscow, Gidrometeizdat, 1958.

Translated by H. Kasha
348

NEUTRON DIFFRACTION INVESTIGATION OF THE ANTIFERROMAGNETISM OF THE CARBONATES OF MANGANESE AND IRON

R. A. ALIKHANOV

Institute of Physics Problems, Academy of Sciences, U.S.S.R.

Submitted to JETP editor February 11, 1959

J. Exptl. Theoret. Phys. (U.S.S.R.) **36**, 1690-1696 (June, 1959)

A procedure is developed for low-temperature powder neutron diffraction. The antiferromagnetic structure of $MnCO_3$ and $FeCO_3$ is investigated. It is shown that in the antiferromagnetic state the spins in $MnCO_3$ lie in the basis plane and in the symmetry plane. In $FeCO_3$ the spins are directed along the rhombohedral axis. According to Dzyaloshinskiĭ, this means that $MnCO_3$ is weakly ferromagnetic and $FeCO_3$ is not.

INTEREST in isomorphous carbonates has been raised in connection with the investigations of the magnetic susceptibility of polycrystalline $MnCO_3$ and $CoCO_3$, carried out by Borovik-Romanov and Orlova,[1] and the theory of the weak antiferromagnetic ferromagnetism observed in these substances, developed by Dzyaloshinskiĭ.[2]

Dzyaloshinskiĭ has analyzed the magnetic symmetry of the crystals and established a connection between the occurrence of weak ferromagnetism and the symmetry of the crystal. For the carbonates of manganese, iron, and cobalt, which crystallize in a rhombohedral system, three types of magnetic symmetry are possible: 1) spins directed along the rhombohedral axis, 2) spins lying in the basis plane and directed along the two-fold axis, 3) spins lying in the basis plane and in the symmetry plane.

There is no weak ferromagnetism in the first case, but it should be observed in the two remaining cases.

Neutron-diffraction procedures, unlike other methods of investigation of magnetism, make it possible to determine directly which of the magnetic structures occurs in a given crystal.

EXPERIMENT

Crystalline carbonates of manganese and iron are difficult to obtain; therefore these substances were investigated by the powder method in a monochromatic neutron beam.

To obtain a monochromatic beam, a white neutron beam from the reactor* was aimed at a lead single crystal (see Appendix). The monoenergetic neutrons with $\lambda = 1.37$ A, reflected at a given angle, were scattered by a polycrystalline specimen, placed in a low-temperature cryostat. The latter was the metallic hydrogen-filled Dewar of Kapitza,[4] in which thin-wall cylindrical aluminum shells, surrounding the specimen, were hermetically connected to the lower portions of the vacuum jacket and of the nitrogen shield. The specimen was placed in an inner aluminum cup, the upper end of which was soldered directly to the vessel with the cooling agent, and the bottom of which was fastened to a carbon resistor* for measuring the temperature.

The instrument, first evacuated to 2×10^{-5} mm mercury, maintained the specimen at helium temperature for two days. The total amount of helium necessary for this purpose, including the cooling of the instrument, amounted to 7.5 liters.

The neutron-scattering pattern was registered with a spectrometer constructed by Abov[5] and adapted for operation with a monochromatic beam.

RESULTS AND THEIR DISCUSSION

$MnCO_3$. Neutron diffraction patterns of $MnCO_3$, obtained with $MnCO_3$ powder at room and hydrogen temperatures, are shown in Fig. 1. As can be seen from this diagram, the diffraction pattern changes as the temperature is decreased. At hydrogen temperature, in addition to a reduction in the diffuse thermal scattering, new reflections are produced at small Bragg angles. Figure 1 shows the reflection indices calculated from the relation for a quadratic form of rhombohedral subsyngony. The lat-

*The work was carried out in the heavy-water reactor of the Institute of Theoretical and Experimental Physics, Academy of Sciences, U.S.S.R.[3]

*We express our gratitude to Yu. V. Sharvin for supplying us with an experimental model of the thermometer.

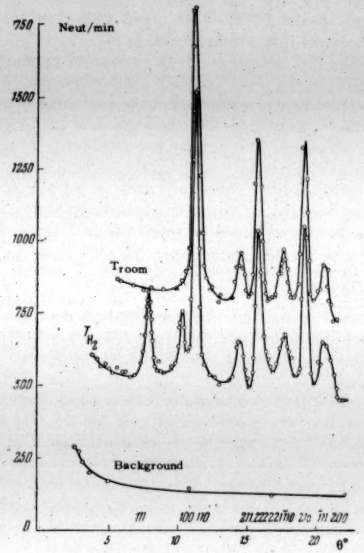

FIG. 1. Neutron diffraction patterns of $MnCO_3$.

tice constants used were[6] a = 5.84 A and α = 47°15′. To verify the overall pattern of nuclear reflections, and for indexing purposes, we calculated the relative intensities of the nuclear peaks.

The coherent-scattering intensity P is given by[7]

$$\frac{P}{I_0} = \frac{BjF^2\, e^{-2W} A_{hkl}}{\sin\theta \sin 2\theta},$$

where I_0 is the number of incident-beam neutrons per minute per square centimeter, B a constant for the given experiment, A_{hkl} the absorption factor, e^{-2W} the thermal coefficient, j the number of equivalent planes, and F the structure factor. The last two quantities vary with scattering angle. The absorption factor A_{hkl} depends in a complicated manner on the coefficient of linear absorption and on the radius of the specimen, which are constant for any given experiment. The thermal coefficient is connected with the characteristic temperature of the substance. The dependence of A_{hkl} and e^{-2W} on θ is very weak and remains practically unchanged for the angle interval under consideration.[7]

Thus, to calculate the relative intensity of nuclear reflections it is necessary to calculate the structure factor. In the general form, the nuclear structure factor is written

$$F_{nuc} = \Sigma b \exp\{2\pi i (hx/a_0 + ky/b_0 + lz/c_0)\},$$

where b is the amplitude of nuclear scattering. According to the data gathered in reference 7,

$$b_{Mn} = -0{,}37 \cdot 10^{-12}\ \text{cm}, \qquad b_O = 0{,}58 \cdot 10^{-12}\ \text{cm},$$
$$b_C = 0{,}66 \cdot 10^{-12}\ \text{cm}$$

respectively for manganese, oxygen, and carbon; x, y, and z are the nuclear coordinates given in reference 6, while a_0, b_0, and c_0 are the dimensions of the elementary crystallographic cell, in this case equal to each other.

After inserting the coordinates of the atoms and after making several transformations, the square of the structural factor for even and odd sums of the Miller indices can be written in the following manner

1) $h + k + l = 2n + 1$ $(n = 0, 1, 2, \ldots)$:

$$F^2_{hkl} = 4b_O^2 [\sin\{2\pi \cdot 0.27\,(h-k)\} + \sin\{2\pi \cdot 0.27\,(l-h)\} + \sin\{2\pi \cdot 0.27\,(k-l)\}]^2. \quad (1)$$

2) $h + k + l = 2n$:

a) $(h + k + l)/2 = 2n$:

$$F^2_{hkl} = 4\{b_C + b_{Mn} + b_O[\cos\{2\pi \cdot 0.27\,(h-k)\} + \cos\{2\pi \cdot 0.27\,(l-h)\} + \cos\{2\pi \cdot 0.27\,(k-l)\}]\}^2.$$

b) $(h + k + l)/2 = 2n + 1$, (2)

$$F^2_{hkl} = 4\{b_C - b_{Mn} + b_O[\cos\{2\pi \cdot 0.27\,(h-k)\} + \cos\{2\pi \cdot 0.27\,(l-h)\} + \cos\{2\pi \cdot 0.27\,(k-l)\}]\}^2. \quad (3)$$

The calculated intensities are listed in Table I, with accuracy to within a constant factor as compared with the observed intensity at hydrogen temperature. The constant factor is obtained by comparison with the two most intense reflections (110), (222).

TABLE I

Index	θ calculated	θ observed	j	Relative intensity calculated	Relative intensity observed
111	7°45′	7°54′	1	0	350
100	9°59′	10°7′	2	0	290
110	11°13′	11°13′	6	1040	1050
211	14°25′	14°25′	6	165	200
222	15°38′	15°40′	2	690	670
221	16°27′	—	6	0	background
110	17°23′	17°30′	3	36	220
210	19°9′	18°59′	12	625	690
111	20°21′	—	6	0	background
200	20°53′	20°27′	6	65	200

An important result is the forbiddenness of nuclear reflections (111) and (100), which follow from formula (1). As can be seen from Fig. 1, these reflections are actually missing at room temperature. However, they do arise as the temperature is reduced to that of hydrogen. It is natural to assume that they are due to magnetic ordering. For the same reason, an increase is seen in the intensity of nuclear reflections ($\bar{1}10$), (210), (200), which are neighbors to the magnetic reflections (221) and ($\bar{1}11$). Certain discrepancies between the compared values for the reflection (211) may be due to insufficient purity of the specimen.

Analysis of magnetic reflections. As shown by Halpern and Johnson,[8] the square of the summary structure factor in both nuclear and magnetic coherent reflection, for unpolarized neutrons, is

$$F^2 = F_{nuc}^2 + q^2 F_m^2 ,$$

where q is the sine of the angle between the magnetization and scattering vectors.

For rhombohedral $MnCO_3$ and $FeCO_3$, in the case of purely antiferromagnetic spin distribution in the elementary cell, the magnetic portion of the square of the structural factor can be represented as

$$q^2 F_m^2 = p^2 \sin^2\beta \, | \, 1 - e^{\pi i (h+k+l)} |^2 , \qquad (4)$$

where $p = (e^2\gamma/mc^2)$ Sf is the magnetic scattering amplitude. The ion form factor f depends on the scattering angle.

When $h + k + l = 2n$, $n = 0, 1, 2, \ldots$, we have

$$q^2 F_m^2 = 0. \qquad (5)$$

It follows from this that reflections with an even number of indices have no magnetic component. For $h + k + l = 2n + 1$

$$q^2 F_m^2 = 4 (e^2\gamma/mc^2)^2 S^2 f^2 \sin^2\beta. \qquad (6)$$

Thus, the scattering picture in the presence of antiferromagnetic ordering should contain, for a given lattice, only magnetic reflections with an odd index sum. However, even in this case $q^2F_m^2$ may vanish if the scattering vector is aligned with the magnetization vector. Such a case is possible in scattering from the (111) plane and antiferromagnetic arrangement of the spins along the rhombohedral axis.

The new reflections on the neutron-diffraction pattern for $MnCO_3$ which occur at hydrogen temperature, are induced precisely by the indices with odd sum (111) and (100). Those following — (221), (210) and ($\bar{1}11$) — are not resolved because of the low intensity. Their presence makes itself felt in a certain change in the bases of the nuclear peaks (222), ($\bar{1}10$), and (200) and in an increase in the intensity of (210).

Since the reflection (111) is present in $MnCO_3$, the first of the three possible antiferromagnetic spin orientation, mentioned at the beginning of this article, namely along the rhombohedral axis, drops out. To choose between the two remaining orientations, it is necessary to compare, in both cases, the calculated and observed ratios of reflection intensities $P_{(100)}/P_{(111)}$. In accordance with the formula for the intensity, this ratio is

$$\frac{P_{(100)}}{P_{(111)}} = \frac{j_{(100)}}{j_{(111)}} \frac{\sin\theta_{(111)} \sin 2\theta_{(111)}}{\sin\theta_{(100)} \sin 2\theta_{(100)}} \frac{f_{(100)}^2}{f_{(111)}^2} \frac{\cos^2\rho_{(100)}}{\cos^2\rho_{(111)}} , \qquad (7)$$

where ρ is the angle between the spin directions [uvw] and the plane $(hkl)(\rho = \pi/2 - \beta)$.

The experimental ratio of the intensities of magnetic reflections is $P_{(100)}/P_{(111)} = 0.82$ (in the calculations we used the data of Shull, Strauser, and Wollan[9] for the form factor of Mn^{++}). On the other hand, the expected values for the spins along the two-fold axis or in the symmetry plane are 1.29 and 0.81 respectively. Thus, the antiferromagnetic spins in $MnCO_3$ lie in the symmetry plane normal to the three-fold axis.

$FeCO_3$. The structure of $FeCO_3$ was studied with a specimen of siderite from the Bokal (U.S.S.R.) deposit. Figure 2 shows the neutron diffraction pattern, taken at hydrogen temperature. The amplitude of nuclear scattering of Fe^{++} is more than double that of Mn^{++}, so that it became possible to record the neutron-scattering pattern with an automatic recording instrument. Table II lists the calculated and measured relative intensities for the first group of peaks.

As in the case of $MnCO_3$, the appearance of the (100) reflection at hydrogen temperature is evidence of the establishment of an antiferromagnetic structure. The absence of the (111) reflection, in accordance with the foregoing, means that the spins in $FeCO_3$ are directed along the rhombohedral axis. This result confirms the conclusions of Bizette[11] concerning the antiferromagnetic structure of iron carbonate. It is interesting to follow also the temperature dependence of the magnetic reflection (100). Figure 3 shows this dependence, plotted as the instrument was heated after evaporation of the hydrogen. As follows from the graph, this specimen of $FeCO_3$ goes into the antiferromagnetic state in the region of 35° K.

I express my deep gratitude to Academician P. L. Kapitza for continuous interest in the work, and also to A. S. Borovik-Romanov for useful advice. I also thank I. E. Dzyaloshinskiĭ for valuable discussion and Yu. G. Abov, for much useful coun-

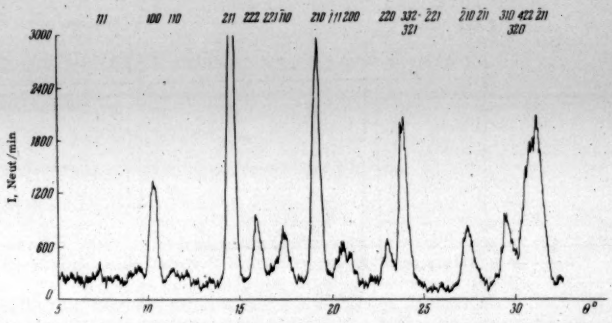

FIG. 2. Neutron diffraction pattern of $FeCO_3$ at liquid-hydrogen temperature.

TABLE II

Index	Relative intensity		Index	Relative intensity	
	calculated	observed		calculated	observed
111	0	background	222	110	117
100	0	150	$\bar{1}10$	117	90
110	5.7	background	210	375	450
211	810	800	$\bar{1}11$	0	80
			200	66	70

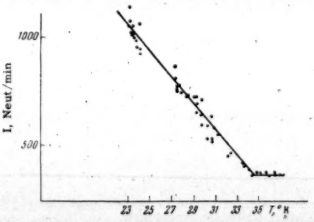

FIG. 3. Temperature dependence of magnetic reflection for $FeCO_3$ (from the Bakal deposit).

sel on the neutronoscopic portion of the investigation.

APPENDIX

1. The crystal area necessary to obtain a monochromatic beam amounts to 100 cm^2. In connection with this, we constructed a special setup to grow, by the Kapitza method,[10] crystals of large area with specified orientation. When successfully grown, the crystal is obtained directly in final form and serves as a monochromator.* The apparatus for growing is arranged as follows (see Fig. 4). A form, 2, of required size was flanged on an aluminum support plate, 1. The form is filled with lead. A glass dome attached to cover 4 permits evacuation of the volume and protects the lead against oxidation during growing, and also affords a certain reduction in heat loss.

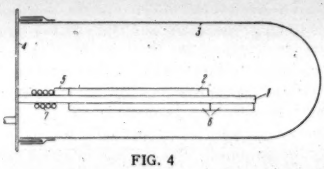

FIG. 4

Located in the narrow channel 5 of the forward cold portion of the mold is a primer, slightly buoyed up by the slowly advancing liquid phase of the lead. The boundary of two phases — the solid and the liquid — moves towards the cold portion which is heated by the small furnaces 6. At the instant when the primer starts floating, the temperature gradient increases rapidly as a result of the passage of compressed air through the cooling coil 7. Dependable single-crystal growth was attained after selecting: a) the shape of the cold portion of the mold, b) the growth rate, and c) the magnitude of the sliding temperature gradient.

The cold portion in final form resembles most closely the projection of a bird's head on a horizontal plane. The growing time did not exceed ten minutes, and the temperature gradient was 200° over the entire length of the crystal (16 cm).

For most effective reflection of the neutrons it is necessary to use the crystal plane with the maximum of atoms. This was the (111) plane, which, when placed in the plane of the plate or close to it,

*The author expresses his gratitude to N. N. Mikhaĭlov for his continuous assistance in growing crystals.

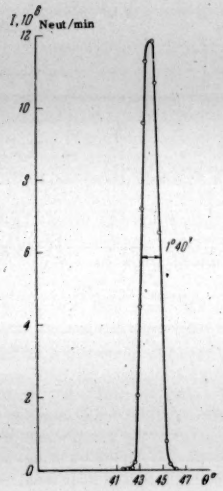

FIG. 5

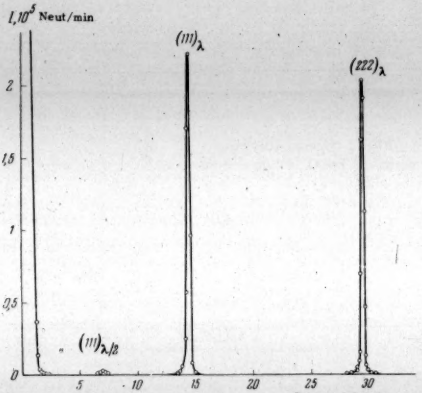

FIG. 6

could be observed during the time of growth by its characteristic light reflection, close to specular. Thus it became possible to control the growing process during the very growth of the crystal.

2. X-ray analysis of the crystals was made by plotting "epigrams." The reflection spots on the epigrams had a unique structure, indicating a considerable mosaic structure in the resultant crystals.

3. Using one such single-crystal plate we obtained a monochromatic beam of neutrons, the reflection curve of which is shown in Fig. 5. The intensity of the beam can be increased above 12×10^6 per minute by greatly narrowing the beam.

An analysis of the monochromatic beam for higher-order reflections is shown in Fig. 6. Worthy of attention is the considerable intensity of reflection (222). The admixture of second-order reflections does not exceed 0.1%.

The properties of grown single crystals will be considered in greater detail in the future.

[1] A. S. Borovik-Romanov and M. P. Orlova, J. Exptl. Theoret. Phys. (U.S.S.R.) **31**, 579 (1957), Soviet Phys. JETP **4**, 531 (1957).

[2] I. E. Dzyaloshinskiĭ, J. Exptl. Theoret. Phys. (U.S.S.R.) **32**, 1547 (1957), Soviet Phys. JETP **5**, 1259 (1957).

[3] Alikhanov, Vladimirskiĭ, Nikitin, et al., Сб. Реакторостроение и теория реакторов (Coll. Reactor Construction and Reactor Theory), U.S.S.R. Acad. Sci. Press, 1955, p. 105.

[4] P. Kapitza and P. Cockroft, Nature **129**, 224 (1932).

[5] Yu. G. Abov, Сб. Сессия АН СССР по мирному использованию атомной энергии (Coll. Session of U.S.S.R. Acad. Sci. on Peaceful Use of Atomic Energy), M., 1955, p. 294.

[6] R. W. G. Wyckoff. The Structure of Crystals, N. Y. Chem. Catalog Co. 1931.

[7] G. E. Bacon, Neutron Diffraction, Oxford Univ. Press, 1955; Russ. Transl. IIL, 1957.

[8] O. Halpern and M. H. Johnson, Phys. Rev. **55**, 898 (1939).

[9] Shull, Strauser, and Wollan, Phys. Rev. **83**, 333 (1951).

[10] P. Kapitza, Proc. Roy. Soc. **119**, 358 (1928).

[11] H. Bizette, J. phys. et radium **12**, 161 (1951).

Translated by J. G. Adashko
349

PRODUCTION OF PIONS BY HIGH-ENERGY COSMIC-RAY ALPHA PARTICLES

A. A. LOKTIONOV and Zh. S. TAKIBAEV

Nuclear Physics Institute, Academy of Sciences, Kazakh S.S.R.

Submitted to JETP editor February 13, 1958; resubmitted January 20, 1959

J. Exptl. Theoret. Phys. (U.S.S.R.) 36, 1697-1702 (June, 1959)

Experimental results are compared with the hydrodynamical theory of multiple meson production. It is shown that, for showers with energy $\gtrsim 10$ Bev per nucleon, the results of an analysis of the parameters of observed stars do not contradict the concept of an interaction between the incident α particle and nucleons filling a tunnel in the target nucleus.

IN the collisions of high-energy nucleons ($\gtrsim 10^{12}$ ev) with atomic nuclei, it is assumed that the nucleons interact with the contents of a tunnel punched by the nucleon in the target nucleus and filled with solid matter; the diameter of the tunnel equals the diameter of the nucleon,* and its length depends on the atomic number of the target nucleus and on the impact parameter. On the basis of such a model of the interaction between the nucleon and the nucleus, one can explain some experimental results for high-energy showers (jets; $\theta_{1/2} \leq 10°$).[2-4]

In the present article, analogous calculations are used for describing the interaction of high-energy α-particles ($\gtrsim 10^{10}$ ev/nucleon) with atomic nuclei. In this case, the idea of a nuclear tunnel as consisting of solid matter will be more correct, since the cross section of the tunnel punched out in the nucleus by the α particle is proportional to $A_\alpha^{2/3}$, and the number of nucleons introduced into the tunnel equals A_α.

In view of that fact, the nucleon density in the interaction volume increases, and the assumption that the time between consecutive collisions of nucleons is smaller than the duration of the interaction is, in that case, more correct.

Showers produced by α particles in a stack of stripped Ilford G-5 emulsions exposed in 1955 in Italy at the altitude of 30 km were selected for the study. In addition, a part of the showers were taken from the published articles by various authors.[5-12] The total number of showers studied equals 67.

1. SHOWER STARS

1. According to the hydrodynamical theory of Landau-Belen'kiĭ,[13,14] the number of particles produced in an interaction of an α-particle with a nucleus is

$$N = N_\alpha (n+1)/2 \quad \text{for } n \leqslant 3.7,$$
$$N = 0.92 N_\alpha \left(n - \tfrac{1}{4}\right)^{3/4} \quad \text{for } n > 3.7,$$
$$N_\alpha = k A_\alpha^{3/4} (E_\alpha / 2M_0c^2)^{1/4}, \tag{1}$$

where N is the sum of produced particles and nucleons involved in the collision, N_α is the same for a collision of two α particles, and $n = M_t/M_\alpha$ is the ratio of the mass of the tunnel punched out in the nucleus by the α particle to the mass of the latter. The relation between the total number of particles N and the number of charged particles n_s is given by the relation

$$N = 1.5 n_s + n + 1. \tag{2}$$

The energy of the primary α particle is equal to

$$E_\alpha = 2nM_\alpha c^2 / \tan^2 \theta_{1/2}. \tag{3}$$

From Eq. (1), using Eqs. (2) and (3), we obtain

$$\tan \theta_{1/2} = A_\alpha^2 (n+1) n^{1/2} (1.5 n_s + n + 1)^{-2} \quad \text{for } n \leqslant 3.7,$$
$$\tan \theta_{1/2} = 3.39 A_\alpha^2 (n - 0.25)^{3/2} n^{1/2} (1.5 n_s + n + 1)^{-2} \quad \text{for } n > 3.7. \tag{4}$$

In the case where the impact parameter is bigger than the difference between the radii of the target nucleus and the α particle, not the entire mass of the α particle takes part in the interaction but only part of it, $M_\alpha^*(b)$ (where b is the impact parameter). The first equation of (4) can then be written in the form

$$\tan \theta_{1/2} = A_\alpha^{*2} (n^* + 1) n^{*1/2} (1.5 n_s + M_t^*/M_\alpha + A^*/4)^{-2},$$
$$n^* = M_t^*/M_\alpha^* \leqslant 3.7. \tag{4'}$$

A_α^*, M_t^*, M_α^* are calculated as the corresponding fractions of the spherical volumes for their partial overlapping; the density of the nuclear matter is assumed to be constant. Formulae (4) and (4') give the relation between the angle $\theta_{1/2}$, from

*One should distinguish between a tunnel in solid nuclear matter from one in the structure of a nucleus;[1] the diameter of the latter is slightly greater than the diameter of the nucleon.

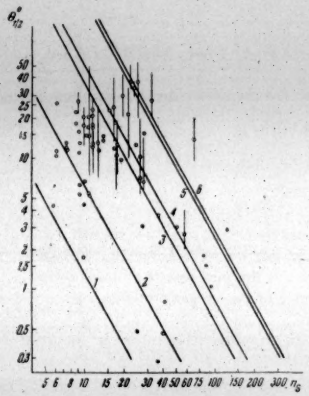

FIG. 1

which the energy of the α particle is determined, and n_s.

The dependence of $\theta_{1/2}$ on n_s for different lengths of tunnels is given in Fig. 1. The smallest possible multiplicity corresponds to the case of a collision between an α particle and a peripherical nucleon of the nucleus, or to a collision of an α particle with a hydrogen nucleus; in both cases the tunnel is punched out by the nucleon in the incident α particle. Averaging over the diameter of the α particle, we obtain $M_t^0/M_0 = 1.6$, where M_t^0 is the mass of the tunnel punched out by the nucleon in the helium nucleus. The dependence of $\theta_{1/2}$ on n_s for that case is given by curve 1. Curve 2 corresponds to the average value of the tunnel length produced by the α particle in a mean light nucleus of emulsion ($\overline{A} = 14$); $n^* = 1.35$. Curve 3 gives the dependence of $\theta_{1/2}$ on n_s for the maximum tunnel length produced by an α particle in an average light nucleus of the emulsion; $n = 2$. Curve 4 gives this dependence for $n^* = 2.77$, which corresponds to the value of the average tunnel length produced by α particles in medium-heavy nuclei of the emulsion ($\overline{A} = 94$). Curves 5 and 6 correspond to a central collision of an α particle with a silver nucleus ($n = 4.41$) and a nucleus of iodine ($n = 4.57$; this corresponds to the maximum tunnel length in photographic emulsion). It should be noted that, for the above selection of tunnel lengths, the experimental points should be grouped in the region between curves 1 and 6. It can be seen from Fig. 1 that this is actually the case.

The errors shown take into account the possible forward-backward asymmetry in the distribution of particles in c.m.s.[15] The errors due to measurement inaccuracy are not given, since the fluctuations are much larger and include these.

2. In heavy nuclei of the emulsion, the maximum tunnel length punched out by the α particle in a nucleus equals 4.57; the maximum length of the tunnel in light elements equals 2.00. It is clear that, for peripheral collisions with a heavy nucleus, the length of the tunnel may be the same as in collisions involving light nuclei of the emulsion. We shall find the ratio N_1 of the number of cases of interaction of α particles with the nuclear matter in a tunnel, the length of which varies from 2.0 to 4.57, to the number of cases of interactions N_2 with tunnels smaller than the maximum tunnel length in light elements.

Assuming the cross section of interaction of α-particles with nuclei being equal to[16]

$$\sigma_i = \pi (R_i + R_\alpha - 2\Delta R), \qquad (5)$$

where R_i is the radius of the target nucleus and R_α the radius of the α particle ($R_i = 1.4 \times 10^{-13} A_i^{1/3}$, $\Delta R = 0.85 \times 10^{-13}$ cm), and taking into account the composition of the emulsion, we find that $N_1/N_2 = 0.6$. The experimental value of this ratio for various energies of the primary α particle, is given in Table I. The data of the table are in good agreement with the calculations.

TABLE I

E, Bev/nucleon	N_1/N_2
$E > 10$	$0.46^{+0.40}_{-0.17}$
$E > 50$	$0.54^{+0.88}_{-0.38}$
$E > 100$	$0.79^{+0.43}_{-0.54}$

It is interesting to compare the results obtained with an analogous calculation carried out for showers produced by nucleons.[15] For this case $(N_1/N_2)_{\text{nucleon}} = 1.45$ and the experimental ratio equals 5.39 ± 0.30 for energies larger than 50 Bev, and 2.92 ± 0.31 for energies > 100 Bev. The observed discrepancy cannot be explained by fluctuations of multiplicity and of the angle $\theta_{1/2}$. The experimental results for showers produced by α particles are therefore in much better agreement with the calculation than for showers produced by nucleons. It should be noted that the conclusion about a purely multiple character of meson production for a given shower cannot be made only on the basis of the fact that a point corresponding to the shower falls into the region of $\theta_{1/2}$ predicted by the hydrodynamical theory. Thus, for instance, the R-star of Kaplon et al.[5] falls on curve 4 (Fig. 1), although, according to the au-

thors, it is produced not in a purely multiple process.

The above analysis points rather towards the meson production being not purely multiple, though predominantly so. A certain contribution of a plural process cannot be excluded. In order to establish the purely multiple character of meson production, it is necessary to carry out additional detailed study of showers.

2. HEAVILY IONIZING STARS

1. Experimental distribution of showers with respect to the number of grey-black tracks N_h is given in Fig. 2 (histogram 1). The distribution has a maximum in the region $3 \leq N_h \leq 5$ and gives one or two cases per interval for $N_h > 6$. The maximum value of N_h observed experimentally equals 26.

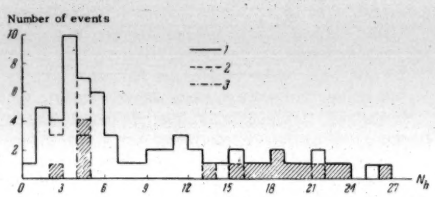

FIG. 2

For total disintegration of light nuclei, the greatest value of N_h equals 8. The ratio of the number of cases with $N_h > 8$ to those with $N_h \leq 8$ equals $n_1(N_h > 8)/n_2(N_h \leq 8) = 0.64$.

It should be noted that Rao et al.[17] found that the mean energy of α particles producing showers equals 10 Bev per nucleon. An analogous ratio found from their data equals 0.6.

Taking the cross section for the interaction of α particles and nuclei according to Eq. (5), we obtain the ratio of the number of interactions with heavy nuclei n_H to the number of interactions with light nuclei of the emulsion n_L equal to 1.87, which is as expected since the cases with $N_h \leq 8$ include the disintegration of both heavy and light nuclei. In the explanation of heavy ionizing stars produced by high-energy α particles, as well as in the explanation of relativistic showers, there is consequently no contradiction between experiment and the idea of the interaction of α particles with a part of the nucleus or with a tunnel punched by the particle in it. The shape of the tunnel is of no importance, the main feature being the fact that the residual nucleus carries away a small fraction of the energy of the primary particle.

2. We shall find the ratio of the number of events $N_h > 8$ to the number of events $N_h \leq 8$ for various values of the primary α particles. The results of such operations are given in Table II.

TABLE II

E, Bev/nucleon	$n_1(N_h>8)/n_2(N_h\leqslant 8)$	$n_1(N_h>8)/n_H$
$\bar{E}=10$	0.6	0.58
$E>10$	0.64 ± 0.01	0.60 ± 0.01
$E>50$	$0.50^{+0.04}_{-0.09}$	$0.51^{+0.03}_{-0.07}$
$E>100$	$0.43^{+0.14}_{-0.05}$	$0.46^{+0.10}_{-0.04}$

It can be seen that, with increasing energy, the fraction of events with $N_h > 8$ decreases and the maximum value of the ratio $n_1(N_h > 8)/n_2(N_h \leq 8)$ is about 0.6. This means that the tunnel model is the more correct the larger the energy of the primary α particle. In the interaction of α particles with light nuclei of the emulsion, $N_h \leq 8$; for peripheral collisions of α particles with heavy nuclei where a tunnel of roughly the same length as in light elements is punched in the nucleus, we also find $N_h < 8$.[18] Consequently, the value $N_h > 8$ is left for the fraction of central and close to central collisions of the α particle with heavy nuclei where the tunnel has maximum length.[17] In other words, the ratio $n_1(N_h > 8)/n_2(N_h \leq 8)$ should not be of greater order of magnitude than 0.6, the value of N_1/N_2. The data of Table II fully confirm this conclusion.

With increasing energy of the α particle, the energy transfer to the residual nucleus (according to the tunnel-effect model) decreases. In consequence, the fraction of cases with $N_h > 8$ will decrease. This conclusion is also confirmed by the results of Table II (column 3), where the ratio of the number of cases with $N_h > 8$ to the number n_H of expected events of collision of α particles with heavy emulsion nuclei is calculated, assuming the validity of Eq. (5).

3. Aside from the general distribution of all showers with respect to N_h, the distribution of showers in which the tunnel length is smaller and larger than the maximum tunnel length in light nuclei is given in Fig. 2, histograms 2 and 3 respectively. It can be seen that histogram 3 begins with $N_h > 13$, and histogram 2 has a maximum for $N_h = 3$ and is practically cut off at $N_h = 12$.

We shall calculate the average value $\overline{N_h}$ as a function of the tunnel length and the energy of the primary α particle. The result is given in Table III. It can be seen that, according to all that was said above, the average value of $\overline{N_h}$ for

TABLE III. Dependence of the number of grey and black tracks on tunnel length and the energy of the primary α particle

E, Bev/nucleon	N_h ($n \leq 2$)	N_h ($n > 2$)
$E > 10$	6.1 ± 2.9	14.3 ± 4.3
$E > 50$	5.3 ± 2.4	12.7 ± 3.8
$E > 100$	2.6 ± 1.5	18.1 ± 1.1

showers with large tunnel length is larger by more than a factor of 2 than the value of $\overline{N}_h$ for showers with small tunnel length; with increasing energy of the primary α particle, this relation becomes more pronounced.

4. Calculating $\overline{N}_h$ in the same manner as was done for showers produced by nucleons,[1] we obtain, for the case of a central collision of the α particle with the average heavy nucleus of the emulsion, $\overline{N}_h = 4.5$, which is considerably smaller than the experimental value. Consequently, the assumption that, in the case of interaction of a high energy particle with heavy nuclei, N_h is determined only by the change of the surface energy of the nucleus and the friction in the tunnel is not correct. In that case, in fact, only about 20% of the nucleons contained in the tunnel are emitted. The redistribution of the residual nucleons in the new nucleus is accompanied by more far-reaching changes than those which are taken into account by the variation of the surface and friction in the tunnel.

CONCLUSIONS

An analysis of the number of particles in showers produced by helium nuclei with energies ≥ 10 Bev per nucleon is in agreement with the tunnel-effect model of the interaction between the incident α particle and continuous nuclear matter.

The energy threshold of the application of such a model of interaction between high-energy α particles and nuclei which in the limiting case is not bigger than 50 Bev/nucleon, is markedly lower than that in the interactions between a nucleon and the nucleus. This can be explained by the fact that, in the case where the primary particle is an atomic nucleus with atomic weight A, $A^{1/3}$ times more nucleons are introduced into the tunnel as compared with the events in which the primary particle is a nucleon. One should therefore expect a better agreement between the theory of multiple meson production and the experiment for showers produced by nuclei heavier than the helium nucleus.

[1] W. Heitler and C. H. Terreaux, Proc. Phys. Soc. **66**, 929 (1953).

[2] I. L. Rozental' and D. S. Chernavskiĭ, Usp. Fiz. Nauk **52**, 185 (1954).

[3] Takibaev, Usik, and Antonova, Dokl. Akad. Nauk SSSR **111**, 341 (1956), Soviet Phys. "Doklady" **1**, 666 (1956).

[4] Zh. S. Takibaev, Вестник АН КазССР, (Bull. Acad. Sci. Kazakh S.S.R.) **1**, 70 (1957).

[5] Bradt, Kaplon, and Peters, Helv. Phys. Acta **23**, 24 (1950).

[6] M. F. Kaplon and D. M. Ritson, Phys. Rev. **58**, 386 (1952).

[7] Daniel, Davies, Mulvey, and Perkins, Phil. Mag. **43**, 753 (1952).

[8] W. Winkler, Helv. Phys. Acta **39**, 267 (1956).

[9] F. Haenni, Helv. Phys. Acta **39**, 281 (1956).

[10] Brisbout, Dahanayake, Engler, Fujimoto, and Perkins, Phil. Mag. **1**, 605 (1956).

[11] G. E. Naygle and P. S. Freier, Phys. Rev. **104**, 804 (1956).

[12] Gramenitskiĭ, Zhdanov, Zamchalova, and Shcherbakova, J. Exptl. Theoret. Phys. (U.S.S.R.) **32**, 936 (1957), Soviet Phys. JETP **5**, 763 (1957).

[13] S. Z. Belen'kiĭ and G. A. Milekhin, J. Exptl. Theoret. Phys. (U.S.S.R.) **29**, 20 (1955), Soviet Phys. JETP **2**, 14 (1956).

[14] S. Z. Belen'kiĭ and L. D. Landau, Usp. Fiz. Nauk **56**, 309 (1955).

[15] San'ko, Takibaev, and Shakhova, J. Exptl. Theoret. Phys. (U.S.S.R.) **35**, 574 (1958), Soviet Phys. JETP **8**, 396 (1959).

[16] Progress in Cosmic Ray Physics, G. Wilson editor, Vol. I, p. 168-170, Amsterdam 1952.

[17] Appa Rao, Daniel, and Neelakantan, Proc. Ind. Acad. **43**, 181 (1956).

[18] J. H. Noon and M. F. Kaplon, Phys. Rev. **92**, 769 (1955).

Translated by H. Kasha
350

EFFECT OF RESONANCE EXCITATION TRANSFER IN THE THEORY OF A LARGE RADIUS EXCITON

É. I. RASHBA

Institute of Physics, Academy of Sciences, Ukrainian S.S.R.

Submitted to JETP editor September 8, 1958

J. Exptl. Theoret. Phys. (U.S.S.R.) **36**, 1703-1708 (June, 1959)

A theory for large-radius excitons is proposed, which takes into account Coulomb as well as resonance interaction. A transition to continuum, made under certain assumptions, leads to an integro-differential equation that contains a nonrelativistic contact term.

THERE are two limiting mechanisms for the travel of an exciton through a crystal. The first, indicated by Frenkel[1] is due to the presence of resonance interaction, and consists of the vanishing of the excitation at one point of the crystal and its occurrence at a different point, while the width of the exciton zone, and consequently also the group velocity of the exciton motion, remain finite as the overlap integrals tend to zero. The second mechanism enters into the Wannier-Mott theory of large-radius excitons[2,3] and consists of the displacement of an electron and a hole through the crystal; the electron and hole are considered as quasi-particles with a specified dispersion law, which describes the structure of a definite electron and a definite hole zone (or a definite group of electron and hole zones). Therefore the width of the exciton zone tends to zero, when the exchange integrals that determine the width of the electron and hole zones become annihilated. The first mechanism of exciton displacement will be called "resonant," and the second "exchange."

In the Wannier-Mott theory no account is taken of the ability of the electron-hole pairs of becoming annihilated or created. Consequently, the dependence of the structure of the exciton zone on the strength of the transition oscillator becomes lost, as do other features, and a contradiction with general theory[4] arises as regards the structure of the exciton band in the vicinity of the point $\mathbf{k} = 0$. In the present communication we introduce annihilation terms in the large-radius exciton theory and consider the results therefrom.

We consider a dielectric, and build up its electron wave function in accordance with the orthogonalized system of the Wannier quasi-atomic functions. Let $\varphi_{\mathbf{pg}}$ and $\varphi_{\mathbf{pe}}$ be the Wannier functions corresponding to g-th and e-th orbits of the p-th elementary cell. Henceforth the functions $\varphi_{\mathbf{pg}}$ will pertain to states which are completely filled in the unexcited crystal, and $\varphi_{\mathbf{ne}}$ will pertain to states which are completely free. The elementary cell may have a complicated structure; for example, it may consist of a series of atoms and ions. We do not take spin interactions into account and consider singlet states. Then the matrix element of the Hamiltonian H of the electron system will be

$$\langle \mathbf{pg},\ \mathbf{ne}\,|\,H\,|\,\mathbf{p}'g',\ \mathbf{n}'e'\rangle = \langle \mathbf{pg}\,|\,H_1\,|\,\mathbf{p}'g'\rangle\,\delta_{\mathbf{ne},\,\mathbf{n}'e'} + \delta_{\rho g,\,\rho' g'}\langle \mathbf{ne}\,|\,H^1\,|\,\mathbf{n}'e'\rangle + M^{\mathbf{ne},\,\mathbf{n}'e'}_{\rho g,\,\rho' g'} + K^{\mathbf{ne},\,\mathbf{n}'e'}_{\rho g,\,\rho' g'}, \quad (1)$$

$$M^{\mathbf{ne},\,\mathbf{n}'e'}_{\rho g,\,\rho' g'} = 2\,\langle \bar{\varphi}_{\rho' g'}(\mathbf{r}_1)\,\bar{\varphi}_{\mathbf{n}e}(\mathbf{r}_2)\,|\,e^2/r_{12}\,|\,\varphi_{\rho g}(\mathbf{r}_2)\,\varphi_{\mathbf{n}'e'}(\mathbf{r}_1)\rangle, \quad (1a)$$

$$K^{\mathbf{ne},\,\mathbf{n}'e'}_{\rho g,\,\rho' g'} = -\,\langle \bar{\varphi}_{\rho' g'}(\mathbf{r}_2)\,\bar{\varphi}_{\mathbf{n}e}(\mathbf{r}_1)\,|\,e^2/r_{12}\,|\,\varphi_{\rho g}(\mathbf{r}_2)\,\varphi_{\mathbf{n}'e'}(\mathbf{r}_1)\rangle. \quad (1b)$$

Here the symbol $|\mathbf{pg},\ \mathbf{ne}\rangle$ denotes the anti-symmetrized wave function of the crystal, in which the electron has been removed from the orbit $\mathbf{pg}$ and transferred to the orbit $\mathbf{ne}$, while the symbols $|\mathbf{ne}\rangle$ and $|\mathbf{pg}\rangle$ are the wave function of a crystal in which the orbit $\mathbf{ne}$ has an excess electron or the orbit $\mathbf{pg}$ lacks an electron; $\langle \mathbf{ne}\,|\,H^1\,|\,\mathbf{n}'e'\rangle$ and $\langle \mathbf{pg}\,|\,H_1\,|\,\mathbf{p}'g'\rangle$ are the matrix elements of the Hamiltonian of a crystal containing a zone electron or a zone hole, respectively. Integrals of the type like $K^{\cdots}_{\cdots}$ and $M^{\cdots}_{\cdots}$ will be called integrals of the Coulomb type or of the resonant type.

In the quantum state, determined by the set of normalized excitation amplitudes $\{a^{\mathbf{ne}}_{\mathbf{pg}}\}$, the crystal energy is

$$E\,[\{a^{\mathbf{ne}}_{\rho g}\}] = \sum_{\mathbf{ne}\,\rho g}\ \sum_{\mathbf{n}'e'\,\mathbf{p}'g'} \bar{a}^{\mathbf{ne}}_{\rho g}\,\langle \mathbf{pg},\ \mathbf{ne}\,|\,H\,|\,\mathbf{p}'g',\ \mathbf{n}'e'\rangle\,a^{\mathbf{n}'e'}_{\mathbf{p}'g'}. \quad (2)$$

The contribution to the first two terms of relation (1) to the sum in the right half of (2) can be readily obtained by going over from the quasi-atomic functions to the zone functions:

$$|\mathbf{k}e\rangle = N^{-1/2}\sum_{\mathbf{n}} e^{i\mathbf{k}\mathbf{n}}|\mathbf{n}e\rangle, \qquad |\mathbf{k}g\rangle = N^{-1/2}\sum_{\mathbf{p}} e^{i\mathbf{k}\mathbf{p}}|\mathbf{p}g\rangle \quad (3)$$

(N is the number of elementary cells in the principal region). Then, if we introduce the notation

$$H^{ee'}(\mathbf{k}) = \langle \mathbf{k}e|H^1|\mathbf{k}e'\rangle, \qquad H_{gg'}(\mathbf{k}) = \langle \mathbf{k}g|H_1|\mathbf{k}g'\rangle, \quad (4)$$

the sum of the two considered terms will be

$$\sum_{\mathbf{pg}}\sum_{\mathbf{n}e e'} \bar{a}^{\mathbf{n}e}_{e\mathbf{g}} H^{ee'}\left(\frac{1}{i}\nabla_{\mathbf{n}}\right) a^{\mathbf{n}e'}_{\mathbf{pg}} + \sum_{\mathbf{n}e}\sum_{\mathbf{p}gg'} \bar{a}^{\mathbf{n}e}_{\mathbf{p}g} H_{gg'}\left(\frac{1}{i}\nabla_{\mathbf{p}}\right) a^{\mathbf{n}e}_{\mathbf{p}g'}; \quad (5)$$

the differentiation of a function of discrete argument $a^{\mathbf{n}e}_{\mathbf{pg}}$ is understood in the sense of differentiation of its representation in the form of a Fourier polynomial.

As can be seen from (1), the quantities $M^{\mathbf{n}e,\mathbf{n}'e'}_{\mathbf{pg},\mathbf{p}'g'}$ are large only when $\mathbf{n}$ and $\mathbf{n}'$ are close to $\mathbf{p}$ and $\mathbf{p}'$, and diminish exponentially with increasing $|\mathbf{n}-\mathbf{p}|$ and $|\mathbf{n}'-\mathbf{p}'|$; when $\mathbf{n}=\mathbf{p}$ and $\mathbf{n}'=\mathbf{p}'$ they go into the ordinary integrals of resonant interaction, which determine the structure of the exciton zones in molecular crystals.[1,5] On the other hand, these quantities decrease slowly with increasing $|\mathbf{p}-\mathbf{p}'|$ and the character of their asymptotic behavior at large $|\mathbf{p}-\mathbf{p}'|$ determines many effects that are connected with far interactions. We shall therefore restrict ourselves* here to the expansion $M^{\mathbf{n}e,\mathbf{n}'e'}_{\mathbf{pg},\mathbf{p}'g'}$ in non-orthogonality integrals, which lead to the relation

$$M^{\mathbf{n}e,\mathbf{n}'e'}_{\mathbf{pg},\mathbf{p}'g'} = U_{\mathbf{pp}'}(\bar{x}^{\mathbf{n}e}_{\mathbf{pg},i}, \bar{x}^{\mathbf{n}e}_{\mathbf{pg},ij}, \ldots | x^{\mathbf{n}'e'}_{\mathbf{p}'g',i}, x^{\mathbf{n}'e'}_{\mathbf{p}'g',ij}\ldots), \quad (6)$$

where

$$x^{\mathbf{n}e}_{\mathbf{pg},i} = V\overline{2}\int \bar{\varphi}_{\mathbf{pg}}(\mathbf{r})(x_i - p_i)\varphi_{\mathbf{n}e}(\mathbf{r})\,d\tau,$$

$$x^{\mathbf{n}e}_{\mathbf{pg},ij} = V\overline{2}\int \bar{\varphi}_{\mathbf{pg}}(\mathbf{r})(x_i - p_i)$$

$$\times(x_j - p_j)\varphi_{\mathbf{n}e}(\mathbf{r})\,d\tau \text{ etc.} \quad (7)$$

where $\mathbf{p} = (p_1, p_2, p_3)$ is the position of the $\mathbf{p}$-th elementary cell and $U_{\mathbf{pp}'}(\ldots|\ldots)$ is the energy of the electrostatic interaction between a system of multipoles (dipole, quadrupole, etc.) located at the point $\mathbf{p}$, with components $\bar{x}^{\mathbf{n}e}_{\mathbf{pg},i}$, $\bar{x}^{\mathbf{n}e}_{\mathbf{pg},ij}$ etc., and a system of multipoles having components $x^{\mathbf{n}'e'}_{\mathbf{p}'g',i}$, $x^{\mathbf{n}'e'}_{\mathbf{p}'g',ij}$ etc. at the point $\mathbf{p}'$. Using (6), and also the fact that the translational symmetry allows us a choice of the amplitudes $a^{\mathbf{n}e}_{\mathbf{pg}}$ in the form $a^{\mathbf{n}e}_{\mathbf{pg}} = N^{-1/2}a^{e}_{\mathbf{g}}(\mathbf{n}-\mathbf{p},\mathbf{k})\exp(i\mathbf{k}\mathbf{p})$, we find the third term of the right half of (2):

$$\sum_{\mathbf{p}'} U_{\mathbf{pp}'}(\overline{X}_i[a], \overline{X}_{ij}[a], \ldots | X_i[a],$$

$$X_{ij}[a], \ldots)\exp\{i\mathbf{k}(\mathbf{p}'-\mathbf{p})\}, \quad (8)$$

where

$$X_i[a] = \sum_{\mathbf{n}-\mathbf{p}}\sum_{eg} a^{e}_{g}(\mathbf{n}-\mathbf{p},\mathbf{k})x^{\mathbf{n}e}_{\mathbf{pg},i} \text{ etc.}$$

These last quantities determine the matrix elements of the coordinates and of their products for a transition from the ground state into the exciton state with $\mathbf{k}=0$. For large-radius excitons they are considerably smaller than the analogous matrix elements in isolated atoms, and a simple estimate shows that in this case expression (8) has a smaller order of magnitude than expression (5), which is on the order of an electron volt. Therefore, in the greater part of the Brillouin zone, allowance for (8) leads only to small numerical corrections.

The situation is quite different in the vicinity of the point $\mathbf{k}=0$, where, owing to the slow convergence of the series, expression (8) becomes a non-analytic and even a discontinuous function of $\mathbf{k}$. In this region the presence of integrals of the resonance type changes the dispersion law qualitatively. The singular portion of (8), which is of principal interest to us, can be segregated by going over to the macroscopic field;[7] the regular portion will be disregarded henceforth. In this approximation, (8) has the form, accurate to terms of order k^2,

$$\frac{4\pi e^2}{vk^2}\left\{\frac{1}{1!\,1!}\overline{X}_i[a]X_j[a]k_ik_j - \frac{i}{1!\,2!}(\overline{X}_i[a]X_{js}[a] - X_i[a]\overline{X}_{js}[a])k_ik_jk_s + \left[\frac{1}{2!\,2!}\overline{X}_{ij}[a]X_{st}[a] - \frac{1}{1!\,3!}(\overline{X}_i[a]X_{jst} + X_i[a]\overline{X}_{jst}[a])\right]k_ik_jk_sk_t + \ldots\right\}. \quad (9)$$

Here v is the volume of the elementary cell of the crystal; repeated coordinate indices imply summation. The first term in (9) is in full agreement with the general result of Pekar.[4] It can also be readily compared with the formula obtained in models that are essentially close to that of Frenkel.[8,9]*

The matrix elements $K^{\mathbf{n}e,\mathbf{n}'e'}_{\mathbf{pg},\mathbf{p}'g'}$ decrease exponentially with increasing $|\mathbf{p}-\mathbf{p}'|$ and $|\mathbf{n}-\mathbf{n}'|$, while the diagonal elements are the ordinary integrals of Coulomb interaction. Since we plan to consider large-radius states, in which the average distance between the electron and the hole exceeds considerably the lattice constant, we expand $K^{\mathbf{n}e,\mathbf{n}'e'}_{\mathbf{pg},\mathbf{p}'g'}$ in non-orthogonality integrals and retain only the first term

$$K^{\mathbf{n}e,\mathbf{n}'e'}_{\mathbf{pg},\mathbf{p}'g'} \approx -\delta_{\mathbf{n}e,\mathbf{n}'e'}\delta_{\mathbf{pg},\mathbf{p}'g'}\frac{e^2}{|\mathbf{n}-\mathbf{p}|},$$

corresponding to the Coulomb attraction between

*The effect of resonance type integrals with $\mathbf{n}=\mathbf{n}'$, $\mathbf{p}=\mathbf{p}'$ on the arrangement of the energy levels of the exciton was investigated by Moskalenko and Tolpygo.[6]

*An error in writing down the system of equations analagous to (1) has crept into the paper by Wannier,[2] and led to a loss of the resonance-type integrals and of all the singularities due to the far-interaction effect.

the point charges, omitting higher terms that lead to the appearance of nondiagonal matrix elements and tensor forces.

Inserting the resultant expressions into (2) and varying over the excitation amplitudes, we obtain an infinite system of equations, from which it is possible to determine in principle the wave functions and the energy spectrum. In practice, however, it is more convenient to carry out a certain transformation, which facilitates further transition to continuum and to the effective-mass approximation.

We use the representations $|\mathbf{ne}\rangle$ and $|\mathbf{pg}\rangle$, and denote by $a^{\mathbf{ne}}(\mathbf{k_n}\nu)$ and $a_{\mathbf{pg}}(\mathbf{k_p}\pi)$ linear combinations of the wave functions of the zone electrons and holes, chosen to form an orthonormal system and to depend analytically on $\mathbf{k_n}$ and $\mathbf{k_p}$; in all other respects the choice of these functions is thus far arbitrary. We expand the wave function of the exciton in a series

$$a^{n\nu}_{\rho g} = \sum_{\mathbf{k_n k_p} \nu\pi} C^{\mathbf{k_n} n\nu}_{\mathbf{k_p}\rho\pi}\, a^{n\mathbf{e}}(\mathbf{k_n}\nu)\, a_{\rho g}(\mathbf{k_p}\pi) \qquad (10)$$

and construct the functions

$$b^{n\nu}_{\rho\pi} = \frac{1}{N} \sum_{\mathbf{k_n k_p}} C^{\mathbf{k_n} n\nu}_{\mathbf{k_p}\rho\pi} \exp\{i(\mathbf{nk_n} + \mathbf{pk_p})\}. \qquad (11)$$

We can then show that (2) is transformed into

$$\begin{aligned} E[\{b^{n\nu}_{\rho\pi}\}] = {} & \sum_{\mathbf{n}\rho\nu\nu'\pi} \bar{b}^{n\nu}_{\rho\pi} H^{\nu\nu'}\Big(\frac{1}{i}\nabla_{\mathbf{n}}\Big) b^{n\nu'}_{\rho\pi} \\ & + \sum_{\mathbf{n}\rho\nu\pi\pi'} \bar{b}^{n\nu}_{\rho\pi} H_{\pi\pi'}\Big(\frac{1}{i}\nabla_{\mathbf{p}}\Big) b^{n\nu}_{\rho\pi'} \\ & - \sum_{\mathbf{np}} \frac{e^2}{|\mathbf{n}-\mathbf{p}|} \sum_{\nu\nu'\pi'} \sum_{eg} \overline{a^e\Big(\frac{1}{i}\nabla_{\mathbf{n}},\ \nu\Big) a_g\Big(\frac{1}{i}\nabla_{\mathbf{p}},\ \pi\Big) b^{n\nu}_{\rho\pi}} \\ & \times a^e\Big(\frac{1}{i}\nabla_{\mathbf{n}},\ \nu'\Big) a_\varepsilon\Big(\frac{1}{i}\nabla_{\mathbf{p}},\ \pi'\Big) b^{n\nu'}_{\lambda\pi'} \\ & + \sum_{\mathbf{npn'}\rho'} \sum_{\nu\pi\nu'\pi'} U_{\mathbf{pp'}} \Big\{ \overline{x^{n\nu}_{\rho\pi,\,i}\Big(\frac{1}{i}\nabla_{\mathbf{n}},\ \frac{1}{i}\nabla_{\mathbf{p}}\Big) b^{n\nu}_{\rho\pi}}, \dots \\ & \dots \Big| x^{n'\nu'}_{\rho'\pi',\,i}\Big(\frac{1}{i}\nabla_{\mathbf{n}'},\ \frac{1}{i}\nabla_{\mathbf{p}'}\Big) b^{n'\nu'}_{\rho'\pi'}, \dots \Big\}, \end{aligned} \qquad (12)$$

where

$$H^{\nu\nu'}(\mathbf{k_n}) = \sum_{ee'} \overline{a^e(\mathbf{k_n}\nu)}\, H^{ee'}(\mathbf{k_n})\, a^{e'}(\mathbf{k_n}\nu'), \qquad (13)$$

$$H_{\pi\pi'}(\mathbf{k_p}) = \sum_{gg'} \overline{a_g(\mathbf{k_p}\pi)} H_{gg'}(\mathbf{k_p})\, a_{g'}(\mathbf{k_p}\pi'), \qquad (14)$$

$$x^{n\nu}_{\rho\pi,\,i}(\mathbf{k_n}\,\mathbf{k_\rho}) = \sum_{eg} x^{ne}_{\rho g,\,i}\, a^e(\mathbf{k_n}\nu)\, a_g(\mathbf{k_p}\pi) \quad \text{etc.} \qquad (15)$$

$$a^e(\mathbf{k_n}\nu) = \sqrt{N} a^{ne}(\mathbf{k_n}\nu)\, e^{-i\mathbf{k_n n}},$$

$$a_g(\mathbf{k_\rho}\pi) = \sqrt{N}\ a_{\rho g}(\mathbf{k_p}\pi)\, e^{-i\mathbf{k_\rho p}}; \qquad (16)$$

the differentiation operators that enter as arguments into the functions a^e, a_g, $x^{ne}_{pg,i}$ etc. act only on the function $b^{n\nu}_{pg}$.

Relation (12) is the principal formula, from which the transition to the macroscopic theory should be carried out in the various cases.

Let us consider one example. It follows from (9) that the greatest interest, from the point of view of the influence of the resonance mechanism, attaches to the investigation of the structure of the exciton zone near the point $\mathbf{k} = 0$; on the other hand, in the effective-mass approximation, which we use here, we can describe only the states near the bottom of the exciton zone. We shall therefore assume that as we neglect the resonance interactions the minimum of the exciton zone is located at the point $\mathbf{k} = 0$.

Let us denote by $\mathbf{k}^0_n$ and $\mathbf{k}^0_p$ the position of the bottom of the lowest electron zone E^0, and the top of the highest hole zone E_0. At the points $\mathbf{k}^0_n$ and $\mathbf{k}^0_p$, generally speaking, contact between several zones can take place. The functions $a^{ne}(\mathbf{k_n}\nu)$ are conveniently chosen such that some (the functions of the first group) belong to the linear envelope of the wave functions of the electron bands that make contact at the point of absolute minimum, and the others (functions of the second group) belong to its orthogonal complement. Analogously, we choose and break up into two groups the functions $a_{pg}(\mathbf{k_p}\pi)$. If the radius of the exciton is sufficiently large, the predominant role in the expansion (10) is assumed by the functions of the first group, and the functions of the second group can be neglected. Henceforth the sums that extend only over the functions of the first group will be designated by primes.

The bottom of the exciton zone is located at the point $\mathbf{k} = 0$, only if the vectors $\mathbf{k} = \mathbf{k}^0_n + \mathbf{k}^0_p$ and $\mathbf{k} = 0$ are equivalent. This can occur actually only when the bottom of the electron zone and the ceiling of the hole zone (or of an entire group of zones) are located at the center of the Brillouin zone ($\mathbf{k_0} = \mathbf{k}^0_n = \mathbf{k}^0_p = 0$), or at one of the symmetry points on its surface ($\mathbf{k_0} = \mathbf{k}^0_n, \mathbf{k}^0_p$). In the latter case we shall assume for simplicity that this point of the extremum is unique, i.e., that all the points to which it goes under the operation of the factor group and the operation of time reversals are equivalent to it.

Introducing the smoothed functions

$$B^{n\nu}_{\pi}(\mathbf{n},\ \mathbf{p}) = \frac{1}{v} b^{n\nu}_{\rho\pi} \exp\{-i\mathbf{k_0}(\mathbf{n}+\mathbf{p})\},$$

assuming that the zone-zone transitions at the point $\mathbf{k_0}$ are allowed, and confining ourselves in

the resonance terms to terms of zero order in $\mathbf{k}$, we obtain, after varying over $B_\pi^\nu(\mathbf{n}, \mathbf{p})$ in the usual effective-mass approximation

$$-\sum_{\nu}{}' D_{ij}^{\nu\nu'} \nabla_{ni} \nabla_{nj} B_\pi^{\nu'}(\mathbf{n}, \mathbf{p}) - \sum_{\pi'}{}' D_{\pi\pi',ij} \nabla_{pi} \nabla_{pj} B_{\pi'}^{\nu}(\mathbf{n}, \mathbf{p})$$

$$-\overline{\frac{e^2}{|\mathbf{n}-\mathbf{p}|}} B_\pi^\nu(\mathbf{n}, \mathbf{p}) + \sum_{\nu'\pi'}{}' \int d\mathbf{n}'\, d\mathbf{p}'\, \delta(\mathbf{n}-\mathbf{p})$$

$$\times \left[\overline{(\mathbf{r}_\pi^\nu(\mathbf{k}_0), \nabla_{\mathbf{p}})\, (\mathbf{r}_{\pi'}^{\nu'}(\mathbf{k}_0), \nabla_{\mathbf{p}'})\, \frac{e^2}{|\mathbf{p}-\mathbf{p}'|}} \right]$$

$$\times \delta(\mathbf{n}'-\mathbf{p}')\, B_{\pi'}^{\nu'}(\mathbf{n}', \mathbf{p}') = \varepsilon B_\pi^\nu(\mathbf{n}, \mathbf{p}), \qquad (17)$$

where

$$\mathbf{r}_\pi^\nu(\mathbf{k}_0) = \sum_{\mathbf{n}} \mathbf{r}_{\rho\pi}^{\eta\nu}(\mathbf{k}_0\, \mathbf{k}_0) \exp\{i\mathbf{k}_0(\mathbf{n}-\mathbf{p})\}, \quad \varepsilon = E - (E^0 - E_0).$$

The first three terms of the left half coincide with the Hamiltonian considered in reference 10. The coefficients $D_{ij}^{\nu\nu'}$ and $D_{\pi\pi',ij}$ determine the structure of the electron and hole zones near the extrema. The connection between the various coefficients, which follows from the symmetry of the crystal, can be found by group-theoretical methods.[11,12] The last term is due to resonance interactions. Thus, introducing resonant interactions into the theory in the approximation considered here leads to the appearance of a characteristic contact term and to the transformation of the differential equation into an integro-differential one.

To solve the equations of (17), which have the form of plane waves with quasi-momentum $\mathbf{k}$, we have $B_\pi^\nu(\mathbf{p}, \mathbf{p}) = B_\pi^\nu(0, 0) \exp(i\mathbf{k}\mathbf{p})$ and the contact term assumes the form

$$\frac{4\pi e^2}{k^2} \sum_{\nu'\pi'}{}' \overline{(\mathbf{r}_\pi^\nu(\mathbf{k}_0), \mathbf{k})(\mathbf{r}_{\pi'}^{\nu'}(\mathbf{k}_0), \mathbf{k})}\, B_{\pi'}^{\nu'}(\mathbf{n}, \mathbf{p})\, \delta(\mathbf{n}-\mathbf{p}). \qquad (18)$$

Although the mean value of the contact term is proportional to $(r_0/r_{exz})^3$, where r_0 and r_{exz} are respectively quantities on the order of the dimensions of the elementary cell and of the radius of the exciton state, this term should be retained, since it is connected directly with the macroscopic characteristic (the oscillator strength for a transition into the exciton state), and leads to a qualitative change in the law of dispersion near the point $\mathbf{k} = 0$. In addition, the resonance term may split the degenerate levels.

An investigation of the higher terms of the expansion in powers of $\mathbf{k}$ in resonance terms and the formulation of a law of dispersion in crystals with a different symmetry are outside the scope of this communication.

For triplet states in a system of equations analogous to (1), there are no terms of the resonance type,[13,6] and consequently the usual form of this theory still applies to them.

The author is grateful to S. I. Pekar for an evaluation of this work.

[1] J. Frenkel, Phys. Rev. **37**, 1276 (1931).
[2] G. H. Wannier, Phys. Rev. **52**, 191 (1937).
[3] F. N. Mott, Trans. Farad. Soc. **34**, 500 (1938).
[4] S. I. Pekar, J. Exptl. Theoret. Phys. (U.S.S.R.) **36**, 451 (1959), Soviet Phys. JETP **9**, 314 (1959).
[5] A. S. Davydov, Теория поглощения света в молекулярных кристаллах (Theory of Absorption of Light in Molecular Crystals), Kiev, 1951.
[6] S. A. Moskalenko and K. B. Tolpygo, J. Exptl. Theoret. Phys. (U.S.S.R.) **36**, 149 (1959), Soviet Phys. JETP **9**, 103 (1959).
[7] M. Born and K. Huang, Dynamical Theory of Crystal Lattices, Oxford 1954, §30.
[8] D. Fox and S. Yatsiv, Phys. Rev. **108**, 938 (1957).
[9] S. I. Pekar, J. Exptl. Theoret. Phys. (U.S.S.R.) **35**, 522 (1958), Soviet Phys. JETP **8**, 360 (1959).
[10] G. Dresselhaus, J. Phys. Chem. Solids **1**, 14 (1956).
[11] Dresselhaus, Kip, and Kittel, Phys. Rev. **98**, 368 (1955).
[12] É. I. Rashba, Физ. тв. тела (Solid State Physics) **1**, 407 (1959).
[13] R. E. Merrifield, J. Chem. Phys. **23**, 402 (1955).

Translated by J. G. Adashko
351

SOVIET PHYSICS JETP VOLUME 36 (9), NUMBER 6 DECEMBER, 1959

ON THE THEORY OF THE ELECTRON SPIN RESONANCE OF F-CENTERS IN CRYSTALS WITH NaCl STRUCTURE

L. A. SHUL' MAN

Tadzhik State University

Submitted to JETP editor October 3, 1958

J. Exptl. Theoret. Phys. (U.S.S.R.) **36**, 1709-1716 (June, 1959)

Two models of the F center are used, the de Boer and the Hilsch-Pohl models. The wave function of the ground state is derived for both models, using the molecular orbital approximation. The hyperfine interaction of the F-center electron with the magnetic moments of the nuclei in the first and second coordination spheres is considered. The coupling constants in the corresponding spin Hamiltonian are calculated. The paramagnetic resonance absorption of radio-frequencies by F centers is examined. The shape and width of the absorption band are obtained. For the KCl crystal, comparison with the experimental data shows agreement of theory and experiment.

INTRODUCTION

THE paramagnetic absorption of radio frequencies by F centers was experimentally discovered by Hutchison.[1,2] The results were interpreted theoretically by Kip et al.,[3] using the de Boer model, according to which the F center is a negative ion vacancy at which an electron is located. The quantum-mechanical description of the F center in reference 3 was made on the basis of the molecular orbital approximation, developed in reference 4. Kip et al. did not take into account the overlap of the eigenfunctions of adjacent ions, as a consequence of which the variation of absorption frequency with crystal orientation relative to the external static magnetic field (the paramagnetic absorption anisotrphy effect) is left out. The existence of such a variation was emphasised by Deĭgen and the author.[5,6] The variation was experimentally discovered by Feher,[7] and a detailed theoretical interpretation of the results was obtained by Deĭgen and Zevin.[8]

Kip et al.[3] introduced into the coupling constant of the spin Hamiltonian a parameter that was determined by a comparison of the theoretical and experimental values of the absorption bandwidth. In references 5, 6, and 9 a method is proposed for calculating, in the macroscopic approximation[10] for the F center, the coupling constants in the spin-Hamiltonian which describes the interaction of the F-center electron (de Boer model) with the magnetic moments of the nuclei in the first and second coordination spheres surrounding the halide vacancy. Glinchuk and Deĭgen[11] considered the F-center in the macroscopic approximation using the Hilsch-Pohl model, according to which the F center is a surplus metallic ion at which an electron is located.

The coupling constants in the spin-Hamiltonian are calculated for the F center below (Sec. 2), taking into account the overlapping of the adjacent ion eigenfunctions in the molecular orbital approximation. The theory is parameterless and permits a comparison of the calculated values with experiment.[7,8] In Sec. 3 the theory of radio wave absorption by F centers is developed for the Hilsch-Pohl model (molecular orbital approximation). The character of the resonance spectrum is qualitatively different for the two models, a fact already remarked on by other authors.[11,12] The possibility therefore exists of deciding from the absorption band shape on the model for F centers in crystals; this is of great importance for silver halides, for example.

1. GROUND STATE OF THE F CENTER

De Boer Model. The wave equation of an electron located at a halide vacancy can be written in the form

$$\left[-\frac{\hbar^2}{2m}\nabla^2+\sum_k V_k(\mathbf{r}-\mathbf{R}_k)+\sum_i V_i(\mathbf{r}-\mathbf{R}_i)-\frac{e^2}{r}\right]\Psi=E\Psi. \tag{1}$$

The adiabatic approximation has already been used in this. Equation (1) is the electronic part of the general Schrödinger equation. The nuclei surrounding the vacancy are assumed fixed. Here $\mathbf{r}$ is the distance from electron to vacancy, $\mathbf{R}_k$ is the dis-

tance from the vacancy to the k-th positive ion, $\mathbf{R}_l$ is the analogous distance for the l-th negative ion, $V_k(\mathbf{r}-\mathbf{R}_k)$ is the potential energy of interaction with the k-th positive ion, $V_l(\mathbf{r}-\mathbf{R}_l)$ is the potential energy of interaction with the l-th negative ion, and $-e^2/r$ is the potential energy of interaction with the positive vacancy. Polarization of the dielectric by the electron is not taken into account.

To find the approximate solution of Eq. (1) we use the variational method. We consider only the electron interaction with the six positive and twelve negative ions nearest to the vacancy.

The energy of the ground state of the system E is determined from the minimum of the function

$$\int \Psi^* \hat{H} \Psi d\tau, \quad \hat{H} = -\frac{\hbar^2}{2m}\nabla^2 + \sum_{k=1}^{6} V_k + \sum_{l=1}^{12} V_l - \frac{e^2}{r},$$

and we use the approximation function customarily employed in the molecular-orbital method,

$$\Psi = N\left[\sum_{k=1}^{6}\psi_k + \gamma\sum_{l=1}^{12}\psi_l\right], \tag{2}$$

$$\int |\Psi|^2 d\tau = 1 \tag{3}$$

where N is a normalizing factor, ψ_k are the normalized eigenfunctions of the isolated atoms in the first coordination sphere, ψ_l are the normalized eigenfunctions of the ions in the second coordination sphere, and γ is the approximation parameter.

We substitute (2) in the variational integral, determine N from (3) and find the parameter γ from the equation $\partial E/\partial\gamma = 0$. In calculating the coefficients entering into the latter equation, we neglect "three-center" integrals (for example, $\int \psi_k V_{k'} \psi_l d\tau$, $k \neq k'$) and also omit terms with $l \neq l'$ by virtue of the rapid fall-off of ψ_l. The calculations on the Hilsch-Pohl model are carried through in the same approximation. The evaluation of the variational integral is simplified if the functions ψ_k and ψ_l, and the potentials V_k and V_l are represented by sums of Gaussian exponentials.

$$\psi_k(\rho_k) = \frac{1}{\sqrt{4\pi}}\sum_i b_i \exp\{-\beta_i \rho_k^2\},$$

$$\psi_l(\rho_l) = \sum_m b_m \exp\{-\beta_m \rho_l^2\},$$

$$V_k(\rho_k) = \sum_p C_p \exp\{-\delta_p \rho_k^2\}, \quad V_l(\rho_l) = \sum_q d_q \exp\{-\varepsilon_q \rho_l^2\},$$

$$\rho_k = \mathbf{r} - \mathbf{R}_k, \quad \rho_l = \mathbf{r} - \mathbf{R}_l. \tag{4}$$

For numerical calculation we use V_k for the K^+ ion from reference 13, and V_l for the Cl^- ion from reference 14; for ψ_k we use the Hartree function with exchange for the 4s electron in the K atom,[15] and for ψ_l the function obtained in reference 14. The error involved in approximation (4) does not exceed 3 or 4% for ψ_k and V_k, and 5 or 6% for ψ_l and V_l. Calculations for the KCl crystal lead to the value of the coefficient $\gamma = -0.08932$, which corresponds to the lowest value of the energy.

Hilsch-Pohl Model. We write the wave function of the electron captured by the additional positive ion in the crystal in the form

$$\left[-\frac{\hbar^2}{2m}\nabla^2 + V_0 + \sum_k V_k + \sum_l V_l\right]\Psi = E\Psi, \tag{5}$$

V_0 is the interaction potential energy of the electron with the additional positive ion; V_k and V_l have the same meanings as before. We neglect the displacement of the ions by the interstitial atom.

The energy of the ground state of the system E is determined by minimizing the variational integral.

$$\int \Psi^* \hat{H} \Psi\, d\tau, \text{ where } \hat{H} = -\frac{\hbar^2}{2m}\nabla^2 + \sum_{k=1}^{4} V_k + \sum_{l=1}^{1} V_l + V_0,$$

i.e., we consider only the interaction of the electron with the interstitial ion and with the four positive and four negative ions of the lattice nearest to it. As the approximate wave function we take the following:

$$\Psi = N\left[\psi_0 + \delta_1\sum_{k=1}^{4}\psi_k + \delta_2\sum_{l=1}^{4}\psi_l\right], \qquad \int |\Psi|^2 d\tau = 1. \tag{6}$$

ψ_0 is the wave function of the interstitial atom; ψ_k and ψ_l have the same meaning as previously; δ_1 and δ_2 are the parameters of the approximation. Substituting (6) in the variational integral and determining N from the normalization conditions we find δ_1 and δ_2 from the equations $\partial E/\partial\delta_i = 0$ $(i = 1, 2)$. The integrals were evaluated using the previous approximations (4). For the KCl crystal with interstitial K^+ ion we find $\delta_1 = -0.3048$ and $\delta_2 = -0.02639$. These parameters correspond to the lowest value of the energy.

2. ELECTRON SPIN RESONANCE OF THE F CENTER. DE BOER MODEL

Following references 5, 6, 8, and 16, the spin-Hamiltonian describing the interaction of the localized electron with the magnetic moments of the six nuclei of the first coordination sphere can lead to the form

$$\hat{H}'_s = \sum_{k=1}^{6}[A_k(\mathbf{I}_k\mathbf{s}) + B_k(\mathbf{I}_k\mathbf{R}_k)(\mathbf{s}\mathbf{R}_k)], \tag{7}$$

where

$$A_k = a_k + A_{22k}, \qquad B_k R_k^2 = A_{33k} - A_{22k},$$

$$a_k = 4\pi \frac{\mu\mu_k}{sI_k} |\Psi(\rho_k = 0)|^2, \quad A_{ppk} = \frac{\mu\mu_k}{sI_k} \int \frac{x_{pk}}{\rho_k^3} \frac{\partial |\Psi|^2}{\partial x_{pk}} d\tau, \tag{8}$$

μ, μ_k, S, and I_k are the magnetic moments and spins of the electron and the k-th nucleus, respectively; $\rho_k = |\mathbf{r} - \mathbf{R}_k|$; the index p = 1, 2, 3 enumerates the axes of the Cartesian system of coordinates (the origin of coordinates is at the k-th site, and the x_{3k} axis is directed along R_k); Ψ is the wave function of the electron.

Similarly, the spin-Hamiltonian describing the interaction of the localized electron with the magnetic moments of the twelve nuclei of the second coordination sphere can be written:[8,9]

$$\hat{H}_s^{II} = \sum_{l=1}^{12} [A_l (\mathbf{I}_l \mathbf{s}) + B_l (\mathbf{I}_l \mathbf{R}_l)(\mathbf{s} \mathbf{R}_l) + C_l I_{lx_l} s_{x_l}], \tag{9}$$

$$A_l = a_l + A_{22l}, \qquad B_l R_l^2 = A_{33l} - A_{22l}, \qquad C_l = A_{11l} - A_{22l},$$

$$a_l = 4\pi \frac{\mu\mu_l}{sI_l} |\Psi(\rho_l = 0)|^2, \qquad A_{ppl} = \frac{\mu\mu_l}{sI_l} \int \frac{x_{pl}}{\rho_l^3} \frac{\partial |\Psi|^2}{\partial x_{pl}} d\tau, \tag{10}$$

μ_l, I_l are the magnetic moment and spin of the l-th nucleus, and $\rho_l = |\mathbf{r} - \mathbf{R}_l|$. Here the Cartesian coordinate system is associated with the l-th site. We bear in mind the following relationships:[8]

$$2A_{22k} + A_{33k} = -a_k, \qquad A_{11k} = A_{22k},$$
$$A_{11l} + A_{22l} + A_{33l} = -a_l. \tag{11}$$

For the wave function we will use (2) with the known parameter γ. We remark that, by ignoring the overlapping of the eigenfunctions of neighboring atoms, we arrive at the results of Kip et al.[3] In fact, in this approximation:

$$A_{33k} = A_{22k}, \qquad B_k R_k^2 = 0, \qquad A_{22k} = -\frac{4\pi}{3} \frac{\mu\mu_k}{sI_k} |\Psi(\rho_k = 0)|^2,$$

$$A_k = \frac{8\pi}{3} \frac{\mu\mu_k}{sI_k} |\Psi(\rho_k = 0)|^2,$$

which agrees exactly with the result of reference 3. When the overlap of eigenfunctions is taken into account, the constants $B_k \neq 0$.

Substituting (2) in (8) and omitting small "three-center" integrals we obtain

$$A_{ppk} = \frac{\mu\mu_k}{sI_k} N^2 \Big[\sum_{n=1}^{6} \int \frac{x_{pk}}{\rho_k^3} \frac{\partial}{\partial x_{pk}} \psi_n^2 d\tau + 2 \sum_{n \neq k} \int \frac{x_{pk}}{\rho_k^3} \frac{\partial}{\partial x_{pk}} (\psi_k \psi_n) d\tau$$
$$+ 2\gamma \sum_{l=1}^{12} \int \frac{x_{pk}}{\rho_k^3} \frac{\partial}{\partial x_{pk}} (\psi_k \psi_l) d\tau + \gamma^2 \sum_{l=1}^{12} \int \frac{x_{pk}}{\rho_k^3} \frac{\partial}{\partial x_{pk}} \psi_l^2 d\tau \Big]. \tag{12}$$

Similarly, substituting (2) in (10) and neglecting "three-center" integrals, we obtain

$$A_{ppl} = \frac{\mu\mu_l}{sI_l} N^2 \Big[\sum_{k=1}^{6} \int \frac{x_{pl}}{\rho_l^3} \frac{\partial}{\partial x_{pl}} \psi_k^2 d\tau + 2\gamma \sum_{k=1}^{6} \int \frac{x_{pl}}{\rho_l^3} \frac{\partial}{\partial x_{pl}} (\psi_k \psi_l) d\tau$$
$$+ 2\gamma^2 \sum_{m \neq l} \int \frac{x_{pl}}{\rho_l^3} \frac{\partial}{\partial x_{pl}} (\psi_l \psi_m) d\tau$$
$$+ \gamma^2 \sum_{m=1}^{12} \int \frac{x_{pl}}{\rho_l^3} \frac{\partial}{\partial x_{pl}} \psi_m^2 d\tau \Big]. \tag{13}$$

To perform the integrations in (12) and (13), approximations (4) are convenient, as well as the approximations for $\psi_k^2(\rho_k)$ and $\psi_l^2(\rho_l)$ used previously;[6,9] thus the coefficients in the spin Hamiltonian of the first and second coordination spheres can be calculated.

We take the external static field along the z axis; then, as in reference 5, we have for the eigenvalues

$$H_s = s_z \Big[\sum_{k=1}^{6} \Delta_k I_k + \sum_{l=1}^{12} \Delta_l I_l \Big],$$

$$\Delta_k = [A_k^2 + B_k R_k^2 p_k^2 (2A_k + B_k R_k^2)]^{1/2},$$

$$\Delta_l = [A_l^2 + B_l R_l^2 m_l^2 (2A_l + B_l R_l^2) + C_l n_l^2 (2A_l + C_l)]^{1/2}. \tag{14}$$

Here $\mathbf{H}$ is the magnitude of the static magnetic field; p_k, m_l, n_l are the cosines of the angles between $\mathbf{H}$ and $\mathbf{R}_k$, $\mathbf{R}_l$, x_l, respectively. The positions of the individual lines in the absorption band are determined by the equation

$$\hbar\Omega = \sum_{k=1}^{6} \Delta_k I_k + \sum_{l=1}^{12} \Delta_l I_l \quad (\Delta I_k = \Delta I_l = 0, \ \Delta s_z = \pm 1). \tag{15}$$

From (14) and (15) we can see the dependence of absorption frequency on crystal orientation relative to the external magnetic field.

In crystals of MgO the interaction of the F-center electron with only one magnetic moment, Mg^{25}, has been observed;[17] the other nuclear magnetic moments in the first coordination sphere were zero. In this case the angular dependence of the line position has the form

$$\hbar\Delta\Omega = [A_k^2 + B_k R_k^2 p_k^2 (2A_k + B_k R_k^2)]^{1/2}, \tag{16}$$

where $\Delta\Omega$ is the separation between two adjacent lines. In reference 17 an empirical dependence of this separation on angle is given:

$$\hbar\Delta\Omega = a + b(3p_k^2 - 1). \tag{17}$$

By comparing (16) and (17) from a and b we determine A_k and $B_k R_k^2$. From (16), using the values found for the coefficients A_k and $B_k R_k^2$, we are satisfied that within the limits of experimental error the empirical angular dependence agrees with our formula (16).

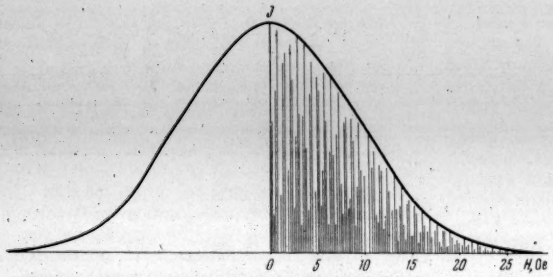

FIG. 1. Shape of the absorption band in KCl crystal (de Boer's model of the F center). The component lines are shown in only one half of the peak.

In references 5 and 6, it was emphasized that the absorption band shape differs somewhat from Gaussian, since I_k and I_l in (15) have different weighting factors. The calculations show that for the crystals considered, the constants $B_kR_k^2$, $B_lR_l^2$ and C_l are several times smaller than the corresponding A constants. Therefore, we can write approximately

$$\hbar\Omega = A_k\Big[\sum_{j=1}^{6} I_j + \varkappa\sum_{i=1}^{12} I_i\Big], \qquad \varkappa = A_l/A_k. \tag{18}$$

The intensities of the lines are proportional to the statistical weights of the energy states. We calculated the statistical weights using formula (18) for $I_j = I_i = 3/2$. For KCl the line shape calculated using (18) is shown in Fig. 1 (only the most intense lines, corresponding to the largest statistical weights, are shown in the given range of magnetic field). The envelope of these most intense lines is almost Gaussian. The half-width of the absorption band, as is known, is determined by the formula

$$\Delta h_{1/2} = 2\sqrt{\frac{\ln 2}{\alpha}}\frac{A_k}{\mu} = 3.37\,\frac{A_k}{\mu}, \tag{19}$$

where α is the parameter of the Gaussian approximation to the absorption band. The maximum width, taking into account the contribution of the second coordination sphere, in unit magnetic field is

$$\Delta h_m = (9A_k/\mu)[1 + 2\varkappa]. \tag{20}$$

Here the constants $B_kR_k^2$, $B_lR_l^2$, and C_l have been left out.

By way of example, the coefficients of the spin-Hamiltonian were calculated for the first and second coordination spheres for the KCl crystal. The half-width and maximum width of the absorption for this crystal were determined from (19) and (20) respectively. These values are given in the table, where the following notation is introduced:

$$\delta = \frac{A_{11k}}{a_k} = -\frac{1+x}{3+x}, \qquad \gamma_1 = \frac{A_{11l}}{a_l} = \frac{z-y-1}{z+y+3},$$

$$\gamma_2 = \frac{A_{22l}}{a_l} = -\frac{y+z+1}{y+z+3},$$

$$x = B_kR_k^2/A_k, \qquad y = B_lR_l^2/A_l, \qquad z = C_l/A_l.$$

It appears from the table that agreement with experiment is better for the molecular-orbital approximation than for the macroscopic approximation (see references 6, 8, and 9). Somewhat poorer agreement with experiment exists for the constants of the second coordination sphere than for the first, which can be explained by the too rapid decrease of the Ψ-function for Cl^{--} used by us.[14] There is satisfactory agreement with experimental data for the ratio of the constants. If we take for $\psi_k^2(0)$, instead of the low Hartree value, the value obtained from radio-spectroscopic data, then $\Delta h_{1/2} = 33$ oersteds, which is already significantly closer to the experimental value.

3. ELECTRON SPIN RESONANCE OF THE F CENTER. HILSCH-POHL MODEL

The spin Hamiltonian describing the interaction of the electron located at the additional positive ion with the ions closest to it has the form

	Theory	Experiment*		Theory	Experiment*
A_k/h Mcs	8.134	20.65	Δh_m, Oe	80.30	218.4
A_l/h Mcs	2.176	6.66	δ	—0.3344	—0.363
$\varkappa$	0.2675	0.323	γ_1	—0.3433	—0.387
$\Delta h_{1/2}$, Oe	19.60	54	γ_2	—0.3110	—0.377

*$\Delta h_{1/2}$ from reference 3, all other data from references 7 and 8.

$$\hat{H}_s = \sum_{k=1}^{3} A_k (\mathbf{I}_k \mathbf{s}) + \sum_{l=1}^{4} A_l (\mathbf{I}_l \mathbf{s}) + A_0 (\mathbf{I}_0 \mathbf{s}) + \sum_{k=1}^{4} \sum_{pq} A_{pqk} I_{pk} s_q$$

$$+ \sum_{l=1}^{4} \sum_{pq} A_{pql} I_{pl} s_q + \sum_{pq} A_{pq0} I_{p0} s_q,$$

$$A_{pqj} = \frac{\mu_1 \mu_j}{s I_j} \int \frac{x_{pj}}{\rho_j^3} \frac{\partial |\Psi|^2}{\partial x_{qj}} d\tau,$$

$$A_j = 4\pi \frac{\mu_1 \mu_j}{s I_j} |\Psi(\rho_j = 0)|^2, \quad j = 0, k, l; \qquad (21)$$

μ_0 and I_0 are the magnetic moment and spin of the interstitial atom.

We use (6) as the wave function. From considerations of symmetry $A_{pqj} = 0$ for $p \neq q$. We take the x_{30} axis along a crystallographic axis, x_{20} along a [110] direction and x_{10} along another similar direction; then $A_{pq0} = 0$ $(p \neq q)$ by virtue of the fact that $|\Psi|^2$ and ρ_0 are even with respect to x_{10} and x_{20}. Directing x_{3k} to the interstitial ion, x_{1k} along the [110] direction, and x_{2k} perpendicular to both these axes, it is easy to show that $A_{pqk} = 0$ $(p \neq q)$, $A_{12k} = A_{21k} = A_{31k} = A_{13k} = 0$ by virtue of the fact that $|\Psi|^2$ and ρ_k are even with respect to x_{1k}. $A_{23k} = A_{32k} = 0$, which is easily shown by rotating the coordinate system about the x_{3k} axis by an angle of 120°. In the same way it can be shown also that $A_{pql} = 0$ $(p \neq q)$.

We proceed with our consideration, ignoring the overlap of the eigenfunctions of neighboring ions. Then (21) takes the form

$$\hat{H}_s = A_0 (\mathbf{I}_0 \mathbf{s}) + A_1 \sum_{k=1}^{4} (\mathbf{I}_k \mathbf{s}) + A_2 \sum_{l=1}^{4} (\mathbf{I}_l \mathbf{s}), \qquad (22)$$

where

$$A_0 = \frac{2\mu_1 \mu_0}{3 s I_0} N^2 \alpha_0^2 \psi_{i0}^2(0), \quad A_1 = \frac{2\mu_1 \mu_1}{3 s I_1} N^2 \alpha_1^2 \psi_{ik}^2(0),$$

$$A_2 = \frac{8\pi}{3} \frac{\mu_1 \mu_2}{s I_2} N^2 \alpha_2^2 \alpha_i^2 (0).$$

In the approximation considered $N = (1 + 4\delta_1^2 + 4\delta_2^2)^{-1}$.

Aligning the z axis with the direction of the static magnetic field and taking into account the selection rules $(\Delta I_{kz} = \Delta I_{lz} = \Delta I_{0z} = 0, \ \Delta s_z = \pm 1)$ in complete analogy with (14) and (15), we obtain the position of the individual lines in the absorption band:

$$\hbar\Omega = A_0 \Big[I_{0z} + \varkappa_1 \sum_{k=1}^{4} I_{kz} + \varkappa_2 \sum_{l=1}^{4} I_{lz} \Big],$$

$$\varkappa_1 = A_1 / A_0, \ \varkappa_2 = A_2 / A_0. \qquad (23)$$

The intensities of the lines are proportional to the statistical weights of the corresponding states calculated in reference 11. The shape of the band is shown in Fig. 2. In the band there are four maxima, corresponding to the interaction of the electron with the nuclear magnetic moment of the interstitial atom. Within the limits of each maximum the shape is close to Gaussian. The effective magnetic field, corresponding to the distance between two adjacent maxima, $\Delta h = A_0/2\mu$. The maximum width of the band (distance between the extreme lines in the spectrum) is

$$\Delta h_m = \frac{3}{2\mu} A_0 [1 + 4(\varkappa_1 + \varkappa_2)], \text{ oe.}$$

By way of example we calculated that for KCl with an additional K^+ ion, $\Delta h_m = 156$ oersteds, $\Delta h = 36.4$ oersteds, $\kappa_1 = 0.09290$, and $\kappa_2 = 0.01461$. Since the distance between maxima is large and their overlap small, these four bands should be resolved experimentally. By the shape of the absorption band it should be possible to distinguish de Boer F centers from Hilsch-Pohl F centers.

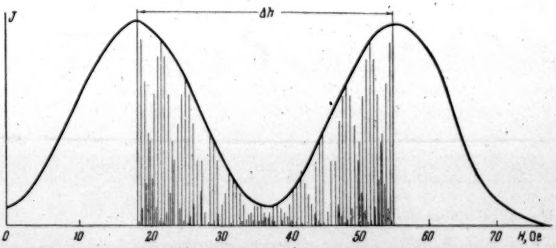

FIG. 2. Shape of the absorption band in KCl crystal (Hilsch-Pohl model of the F center). Only two maxima are shown, in each of which only the lines in one half are indicated. Two maxima omitted are disposed symmetrically relative to the origin of coordinates.

In conclusion I express my sincere gratitude to M. F. Deĭgen for the suggestion of and constant interest in the work.

[1] C. A. Hutchison, Jr., Phys. Rev. **75**, 1769 (1949).

[2] C. A. Hutchison, Jr., and G. A. Nobel, Phys. Rev. **87**, 1125 (1952).

[3] Kip, Kittel, Levy, and Portis, Phys. Rev. 91, 1066 (1953).

[4] T. Muto, Progr. Theor. Phys. **4**, 211 (1949). T. Inui and I. Uemura, Progr. Theor. Phys. **5**, 252, 395 (1950).

[5] M. F. Deĭgen and L. A. Shul'man, Оптика и спектроскопия (Optics and Spectroscopy) **3**, 21 (1957).

[6] M. F. Deĭgen, J. Exptl. Theoret. Phys. (U.S.S.R.) **33**, 773 (1957), Soviet Phys. JETP **6**, 594 (1958).

[7] G. Feher, Phys. Rev. **105**, 1122 (1957).

[8] M. F. Deĭgen and V. Ya. Zevin, J. Exptl. Theoret. Phys. (U.S.S.R.) **34**, 1142 (1958), Soviet Phys. JETP **7**, 790 (1958).

[9] L. A. Shul'man, Оптика и спектроскопия (Optics and Spectroscopy) **4**, 684 (1958).

[10] S. I. Pekar, Исследования по электронной теории кристаллов, (Studies on the Electronic Theory of Crystals) M.-L. GITTL, (1951).

[11] M. D. Glinchuk and M. F. Deĭgen, J. Tech. Phys. (U.S.S.R.) **28**, 1981 (1958), Soviet Phys. "Tech. Phys." **3**, 1819 (1958).

[12] F. Seitz, Revs. Modern Phys. **26**, 7 (1954).

[13] D. R. Hartree and W. Hartree, Proc. Roy. Soc. **166**, 450 (1938).

[14] K. B. Tolpygo and O. F. Tomasevich, Укр. физ. журн. (Ukr. Phys. J.) **3**, 1 (1958).

[15] D. R. Hartree and W. Hartree, Proc. Cam. Phil. Soc. **34**, 550 (1938).

[16] V. Ya. Zevin, Оптика и спектроскопия (Optics and Spectroscopy) **3**, 660 (1957).

[17] Wertz, Auzins, Weeks, and Silsbel, Phys. Rev. **107**, 1535 (1957).

Translated by K. F. Hulme
352

NUCLEON-NUCLEON SCATTERING IN HIGH ANGULAR MOMENTUM STATES

A. F. GRASHIN

Moscow Engineering Physics Institute

Submitted to JETP editor November 18, 1958

J. Exptl. Theoret. Phys. (U.S.S.R.) 36, 1717-1724 (June, 1959)

The properties of the one-meson approximation to elastic nucleon-nucleon scattering are considered in detail, and the scattering phase shifts are calculated. A new method of phase-shift analysis is proposed, which should lessen the ambiguity of the solution and make it possible to get more accurate values of the experimental phase shifts.

OKUN' and Pomeranchuk[1] have shown that, since peripheral interactions of a particle involve effectively the minimum possible number of π mesons, processes involving large orbital angular momenta can be calculated on the basis of the present meson theory.

Let us examine nucleon-nucleon scattering in greater detail. For the part of the amplitude that corresponds to sufficiently large orbital angular momenta l there are contributions only from diagrams in which a single π meson is exchanged.* In the one-meson approximation with the symmetric pseudoscalar meson-nucleon interaction the nucleon-nucleon scattering is described in the center-of-mass system by the amplitude ($\hbar = c = 1$)

$$\langle \mathbf{k}', s_1', s_2', \tau_1', \tau_2' | \mathbf{M} | \mathbf{k}, s_1, s_2, \tau_1, \tau_2 \rangle = \frac{g^2}{4m\gamma} \left\{ \frac{\langle 1', 2' | (\tau_1\tau_2)(\sigma_1\mathbf{q})(\sigma_2\mathbf{q}) | 1, 2 \rangle}{q^2 + \mu^2} - \frac{\langle 2', 1' | (\tau_1\tau_2)(\sigma_1\mathbf{p})(\sigma_2\mathbf{p}) | 1, 2 \rangle}{p^2 + \mu^2} \right\},$$

$$\mathbf{q} = \mathbf{k} - \mathbf{k}', \quad q = 2k \sin \theta/2, \quad \mathbf{p} = \mathbf{k} + \mathbf{k}',$$

$$p = 2k \cos \theta/2, \quad \gamma = \sqrt{m^2 + k^2/m}, \qquad (1)$$

The absolute square of this amplitude gives the differential cross-section for the transition between states prescribed by the momentum of one of the nucleons, the components of the spins of both nucleons along the initial momentum, and the isotopic spin components of both nucleons.

Here the notations are: g is the the renormalized meson-nucleon interaction constant ($g^2 \approx 15$), m the mass of the nucleon, μ the mass of the π meson, τ_1 and σ_1 the Pauli matrices in the isotopic and spin spaces, respectively, of the first nucleon, τ_2 and σ_2 the analogous matrices for the second nucleon, and θ the scattering angle. Strictly speaking, the amplitude (1), is only the main part of the exact one-meson amplitude, since the only one of the effects caused by the use of the exact vertex part and the exact Green's function that has been taken into account is the renormalization of the interaction constant. Besides this the exact one-meson amplitude contains a contribution of the same type as is given by many-meson diagrams, which need not be used (this is proved in reference 1). In nonrelativistic approximation the amplitude (1) corresponds to the well known one-meson interaction of nucleons, which is obtained in the lowest order of perturbation theory (cf. e.g., references 3* and 4). The part of the exact one-meson amplitude that has been omitted corresponds to an interaction that vanishes at infinity like $\exp(-3\mu r)$.

To make the change to the representation of the total spin and total isotopic spin ($\mathbf{k}$, S, S_z, T, T_3) we must reconstruct the scattering operator M, for which the amplitude (1) is the matrix element in the representation $\mathbf{k}$, s_1, s_2, τ_1, τ_2. It is not hard to verify that the scattering operator has the form

$$\mathbf{M} = \frac{g^2}{4m\gamma} \frac{3 - (\tau_1\tau_2)}{4} \frac{p^2}{p^2 + \mu^2} \{ -1 + (\sigma_1\mathbf{n})(\sigma_2\mathbf{n}) - (\sigma_1\mathbf{l})(\sigma_2\mathbf{l}) \} + \frac{g^2}{4m\gamma} \left\{ (\tau_1\tau_2) \frac{q^2}{q^2 + \mu^2} + \frac{3 - (\tau_1\tau_2)}{4} \frac{p^2}{p^2 + \mu^2} \right\} (\sigma_1\mathbf{m})(\sigma_2\mathbf{m}), \qquad (2)$$

where $\mathbf{n} = [\mathbf{k} \times \mathbf{k}']/k^2$, $\mathbf{l} = \mathbf{p}/p$, $\mathbf{m} = \mathbf{q}/q$. We note

*A calculation of the contribution from diagrams with two mesons exchanged, made by Galanin, Grashin, Ioffe, and Pomeranchuk, provides an estimate of the accuracy of the one-meson approximation for various values of l. It turns out that for nonrelativistic energies (up to 100 – 300 Mev) the one-meson approximation makes the main contribution even for the relatively small values $l = 3$, 4. The results of an analysis of the experimental data[2] for 90 and 150 Mev agree with these estimates.

*We take occasion to point out that Eqs. (47.10) and (47.13) of reference 3 contain a superfluous factor 3 in the central part of the potential.

the following fact. In the amplitude (1) the second (exchange) term exists only for identical particles. For different particles, keeping the former interaction of the two particles with the meson, we should have simply

$$\mathbf{M}=\frac{g^2}{4m\gamma}(\tau_1\tau_2)\frac{q^2}{q^2+\mu^2}(\sigma_1\mathbf{m})(\sigma_2\mathbf{m}).$$

Comparison with Eq. (2) shows that inclusion of the symmetry changes the interaction. This is indeed not surprising, since inclusion of the symmetry in fact means the introduction of a new (exchange) interaction, to describe which additional terms in the scattering operator are required.

The scattering operator is diagonal in the total spin and the total isotopic spin, and therefore we shall denote its matrix elements by the symbol M (S, β, α, T), where α and β are the initial and final components of the total spin along the initial momentum. Calculation gives the following scattering amplitudes:

$$\left.\begin{aligned}M(1,\beta,\alpha,1)&=M_{\beta\alpha}(\theta,\varphi)-M_{\beta\alpha}(\pi-\theta,\varphi+\pi)\\M(0,0,0,1)&=M(\theta)+M(\pi-\theta)\end{aligned}\right\}\quad T=1,$$

$$\left.\begin{aligned}M(1,\beta,\alpha,0)&=-3[M_{\beta\alpha}(\theta,\varphi)+M_{\beta\alpha}(\pi-\theta,\varphi+\pi)]\\M(0,0,0,0)&=-3[M(\theta)-M(\pi-\theta)]\end{aligned}\right\}\quad T=0,\tag{3a}$$

where the matrices $M_{\beta\alpha}(\theta,\varphi)$ and $M(\theta)$, combined into a single four-row matrix, have the form

$$M_{\beta\alpha}(\theta,\varphi)=-M(\theta)L_{\beta\alpha}(\theta,\varphi)\qquad(\alpha,\beta=1,0,-1,0);\qquad M(\theta)=\frac{1}{\mu}\,G\frac{\cos\theta-1}{x-\cos\theta},\qquad G=\frac{g^2\mu}{4m\gamma},\qquad x=1+\frac{1}{2}\left(\frac{\mu}{k}\right)^2;$$

$$L_{\beta\alpha}(\theta,\varphi)=\begin{pmatrix}(1-\cos\theta)/2 & -\sin\theta e^{-i\varphi}/\sqrt{2} & (1+\cos\theta)e^{-2i\varphi}/2 & 0\\ -\sin\theta e^{i\varphi}/\sqrt{2} & \cos\theta & \sin\theta e^{-i\varphi}/\sqrt{2} & 0\\ (1+\cos\theta)e^{2i\varphi}/2 & \sin\theta e^{i\varphi}/\sqrt{2} & (1-\cos\theta)/2 & 0\\ 0 & 0 & 0 & -1\end{pmatrix}.\tag{3b}$$

Here φ is the azimuthal angle of the scattering, and the fourth value of α and β corresponds to the singlet.

Since for our purpose it is important to separate the large orbital angular momenta l, which are well described by the one-meson amplitude, from the small angular momenta, for which many-meson diagrams must be included, we shall go over to the representation J, m_J, l, S, T, T_3 (J and m_J are the total angular momentum and its component along the initial momentum). In the representation of the total angular momentum the scattering is described by a matrix $S^{JT}_{l',l}$, diagonal in J, m_J, S, T, T_3 and independent of m_J and T_3 (cf., e.g., reference 5). The index for the total spin is omitted, since the singlet is distinguished from the triplet by the use of the notation S^T_l. The scattering amplitude in the representation $\mathbf{k}$, S, S_z, T, T_3 is connected with the matrix $S^{JT}_{l',l}$ by the following general relation:*

$$M(S,\beta,\alpha,T)=\frac{1}{ik}\sum_{l'}^{\infty}\sum_{J}^{\infty}\sum_{l}^{\infty}\sqrt{4\pi(2l+1)}\,i^{l-l'}Y^{(\alpha-\beta)}_{l'}(\theta,\varphi)$$
$$\times(l,S,0,\alpha\,|\,l,S,J,\alpha)$$
$$\times(l',S,\alpha-\beta,\beta\,|\,l',S,J,\alpha)(S^{JT}_{l',l}-\delta_{l',l}),\tag{4}$$

where $(l, S, m_l, m_S \,|\, l, S, J, m_J)$ are Clebsch-Gordan coefficients in the notation of Condon and Shortley.[6] This relation enables us to express the scattering matrix and the scattering phase shifts in terms of the coefficients of the expansion of the amplitudes M (S, β, α, T) in associated Legendre polynomials:

$$M(S,\beta,\alpha,T)=\frac{2}{k}e^{i(\alpha-\beta)\varphi}\sum_{l=|\alpha-\beta|}^{\infty}(2l+1)P_l^{(\alpha-\beta)}$$
$$\times(\cos\theta)\,a_l(S,\beta,\alpha,T).\tag{5}$$

Let us introduce the following notations for the non-vanishing elements of the scattering matrix:

$$S^{JT}_{l,l}-1=2i\eta^{JT}_l$$
$$S^{T}_{J-1,J+1}=S^{T}_{J+1,J-1}=2i\xi^{T}_J\qquad\text{for the triplet,}$$
$$S^{T}_{l}-1=2i\eta^{T}_l\qquad\text{for the singlet.}$$

For T = 1 only the matrix elements with odd l in the triplet and even l in the singlet are different from zero, and the reverse is the case for T = 0; therefore the index for the total isotopic spin can be omitted (in the triplet coefficients of the expansion of the amplitudes we shall also omit the index for the total spin, and in the singlet coefficients, all spin indices). In the case in which $|\eta^J_l|$, $|\xi_J|$, $|\eta_l| \ll 1$, i.e., for large orbital angular momenta, the real parts of these quantities are respectively the same as the matrix phases $\bar{\delta}_{l,J}$, $\bar{\epsilon}_J$, $\bar{\delta}_l$ (bar phase shifts) introduced by Stapp and others.[7] If we parametrize the scattering matrix by means of the proper phase shifts[5] δ^J_l, ϵ_J, δ_l, then for large orbital angular momenta

*We call attention to the fact that the right member of Eq. (4) is doubled as compared with the analogous expression for nonidentical particles. The right side of Eq. (5) is also doubled.

$$\mathrm{Re}\,\eta_{li} = \delta_i \equiv \overline{\delta}_l, \qquad \mathrm{Re}\,\eta_{lj}^{J} = \delta_j' \equiv \overline{\delta}_{J,J},$$

$$\mathrm{Re}\,\eta_{lJ\pm1}^{J} = \cos^2\varepsilon_J \cdot \delta_{J\pm1}' + \sin^2\varepsilon_J \cdot \delta_{J\mp1}',$$

$$\mathrm{Re}\,\xi_J = \tfrac{1}{2}\sin 2\varepsilon_J\,(\delta_{J-1}' - \delta_{J+1}').$$

We note that the mixing parameters ϵ_J are usually large, so that the quantities $\eta_{J\pm1}^{J}$ can be decidedly different from the corresponding proper phase shifts $\delta_{J\pm1}^{J}$.

Solving Eqs. (4) and (5) for η and ξ, we get for the quantities different from zero

$$\begin{aligned}
(2l-1)\,\eta_{li}^{l-1} &= (l-1)\,a_l(1,1) + \sqrt{2}\,(l+1)\,a_l(1,0)\\
&+ (l-1)(l+1)(l+2)\,a_l(-1,1) + l a_l(0,0)\\
&+ (l-1)(l+1)[a_l(1,0) + a_l(0,1)]\sqrt{2},\\
\eta_{li}^{l} &= a_l(1,1) - \sqrt{2}\,a_l(1,0) - (l-1)(l+2)\,a_l(-1,1)\\
&+ [a_l(1,0) + a_l(0,1)]\sqrt{2},\\
(2l+3)\,\eta_{li}^{l+1} &= (l+2)\,a_l(1,1)\\
&+ \sqrt{2}\,l a_l(1,0) + (l-1)\,l\,(l+2)\,a_l(-1,1)\\
&+ (l+1)\,a_l(0,0) - l(l+2)[a_l(1,0) + a_l(0,1)]\sqrt{2},\\
\xi_J &= \frac{\sqrt{J(J+1)}}{2J+1}\{-a_{J-1}(1,1) - 2\sqrt{2}\,(J-1)\,a_{J-1}(1,0)\\
&- (J-2)(J-1)\,a_{J-1}(-1,1) + a_{J-1}(0,0)\\
&+ (J-1)[a_{J-1}(1,0) + a_{J-1}(0,1)]\sqrt{2}\}\\
&= \frac{\sqrt{J(J+1)}}{2J+1}\{-a_{J+1}(1,1) + 2\sqrt{2}\,(J+2)\,a_{J+1}(1,0)\\
&- (J+2)(J+3)\,a_{J+1}(-1,1) + a_{J+1}(0,0)\\
&- (J+2)[a_{J+1}(1,0) + a_{J+1}(0,1)]\sqrt{2}\},\\
\eta_{li} &= a_i.
\end{aligned} \tag{6}$$

We emphasize that the relations (6) are of a general character, i.e., are valid in any approximation as to the number of mesons, since no specific properties of the scattering amplitude were used in deriving them. In the one-meson approximation $a_l(1,0) + a_l(0,1) = 0$, which is equivalent to the equation $e^{-i\varphi}M(1,0,1,T) = e^{i\varphi}M(1,1,0,T)$; this leads to some simplification in the equations (6) (the last terms vanish), and also to a linear relation between the triplet elements with the same l but different J:

$$(l+1)(2l-1)\,\eta_{li}^{l-1} + (2l+1)\,\eta_{li}^{l} - l(2l+3)\,\eta_{li}^{l+1} = 0. \tag{7}$$

Substituting in Eq. (6) the expansion coefficients of the amplitudes (3)

$$\begin{aligned}
a_l(1,1) &= \tfrac{1}{2}\,G\,\frac{k}{\mu}\left\{(2-x)\,\delta_{l0} - \tfrac{1}{3}\,\delta_{l1} + (x-1)^2 Q_l\right\} E_l,\\
a_l(1,0) &= \frac{Gk/\mu}{\sqrt{2}\,l\,(l+1)}\left\{\frac{2}{3}\,\delta_{l1} + l(x-1)\,[xQ_l - Q_{l-1}]\right\} E_l,\\
a_l(-1,1) &= \frac{Gk/\mu}{2(l-1)(l+1)(l+2)}\{[(l-1)(x^2-1)-2]\\
&\times Q_l + 2xQ_{l-1}\}\,E_l,\\
a_l(0,0) &= G\,\frac{k}{\mu}\left\{(x-1)\,\delta_{l0} + \frac{1}{3}\,\delta_{l1} - x(x-1)\,Q_l\right\} E_l,\\
a_l &= G\,\frac{k}{\mu}\{(x-1)\,Q_l - \delta_{l0}\}\,E_l,
\end{aligned} \tag{8}$$

where the projection function

$$E_l \equiv E_l(S,T) = -\tfrac{3}{2} + 2T + (1-2S)(\tfrac{3}{2} - T)(-1)^l$$

takes the values 1, 0, −3, depending on the spin and parity, we get

$$\begin{aligned}
\eta_{li}^{l-1} &= \frac{Gk/\mu}{2l-1}\{Q_{l-1} - Q_l\}\,E_l,\\
\eta_{li}^{l} &= -\frac{Gk/\mu}{l+1}\{[l(x-1)-1]\,Q_l + Q_{l-1}\}\,E_l, \quad \text{for } l \geqslant 2;\\
\eta_{li}^{l+1} &= \frac{Gk/\mu}{2l+3}\{Q_l - Q_{l+1}\}\,E_l;\\
\xi_J &= \frac{Gk/\mu}{2J+1}\sqrt{\frac{J}{J+1}}\{[1-(2J+1)(x-1)]\,Q_J - Q_{J-1}\}\,E_{J-1},\\
\eta_{li} &= G\,\frac{k}{\mu}\{(x-1)\,Q_l - \delta_{l0}\}\,E_l.
\end{aligned} \tag{9}$$

For the ^3S and ^3P states we have

$$\begin{aligned}
\eta_1^0 &= G\,\frac{k}{\mu}[1-(x-1)\,Q_0],\\
\eta_1^1 &= -\frac{1}{2}\,G\,\frac{k}{\mu}[1-(x-1)(Q_0 - Q_1)], \quad \text{for } T=1;\\
\eta_1^2 &= 0.1\,G\,\frac{k}{\mu}[1-(x-1)(Q_0 + 3Q_1)];\\
\eta_0^1 &= -G\,\frac{k}{\mu}[1-(x-1)\,Q_0] \quad \text{for } T=0.
\end{aligned} \tag{10}$$

In Eqs. (8) – (10) the following notations have been used: δ_{l0} and δ_{l1} are Kronecker symbols, and $Q_l \equiv Q_l(x)$ is the Legendre function of the second kind. For small energies ($k/\mu \ll 1$, which corresponds to laboratory energies $E \ll 40$ Mev)

$$Q_l \approx [l!\,2^{l+1}/(2l+1)!!\,](k/\mu)^{2l+2}.$$

In determining the accuracy of the one-meson approximation for the various quantities we must take into account the following properties of these quantities. The off-diagonal element ξ_J can be expressed in terms of the $(J+1)$st coefficients of the expansion of the amplitudes [cf. Eq. (6)]. These same coefficients occur in the expressions for the diagonal elements corresponding to the orbital angular momentum $l = J+1$, and thus, generally speaking, the errors incurred in all

TABLE I. Values of η_l, η_l^J, ξ_J for T = 1 (the usual spectroscopic notations are used for the diagonal elements η_l, η_l^J)

E, Mev	10	17	40	100	200	300	400	670
x	$\sqrt{3}$	2.165	1.5	1.2	1.1	1.0675	1.05	1.03
$^1S_0$	—4.8	—8.6	—19	—37	—57	—70	—82	—100
$^1D_2$	0.17	0.38	0.99	1.9	2.4	2.5	2.6	2.5
$^1G_4$	0.004	0.018	0.11	0.41	0.75	0.94	1.1	1.2
$^3P_0$	4.8	8.6	19	37	57	70	82	100
$^3P_1$	—3.0	—5.3	—11	—21	—31	—37	—43	—54
$^3P_2$	0.11	0.28	0.89	2.4	4.3	5.7	6.9	9.2
ξ_2	—0.23	—0.53	—1.5	—3.5	—5.4	—6.7	—7.7	—9.5
$^3F_2$	0.015	0.052	0.27	1.0	2.1	3.0	3.8	5.3
$^3F_3$	—0.037	—0.13	—0.58	—1.9	—3.6	—4.9	—5.9	—7.9
$^3F_4$	0.001	0.006	0.048	0.25	0.62	0.94	1.2	1.9
ξ_4	—0.004	—0.021	—0.14	—0.59	—1.2	—1.7	—2.1	—2.7
$^3H_4$	$2\cdot10^{-4}$	0.001	0.016	0.12	0.35	0.57	0.78	1.3
$^3H_5$	$-8\cdot10^{-5}$	—0.005	—0.056	—0.35	—0.88	—1.4	—1.8	—2.6
$^3H_6$	$2\cdot10^{-5}$	$2\cdot10^{-4}$	0.004	0.039	0.14	0.23	0.35	0.60

these quantities (ξ_J, η_{J+1}^J, a_{J+1}) owing to the use of the one-meson approximation are of the same order of magnitude. For small energies $|\xi_J| \gg |\eta_{J+1}^J|$; evidently a similar relation will also hold in this range of energies for the corresponding corrections to the one-meson approximation. Furthermore, for a very wide range of energies in the one-meson approximation $|\eta_l^{l+1}| \ll |\eta_l^{l-1}|$, $|\eta_l^l|$ (we note that for small energies η_l^{l-1}, $\eta_l^l \sim k^{2l+1}$, and $\eta_l^{l+1} \sim k^{2l+3}$), and therefore the fractional accuracy of the quantity η_l^{l+1} must be much lower than those of η_l^{l-1} and η_l^l. For small energies ($k/\mu \lesssim 1$) the one-meson approximation can be quite useless for the determination of η_l^{l+1}. This must be particularly noticeable for small l ($^3P_2$, $^3D_3$). On going over to the proper phases we get δ_{J+1}^J and ϵ_J in the one-meson approximation with the errors characteristic of the (J − 1)st coefficients, since these phases depend on η_{J-1}^J. In order not to introduce these artificial errors into the calculation it is better to use the Stapp parametrization or to use the coefficients (8) directly.

These remarks show that the accuracy of calculations in the one-meson approximation of the various measurable quantities corresponding to a given orbital angular momentum l is determined by the accuracy of the elements η_l^{l-1}, η_l^l, ξ_{l-1}, η_l, except in those special cases in which through cancellations a measurable quantity will actually depend only on η_l^{l+1}. In principle other types of cancellations are possible, for example if the triplet elements occur only in the form of the linear combination (7), which vanishes in the one-meson approximation. In these cases there is a corresponding decrease in the accuracy of the calculations. Besides this, in the one-meson approximation all the quantities are real, and therefore they cannot be used in cases in which the imaginary part of the scattering amplitude cannot be neglected.

Table I shows the values in degrees of η and ξ for T = 1, as calculated from Eqs. (9), (10) with $G = 0.55/\gamma$ for a number of energies E (in the laboratory system), and Table II shows the values of η and ξ for T = 0. The tables begin with $l = 0$, although it is obvious that for small values of l the one-meson approximation can be quite useless.

An estimate of the accuracy of the one-meson approximation found by calculation of the two-meson phase shifts shows that with good accuracy (of the order of 20 percent) one can use the one-meson F and G phase shifts for $E \lesssim 200$ Mev; their accuracy improves with decrease of the energy. For a fixed energy the accuracy of the various phase shifts increases exponentially with increase of l. The D phase shifts are given with good accuracy by the one-meson approximation for $E \lesssim 50$ Mev. To determine the goodness of the one-meson S and P phase shifts one would have to study many-meson diagrams,* and this has not been done so far. There is evidently no region of applicability of the one-meson S phase shifts, since for small energies these phases are $\delta_1 = \delta_0^1 \sim k^3$ and cannot provide the main contribution. An analogous situation exists for the $^3P_2$ phase shifts.

For a comparison of the one-meson phase shifts with the experimental values one needs a rather precise phase-shift analysis of the experi-

*We emphasize that it is necessary to study the exact many-meson diagrams; calculations in low orders of perturbation theory (cf., e.g., reference 4) cannot serve as a reliable basis for estimating the corrections to the one-meson phase shifts.

TABLE II. Values of η_l, η_l^J, ξ_J for T = 0

E, Mev	10	17	40	100	200	300	400	670
x	3	2.165	1.5	1.2	1.1	1.0675	1.05	1.03
$^1P_1$	−3.8	−5.9	−9.7	−13	−14	−13	−13	−12
$^1F_3$	−0.08	−0.24	−0.98	−2.6	−3.9	−4.6	−4.9	−5.1
$^1H_5$	−0.002	−0.012	−0.12	−0.60	−1.3	−1.8	−2.1	−2.6
$^3S_1$	−4.8	−8.6	−19	−37	−57	−70	−82	−100
ξ_1	6.0	10	20	35	50	59	67	81
$^3D_1$	−0.54	−1.4	−4.5	−12	−22	−29	−34	−46
$^3D_2$	0.88	2.1	6.5	16	26	33	40	51
$^3D_3$	−0.032	−0.11	−0.57	−2.1	−4.5	−6.4	−8.0	−11
ξ_3	−0.093	0.31	1.3	4.1	7.3	9.4	11	14
$^3G_3$	−0.003	−0.024	−0.18	−0.96	−2.4	−3.6	−4.8	−7.3
$^3G_4$	−0.016	−0.075	−0.53	−2.3	−5.2	−7.3	−9.3	−13
$^3G_5$	$-4\cdot10^{-4}$	−0.003	−0.039	−0.28	−0.85	−1.4	−1.9	−3.1

mental data, including phase shifts for high angular momenta. The usual procedure in phase-shift analysis is as follows: all the measured quantities are written as functions of the phase shifts with $l \leq l_{\max}$, and all the phase shifts for $l > l_{\max}$ are assumed to be zero. The nonvanishing phase shifts are then varied to get the best agreement with the experimental data. The main shortcoming of such a procedure as applied to the existing data is the ambiguity of the solution, caused by the large number of variable parameters and the incompleteness of the set of measurements. Thus in the analysis of the data on p-p scattering at 310 Mev with $l_{\max} = 5$ (14 parameters)[7] eight acceptable solutions are obtained, more precisely eight more or less broad many-dimensional regions (of ellipsoidal type) centered on the solutions. In analyzing the data for 150 Mev Ohnuma and Feldman[8] obtained 11 such regions, some of them connecting continuously with each other. The analysis for 40 Mev[9] leaves so much arbitrariness in the allowed solutions that it is practically impossible to get any sort of quantitative estimate of the phase shifts.

Besides this difficulty, which in principle can be removed by an increase of the amount of experimental data, there remains the problem of the stability of the solutions with respect to the inclusion of the phases that have been dropped (with $l > l_{\max}$). It is obvious that the least stable values (we are speaking in terms of fractional stability) will be the last of the included phase shifts with $l \approx l_{\max}$, which are those of interest to us here. Therefore, for example, for a comparison of the phase shifts with $l = 4$ we need an analysis with at least $l_{\max} = 5$, and to test the stability of these phase shifts it is desirable to continue the analysis to $l_{\max} = 6$. It is obvious that the analysis then becomes cumbersome and practically not feasible.

It seems reasonable to us to propose a different method of phase-shift analysis, which would take into account our knowledge of the phases with large l: to use the phase shifts for $l \leq l_1$ as unknown parameters and take for all the others (with $l > l_1$) the values in the one-meson approximation. The simplest way to do this is to write the measured quantities as functions of the "corrected" amplitudes

$$M'(S, \beta, \alpha, T) = M(S, \beta, \alpha, T) - \frac{2}{k} e^{i(\alpha-\beta)\varphi} \sum_{l=|\alpha-\beta|}^{l_1} (2l+1) P_l^{(\alpha-\beta)}(\cos\theta)\, a_l(S, \beta, \alpha, T) + \frac{1}{ik} \sum_{l'=0}^{l_1} \sum_{J=0}^{l_1+1} \sum_{l=0}^{l_1+2} \sqrt{4\pi(2l+1)}\, i^{l-l'} Y_{l'}^{(\alpha-\beta)}(\theta, \varphi) \times (l, S, 0, \alpha | l, S, J, \alpha)(l', S, \alpha-\beta, \beta | l', S, J, \alpha) \times (S_{l',l}^{JT} - \delta_{l',l}), \quad (11)$$

where $M(S, \beta, \alpha, T)$ and $a_l(S, \beta, \alpha, T)$ are respectively the amplitudes (3) and their expansion coefficients (8), and the rest of the right member is the usual expression for the matrix elements* in terms of a finite number of phase shifts ($l_{\max} = l_1$). The off-diagonal elements of the scattering matrix, corresponding to $J \geq l_1$, which will be involved in this part, must be included in the one-meson approximation. For example one can begin the analysis for 310 Mev with $l_1 = 2$, in view of the satisfactory accuracy of the F phase shifts. There are then in all 5 variable parameters (instead of the 14 parameters of reference 7); the analysis is much easier and, what is more important, the number of solutions must be smaller. To test the stability of the solutions with respect to errors in the phase shifts with $l > l_1$, which have been included in the one-meson approximation,

*Expressions for the various measurable quantities in terms of the amplitudes M′, and the parts of the amplitudes (11) required for the "correction," with effects of the Coulomb interaction included, can be found in reference 7.

and to improve the solution, one must repeat the analysis with $l_1 = 3$ (9 parameters) and examine the displacement of the solutions found previously. If new solutions (isolated from the former ones) appear, they must be rejected. It may turn out that the value $l_1 = 2$ is too low for the case in question, and that the solution found in the first step is not accurate enough. Nevertheless successive stages of the analysis with $l_1 = 3$ and $l_1 = 4$ must give better results than those obtained by Stapp and others[7] by the usual method. Furthermore the analysis is less cumbersome and is a natural physical scheme for breaking up the analysis into several stages and thus reducing the volume of the calculations. Even from the experimental data available at present the proposed procedure of phase-shift analysis should give more definite and accurate information about the phase shifts.*

In conclusion I express my gratitude to L. B. Okun', I. Ya. Pomeranchuk, and Ya. A. Smorodinskiĭ for a discussion and helpful comments.

*From the example of the phase-shift analysis for E < 40 Mev with $l_{max} = 2$ carried out by MacGregor[10] we can see how an inspection of the one-meson approximation to the higher phase shifts (in this case $^3P_0$, $^3P_1$, $^1D_2$) can reduce the number of solutions. On the other hand, the analysis[9] for 40 Mev shows what a large effect can come from the neglect of the phase shifts with $l > l_{max}$ and what difficulties arise from the inclusion of additional phase shifts as arbitrary parameters.

[1] L. B. Okun' and I. Ya. Pomeranchuk, J. Exptl. Theoret. Phys. (U.S.S.R.) **36**, 300 (1959), Soviet Phys. JETP **9**, 207 (1959).

[2] S. Otsuki, Prog. Theor. Phys. **20**, 171 (1958). W. Watari, Prog. Theor. Phys. **20**, 181 (1958). R. Tamagaki, Prob. Theor. Phys. **20**, 505 (1958).

[3] H. Bethe and F. de Hoffmann, Mesons and Fields, vol. II, Evanston, Ill., Row Peterson and Co., 1955, Russ. Transl. IIL 1958.

[4] Prog. Theor. Phys. (Japan) Suppl. III (1956).

[5] J. Blatt and L. Biedenharn, Rev. Mod. Phys. **24**, 258 (1952), Russ. Transl. in Пробл. совр. физ. (Problems of Modern Phys.) **6** (1955).

[6] E. Condon and G. Shortley, The Theory of Atomic Spectra, Cambridge, 1944, Russ. Transl. IIL 1949.

[7] Stapp, Ypsilantis, and Metropolis, Phys. Rev. **105**, 302 (1957).

[8] S. Ohnuma and D. Feldman, Phys. Rev. **102**, 1641 (1956).

[9] H. P. Noyes and M. H. MacGregor, Phys. Rev. **111**, 223 (1958).

[10] M. MacGregor, Phys. Rev., preprint.

Translated by W. H. Furry
353

COMPARISON OF THE DIFFERENTIAL CROSS SECTIONS FOR THE (dp) AND (dt) REACTIONS

A. B. KUREPIN and V. G. NEUDACHIN

Nuclear Physics Institute, Moscow State University

Submitted to JETP editor November 24, 1958

J. Exptl. Theoret. Phys. (U.S.S.R.) **36**, 1725-1730 (June, 1959)

The (dt) reaction is considered as a special case of a stripping reaction involving two complex systems. The reduced widths derived from the (dt) and (dp) reactions by choosing various triton wave functions are compared. The neutron wave function relative to the deuteron in the triton, which yields the best agreement with experiment is found. A value of ≈ 0.40 is derived for the probability of finding the triton in the (deuteron + neutron) state.

THE analysis of the angular distribution of the triton in the reaction (dt) shows that the mechanism of the reaction at deuteron energies of the order of several Mev is similar to the mechanism of the (dp) reaction, i.e., a stripping reaction is encountered. In connection with this, two interrelated problems arise: a) the comparison of the "reduced widths" γ^2 obtained for the reactions (dp) and (dt), and b) the determination of that part of the wave function of the triton which corresponds to the state (deuteron + neutron). Below, we consider both problems, and a part of the results is compared with results of other authors.[1,2]

As the analysis of the experimental data obtained in recent years shows (Belyaev, Zakhar'ev, and Neudachin, to be published), the "reduced width" γ^2 in the formulae of Butler does not represent the "square of the amplitude of the wave function of a nucleon on the surface of the nucleus" since it is not constant for varying energy of the deuteron but varies very rapidly. It is possible that this is due to the influence of the exchange effect in the stripping reaction.[3] The comparison of γ^2 from the (dp) and (dt) reactions is interesting as a check on the analogy between the two mechanisms, complementing the comparison of the angular distributions.

In contrast to the deuteron, the triton and He^3 are compound particles, on the wave functions of which one has to impose, apart from the vector coupling of the moments, the requirements of antisymmetry. The calculation was carried out by means of the Born approximation using plane waves which, for the ratio of the reduced widths, gives about the same results as the calculation with distorted waves.

The general expression for a stripping reaction between two coupled systems applied to the reaction (dt) is of the form (see also reference 1)

$$\frac{d\sigma}{d\Omega} = \frac{\mu_d \mu_t}{4\pi\mu_n^2} \frac{k_t}{k_d} \frac{(2S_t+1)}{(2S_d+1)(2S_n+1)} \times n_t |\langle s^3\alpha | s^2\alpha_0\rangle|^2 |G(p)|^2 Z^{-2} \times [j_t'(Za) - g_l(\chi a) j_l(Za)]^2 (2\mu_n/\hbar^2)\gamma_c^2, \quad (1)$$

where $|\langle s^3\alpha | s^2\alpha_0\rangle|^2 = \frac{1}{2}$ is the parentage coefficient of the transition from the state s^2 of the deuteron with quantum numbers α_0 to the state s^3 of the triton with quantum numbers α; n_t is the number of nucleons in the triton; S_t, S_d, S_n — are the spin of the triton, deuteron, and neutron respectively; γ_c^2 is the reduced width;

$$\mu_d = M_d M_i/(M_i + M_d), \quad \mu_t = M_t M_f/(M_f + M_t),$$
$$\mu_n = M_n M_f/(M_f + M_n),$$

M_i and M_f are the masses of the initial and final nuclei; k_t, k_d are the wave numbers,

$$k_d = \left(\frac{2M_d}{\hbar^2}\frac{M_i^2}{(M_i+M_d)^2} E_{d\,\mathrm{lab}}\right)^{1/2};$$

$$\mathbf{p} = \mathbf{k}_t/3 - \mathbf{k}_d/2, \quad \mathbf{Z} = \mathbf{k}_t - \mathbf{k}_d M_f/(M_j + M_n),$$
$$\chi = (2\mu_n |E_b|)^{1/2}/\hbar,$$

and E_b is the binding energy of the neutron in the initial nucleus. The interaction radius α is chosen for the best fit of the theoretical angular distribution with the experimental one. The function $j_l(x)$ can be expressed by a Bessel function of half-integral order:

$$j_l(x) = \sqrt{\pi x/2}\, J_{l+1/2}(x) = x j_{lC}(x),$$

where $j_{lC}(x)$ is the spherical Bessel function; $j'_l(x)$ is the derivate with respect to the radius: $j'_l(Za) = Z dj_l(x)/dx$ for $x = Za$; and $g_l(\chi a)$ are logarithmic derivatives on the boundary of the nucleus. These are given for $l = 0$, 1, and 2 by Yoshida.[4] The reduced widths can be expressed in units of the sum $\sum_c \gamma_c^2$ over all reaction channels, and one can obtain the non-dimensional quantity θ:

$$\theta^2 = (a2\mu_n/3\hbar^2)\gamma_c^2.$$

Furthermore, $(2\pi)^{-3/2} G(p)$ is the Fourier transform of a function whose square expresses the probability of finding a triton in the state (deuteron + neutron). We shall denote the neutron contained in the deuteron by n_0, the captured neutron by n_1, and the distances in the triton as $(n_0 p) = x$, $(p n_1) = y$, and $(n_1 n_0) = z$. We then have

$$G(p) = \int \exp\{i\mathbf{p}(2\mathbf{y} - \mathbf{x})\}\, \psi_t(p, n_0, n_1)\, \psi_d(p, n_0)\, d\tau$$

(the integration is carried out over all internal coordinates of the triton). For the deuteron, we assume the Hulthen wave function

$$\psi_d(p, n_0) = N_d (e^{-\alpha x} - e^{-\beta x})/x,$$

$$N_d^2 = [4\pi\ (1/2\alpha - 2/(\alpha+\beta) + 1/2\beta)]^{-1},$$

$$\alpha = 0.23 \cdot 10^{13}\ \text{cm}^{-1}, \quad \beta = 1.63 \cdot 10^{13}\ \text{cm}^{-1}.$$

The problem of the triton has been studied to a much lesser extent than that of the deuteron. Therefore, there is still no acceptable wave function for the triton. We assume a function which is in good agreement with experimental values of the binding energies of H^3 and He^3, and with the difference of the binding energies of H^3 and He^3 for a certain choice of potential parameters. These are the Gaussian function

$$\psi_t(p, n_0, n_1) = N_{t_1} \exp\{-\gamma^2 (x^2 + y^2 + z^2)\},$$
$$N_{t_1}^2 = 24 \sqrt{3}\, \pi^{-3} \gamma^6, \qquad \gamma = 0.25 \cdot 10^{13}\ \text{cm}^{-1}\ [5]$$

and the wave function of Irving[6]

$$\psi_t(p, n_0, n_1) = N_{t_2} \exp\{-\lambda(x^2 + y^2 + z^2)^{1/4}\} / (x^2 + y^2 + z^2)^n,$$
$$n = \tfrac{1}{4}, \quad \lambda = 0.759 \cdot 10^{13}\ \text{cm}^{-1}, \quad N_{t_2}^2 = 4 \sqrt{3}\, \pi^{-2} \lambda^5.$$

It is shown in several papers that the angular distribution of the reaction (dt) is well described by this function for a suitable choice of the interaction radius. In the present work, we have studied the applicability of the Gaussian and Irving wave functions to a calculation of the reduced width and of the angular distribution. For this purpose, it is necessary to know, apart from the dependence on p, the absolute value of G(p).

We shall give the results of the calculation of G(p): 1) for the triton, we assumed the Gaussian wave function

$$G(p) = 42.5 \cdot 10^{-20} \exp\{-p^2/2\gamma^2\};$$

2) for the triton we used the Irving function

$$G(p) = N_d N_{t_2} (8\pi^2/3)\, \Gamma(7/2) \lambda^{-7/2} [I(\alpha) - I(\beta)]/p,$$

where

$$I(\alpha) = \int_0^1 (A^2 + B^2)^{-7/4} \sin\left(\frac{7}{2} \tan^{-1} \frac{B}{A}\right) u\, du,$$

$$B = \frac{\sqrt{2}\, p}{\lambda} (1 - u^2)^{1/2}, \qquad A = 1 + \sqrt{\tfrac{2}{3}}\, \frac{\alpha}{\lambda} u$$

(see also reference 7).

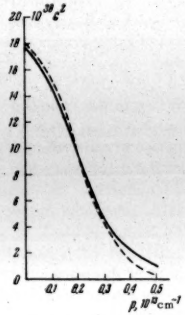

FIG. 1. $|G(p)|^2$ for two cases: Solid curve represents the triton function according to Irving; dotted curve – the Gaussian wave function.

The final results are given in Fig. 1. It can be seen from the figure that the value of the differential cross section depends very slightly on the choice (between variants 1 and 2) of the triton wave function. Therefore, in Table I, where the values of θ^2 calculated from the reaction (dt) according to formula (1) are compared with the reduced widths calculated from the reactions (dp), (pd), and (nd), the Irving function was used to calculate θ^2_{dt} for the corresponding levels. (Formulae for the cross sections are given, e.g., in reference 8.)

We have assumed that, for the choice of a good triton wave function, the interaction radius chosen to describe the angular distribution of the (dt) reaction should coincide with the interaction radius for the corresponding (pd) reaction[14] and the reduced widths obtained from the (dt) reaction should be approximately equal to θ^2_{pd}. Since the accuracy of the ratio θ^2 for identical targets and for different states of the final nucleus is greater than the accuracy of the absolute values, then the ratio θ^2 for two levels of Li from reactions (dt) and (pd) should coincide even better. It can be seen from Table I that all these requirements are

TABLE I

Reaction	E_d, Mev c.m.s.	a, f	θ^2	Error, %	Reference
$Li^7(pd)Li^6$	7.7	5.5	0.052	20	[9]
$Li^7(pd)Li^{6*}$	6.07	5.5	0.036	20	[9]
$C^{12}(dp)C^{13}$	5.87	5.3	0.060	10	[10]
	2.02	5.8	0.030	3	[13]
$Li^6(nd)He^5$	6.48	4.5	0.090	5	[11]
$Be^9(pd)Be^8$	12.3	3	0.025	20	[9]
$Li^7(dt)Li^6$	8.7	6	0.067	20	[12]
$Li^7(dt)Li^{6*}$	8.7	6.5	0.038	20	[12]
$C^{13}(dt)C^{12}$	2.47	6.25	0.050	3	[13]
$Li^6(dt)Li^5$	11.3	5.5	0.140	20	[14]
$Be^9(dt)Be^8$	13.4	4.0	0.061	20	[14]

*Transition to the 2.187-Mev level; in all other cases, transition to the ground state.

fulfilled for wave functions of a triton in both Irving and Gaussian forms. Besides, the functions do not give the correct asymptotic behavior of the wave function f_0 of the neutron in the triton with respect to a deuteron described by the function $\exp(-\lambda R)/R$, where $\lambda = 0.45$ as calculated from the binding energy of the neutron in the triton.

One can try to determine the function f_0 which best satisfies the condition given above directly from experimental data.

Making use of the series expansion (see reference 15).

$$\psi_t(\mathbf{r}\mathbf{R}S_tM_{S_t}) = \sum_{i,\,M_{S_d}m_{S_n}} A_{iM_{S_d}m_{S_n}}\psi_{d_i}(\mathbf{r}S_dM_{S_d})\,C_if_i(\mathbf{R}S_nm_{S_n})$$

(where $\mathbf{r}$ is the vector between the particles in the deuteron, $\mathbf{R}$ is the distance from the middle of $\mathbf{r}$ to the second neutron in the triton, C_if_i is the wave function of this neutron with a normalization factor, and i denotes the different states of the deuteron in the triton), we can substitute in the formula for the cross section of the (dt) reaction:

$$G^2(p)\,\theta^2_{dt} = (2\pi)^3A_0^2C_0^2\Phi^2(k)\,\theta^2_{dt}. \qquad (2)$$

where $k = 2p$ is the momentum of the neutron in the triton with respect to the deuteron, $\Phi(k)$ is the Fourier transform of the function $f_0(R)$, chosen to be equal to one for $k = 0$, and A_0^2 is the probability of finding a triton in the state (deuteron + neutron).

Vlasov and Oglobin[14] give the variation of $\Phi^2(k)$ for $k = (0.3-0.55)\times 10^{13}$ cm^{-1}, and mention that $\Phi^2(k)$ describes the angular distribution of the reaction $Li^7(dt)Li^6$ and $Li^7(dt)Li^{6*}$ with the same interaction radius. For $k \approx 0$ to 0.34, according to data of Holmgren et al.,[13] $\Phi(k) = 1/(k^2+\lambda^2)$ and $\lambda = 0.45$, which gives the correct asymptotic exponential behavior of $f_0(R)$ (see also reference 1). It was also found that $\Phi(k)$ for small and large k join smoothly (see Fig. 2,

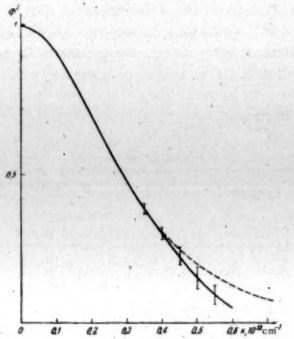

FIG. 2. Fourier transform $\Phi^2(k)$ determined from experimental data (solid curve). Dotted curve – transform $(k^2+\lambda^2)^{-2}$ of the asymptote of f_0.

where, for large k, an average $\Phi(k)$ is taken for $Li^7(dt)Li^6$ at $E_d = 20$ Mev and $E_d = 14.4$ Mev).

Choosing in a rather arbitrary way the asymptotic behavior of $\Phi^2(k)$ for large momenta (which, however, does not introduce a large error), we find the distribution $Rf_0(R)$, Fig. 3. It has a maximum for $R = 3f$, and, beginning with $R \approx 4.5f$, gives the asymptotic dependence $\exp(-\lambda R)$. Thus, $f_0(R)$ satisfies the physical requirements

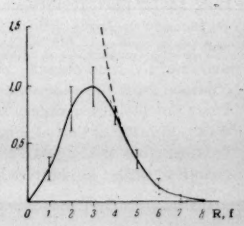

FIG. 3. The function $R^2f_0^2(R)$ (solid curve) and the function proportional to $\exp(-2\lambda R)$ (dotted curve). Arbitrary units.

of the proper asymptotic behavior at large distances and has a maximum for R of the order of the deuteron radius. These properties of functions $f_0(R)$ are mentioned by Werner,[1] who calculated f_0 by solving the Schrödinger equation for the second neutron in the triton with a Gaussian potential. The normalizing coefficient of the function f_0 is given by the equation

$$C^2 = \left(4\pi \int_0^\infty f_0^2(R)\, R^2\, dR\right)^{-1} = 4 \cdot 10^{-39}\ \text{cm}^{-1}.$$

We can now find A_0^2 from different experiments. The interaction radius and the reduced width for the (dt) reaction were taken from the corresponding (dp), (pd), and (nd) reactions (see Table II). The low accuracy of the experimental data obtained from the (pd) reactions involving Be and from the reactions of low-energy deuterons with carbon should be noted. The average value $A_0^2 = 0.37$ (20% error) is greater than the upper limit 0.11 given by Werner.

TABLE II

Reaction	a, f	$\theta_{dt}^2 = \theta_{pd}^2$	A_0^2	Reference
$Li^7(dt)Li^6$	5.5	0.052	0.360	[9, 12]
$Li^7(dt)Li^{6*}$	5.5	0.036	0.377	[9, 12]
$Li^6(dt)Li^5$	4.5	0.090	0.372	[11, 14]
$Be^9(dt)Be^8$	3.0	0.025	0.390	[9, 14]
$C^{13}(dt)C^{12}$	5.8	0.030	0.330	[13]

*See footnote for Table I.

We note that Werner has compared the (dt) and (pd) reactions for different energies; if the comparison is made at the same energy using the data of Holmgren et al.[13] the value 0.11 should be increased by a factor of two.

The deviation from our value of 0.4 can be explained by the fact that the function f_0, and consequently the normalizing coefficient for it, have been obtained from experimental data and are different from f_0 and C^2 calculated by Werner for a definite choice of the interaction.

Recently El Nadi and Hadid[2] estimated A_0^2, using the calculations of Werner, from the reaction $Li^7(dt)Li^6$ (reference 12) and $Li^7(pd)Li^6$ (reference 9) from $F^{19}(dt)F^{18}$ (reference 16), and from $F^{19}(pd)F^{18}$ (reference 9) for the ground states of the final nuclei. The estimate $A_0^2 < 0.06$ obtained from the reactions with Li is doubtful, since the authors maintain that, for a choice of $\Phi(k)$ similar to that of Werner, the value $a = 6\phi$ describes the angular distribution of the (dt) reaction, while, in references 12 and 17, $a = 6$ is assumed for $\Phi(k)$ calculated from the wave function of the triton according to Irving. From the reactions involving fluorine a still smaller value $A_0^2 < 0.02$ has been obtained in reference 2. From the same experimental data, we obtain $A_0^2 \approx 0.06$. This value is in disagreement with five values of A_0^2, two of which are in agreement between themselves, obtained from data of three experiments[12-14] (see Table II).

To obtain a correct formula for the experimental angular distribution of the (dt) reaction with the same interaction radii as in the corresponding (pd) reaction, and to calculate the reduced width θ_{dt}^2, it is necessary to substitute Eq. (2) into Eq. (1) and to substitute the above-given values of A_0^2 and C_0^2.

The authors thank N. A. Vlasov and A. A. Ogloblin for their helpful discussion.

Note added in proof (April 29, 1959): The angular distribution of the reaction $C^{13}(dp)C^{14}$ for the ground state of C^{14} (reference 18), and the reaction $C^{14}(dt)C^{13}$ (reference 19) for the ground state of C^{13} and the 3.08-Mev and 3.68-Mev excited states are satisfactorily described by the choice $a = 5.4\phi$. The value of A_0^2 is 0.3 (100% error).

[1] A. Werner, Nucl. Phys. **1**, 9 (1956).

[2] M. El Nadi and L. Abou Hadid, Nucl. Phys. **8**, 51 (1958).

[3] A. P. French, Phys. Rev. **107**, 1655 (1957). N. Evans and A. P. French, Phys. Rev. **109**, 1272 (1958). T. Fulton and G. Owen, Phys. Rev. **108**, 789 (1957). V. G. Neudachin, J. Exptl. Theoret. Phys. (U.S.S.R.) **35**, 1165 (1958), Soviet Phys. JETP **8**, 815 (1959). Neudachin, Teplov, and Shevchenko, J. Exptl. Theoret. Phys. (U.S.S.R.) **36**, 850 (1959), Soviet Phys. JETP **9**, 599 (1959).

[4] S. Yoshida, Prog. Theor. Phys. **10**, 1 (1953).

[5] B. Bruno, Ark. Mat. Astr. Fys. **A36**, 8 (1948).

[6] J. Irving, Phil. Mag. **42**, 338 (1951).

[7] H. C. Newns, Proc. Phys. Soc. **A65**, 916 (1952).

[8] Fujimoto, Kikuchi, and Yoshida, Prog. Theoret. Phys. **11**, 264 (1954).

[9] J. B. Reynolds, and K. G. Standing, Phys. Rev. **101**, 158 (1956).

[10] J. Rotblat, Nature **167**, 1027 (1951).

[11] G. M. Frye Jr., Phys. Rev. **93**, 1086 (1954).

[12] Levine, Bender, and McGruer, Phys. Rev. **97**, 1249 (1955).

[13] Holmgren, Blair, Simmons, Stratton, and Stuart, Phys. Rev. **95**, 1544 (1954).

[14] N. A. Vlasov and A. A. Ogloblin, Paper presented at the Paris Conference on Nuclear Reac-

tions and Nuclear Structure, 1958.

[15] S. T. Butler and E. E. Salpeter, Phys. Rev. **88**, 133 (1952).

[16] F. A. El Bedewi and I. Hussein, Proc. Phys. Soc. **A70**, 233 (1957).

[17] J. B. French and A. Fujii, Phys. Rev. **105**, 652 (1957).

[18] McGruer, Warburton, and Bender, Phys. Rev. **100**, 235 (1955).

[19] Moore, McGruer, and Hamburger, Phys. Rev. Let. **1**, 29 (1958).

Translated by H. Kasha
354

AN EQUATION FOR THE DIFFUSION IN PHASE SPACE FOR NONLINEAR SYSTEMS

V. B. MAGALINSKIĬ and Ya. P. TERLETSKIĬ

Moscow State University

Submitted to JETP editor November 25, 1958

J. Exptl. Theoret. Phys. (U.S.S.R.) **36**, 1731-1735 (June, 1959)

We have generalized the method developed in references 1 and 2, which is based upon Gibbs' method, to the case of diffusion in phase space. Starting only from the general rules of statistical mechanics and an assumption about the form of the averaged nonlinear macroscopic equation of motion for the system, we derive a general space-velocity equation of motion for the probability density. In the particular case of a linear law of friction this equation is the same as the well-known Einstein-Fokker-Planck space-velocity equation. For a system with a non-linear frictional force which does not depend on the coordinates in a uniform external field we obtain the general solution of the diffusion equation obtained here.

INTRODUCTION

We have shown in previous papers[1,2] that one can derive by Gibbs' method not only the exact formulae of the theory of Brownian motion for fluctuations and correlations,[3,4] but also a general expression for the transition probability density in configuration space, and also equations for this probability density in the case of essentially nonlinear systems.

We shall show below that the general statistical method developed by us can also be applied to derive a general equation of motion for the probability density in the phase space of the coordinates and momenta (or velocities) for arbitrary nonlinear systems.

To obtain such a diffusion equation it is sufficient to make only an assumption about the form of the averaged macroscopic equation of motion for the coordinate and momentum of the particle and there is no necessity to introduce any assumption about the correlations of the random forces or about the character of the stochastic process.

TRANSITION PROBABILITY DENSITY IN PHASE SPACE

Let $Q(X)$ and $P(X)$ be the generalized coordinate and its conjugate generalized momentum of interest to us, where X is the totality of all canonical variables of the microsystem. We denote by $W(Q, P, t; Q_0, P_0, t_0)$ the probability density for a transition of the system from the state $Q(X) = Q_0$, $P(X) = P_0$ at the initial moment t_0 to the state $Q(X) = Q$, $P(X) = P$ at time t. The probability density for the equilibrium values of Q and P in a Gibbs ensemble

$$w(X) = \exp\{[\Psi - H(X)]/\Theta\}$$

will be denoted by $W_0(Q, P)$. We have then, in accordance with reference 5

$$W(Q, P, t; Q_0, P_0, t_0) = \int_{(X^0)} \delta\{Q - Q(X^t)\}\,\delta\{P - P(X^t)\}\,\frac{\exp\{[\Psi - H(X^0)]/\Theta\}}{W_0(Q_0, P_0)} \times \delta\{Q_0 - Q(X^0)\}\,\delta\{P_0 - P(X^0)\}\,dX^0, \quad (1)$$

where X^t and X^0 are the canonical variables of the system at times t and t_0, which are connected through the relations $X^t = x(t; X^0, t_0)$ which are solutions of the dynamical equations with a Hamiltonian $H(X)$. From (1) we have clearly, for $t = t_0$,

$$W(Q, P, t_0; Q_0, P_0, t_0) = \delta(Q - Q_0)\,\delta(P - P_0).$$

If initially, at $t = t_0$, Q and P are given not exactly, but corresponding to some probability density $\rho(Q, P)$ the probability density at an arbitrary moment t will be defined as

$$W(Q, P, t) = \int_{(Q_0)}\int_{(P_0)} W(Q, P, t; Q_0, P_0, t_0)\,\rho(Q_0, P_0)\,dQ_0\,dP_0 = \int_{(X^0)} \delta\{Q - Q(X^t)\}\,\delta\{P - P(X^t)\} \times \exp\left\{\frac{1}{\Theta}[\Psi - H(X^0)]\right\}\frac{\rho\{Q(X^0), P(X^0)\}}{W_0\{Q(X^0), P(X^0)\}}\,dX^0. \quad (2)$$

Expression (1) is obtained from (2) for $\rho(Q, P)$

$= \delta(Q - Q_0)\,\delta(P - P_0)$. Similarly to what was done in reference 1, Eq. (2) can be written in the form

$$W(Q, P; t) = (2\pi)^{-2} \int_{-\infty}^{+\infty} \exp[i(\xi Q + \eta_i P)]\,\varphi(\xi, \eta_i; t)\,d\xi\,d\eta, \tag{3}$$

where φ is the characteristic function:

$$\varphi(\xi, \eta_i; t) = \int_{(X^0)} R\{Q(X^0), P(X^0)\} \exp\left\{-i[\xi Q(X^t) + \eta_i P(X^t)] + \frac{1}{\Theta}[\Psi - H(X^0)]\right\} dX^0, \tag{4}$$

$$R(Q, P) = \rho(Q, P) / W_0(Q, P). \tag{5}$$

It is obvious that the moments of the distribution (3) can be expressed in terms of φ as follows

$$\overline{Q^m P^n} = i^{m+n} \partial^{m+n}\varphi / \partial\xi^m \partial\eta_i^n |_{\xi,\,\eta=0}. \tag{6}$$

One can also give the funtions φ a different physical meaning. Let us introduce the quantity

$$Z(a, b; t) = \int_{(X^0)} R\{Q(X^0), P(X^0)\} \times \exp\left\{-\frac{1}{\Theta}[H(X^0) + aQ(X^t) + bP(X^t)]\right\} dX^0. \tag{7}$$

It is clear that for $a = i\xi\Theta$, $b = i\eta\Theta$

$$\varphi = e^{\Psi/\Theta} Z. \tag{8}$$

In the integrand of Eq. (7) we can replace $H(X^0)$ by $H(X^\tau)$ because of the conservation of energy, and dX^0 by dX^τ by virtue of Liouville's theorem. We can then consider the expression

$$\omega(X^\tau, \tau) = \frac{1}{Z} R\{Q(X^0), P(X^0)\} \times \exp\left\{-\frac{1}{\Theta}[H(X^\tau) + aQ(X^t) + bP(X^t)]\right\} \tag{9}$$

where we take into account that $X^t = x(t; X^\tau, \tau)$ and $X^0 = x(t_0; X^\tau, \tau)$, as the microscopic probability density for some non-equilibrium process satisfying the equation of motion for a phase ensemble:

$$\frac{\partial w}{\partial \tau} = [H, w]. \tag{10}$$

The moments taken over the ensemble (9) are obviously defined by the relations

$$\overline{Q^m P^n}^{a,b} = \frac{(-\Theta)^{m+n}}{Z} \frac{\partial^{m+n} Z}{\partial a^m\,\partial b^n}. \tag{11}$$

For a, b = 0 Eq. (11) is the same as (6).

Differentiating Z with respect to t we get also the relation

$$a\bar{Q}^{a,b} + b\bar{P}^{a,b} = -\frac{\Theta}{Z}\frac{\partial Z}{\partial t}. \tag{12}$$

We can thus evaluated φ and consequently also W if we know the moments (11) evaluated with respect to the non-equilibrium ensemble (9). Any information about these moments can only be obtained from a macroscopic experiment. A macroscopic experiment cannot give us, however, all moments, but only information about the change of the average values of Q and P in well defined non-equilibrium processes or the averaged equations of motion for these quantities. The problem thus arises of determining the equations of motion for Z and then also for W from the macroscopic equations of motion for Q and P.

THE EQUATION OF MOTION FOR THE PROBABILITY DENSITY

We shall write Eq. (9) for the microscopic probability density at time $\tau = t$ in the form

$$\omega(X^t, t) = \frac{1}{Z} R\{Q(X^0), P(X^0)\} \times \exp\left\{-\frac{1}{\Theta}[H(X^t) + aQ(X^t) + bP(X^t)]\right\}, \tag{13}$$

where $X^0 = x(t_0; X^t, t)$. This expression can be considered to be the non-equilibrium probability for a phase ensemble which is formed from an equilibrium ensemble with a Hamiltonian $H(X^t) + aQ(X^t) + bP(X^t)$ through a well defined fixing of the canonical variables X^t at time t by a given function $R\{x(t_0; X^t, t)\}$.

If we take into account that the momentum P enters into the Hamiltonian H only in the form of a term $P^2/2M$, as usual, we can consider an equilibrium system with a Hamiltonian H + aQ + bP as being under the action of an additional force $-a + M\dot{b}$, since

$$H + aQ + bP = H_1 + P^2/2M + bP + aQ = H_1 + (P + Mb)^2/2M - Mb^2/2 + aQ, \tag{14}$$

and hence

$$\dot{Q} = P/M + b, \quad \dot{P} = -\partial H_1/\partial Q - a,$$

or

$$M\dot{Q} = -\partial H_1/\partial Q - a + M\dot{b}. \tag{15}$$

If $\rho = W_0$, i.e., R = 1, the ensemble (13) with the Hamiltonian (14) is an equilibrium one and the average values of Q and P, determined from (15) are therefore equal to zero. If however, $\rho \neq W_0$, the averages $\bar{Q}^{a,b}$ and $\bar{P}^{a,b}$ are, clearly, different from zero since such an ensemble is not an equilibrium one. We shall determine these averages from a macroscopic experiment.

Let the macroscopic equations of motion for the particle be of the form

$$\dot{P} = F(\dot{Q}, Q) - a, \quad \dot{Q} = P/M - b. \tag{16}$$

where F is the sum of an external force of the potential type and a dissipative force, which depends in some arbitrary way on both $\dot{Q}$ and on Q. We shall assume that the motion averaged over the ensemble (13) is described by the Eqs. (16), i.e.,

$$\overline{P}^{a,b} = \overline{F(Q,\dot{Q})}^{a,b} = a, \quad \overline{\dot{Q}}^{a,b} = \overline{P}^{a,b}/M + b. \quad (17)$$

This is a natural physical assumption which is common to all theories developed so far, in any case for systems which are not too far from an equilibrium situation.

Combining (11), (12), and (17), using a transformation similar to the one used in reference 2, and introducing the velocity $V = P/M$ instead of the momentum we get for W the equation

$$\frac{\partial W}{\partial t} + V\frac{\partial W}{\partial Q} = \frac{1}{M}\frac{\partial}{\partial V}\sum_{n=0}^{\infty}\frac{(\Theta/M)^n}{n!}\frac{\partial^n}{\partial V^n}\left[W\frac{\partial^n}{\partial V^n}F(Q,V)\right]. \quad (18)$$

We have thus obtained a more general equation for the diffusion in coordinate-velocity space for a system with an arbitrary form of the macroscopic dissipative and potential forces.

It is evident that the expression for the transition probability density $W(Q, P, t; Q_0, P_0, t_0)$ can be obtained as a solution of Eq. (18) with the initial condition $W(Q, P; t_0) = \delta(Q - Q_0)\,\delta(P - P_0)$.

If

$$F(Q,V) = K(Q) + \gamma(Q)V, \quad (19)$$

Eq. (18) goes over into the usual Einstein-Fokker-Planck space-velocity equation of the form (see, e.g., reference 6)

$$\frac{\partial W}{\partial t} + V\frac{\partial W}{\partial Q} + \frac{K}{M}\frac{\partial W}{\partial V} = \frac{\gamma}{M}\frac{\partial}{\partial V}(VW) + \frac{\gamma\Theta}{M^2}\frac{\partial^2 W}{\partial V^2}. \quad (20)$$

In contradistinction to all known methods of deriving equations for the probability density, Eqs. (18) and (20) have been obtained by using only the general rules of statistical mechanics and a single assumption (17) about the averaged equations of motion. We have not made any assumptions about the Markov character of the random process or about the character of the correlations of the random collisional forces. We have thus obtained Eq. (18) starting from the most general assumptions.

THE GENERAL SOLUTION OF EQ. (18) FOR ONE PARTICULAR CASE

If the external force and the frictional force do not depend on the coordinates, i.e., $F(Q, V) = K + G(V)$, then Eq. (18), like Eq. (9) in reference 2, can be integrated by quadratures. The corresponding formula for the source function is of the form

$$W(q, v, \tau;\ q_0, v_0, \tau_0) = (2\pi i)^{-2}\int_{-i\infty}^{+i\infty}\int_{-i\infty}^{+i\infty}\exp\left\{\frac{1}{2}(p - v_0)^2 - \frac{1}{2}(s - v)^2 + \sigma\left[q - q_0 + \int_{p}^{s}\frac{\xi\,d\xi}{\overline{G}_1(\xi) + \sigma - K}\right]\right\}dp\,d\sigma,$$

$$\tau - \tau_0 = \int_{p}^{s(p,\sigma;\tau)} d\xi/[\overline{G}_1(\xi) + \sigma - K] = 0,$$

$$\overline{G}_1(\xi) = \frac{1}{\sqrt{2\pi}}\int_{-\infty}^{+\infty} e^{-(v-\xi)^2/2}\,G_1(v)\,dv, \quad (21)$$

where we have introduced the notation

$$\tau = t/\sqrt{M\Theta}, \quad v = V\sqrt{M/\Theta}, \quad q = Q/\Theta, \quad G_1(v) = G(v\sqrt{\Theta/M});$$

the function $s(p, \sigma; \tau)$ is determined by the second of Eqs. (21).

Following the method given here one can easily obtain equations similar to Eq. (18) also for other, non-mechanical, physical systems by suitably choosing in each concrete case the generalized coordinates, velocities and forces.

[1] V. B. Magalinskiĭ and Ya. P. Terletskiĭ, J. Exptl. Theoret. Phys. (U.S.S.R.) **34**, 729 (1958), Soviet Phys. JETP 7, 501 (1958).

[2] V. B. Magalinskiĭ, J. Exptl. Theoret. Phys. (U.S.S.R.) **36**, 1942 (1959), Soviet Phys. JETP **9**, 1381 (1959), this issue.

[3] V. V. Vladimirskiĭ, J. Exptl. Theoret. Phys. (U.S.S.R.) **12**, 199 (1942).

[4] Ya. P. Terletskiĭ, Nuovo cimento **7**, 308 (1958).

[5] Ya. P. Terletskiĭ, Динамические и статистические законы физики, (Dynamical and Statistical Laws of Physics), Moscow State Univ. Press, 1949.

[6] S. Chandrasekhar, Revs. Modern Phys. **15**, 1 (1943) (Russ. Transl. "Stochastic Problems in Physics and Astronomy," IIL 1949).

Translated by D. ter Haar
355

ELECTRICAL, OPTICAL AND ELASTIC PROPERTIES OF DIAMOND TYPE CRYSTALS
IV. INTERACTION BETWEEN CONDUCTION ELECTRONS AND LATTICE VIBRATIONS

V. S. MASHKEVICH

Kiev Polytechnic Institute

Submitted to JETP editor December 4, 1958

J. Exptl. Theoret. Phys. (U.S.S.R.) **36**, 1736-1742 (June, 1959)

We consider the interaction produced between conduction electrons and lattice vibrations by the polarization due to these vibrations. The possibility of existence of polaron states is investigated. The electron mobility is evaluated.

THE interaction of an electron with the lattice vibrations of an ionic crystal can be considered by taking into account the polarization caused by the vibrations even in the approximation of point-like ions. In the case of homeopolar crystals, there is no polarization in this approximation. This forces us to use either the Bloch potential, which does not completely represent the interaction,[1] or, as is commonly done lately, to use the deformation potential.[2,3] But, as shown in reference 4 (henceforth referred to as II,) consideration of the dipole moment of the atoms leads to a polarization due to lattice vibrations. This polarization should cause an interaction between the electron and the lattice vibrations. In this paper we develop on this basis a quantitative theory of the interactions. This theory is used to investigate the existence of polarons in the homeopolar crystals and to evaluate the mobility of the conduction electrons.

To simplify the calculation we do not take into the consideration the complexity of the isoenergetic surfaces in the conduction band,[5] but adopt a simple model of spherically symmetric surfaces with the center at $\mathbf{k} = 0$. This simplification is not a principal one, and can be got rid of by known methods.[6]

1. INERTIAL POLARIZATION OF THE CRYSTAL

We consider forced lattice vibrations at zero frequency, i.e., atomic displacement and dipole moments due to a constant external field. Let $\mathbf{D}'(\mathbf{r})$ be the intensity of the external electric field, $\mathbf{D}'_s(\mathbf{K})$ and $\mathbf{D}'(\mathbf{K})$ the Fourier coefficients in the expansion of $\mathbf{D}'(\mathbf{r}^l_s)$ in terms of reduced and free wave vectors:

$$\mathbf{D}'(\mathbf{r}^l_s) = \sum_{\mathbf{K}} \mathbf{D}'_s(\mathbf{K}) \exp(i\mathbf{K}\mathbf{r}^l_s), \qquad (1)$$

$$\mathbf{D}'_s(\mathbf{K}) = \sum_{\mathbf{b}} \mathbf{D}'(\mathbf{K} + 2\pi\mathbf{b}) \exp(i2\pi\mathbf{b}\mathbf{r}_s), \qquad (2)$$

where $\mathbf{r}^l_s$ are the coordinates of the s-th atom in the l-th cell, b the vector of the reciprocal lattice. Introducing the dimensionless Fourier coefficients

$$\mathbf{D}_s = (d^2/e)\mathbf{D}'_s, \quad \mathbf{D} = (d^2/e)\mathbf{D}'$$

(d is the lattice constant and e is the electron charge) we get the equations of vibrations, which we are interested in, from (4,II), in which we use a frequency $\Omega = 0$ and subtract $\mathbf{D}_1$ from the left hand side of the second equation:

$$L(\mathbf{v}_1 - \mathbf{v}_2) + F(\mathbf{w}_1 - \mathbf{w}_2) = i\mu\varkappa\,[(D/2)(\mathbf{s} \overset{+}{\times} \mathbf{v}_2) + (C/2)(\mathbf{s} \overset{+}{\times} \mathbf{w}_2)] - \mu^2\varkappa^2\varphi(\mathbf{v}_2; \mathbf{w}_2);$$

$$A\mathbf{w}_1 + F(\mathbf{v}_1 - \mathbf{v}_2) - (16\pi/3)\mathbf{w} + 16\pi(\mathbf{w}, \mathbf{s})\mathbf{s} - \mathbf{D}_1 = i\mu\varkappa \times [(C/2)(\mathbf{s} \overset{+}{\times} \mathbf{v}_2) + S(\mathbf{s} \overset{+}{\times} \mathbf{w}_2)] + \mu^2\varkappa^2\mathbf{f}(\mathbf{v}_2; \mathbf{w}_1; \mathbf{w}_2), \qquad (3)$$

where $\mathbf{v}_S$, $\mathbf{w}_S$ are the dimensionless amplitudes of the displacements and of the dipole moments; L, F, D, C, and A are the parameters of the theory; $\mu \sim 10^{-5}$ is the small parameter of the expansion; κ is the modulus of the dimensionless wave vector and $\mathbf{s}$ is the unit vector in its direction; φ and $\mathbf{f}$ linear functions of the amplitudes; $\mathbf{w} = \mathbf{w}_1 + \mathbf{w}_2$; S = 20 and 11. We can get two other equations by permuting the indices 1, 2 and by interchanging i and $-i$. The symbol $\overset{+}{\times}$ denotes as in the previous articles of this series,

$$(\mathbf{s} \overset{+}{\times} \mathbf{v}) = \mathbf{i}(s_y v_z + s_z v_y) + \ldots.$$

To investigate the polaron states we must (see references 7 and 8) find the inertial part of the crystal polarization. To find the amplitudes $\mathbf{w}^{(i)}_S$ of the dipole moments of the inertial polarization, we must solve Eq. (3) for $\mathbf{v}_S$, and holding these values constant, we put $\mathbf{D}_S = 0$. This gives us equations for $\mathbf{w}^{(i)}_S$, from which we can find

$$\mathbf{w}^{(i)}\,\mathbf{s} = 2\mu^2\varkappa^2\,(A + 64\pi/3)^{-1}\,[\gamma_1\,(\mathbf{v}_1^0 \overset{+}{\times} \mathbf{s}) \overset{+}{\times} \mathbf{s}$$

$$+ (\gamma_2 - S^2/A)\,(\mathbf{w}_1^0 \overset{+}{\times} \mathbf{s}) \overset{+}{\times} \mathbf{s} + \mathbf{f}\,(\mathbf{v}_1^0; 0; 0)]\,\mathbf{s},$$

$$\gamma_3\,(\mathbf{v}_1^0 \overset{+}{\times} \mathbf{s}) \overset{+}{\times} \mathbf{s} + \gamma_4\,(\mathbf{w}_1^0 \overset{+}{\times} \mathbf{s}) \overset{+}{\times} \mathbf{s} + \varphi\,(\mathbf{v}_1^0; \mathbf{w}_1^0) = 0,$$

$$\mathbf{w}_1^0 = \{\mathbf{D}_1 + \mathbf{D}_2 - [32\pi/(A + 64\pi/3)]\,(\mathbf{D}_1 + \mathbf{D}_2, \mathbf{s})\,\mathbf{s}\}$$

$$\times\,[2\,(A - 32\pi/3)]^{-1}, \qquad (4)$$

with the γ_i ($i = 1, 2, 3, 4$) expressed in terms of the parameters of the theory.

2. THE QUESTION OF THE EXISTENCE OF THE POLARON OF LARGE RADIUS

To investigate the polaron states we must vary the functional (see references 7 and 8)

$$J[\psi] = (\hbar^2/2m^*)\int |\nabla\psi|^2\,d\tau - \tfrac{1}{2}\sum_{ls} \mathbf{P}_s^l\,\mathbf{D}'\,(\mathbf{r}_s^l) = T + U,$$

$$\mathbf{P}_s^l = ed\sum_{\mathbf{K}} \mathbf{w}_s^{(i)}\,\exp\,(i\mathbf{K}\mathbf{r}_s^l), \qquad (5)$$

where m^* is the effective mass of the electron, and $\mathbf{D}'(\mathbf{r})$ is the induction produced by the electron in the state with wave function ψ.

Inserting (1) into (5) and summing over l, we get,

$$U = -\tfrac{1}{2}\,Ned\sum_{s\mathbf{K}} \mathbf{w}_s^{(i)}\,(\mathbf{K})\,\mathbf{D}'_s\,(-\mathbf{K}),$$

where N is the number of cells in the basic domain. In the case of states of large radius, $\mathbf{D}'(\mathbf{r})$ is a smooth function of the coordinates. In this case the Fourier coefficients are small for large values of the wave vector and we can discard in Eq. (2) the terms with $\mathbf{b} \neq 0$, thus getting

$$U = -\tfrac{1}{2}\,Ned\sum_{\mathbf{K}} \mathbf{w}^{(i)}\,(\mathbf{K})\,\mathbf{D}'\,(-\mathbf{K}).$$

We set, following Pekar,[7]

$$\psi\,(\mathbf{r}) = \gamma\,(1 + \alpha r)\,e^{-\alpha r}.$$

This leads to

$$J[\psi] = T_0\alpha^2 - U_0\alpha^3, \qquad T_0 = 3\hbar^2/14\,m^*,$$

$$U_0 = \frac{437\,e^2d^2}{(1792\,\pi)^2}\left(\frac{n_0^2 - 1}{n_0^2}\right)^2\int [\gamma_1\,(\mathbf{v}\overset{+}{\times}\mathbf{s})\overset{+}{\times}\mathbf{s}$$

$$+ \mathbf{f}\,(\mathbf{v}; 0; 0) + (\gamma_2 - S^2/A)\,(\mathbf{s}\overset{+}{\times}\mathbf{s})\overset{+}{\times}\mathbf{s}]\,s\,d\Omega, \qquad (6)$$

where $d\Omega$ is the element of solid angle in $\mathbf{K}$-space, $\mathbf{v}$ is determined from the equation

$$\gamma_3\,(\mathbf{v}\overset{+}{\times}\mathbf{s})\overset{+}{\times}\mathbf{s} + \gamma_4\,(\mathbf{s}\overset{+}{\times}\mathbf{s})\overset{+}{\times}\mathbf{s} + \varphi\,(\mathbf{v};\ s) = 0,$$

and n_0 is the index of refraction for waves of the largest wavelengths.

The results from above fit qualitatively with the results of Deĭgen and Pekar[3] and this indicates stability (or metastability) of the band state of the electron and also shows the absence of a polaron of large radius: $J[\psi]$ has a minimum at $\alpha = 0$.

3. INTERACTION OF THE ELECTRON WITH LATTICE VIBRATIONS AS A PERTURBATION

The mobility of the electrons, in the crystal under investigation, is large. This shows that the interaction of the electrons with the lattice vibrations is rather weak. This fact together with the absence of polarons permits one to consider the band electrons as the carriers and to consider their interaction with the lattice vibrations by perturbation-theory methods. The operator of this interaction is

$$\hat{V} = -\sum_{ls} \mathbf{P}_s^l\,\mathbf{D}'\,(\mathbf{r}_s^l), \qquad (7)$$

where $\mathbf{D}'$ is the intensity of the electric field of the electron. We introduce normal coordinates $q^\alpha(\mathbf{K})$:

$$\mathbf{P}_s^l = ed\sum_{\alpha\mathbf{K}} q^\alpha\,(\mathbf{K})\,\mathbf{w}_{s\alpha}\,(\mathbf{K})\exp\,(i\mathbf{K}\mathbf{r}_s^l), \qquad (8)$$

where α is the number of the branch of the spectrum of vibration. Inserting (8) and (1) into (7) and summing over l, we get

$$\hat{V} = -edN\sum_{s\alpha\mathbf{K}} q^\alpha\,(\mathbf{K})\,\mathbf{w}_{s\alpha}\,(\mathbf{K})\,\mathbf{D}'_s\,(-\mathbf{K}), \qquad (9)$$

$$\mathbf{D}'_s\,(\mathbf{K}) = \frac{4\pi ie}{V}\exp\,(-i\mathbf{K}\mathbf{r})\sum_{\mathbf{b}}\frac{\mathbf{K} + 2\pi\mathbf{b}}{|\mathbf{K} + 2\pi\mathbf{b}|^2}$$

$$\times\,\exp\,[i\,2\pi\mathbf{b}\,(\mathbf{r}_s - \mathbf{r})], \qquad (10)$$

where $\mathbf{r}$ are the coordinates of the electron and V is the volume of the basic domain.

The probability of transition per unit time due to perturbation (9) is

$$P_{\alpha'\mathbf{K}'}\,[\mathbf{p}, n_\alpha\,(\mathbf{K})]$$

$$= \frac{2\pi}{\hbar}\,|(\mathbf{p}, n_\alpha\,(\mathbf{K})\,|\,\hat{V}\,|\,\mathbf{p}^0, n^0{}_\alpha\,(\mathbf{K}))|^2\,\delta\,(E - E^0), \qquad (11)$$

where $\mathbf{p}^0$ and $\mathbf{p}$ are the quasi-momenta of the electron in the initial and final state; while $n^0_\alpha(\mathbf{K})$, $n_\alpha(\mathbf{K})$ are the corresponding numbers of phonons, with

$$n_\alpha\,(\mathbf{K}) = n_\alpha^0\,(\mathbf{K}) \mp \delta_{\alpha\mathbf{K},\,\alpha'\mathbf{K}'};$$

E^0 and E are the energies of the initial and final state. The reciprocal of the lifetime of the initial state is

$$\frac{1}{\tau_0} = \sum_{\mathbf{p},\, n_\alpha,\, \alpha',\, \mathbf{K}'} P_{\alpha'\mathbf{K}'}\, [\mathbf{p} n_\alpha(\mathbf{K})]$$

$$= \frac{2\pi}{\hbar} \sum_{\mathbf{p}\alpha\mathbf{K}}{}' \sum_{ijl}^{1,2} \left| F_\alpha(-1)^j \mathbf{K}, \mathbf{p}, \mathbf{p}^0) \right|^2 |(n^0_\alpha((-1)^j \mathbf{K})$$

$$+ (-1)^l | q^\alpha((-1)^j \mathbf{K})| \, n^0_\alpha((-1)^j \mathbf{K}))|^2 \delta(E - E^0), \quad (12)$$

where the prime means that the summation is to be taken over the half-space $\mathbf{K}$, and

$$F_\alpha(\mathbf{K}, \mathbf{p}, \mathbf{p}^0) = -ed \sum_s \mathbf{w}_{s\alpha}(\mathbf{K})$$

$$\times \int \mathbf{D}'(-\mathbf{K}) \exp\left(i \frac{\mathbf{p}^0 - \mathbf{p}}{\hbar} \mathbf{r}\right) u^*_{\mathbf{p}} u_{\mathbf{p}^0} d\tau, \quad (13)$$

and $u_{\mathbf{p}}$ is the Bloch function normalized to unity for the elementary cell Δ.

The integral in (13) differs from zero only if

$$\mathbf{K} + (\mathbf{p}^0 - \mathbf{p})/\hbar = 2\pi \mathbf{b}.$$

The transitions for which $\mathbf{b} \neq 0$ are the Peierls "Umklapp" processes. In the simple band model,[5] in the case of semiconductors with not very high temperatures, these processes can be ignored. In this case, inserting (10) into (13), we get

$$F_\alpha(\mathbf{K}, \mathbf{p}, \mathbf{p}^0) = \frac{4\pi i e^2 d}{\Delta} \sum_s \mathbf{w}_{s\alpha}(\mathbf{K}) \sum_b \frac{\mathbf{K} + 2\pi\mathbf{b}}{|\mathbf{K} + 2\pi\mathbf{b}|^2} \exp(-i 2\pi \mathbf{b} \mathbf{r}_s)$$

$$\times \delta_{\mathbf{K},\,(\mathbf{p}-\mathbf{p}^0)/\hbar} \int_{(\Delta)} \exp(i\, 2\pi \mathbf{b}\mathbf{r}) u^*_{\mathbf{p}} u_{\mathbf{p}^0} d\tau.$$

For most electrons the difference $\mathbf{p} - \mathbf{p}^0$ is small, therefore we can expand $u_{\mathbf{p}}$ in powers of this difference and retain only the linear factor. For $\mathbf{b} \neq 0$ the integral can be ignored, as it contains a rapidly oscillating term. When $\mathbf{b} = 0$ the term linear in $\mathbf{p} - \mathbf{p}^0$ vanishes because of the central symmetry of the crystals under investigation,[7] therefore the integral equals unity. So,

$$F_\alpha(\mathbf{K}, \mathbf{p}, \mathbf{p}^0) = \frac{4\pi i e^2 d}{\Delta} \frac{\mathbf{w}_\alpha(\mathbf{K})\, \mathbf{s}}{K} \delta_{\mathbf{K},\,(\mathbf{p}-\mathbf{p}^0)/\hbar}. \quad (14)$$

If we normalize the amplitude according to $I_{\alpha\alpha} = md^2$, (see reference 9, henceforth denoted by III), we get for the matrix elements in (12)

$$|(n_\alpha | q^\alpha | n_\alpha + 1)| = |(n_\alpha + 1 | q^\alpha | n_\alpha)|$$

$$= \tfrac{1}{2} [\hbar (n_\alpha + 1)/N m d^2 \omega_\alpha]^{1/2}, \quad (15)$$

where m is the atomic mass and ω_α is the frequency of vibration of the α branch. Inserting (15) and (14) into (12), summing up over $\mathbf{K}$, and passing from summation over $\mathbf{p}$ to integration, we get

$$\frac{1}{\tau^0} = \frac{e^4}{m\Delta\hbar^3} \sum_\alpha \int \frac{|\mathbf{w}_\alpha(\mathbf{K})\, \mathbf{s}|^2}{K^2 \omega_\alpha(\mathbf{K})} \sum_{i=1,2} [n^0_\alpha(\mathbf{K}) + n^0_\alpha(-\mathbf{K}) + 2\delta_{i1}]$$

$$\times \delta[E(\mathbf{p}) - E(\mathbf{p}^0) - \hbar\omega_\alpha(\mathbf{K})(1 - 2\delta_{i1})]\, p^2 dp d\Omega,$$

$$\mathbf{K} = (\mathbf{p} - \mathbf{p}^0)/\hbar, \; E(\mathbf{p}) = p^2/2m. \quad (16)$$

4. MOBILITY OF ELECTRON

According to II, the frequency of light oscillations is a rapidly growing function of the wave vector, therefore the scattering of electrons by these vibrations is practically insignificant.

In the case of acoustic vibrations the phonon energy can be ignored over a wide range of temperatures.[10] We can also ignore unity as compared with n^0_α and put

$$n^0_\alpha(\mathbf{K}) = kT/\hbar\omega_\alpha(\mathbf{K}).$$

Using all these simplifications and integrating in (16) over $\mathbf{p}$, we get for the reciprocal of the time of free path in the state $\mathbf{p}_0$, due to the scattering by the acoustical vibrations,

$$\frac{1}{\tau^0_{ac}} = \frac{4e^4 kT m^* p^0}{m\Delta\hbar^4} \sum_{\alpha\,(ac)} \int \frac{|\mathbf{w}_\alpha(\mathbf{K})\, \mathbf{s}|^2}{K^2 \omega^2_\alpha(\mathbf{K})} d\Omega,$$

$$\mathbf{K} = (\mathbf{p} - \mathbf{p}^0)/\hbar, \quad p = p^0. \quad (17)$$

From II, we get for the acoustical vibrations

$$\omega_\alpha(\mathbf{K}) = \Gamma \mu \varkappa \zeta_\alpha(\mathbf{s}), \quad \Gamma = em^{-1/2} d^{-1/2},$$

where $\zeta_\alpha \equiv \Omega_2/\kappa$ is the solution of the characteristic equation of the system (12,II),

$$\mathbf{w}_\alpha(\mathbf{K})\, \mathbf{s} = \mu^2 \varkappa^2 \Psi(\mathbf{s};\, \mathbf{v}^0_{1\alpha}),$$

$$\Psi(\mathbf{s}; \mathbf{v}) = 2[\gamma_1 (\mathbf{v} \overset{+}{\times} \mathbf{s}) \overset{+}{\times} \mathbf{s} + \mathbf{f}(\mathbf{v}; 0; 0)]\, \mathbf{s}/(A + 64\pi/3).$$

Inserting these results into (17) and averaging over the initial states of the electron, we get

$$\frac{1}{\tau_{ac}} = \frac{\sqrt{3}\, e^2 d^2}{\pi\hbar^4} \frac{(m^* k)^{3/2} T^{3/2}}{}$$

$$\times \sum_{\alpha\,(ac)} \int \zeta_\alpha^{-2}(\mathbf{s}) |\Psi(\mathbf{s}; \mathbf{v}^0_{1\alpha})|^2 d\Omega d\Omega^0. \quad (18)$$

The integration is performed here over all directions $\mathbf{p}^0$ (element of solid angle $d\Omega^0$) and over all directions $\mathbf{p}$.

Since the limiting frequency of the optical vibrations $\omega_{\lim}$ in the crystals under investigation is large, we can consider only the range $T < \hbar\omega_{\lim}/k$ in calculating the scattering of the electrons on the optical vibrations. In this case the creation of phonons is practically impossible and the second term in the brackets of Eq. (16) vanishes. For all three optical branches we can put

$$\omega_\alpha(\mathbf{K}) = \omega_{\lim}, \quad n^0_\alpha(\mathbf{K}) = [\exp(\hbar\omega_{\lim}/kT) - 1]^{-1}.$$

Inserting this into (16) and integrating over $\mathbf{p}$, we get

$$\frac{1}{\tau^0_{opt}} = \frac{2e^4 m^* [(p^0)^2 + 2m^* \hbar\omega_{\lim}]^{1/2}}{m\Delta\hbar^3 \omega_{\lim} [\exp(\hbar\omega_{\lim}/kT) - 1]} \sum_{\alpha\,(opt)} \int \frac{|\mathbf{w}_\alpha(\mathbf{K})\, \mathbf{s}|^2}{K^2} d\Omega,$$

$$\mathbf{K} = (\mathbf{p} - \mathbf{p}^0)/\hbar, \quad p^2 = (p^0)^2 + 2m^* \hbar\omega_{\lim}. \quad (19)$$

From II we get for optical vibrations

$w_a(\mathbf{K})\,\mathbf{s} = i\mu\varkappa[R_1/\varkappa_0^3(n_0^2-1)](\mathbf{v}_{1a}^0 \times \mathbf{s})\,\mathbf{s}, \quad \varkappa_0 = n_0\omega_{lim}/\Gamma,$

where R_1 is a combination of theory parameters, which appears in (30a,II). Inserting this result into (19) and averaging over $\mathbf{p}^0$, we get approximately

$$\frac{1}{\tau_{opt}} = \frac{e^4\gamma\,(m^*)^{3/2}\sqrt{2\hbar\omega_{lim}+3kT}}{16\pi^2\varkappa_0^4 n_0^2 m d\hbar^3\omega_{lim}[\exp(\hbar\omega_{lim}/kT)-1]} \times \sum_{a\,(opt)}\int|(\mathbf{v}_{1a}^0 \times \mathbf{s})\,\mathbf{s}|^2\,d\Omega d\Omega^0, \qquad (20)$$

where γ is expressed in terms of the parameters of the theory according to (16,III).

The mobility of the electron is

$$u = \tau e/m^*, \quad 1/\tau = 1/\tau_{ac} + 1/\tau_{opt}. \qquad (21)$$

According to (18), if we consider the scattering by acoustic vibrations only, we get for the temperature dependence of mobility the well known $^3/_2$ law. But the scattering by optical vibration gives, according to (20), a deviation from this law.

5. NUMERICAL RESULTS. COMPARISON OF THEORY WITH EXPERIMENT.

We represent u from (21), (18), and (20) in the form

$$u = (m^0/m^*)^{5/2}(e/N_1 m^0)[T^{3/2} + N_2 f(T)]^{-1}, \qquad (22)$$

where m^0 is the electron mass,

$$f(T) = (2\hbar\omega_{lim} + 3kT)^{1/2}[\exp(\hbar\omega_{lim}/kT) - 1]^{-1},$$

and the coefficients N_1 and N_2 are expressed in terms of a sum of integrals which appear in (18) and (20). These sums are calculated approximately in reference 11; the numerical values of the other parameters which enter in N_1 and N_2 are found in III. The numerical values of N_1 and N_2 are given in Table I.

TABLE I

	Diamond	Si	Ge
N_1	$0.5\cdot10^9$	$0.5\cdot10^9$	$0.5\cdot10^9$
N_2	$3.6\cdot10^{10}$	$1.3\cdot10^{10}$	$0.93\cdot10^{10}$

The presence of the term $N_2 f(T)$ in (22) causes a deviation from the $^3/_2$ law. For room temperatures and below, this deviation is most remarkable for germanium, because although N_2 increases in the direction from germanium to diamond, ω_{lim} also increases in this direction, and the latter is much more important. In the case of diamond and silicon, there was no deviation in the experiment from the $^3/_2$ law.[12,13] According to (22) these deviations should be insignificant for temperatures below 300° K. For germanium, according to the experimental data,[14] we can consider $u \sim T^{-1.65}$ in the temperature range 20 to 300° K. Table II lists the values of the ratio $T^{1.65}/F(T)$ [where $F(T) = T^{3/2} + N_2 f(T)$] for germanium in the range of 25 to 300° K. This ratio remains practically constant in the range 75 to 300° K (the experimental data are accurate to two significant figures; at this accuracy the ratio in the foregoing range is 1.9). For $T \lesssim 50°$ K the ratio slightly decreases with decreasing temperature. This is caused by the fact that for such low temperatures the optical vibrations play no role. For comparison, Table II lists also the values of the ratio $T^{3/2}/F(T)$, [which reduce to $T^{1.65}/F(T)$ at 150° K]. It can be seen that $T^{3/2}/F(T)$ changes in the temperature range under investigation even in the second significant figure.

In Table III the experimental values[12,14,15] of the mobility at 300° K are given together with the values of m^*/m^0 calculated from the values of mobility, using (22). The results lie in the range of values which, according to the experimental data, m^*/m^0 takes on for different directions in the crystal.

TABLE III. Computed values of effective mass

	Diamond	Si	Ge
u, (cm²/v sec)	1800	1900	4000
m^*/m^0	0.69	0.65	0.44

Therefore, the value of the mobility, calculated from the polarization that accompanies the lattice vibrations, is quite satisfactory. This opposes Shockley's point of view,[10] according to which the electric fields connected with the lattice vibrations are insignificant, as far as the interaction of the electron with lattice vibration is concerned. According to the results obtained above, the effect caused by these fields (which is the same as that caused by polarization) is almost the dominating one.

TABLE II. Temperature dependence of mobility in germanium

T, °K	300	250	200	150	100	75	50	25
$T^{1.65}/F(T)$	1.92	1.93	1.94	1.94	1.94	1.89	1.80	1.62
$T^{3/2}/F(T)$	2.16	2.10	2.04	1.94	1.84	1.76	1.65	1.49

5. CONCLUSIONS

1. The interaction between the conduction electrons and lattice vibrations of a homeopolar crystal can be investigated on the basis of the polarization due to these vibrations.

2. In homeopolar crystals the band state of electrons is stable (or metastable), and polarons of large radius should be missing.

3. The method developed in this paper to calculate the interaction gives correct results for the values of mobility and its temperature dependence.

This gives grounds for believing that the interaction between the electron and the electric fields due to the lattice vibrations plays a significant role.

The author thanks K. B. Tolpygo for a discussion of the results of this paper.

[1] F. Seitz, Phys. Rev. **73**, 549 (1948).

[2] W. Shockley and J. Bardeen, Phys. Rev. **77**, 407 (1950); J. Bardeen and W. Shockley, Phys. Rev. **80**, 72 (1950).

[3] M. F. Deigen and S. E. Pekar, J. Exptl. Theoret. Phys. (U.S.S.R.) **21**, 803 (1951).

[4] V. S. Mashkevich, J. Exptl. Theoret. Phys. (U.S.S.R.) **32**, 866 (1957), Soviet Phys. JETP **5**, 707 (1957).

[5] C. Herring, Bell System Techn. J. **34**, 237 (1955).

[6] W. P. Dumke, Phys. Rev. **101**, 531 (1956); C. Herring and E. Vogt, Phys. Rev. **101**, 944 (1956).

[7] S. E. Pekar, Исследования по электронной теории кристаллов (Investigation in the Electron Theory of Crystals), GITTL, M. 1951.

[8] K. B. Tolpygo, Dissertation, Kiev 1947.

[9] V. S. Mashkevich, J. Exptl. Theoret. Phys. (U.S.S.R.) **36**, 108 (1959). Soviet Phys. JETP **9**, 76 (1959).

[10] W. Shockley, The Theory of Electronic Semiconductors (Russ. Transl.) IIL, M. 1953.

[11] V. S. Mashkevich, Dissertation, Kiev 1956.

[12] A. G. Redfield, Phys. Rev. **94**, 256 (1954).

[13] M. B. Prince, Phys. Rev. **93**, 1204 (1954).

[14] F. J. Morin, Phys. Rev. **93**, 62 (1954); P. P. Debye and E. M. Conwell, Phys. Rev. **93**, 693 (1954).

[15] P. P. Debye and T. Kohane, Phys. Rev. **94**, 724 (1954); H. Welker, Physica **20**, 893 (1954).

[16] Dexter, Lax, Kip, and Dresselhaus, Phys. Rev. **96**, 222 (1954); Lax, Zeiger, and Dexter, Physica **20**, 818 (1954); C. Kittel, Physica **20**, 829 (1954).

Translated by S. Kotz
356

ON THE THEORY OF LATTICE SPIN RELAXATION

K. A. VALIEV

Kazan' Pedagogical Institute

Submitted to JETP editor December 8, 1958

J. Exptl. Theoret. Phys. (U.S.S.R.) **36**, 1743-1749 (June, 1959)

A theoretical discussion is given of relaxation in systems containing two types of interacting spins with very different values of their lattice relaxation times. The correlation function method is applied to the fast relaxing spin variables of the system.

1. INTRODUCTION

THE lattice relaxation of nuclear spins in diamagnetic crystals and liquids is the result of the modulation by heat motion of the magnetic dipole-dipole interactions between spins or of the interaction of the nuclear quadrupole moment with the non-uniform field of the charges surrounding the nucleus. Waller[1] constructed a theory of relaxation based on the magnetic interaction of particles for cubic crystals. Bloembergen et al.[2] were the first to give a theoretical consideration of relaxation through dipole interactions between particles in liquids. It was later shown that Bloembergen's theory also describes satisfactorily relaxation processes for spins in molecular diamagnetic crystals, for instance, in solid hydrogen.[3]

It is very characteristic for lattice relaxation in liquids that the changes in the coordinates which describe the heat motion of the system are fluctuating in time. If one considers the relaxation through the dipole interactions between particles, such randomly changing coordinates are the distances between the particles and the angles which the radius vector makes with the axes of the laboratory system of coordinates. In the paper[4] by Al'tshuler and the author devoted to the longitudinal relaxation of electron spins of paramagnetic ions which in a solution form octahedral complexes of the form XY_6 (X is the paramagnetic ion; Y is a molecule of the solvent or an anion) we considered as such randomly changing functions of the time the normal coordinates for the vibrations of the complex. The theoretical discussion of the relaxation process is facilitated by the fact that only a small number from the vast number of lattice coordinates will interact with each particular spin. Thus, with the spin of the X ion in the XY_6 complex only the coordinates of the normal vibrations of the complex will interact. The influence of the other "thermal" degrees of freedom of the system is manifest in producing the random character of the changes in all the other coordinates. The period of correlation for consecutive values for different coordinates must be determined separately and in each case individually.

In this paper we consider the relaxation process for spins of one kind which are connected through exchange of magnetic dipole forces with spins of another kind; the latter are assumed to relax independently of the former and very rapidly. Such a situation is realized in the following cases. The lattice relaxation of nuclei with a quadrupole moment takes place in molecular liquids through the interaction of the quadrupole moment with the electrical field of the surrounding charges, is fast, and is independent of the interaction with the spins of the other nuclei. At the same time, the relaxation of spins of nuclei without a quadrupole moment (protons) goes slowly and may depend strongly on the interaction with the spin of a nucleus with a quadrupole moment. This is confirmed by experiments studying the highly resolved nuclear magnetic resonance spectra: those lines in the spectrum which are caused by the protons which are chemically connected with the N^{14} nitrogen atoms are appreciably wider than the lines due to the other protons.[5] Another interesting example is the relaxation of the spins of the nuclei of paramagnetic atoms which takes place through the hyperfine interaction with the spins of the electron shells of the same atom. The lattice relaxation of the electron spin takes place independently of its interaction with the nuclear spins and with an appreciably larger speed than the relaxation of the nuclear spin. The situation is similar to the one discussed both in paramagnetic crystals and in liquids: the relaxation of the nuclear spins of diamagnetic atoms in such media takes place due to their coupling with the spins of the paramagnetic atoms, as is found out in the study of proton relaxation.[6]

We consider the fast relaxing spin variables of the system as randomly changing quantities, which can take on a number of discrete values, and treat them in the same way as fluctuating lattice coordinates that interact with relaxing spins. Such a representation of a part of the spin variables of the system simplifies the theoretical study of the relaxation process very greatly by making it very clear. From a thermodynamical point of view such a representation is completely permissible: it simply means assigning to the lattice structure those spins which interact strongly with it and separating into the "spin system" structure the spins that are weakly coupled to the lattice. It is clear that one must consider the lattice relaxation times of those spins which are assigned to the lattice as their correlation times. Since these spin variables are random functions of the time, we apply to them the method of correlation functions — both in the case of liquids and in the case of crystals.

Rivkind[6] and slightly later Bloembergen[7] have stated some of the methods used in our paper for the nuclear relaxation process to explain the experimental results on proton relaxation in liquid solutions of paramagnetic salts. Rivkind assumed that in a certain volume around the paramagnetic ion (in the solvate atmosphere of the ion) the mobility of the molecules of the solvent is limited and that in that volume the "change in quantization of the electron spin relative to an external static magnetic field" is a very fast process. Rivkind succeeded in explaining qualitatively his own experimental results by substituting in the formulae of Bloembergen et al.[2] for the electron spin relaxation time τ_e the correlation time for the thermal motion of the particles in the liquid τ_c. Bloembergen[7] assumed the existence of an exchange interaction of the form $A(\mathbf{I}\cdot\mathbf{S})$ between the spin of a proton in the first hydrate shell of the ion and the spin of the paramagnetic ion; such an assumption makes it possible to explain the difference between the times T_1 and T_2 for protons in solutions of Mn^{2+}, Gd^{3+}, and Fe^{3+} ions.

2. PROTON-RESONANCE QUADRUPOLE LINE BROADENING IN LIQUIDS

The indirect interaction between spins $\mathbf{I}_i$ and $\mathbf{I}_j$ belonging to nuclei in the structure of one molecule arises from taking into account the exchange overlap of the electron shells of atoms i and j. The energy of the resulting spin-spin interaction can be written in the form

$$\mathcal{H} = \hbar \sum_{i<j} A_{ij}\, \mathbf{I}_i \mathbf{I}_j \qquad (1)$$

The Hamiltonian (1) is invariant under rotations of the system of coordinates since a rotation of the molecule does not change its energy and therefore does not produce relaxation. We pick out from among all the nuclear spins in one separate molecule the spin $\mathbf{I}_k$ of the nucleus k which relaxes through quadrupole interaction with an appreciably greater speed than the spins of the other nuclei of the molecule. In accordance with what we have said a moment ago we can assume the spin $\mathbf{I}_k$ to be a variable which varies randomly with time; we can then take from (1) the part which depends on time and which leads to the relaxation of the spins $\mathbf{I}_i$:

$$\mathcal{H}'(t) = \hbar \sum_i A_{ik} [I_{zi} I_{zk}(t) + I_{xi} I_{xk}(t) + I_{yi} I_{yk}(t)]. \qquad (2)$$

The correlation times of the quantities I_{zk} and I_{xk}, I_{yk} will be equal to the longitudinal (τ_z) and transverse (τ_x, τ_y) relaxation times of the spin $\mathbf{I}_k$, respectively. For a liquid $\tau_x = \tau_y = \tau_z = \tau_k$ because of the fast thermal motion of the particles.

We shall denote the wave functions of the proton spin in a strong magnetic field by $\varphi_i(I_z = \frac{1}{2}) = |+\rangle$ and $\varphi_i(I_z = -\frac{1}{2}) = |-\rangle$; the wave functions of I_{xi} corresponding to the eigenvalues $I_{xi} = \frac{1}{2}$ and $-\frac{1}{2}$ can then be written in the form of linear combinations

$$\psi_i(\alpha) = (|+\rangle + |-\rangle)/\sqrt{2},$$
$$\psi_i(\beta) = (|+\rangle - |-\rangle)/\sqrt{2}. \qquad (3)$$

The probability that the system makes during 1 sec a transition from the state l to a state k under the action of the perturbation $\mathcal{H}'(t)$ can then be evaluated from the equation[8]

$$W_{lk} = \frac{1}{t\hbar^2} \left| \int_0^t \langle l | \mathcal{H}'(t') | k \rangle\, e^{-i\omega_{lk} t'}\, dt' \right|^2. \qquad (4)$$

The matrix elements corresponding to a transition between states of the spins $\mathbf{I}_i$ and $\mathbf{I}_k$ are equal to

$$\langle + | \mathcal{H}'(t') | - \rangle = \tfrac{1}{2} A\hbar\, [I_{kx}(t') - i I_{ky}(t')]_{m_k, m_k+1},$$
$$\omega_{lk} = \omega_i - \omega_k; \qquad (5)$$

$$\langle \alpha | \mathcal{H}'(t') | \beta \rangle = \tfrac{1}{2} A\hbar\, I_{zk}(t'), \qquad \omega_{lk} = 0. \qquad (6)$$

The matrix element (5) corresponds to a simultaneous change in orientation of the proton spin and the spin of the nucleus k; the generalized kinetic moment of the system is then conserved.

The lifetime of the proton spin in a state characterized by a well determined value of I_z is commonly called the longitudinal relaxation time T_1, and the life time in a state with a well defined value of I_x—the transverse relaxation time T_2.

Using the well known relation between transition probabilities and relaxation times[2] we get from (4), (5), and (6):

$$\frac{1}{2T_1} = W_{+-} = \frac{A^2}{4\hbar}\left|\int_0^t [I_{kx}(t') - iI_{ky}(t')]_{m_k, m_k+1} e^{-i(\omega_i - \omega_k)t'}\, dt'\right|^2, \quad (7)$$

$$\frac{1}{2T_2} = W_{\alpha,\beta} = \frac{A^2}{4\hbar}\left|\int_0^t I_{zk}(t')dt'\right|^2 \quad (8)$$

We shall perform the further evaluations of the integrals by taking an exponential law for the change of the correlation functions of the quantities I_{zk}, I_{xk}, I_{yk} with the same correlation time τ_k:

$$\langle I_{zk}(t')\, I_{zk}(t'+\tau)\rangle = \tfrac{1}{3} I_k(I_k+1)\exp(-\tau/\tau_k); \quad (9)$$

$$\langle I_{xk}(t')\, I_{xk}(t'+\tau) + I_{yk}(t')\, I_{yk}(t'+\tau)\rangle = \tfrac{2}{3} I_k(I_k+1)\exp(-\tau/\tau_k). \quad (10)$$

The relaxation times T_1 and T_2 obtained in this way are quantities which are averaged over all the protons in the specimen:

$$T_1^{-1} = \tfrac{2}{3} A^2 I_k(I_k+1)\tau_k/[1 + (\omega_i - \omega_k)^2\tau_k^2]; \quad (11)$$

$$T_2^{-1} = A^2 I_k(I_k+1)\tau_k/3. \quad (12)$$

If the condition $A\tau_k \lesssim 1$ is fulfilled Eqs. (11) and (12) are applicable. This condition is similar to inequality (6.24) from the paper by Kubo and Tomita[9] and is the criterion that one broad line exists instead of a spectrum of discrete lines; if the inequality is strengthened to $A\tau_k \ll 1$, a "narrowing of the line by motion" arises. Such a change occurs, for instance, in the spectrum of the hyperfine structure lines of electron resonance under the action of a fast exchange motion in the spin system,[10] and a narrowing of the nuclear resonance lines due to a fast molecular motion in liquids has been theoretically established already in reference 2. Equations (11) and (12) demonstrate a new example of similar changes in a spectrum produced by the fast relaxation of one of the interacting spins. If $A > \tau_k^{-1}$ the proton line will be split into $2I_k + 1$ components; if $A \lesssim \tau_k^{-1}$ the components merge together, forming one line; and if $A \ll \tau_k^{-1}$ the proton lines narrow because of the fast relaxation of the spin I_k.

Let us now make a numerical estimate of the relaxation times T_1 and T_2. The relaxation time τ_k of the spins which are coupled with the thermal motion through the nuclear quadrupole moment is in liquids $\sim 10^{-4}$ sec, $|\omega_i - \omega_k| = 10^7$ cps. The value of the spin-spin coupling constant depends on the number of chemical bonds which separate the nuclei and is of the order of 200, 50, and 10 cps if the proton and the nucleus k are separated by one, two, and three chemical bonds, respectively.[11] If the proton is directly joined to an atom, the nucleus of which possesses a quadrupole moment, the values calculated with Eq. (11) are $T_1 = 10^5$ sec and $T_2 = 0.3$ sec. The contribution from the spin-spin coupling of the protons and the other nuclei to the longitudinal relaxation is thus extremely small compared to the contribution to this relaxation from the dipole-dipole interaction of the nuclei. It is clear that the broadening of the "spread out" proton lines is caused by the strengthening of the transverse relaxation of the proton spins, i.e., by the occurrence of an unresolved structure due to the spins of nuclei which possess a quadrupole moment; this broadening is of the order $1/T_2 \approx 10$ cps which agrees well with the observed line width. Since the longitudinal relaxation of the protons which give a broad line takes place through magnetic dipole interactions, the ratio T_1/T_2 for them must differ considerably from unity.

Equation (12) makes it possible to determine the value of the spin-spin coupling constant A_{ik} from the broadening of the proton lines produced by this coupling. This method is possibly unique since the spin-spin coupling with a fast relaxing spin does not produce a splitting of the lines. We must note that the produced broadening depends essentially on the relaxation time of the spins I_k.

3. RESONANCE PHENOMENA IN SPIN-LATTICE RELAXATION

The systems considered by us contain two kinds of spins: the spins of the first kind have a long lattice relaxation time, and the spins of the second kind have an appreciably shorter time. In such systems the relaxation time of the first spins is shortened when the energy intervals between the sublevels of these and of the other spins are the same. This experimental fact can be explained using Eq. (11). We shall put $\omega_i = \omega_k$; we have then:

$$T_1^{-1} = \tfrac{2}{3} A^2 I_k(I_k+1)\tau_k. \quad (18)$$

The quantity A characterizes the interaction energy of spins with different relaxation times. In this way we get for the case of a coupling between protons and nuclei with a quadrupole moment, which we considered above, for the same values of the parameters, $T_1 \approx 0.1$ sec. The value of T_1 which characterizes the relaxation of protons through dipole interactions is in molecular liquids about 10 sec. The time T_1 can thus be decreased

by a factor 100 in the case of "relaxation resonance" for a proton and a nucleus relaxing through a quadrupole moment.

From this example the nature of relaxation resonance is clear although it is apparently not possible to realize it, because in liquids the quadrupole interaction of a nucleus does not lead to a constant contribution in the splitting of the spin levels and the intervals between those are determined by the Zeeman energy of the spins. The intervals $\Delta E(m_i, m_i \pm 1)$ and $\Delta E(m_k, m_k \pm 1)$ between pairs of levels of two spins I_i and I_k belonging to nuclei of the foregoing two kinds, which are unequal for one value of the field, may become equal for another value of the field only if there is already a splitting of the levels: the quadrupole splitting of nuclear spin levels in diamagnetic crystals or the electrical splitting of electron spin levels in paramagnetic crystals. It is clear that the strongest interaction between the nuclear spins in diamagnetic crystals will be the magnetic dipole interactions. The latter, and also an exchange interaction of the form (1), can provide a transfer of energy absorbed by one kind of spins to spins of the other kind which are strongly coupled to the thermal motion in the lattice. The absorbed energy goes over from the latter into the thermal motion of the particles in the system.

If such a mechanism is present resonance phenomena can arise in relaxation processes. Such an occurrence was observed experimentally in crystals of paradichlorobenzene.[12] In these crystals the proton lattice relaxation time T_{1p} was greatly decreased at the moment when the proton resonance frequency ν_p became the same as the interval ν_Q between a pair of nuclear spin levels of chlorine. We can estimate the proton relaxation time T_{1p} when there is relaxation resonance with the chlorine nucleus: $\nu_p = \nu_Q$. The matrix element corresponding to the transition $(m_p = \frac{1}{2}, m_k;\ m_p = -\frac{1}{2},\ m_k + 1)$ which is produced by the dipole interaction is equal to[2]

$$\langle \tfrac{1}{2}, m_k | V_{ik} | -\tfrac{1}{2}, m_k + 1 \rangle = -\tfrac{1}{4} g_i g_k \beta_N^2 r_{ik}^{-3} (1 - 3\cos^2\theta_{ik}) \times \sqrt{(I_k - m_k)(I_k + m_k + 1)}. \quad (19)$$

Here g_i and g_k are the g-factors of the nuclei i and k, while β_N is the nuclear magneton. The angle θ_{ik} and the distance r_{ik} between the nuclei are constant quantities since the crystal retains its orientation in a static magnetic field. If $\omega_i = \omega_k$ we get instead of Eq. (18) the equation

$$W_{+,-} = \hbar^{-2} (g_i g_k \beta_N^2 r_{ik}^{-3})^2 (1 - 3\cos^2\theta_{ik})^2 I_k (I_k + 1)/12. \quad (20)$$

The energy of the dipole interaction between two nuclear spins is of the order of 10^{-23} erg and the lattice relaxation time of Cl nuclei at room temperature is of the order 10^{-2} sec. Substituting these quantities into (20) we get $T_{1p} = 10^{-1}$ sec for the proton relaxation time under the conditions of relaxation resonance, while T_{1p} would be of the order of a minute if there were no resonance. The relaxation resonance observed in crystals containing two kinds of paramagnetic ions with different lattice relaxation times is apparently caused also by the dipole-dipole interaction between them (the effect is observed in crystals containing the ions[13] Co^{2+} and Fe^{2+} and the ions[14] Gd^{3+} and Ce^{3+}). The matrix element of the energy of the dipole interaction between two particles is in that case $|V_{ij}| \sim 10^{-17}$ erg; we can take $\tau_e = 10^{-11}$ sec for the lattice relaxation time of spins tightly coupled to the lattice. We then get for relaxation times of spins, which under normal conditions have a long time T_1, under resonance conditions,

$$T_{1\,res}^{-1} \sim |V_{ij}|^2 \hbar^{-2} \tau_e \sim 10^6\ \text{sec}^{-1}. \quad (20a)$$

It is clear that one can estimate using Eq. (20a) very short relaxation times τ_e which cannot be measured by other methods; to do this it is necessary to determine the very long time $T_{1\,res}$ and to estimate the magnitude of the matrix element (19). We note that the applicability of Eqs. (20) and (20a) is determined by criteria which are similar to those stated when we discuss Eqs. (11) and (12).

4. LATTICE RELAXATION OF NUCLEI CONNECTED WITH PARAMAGNETIC ATOMS

One can study also the lattice relaxation of spins of nuclei of paramagnetic atoms in a way similar to the one above. This problem was considered by perturbation theory methods in the papers by the author[15] and Bashkirov.[16] The electron spin of paramagnetic ions in condensed media relaxes with a velocity $1/\tau_e$ which is appreciably larger than the velocity of the relaxation of the nuclear spin of the paramagnetic ion. The relaxation of the latter takes place through a hyperfine interaction with electron spins. The components of the electron spin entering into the hyperfine interaction energy can be considered to be quantities which change rapidly and in a random fashion:

$$H'(t) = A I_z S_z(t) + B[I_x S_x(t) + I_y S_y(t)]. \quad (21)$$

The probability for a relaxation transition between the sublevels of the nuclear spin energy can be expressed through a formula analogous to (7):

$$W_{m,m-1} = \frac{B^2}{4\hbar^2 I}\left|\int_0^t [S_x(t') - iS_y(t')]_{M-1,M} e^{-i(\omega_N-\omega_S)t'}\,dt'\right|^2$$

$$\times (I+m)(I-m+1). \qquad (22)$$

If we consider a medium with a small concentration of magnetic particles we can neglect the dipole-dipole and exchange effects and assume the correlation times of the quantities S_x, S_y, and S_z to be the spin-lattice relaxation time of the electron spin τ_e. We get then from (22), similar to (11):

$$W_{m,m-1} = B^2(I+m)(I-m+1)$$

$$\times S(S+1)\tau_e/3\hbar^2(1+(\omega_N-\omega_S)^2\tau_e^2). \qquad (23)$$

In the practically important case $\omega_S = g_e\beta H_0/\hbar \geq \tau_e^{-1}$, $\omega_S \gg \omega_N$ we have

$$W_{m,m-1} = B^2(I+m)(I-m+1)$$

$$\times S(S+1)/3\hbar^2(g_e\beta H_0)^2\tau_e, \qquad (24)$$

which agrees with the result of the calculation by the perturbation-theory method.[13,14] We can also use Eqs. (23) and (24) to evaluate the relaxation of the nuclei of paramagnetic atoms in liquids. The evaluation of τ_e for that case was given in reference 4.

In paramagnetic media at high temperatures the condition $\omega_e < \tau_e^{-1}$ is also often realized, when it becomes impossible to observe magnetic resonance. Under those conditions

$$W_{m,m-1} = B^2(I+m)(I-m+1)$$

$$\times S(S+1)\tau_e\hbar^{-2}/3 \sim 10^7 \text{ sec}^{-1}, \qquad (25)$$

($B = 3\times10^{-3}$ cm^{-1}, $\tau_e = 3\times10^{-11}$ sec). Such a fast nuclear relaxation can show up when one studies angular correlations of the radioactivity from nuclei: the angular correlation between the directions of two consecutive processes of emission by the nucleus will occur within a time interval[8] $\tau \leq W_{m-1,m}^{-1}$.

The transverse relaxation time of the spins of the nuclei of paramagnetic ions is determined by a formula similar to (12):

$$T_{2N}^{-1} \approx 4A^2\hbar^{-2}S(S+1)I(I+1)\tau_e/9. \qquad (26)$$

One can interpret this quantity as follows. The nuclear resonance line for paramagnetic atoms has a fine structure of $2I(2S+1)$ components in accordance with the fact that for each of the $2S+1$ electron spinlevels of each atom there are $2I$ energy intervals $\Delta E_{m,m-1}$ between which nuclear magnetic dipole transitions are allowed. Due to the fast relaxation of the electron spin in this spectrum there occurs a change which is similar, for instance, to the change in the hyperfine structure of the electron resonance lines caused by the fast exchange motion of the spins: if $A/\hbar \gg \tau_e^{-1}$ all lines will be observed to be separate (the conditions for Eq. (26) are then, generally speaking, not fulfilled); if $\hbar^{-1}A \lesssim \tau_e^{-1}$, the components of the line merge together giving a line of width $\Delta\nu \sim T_{2N}^{-1} + T_{1N}^{-1}$; finally, if $A/\hbar \ll \tau_e^{-1}$, a strong narrowing of the nuclear resonance line sets in, owing to the fast lattice relaxation of the electron spin. It would be very interesting to carry out an experiment on nuclear resonance in paramagnetic atoms under the conditions of a strong relaxation narrowing. Such experiments, in our opinion, are most easily carried out on impurity paramagnetic atoms in crystalline silicon. It is clear that the experiments can be successful if the relaxation times of the nuclear spins T_{1N} and T_{2N} are not shorter than 10^{-5} sec. For a Li atom in silicon[17] $A/\hbar = B/\hbar = 0.85$ Mcs. We then get from Eqs. (24) and (26) the values $T_{1N} = 2\times10^{-2}$ sec and $T_{2N} = 1.4\times10^{-5}$ sec, if $\omega_S = 10^{10}$ cps and $\tau_e = 10^{-8}$ sec (the time τ_e can be decreased by increasing the temperature of the crystal).

We can similarly establish the conditions for a strong narrowing of the magnetic resonance line for nuclei of paramagnetic atoms (ions) of the iron group and of the rare earths in crystals of salts.

In conclusion the author expresses his deep gratitude to Professor S. A. Al'tshuler and Professor B. M. Kozyrev for discussing his results.

[1] I. Waller, Z. Physik **79**, 370 (1932).
[2] Bloembergen, Purcell, and Pound, Phys. Rev. **73**, 679 (1948).
[3] T. Sugawara, Sc. Repts. Res. Inst. Tohoku Univ. **A8**, 95 (1956).
[4] S. A. Al'tshuler and K. A. Valiev, J. Exptl. Theoret. Phys. (U.S.S.R.) **35**, 947 (1958), Soviet Phys. JETP **8**, 661 (1959).
[5] J. D. Ray and R. A. Ogg, J. Chem. Phys. **26**, 1452 (1957); R. A. Ogg and J. D. Ray, J. Chem. Phys. **26**, 1515 (1957).
[6] A. I. Rivkind, Dokl. Akad. Nauk SSSR **102**, 1197 (1955).
[7] N. Bloembergen, J. Chem. Phys. **27**, 572 (1957).
[8] A. Abragam and R. V. Pound, Phys. Rev. **92**, 943 (1953).
[9] R. Kubo and K. Tomita, J. Phys. Soc. Japan **9**, 888 (1954).
[10] D. Kivelson, J. Chem. Phys. **27**, 1087 (1957).
[11] C. H. Holm, J. Chem. Phys. **27**, 707 (1957).
[12] M. Goldman, Compt. rend. **246**, 1038 (1958).

[13] T. Haseda, Physica **24**, 93 (1958).
[14] G. Feher and H. E. D. Scovil, Phys. Rev. **105**, 760 (1957).
[15] K. A. Valiev, Физика металлов и металловедение (Phys. of Metals and Metal Research) **6**, 193 (1958).
[16] Sh. Sh. Bashkirov, Уч. зап. Казанск. ун-та, (Sci. Notes, Kazan' Univ.) **117** (No. 9), 154, 157 (1957).
[17] G. Feher, Phys. Rev. **103**, 834 (1956).

Translated by D. ter Haar
357

USE OF SCATTERING AMPLITUDE TO RECONSTRUCT THE POTENTIAL NEAR ITS BOUNDARY

A. G. CHICHERIN

Submitted to JETP editor December 1958

J. Exptl. Theoret. Phys. (U.S.S.R.) **36**, 1750-1757 (June, 1959)

The "asymptotic Born approximation" is formulated from the scattering amplitude for a potential that coincides with the true potential at sufficiently large radii. The order of magnitude of the relative error in the determination of the scattering potential at a point r is $\int_r^\infty U(r')\,r'dr'$. The case where the scattering amplitude is given in a finite energy interval is considered.

INTRODUCTION

THE methods presented in the literature for solving the problem of potential reconstruction use, as data on scattering, the phase corresponding to one of the values of the orbital momentum.[1-3] An exception is the work of Moses,[4] who uses the amplitude of the backward scattering. The use of the scattering amplitude instead of the phase is more logical, first because it may, in principle, be determined from the scattering cross section without a phase analysis,[5] and second because the use of the scattering amplitude makes it possible to consider arbitrary and not only spherically symmetric potentials.

In the case of an arbitrary potential, the scattering amplitude depends on five values: the energy and the components of two unit vectors, in the directions of the initial and final momenta. The potential depends only on three components of the radius vector. The resulting indeterminacy of the inverse problem is easiest to eliminate for weak potentials: in that case, the scattering amplitude depends, in first approximation, only on the vector of momentum transfer, i.e., on three parameters. A simple Fourier transformation is then sufficient to reconstruct the potential simultaneously in the whole space. For strong potentials, the first Born approximation for the scattering amplitude is correct only for large energies and for not very small vectors of momentum transfer. This means that, in the case of strong potentials, the first Born approximation for the potential is meaningless.

In the present paper we shall construct an "asymptotic Born approximation" for a potential having the following properties: in the case of weak potentials, it coincides with the usual first approximation and yields the real potential simultaneously in the whole space. As the potential increases, the accuracy of the approximation decreases, but not uniformly; it decreases faster near the central regions and slower near the potential boundary. (Only potentials lying wholly in a certain finite region of the space are considered.) Thus, the "asymptotic approximation" for a potential of any value will correctly reconstruct its behavior in a certain layer near the boundary; the thickness of the layer is determined by the value of the potential.

The simplicity of constructing the "asymptotic approximation" makes it easily possible to assess errors introduced by the finiteness of the energy interval in which the scattering amplitude is given. Thus, in the framework of this approximation, one can disregard the academic problem of determining the potential from data at all energies from zero to infinity, and approach the solution of the practical problem formulated by Smorodinskiĭ,[6] that of reconstructing the potential from a scattering amplitude given in a finite energy interval. The over-determination of the problem is also removed in this approximation. It is found that, in order to construct the "asymptotic approximation," only the dependence of the scattering amplitude on the momentum transfer vector is essential.

All proofs use the representation of the scattering amplitude by a Born approximation series (the derivation of which can be seen for instance, in the paper by Moses,[4] Sec. 5). The one-dimensional Fourier transformation of this series for fixed directions of the incident and scattering particle was used by Wong[7] to obtain the dispersion relations in the nonrelativistic case. In the same

paper, a method of determining the potential boundary from the scattering amplitude is given.

Strictly speaking, all assumptions of the present paper are correct only for potentials for which the Born approximation series converges uniformly for all energies. However, the character of the results makes it possible to assume that the use of these series is only a subsidiary means, which makes the proof simpler, but the basic result is correct also for potentials for which the Born approximation series for the scattering amplitude is divergent.

1. FOURIER TRANSFORMATION

The scattering amplitude is a function of the wave number k and the two unit vectors $\mathbf{n}_1$ and $\mathbf{n}_2$ in the direction of the initial and final momentum of the particle, defined only for positive values of k. It will be convenient, however, to consider a definition extended to the negative values of k by means of the equation

$$f(\mathbf{n}_2, k, \mathbf{n}_1) = f^*(\mathbf{n}_2, |k|, \mathbf{n}_1), \quad k < 0. \tag{1}$$

We shall introduce new variables $\mathbf{n}$ and $\mathbf{N}$:

$$\mathbf{n} = \mathbf{n}_2 - \mathbf{n}_1, \qquad n \leqslant 2, \tag{2}$$

$$\mathbf{N} = (\mathbf{n}_2 + \mathbf{n}_1)/2, \qquad N \leqslant 1, \tag{3}$$

and the momentum transfer vector $\mathbf{q}$:

$$\mathbf{q} = k\,\mathbf{n}_2 - k\,\mathbf{n}_1 = k\,\mathbf{n}, \qquad \mathbf{q}_0 = \mathbf{q}/q, \tag{4}$$

The vectors $\mathbf{n}$ and $\mathbf{N}$ are orthogonal and their absolute values are determined by the polar scattering angle ϑ:

$$\cos\vartheta = (\mathbf{n}_2\mathbf{n}_1), \qquad n = 2\sin(\vartheta/2), \qquad N = \cos(\vartheta/2). \tag{5}$$

The scattering amplitude can also be considered as a function of the new variables q, $\mathbf{q}_0$, and $\mathbf{N}$ where, according to Eq. (1), the value q takes all possible values $-\infty < q < \infty$.

We shall fix the direction of the initial and final momenta or, which is the same, of the vectors $\mathbf{q}_0$ and $\mathbf{N}$, and we shall perform the following Fourier transformation:

$$F(\rho, \mathbf{q}_0, \mathbf{N}) = 2\int_{-\infty}^{\infty} f(q, \mathbf{q}_0, \mathbf{N}) \exp(iq\rho)\, dq$$

$$\equiv 2\int_{-\infty}^{\infty} f(\mathbf{n}_2, k, \mathbf{n}_1) \exp(ik\mathbf{n}\rho)\, d(kn). \tag{6}$$

The function F may be written as a series

$$F(\rho, \mathbf{q}_0, \mathbf{N}) = (4\pi)^{-1} \sum_{l=1}^{\infty} (-1)^l U_l(\rho, \mathbf{q}_0, \mathbf{N}), \tag{7}$$

the terms of which are determined by the scattering potential U(r), and which represent the Fourier transformations of the terms of the Born approximation series

$$U_l(\rho, \mathbf{q}_0, \mathbf{N}) = 2\int_{-\infty}^{\infty} B_l(\mathbf{n}_2, k, \mathbf{n}_1) \exp(ik\mathbf{n}\rho)\, n\, dk. \tag{8}$$

Because of the exponential dependence of B_l on k, after integrating over dk in the expression for U_l, the one-dimensional δ-function appears under the sign of integration over the coordinates:

$$U_1(\rho, \mathbf{q}_0) = \int U(\mathbf{r})\, \delta(-\mathbf{q}_0\mathbf{r} + \rho)\, d\mathbf{r}, \tag{9}$$

$$U_l(\rho, \mathbf{q}_0, \mathbf{N}) = (4\pi)^{-l+1}$$

$$\times \int \frac{U(\mathbf{x})\, U(\mathbf{z}_1) \ldots U(\mathbf{z}_{l-2})\, U(\mathbf{y})}{|\mathbf{x} - \mathbf{z}_1| \ldots |\mathbf{z}_{l-2} - \mathbf{y}|}\, \delta(-\mathbf{n}_2\mathbf{x} + |\mathbf{x} - \mathbf{z}_1| + \ldots$$

$$\ldots + |\mathbf{z}_{l-2} - \mathbf{y}| + \mathbf{n}_1\mathbf{y} + n\rho)\, n\, dk \ldots d\mathbf{y}. \tag{10}$$

Setting the arguments of the δ-function equal to zero, we obtain equations that determine the range of integration over the coordinates.

The first term is especially simpie

$$U_1(\rho, \mathbf{q}_0) = \int_{\mathbf{r}\mathbf{q}_0 = \rho} U(\mathbf{r})\, dS, \tag{11}$$

and reduces to a double integral of the potential in the plane determined by the following equation:

$$\mathbf{r}\mathbf{q}_0 = \rho. \tag{12}$$

This plane is perpendicular to the vector $\mathbf{q}_0$, and its distance from the point of origin of the coordinates is equal to ρ if we consider the direction of $\mathbf{q}_0$ as positive.

The remaining terms are analyzed in detail in the Appendix, where it is shown that the integration over all variables is carried out only in that part of the space where

$$\mathbf{r}\mathbf{q}_0 \geqslant \rho. \tag{13}$$

The first conclusion we can draw is that if the plane (12) lies beyond the potential boundaries (see figure, straight line 1), then the transforma-

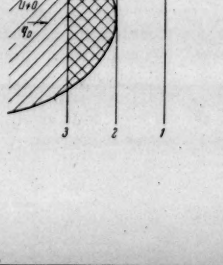

tion (6) of the scattering amplitude equals zero:

$$F(\rho, \mathbf{q}_0, \mathbf{N}) \equiv 0, \quad \rho \geqslant R(\mathbf{q}_0). \tag{14}$$

The radius of the potential in the direction $\mathbf{q}_0 R(\mathbf{q}_0)$ is equal to that value of ρ for which the plane (12) is tangent to the potential boundary (straight line 2 in the figure). Equation (13) was first obtained by Wong.[7]

In the Appendix it is also shown that, for $\rho < R(\mathbf{q}_0)$, the value of the first term in the series (7) and the sum of the other terms can be estimated in the following way:

$$|U_1(\rho, \mathbf{q}_0)| \approx \overline{U r}^2, \tag{15}$$

$$\left|\sum_{l=r}^{\infty} U_l\right| \approx (\overline{U r^2})\,(\overline{U \Delta^2}), \tag{16}$$

where $\overline{r}$ represents the mean linear dimensions of the area cut in the region $U \neq 0$ by the plane (12). These estimates are basically correct only for small values of the difference Δ:

$$\Delta = R(\mathbf{q}_0) - \rho. \tag{17}$$

The value of $\overline{\Delta}$ in Eq. (16) is equal to the smallest of the numbers $\overline{r}$, Δ

$$\overline{\Delta} = \min\{\overline{r}, \Delta\}. \tag{18}$$

From the estimates (15) and (16), it follows that in the equation

$$F(\rho, \mathbf{q}_0, \mathbf{N}) = U_1(\rho, \mathbf{q}_0)[1 + \varepsilon(\rho, \mathbf{q}_0, \mathbf{N})] \tag{19}$$

the value of ϵ for sufficiently small Δ is determined by the following approximate relations

$$|\varepsilon(\rho, \mathbf{q}_0, \mathbf{N})| \approx \overline{U}\,\overline{\Delta}^2 \leqslant \overline{U}\,\overline{r}^2$$

$$\approx |U_1(\rho, \mathbf{q}_0)| \approx |F(\rho, \mathbf{q}_0, \mathbf{N})|. \tag{20}$$

We summarize the results of this section: Let the scattering amplitude be given in such a way that the vector $\mathbf{q}_0$ assumes all possible directions and the length of the momentum-transfer vector goes through all possible values from zero to infinity for each direction of $\mathbf{q}_0$. In such a case, the scattering amplitude permits us to construct a function $F(\rho, \mathbf{q}_0, \mathbf{N})$ for all values of ρ and directions $\mathbf{q}_0$. According to Eq. (14), this function is identically equal to zero for sufficiently large values of ρ. The largest value of ρ for which F is different from zero determines the potential boundary in the direction $\mathbf{q}_0$, namely the value $R(\mathbf{q}_0)$. It is evident that the envelope of all tangential planes obtained in such a way determines the exact potential boundary. For values of ρ smaller than $R(\mathbf{q}_0)$ but sufficiently close to it, and where the value of Δ is small, the following approximate equation is correct:

$$F(\rho, \mathbf{q}_0, \mathbf{N}) \approx U_1(\rho, \mathbf{q}_0), \tag{21}$$

which determines the integral of the potential in the plane (12). The relative error of Eq. (21) is equal to the absolute value of the function F, i.e., the integrals of the potential in planes cutting its external layers are determinated very accurately, but only rather roughly in planes which encompass the central regions.

We shall note that, for a centrally symmetric potential, the value $U_1(\rho, \mathbf{q}_0)$ is given by the integral

$$U_1(\rho, \mathbf{q}_0) = 2\pi \int_{\rho}^{\infty} U(r)\, r\, dr, \tag{22}$$

which determines the accuracy of Eq. (21).

It is interesting to obtain equations which determine the potential of $U(\mathbf{r})$ itself rather than integrals of it. It will be shown below that Eq. (21) makes it possible to construct a certain approximate potential F which has the same boundary as the true scattering potential and coincides with the boundary with an accuracy given by Eq. (20).

2. THE ASYMPTOTIC BORN APPROXIMATION

We shall make use of the approximate expression (21) for the inverse transition from the function U_1 to the potential $U(\mathbf{r})$. If the function $U_1(\rho, \mathbf{q}_0)$ were known accurately, then, for a single-valued reconstruction of the potential, it would be sufficient to perform two Fourier transformations on it:

$$U(\mathbf{q}) = \int U_1(\rho, \mathbf{q}_0) \exp(-iq\rho)\, d\rho, \quad q > 0 \tag{23}$$

and

$$U(\mathbf{r}) = (2\pi)^{-3} \int U(\mathbf{q}) \exp(i\mathbf{q}\mathbf{r})\, d\mathbf{q}. \tag{24}$$

It can easily be seen that the function $F(\rho, \mathbf{q}_0, \mathbf{N})$ is not a transformation of the type $U_1(\rho, \mathbf{q}_0)$ of any fictitious potential and, consequently, it is impossible to apply transformations (23) and (24) to it directly. In fact, were such a fictitious potential to exist, the function F would have the form of a double integral

$$F(\rho, \mathbf{q}_0, \mathbf{N}) = \int\limits_{\mathbf{r}\mathbf{q}_0 = \rho} F(\mathbf{r})\, dS, \tag{25}$$

and would therefore satisfy the condition

$$F(\rho, \mathbf{q}_0, \mathbf{N}) = F(-\rho, -\mathbf{q}_0, \mathbf{N}). \tag{26}$$

As can be seen from Eq. (13), which determines the region of integration, $F(\rho, \mathbf{q}_0, \mathbf{N})$ depends on the behavior of the potential in the region $\mathbf{r}\mathbf{q}_0 \geq \rho$, and $F(-\rho, -\mathbf{q}_0, \mathbf{N})$ depends on the behavior of the potential when $\mathbf{r}\mathbf{q}_0 \leq \rho$, so that condition (26) cannot be

satisfied. However, it is clear from these considerations how to circumvent this difficulty. To this end, we introduce a new function F by means of the two equations

$$F(\rho, \mathbf{q}_0, \mathbf{N}) = \begin{cases} f(\rho, \mathbf{q}_0, \mathbf{N}), & \rho > 0, \\ f(-\rho, -\mathbf{q}_0, \mathbf{N}) & \rho < 0. \end{cases} \quad (27)$$

A certain approximate potential $F(\mathbf{r}, \mathbf{N})$ corresponds to the new function. To obtain a three-dimensional Fourier component of this potential, we substitute Eq. (27) in Eq. (23) and make use of the definition (6) of the function F. We have

$$f^+(\mathbf{q}, \mathbf{N}) \equiv \int F(\rho, \mathbf{q}_0, \mathbf{N}) \exp(-iq\rho)\, d\rho = \int [f(q', \mathbf{q}_0, \mathbf{N}) \times \delta_+(q' - q) + f^*(q', -\mathbf{q}_0, \mathbf{N})\, \delta_+(q - q')]\, dq'. \quad (28)$$

The final result can be formulated in the following manner: If the scattering amplitude is transformed according to Eq. (28), and we then use the transformed amplitude for constructing the first Born approximation for the potential, then the approximation obtained will have exactly the same boundary as the true potential and will coincide with it near the boundary with an accuracy of order of magnitude equal to the product

$$\overline{U(\mathbf{r})}\, \Delta^2(\mathbf{r}),$$

where Δ is the shortest distance from the point at which the potential is determined to the boundary, and $\overline{U}$ is the average value of the potential between the point $\mathbf{r}$ and the boundary.

Let us return to the experimental data necessary for reconstructing the potential. It is clear that the unit vector $\mathbf{q}_0$ does not determine the scattering amplitude in a unique way: there still remains an ambiguity in the choice of the vector $\mathbf{N}$. According to Eq. (19) – (21), for any choice of the vector $\mathbf{N}$, the reconstructed potential will coincide with the true one in a single layer near the boundary with the same accuracy. This means that not only the potential is obtained, but also the condition which should be satisfied by the scattering amplitude of any potential. The transformed scattering amplitude determines a fictitious potential $F(\mathbf{r}, \mathbf{N})$, the value of which is independent of the vector $\mathbf{N}$ within the limits of the error (20).

In any practical case, the scattering amplitude will be given only up to a certain finite value of q_{max}. It is evident that the replacing of the infinite range of integration by a finite one leads to the averaging of the approximate potential $F(\mathbf{r})$ over a certain volume, the linear dimensions l of which are determined by the value q_{max}:

$$l q_{max} \sim \pi. \quad (29)$$

If it is necessary that the relative error in the determination of the potential be smaller than ϵ, then the value of l should satisfy the condition

$$l \leqslant \Delta, \quad (30)$$

where $\Delta = \Delta(\epsilon)$ is determined by the condition that, in a layer at the depth Δ near the boundary, the approximate potential $F(\mathbf{r})$ is equal to the true potential $U(\mathbf{r})$ with the relative error not bigger than ϵ. This condition is satisfied if

$$\overline{U}\Delta^2 \leqslant \varepsilon. \quad (31)$$

From Eqs. (29), (30), and (31), and substituting for q_{max} the maximum energy up to which the scattering amplitude is known,

$$E_{max} = k^2_{max} = q^2_{max} [2 \sin(\vartheta/2)]^{-2}, \quad (32)$$

we obtain a new inequality

$$E_{max} \geqslant (\pi^2/4) |\overline{U}| \varepsilon^{-1} \sin^{-2}(\vartheta/2). \quad (33)$$

From this inequality it follows that, in practice, it is more convenient to use the backward scattering amplitude, in which case it is necessary to measure it in a minimum energy interval.

Thus, for instance, for a rough determination of the order of magnitude, for the case where $\epsilon \approx 1$, the backward scattering amplitude should be measured to the value

$$E_{max} > 2 |\overline{U}(\mathbf{r})| \quad (34)$$

and, to the contrary, if the scattering amplitude at an angle π is known up to the energy E_{max}, then, on this basis, it is impossible, to reconstruct the potential in that region even roughly, if its order of magnitude is bigger than or equal to E_{max}.

CONCLUSION

All the results of the present paper are also applicable to the scattering of particles with spin, but in that case it is necessary to consider the potential in a form of a matrix and to introduce the spin function into all plane waves.

Strictly speaking, all the above results have been proven only for bounded potentials for which the Born approximation series converges for all energies. However, the series may diverge, owing to integration over the whole range where the potential is different from zero, while in the series (6) the integration extends only over the external segment of the potential. Therefore, it seems highly probable that the divergence of the series (7) is quite independent of the behavior of the potential in the deep regions, since the use of the total series of the Born approximations is simply

the most convenient method of proof.

In that case, in order that the theorems be correct it is only necessary that the transformation $U_1(\rho, \mathbf{q}_0)$ tend to zero for $\rho \to \infty$, which is the case for all potentials that decrease at infinity so that $r^2U(\mathbf{r}) \to 0$ for $r \to \infty$.

The author wishes to express his deep gratitude to Prof. Ya. A. Smorodinskiĭ for valuable advice and discussion in the course of the work.

APPENDIX

The sum $-\mathbf{n}_2\mathbf{x} + \mathbf{n}_1\mathbf{y}$ expressed in terms of the variables (2) — (4) in the new coordinates $\mathbf{Z}$ and $\mathbf{z}$

$$\mathbf{Z} = (\mathbf{x} + \mathbf{y})/2, \tag{A1}$$

$$\mathbf{z} = (\mathbf{x} - \mathbf{y})/2, \tag{A2}$$

can be written in the following way:

$$-\mathbf{n}_2\mathbf{x} + \mathbf{n}_1\mathbf{y} = -(n\,\mathbf{q}_0\mathbf{Z} + 2\,\mathbf{N}\mathbf{z}). \tag{A3}$$

The sum $|\mathbf{x} - \mathbf{z}_1| + |\mathbf{z}_1 - \mathbf{z}_2| + \ldots + |\mathbf{z}_{l-2} - \mathbf{y}|$ represents the length of a broken line connecting the ends of the vectors $\mathbf{x}$ and $\mathbf{y}$; it is greater than the length of the vector $\mathbf{x} - \mathbf{y} = 2\mathbf{z}$:

$$|\mathbf{x} - \mathbf{z}_1| + \ldots + |\mathbf{z}_{l-2} - \mathbf{y}| = 2z + \beta,\ \beta \geqslant 0. \tag{A4}$$

Making use of all these transformations, we shall express the vanishing of the argument of the δ-function in the l-th term of the series (7) [see Eq. (10)] in the following way:

$$n[\mathbf{q}_0\mathbf{Z} - \rho] = 2[z + \mathbf{N}\mathbf{z}] + \beta. \tag{A5}$$

On the right-hand side we have a sum of positive values [see Eq. (3)]. Therefore the difference on the left hand side should also be positive.

$$\mathbf{q}_0\mathbf{Z} \geqslant \rho. \tag{A6}$$

For a fixed $\mathbf{Z}$ and β, the projection of the vector $\mathbf{z}$ on the direction $\mathbf{q}_0$ may be expressed as a function of the angle α between the vectors $\mathbf{N}$ and $\mathbf{z}$:

$$|\mathbf{q}_0\mathbf{z}| = \sin\alpha\,[n(\mathbf{q}_0\mathbf{Z} - \rho) - \beta]/[2(1 - N\cos\alpha)]. \tag{A7}$$

In the last equation, we make use of the orthogonality of the vectors $\mathbf{q}_0$ and $\mathbf{N}$. This function has a maximum if $\cos\alpha = \mathrm{N}$. Making use of expressions (5) for N and n, we obtain for the maximum value of this projection

$$|\mathbf{q}_0, \mathbf{z}|_{max} = \mathbf{q}_0\mathbf{Z} - \rho, \tag{A8}$$

from which follows the required limitation of the integration region over variables $\mathbf{x}$ and $\mathbf{y}$:

$$\mathbf{x}\mathbf{q}_0 \geqslant \rho, \quad \mathbf{y}\mathbf{q}_0 \geqslant \rho. \tag{A9}$$

The variables $\mathbf{z}_i$ remain to be considered. It is clear that any of the vertices of the broken line $2z + \beta$ cannot deviate from the end of vector $\mathbf{Z}$ in the direction $\mathbf{q}_0$ by more than $z + \beta/2$, while the maximum deviation is attained when the directions of the vectors $\mathbf{q}_0$ and $\mathbf{z}$ coincide; in that case $\mathbf{z}\mathbf{N} = 0$. The last equation makes it possible to estimate the sum $z + \beta/2$ from Eq. (A6)

$$z + \beta/2 = \sin(\vartheta/2)\,[\mathbf{q}_0\mathbf{Z} - \rho]. \tag{A10}$$

Whence follows the proof:

$$\mathbf{z}_i\mathbf{q} \geqslant \rho. \tag{A11}$$

Thus, the range of integration over the variables $\mathbf{x}$ and $\mathbf{y}$ extends over the crosshatched segment. The contribution of the integral over these variables to the total integral U_l can be estimated as the product

$$(\bar{U}\bar{r}^2)(\bar{U}\bar{\Delta}^2). \tag{A12}$$

For fixed vectors $\mathbf{x}$ and $\mathbf{y}$, the vectors $\mathbf{z}_i$ all lie in a sphere of radius

$$\sin(\vartheta/2)\,[\mathbf{q}_0\mathbf{Z} - \rho],$$

with its center at $\mathbf{Z}$, and therefore the integral over these variables contains no $\bar{r}$ but a certain $\bar{\Delta}$ equal to the smallest of the numbers $\bar{r}$, Δ.

The total integral U_l can be estimated in the following way:

$$U_l \approx (\bar{U}\bar{r}^2)(\bar{U}\bar{\Delta}^2)^{l-1} \tag{A13}$$

If the expressions obtained are summed up over l from $l = 2$ to ∞, we obtain the following estimate for the sum of all terms of the series (7) without the first one:

$$\left|\sum_{l=2}^{\infty} U_l\right| \approx (\bar{U}\bar{r}^2)(\bar{U}\bar{\Delta}^2)\,[1 - (\bar{U}\bar{\Delta}^2)]. \tag{A14}$$

[1] I. M. Gel'fand and B. M. Levitan, Izv. Akad. Nauk SSSR, Ser. Mat. **15**, 309 (1951).

[2] V. A. Marchenko, Dokl. Akad. Nauk SSSR **104**, 695 (1955).

[3] R. G. Newton, Phys. Rev. **100**, 412 (1955).

[4] H. E. Moses, Phys. Rev. **102**, 559 (1956).

[5] Puzikov, Ryndin, and Smorodinskiĭ, J. Exptl. Theoret. Phys. (U.S.S.R.) **32**, 592 (1957), Soviet Phys. JETP **5**, 489 (1957).

[6] Ya. A. Smorodinskiĭ, J. Exptl. Theoret. Phys. (U.S.S.R.) **34**, 1333 (1958), Soviet Phys. JETP **7**, 920 (1958).

[7] D. Y. Wong, Phys. Rev. **107**, 302 (1957).

Translated by H. Kasha
358

SLIPPING AND TEMPERATURE DISCONTINUITY AT THE BOUNDARY OF A GAS MIXTURE

R. Ya. KUCHEROV and L. É. RIKENGLAZ

Submitted to JETP editor December 10, 1958

J. Exptl. Theoret. Phys. (U.S.S.R.) **36**, 1758-1761 (June, 1959)

Boundary conditions have been obtained for the hydrodynamical transport equations for a gas mixture. The conditions take into account slipping and the temperature jump at the boundary with a solid surface.

1. As is known, corrections due to the finite mean free path appear in the boundary conditions for hydrodynamic transport equations before they appear in the equations themselves.[1] Therefore, when making the transition from hydrodynamic flow to molecular flow, there exists a region of values $l/a < 1$ (l is the mean free path and a is the characteristic dimension of the problem), where these equations can still be used, but the boundary-condition corrections linear in l/a cannot be neglected. Furthermore, these corrections may prove to be substantial even at high pressures, if they lead to the appearance of noticeable additions to the convective terms in the transport equations (see, for example, reference 2).

Corrections to boundary conditions for a one-component gas were investigated by many authors.[3,4] The most thorough method for obtaining them was developed by Grad.[5] In this paper we shall generalize this method to find corresponding boundary conditions for a binary inhomogeneous gas mixture on a non-absorbing solid surface.

2. We describe a binary mixture of gases by distribution functions $f_\alpha(\mathbf{r}, \boldsymbol{\xi}, t)$, normalized for the density of the molecules of the α component. Here $\mathbf{r}$ is the radius vector of the molecule, $\boldsymbol{\xi}$ its velocity, and t the time. The internal degrees of freedom of the molecules are neglected.

The principal macroscopic quantities will be introduced with the aid of the equalities:

$$n_\alpha(\mathbf{r}, t) = \int f_\alpha(\mathbf{r}, \boldsymbol{\xi}, t)\, d\boldsymbol{\xi}, \qquad \rho_\alpha(\mathbf{r}, t) = m_\alpha n_\alpha, \qquad \rho = \sum_\alpha \rho_\alpha,$$

$$\mathbf{u}_\alpha(\mathbf{r}, t) = \frac{1}{n_\alpha}\int \boldsymbol{\xi} f_\alpha(\mathbf{r}, \boldsymbol{\xi}, t)\, d\boldsymbol{\xi}, \quad \mathbf{u}(\mathbf{r}\ t) = \frac{1}{\rho}\sum_\alpha \rho_\alpha \mathbf{u}_\alpha, \qquad (1)$$

where n_α, ρ_α, and $\mathbf{u}_\alpha$ are respectively the density of the molecules, the mass density, the local velocity of the α component; ρ and $\mathbf{u}$ are the mass density and velocity of the local center of intertia of the mixture, and m_α is the mass of a molecule of type α.

Introducing the relative velocity $\mathbf{c} = \boldsymbol{\xi} - \mathbf{u}$, we form the moments

$$R_{\alpha,i} = m_\alpha \int c_i f_\alpha\, d\boldsymbol{\xi}, \qquad P_{\alpha,ij} = m_\alpha \int c_i c_j f_\alpha\, d\boldsymbol{\xi},$$

$$S_{\alpha,i} = (m_\alpha/2)\int c^2 c_i f_\alpha\, d\boldsymbol{\xi}. \qquad (2)$$

The physical meaning of these moments is obvious.

The partial pressure p_α, the mixture pressure p, the stress tensor of the mixture p_{ij}, and the mixture temperature T are

$$p_\alpha = \tfrac{1}{3} P_{\alpha,ii}, \qquad p = \sum_\alpha p_\alpha, \qquad p_{\alpha,ij} = P_{\alpha,ij} - p_\alpha \delta_{ij},$$

$$p_{ij} = \sum_\alpha P_{\alpha,ij} - p\,\delta_{ij}, \qquad p_\alpha = n_\alpha k T. \qquad (3)$$

Repeated Latin indices will henceforth be summed.

3. We expand $f_\alpha(\mathbf{r}, \boldsymbol{\xi}, t)$ in a series of Hermite vector polynomials. Confining ourselves to the third approximation, we obtain after transformations analogous to those used by Grad[5]

$$f_\alpha(\mathbf{r}, \boldsymbol{\xi}, t) = f_{\alpha 0}\left[1 + \frac{R_{\alpha,i}}{p_\alpha} c_i + \frac{m_\alpha}{2kT}\frac{P_{\alpha,ik}}{p_\alpha} c_i c_k + \frac{1}{10}\left(\frac{2m_\alpha}{kT} S_{\alpha,i} - 5R_{\alpha,i}\right)\left(\frac{m_\alpha}{kT} c^2 - 5\right)\frac{c_i}{p_\alpha}\right], \qquad (4)$$

where

$$f_{\alpha 0} = n_\alpha (m_\alpha/2\pi kT)^{3/2} \exp(-m_\alpha c^2/2kT). \qquad (5)$$

4. We consider two-dimensional flow of gas near the surface $x = 0$ (the x axis is directed along the outward normal to the surface, the y axis in the flow direction). If the gas is in equilibrium with the wall, then, in the narrow boundary layer whose thickness is on the order of the length of the mean free path of the molecule, the distribution of the molecules that collide with the wall differs from the distribution of the molecules that are directed toward it. It is natural to introduce in this layer two distribution functions $f^+_\alpha(\mathbf{r}, \boldsymbol{\xi}, t)$ for molecules with $\xi_x > 0$, and $f^-_\alpha(\mathbf{r}, \boldsymbol{\xi}, t)$ for molecules with $\xi_x < 0$. These "parts" of the dis-

tribution function will be related to the general distribution function by the equation

$$f_\alpha(\mathbf{r}, \boldsymbol{\xi}, t) = f_\alpha^+(\mathbf{r}, \boldsymbol{\xi}, t) + f_\alpha^-(\mathbf{r}, \boldsymbol{\xi}, t),$$

$$f_\alpha^+(\mathbf{r}, \boldsymbol{\xi}, t) = 0 \quad \text{for } \xi_x < 0,$$

$$f_\alpha^-(\mathbf{r}, \boldsymbol{\xi}, t) = 0 \quad \text{for } \xi_x > 0. \tag{6}$$

By way of a kinetic boundary condition we assume that some of the molecules incident on the wall are specularly reflected, while the others are absorbed on the wall and are then emitted with a Maxwellian distribution corresponding to a wall temperature T_0, i.e.,

$$f_\alpha^+(\xi_x, \xi_y, \xi_z) = \beta_\alpha f_\alpha^-(-\xi_x, \xi_y, \xi_z) + \varkappa_\alpha \exp(-m_\alpha \boldsymbol{\xi}^2/2kT_0) \quad \text{for } x = 0. \tag{7}$$

The parameters β_α and κ_α are not independent, since they are related by the condition that no molecules accumulate on the wall.

Supplementing (7) with the condition $\kappa_\alpha = 0$ at $\xi_x < 0$, we can expand (7) in a series of Hermite vector polynomials. Equating the coefficients of the corresponding polynomials, we obtain an infinite number of boundary conditions for the moments of distribution function. However, in view of the fact that the distribution function is approximated by a finite number of terms in the expansion in Hermite polynomials, all these conditions cannot be satisfied simultaneously.

From simple physical considerations it is clear that it is necessary to retain only the conditions connected with the mass, energy, and tangential momentum fluxes that are normal to the wall, since the wall "deforms" precisely these fluxes.

The first of these boundary conditions expresses the fact that the solid surface absorbs no molecules,

$$u_{\alpha x}\big|_{x=0} = 0. \tag{8}$$

We insert the distribution function (4) into the kinetic boundary condition (7). We then multiply (7) successively by c_x, $c_x c_y$, $c^2 c_x$, and integrate in velocity space, thus obtaining the second and third boundary conditions:

$$\tfrac{1}{2} p_{\alpha,\, xy}(1+\beta_\alpha) + (1-\beta_\alpha)(S_{\alpha y}/5\sqrt{\pi}\, q_\alpha + R_{\alpha y} q_\alpha/4\sqrt{\pi}) + \tfrac{1}{2}\pi \varkappa_\alpha u_y q_{\alpha 0}^4 = 0; \tag{9}$$

$$(1+\beta_\alpha) S_{\alpha,\, x} + (1-\beta_\alpha)(4 p_{\alpha,\, xx} + 3p_{\alpha,\, xx}) q_\alpha/2\sqrt{\pi} - \pi \varkappa_\alpha q_{\alpha 0}^6 = 0, \tag{10}$$

where

$$\varkappa_\alpha = (2/\pi^{1/2} q_{\alpha 0}^4 q_\alpha)(1-\beta_\alpha)(p_\alpha + \tfrac{1}{2} p_{\alpha,\, xx}),$$

$$q_{\alpha 0}^2 = 2kT_0/m_\alpha, \qquad q_\alpha^2 = 2kT(0)/m_\alpha, \tag{11}$$

$T(0)$ is the temperature of the mixture at the boundary.

It is more convenient, however, to have boundary conditions for the entire mixture and one of the components, instead of boundary conditions that pertain to each component separately. To simplify the notation, we shall confine ourselves to the case when the gas molecules are only diffusely scattered by the wall, i.e., $\beta_\alpha = 0$. We obtain from (8)

$$u_x\big|_{x=0} = 0. \tag{12}$$

Summing (9) and (10) over α and neglecting small terms of second order, we obtain

$$u_y\big|_{x=0} = -\frac{\pi^{1/2}(p_{1,\, xy} + p_{2,\, xy}) + {}^2/_5 (S_{1y}/q_1 + S_{2y}/q_2) + {}^1/_2 (R_{1y} q_1 + R_{2y} q_2)}{2(p_1/q_1 + p_2/q_2) + (p_{1,\, xx}/q_1 + p_{2,\, xx}/q_2)}; \tag{13}$$

$$\frac{T_0 - T(0)}{T(0)} = \frac{(2\pi)^{1/2}}{4(kT_0)^{3/2}} \frac{S_x + (kT_0/2\pi)^{1/2}(p_{1,\, xx}/m_1^{1/2} + p_{2,\, xx}/m_2^{1/2})}{n_1 m_1^{1/2} + n_2 m_2^{1/2}}. \tag{14}$$

These formulas determine the speed and temperature of the gas mixture at a boundary with a solid surface. We use these to obtain boundary conditions for the equations of hydrodynamics. For this purpose we assume that the hydrodynamic approximation, which is correct only for $x \gg l$, is applicable all the way to the boundary, and we express the fluxes contained in (13) and (14) in terms of the corresponding gradients. Using the Chapman and Enskog formulas[6] and neglecting terms that contain the small quantities $p_{\alpha,xx}$, we find

$$\frac{T_0 - T(0)}{T(0)} = \frac{(2\pi)^{1/2}\lambda}{4(kT)^{3/2}(n_1 m_1^{1/2} + n_2 m_2^{1/2})} \frac{dT}{dx}\bigg|_{x=0}, \tag{15}$$

$$u_y\big|_{x=0} = \frac{\eta\sqrt{\pi/2kT}}{n_1 m_1^{1/2} + n_2 m_2^{1/2}} \frac{du_y}{dx}\bigg|_{x=0} + \frac{\lambda}{5p} \frac{dT}{dy}\bigg|_{x=0} - \left[\frac{k_T}{5} + \frac{n_1 n_2 m_1 m_2 (m_1^{1/2} - m_2^{1/2})}{\rho(n_1 m_1^{1/2} + n_2 m_2^{1/2})}\right](c_{1y} - c_{2y})\bigg|_{x=0} + \frac{\sqrt{m_2} + \sqrt{m_1}}{2p(n_1 m_1^{1/2} + n_2 m_2^{1/2})}[X_{1y} n_2 - X_{2y} n_1], \tag{16}$$

where η is the coefficient of viscosity of the mixture, k_T is the thermal diffusion ratio, λ the coefficient of heat conduction of the mixture,

$$X_{\alpha y} = {}^{2}/_{5} S_{\alpha y} - {}^{1}/_{2} R_{\alpha y} q_{\alpha}^{2},$$

$$c_{1y} - c_{2y} = \frac{n^2}{n_1 n_2} D_{12} \left\{ \frac{\partial \gamma}{\partial y} + \frac{n_1 n_2 (m_2 - m_1)}{n\rho} \frac{\partial \ln p}{\partial y} \right.$$

$$\left. + \frac{\rho_1 \rho_2}{p\rho} (F_{1y} - F_{2y}) + k_T \frac{\partial \ln T}{\partial y} \right\},$$

D_{12} is the coefficient of mutual diffusion, F_α is the force acting per unit mass of the α component, $n = n_1 + n_2$, and $\gamma = n_1/n$.

Formula (15) determines the temperature discontinuity at the boundary of the gas mixture and the solid body, while Eq. (16) determines the slipping speed.

The first term in (16) describes Maxwellian viscous slipping for a boundary mixture, while the third describes diffuse slipping, due to the presence of concentration, pressure, and temperature gradients in the mixture and also due to the presence of an external field.

The second and fourth terms are due to thermal slipping. The fluxes $X_{\alpha y}$ contained in the fourth term cannot be expressed in terms of known kinetic coefficients. They can be calculated, for example, by a variational method.[7]

It is interesting to note that, owing to diffuse slipping, a body placed in a mixture of gases of inhomogeneous concentration should be set in motion. This phenomenon is to some extent analogous with the radiometric effect.

[1] L. D. Landau and E. M. Lifshitz, Механика сплошных сред (Mechanics of Continuous Media) M-L, Gostekhizdat, 1944.

[2] R. Ya. Kucherov, J. Tech. Phys. **27**, 2158 (1957), Soviet Phys. "Tech. Phys." **2**, 2001 (1957).

[3] J. C. Maxwell, The Scientific Papers of James Clark Maxwell, Cambridge 1890.

[4] M. Smolukhovski, Sitz. Ber. Akad. Wiss. Wien, **108**, 5 (1899).

[5] H. Grad, Comm. Pure and Appl. Math. **2**, 231 (1949); cf. also the collection Механика (Mechanics), **4** (14), 71 (1952).

[6] S. Chapman and T. Cowling. The Mathematical Theory of Non Uniform Gases, Cambridge, 1939.

[7] C. F. Curtiss and J. O. Hirschfelder, J. Chem. Phys. **17**, 550 (1949).

Translated by J. G. Adashko
359

SOVIET PHYSICS JETP VOLUME 36 (9), NUMBER 6 DECEMBER, 1959

RESONANCE EFFECTS IN THE SCATTERING OF PARTICLES NEAR A REACTION THRESHOLD

A. I. BAZ'

Submitted to JETP editor December 10, 1958

J. Exptl. Theoret. Phys. (U.S.S.R.) **36**, 1762-1770 (June, 1959)

The energy dependence of the cross-section for the scattering X(aa)X near the threshold E_{th} of the reaction X(ab)Y (X, a, b, Y are arbitrary particles) is studied on the assumption that there are long-range attractive forces between particles b and Y. It is shown that if these forces are capable of producing bound states of the particles b + Y there are resonances in the scattering cross-section. These resonances lie below the threshold of the reaction X(ab)Y. A detailed study is made of the case in which attractive Coulomb forces act between b and Y. For this case the number of resonances is infinite, and the density of the resonances approaches infinity as the threshold is approached from below.

INTRODUCTION

IN a previous paper[1] the writer has studied the energy dependence of the cross-section for the scattering X(aa)X near the threshold of the reaction X(ab)Y. It was found that if there is no Coulomb interaction between b and Y the scattering cross-section has a characteristic singularity at the threshold point. In this connection it is interesting to examine the case in which long-range (for example, Coulomb) forces exist between b and Y. The present paper is devoted to the study of this problem.

Let us look at the statement of the problem in more detail. We shall study the energy dependence of the cross-section for the scattering X(aa)X near the threshold E_{th} for the reaction X(ab)Y. No restrictions are placed on the nature of the particles X, a, b, Y, except that for simplicity we shall regard them as spinless. Let us introduce one more simplification: we shall assume that there are no other inelastic processes besides the reaction X(ab)Y in the range of energies with which we are concerned. We shall free ourselves from this restriction in Sec. 3.

The reason that some sort of anomalies in the scattering cross-section are to be expected near E_{th} is as follows. Suppose the long-range potential between b and Y is an attractive one and is capable of leading to the formation of a bound state with binding energy Δ. If such a state exists, then it can be formed in the collision of particles X and a (because the reaction X(ab)Y exists), and consequently the scattering cross-section must have a resonance at the energy of formation of the bound state, $E = E_{th} - \Delta$. Breit[2] was the first to call attention in the literature to the possibility of such an effect. It is clear that it is possible only if the size of the long-range potential is much larger than r_0, the radius outside which one can neglect specifically nuclear forces. We shall always assume that this condition is fulfilled.

The general theory of the effect is presented in Sec. 1. The second section is devoted to a detailed study of the case in which an attractive Coulomb potential acts between b and Y. This situation is encountered whenever differently charged particles can arise from the reaction. Section 3 contains a discussion of the effects that appear when one of the particles formed in the reaction has a finite lifetime.

1. GENERAL THEORY

Let us consider the general problem of the behavior of the cross-section for the elastic scattering X(aa)X near the threshold E_{th} for a reaction X(ab)Y. We consider a state with a given total angular momentum I; in the region outside the action of nuclear forces ($r > r_0$) the wave function has the form

$$\Psi = \Phi(a, X)(R_k^{(-)}(r) - S_l R_k^{(+)}(r))Y_{l0} - \Phi(b, Y) M_l \mathcal{R}_{k_1}^{(+)}(r) Y_{l0}, \quad (1.1)$$

where $\Phi(a, X)$ and $\Phi(b, Y)$ are the internal wave functions of particles a and X and of b and Y, respectively; $R_k^{(\pm)}(r)$ is the radial function for the relative motion of particles a and X with the wave number k (the signs ± refer

to diverging and converging waves); $\mathcal{R}^{(*)}_{k_1}(r)$ is the radial function for the diverging particles b and Y with the wave number k_1; Y_{l0} is the angular part of the wave functions, normalized to unity; and S_l and M_l are the elements of the scattering matrix, whose energy dependence we have to determine. The wave numbers k and k_1 are connected by the relation

$$\hbar^2k^2/2\mu = \hbar^2k_1^2/2\mu_1 + E_{th}$$

[μ and μ_1 are the reduced masses of (a+X) and (b+Y)].

The radial functions $R^{(*)}_k$ are determined in the usual way. They are combinations of Bessel functions if a and X can be regarded as free in the region $r > r_0$, and Coulomb functions if the particles a and X are charged. As for $\mathcal{R}^{(*)}$, this is the function that describes the motion of particles b and Y in the field of the long-range potential that acts between them. At infinity it must behave like e^{ik_1r}/r. Hereafter we shall always suppose that $R^{(*)}$ and $\mathcal{R}^{(*)}$ are normalized to unit flux.

The scattering cross-section is given by

$$\sigma(\theta, E) = \frac{1}{4k^2}\left|\sum_l (2l+1)(S_l - 1)P_l(\cos\theta)\right|^2.$$

In order to determine the dependence of S_l on the energy, we use a formula proved in the Appendix, according to which

$$S_l = (a + b\varkappa_b^{(+)})/(a^* + b^*\varkappa_b^{(+)}), \qquad (1.2)$$

where the quantities a and b can be supposed independent of the energy near the threshold, and

$$\varkappa_b^{(+)} = \frac{d}{dr}\ln \mathcal{R}^{(+)}_{k_1}\Big|_{r=r_0}. \qquad (1.3)$$

Thus for our problem it suffices to determine the energy dependence of the function $\kappa_b^{(*)}$. We shall first consider the range of energies $E < E_{th}$.

For $r > r_0$ the function $\mathcal{R}^{(*)}_{k_1} \equiv \chi/r$ satisfies the usual Schrödinger equation

$$d^2\chi/dr^2 + [k_1^2 - l(l+1)/r^2 - (2\mu_1/\hbar^2)V(r)]\chi = 0, \qquad (1.4)$$

where V is the long-range potential between particles b and Y. We are interested in the solution of this equation that behaves like e^{ik_1r} at infinity. Since $E < E_{th}$ and k_1 is pure imaginary, this asymptotic form assures the finiteness of χ for $r \to \infty$. As is well known from the general theory of the Schrödinger equation,[3] the function χ for small r can be represented in the form

$$\chi = \xi[(k_1r)^{l+1} + i\varepsilon(k_1r)^{-l}], \qquad (1.5)$$

where ξ and ϵ are functions of k_1; the concrete form of these functions is determined by the potential V. The function ϵ is real, since both the equation (1.4) and the boundary condition at infinity, $\chi \sim e^{ik_1r} = e^{-|k_1|r}$, are real. Some general conclusions can be drawn about the energy dependence of the function ϵ. Indeed, let us continue equation (1.4) into the region $r < r_0$. If it admits of the existence of bound states with binding energies Δ_m, then the function ϵ must go to zero at the values $k_1 = (k_1)_m = (\Delta_m/2\mu_1\hbar^2)^{1/2}$, since only under this condition is χ regular at the origin. Thus as a function of the energy E of the particles a + X the quantity ϵ has the form shown schematically in Fig. 1. Sometimes, as for example in the case of the Coulomb field, considered in Sec. 2, ϵ goes to infinity in the intervals between the values Δ_m. This makes no difference, however, in the following arguments.

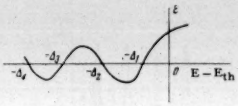

FIG. 1

Let us calculate the logarithmic derivative $\kappa_b^{(*)}$. From Eqs. (1.3) and (1.5) we get

$$\varkappa_b^{(+)} = \frac{1}{r_0}\left[l - \frac{i(2l+1)\varepsilon}{i\varepsilon + (k_1r_0)^{2l+1}}\right]. \qquad (1.6)$$

Let us examine the behavior of $\kappa_b^{(*)}$ near one of the bound states. Since we are considering the region near the threshold, where (k_1r) is small, it follows from Eq. (1.6) that the function $\kappa_b^{(*)}$ is practically constant and equal to $-(l+1)/r_0$ everywhere except in narrow intervals of energy around the energies Δ_m of the bound states. In these intervals, defined by the condition $|\epsilon| \lesssim |(k_1r_0)^{2l+1}|$, $\kappa_b^{(*)}$ changes very rapidly, running through the entire range of values from $-\infty$ to $+\infty$. This is shown schematically in Fig. 2.

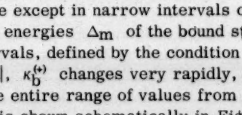

FIG. 2

Substituting Eq. (1.6) in the formula (1.2) for S_l, and noting that $\kappa_b^{(*)}$ is real for $E < E_{th}$, we

can write S_l in the form $e^{2i\varphi}$, where φ is the real phase of the scattering S_l.

The energy dependence of φ can be seen from the formula

$$\varphi = \tan^{-1} \frac{\mathrm{Im}(a + b\varkappa_b^{(+)})}{\mathrm{Re}(a + b\varkappa_b^{(+)})}. \qquad (1.7)$$

Using the energy dependence of $\kappa_b^{(+)}$ obtained above (see Fig. 2), we easily see that the scattering phase shift φ remains constant everywhere except in narrow regions around the bound-state energies $E = E_{th} - \Delta_m$, where it changes by π. As can be seen from the formula for the scattering cross-section

$$\sigma_l = 4\pi k^{-2}(2l+1)\sin^2\varphi,$$

to such changes of the phase shift there correspond resonance peaks of the scattering cross-section at energies close to $E_m = E_{th} - \Delta_m$, and the scattering cross-section has the shape shown in Fig. 3.

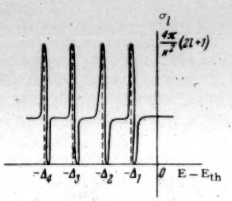

FIG. 3

We can determine the width and shape of the resonance peaks. For this purpose we rewrite S_l in the following way:

$$S_l = \frac{b}{b^*}\frac{c+\varepsilon}{c^*+\varepsilon} = \frac{b}{b^*}\left[1 - \frac{2ic_2}{(c_1+\varepsilon)+ic_2}\right],$$
$$c \equiv c_1 - ic_2, \qquad (1.8)$$

where the complex constants c and b are expressed in an obvious way in terms of the constants appearing in Eqs. (1.2) and (1.6). We note further that near the m-th bound state the quantity ϵ can be expanded in a series in powers of the energy difference,

$$\varepsilon = A[E - (E_{th} - \Delta_m)] + \ldots \qquad (1.9)$$

Substituting Eq. (1.9) in Eq. (1.8), we get for S_l

$$S_l = \frac{b}{b^*}\left[1 - \frac{2i\Gamma_e}{(E - E_m') + i\Gamma_e}\right],$$
$$\Gamma_e = \frac{c_2}{A}, \qquad E_m' = E_{th} - \Delta_m - \frac{c_1}{A}. \qquad (1.10)$$

This equation has the form of the usual Breit-Wigner formula (cf. reference 3), with Γ_e playing the role of the elastic width, which in our case is the total width, and the constant c_1/A is the shift of the resonance maximum relative to the energy of the bound state. Thus the general shape of the resonance peaks is described by the Breit-Wigner formula. The parameters of the resonances (Γ_e and c_1/A) cannot be calculated, since through the constants c_1 and c_2 they depend on the form of the wave function for $r < r_0$.

This picture corresponds exactly to the resonance scattering that is well known from the theory of nuclear reactions. The part of the quasistationary states is played by the bound states of particles b + Y in the field of the long-range potential. There is no absorption, since for $E < E_{th}$ there are no inelastic processes, and therefore at its maxima the cross-section reaches the maximum value $4\pi k^{-2}(2l+1)$.

Up to now we have spoken only of the region $E < E_{th}$. What will happen at the threshold point itself and above it? Here we must distinguish two cases: for large r the long-range potential falls off either a) faster than $1/r$, or b) as $1/r$. In the first case the theory developed in reference 1 applies, and at the threshold point the differential cross-section has a singularity (a peak, an inverted peak, or a finite discontinuity), and above the threshold it is a smooth function of the energy. The width of the singularity at the threshold point is very small: $|k_1| < R^{-1}$, where R is the radius of the long-range potential. Case b) is treated in the next section. Looking ahead, we can state that the threshold is a point of condensation of the resonances, and above the threshold the cross-section is constant.

2. CASE OF ATTRACTIVE COULOMB FORCE BETWEEN b AND Y

The case of a Coulomb attraction can be studied exhaustively, since the analytic properties of the Coulomb functions are known. Using the method of reference 4, we find without difficulty that for $|k_1| \to 0$ the following formulas hold:

$$\mathcal{R}_{k_1}^{(+)} = \frac{1}{r}(G_l + iF_l) = \frac{1}{r}C_0^{-1}[-2A(\ln(-iz) + f(x) - C_0^2/2x) + B], \qquad (2.1)$$

where

$$x = ie_1e_2\mu_1/\hbar^2k_1, \qquad z = 2ik_1r,$$
$$A = \frac{(-)^l}{2}\sum_{n=0}^{\infty}(-xz)^{n+l+1}/n!\Gamma(2l+n+2),$$
$$B = \sum_{t=0}^{2l}\frac{(xz)^{t-l}}{t!}\Gamma(2l+1-t) + \sum_{n=1}^{\infty}\frac{(-xz)^{n+l+1}}{n!}\frac{(-)^{l+1}}{\Gamma(2l+2+n)} \times\left[-2\gamma + \sum_{s=1}^{n}\frac{1}{s} + \sum_{s=1}^{n+2l+1}\frac{1}{s}\right],$$
$$C_0 = [\pi x e^{\pi x}/\sin\pi x]^{1/2}, \qquad 2f(x) = \psi(x) + \psi(-x),$$

e_1 and e_2 are charges of particles b and Y, γ is the Euler constant, and ψ is the logarithmic derivative of the Γ function. As can be seen from the formulas, A and B are real and do not depend on the energy (the product xz does not contain k_1). Let us consider the quantity

$$T \equiv \ln(-iz) + f(x) - C_0^2/2x.$$

From the properties of the ψ function[5]

$$\psi(y) - \psi(-y) \approx -\pi \cot \pi y,$$
$$\psi(y) \approx \ln y \quad \text{for } |y| \to \infty;\ |\arg y| < \pi$$

it follows that

$$T = \ln(xz) + \begin{cases} -i\pi, & E > E_{\text{th}}, \\ -\pi \cot \pi x, & E < E_{\text{th}}. \end{cases} \tag{2.2}$$

Substituting Eq. (2.2) in Eq. (2.1) and calculating the logarithmic derivative, we get

$$x_b^{(+)} = \begin{cases} (p + is)/r_0(p_1 + is_1), & E > E_{\text{th}}, \\ (p + s\cot \pi x)/r_0(p_1 + s_1 \cot \pi x), & E < E_{\text{th}}, \end{cases} \tag{2.3}$$

where p, p_1, s, and s_1 are constants that can be expressed simply in terms of A, B, and their derivatives with respect to (xz).

Substituting Eq. (2.3) in Eq. (1.2), we get for S_l

$$S_l = \begin{cases} (\alpha + i\beta)/(\alpha^* + i\beta^*), & E > E_{\text{th}}, \\ (\alpha + \beta \cot \pi x)/(\alpha^* + \beta^* \cot \pi x), & E < E_{\text{th}}. \end{cases} \tag{2.4}$$

Here α and β are constants made up from a, b, p, s, p_1, and s_1. We now have assembled all the formulas needed for the study of the behavior of the elastic scattering.

Let us consider the region above the threshold. Here two processes are possible: elastic scattering and the reaction. The cross-section for elastic scattering is given by

$$\sigma_s = \frac{\pi}{k^2}(2l+1)|S_l - 1|^2$$
$$= \frac{\pi}{k^2}(2l+1)\left|\frac{\alpha + i\beta}{\alpha^* + i\beta^*} - 1\right|^2, \tag{2.5}$$

and the reaction cross-section by

$$\sigma_r = \frac{\pi}{k^2}(2l+1)[1 - |S_l|^2]$$
$$= \frac{\pi}{k^2}(2l+1)\left[1 - \left|\frac{\alpha + i\beta}{\alpha^* + i\beta^*}\right|^2\right]. \tag{2.6}$$

The total cross-section is

$$\sigma_t = \sigma_r + \sigma_s = \frac{2\pi}{k^2}(2l+1)\left[1 - \mathrm{Re}\frac{\alpha + i\beta}{\alpha^* + i\beta^*}\right]. \tag{2.7}$$

Since α and β do not depend on the energy, all three cross-sections are constants. For σ_r this has been known for a long time.[6]

Let us now go on to the region below the threshold. From Eq. (2.4) we get

$$\sigma_s = \frac{2\pi}{k^2}(2l+1)\left[1 - \mathrm{Re}\frac{\alpha + \beta\cot \pi x}{\alpha^* + \beta^* \cot \pi x}\right],$$

$$x = \frac{e_1 e_2}{\hbar}\sqrt{\frac{\mu_1}{2(E_{\text{th}} - E)}} \tag{2.8}$$

and the scattering cross-section has the form shown in Fig. 4. When the cotangent is large, the cross-section is constant (the plateaus between the resonances in Fig. 4), and is given by

$$\sigma_{s0} = 4\pi k^{-2}(2l+1)(\sin \beta)^2 |\beta|^{-2}.$$

The sharp changes in the cross-section occur only for $\cot \pi x \approx -\mathrm{Re}(\alpha/\beta)$; in such a place the cross-section runs through the whole range of possible values from zero to $4\pi k^{-2}(2l+1)$. Corresponding to the nature of the Coulomb spectrum the cross-section has an infinite number of resonances, which are more and more closely spaced as we approach

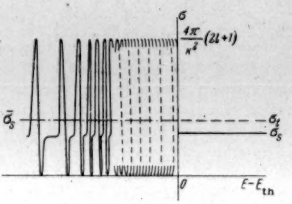

FIG. 4

the threshold point. The width of the resonance region is obviously given by the energy of the first Coulomb level, i.e., the quantity $e_1^2 e_2^2 \mu_1/2\hbar^2$. For heavy particles the width can be large. Thus if b and Y are singly charged and their masses are of the order of the nucleon mass the width is ~50 kev. A quantity of interest is the average value of the cross section:

$$\bar{\sigma}_s = \frac{1}{2\Delta}\int_{E-\Delta}^{E+\Delta} \sigma_s dE$$
$$= \frac{2\pi}{k^2}(2l+1)\,\mathrm{Re}\left\{\frac{1}{\pi}\int_{-\infty}^{\infty}\left[1 - \frac{\alpha + \beta y}{\alpha^* + \beta^* y}\right]\frac{dy}{1+y^2}\right\}$$
$$= \frac{2\pi}{k^2}(2l+1)\left[1 - \mathrm{Re}\frac{\alpha + i\beta}{\alpha^* + i\beta^*}\right] = \sigma_t. \tag{2.9}$$

In the integration one must use the inequality $i(\alpha\beta^* - \alpha^*\beta) > 0$, which follows from the fact that above the threshold the condition $|S_l| \leq 1$ must hold. Equation (2.9) leads to a remarkable result: the average scattering cross-section below the threshold is equal to the total cross-section above the threshold. Thus the total cross-section (below the threshold it is just the elastic cross-section) is in a certain sense continuous as we go through the threshold point, whereas the aver-

age elastic cross-section decreases discontinuously at this point.

3. CASE OF PRODUCTION OF AN UNSTABLE PARTICLE IN THE REACTION

It has been assumed so far that the particles b and Y are stable. We shall now consider the case in which one of them (Y) has a finite lifetime τ. It is not hard to see that the instability of Y can decidedly change the shape of the cross-section for the elastic scattering X(aa)X below the threshold. In fact, let us recall how the scattering process occurs: in the collision of a with X there is formed a certain intermediate state of the particles a, X and b, Y, which then decays to a state a + X (below threshold) or to a + X and b + Y (above threshold). If Y is unstable, it can decay during the time t of existence of the intermediate state. As a rule, however, this can be neglected, since t is usually small (of the order of nuclear times). The only exception is the case of formation of a bound state of the particles b + Y, about which we spoke in Sec. 1. The time of existence of this state can reach large values; if it is comparable with τ, an appreciable part of the Y in the intermediate state has time to decay, and this leads to a corresponding decrease of the scattering cross section. This effect is important only near the resonance maxima of the scattering cross-section and can produce a decided smoothing-out of these maxima. We also note one other conclusion from these considerations: the cross-section of the reaction

$$X(ab)Y^* \tag{3.1}$$

(Y* means the products of the decay of particle Y) will have maxima near the energies for formation of the bound states of the particles b + Y.

It is not hard to obtain formulas for the scattering cross-section and the cross-section for the reaction (1.3). To do so we must substitute in Eq. (1.10) in place of E_{th} the quantity $E_{th} - i\Gamma$ (Γ is the energy width of particle Y). We then get

$$S_l = \frac{b}{b^*}\left[1 - \frac{2i\Gamma_e}{(E - E_m^1) + i(\Gamma_e + \Gamma)}\right]. \tag{3.2}$$

This formula, like Eq. (1.10) has the usual Breit-Wigner form, but now the total width is not just the elastic width. The cross-sections for scattering and for the reaction (3.1) are obtained by substitution of Eq. (3.2) in Eqs. (2.5) and (2.6). They are just the usual Breit-Wigner formulas, and we shall not write them out here. We note only that if $\Gamma > \Gamma_e$, then at the maximum the cross-section for the reaction (3.1) will be larger than the scattering cross-section.

Like Eq. (1.10), Eq. (3.2) is valid only in the immediate neighborhood of the energy of a bound state: $E - (E_{th} - \Delta_m) \ll \delta$ (δ is the distance between resonances). Far from the resonances, however, the instability of Y can be neglected, as we have seen. The cross-section of the reaction (3.1) is equal to zero for such energies, and the scattering cross-section is constant. The approximate character of Eq. (3.2) also shows itself in the fact that it is true only if $\Gamma < \delta$.

It is easy to generalize the theory of Sec. 1 to the case in which for $E < E_{th}$ some other reactions are possible besides elastic scattering. To do this we must take the point of view of the usual resonance theory of nuclear reactions and regard the bound states of the particles b + Y as intermediate states of our system. Then introducing the partial widths for decay of a bound state into various channels, we easily obtain the generalization of the results of Sec. 1: the cross-sections for all the processes will have resonances at the energies $E \approx E_{th} - \Delta_m$; the heights of the resonances will be determined by the partial widths for the respective channels; and the width of each resonance will be the total width.

In conclusion I would like to thank Ya. A. Smorodinskiĭ for his constant interest in this work and L. A. Maksimov for reading the manuscript of the paper and making a number of comments.

APPENDIX

In the region outside the radius of action of nuclear forces ($r > r_0$) the most general wave function with a given angular momentum l has the form

$$\Psi = (R^{(-)\prime} - SR^{(+)\prime})\Phi(a, X)Y_{l0} - D(R^{(-)} - \Omega R^{(+)})\Phi(b, Y)Y_{l0}, \tag{A.1}$$

where S, Ω, and D are certain constants. The coefficient of $R^{(-)}$ is set equal to unity, since Ψ can be multiplied by any number. For $r = r_0$ this function must join on to the internal wave function. Then in general the internal wave function will not satisfy the conditions of regularity. These conditions will be satisfied only if S, Ω, and D take certain definite values. Corresponding to the two possible channels (scattering and the reaction) there must exist two and only two sets of values of S, Ω, and D for which Ψ is regular. Let us denote these values by S_i, Ω_i, D_i ($i = 1, 2$), and the two corresponding regular functions by Ψ_1 and Ψ_2. The quantities S_i, Ω_i, and D_i can be expressed in terms of the values of the wave

function and its derivative at the surface of the nucleus. To do this we must consider separately the radial functions for the particles a + X and b + Y in Eq. (A.1), and match their logarithmic derivatives, and also the ratio of these two functions, at $r = r_0$ to the corresponding quantities formed from the internal wave function. We thus get

$$\left.\frac{R^{(-)\prime} - S_l R^{(+)\prime}}{R^{(-)} - S_l R^{(+)}}\right|_{r=r_0} = \tau_l, \quad \left.\frac{\mathcal{R}^{(-)\prime} - \Omega_l \mathcal{R}^{(+)\prime}}{\mathcal{R}^{(-)} - \Omega_l \mathcal{R}^{(+)}}\right|_{r=r_0} = \rho_l,$$
$$\left.\frac{R^{(-)} - S_l R^{(+)}}{D_l(\mathcal{R}^{(-)} - \Omega_l \mathcal{R}^{(+)})}\right|_{r=r_0} = \sqrt{\frac{\mu}{\mu_1}}\,\sigma_l, \qquad (A.2)$$

where the prime indicates differentiation with respect to r; τ_l, ρ_l, and σ_l are determined by the internal function; and μ and μ_1 are the reduced masses for the particles a + X and b + Y. From Eq. (A.2) we easily get

$$S_l = \frac{\varkappa_a^{(-)} - \tau_l}{\varkappa_a^{(+)} - \tau_l}, \quad \Omega_l = \frac{\varkappa_b^{(-)} - \rho_l}{\varkappa_b^{(+)} - \rho_l},$$
$$D_l = \frac{1}{\sigma_l}\sqrt{\frac{\mu}{\mu_1}}\,\frac{\mathcal{R}^{(+)}\varkappa_b^{(+)} - \rho_l}{R^{(+)}\varkappa_a^{(+)} - \tau_l}, \qquad (A.3)$$

where

$$\varkappa_a^{(\pm)} = (R^{(\pm)\prime}/R^{(\pm)})|_{r=r_0}, \quad \varkappa_b^{(\pm)} = (\mathcal{R}^{(\pm)\prime}/\mathcal{R}^{(\pm)})|_{r=r_0}.$$

We note that by using the law of conservation of numbers of particles and the reversibility of the time one can show that the quantities τ_l, ρ_l, and σ_l are real, and that furthermore one can choose the functions in such a way that $\tau_l = \rho_l$ and $\sigma_l\sigma_2 = -1$. This must be kept in mind in order to assure ourselves that the scattering matrix obtained below is unitary and symmetric, as a scattering matrix should be.†

We can now determine the scattering matrix of our problem. To do this we take the general wave function

$$A_1\psi_1 + A_2\psi_2 = \Phi(a, X)[(A_1 + A_2)R^{(-)} - (A_1S_1 + A_2S_2)R^{(+)}]Y_{l0} + \Phi(b, Y)[(A_1D_1 + A_2D_2)\mathcal{R}^{(-)} - (A_1D_1\Omega_1 + A_2D_2\Omega_2)\mathcal{R}^{(+)}]Y_{l0} \qquad (A.4)$$

and require that it describe the processes occurring in the collision of particles a + X. To this statement of the problem there corresponds a function that does not contain converging waves of particles b + Y. In order to get such a function, we impose on the amplitudes A_1 and A_2 the condition

$$A_1D_1 + A_2D_2 = 0. \qquad (A.5)$$

Then, setting $A_1 + A_2 = 1$, we can write the function (A.4) in the form

$$[R^{(-)} - SR^{(+)}]\Phi(a, X)Y_{l0} - M\mathcal{R}^{(+)}\Phi(b, Y)Y_{l0},$$

where the quantities S and M that are the amplitudes of the outgoing waves of particles a + X and b + Y are given by:

$$S = \frac{D_1S_2 - D_2S_1}{D_1 - D_2}, \quad M = -\frac{\Omega_1 - \Omega_2}{D_1 - D_2}D_1D_2. \qquad (A.6)$$

Substituting Eq. (A.3) in Eq. (A.6), we get for S:

$$S = \left.\frac{(\tau_2 - \varkappa_a^{(-)})(\tau_1 - \varkappa_b^{(+)}) + \sigma_1^2(\tau_2 - \varkappa_b^{(+)})(\tau_1 - \varkappa_a^{(-)})}{(\tau_2 - \varkappa_a^{(+)})(\tau_1 - \varkappa_b^{(+)}) + \sigma_1^2(\tau_2 - \varkappa_b^{(+)})(\tau_1 - \varkappa_a^{(+)})}\,\frac{R^{(-)}}{R^{(+)}}\right|_{r=r_0}. \qquad (A.7)$$

From this formula we can determine the energy dependence of S near the reaction threshold. We begin by noting that near the threshold the entire energy dependence is determined by the function $\varkappa_b^{(+)}$, and all the other quantities in Eq. (A.7) can be regarded as constants. Let us prove this. By definition $\varkappa_b^{(+)}$ is the logarithmic derivative of the radial function of particles b + Y at $r = r_0$. This function has a singularity at $k_1r_0 \to 0$, and consequently $\varkappa_b^{(+)}$ changes rapidly even for small values of k_1r_0. As for the other quantities in S, $\varkappa_a^{(\pm)}$ and $R^{(\pm)}$ by definition have no singularity at the threshold and depend only on k, which near the threshold is a quadratic function of k_1:

$$k \approx \sqrt{\frac{2\mu E_{th}}{\hbar^2}}\left(1 + \frac{1}{2}\frac{\hbar^2k_1^2}{2\mu_1E_{th}}\right).$$

The situation is also similar for the quantities τ_1, τ_2, and σ_1. They are determined by the form of the wave function inside the sphere $r < r_0$, where the specifically nuclear forces are large, and therefore these quantities cannot change much for small changes of the energy of the system near the threshold. This conclusion is invalid only if there exists near the reaction threshold E_{th} some level of the system that owes its occurrence to the nuclear forces.

Changing the designations of the constants, we now get the formula for S_l given in Sec. 1.

This formula for S_l is valid both above and below the threshold. In fact, only two assumptions have been made in its derivation: 1) the quantities τ_l, ρ_l, and σ_l are real and related as stated above, and 2) the complete wave function must not contain $\mathcal{R}^{(+)}$. Strictly speaking the first assumption is valid only above the threshold, but owing to the constancy of the quantities τ_l, ρ_l, and σ_l, which has been proved, it remains true in a small region for $E < E_{th}$. The second condition holds equally well for both regions, above and below the threshold. For $E > E_{th}$ it corresponds to the absence of converging waves of b + Y, and for $E < E_{th}$

(k_1 imaginary) it is required for the finiteness of the wave function at infinity.

[1] A. I. Baz', J. Exptl. Theoret. Phys. (U.S.S.R.) **33**, 923 (1957), Soviet Phys. JETP **6**, 709 (1958).

[2] G. Breit, Phys. Rev. **107**, 1612 (1957).

[3] L. D. Landau and E. M. Lifshitz, Квантовая механика, (Quantum Mechanics), pp. 134, 505. GITTL, 1948 (Engl. Transl., Pergamon, 1958).

[4] Yost, Wheeler, and Breit, Phys. Rev. **49**, 174 (1936).

[5] Higher Transcendental Functions, vol. 1. N.Y., McGraw-Hill, 1953.

[6] E. P. Wigner, Phys. Rev. **73**, 1002 (1948).

[7] J. Blatt and V. Weisskopf, Theoretical Nuclear Physics, Wiley, 1952; Russ. Transl. IIL, 1954.

Translated by W. H. Furry
360

MONTE CARLO CALCULATIONS OF ELECTROMAGNETIC CASCADES WITH ACCOUNT OF THE INFLUENCE OF THE MEDIUM ON BREMSSTRAHLUNG

A. A. VARFOLOMEEV and I. A. SVETLOLOBOV

Submitted to JETP editor December 12, 1958

J. Exptl. Theoret. Phys. (U.S.S.R.) **36**, 1771-1781 (June, 1959)

Calculations of electromagnetic cascades, initiated by primary electrons with energies of 10^9, 10^{10}, 10^{11}, 5×10^{11}, 10^{12} and 3×10^{12} ev, have been performed for depths up to 2.8 radiation units. The Monte Carlo method was used. Actual cross sections (not asymptotic) for the elementary electromagnetic processes in the nuclear emulsions were employed. Two types of calculations were carried out: those using the Bethe-Heitler formula and those based on formulae that take into account the influence of multiple scattering and polarization of the medium on bremsstrahlung.

1. INTRODUCTION

THE method of irradiating stacks of photoemulsion plates in the stratosphere is used for the experimental investigation of electron-photon showers at high energy. Nuclear emulsions represent a sufficiently dense medium: the radiation unit length (shower) in emulsions being $t_0 = 2.9$ cm. At the present time, individual electron-photon showers, with primary energies up to $\sim 10^{12}$ ev, can be registered with adequate efficiency over several radiation lengths in several liters of emulsion.

Special interest is focused on investigations of electromagnetic cascades at high energies at the beginning of their development (in the first radiation length) where the characteristics of the cascade are determined by the basic processes at energies near to the initial energies of the particles initiating the cascade shower.

One of the basic difficulties in interpreting experimental data, obtained in investigations of this kind, is the absence of theoretical calculations of cascades with allowance for the peculiarities of nuclear emulsions. A number of workers[1-3] have carried out calculations of cascades analogous to nuclear emulsion experiments. However, these calculations cannot be considered satisfactory because they were carried out in the so-called A-approximation (see reference 4), which neglects electron collisions, except for the formation of pairs and bremsstrahlung, making use of asymptotic formulae.

Such assumptions are not justified at small depths near the vertex of the shower, particularly in the domain of low energy electron cascades. Besides, in these calculations not all elementary processes are taken into account, which can have a noticeable influence on the characteristics of the cascade.

Recently, there have appeared several papers devoted to improving the calculations of cascades and, in particular, to take into account some of the peculiarities of the emulsion method. Gardner[5] considered the influence of immediate formation of electron pairs on the different cascade processes. Several papers are devoted to the derivation[6,7] and solution[3,8] of the diffusion equations in order to obtain the energy spectrum of electrons formed in all ways (the number at small depths[3]) and taking into account ionization loss.[7] However, all these works only touch upon the separate question of developing cascades and usually do not solve the problem in view of the complexity of the calculations.

There are other difficulties which excuse the abscence of calculations on the fluctuations in cascades at small depths.

It is clear that the majority of the indicated difficulties in the calculation can be circumvented by applying the Monte Carlo method.

Of course, for a complete solution of the problem it is necessary to take into account the spatial description of the cascade. However, at high energies, primary particles develop showers in a very narrow cone. As a result, the track of the electron is effectively registered in the emulsion and it is possible to reconstruct the spatial description of the shower, at any rate, over several centimeters near the vertex of the shower. This confines calculations of the problem to small depths.

In the present work, calculations of longitudinal electromagnetic cascades were carried out down to

depths of 2.8 t_0. The calculations were carried out by the Monte Carlo method. The conditions of the calculation were chosen in accordance with the experimental peculiarities of the photoemulsion method. (Preliminary results were reported in references 9 and 10.)

2. INFLUENCE OF THE MEDIUM ON BREMSSTRAHLUNG IN NUCLEAR EMULSIONS

Landau and Pomeranchuk[11] have shown that the Bethe-Heitler theory of bremsstrahlung breaks down in condensed media at sufficiently high energies. As a consequence of multiple scattering in the medium, the bremsstrahlung process is disturbed, leading to a decreased probability for soft photon emission (particularly in the domain of small frequencies).

Ter-Mikaelyan,[12] in turn, showed that there was an additional weakening of the intensity of the soft bremsstrahlung due to the polarization of the medium.

Rigorous formulae, taking both effects into account, and valid for electron energies $E \gg mc^2$, were obtained by Migdal[13] (for a survey, see reference 14).

The graphs of the intensity of electron bremsstrahlung in nuclear emulsions according to the Bethe-Heitler formula (total screening) and according to Migdal's formula, taking into account both effects of the medium for electrons with energies from 10^{11} to 10^{13} ev, are presented in Fig. 1. For comparison, the dotted curve gives the intensity only taking the polarization effect into account. It is clear that at $E = 10^{12}$ ev the influence of the medium on radiation quanta with energy $\hbar\omega \leq 10^9$ ev is considerable.

To determine the influence of these effects on the energy spectra of particles in electromagnetic cascades and to clarify the possibility of experimentally revealing these effects, it was decided to carry out two types of calculations: using the Bethe-Heitler formula and applying Migdal's formula, taking into account both influences of the medium on the bremsstrahlung. Since the influence of the medium manifests itself more strongly the smaller the energies of the radiated quanta, it was decided to calculate spectra of cascade electrons and pairs up to energies $\sim 10^6$ ev, valid at small depths t in the emulsion. This required the actual (not asymptotic) cross sections for the elementary processes.

3. ELEMENTARY CROSS SECTIONS OF THE ELECTROMAGNETIC PROCESSES, USED IN THE CALCULATION

The following electromagnetic processes in the fields of the nuclear and electronic components of the emulsion were taken into account in the calculation: bremsstrahlung, pair production by photons, pair production by electrons, the Compton effect, photonuclear absorption and ionization deceleration of the electron. The spatial distribution of the particles was neglected in the calculation. We therefore used for all the elementary processes differential cross sections integrated over the angle, and dependent only on the energy of the particles. That is, cross sections of the type $d\sigma = f(\alpha, \beta)\,d\alpha$, where β is the energy of the primary particle and α is the energy of one of the formed particles.

The Bethe-Heitler formula in the Born approximation, taking screening into account by using the Thomas-Fermi model, was used for the differential cross section for bremsstrahlung and pair formation in the field of the nucleus. The screening function was approximated by an analytic expression to within 1 to 2 per cent. The Thomas-Fermi approximation is considered sufficient for the problem under consideration, because the electromagnetic processes in emulsions take place principally in the heavy nuclei Ag and Br.

We took into account the corrections necessi-

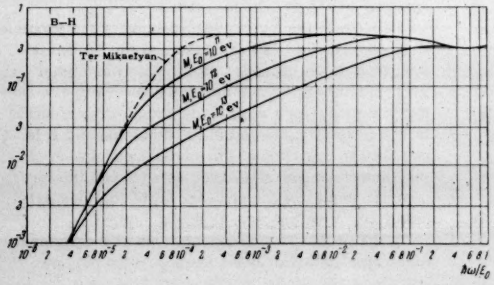

FIG. 1. Energy dependence of electron bremstrahlung in emulsions, in accordance with the Bethe-Heitler formula (B-H) and Migdal's formula (M) for electrons with energies 10^{11} to 10^{13} ev. Ordinate: intensity of the radiation $(\hbar\omega/E_0)/\lambda(\omega)$, where $\lambda(\omega)$ is the free passage of electrons in emulsions for radiation of quanta with frequency between ω and $\omega + d\omega$. E_0 is the energy of the electron.

tated by failure of the Born approximation. In the expression for the differential cross section for pair formation, the corrections introduced by Davies et al.[15] are independent of the screening:

$$\Delta\sigma = -\frac{28}{9}\frac{Z^2 r_0^2}{137} f(Z), \qquad f(Z) = a^2 \sum_{\nu=1}^{\infty} \frac{1}{\nu(\nu^2+a^2)},$$

where $a = Ze^2/\hbar c$ and Z is the nuclear charge. For the heavy elements of emulsions $f(Z) = 0.59 \times 10^{-4} Z^2$. In accordance with Olsen and Brown,[16] analogous corrections were introduced into the expressions for bremsstrahlung.

The total cross section σ for pair production by photons with energy $\hbar\omega \leq 10$ Mev was calculated using the known numerical data,[17] by means of analytic integration of the cross section, $d\sigma$, without taking into account the screening in the Born approximation. Then corrections to the Born approximation, σ_b, were introduced in accordance with the experimental results of Dayton.[18]

$$\Delta\sigma = +1.59 \cdot 10^{-4} Z^2 \sigma_B \quad \text{for} \quad \hbar\omega = 1.33 \text{ Mev},$$

$$\Delta\sigma = +3.39 \cdot 10^{-5} Z^2 \sigma_B \quad \text{for} \quad \hbar\omega = 2.62 \text{ Mev}.$$

Also, in accordance with reference 19, $\Delta\sigma = 0$ at $\hbar\omega = 5$ Mev and $\Delta\sigma = -0.04\ \sigma_B$ at $\hbar\omega = 10$ Mev.

The total cross section for pair production by photons at $\hbar\omega > 10$ Mev in the nuclear field was obtained from numerical integration of the Bethe-Heitler formula, taking screening and the corrections due to Davies[15] into account. The integration was performed on an electronic computer for separate groups of elements with charges Z = 47.35, 7, and 1.

The cross section for bremsstrahlung was calculated in an analogous way: numerical integration of the expression $d\sigma$, with the corrections.[15]

In determining the total cross sections for elements, Z_i, pair production and bremsstrahlung in the electron field were also taken into account. The formula of Wheeler and Lamb[20] was used, taking screening into account correctly, generally speaking, for nuclei with charge Z = 1. For pair production, we follow Bethe and Ashkin[21] obtained by means of numerical integration of the cross section subtracted from the different total cross sections in a nuclear field Z = 1 and in the electron field, determined from the results of Borsellino.[21]

The so-called absorption coefficient, τ, is defined as $\tau = \sum n_i \sigma_i$, where σ_i is the total cross section for the interactions under consideration in atoms Z_i, while n_i is the number of atoms Z_i per cm^3 of medium. The value of n_i is determined in accordance with the composition of the emulsion Ilford G-5 at 58 per cent humidity.[22] The composition of the R-NIKFI emulsion is nearly the same.[23]

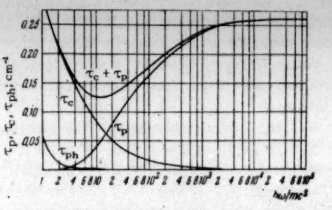

FIG. 2. Absorption coefficients for photons in emulsions for pair production (τ_p), Compton effect (τ_c) and photo-electric effect (τ_{ph}).

The calculated values of the absorption coefficients of γ quanta in emulsions after counting pair production (in the fields of the nuclear and electronic components of the emulsion) and Compton effect are presented in Fig. 2. For comparison, the value of τ_{ph} for the usual photo-effect is presented.

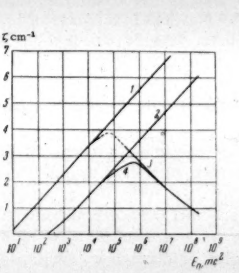

FIG. 3. The coefficient $\tau = 1/\lambda$, for electrons with energy E_0 for the radiation of quanta with energy $\hbar\omega \to \varepsilon$ calculated for emulsions according to the Bethe-Heitler (B – H) and Migdal's (M) formulae. 1) B – H, $\varepsilon = 1.5 \times 10^6$ ev, 2) B – H, $\varepsilon = 10^8$ ev, 3) M, $\varepsilon = 1.5 \times 10^6$ ev, 4) M, $\varepsilon = 10^8$ ev.

The τ coefficients for radiation quanta with energies exceeding the minimum value ϵ (1.5×10^6 ev and 10^8 ev) are given in Fig. 3. Curves 3 and 4 were obtained by numerically integrating Migdal's[13] formula for the differential cross section. The composition of the medium, in this case, is allowed for in the following way. Since the probability of radiation depends on the medium through the quantity $Z^2 \ln(190\ Z^{-1/3})$. We determine for emulsions an effective value $Z_{eff} = 20.54$, and then the parameter $s_1 = (Z_{eff}^{1/3}/190)^2$, which enters

into Migdal's formula. The effect of polarization was accounted for by introducing into the formula the parameter $q = s\gamma$ instead of s and dividing the expression for the probability of radiation by γ, where $\gamma = 1 + 5.1 \times 10^{-9} (\hbar\omega)^{-2} E^2$, a parameter that takes into account the deviation of the dielectric constant of the emulsion from unity.

The value of the coefficient τ for electron pair production by electrons was determined in the following way: in the electron energy range $E < 10^7$ ev, the formula of Bhabha,[24] neglecting shielding, was used; in the range 10^7 ev $\leq E \leq 10^9$ ev we used the modified Bhabha formula,[25] and in the range $E > 10^9$ ev we used the Racah[26] formula, taking shielding into account (see reference 25).

Ionization loss of the electrons was considered constant and equal to 7 Mev/cm (the loss on the ionization plateau[27]). The loss of electron energy in radiating soft quanta with energies $\hbar\omega < \epsilon$ was not considered in the calculation of the cascade. As shown in the actual calculations, these losses can be considered constant to an accuracy of 1 or 2 per cent for electrons with energies $> 10\,\epsilon$. The usual energy loss for electrons was considered to be equal to 7.6 Mev/cm in the case of $\epsilon = 1.5 \times 10^6$ ev and 50 Mev/cm in the case $\epsilon = 10^8$ ev.

4. CONDITIONS OF THE CASCADE CALCULATION

The primary particles initiating the cascade were taken to be electrons with initial energies E_0 of 10^8, 10^{10}, 10^{11}, 5×10^{11}, 10^{12}, and 3×10^{12} ev.

Several problems were calculated simultaneously. Along the t axis of the shower, all secondary particles (electrons and photons) having a total energy greater than some value ϵ (1.5×10^6 or 10^8 ev) were investigated. Results were obtained for four values of the cascade depth t (calculated from the vertex of the shower): $t_1 = 1.0\,t_0$, $t_2 = 1.5\,t_0$, $t_3 = 2.1\,t_0$, and $t_4 = 2.8\,t_0$.

We note that the quantity $t_0 = 2.9$ cm is only used as a unit of length. The probability of different processes is calculated according to the elementary cross sections (see the preceding section).

Two of the elementary processes taken into account — bremsstrahlung and γ-quantum pair production — were performed for definite Z_i. The value Z_i corresponding to the four groups of elements in the emulsion: hydrogen ($Z = 1$), the group of light elements ($Z = 7$), bromine ($Z = 35$), and silver ($Z = 47$). The remaining processes were performed with cross sections, averaged according to the composition of the emulsion.

The values of the coefficients τ_j were specified at the following values of the total energies of the particles, expressed in units of the electron rest mass mc^2: 3, 7, 10, 20, 60, 200, 600, 2×10^3, 6×10^3, 2×10^4, 2×10^5, 2×10^6, and 2×10^8. Linear interpolation was used for intermediate values of the energy.

The sequence of selecting the processes for photons was performed in the following way:

1. Select the distance x, which the photon covers prior to an interaction, in accordance with the total absorption coefficient for all the elements of the emulsion.

2. Select the form of the process. Each of the six processes taken into account (pair production at a fixed Z_i, absorption, and Compton effect) was given its statistical weight.

3. In the case of pair production, the energy of the pair and the depth t at the place of production were noted in the results. Then the relative energy of the components of the pair were selected according to the formula for the differential cross section at a fixed Z_i.

4. For the Compton effect, the Klein-Nishina formula was used to determine the scattering angle of the photon, the angle of the ejected electron and the energies of the photon and electron. We chose for further investigation photons whose scattering angle did not exceed 0.01 radians and electrons with a scattering angle $< 30°$. The electron yield, independent of the scattering angle, was noted in the appropriate energy intervals.

The scheme for choosing the electron processes was the following:

1. Select the distance x, which the electron covers prior to one of the processes, with the help of the total coefficient τ, taking into account bremsstrahlung with energy $> \epsilon$ and electron pair production.

2. Determine the energy of the electron at the point of interaction, taking into account energy losses by ionization and soft bremsstrahlung with energy $< \epsilon$, along the path x.

3. As the electrons passed through depths t_i ($i = 1, 2, 3, 4$), determine the energies at these depths and record the results in appropriate energy intervals.

4. Select the nature of the process (five possibilities) in accordance with their statistical weights τ_i/τ.

5. Select the radiation energy according to the

TABLE I. Differential energy spectrum of electrons and electron pairs in cascade showers initiated by electrons with energy E_0

Energy interval, ev	Number of pairs down to depths				Number of electrons to depths			
	t_1	t_2	t_3	t_4	t_1	t_2	t_3	t_4
			$E_0 = 10^8$ ev					
$1.5 \cdot 10^8$—$3.5 \cdot 10^8$	0.06	0.09	0.16	0.24	0.18	0.34	0.68	0.65
$3.5 \cdot 10^8$—10^7	0.11	0.30	0.70	1.21	0.30	0.61	0.84	1.16
10^7—$3 \cdot 10^7$	0.21	0.52	1.05	1.85	0.41	0.88	1.37	1.42
$3 \cdot 10^7$—10^8	0.27	0.62	1.15	1.74	0.60	1.05	1.06	1.22
10^8—$3 \cdot 10^8$	0.27	0.52	0.76	1.12	0.45	0.56	0.64	0.62
$3 \cdot 10^8$—10^9	0.21	0.28	0.46	0.62	0.68	0.45	0.27	0.14
			$E_0 = 10^{10}$ ev					
$1.5 \cdot 10^8$—$3.5 \cdot 10^8$	0	0.08	0.16	0.40	0.18	0.46	1.13	2.05
$3.5 \cdot 10^8$—10^7	0.13	0.41	0.94	2.31	0.28	0.96	1.90	3.59
10^7—$3 \cdot 10^7$	0.22	0.63	1.72	3.76	0.71	1.24	2.62	4.69
$3 \cdot 10^7$—10^8	0.37	0.96	2.35	4.71	0.60	1.33	3.14	5.13
10^8—$3 \cdot 10^8$	0.30	0.70	1.59	3.24	0.54	1.14	2.33	3.47
$3 \cdot 10^8$—10^9	0.33	0.78	1.63	2.82	0.49	1.14	1.46	1.99
10^9—$3 \cdot 10^9$	0.19	0.36	0.73	1.20	0.56	0.61	0.68	0.65
$3 \cdot 10^9$—10^{10}	0.23	0.41	0.55	0.63	0.63	0.49	0.41	0.20

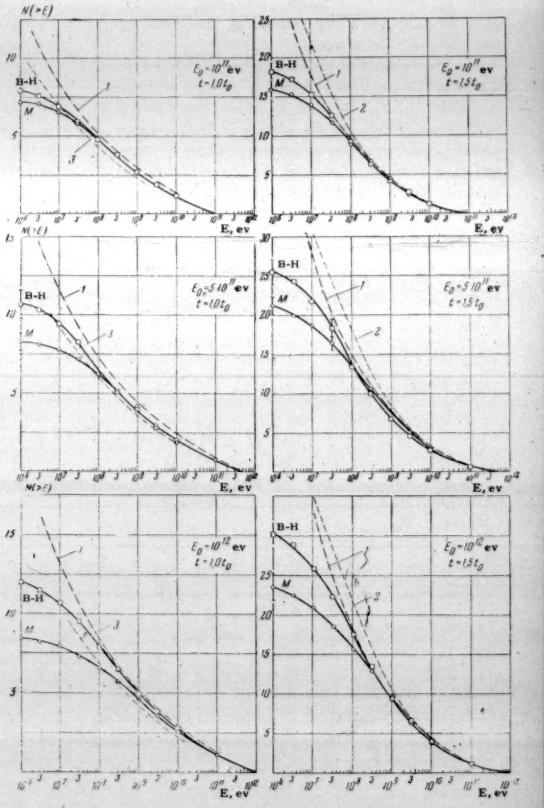

FIG. 4. Integrated energy spectrum of N(> E) electrons to depths t in the cascade shower, initiated by electrons with energy E_0. B–H) calculated according to Bethe-Heitler for emulsions, M) calculated according to Migdal's formula, 1) results of Arley,[1] 2) results of Janossy and Messel,[2] 3) results of Srinivasan et al.[3]

differential cross section, taking screening into account.

6. Select the pair energy and select the energies of the components of the pair according to Rossi's formula[28] (using the average Z of the emulsion).

In all cases, the selection must be performed with respect to a complicated formula, which does not allow a simple converse transformation. Therefore, we used the following method of selection with a double series of random numbers:[29]

The first random number, ξ_1, fixes the value u_1 of the argument of the differential probability $f(u)$. The value $f(u_1)$ is then compared with a second random number ξ_2. If $f(u_1) < \xi_2$, the operation is repeated. We generate the following pair of random numbers ξ_3 and ξ_4 which determines u_3 and carry out the comparison of $f(u_3)$ with ξ_4 and so on, until the condition $f(u_k) > \xi_{k+1}$ is satisfied. The values u_k are used as the generated argument.

As the results of the data are distributed about a number of particles in twelve energy intervals, to depths t_1, t_2, t_3, and t_4. The limits of the intervals coincide with the values of the energies, in which is assigned the numerical value τ_i (see above). The calculation of the cascade was carried out on the "Strela" electronic computer.

5. RESULTS

The purpose of the calculation was to obtain the following characteristics of electromagnetic cascades in their first stages of development in nuclear emulsions:

1. Energy spectrum of cascade electrons reaching depths t_1, t_2, t_3, and t_4.

2. Energy spectrum of electron-positron pairs produced by photons down to depths t_1, t_2, t_3, and t_4.

3. Energy spectrum of the Compton electron yield to depths down to t_1 and t_2.

4. The number of pairs formed by electrons (tridents) with energy corresponding more or less to 3×10^7 ev in depths $\leq t_2$.

Besides this, the fact that the cascade calculations covered all particles and not merely a separate single branch of the cascade tree has allowed us to obtain information on fluctuations in the cascade.

A total of more than 1000 cascade trees were followed. At $E_0 = 10^{12}$ ev, 179 cascade trees were calculated using the Bethe-Heitler formula, in the remaining cases, an average of 80 to 100 trees were followed.

The results of the calculations for primary energies $E_0 = 10^9$ and 10^{10} ev are presented in Table I. The influence of the medium is absent at so small E_0. The data can be useful for work with electrons obtained in accelerators.

Figure 4 shows the integrated energy spectrum for cascade electrons at depths t_1 and t_2 at primary energies $E_0 \geq 10^{11}$ ev. It is seen that the total number of electrons in the Bethe-Heitler formula (B-H) is 10 to 40 per cent higher than that calculated by Migdal's formula (M), if the influ-

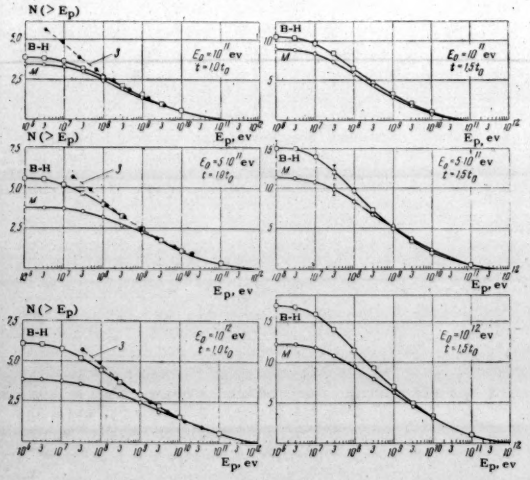

FIG. 5. Integrated energy spectrum $N(>E_p)$ of electron-positron pairs to depths t in cascade showers, formed by electrons with energy E_0 [Notation is the same as in Fig. (4)].

ence of the medium is taken into account. From a comparison of the graphs it is possible to see how much this difference depends on the primary energy E_0 and the considered depth t. For comparison, the cascade curves of Arley,[1] Janossy and Messel,[2] and Srinivasan et al.[3] are also presented. It is seen that the essential difference between our results and the others occurs for low energy electrons.

The errors indicated in Fig. 4 (as in all subsequent figures) are statistical. They are determined from the results of calculations on the distribution of tree cascades with respect to the number of electrons in the cascade, N(>E).

The integrated energy spectrum of electron-positron pairs N(>E) is presented in Fig. 5, formed in depths down to t_1 and t_2 at different E_0. The difference between the Bethe-Heitler and Migdal variants in this case is from 10 to 60 per cent, i.e., visibly greater than in the electron spectrum at high E_0. If we take into consideration that the effectiveness of counting a pair is greater than for electrons only, it becomes clear to what extent it is advantageous to measure electron-positron pairs in order to investigate the influence of the medium.

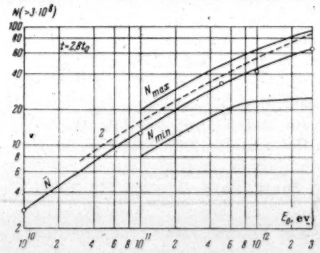

FIG. 6. Number of electrons N, depth t_4 with energy $E > 3 \times 10^8$ ev as a function of the energy, E_0, of the electron initiating the shower. N, N_{max} and N_{min} are the average, the maximum and the minimum number of electrons using Migdal's formula. 2) The results of Janossy and Messel.[2]

Curve 3 in Fig. 5 is drawn from the results of Srinivasan et al.[3] It is seen that it is little different from our results for high energy pairs using the Bethe-Heitler formulation, particularly at $E_0 = 10^{11}$ ev, but very different for low-energy pairs.

In Fig. 6 we present the curves for the number of electrons at depth t_4 with energy $> 3 \times 10^8$ ev as a function of the primary energy E_0. Curves N_{max} and N_{min} tend to the limiting value N in different cascades. The probability that N lies between the limits N_{max} to N_{min} is 0.7. See reference 10 for the determination of N_{max} and N_{min}.

Table II gives the results of the calculation for the number of pairs formed by electrons (tridents) at depths $t \leq 1.55\,t_0$.

In Fig. 7 we present a histogram of the distribution of cascade electrons, depth t_2 with energy $E > 1.5 \times 10^6$ ev ($E_0 = 10^{12}$ ev, B-H variant).

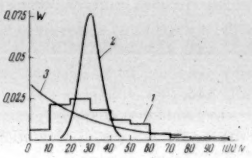

FIG. 7. Probability, W, of finding N electrons with energy $E > 3 \times 10^8$ ev at depth t_2 in a cascade shower, formed by electrons with energy $E_0 = 10^{12}$ ev. 1) Results of the calculation using the Bethe-Heitler formula. 2 and 3) The Poisson and Furry[30] distributions, respectively, at average value $\bar{N}$, determined in the calculation.

For comparison, we also show the curves for Poisson and Furry[30] distributions for the corresponding average $\bar{N}$. It is seen that the Furry curve agrees better with the distribution than the Poisson curve.

Taking the fluctuations in the cascade into account, it is possible to say that in order to detect, experimentally, the influence of the medium on bremsstrahlung from the energy spectrum of

TABLE II. Number of electron-positron pairs with total energy $\geq 1.5 \times 10^6$ ev, produced immediately by electrons in cascade showers, initiated by electrons with energy E_0, to depths $t \leq 1.55\,t_0$. The number of pairs with energies 1.5×10^6 to 3×10^7 ev is indicated in parentheses

E_0, ev	B–H	M.	E_0, ev	B–H	M.
10^9	0.04 (0.02)		$5 \cdot 10^{11}$	0.52 (0.20)	0.34 (0.05)
10^{10}	0.14 (0.08)		10^{12}	0.56 (0.18)	0.51 (0.15)
10^{11}	0.28 (0.07)	0.27 (0.11)			

pairs in electron-photon showers, it is necessary to have not less than 8 to 10 showers with energy $\sim 10^{12}$ ev.

We express our thanks to I. I. Gurevich for his attention and interest in the work, to A. B. Migdal and to P. Nemirovskiĭ for valuable consultation, to A. A. Dorodnitsin for use of the computer, and to D. I. Golenko for programming the problem.

[1] N. Arley, Proc. Roy. Soc. **A168**, 519 (1938).

[2] L. Janossy and H. Messel, Proc. Roy. Irish. Acad. **A54**, 217 (1951).

[3] Srinivasan, Butcher, Chartres, and Messel, Nuovo cimento **9**, 77 (1958).

[4] B. Rossi and K. Greisen, Revs. Modern Phys. **13**, 240 (1941).

[5] J. W. Gardner, Nuovo cimento **7**, 10 (1958).

[6] A. Ramakrishnan and S. K. Srinivasan, Proc. Ind. Acad. Sci. **A44**, 263 (1956); S. K. Srinivasan and N. R. Ranganatham, Proc. Ind. Acad. Sci. **A45**, 69 (1957).

[7] A. Ramakrishnan and S. K. Srinivasan, Proc. Ind. Acad. Sci. **A45**, 133 (1957).

[8] S. K. Srinivasan and N. R. Ranganatham, Proc. Ind. Acad. Sci. **A45**, 268 (1957).

[9] Varfolomeev, Golenko, and Svetlolobov, Dokl. Akad. Nauk SSSR **122**, 785 (1958), Soviet Phys. "Doklady" **3**, 977 (1959).

[10] Varfolomeev, Gerasimova, Gurevich, Makar'ina, Romantseva, Svetlolobov, and Chueva, Proc. of the 1958 Ann. Roch. Conf. on High Energy Physics, CERN, 297 (1958).

[11] L. D. Landau and I. Ya. Pomeranchuk, Dokl. Akad. Nauk SSSR **92**, 535, 735 (1953).

[12] M. L. Ter-Mikaelyan, Dokl. Akad. Nauk SSSR **94**, 1033 (1954).

[13] A. B. Migdal, Phys. Rev. **103**, 1811 (1956); J. Exptl. Theoret. Phys. (U.S.S.R.) **32**, 633 (1957), Soviet Physics JETP **5**, 527 (1957).

[14] E. L. Feĭnberg, Usp. Fiz. Nauk **58**, 193 (1956); E. L. Feĭnberg and I. Ya. Pomeranchuk, Suppl. Nuovo cimento **3**, 652 (1956).

[15] Davies, Bethe, and Maximon, Phys. Rev. **93**, 788 (1954).

[16] H. Olsen, Phys. Rev. **99**, 1335 (1955). K. L. Brown, Phys. Rev. **103**, 243 (1956).

[17] W. Heitler, The Quantum Theory of Radiation (Russ. Transl.) IIL, M. 1956, p. 297, [Oxford, 1953]. P. V. C. Hough, Phys. Rev. **73**, 266 (1948).

[18] I. E. Dayton, Phys. Rev. **89**, 544 (1953).

[19] S. A. Colgate, Phys. Rev. **87**, 592 (1952). Rosenblum, Shrader, and Warner, Phys. Rev. **88**, 612 (1952). H. I. West, Phys. Rev. **101**, 915 (1956).

[20] J. A. Wheeler and W. E. Lamb, Phys. Rev. **55**, 858 (1939).

[21] E. Segre ed., Experimental Nuclear Physics, Vol. 1 (Russ. Transl.) IIL, M. 1955, p. 279 [Wiley, 1953].

[22] A. J. Swinnerton and C. Waller, Sci. et inds. photogr. **28**, 481 (1957).

[23] M. F. Rodicheva, Научн. и прикл. фотогр. и кинематогр. (Scient. and Appl. Photogr. and Cinematogr.) **3**, 286 (1958).

[24] H. J. Bhabha, Proc. Roy. Soc. **A152**, 559 (1935).

[25] Block, King, and Wada, Phys. Rev. **96**, 1627 (1954).

[26] G. Racah, Nuovo cimento **14**, 93 (1937).

[27] Varfolomeev, Gerasimova, Makar'ina, Romantseva, and Chueva, J. Exptl. Theoret. Phys. (U.S.S.R.) **36**, 707 (1959), Soviet Phys. JETP **9**, 495 (1959).

[28] B. Rossi, High Energy Particles (Russ. Transl.) IIL, M. 1955, p. 108 [Prentice-Hall, 1952].

[29] A. S. Householder, Ed., Nat. Bur. Stand., Appl. Math. Ser. **12**, 33 (1951).

[30] W. H. Furry, Phys. Rev. **52**, 569 (1937).

Translated by Kenneth Smith
361

CYLINDRICAL AND PLANE MAGNETOHYDRODYNAMIC WAVES

K. P. STANYUKOVICH

Bauman Higher Technical School

Submitted to JETP editor December 13, 1958

J. Exptl. Theoret. Phys. (U.S.S.R.) **36**, 1782-1787 (June, 1959)

Cylindrical waves produced in a conducting medium by a magnetic field are considered. The two cases when the field is directed along the z axis and along the angle φ are analyzed. Special attention is paid to "sound" waves as well as to those possessing velocities close to that of light.

A study of plane and particularly cylindrical magnetohydrodynamic waves is of considerable interest both from the physical and from the analytical points of view.

In the present paper we confine ourselves to the case of infinite conductivity and isentropic motion, with the condition that the magnetic field is perpendicular to the velocity. We shall carry out the study first in the general relativistic form with strong fields and large energy densities, and shall then proceed to examine "classical" relatively weak waves.

1. FUNDAMENTAL EQUATIONS

The fundamental equations of isentropic cylindrical waves can be written in the relativistic case

$$\frac{1}{\theta^2}\left(\frac{\partial a}{\partial t}+a\frac{\partial a}{\partial r}\right)+c^2\left(\frac{\partial \ln w^*}{\partial r}+\frac{a}{c^2}\frac{\partial \ln w^*}{\partial t}\right)=0, \tag{1}$$

$$-\left(\frac{\partial \ln V}{\partial t}+a\frac{\partial \ln V}{\partial r}\right)+\frac{1}{\theta^2}\left(\frac{\partial a}{\partial r}+\frac{a}{c^2}\frac{\partial a}{\partial t}\right)-\frac{Na}{r}=0. \tag{2}$$

Here a is the velocity, w* the total heat content, V the specific volume, $\theta^2 = 1 - a^2/c^2$, N = 1 for cylindrical waves, and N = 0 for plane waves. The equations can be derived by using the condition $\partial T_{ik}/\partial x_k = 0$, where T_{ik} is the total energy-momentum tensor of the field and of the medium.[1]

If the magnetic-field vector is perpendicular to the plane of motion of the medium, we have

$$HV = b = \text{const}. \tag{3}$$

If the magnetic-field vector lies in the plane of motion (but is, naturally, perpendicular to the velocity vector), then

$$\frac{HV}{r} = b = \text{const}. \tag{4}$$

Relations (3) and (4) can be combined into one,

$$HV = br^m, \tag{5}$$

where m = 0 when N = 0 and m = 0 or 1 when N = 1. From the relation $dw^* = Vd(p + p') = V\,dp^*$, where

$$dp' = \frac{Hr^{-m}}{4\pi}d(Hr^m) = \frac{1}{4\pi V}d(iH^2V) \tag{6}$$

(p' is the supplementary field pressure), we obtain

$$w^* = pV + \rho Vc^2 + \frac{H^2V}{4\pi}. \tag{7}$$

Inserting now the value of H from (5) we get

$$dw^* = V\,dp - \frac{b^2}{4\pi V^2}r^{2m}\,dV + \frac{2mb^2r^{2m-1}}{4\pi V}\,dr$$

$$= V\,dp - \frac{H^2\,dV}{4\pi} + \frac{2mH^2V\,dr}{4\pi r}. \tag{8}$$

Now Eq. (1) can be rewritten

$$\frac{1}{\theta^2}\left(\frac{\partial a}{\partial t}+a\frac{\partial a}{\partial r}\right)$$

$$-\omega^{*2}\left(\frac{\partial \ln V}{\partial r}+\frac{a}{c^2}\frac{\partial \ln V}{\partial t}\right)+\frac{2mc^2VH^2}{4\pi r w^*}=0. \tag{9}$$

The characteristics of the system of equations (9) and (2) can be written

$$\frac{dr}{dt}=\frac{a\pm\omega^*}{1\pm a\omega^*/c^2}. \tag{10}$$

The following relations hold along the lines

$$\frac{da}{\theta^2}=\pm\omega^*\,d\ln V\mp\omega^*\frac{Na}{r}\,dt-\frac{2mc^2VH^2}{4\pi r w^*}\,dt$$

$$=\pm\omega^*\,d\ln V\mp\omega^*\frac{Na}{r}\,dt-\frac{2mc^2b^2r}{4\pi V w^*}\,dt, \tag{11}$$

where

$$\frac{\omega^{*2}}{c^2}=\frac{V}{w^*}\left(-V\frac{dp}{dV}+\frac{H^2}{4\pi}\right); \tag{12}$$

ω^* is the magneto-gasdynamic velocity of sound. Inasmuch as

$$\frac{V}{w^*}=\frac{1}{p+\rho c^2+H^2/4\pi},\qquad -V\frac{dp}{dV}=\frac{\omega^2}{c^2}(p+\rho c^2),$$

where $\omega = (dp/d\rho)^{1/2}$ is the ordinary velocity of sound, we get

$$\frac{\omega^{*2}}{c^2} = \frac{(p+\rho c^2)\,\omega^2/c^2 + H^2/4\pi}{p+\rho c^2 + H^2/4\pi}. \qquad (13)$$

Let us now calculate the value of ω^{*2}/c^2 for an ideal gas, assuming that for the isentropic process $p = AV^{-k}$, where A is a constant. Here, starting with the relation $-dV/V = c^2 d\rho/(p+\rho c^2)$, we obtain

$$\rho V = \alpha + \frac{pV}{(k-1)\,c^2}, \qquad \alpha = \rho_a V_a \left(1 - \frac{p_a}{(k-1)\,\rho_a c^2}\right),$$

where ρ_a and V_a are the initial values of ρ and V at $p = p_a$. It is obvious that

$$\frac{\omega^{*2}}{c^2} = \frac{kAV^{2-k} + r^{2m}b^2/4\pi}{\alpha Vc^2 + kAV^{2-k}/(k-1) + r^{2m}b^2/4\pi}.$$

For ordinary gas $\alpha = 1$; for an ultrarelativistic or a photon gas, when $p = (k-1)\rho c^2$, we get $\alpha = 0$.

Let us proceed now to examine several problems.

2. STATIONARY FLOWS

In the case of stationary flows the system (1) and (2) admits of the following integrals

$$w^*/\theta = w_0 = \text{const}, \qquad (14)$$

$$\frac{ar^N}{V\theta} = \frac{\overline{m}}{A} = m = \text{const}, \qquad (15)$$

where w_0^* is the heat contents at rest, $A = 1$ or 2π respectively for $N = 0$ or 1, and $\overline{m}$ is the total mass flow per second.

Relations (14) and (15) can be rewritten

$$\frac{a^2}{c^2} = \left(1 + \frac{c^2 r^{2m}}{m^2V^2}\right)^{-1} = 1 - \frac{w^{*2}}{w_0^{*2}}$$

$$= 1 - \frac{1}{w_0^{*2}}\,(pV + \rho Vc^2 + H^2V/4\pi)^2. \qquad (16)$$

From (16) we obtain an expression for V

$$\left(\alpha c^2 + \frac{kA}{k-1}V^{1-k} + \frac{b^2 r^{2m}}{4\pi V}\right)^2 = w_0^{*2}\left(1 + \frac{m^2V^2}{c^2 r^{2m}}\right)^{-1}.$$

The case when $N = 0$ (and consequently $m = 0$) is of no interest; in this case $V = \text{const}$.

Let us consider two interesting types of motion, when $N = 1$ and $m = 0$ and 1. It is easy to explain first that the motion in these cases can be defined only within a certain region. In fact, since

$$r^{2m} = (m/c)^2 w^{*2}V^2/(w_0^{*2} - w^{*2}),$$

we have at $dr^{2m} = 0$

$$-d\ln w^*/d\ln V = 1 - w^{*2}/w_0^{*2} = a^2/c^2.$$

Furthermore

$$dw^* = V\,dp - \frac{H^2\,dV}{4\pi}, \qquad -\frac{d\ln w^*}{d\ln V} = \frac{\omega^{*2}}{c^2},$$

so that

$$\frac{\omega^{*2}}{c^2} = \frac{\omega_{cr}^{*2}}{c^2} = \frac{a_{cr}^2}{c^2} = 1 - \frac{w_{cr}^{*2}}{w_0^{*2}},$$

i.e., the condition of critical flow is obtained.

If $m = 0$, we can readily determine $V = V_{cr}$; $r = r_{cr} = r_{min}$, and the motion is defined in the region $r_{min} \le r < \infty$. When $\alpha \neq 0$ and $r \to \infty$ we have $V \to \infty$; $a = a_{max} < c$, with

$$r_{min} \approx \frac{mV}{c}\,\frac{\alpha c^2}{(w_0^{*2} - a^2c^4)^{1/2}}.$$

If $\alpha = 0$, then

$$r \approx \frac{m}{cw_0^*}\left(\frac{kA}{k-1}\right)^{1/2} V^{(2-k)/2}$$

and

$$a \to a_{max} = c.$$

If $m = 1$, we obtain by eliminating r^2

$$\left[\frac{k}{k-1}AV^{1-k} + \alpha c^2 + \frac{b^2m^2V}{4\pi c^2} + \frac{1}{-1 + \left\{\left[kAV^{1-k}\,\frac{2-k}{k-1} + \alpha c^2\right]\Big/ w_0^{*2}\right\}^{-1/2}}\right]^2$$

$$= w_0^{*2}\left(\frac{2-k}{k-1}\,kAV^{1-k} + \alpha c^2\right),$$

which determines $V = V_{cr}$.

If $\alpha \neq 0$, then, as seen from an analysis of this equation, we have two values of $V = V_{cr}$, corresponding to two extremal values of r, $r = r_{min}$ and $r = r_{max}$. Thus, the motion will be defined in the region $r_{min} \le r \le r_{max}$. When $r \ge r_{max}$, the stationary mode of flow is no longer possible, and the current will pulsate there.

If $\alpha = 0$ (ultrarelativistic gas), then $r_{max} \to \infty$, and thus the stationary flow will be defined in the region $r_{cr} \le r < \infty$.

3. NONSTATIONARY WAVES

We shall study strong "sound" waves in an ultrarelativistic gas, when the pulsation occurs at velocities of flow close to the velocity of light so that $1 - a/c \ll 1$. Now Eqs. (2) and (9) become

$$\frac{1}{\theta^2}\left[\frac{\partial(a/c)}{c\partial t} + \frac{\partial(a/c)}{\partial r}\right] = \frac{\omega^{*2}}{c^2}\left(\frac{\partial\ln V}{c\partial t} + \frac{\partial\ln V}{\partial r}\right)$$

$$-\frac{2mH^2V}{4\pi r w^*} = -\frac{N}{r} + \frac{\partial\ln V}{c\partial t} + \frac{\partial\ln V}{\partial r}. \qquad (17)$$

Hence, since $H^2V = b^2r^{2m}/V$, we have

$$\left(1 - \frac{\omega^{*2}}{c^2}\right)\left(\frac{\partial\ln V}{c\,\partial t} + \frac{\partial\ln V}{\partial r}\right) = \frac{N}{r} - \frac{2mb^2r^{2m}}{4\pi V r w^*}. \qquad (18)$$

Here

$$1-\frac{\omega^{*2}}{c^2}=\frac{kAV^{1-k}(2-k)/(k-1)+\alpha c^2}{kAV^{1-k}/(k-1)+\alpha c^2+b^2r^{2m}/4\pi V},$$

$$w^*=\frac{kAV^{1-k}}{k-1}+\alpha c^2+\frac{b^2r^{2m}}{4\pi V}.$$

The solution of Eq. (18) involves no great difficulties in the case of an ultrarelativistic gas, $\alpha = 0$. In the case when $N = 0$, we have $V = F(r - ct)$, but a more detailed analysis is of no interest.

Let us consider the case when $N = 1$:

$$\frac{\partial \ln V}{c\partial t}+\frac{\partial \ln V}{\partial r}=\frac{1}{(2-k)r}\left[1+\frac{(k-1)b^2r^{2m}}{4\pi kAV^{2-k}}(1-2m)\right],$$

$$V^{2-k}=r\left[F(r-ct)-(k-1)b^2r^{2m-1}/4\pi kA\right]; \qquad (19)$$

with this

$$\frac{1}{\theta^2}\left[\frac{\partial(a/c)}{c\partial t}+\frac{\partial(a/c)}{\partial r}\right]$$

$$=-\frac{N}{r}+\frac{1}{(2-k)r}\left[\frac{4\pi kArF(r-ct)-2m(k-1)b^2r^{2m}}{4\pi kArF(r-ct)-(k-1)b^2r^{2m}}\right].$$

The solution of this equation is of the form

$$1-\frac{a}{c}=r^{-2(k-1)/(2-k)}f(r-ct)$$

$$\times\left[1-\frac{(k-1)b^2r^{2m-1}}{4\pi kAF(r-ct)}\right]^{-2/(2-k)}. \qquad (20)$$

It is obvious that

$$1-\frac{a}{c}=r^{-2(k-1)/(2-k)}\frac{f_1(r-ct)}{V^2}r^{2/(2-k)}=f_1(r-ct)\frac{r^2}{V^2}.$$

It follows from this that when $a \approx c$ we also have

$$\frac{\sigma r}{V\theta}=f_1(r-ct),$$

which is an analogue of the continuity equation for the stationary case, when $f_1(r - ct) = \text{const}$. In this case we deal with a source of variable flow.

An investigation of relation (19) and (20) shows that when $m = 0$ the motion is defined over the entire space $0 < r < \infty$.

When $m = 1$, waves of this type can exist only at $0 \le r \le r_{max}$, when $1 - a/c \to 1$ and $V \to 0$. When $r > r_{max}$, motions can exist only when $a/c \ll 1$.

We now show that if there is no magnetic field, Eqs. (17) assume the form

$$\frac{1}{\theta^2}\left[\frac{\partial(a/c)}{c\partial t}+\frac{\partial(a/c)}{\partial r}\right]$$

$$=\frac{N}{r}\frac{\omega^2/c^2}{1-\omega^2/c^2}=\frac{\omega^2}{c^2}\left(\frac{\partial \ln V}{c\partial t}+\frac{\partial \ln V}{\partial r}\right). \qquad (21)$$

In the case $\alpha = 0$ we have $\omega^2/c^2 = k - 1$, and therefore Eq. (21) can be rewritten

$$\frac{1}{\theta^2}\left[\frac{\partial(a/c)}{c\partial t}+\frac{\partial(a/c)}{\partial r}\right]=\frac{k-1}{2-k}\frac{N}{r},$$

$$\frac{\partial \ln V}{c\partial t}+\frac{\partial \ln V}{\partial r}=\frac{N}{(2-k)r}.$$

The solution of these equations is

$$1-\frac{a}{c}=f(r-ct)r^{-2N(k-1)/(2-k)}, \quad V=\varphi(r-ct)r^{N/(2-k)}.$$

Obviously the following relations hold

$$\frac{ra}{V\theta}=f_1(r-ct), \quad \frac{w}{\theta}=f_2(r-ct).$$

The second relation is an analogue of the Bernoulli equation. With this

$$p=AV^{-k}=\Phi(r-ct)r^{-kN/(2-k)}.$$

If $N = 2$ and $k = 4/3$,

$$p=\Phi(r-ct)r^{-4}, \qquad (22)$$

hence

$$4\pi r^2p=F=\frac{\Phi(r-ct)}{r^2}, \qquad (23)$$

where F is the force acting on the surface $4\pi r^2$. This force is inversely proportional to the square of the distance r from the center of the body that radiates the ultrarelativistic (or photon) gas.

Let us proceed now to investigate sound waves. The principal equations for sound waves, when $a \ll c$, become

$$\frac{\partial a}{\partial t}-\omega^{*2}\frac{\partial \ln V}{\partial r}+\frac{2mV\dot{H}^2c^2}{4\pi r\omega^*}=0, \qquad (24)$$

$$-\frac{\partial \ln V}{\partial t}+\frac{\partial a}{\partial r}+\frac{Na}{r}=0. \qquad (25)$$

if $m = 0$, the problem of investigating sound wave is simply solved. Here $\omega^* = \omega_0^* = \text{const}$, and the system (24) and (25) can be written

$$\frac{\partial a}{\partial t}=\frac{\omega_0^{*2}}{V_0}\frac{\partial V}{\partial t}, \quad \frac{\partial V}{V_0\partial t}=\frac{\partial a}{\partial r}+\frac{Na}{r},$$

with $V = V_0 + \Delta V$. Hence, introducing the velocity potential defined by the relations

$$a=\frac{\partial\varphi}{\partial r}, \quad V=\frac{V_0}{\omega_0^{*2}}\frac{\partial\varphi}{\partial t},$$

we arrive at the classical wave equation

$$\omega_0^{*-2}\frac{\partial^2\varphi}{\partial t^2}=\frac{\partial^2\varphi}{\partial r^2}+\frac{N}{r}\frac{\partial\varphi}{\partial r}$$

(where $N = 0$ or 1), the solution of which is well known.

If we have $m = 1$ and when $N = 1$, the problem is much more complicated. Since $HV = br$, then $HV \to \infty$ when $r \to \infty$. We may have here $p \approx \rho c^2$ and $H^2 = \rho c^2$. It is therefore necessary to inte-

grate the system

$$\frac{\partial a}{\partial t} + \frac{b^2 c^2 r}{2\pi V w^*} = \omega^{*2} \frac{\partial \ln V}{\partial r}, \tag{26}$$

$$\frac{\partial \ln V}{\partial t} = \frac{\partial a}{\partial r} + \frac{a}{r}. \tag{27}$$

In considering sound waves, we should put

$$V = V_0(r) + \Delta V, \quad H = H_0(r) + \Delta H,$$

Since $H_0 V_0 = HV = br$, then

$$\Delta H = -\Delta V \frac{H_0}{V_0} = -\Delta V \frac{br}{V_0^2}, \quad H = \frac{br}{V_0}\left(1 - \frac{\Delta V}{V_0}\right).$$

With this, the system of equations beomes

$$\frac{\partial \xi}{\partial r} = \frac{r}{V_0} \frac{\partial \Delta V}{\partial t},$$

$$\frac{\partial \xi}{\partial t} = -\frac{b^2 c^2 r^2}{2\pi V_0 \omega_0^*} + \frac{r\omega_0^{*2}}{V_0} \frac{\partial \Delta V}{\partial r}, \quad \text{where } \xi = ar.$$

It is obvious that, by introducing

$$\eta = \Delta V - \frac{b^2 c^2}{2\pi} \int \frac{r\,dr}{w_0^* \omega_0^{*2}} = \Delta V - \frac{b^2}{4\pi} \int \frac{V_0\, dr^2}{AkV_0^{2-k} + b^2 r^2 / 4\pi}, \tag{28}$$

we arrive at a simpler system of equations

$$\frac{\partial \xi}{\partial r} = \frac{r}{V_0} \frac{\partial \eta}{\partial t}, \quad \frac{\partial \xi}{\partial t} = \frac{r}{V_0} \omega_0^{*2} \frac{\partial \eta}{\partial r}.$$

Hence, eliminating η, we obtain the equation

$$\frac{\partial^2 \xi}{\partial r^2} + \frac{d \ln (V_0 / r)}{dr} \frac{\partial \xi}{\partial r} = \frac{c^2}{\omega_0^{*2}} \frac{\partial^2 \xi}{c^2 \partial t^2},$$

the solution of which is also possible in explicit form for the set of relations $V_0 = V_0(r)$.

Relation (28) can be meaningful only under the condition that both terms in the right half are of the same order of smallness. This can occur either if b is small, i.e., the field is weak, or if we assume that

$$\frac{\partial \Delta V}{\partial r} \sim \frac{b^2}{2\pi} \frac{V_0 r}{kAV_0^{2-k} + b^2 r^2 / 4\pi},$$

i.e., by assuming that the derivatives of the functions ΔV and ξ can be arbitrary when b is arbitrary, a fact that leads to high frequency waves of low amplitude.

Depending on the law $V_0 = V_0(r)$, the velocity of sound ω_0^* may increase with the distance, decrease with it, or remain constant as a particular case.

Assuming $\alpha \neq 0$ and specifying $V_0 = \beta r^\nu$ at $k > 1$, we find that if $\nu < 2$, we get $\omega_0^* \to c$ as $r \to \infty$.

If $\nu > 2$, then $\omega_0^* \to 0$ as $r \to \infty$; when $r = 0$ we get in both cases $\omega_0^* = \sqrt{k-1}\, c$. If $\alpha = 0$, we have $\omega_0^* = \text{const}$ when $\nu = 2/(2-k)$.

When $\nu < 2/(2-k)$ and $r \to \infty$ we get $\omega_0^* \to c$; when $r = 0$ we get $\omega_0^* = \sqrt{k-1}\, c$.

When $\nu > 2/(2-k)$ and $r \to \infty$, we have $\omega_0^* = \sqrt{k-1}\, c$; when $r = 0$ we get $\omega_0^* \to c$.

We can, in particular, assume the field to be constant everywhere; then $V_0 \sim r$, i.e., $\nu = 1$.

[1] Baum, Kaplan, and Stanyukovich, Введение в космическую газодинамику (Introduction to Cosmic Gas Dynamics), Part 3, Ch. 2, Fizmatizdat, 1958.

Translated by J. G. Adashko
362

SOVIET PHYSICS JETP VOLUME 36 (9), NUMBER 6 DECEMBER, 1959

TRANSITION PROBABILITIES BETWEEN THE LEVELS OF THE ROTATIONAL BAND OF NON-AXIAL NUCLEI

A. S. DAVYDOV and V. S. ROSTOVSKIĬ

Moscow State University

Submitted to JETP editor December 16, 1958

J. Exptl. Theoret. Phys. (U.S.S.R.) **36**, 1788-1796 (June, 1959)

The energies and the wave functions of the rotational states ($J \geq 4$) of non-axial nuclei are calculated, and the reduced probabilities for E2 transitions between these states are derived. Conditions under which the rotational states can be characterized by a quantum number K are ascertained. It is shown that, when the shape of the nucleus deviates from axial symmetry, the interval rule $1-3.3-7-12$ observed in the rotational band of axial nuclei is violated. The theory is compared with experiment.

THE rotational states of even-even nuclei have been studied by Davydov and Filippov[1-3] under the assumption that the equilibrium shape of the nucleus can be represented by a tri-axial ellipsoid. Analytical expressions for the energy of the rotational states with spin 2, 3, and 5 were found, and the transition probabilities between these states were calculated. In particular, it was shown that the theory made it possible to find a single-valued relation between the ratio of the energy of the two levels with spin 2 and the ratio of the reduced probabilities of E2 transitions from the second level ($J = 2$) to the first level (cascade transition) and directly to the ground state (direct transition).

In the present work, results are presented of numerical calculations of the energy of rotational states with spin 4, 6, and 8 for different values of the parameter γ which determines the deviation of the shape of the nucleus from axial symmetry.[4] The wave functions of these excited states and the transmission probabilities between them are calculated. In Sec. 3 the conditions are given under which the rotational states of nuclei may be described by approximate wave functions corresponding to states with a given value of the projection of the total momentum on axis 3 of the nucleus. Approximate formulae which determine the reduced probabilities of E2 transitions between rotational states of nuclei whose shape does not differ greatly from axially symmetric are derived. The theory is compared with experimental data in Sec. 4.

1. ENERGY OF EXCITED STATES WITH SPIN 4, 6, AND 8

The energy of rotation of a non-spherical even-even nucleus is given, in the adiabatic approximation, by the Schrödinger equation

$$(H-\varepsilon)\psi = 0, \tag{1.1}$$

where ϵ is measured in units of $\hbar^2/4B\beta^2$, and the operator H is given by the formula

$$H = \tfrac{1}{2}\sum_{\lambda=1}^{3} j_\lambda^2 \sin^{-2}(\gamma - \lambda 2\pi/3), \tag{1.2}$$

where J_λ are the projections of the operator of the total angular momentum on the axes of the coordinate system fixed in the nucleus. The wave function corresponding to the state with total moment J, and fulfilling the conditions of symmetry found by Bohr,[4] can be represented in the form

$$\psi_{JM} = \sum_{K\geq 0} |JK\rangle A_K, \tag{1.3}$$

where

$$|JK\rangle = [(2J+1)/16\pi^2(1+\delta_{K0})]^{1/2} \times \{D^J_{MK} + (-1)^J D^J_{M,-K}\}. \tag{1.4}$$

The functions D^J_{MK} in Eq. (1.4) are functions of the Euler angles that determine the orientation of the principal axes of the nucleus in space. It can be shown that the wave functions (1.3) form the basis of a totally symmetric representation of the group D_2 (see reference 1), the elements of which are the rotation through 180° around each of the three principal axes of the nucleus.

Substituting Eq. (1.3) in Eq. (1.1), and making use of the value of the matrix element of the operator of the rotational energy (1.2) acting on the wave functions (1.4),

$$\langle JK|H|JK\rangle = \frac{\alpha+\beta}{4}[J(J+1)-K^2]+\frac{\delta K^2}{2},$$

$$\langle JK+2|H|JK\rangle = \frac{\alpha-\beta}{8}((1+\delta_{K0})(J-K)$$

$$\times (J-K-1)(J+K+1)(J+K+2))^{1/2},$$

$$\alpha = \sin^{-2}(\gamma-2\pi/3),\quad \beta = \sin^{-2}(\gamma+2\pi/3),$$

$$\delta = \sin^{-2}\gamma,\quad \delta_{K0} = \begin{cases} 0, & \text{for } K\neq 0 \\ 1, & \text{for } K=0 \end{cases},$$

we obtain for each value of J a system of algebraic equations for the value of the coefficients A_K in the wave functions (1.3). For instance, for J = 4, the Schrödinger equation (1.1) is reduced to a system of equations

$$[5(\alpha+\beta)-\varepsilon]A_0+(3\sqrt{5}/2)(\alpha-\beta)A_2=0,$$

$$(3\sqrt{5}/2)(\alpha-\beta)A_0+[4(\alpha+\beta)+2\delta-\varepsilon]A_2$$

$$+(\sqrt{7}/2)(\alpha-\beta)A_4=0,$$

$$(\sqrt{7}/2)(\alpha-\beta)A_2+[(\alpha+\beta)+8\delta-\varepsilon]A_4=0. \qquad (1.5)$$

The energy of the corresponding rotational states is determined from the condition that the system (1.5) has a solution. Having solved each of the systems of equations (for corresponding values of ϵ) we can determine the wave functions of these states.

The wave function (1.3) and the values of the energy of the states with spin 2, 3, and 5 can be expressed in terms of the parameter γ by analytical functions. The formulae are given in references 1 and 2. For the energy of the states with spin 4, 6, and 8, equations containing the third, fourth, and fifth power of ϵ are obtained respectively.

The results of a numerical solution of these equations for several values of γ are given in Table I. The number in parentheses next to ϵ indicates the value of the spin in the excited state, whereas the index below denotes the number of the level with a given spin.

2. PROBABILITIES OF ELECTRIC QUADRUPOLE TRANSITIONS IN THE ROTATIONAL BAND

The reduced probability of electric quadrupole transitions between the two states described by the functions ψ_{Jmi} and $\psi_{J'm'f}$ is given by the expression

$$B(E2;\ i\to f) = \frac{5}{16\pi(2J+1)}\sum_{m'um}|(J'm'f|\hat{Q}_{2u}|Jmi)|^2, \qquad (2.1)$$

where

$$\hat{Q}_{2u} = eQ_0\left\{D^2_{u0}\cos\gamma+\frac{1}{\sqrt{2}}(D^2_{u2}+D^2_{u,-2})\sin\gamma\right\},$$

$$Q_0 = 3Z\beta R^2/\sqrt{5\pi}.$$

The wave functions of the states with spin 2 and 3 are given in reference 1. Coefficients A_K of the wave functions of the state with spin 4

$$\psi_{4mi} = \sqrt{9/8\pi^2}\left\{A_{0i}D^4_{m0}+\frac{1}{\sqrt{2}}A_{2i}(D^4_{m2}+D^4_{m,-2})\right.$$

$$\left.+\frac{1}{\sqrt{2}}A_{4i}(D^4_{m4}+D^4_{m,-4})\right\}, \qquad (2.2)$$

can be calculated by solving the system of equation (1.5) for each of the three roots of the equation determining the value of the energy of these levels. The values of the coefficients A_{Ki} for three levels with spin 4 are given in Table II. Also presented in the table are the values of the coefficients B_{Ki} of the wave functions

$$\psi_{6mi} = \sqrt{13/8\pi^2}\left\{B_{0i}D^6_{m0}+\frac{1}{\sqrt{2}}B_{2i}(D^6_{m2}+D^6_{m,-2})\right.$$

$$+\frac{1}{\sqrt{2}}B_{4i}(D^6_{m4}+D^6_{m,-4})$$

$$\left.+\frac{1}{\sqrt{2}}B_{6i}(D^6_{m6}+D^6_{m,-6})\right\} \qquad (2.3)$$

of the states with spin 6.

Using Eq. (2.1) and the wave function with J = 2 and 4, one can calculate the reduced transition probabilities between these states. Thus, for the electric quadrupole transition, the reduced probabilities (in units of $e^2Q_0^2/16\pi$) are given by

TABLE I. Dependence of the rotational energy (in units of $\hbar^2/4B\beta^2$) of even-even nuclei on the parameter γ

γ°	0	5	10	15	20	22.5	25	27.5	30	
$\varepsilon_1(4)$	13.33	13.54	14.12	15.00	15.81	16.01	16.06	16.02	16	
$\varepsilon_2(4)$	∞	274.1	77.73	42.48	32.26	30.92	31.21	32.69	34	
$\varepsilon_3(4)$	∞	1056	268.1	122.5	71.92	58.51	49.20	42.85	40	
$\varepsilon_1(6)$	28	28.42	29.51	30.65	30.78	30.51	30.33	30.06	30	
$\varepsilon_2(6)$	∞	270.5	93.51	60.46	54.52	55.74	57.33	59.71	60	
$\varepsilon_1(8)$	48	48.60	50.26	50.87	49.60	48.94	48.38	48.10	48	

TABLE II. Coefficients determining the wave functions (2.2) and (2.3) of states with spin 4 and 6 respectively

γ°	0	5	10	15	20	22.5	25	27.5	30
A_{01}	1	1	0.999	0.993	0.955	0.909	0.852	0.792	0.739
A_{21}	0	0.003	0.030	0.114	0.296	0.414	0.522	0.605	0.661
A_{41}	0	10^{-6}	10^{-4}	0.001	0.010	0.022	0.042	0.076	0.125
A_{02}	0	−0.003	−0.03	−0.114	−0.296	−0.415	−0.523	−0.602	−0.559
A_{22}	1	1	0.999	0.993	0.954	0.907	0.842	0.754	0.500
A_{42}	0	$5\cdot10^{-4}$	0.004	0.015	0.043	0.074	0.128	0.264	0.661
B_{01}	1	1	0.998	0.973	0.878	0.817	0.766	0.714	0.672
B_{21}	0	0.0075	0.065	0.232	0.476	0.570	0.633	0.674	0.695
B_{41}	0	10^{-4}	$6\cdot10^{-4}$	$8\cdot10^{-5}$	0.043	0.081	0.113	0.189	0.254
B_{61}	0	10^{-7}	10^{-6}	$6\cdot10^{-5}$	$9\cdot10^{-4}$	$2.8\cdot10^{-3}$	$6.1\cdot10^{-3}$	0.015	0.031

the formula

$$b(E2;\ 4i \to 2f) = \tfrac{5}{126}\{\cos\gamma\cdot[6A_{0i}a_f + \sqrt{15}\,A_{2i}b_f] + \sin\gamma\cdot[\sqrt{15}\,A_{2i}a_f + A_{0i}b_f + \sqrt{35}\,A_{4i}b_f]\}^2, \quad (2.4)$$

where a_f and b_f are coefficients that determine the wave functions of spin 2 (see reference 1). The reduced transition probabilities between states with spin 4 are given by the expression

$$b(E2;\ 4i \to 4f) = (77)^{-1}\{2\cos\gamma\cdot[7A_{4i}A_{4f} - 5A_{0i}A_{0f} - 2A_{2i}A_{2f}] + \sqrt{3}\sin\gamma\cdot[3\sqrt{5}(A_{2i}A_{0f} + A_{0i}A_{2f}) + \sqrt{7}(A_{2i}A_{4f} + A_{4i}A_{2f})]\}^2. \quad (2.5)$$

The reduced probabilities of a transition between states with spin 4 and 3 are given by the expression

$$b(E2;\ 4i \to 3) = \tfrac{1}{9}\{2\sqrt{3}\cos\gamma\cdot A_{2i} + \sin\gamma[\sqrt{5}\,A_{0i} - \sqrt{7}\,A_{4i}]\}^2. \quad (2.6)$$

Finally, we shall give the equation determining the reduced probabilities for the transition 6i → 4f:

$$b(E2;\ 6i \to 4f) = \tfrac{5}{143}\{\cos\gamma[3\sqrt{5}\,B_{0i}A_{0f} + 4\sqrt{2.1}\,B_{2i}A_{2f} + 3B_{4i}A_{4f}] + \sin\gamma[\sqrt{3}\,B_{0i}A_{2f} + B_{2i}A_{4f}/\sqrt{10} + \sqrt{14}\,B_{2i}A_{0f} + \sqrt{21}\,B_{4i}A_{2f} + \sqrt{49.5}\,B_{6i}A_{4f}]\}^2. \quad (2.7)$$

For the sake of brevity, we shall call the energy levels 0, 21, 41, 61, and 81 (where the first figure denotes the spin of the level and the second the number of the level) the levels of the "principal rotational band." These energy levels are represented in the figure by solid lines. For $\gamma \to 0$, the states of the "principal rotational band" pass over to the levels of the axially symmetrical nucleus. All other energy levels represented in the figure (by dotted lines) tend to infinity for $\gamma \to 0$. We shall call these energy levels "anomalous."

Using the values of coefficients determining the wave functions, one can calculate from Table II and reference 1 the probabilities of electric quadrupole transitions between various rotational states of the nucleus. The values of some of these probabilities are given in Table III.

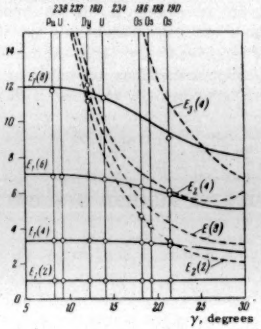

Taking the results of reference 1 and the data of Table III into account, we see that the values of reduced probabilities for electric quadrupole transitions between different rotational states of an even-even nucleus can be split into three types:

1. Transitions with reduced probabilities (in units of $e^2Q_0^2/16\pi$) on the order of unity. These transitions include the cascade transitions between the levels of the principal rotational band and the cascade transitions between "anomalous" rotational levels. For example, the transitions 3 → 22, 42 → 3, and 42 → 22 belong to this type.

2. Transitions beween the levels of the principal rotational band and "anomalous" rotational levels with another value of the spin. Examples of this are the transitions 3 → 21, 41 → 22, 42 → 21, and 61 → 42. The reduced probabilities of such transitions are equal to 0 for $\gamma = 0°$ or 30°, and are unlikely to occur for other values of γ.

TABLE III. Reduced probabilities for electric quadrupole transitions (in units of $e^2Q_0^2/16\pi$) between certain rotational states of even-even nuclei

γ°	0	5	10	15	20	22.5	25	27.5	30
$b(E2;\ 3 \to 41)$	0	0.0060	0.034	0.130	0.406	0.619	0.821	0.955	1.00
$b(E2;\ 41 \to 21)$	1.429	1.418	1.395	1.377	1.371	1.366	1.365	1.378	1.389
$b(E2;\ 41 \to 22)$	0	$3.5\cdot10^{-4}$	0.0023	0.010	0.033	0.044	0.039	0.016	0
$b(E2;\ 42 \to 21)$	0	$4.1\cdot10^{-3}$	0.011	0.008	$4\cdot10^{-4}$	0.009	0.021	0.018	0
$b(E2;\ 42 \to 22)$	0.595	0.591	0.575	0.543	0.481	0.447	0.435	0.484	0.595
$b(E2;\ 42 \to 3\ )$	1.333	1.323	1.282	1.172	0.978	0.680	0.448	0.210	0
$b(E2;\ 42 \to 41)$	0	0.0138	0.0624	0.167	0.313	0.339	0.311	0.271	0.273
$b(E2;\ 61 \to 41)$	1.573	1.563	1.547	1.562	1.623	1.671	1.703	1.725	1.731
$b(E2;\ 61 \to 42)$	0	10^{-3}	$7.7\cdot10^{-3}$	0.035	0.052	0.033	0.011	0.0023	0

3. Transitions between levels with identical value of the spin. Examples of this are the transitions $22 \to 21$ and $42 \to 41$. The reduced probabilities of such transitions are equal to 0 for $\gamma = 0°$, and then markedly increase with increasing γ, attaining maximum values of the order of unity for $\gamma = 30°$. The transition $3 \to 41$ belongs to this group.

3. THE QUANTUM NUMBER K AND ITS SELECTION RULE

The wave functions (1.3) of rotational states of even-even nuclei are represented by linear combinations* of functions (1.4) corresponding to a state with a given value of the projection of the total momentum (quantum number K) of the nucleus on the axis 3 of the coordinate system fixed in the nucleus. The value of the coefficients that determine the contribution of different terms of such linear combination depends on the parameter γ.

As can be seen from Table II and reference 1, the wave functions of the rotational states of the nucleus can be approximated for $\gamma < 15°$ by expressions containing only one value of K. Thus, the wave function of states having spin 2 for $\gamma < 15°$ can be replaced by the approximate functions

$$\varphi^0_{21} = |20\rangle = (5/8\pi^2)^{1/2} D^2_{m0},$$
$$\varphi^0_{22} = |22\rangle = (5/16\pi^2)^{1/2}(D^2_{m2} + D^2_{m,-2}). \qquad (3.1)$$

Under the same condition, the wave function of states having spin 4 are approximated by the expression

$$\varphi^0_{41} = |40\rangle = (9/8\pi^2)^{1/2} D^4_{m0},$$
$$\varphi^0_{42} = |42\rangle = (9/16\pi^2)^{1/2}(D^4_{m2} + D^4_{m,-2}),$$
$$\varphi^0_{43} = |44\rangle = (9/16\pi^2)^{1/2}(D^4_{m4} + D^4_{m,-4}) \qquad (3.2)$$

and so on.

In the cases ($\gamma < 15°$) where the rotational motion of the nucleus can be described by approximate functions of type (3.1) and (3.2), the rotational states can be characterized by two quantum numbers J and K. In this approximation, the levels of the principal rotational band are characterized by the value K = 0. "Anomalous" rotational states can then also be subdivided into system of levels with various K = 2, 4, 6 ...

The reduced probabilities of electric quadrupole transition between states described by approximate functions $|JK\rangle$ different from 0 (in units of $e^2Q_0^2/16\pi$) have the form

$$b_0(E2;\ JK \to J'K) = 5(2\,J\,0\,K\,|\,J'K)^2\cos^2\gamma,$$

$$b_0(E2;\ JK \to J',\ K+2) = \tfrac{5}{2}(1+\delta_{K0})(2\,J\,2\,K\,|\,J',\ K+2)^2\sin^2\gamma,$$

$$b_0(E2;\ JK \to J',\ K-2) = \tfrac{5}{2}(1+\delta_{K2})(2\,J,\ -2\,K,|\,J',\ K-2)^2\sin^2\gamma.$$

The rules with respect to the probabilities of transitions given at the end of the last paragraph are, in this approximation, reduced to the selection rule

$$\Delta K = 0 \qquad (3.3)$$

for the most probable transitions. Transitions violating the condition (3.3) are called K-forbidden transitions.

In view of the fact that the quantum number K is an approximate one, Eq. (3.3) is applicable only for nuclei with $\gamma < 15°$. For $\gamma > 15°$, one should use the accurate functions (1.3). The results of Sec. 2 make it possible to estimate the error which occurs when the approximate functions (3.1) and (3.2) are used instead of the accurate function (1.3).

It should be mentioned that in several of papers,[5-8] in the analysis of the relative transition intensities, certain excited states with spin 2 and 3 were assigned the quantum number K = 2.

*Only the function of the rotational state with spin 3 corresponds to a given value of K = 2 (see reference 1).

The authors of these papers regarded these excited states as so-called γ-oscillations, and arbitrarily assumed the frequency of these oscillations. If we consider such states as rotational states of a non-axial nucleus, then the mutual position of states and the relative transition probabilities between them can be readily explained. In that case, the theory used only one parameter γ, which is determined in an unique way from the ratio of the energy of two levels with spin 2 (see following section).

4. COMPARISON WITH EXPERIMENT

In order to facilitate the comparison of the results obtained with experimental data, we show in the figure the ratio of the energy of rotational states with different values of spin to the energy of the first excited state plotted as a function of the parameter γ. The parameter γ is determined in an unique* way in the interval $0 < \gamma < 30°$ from the ratio of the energies of two levels with spin 2 by means of the formula

$$E_2(2)/E_1(2) = \left[1 + \sqrt{1 - \tfrac{8}{9}\sin^2 3\gamma}\,\right] \times \left[1 - \sqrt{1 - \tfrac{8}{9}\sin^2 3\gamma}\,\right]^{-1}. \quad (4.1)$$

Having thus determined the value of γ, we can, with the help of the figure, find the position of the remaining rotational states with different values of the spin. It can be seen from the figure that the deviation of the shape of the nucleus from a rotational ellipsoid leads to the violation of the interval rule $1 - 3.3 - 7 - 12$ in the principal band, which can be observed in the rotational band of axially symmetrical nuclei. Thus, for instance for $\gamma = 30°$, the principal rotation level should satisfy the interval rule $1 - 2.67 - 5 - 8$.

The experimental values of the ratios of the excitation energy of nuclei Os^{190}, Dy^{160}, U^{232}, Pu^{238} (data of reference 9), U^{234} (data of reference 10) and Os^{188}, Os^{186} (data of reference 14) to the energy of their first excited state are denoted by points in the figure. It can be seen that the theory predicts correctly the sequence of spins and the experimental energy ratios. A slight deviation of the experimental points from theoretical values can be accounted for by introducing a correction term

$$-aJ^2(J+1)^2, \quad (4.2)$$

which takes the connection between the rotation and internal excitation of the nucleus into account. The value of this correction term can be used as a criterion of the applicability of the adiabatic approximation. It should be noted that, in an analysis of rotational spectra from the point of view of the assumption about the actual form of the nucleus, the deviation of experimental energy ratios from the interval rule $1 - 3.3 - 7 - 12$ was assumed to be wholly due to the violation of the adiabatic condition. This has led to a great overestimate of the role of the correction term (4.2). In fact, the deviation from the interval rule for axial nuclei is mainly due to the violation of the axial symmetry of the nucleus. Of special interest, in that respect, are the experimental data on the levels 2, 4, 6, and 8 of the Os^{190} nucleus, the position of which has been determined by Scharf-Goldhaber et al.[11] and Aten et al.[12] in the study of cascade γ transtions in the decay of the isomere Os^{190} with a decay time of ten minutes and spin 10^-. As has been noticed by the authors,[11,12] the experimentally-observed sequence of spins corresponds well to the sequence of spins of the levels of the nucleus Hf^{180}, which has a well-defined rotational spectrum. However, the observed ratios of energies are substantially different from those obtained theoretically for axially symmetrical nuclei. It has been mentioned in this paper that the experimentally observed ratios $1 - 2.93 - 5.62 - 8.93$ cannot be obtained theoretically even by applying the correction (4.2).

Apart from the variation of the interval rule for the levels of the principal rotational band, the violation of axial symmetry of a nucleus leads to the appearance of new rotational levels ("anomalous"), such as, for instance, the second levels with spin 2 and 4 in Os^{190}. These levels do not appear in the decay of the isomer of Os^{190} with ten minutes half life, but they appear in the K-capture decay of Ir^{190}.

The features of the spectrum of the Os^{190} nucleus are due to the large value of $\gamma = 21.4°$ corresponding to an experimental ratio of energies $E_{22}/E_{21} = 3.15$. Using the value of $\gamma = 21.4$, one can calculate the values of the given probabilities and the relative probabilities of electric quadrupole transitions in the nucleus Os^{190}. These values are given in Table IV, together with the transitions connected with the theoretical level with spin 3, a level which has not yet been observed experimentally. With Os^{190} nucleus as an example we have shown that the theory of non-axial nuclei makes it possible to calculate the relative probabilities of electric quadrupole transitions

*We disregard the ambiguity due to the fact that, in even-even nuclei, the rotational energy and the transition probability between them are the same for various γ and $\pi/3 - \gamma$ (see reference 1 and 3).

TABLE IV. Relative transition probabilities between various rotational levels of the Os^{190} nucleus

E2-transition	Transition energy (kev)	Reduced probability ($e^2Q_0^2/16\pi$)	Relative probability	E2-transition	Transition energy (kev)	Reduced probability ($e^2Q_0^2/16\pi$)	Relative probability
$21 \to 0$	186	0.934	1	$3 \to 41$	244	0.515	2.14
$41 \to 21$	360	1.33	39.3	$61 \to 41$	500	1.6	254
$22 \to 21$	400	0.467	21.5	$42 \to 22$	540	0.461	100
$22 \to 0$	586	0.066	21.9	$42 \to 41$	580	0.319	100
$22 \to 41$	40	0.071	$3.5 \cdot 10^{-5}$	$42 \to 21$	940	0.007	24.6
$3 \to 21$	604	0.18	69	$42 \to 3$	336	0.813	16.5
$3 \to 22$	204	1.60	2.9	$42 \to 61$	80	0.06	$9 \cdot 10^{-4}$

between all rotational states. The values of the relative transition intensities found provide a qualitative explanation for the observed decay schemes of the excited states of Os^{190}. Thus, for instance, a decay of the isomeric state of Os^{190} takes place only through the series of cascade transitions through rotational levels of the main rotational band without a marked excitation of the "anomalous" rotational levels. The "anomalous" rotational levels 4^+ and 2^+ are excited in the K-capture decay of the Ir^{190} nucleus. It follows from Table IV that the nucleus, after emitting an E2 photon, can pass from the excited states corresponding to an "anomalous" rotational level 4^+ either into the rotational level with spin 4^+ in the principal rotational band with subsequent cascade emission of 2 photons, or (with the same probability) into the level 2^+ corresponding to an "anomalous" rotational level. From this state, the transition either occurs to the state with spin 2^+ of the principal rotational band, or (roughly with the same probability) directly to the ground state. According to the theory, the Os^{190} nucleus should have an excited state (~ 790 kev) with spin 3^+. However, as can be seen from Table IV, the excitation of this rotational level is not very probable since, from the higher levels 4^+ and 6^+, transitions to other rotational states are much more probable. It is possible that, because of that, this rotational state has so far not been discovered.

In reference 1, a comparison has already been made of the theoretical values for transition probabilities with experimental data for levels having spin 2 and 3. Since the writing of reference 1 new experimental data have appeared on the ratio of the reduced probabilities of cascade and direct transitions. Table V presents the experimental data (McGowan[13,6]) and theoretical values, obtained from the formula

$$\frac{b(E2;\ 22 \to 21)}{b(E2;\ 22 \to 0)} = \frac{20 \sin^2 3\gamma}{7\,(9 - 8\sin^2 3\gamma - [3 - 2\sin^2 3\gamma]\sqrt{9 - 8\sin^2 3\gamma})}.$$

The parameter γ is determined from the ratio (4.1). The experimental data[13] and theoretical values

$$\frac{b(E2;\ 22 \to 21)}{b(E2;\ 21 \to 0)} = \frac{20 \sin^2 3\gamma}{7\,(9 - 8\sin^2 3\gamma + [3 - 2\sin^2 3\gamma]\sqrt{9 - 8\sin^2 3\gamma})}$$

are also given for the ratio of the reduced transition probabilities $(22 \to 21)$ and $(21 \to 0)$. It can be concluded from Table V that this theory makes it possible to establish a single-valued relation between the given ratio of the reduced transition probabilities and the ratio of the energy of both levels with spin 2.

Experimental values of the ratio of intensity of E2 transitions $3 \to 41$ and $3 \to 21$ in the Sm^{152} nucleus are given by Nathan and Waggoner.[5]

TABLE V. Ratio of the reduced probabilities of electric quadrupole transitions for certain nuclei

Nucleus	E_{21}/E_{41}	γ	$b(E2;\ 22 \to 21)/b(E2;\ 22 \to 0)$		$b(E2;\ 22 \to 21)/b(E2;\ 21 \to 0)$	
			Theory	Experiment	Theory	Experiment
Th^{232}	15.4	10.3	1.7	1.8	0.052	0.014
Gd^{154}	8.11	14.0	2.6	1.94	—	—
W^{184}	8.02	14.1	3.0	2.36	0.18	0.12
Os^{188}	4.08	19.3	4.5	2.7	0.32	0.19
Os^{190}	2.98	21.4	7.1	9.7	0.50	0.52
Os^{192}	2.37	25.4	21	9.1	0.90	0.68
Te^{122}	2.23	26.3	40	30	1.29	2.8

This ratio corresponds to the ratio of reduced probabilities

$$\{b(E2;\ 3\to 41)/b(E2;\ 3\to 21)\}_{\text{exp}} = 1.88.$$

From the ratio $E_{22}/E_{21} = 8.9$ for Sm^{152} nucleus, it follows that $\gamma = 13.5°$. The theory then leads to the value

$$\{b(E2;\ 3\to 41)/b(E2;\ 3\to 21)\}_{\text{theor}} = 1.37,$$

which is in agreement with the experimental ratio.

[1] A. S. Davydov and G. F. Filippov, J. Exptl. Theoret. Phys. (U.S.S.R.) **35**, 440 (1958), Soviet Phys. JETP **8**, 303 (1959).

[2] A. S. Davydov and G. F. Filippov, J. Exptl. Theoret. Phys. (U.S.S.R.) **35**, 703 (1958), Soviet Phys. JETP **8**, 488 (1959).

[3] A. S. Davydov and G. F. Filippov, Nuclear Phys. **8**, 237 (1958).

[4] A. Bohr, Dan. Mat.-Fys. Medd. **27**, 14 (1952). A. Bohr and B. Mottelson, Dan. Mat.-Fys. Medd. **27**, 16 (1953).

[5] O. Nathan and M. Waggoner, Nuclear Phys. **2**, 548 (1956/57).

[6] O. Nathan, Nuclear Phys. **4**, 125 (1957).

[7] J. Juliano and F. Stephens, Phys. Rev. **108**, 341 (1958).

[8] G. Hickman and M. Wiedenbeck, Phys. Rev. **111**, 539 (1958).

[9] B. S. Dzhelepov and L. K. Peker, Схемы распада радиоактивных ядер, (Decay Schemes of Radioactive Nuclei) U.S.S.R. Acad. Sci. Press 1958.

[10] Strominger, Hollander, and Seaborg, Revs. Modern Phys. **30**, 585 (1958).

[11] Scharf-Goldhaber, Alburger, Harbottle, and McKeown, Bull. Amer. Phys. Soc. **2**, 25 (1957); preprint, 1958.

[12] Aten, de Feyfer, Sterk, and Wapstra, Physica **21**, 740, 990 (1955).

[13] F. McGowan, Paper presented at the International Nuclear Physics Conference in Paris, July 1958.

[14] F. McGowan and P. Stelson, Bull. Amer. Phys. Soc. **3**, 228 (1958).

[15] R. Diamond and J. Hollander, Nuclear Phys. **8**, 143 (1958).

Translated by H. Kasha
363

VAN DER WAALS FORCES IN AN INHOMOGENEOUS DIELECTRIC

I. E. DZYALOSHINSKIĬ and L. P. PITAEVSKIĬ

Institute of Physical Problems, U.S.S.R. Academy of Science

Submitted to JETP editor December 17, 1958

J. Exptl. Theoret. Phys. (U.S.S.R.) **36**, 1797-1805 (June, 1959)

The non-additive part of the free energy of an inhomogeneous dielectric, related to the presence of long wavelength fluctuations of the electromagnetic field in it, is calculated with the aid of the diagram technique. The corresponding part of the stress tensor (the van der Waals force stress tensor) is also calculated. In addition, formulas for the Green's functions of an electromagnetic field in an absorbing medium are adduced.

INTRODUCTION

THIS work is devoted to the calculation of additional forces arising in an inhomogeneous dielectric* due to the presence of a long-wave fluctuating the electromagnetic field in it. These forces may be called van der Waals forces since they have the same character as the van der Waals forces of attraction between molecules at large distances.

The contribution of the long wave fluctuations to the free energy is small compared with the total free energy of the body. However, they lead to a qualitatively new effect: the non-additivity of the free energy of the body. Indeed, each change of the density and, consequently, in the dielectric constant of the body in a certain region leads to a change of the fluctuating electromagnetic field within this region by virtue of the Maxwell equations. Thus the part of the free energy under consideration is not determined by the properties of the substance at the given point alone. Therefore, for example, the chemical potential of a thin film of liquid on the surface of a solid depends on the thickness of the film. (A rough calculation based on the assumption that the interaction between the liquid molecules and the underlying substance obeys the van der Waals law leads to the dependence[1] $\mu = \text{const} - a/d^3$). These same effects lead to the appearance of forces of mutual attraction between solids, i.e., to a dependence of the free energy of bodies on the distance between them. Such forces were calculated rigorously by E. M. Lifshitz[2] (see also reference 3).

*To avoid misunderstandings we emphasize that in the present paper inhomogeneous bodies are understood, in particular, to include bounded bodies even though these are homogeneous over their entire volume.

Here, evidently, fluctuations with wavelengths of the order of the dimensions of the inhomogeneities are significant (for example, of the order of the film thickness or of the distance between the attracting solids). This makes possible a macroscopic analysis for macroscopic bodies and to express the results in terms of ϵ, the dielectric constant of the body.

Of course, the corrections to the free energy, necessitated by the fluctuations of the electromagnetic field, cannot be calculated by means of simple average expressions for the energy of the electromagnetic field in the medium — for variable fields in an absorbing medium such a concept is generally meaningless in view of the presence of dissipation. It is therefore necessary to determine directly the correction to the free energy of the body, necessitated by the interaction of the particles of the body with the long-wavelength electromagnetic radiation. We shall calculate here the corrections to the free energy by the Matsubara technique[4] as modified by Abrikosov, Gor'kov and Dzyaloshinskiĭ, and Fradkin.[5] We remark at once that this method makes it possible to recast the whole of the quantum theory of fluctuations in a considerably more convenient form. In the following sections we shall describe the properties of certain functions encountered in the application of the indicated methods to the electromagnetic field in an inhomogeneous absorbing medium. In this connection we shall make wide use of the results of reference 5.

PROPERTIES OF THE GREEN'S FUNCTIONS OF AN ELECTROMAGNETIC FIELD IN AN ABSORBING MEDIUM

A basic role will be played in our work by the temperature or "Matsubara" Green's functions for

the electromagnetic field, defined by the formula*

$$\mathfrak{D}_{\alpha\beta}(\mathbf{r}_1, \mathbf{r}_2, \tau_1-\tau_2) = \begin{cases} -\operatorname{Sp}\{e^{(\hat{F}-\hat{H})/T} e^{\hat{H}(\tau_1-\tau_2)} \hat{A}_\alpha(\mathbf{r}_1) e^{-\hat{H}(\tau_1-\tau_2)} \hat{A}_\beta(\mathbf{r}_2)\}, & \tau_1 > \tau_2, \\ -\operatorname{Sp}\{e^{(\hat{F}-\hat{H})/T} e^{-\hat{H}(\tau_1-\tau_2)} \hat{A}_\beta(\mathbf{r}_2) e^{\hat{H}(\tau_1-\tau_2)} \hat{A}_\alpha(\mathbf{r}_1)\}, & \tau_1 < \tau_2. \end{cases} \quad (1)$$

Here $\hat{\mathbf{A}}_\alpha(\mathbf{r})$ is the 4-vector potential operator in the Schrödinger representation, $\hat{H}$ is the system Hamiltonian, and $\hat{F}$ is the free energy of the body.

By virtue of the reality of the electromagnetic field, the operator $\hat{\mathbf{A}}_\alpha(\mathbf{r})$ is Hermitian. This permits the components of the expansion of $\mathfrak{D}_{\alpha\beta}$ in a Fourier series in $\tau_1 - \tau_2$ to be determined from the equation

$$\mathfrak{D}_{\alpha\beta}(\mathbf{r}_1, \mathbf{r}_2, \omega_n) = \frac{1}{2}\int_{-1/T}^{1/T} e^{i\omega_n\tau} \mathfrak{D}_{\alpha\beta}(\mathbf{r}_1, \mathbf{r}_2, \tau)\, d\tau, \quad (2)$$

which satisfies the relation

$$\mathfrak{D}_{\alpha\beta}(\mathbf{r}_1, \mathbf{r}_2, \omega_n) = \mathfrak{D}^*_{\beta\alpha}(\mathbf{r}_2, \mathbf{r}_1, -\omega_n). \quad (3)$$

(The asterisk denotes the complex conjugate quantity.) The temperature Green's function $\mathfrak{D}_{\alpha\beta}$ is connected by a simple relation with the so-called "retarded" Green's function $D^R_{\alpha\beta}$, defined by the formula

$$D^R_{\alpha\beta}(\mathbf{r}_1, \mathbf{r}_2, t_1-t_2) = \begin{cases} -i\operatorname{Sp}\{e^{(\hat{F}-\hat{H})/T}[\hat{A}_\alpha(\mathbf{r}_1, t_1)\hat{A}_\beta(\mathbf{r}_2, t_2) - \hat{A}_\beta(\mathbf{r}_2, t_2)\hat{A}_\alpha(\mathbf{r}_1, t_1)]\}, & t_1 > t_2, \\ 0, & t_1 < t_2. \end{cases} \quad (4)$$

Arguments analogous to those brought forth in reference 5 for the homogeneous medium case lead to the conclusion that $\mathfrak{D}_{\alpha\beta}(\mathbf{r}_1, \mathbf{r}_2, \omega)$ can be expressed in terms of the Fourier components of $D^R_{\alpha\beta}$. Indeed, if we define $D^R_{\alpha\beta}(\mathbf{r}_1, \mathbf{r}_2, \omega)$ by

$$D^R_{\alpha\beta}(\mathbf{r}_1, \mathbf{r}_2, \omega) = \int_{-\infty}^{\infty} e^{i\omega t} D^R_{\alpha\beta}(\mathbf{r}_1, \mathbf{r}_2, t)\, dt,$$

then $\mathfrak{D}_{\alpha\beta}(\mathbf{r}_1, \mathbf{r}_2, \omega_n)$ and $D^R_{\alpha\beta}(\mathbf{r}_1, \mathbf{r}_2, \omega)$ are connected for $\omega_n > 0$ by the relation

$$\mathfrak{D}_{\alpha\beta}(\mathbf{r}_1, \mathbf{r}_2, \omega_n) = D^R_{\alpha\beta}(\mathbf{r}_1, \mathbf{r}_2, i\omega_n). \quad (5)$$

We remark that it follows from the very definition (3) that $D^R_{\alpha\beta}(\mathbf{r}_1, \mathbf{r}_2, \omega)$ is an analytic function of ω, having no singularities in the upper half-plane.

The tensor $D^R_{\alpha\beta}$ (or $\mathfrak{D}_{\alpha\beta}$) has ten independent components. However, we have at our disposal a considerable arbitrariness connected with the gauge invariance. Indeed, it is not the quantities $D^R_{\alpha\beta}$, made up of the components of the vector potential $\hat{\mathbf{A}}_\alpha$, that have a physical significance, but only the six corresponding quantities made up of the components of the electric field intensity $\hat{\mathbf{E}}_i$. Thus, only six physical conditions are imposed on the ten quantities. The remaining arbitrariness may be made use of in order to set the components D^R_{00} and D^R_{01} equal to zero. Obviously, this corresponds to a gauge with a scalar potential equal to zero. We shall henceforth assume such a gauge (except for the Appendix), since it is the most convenient for the case of a spatially inhomogeneous medium. With this gauge, the Heisenberg operators $\hat{\mathbf{E}}$ and $\hat{\mathbf{H}}$ are related to $\hat{\mathbf{A}}$ by the formulas

$$\hat{\mathbf{E}} = -\partial\hat{\mathbf{A}}/\partial t, \qquad \hat{\mathbf{H}} = \operatorname{curl}\hat{\mathbf{A}}, \quad (6)$$

and the operator $\hat{\mathbf{A}}(\mathbf{r}, t)$ itself, in the case of long wavelengths when a macroscopic description of the medium can be used, satisfies the equation*

$$\frac{\partial}{\partial t}\left(\varepsilon\frac{\partial\hat{\mathbf{A}}}{\partial t}\right) + \operatorname{curl}\operatorname{curl}\hat{\mathbf{A}} = 0. \quad (7)$$

(As always, the dielectric constant ϵ is a time-dependent linear operator in the presence of dispersion. We neglect the magnetic properties of matter, since they are completely inessential in the frequency region of interest.)

Differentiating (4) with respect to time, taking into account Eq. (7) and the commutation rule for the vector potential, which has the form

$$\left[\frac{\partial\hat{A}_i(\mathbf{r}, t)}{\partial t}\hat{A}_k(\mathbf{r}', t) - \hat{A}_k(\mathbf{r}', t)\frac{\partial\hat{A}_i(\mathbf{r}, t)}{\partial t}\right] = -4\pi i\delta(\mathbf{r}-\mathbf{r}')\delta_{ik}, \quad (8)$$

and going over to the Fourier components in terms of t, we obtain an equation for D^R_{ik}:

$$[\varepsilon(\mathbf{r}, \omega)\omega^2\delta_{il} + \delta_{il}\partial^2/\partial x_m^2 - \partial^2/\partial x_i\partial x_l]\, D^R_{lk}(\mathbf{r}_1, \mathbf{r}_2, \omega) = 4\pi\delta(\mathbf{r}-\mathbf{r}')\delta_{ik}. \quad (9)$$

Substituting $i\omega_n$ for ω in (9), we find that the function $\mathfrak{D}_{ik}$ satisfies the following equation for $\omega_n > 0$:

*Here and below Greek indices $\alpha, \beta, \ldots = 0, 1, 2, 3$ denote the components of 4-vectors and tensors, and Latin ones, i, k, ... = 1, 2, 3, denote the components of 3-vectors and tensors.

*We use a system of units in which $\hbar = c = 1$. For the sake of simplicity, we assume everywhere that the dielectric is a fluid and consequently isotropic. All formulas are easily generalized to the case of a solid anisotropic dielectric.

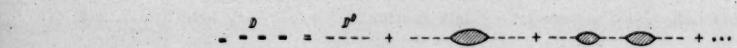

FIG. 1

$$\{\varepsilon(\mathbf{r}, i\omega_n)\omega_n^2\delta_{il} - \delta_{il}\partial^2/\partial x_m^2 + \partial^2/\partial x_i\partial x_l\}\,\mathfrak{D}_{lk}(\mathbf{r}_1, \mathbf{r}_2, \omega_n)$$

$$= -4\pi\delta(\mathbf{r}_1 - \mathbf{r}_2)\delta_{ik}. \qquad (10)$$

We note that since $\epsilon(i\omega_n)$ is, as is well known, a real quantity, the operator acting on $\mathfrak{D}_{ik}$ on the left-hand side of (10) is Hermitian even in an absorbing medium. Equation (10) defines $\mathfrak{D}_{ik}(\mathbf{r}, \mathbf{r}', \omega_n)$ for $\omega_n > 0$. $\mathfrak{D}_{ik}$ for $\omega_n < 0$ can then be found with the aid of relation (3). It is necessary to bear in mind here that the function $\mathfrak{D}_{ik}$ satisfies a real equation and is therefore real.

Thus, solving Eq. (10) for the given body, we find $\mathfrak{D}_{ik}$.

On the other hand, $\mathfrak{D}_{ik}$ can also be calculated not from (10), but according to the general rules of the Matsubara technique. We separate from the complete system Hamiltonian the part corresponding to the interaction of the particles of the body with the long-wave electromagnetic radiation:

$$\hat{H} = \hat{H}_0 + \hat{H}_{int} = \hat{H}_0 + \int \hat{A}_\alpha(\mathbf{r})\,\hat{j}_\alpha(\mathbf{r})\,d^3\mathbf{r}. \qquad (11)$$

Here $\hat{H}_0$ is the sum of the Hamiltonian of the free electromagnetic field in vacuum and the Hamiltonian of the particles of the solid, i.e., we consider that all interactions between particles are included in $\hat{H}_0$, except for the interactions with the long-wave radiation. $\hat{j}_\alpha(\mathbf{r})$ is the system total current operator. We can now calculate $\mathfrak{D}_{\alpha\beta}$ by the usual diagram technique.[5] Here, however, it is necessary to bear in mind that since we include in $\hat{H}_{int}$ only the interaction with the long-wave oscillations, we must consider that all integrals over the momenta of the long-wave photons are cut off at a momentum k_0 that is much smaller than the reciprocal of the interatomic distance, $1/a$. (We shall not introduce this cutoff explicitly, since the final answer will be formulated in a manner independent of the nature of the cutoff.) Obviously, each long-wave photon line, along which an integration is carried out, will therefore bring in an additional smallness $\sim k_0 a$ and we must restrict ourselves in $D_{\alpha\beta}$ to only those graphs in which no integration is carried out along the long-wave photon lines, i.e., to summing the following series (see Fig. 1)

$$\mathfrak{D}_{ik}(\mathbf{r}, \mathbf{r}', \omega_n) = \mathfrak{D}^0_{ik}(\mathbf{r} - \mathbf{r}', \omega_n)$$
$$+ \int \mathfrak{D}^0_{il_1}(\mathbf{r} - \mathbf{r}_1, \omega_n)\,\Pi_{l_1l_2}(\mathbf{r}_1, \mathbf{r}_2, \omega_n)$$
$$\times \mathfrak{D}^0_{l_2k}(\mathbf{r}_2 - \mathbf{r}', \omega_n)\,d^3\mathbf{r}_1 d^3\mathbf{r}_2$$
$$+ \int \mathfrak{D}^0_{il_1}(\mathbf{r} - \mathbf{r}_1, \omega_n)\,\Pi_{l_1l_2}(\mathbf{r}_1, \mathbf{r}_1, \omega_n)$$
$$\times \mathfrak{D}^0_{l_2l_3}(\mathbf{r}_2 - \mathbf{r}_3, \omega_n)\,\Pi_{l_3l_4}(\mathbf{r}_3, \mathbf{r}_4, \omega_n)$$
$$\times \mathfrak{D}^0_{l_4k}(\mathbf{r}_4 - \mathbf{r}', \omega_n)\,d^3\mathbf{r}_1 d^3\mathbf{r}_2 d^3\mathbf{r}_3 d^3\mathbf{r}_4 + \ldots. \qquad (12)$$

Here $\Pi_{ik}(\mathbf{r}, \mathbf{r}', \omega_n)$ is the Fourier component of the system polarization operator, denoted in the graph by a crosshatched loop. It is understood that all graphs not containing long-wave photon lines must be included; the inclusion of graphs with these lines would exceed the accuracy.

Summing the series (12), we obtain an equation for $\mathfrak{D}_{ik}$:*

$$\mathfrak{D}_{ik}(\mathbf{r}, \mathbf{r}', \omega_n) = \mathfrak{D}^0_{ik}(\mathbf{r} - \mathbf{r}', \omega_n) + \int \mathfrak{D}_{il_1}(\mathbf{r}, \mathbf{r}_1, \omega_n)$$
$$\times \Pi_{l_1l_2}(\mathbf{r}_1, \mathbf{r}_2, \omega_n)\,\mathfrak{D}^0_{l_2k}(\mathbf{r}_2 - \mathbf{r}', \omega)\,d^3\mathbf{r}_1 d^3\mathbf{r}_2. \qquad (13)$$

We apply to Eq. (13) by the operators

$$\{\varepsilon(\mathbf{r}, i\omega_n)\omega_n^2\delta_{il} - \delta_{il}\partial^2/\partial x_m^2 + \partial^2/\partial x_i\partial x_l\},$$
$$\{\omega_n^2\delta_{qk} - \delta_{qk}\partial^2/\partial x_m'^2 + \partial^2/\partial x_k'\partial x_q'\}. \qquad (14)$$

Taking into account that $\mathfrak{D}_{ik}$ satisfies Eq. (10), and $\mathfrak{D}^0_{ik}$ satisfies the same equation with $\epsilon = 1$, we find, taking Eq. (3) into account,

$$\Pi_{ik}(\mathbf{r}, \mathbf{r}', \omega_n) = \frac{\varepsilon(\mathbf{r}, i|\omega_n|) - 1}{4\pi}\,\omega_n^2\delta_{ik}\delta(\mathbf{r} - \mathbf{r}'). \qquad (15)$$

The fact that $\Pi_{ik}(\mathbf{r}, \mathbf{r}', \omega_n)$ turns out to be proportional to $\delta(\mathbf{r} - \mathbf{r}')$ is connected with the neglect in the macroscopic theory of correlation effects, i.e., of the spatial dispersion of ϵ. It is seen from (15) that to calculate ϵ by the Matsubara technique it is sufficient to calculate the system polarization operator. (Such a method of calculating ϵ was first used by Abrikosov and Gor'kov in their work on the theory of superconducting alloys.[6])

CALCULATION OF THE STRESS TENSOR

We now calculate the corrections to the system free energy, necessitated by the interactions with

*Equation (13) is, evidently, the Dyson equation for the function $\mathfrak{D}_{ik}$

FIG. 2

the long-wave electromagnetic field. The calculations may be performed by summing the Matsubara diagrams for F, i.e., by summing the series of diagrams shown in Fig. 2, where the polarization operator $\Pi_{ik}(\mathbf{r}, \mathbf{r}', \omega_n)$ can be taken to the same approximation as in the calculation of $\mathfrak{D}_{ik}$. Making use of the general rules for writing the diagrams and taking expression (15) for the polarization operator into account, we find that the free energy is given by the series

$$F = F_0 + F_b - \frac{T}{2}\sum_{n=-\infty}^{\infty}\left\{\int\frac{\varepsilon(\mathbf{r}, i|\omega_n|)-1}{4\pi}\omega_n^2\mathfrak{D}_{ii}^0(\mathbf{r}, \mathbf{r}, \omega_n)\,d^3\mathbf{r}\right.$$
$$+\frac{1}{2}\iint\frac{\varepsilon(\mathbf{r}, i|\omega_n|)-1}{4\pi}\omega_n^2\mathfrak{D}_{il}^0(\mathbf{r}-\mathbf{r}_1, \omega_n)\times\frac{\varepsilon(\mathbf{r}_1, i|\omega_n|)-1}{4\pi}$$
$$\left.\times\omega_n^2\mathfrak{D}_{li}^0(\mathbf{r}_1-\mathbf{r}, \omega_n)\,d^3\mathbf{r}d^3\mathbf{r}_1+\ldots\right\}. \quad (16)$$

Here F_0 is the free energy without allowance for the long-wave electromagnetic field, and F_b is the free energy of black-body radiation in vacuum. The appearance of this term is due to the fact that the energy of the electromagnetic field in vacuum enters into $\hat{H}_0$. The summation is taken over the values of the imaginary frequency $\omega_n = 2\pi nT$.

The series (16) is not summed directly, but to calculate the forces we need not the quantity F, but its variational derivative with respect to ϵ. Making the variation and comparing it with expression (12) for $\mathfrak{D}_{ik}$, we find that

$$\delta F = -\frac{T}{8\pi}\sum_{n=-\infty}^{\infty}\omega_n^2\int\mathfrak{D}_{ii}(\mathbf{r}, \mathbf{r}, \omega_n)\,\delta\varepsilon(\mathbf{r}, i|\omega_n|)\,d^3\mathbf{r}. \quad (17)$$

Making use of Eq. (3) we can go over to summation over n from 0 to ∞. Here all terms except the zero term are doubled. The prime on the summation sign will henceforth denote that the zero term is taken with a halved weight:*

$$\delta F = -\frac{T}{4\pi}\sum_{n=0}^{\infty}{}'\omega_n^2\int\mathfrak{D}_{ii}(\mathbf{r}, \mathbf{r}, \omega_n)\,\delta\varepsilon(\mathbf{r}, i\omega_n)\,d^3\mathbf{r}. \quad (18)$$

*As shown by E. M. Lifshitz,[3] a sum of the same kind as that in (18) arises also when the forces of attraction between solid bodies is calculated to the usual scheme of the quantum theory of fluctuations.

Equation (18) is completely analogous to the known formula for the variation of the free energy in a dispersionless medium with specified field sources [see, for example reference 3, Eq. (14.1)]:

$$\delta F = -\int\frac{E^2(\mathbf{r})}{8\pi}\,\delta\varepsilon(\mathbf{r})\,d^3\mathbf{r}. \quad (19)$$

Making use of the Maxwell equations, it is possible to obtain from (19), as is well known, an expression for the stress tensor in a nondispersive medium:

$$\sigma_{ik} = -p_0\delta_{ik} - \frac{E^2}{8\pi}\left[\varepsilon-\rho\left(\frac{\partial\varepsilon}{\partial\rho}\right)_T\right]\delta_{ik} + \frac{\varepsilon E_i E_k}{4\pi} - \frac{H^2}{8\pi}\delta_{ik} + \frac{H_i H_k}{4\pi}. \quad (20)$$

In our case the function $\mathfrak{D}_{ik}(\mathbf{r}, \mathbf{r}', \omega_n)$ satisfies Eq. (10) with respect to each of its variables. Equation (10) is analogous to the usual equation for the vector potential, but is inhomogeneous, for its right-hand side is proportional to a delta-function. This analogy permits finding an expression for the tensor of the additional stresses by the same transformations as used in the ordinary case. This expression turns out to be formally similar to the usual expression (20). The terms arising from the presence of the right-hand half of Eq. (10) are found to cancel. We omit these simple, although rather cumbersome, calculations and give directly the expression for the additional part of the stress tensor. Here we introduce the notation

$$\mathfrak{D}_{ik}^E(\mathbf{r}, \mathbf{r}', \omega_n) = -\omega_n^2\mathfrak{D}_{ik}(\mathbf{r}, \mathbf{r}', \omega_n),$$
$$\mathfrak{D}_{ik}^H(\mathbf{r}, \mathbf{r}', \omega_n) = e_{ilp}e_{kmq}\frac{\partial^2}{\partial x_l\partial x'_m}\mathfrak{D}_{pq}(\mathbf{r}, \mathbf{r}', \omega_n), \quad (21)$$

e_{ikl} is a unit tensor, antisymmetric in all its indices. The quantities $\mathfrak{D}_{ik}^E$ and $\mathfrak{D}_{ik}^H$ evidently represent the "Matsubara" averages of certain quadratic combinations of the vectors **E** and **H**, respectively.

In this notation the expression for the stress tensor becomes

$$\sigma_{ik}(\mathbf{r}) = -2T\sum_{n=0}^{\infty}{}'\left\{-\frac{\delta_{ik}}{8\pi}\left[\varepsilon(\mathbf{r}, i\omega_n)-\rho\frac{\partial\varepsilon(\mathbf{r}, i\omega_n)}{\partial\rho}\right]\times\mathfrak{D}_{ll}^E(\mathbf{r}, \mathbf{r}, \omega_n) + \frac{\varepsilon(\mathbf{r}, i\omega_n)}{4\pi}\mathfrak{D}_{ik}^E(\mathbf{r}, \mathbf{r}, \omega_n) - \frac{\delta_{ik}}{8\pi}\mathfrak{D}_{ll}^H(\mathbf{r}, \mathbf{r}, \omega_n) + \frac{\mathfrak{D}_{ik}^H(\mathbf{r}, \mathbf{r}, \omega_n)}{4\pi}\right\}. \quad (22)$$

Equation (22), however, cannot have a direct physical significance, since the quantities $\mathfrak{D}_{ik}^E$ and $\mathfrak{D}_{ik}^H$ entering into it are infinite when $\mathbf{r} = \mathbf{r}'$. This is

connected with the fact that (unless a corresponding cutoff is explicitly introduced) σ_{ik} receives an infinite contribution from short-wave fluctuations that have no relation to the inhomogeneities of the body in the sense that their contribution to the pressure at a given point is the same in a homogeneous body as in an inhomogeneous body having the same dielectric constant at that point. To recast Eq. (22) in a form independent of the nature of the cutoff, we therefore must subtract from $\sigma_{ik}(\mathbf{r})$ the analogous expression for the homogeneous solid. These "homogeneous" terms can always be included in that part of the pressure which is defined by the properties of the body only at the given point.

Mathematically this subtraction can be carried out more simply by introducing a Green's function $\overline{\mathfrak{D}}_{ik}(\mathbf{r}-\mathbf{r}', \omega_n; \mathbf{r}_0)$ for a homogeneous infinite body having the same dielectric constant at the point $\mathbf{r}_0$ as the inhomogeneous solid under consideration. Such a function obviously satisfies the equation

$$\{\varepsilon(\mathbf{r}_0, i|\omega_n|)\,\omega_n^2\delta_{il} - \delta_{il}\partial^2/\partial x_m^2 + \partial^2/\partial x_i\partial x_l\}$$

$$\times\,\overline{\mathfrak{D}}_{lk}(\mathbf{r}-\mathbf{r}', \omega_n; \mathbf{r}_0) = -4\pi\delta(\mathbf{r}-\mathbf{r}')\,\delta_{ik}. \qquad (23)$$

This equation, as is well known, can be integrated explicitly (for example, by means of resolving it into a Fourier integral in $\mathbf{r}-\mathbf{r}'$, see the Appendix). After expressing in terms of $\overline{\mathfrak{D}}_{ik}$ the corresponding functions $\overline{\mathfrak{D}}^E_{ik}$ and $\overline{\mathfrak{D}}^H_{ik}$, by means of Eq. (31) (where all differentiations must, of course, be carried out at constant $\mathbf{r}_0$), and subtracting from σ_{ik} the analogous expression expressed in terms of $\overline{\mathfrak{D}}^E_{ik}$ and $\overline{\mathfrak{D}}^H_{ik}$, we finally obtain for the stress tensor an expression containing no divergences:

$$\sigma_{ik}(\mathbf{r}) = -2T\sum_{n=0}^{\infty}{}'\lim_{\mathbf{r}\to\mathbf{r}'}\left\{-\frac{\delta_{ik}}{8\pi}\left[\varepsilon(\mathbf{r}, i\omega_n) - \rho\frac{\partial\varepsilon(\mathbf{r}, i\omega_n)}{\partial\rho}\right]\right.$$

$$\times\left[\mathfrak{D}^E_{ll}(\mathbf{r}, \mathbf{r}', \omega_n) - \overline{\mathfrak{D}}^E_{ll}(\mathbf{r}-\mathbf{r}', \omega_n; \mathbf{r})\right]$$

$$+\frac{\varepsilon(\mathbf{r}, i\omega_n)}{4\pi}\left[\mathfrak{D}^E_{ik}(\mathbf{r}, \mathbf{r}', \omega_n) - \overline{\mathfrak{D}}^E_{ik}(\mathbf{r}-\mathbf{r}', \omega_n; \mathbf{r})\right]$$

$$-\frac{\delta_{ik}}{8\pi}\left[\mathfrak{D}^H_{ll}(\mathbf{r}, \mathbf{r}', \omega_n) - \overline{\mathfrak{D}}^H_{ll}(\mathbf{r}-\mathbf{r}', \omega_n; \mathbf{r})\right]$$

$$\left.+\frac{1}{4\pi}\left[\mathfrak{D}^H_{ik}(\mathbf{r}, \mathbf{r}', \omega_n) - \overline{\mathfrak{D}}^H_{ik}(\mathbf{r}-\mathbf{r}', \omega_n; \mathbf{r})\right]\right\}. \qquad (24)$$

We note that at imaginary frequencies the value of the dielectric constant in (24) is related to the imaginary part of $\epsilon(\omega)$ by the relation[3]

$$\varepsilon(i\xi) - 1 = \frac{2}{\pi}\int_0^\infty \frac{\omega\varepsilon''(\omega)d\omega}{\xi^2+\omega^2}.$$

The authors express their thanks to Academician L. D. Landau for his constant interest in the work and for his advice, and to E. M. Lifshitz for his discussions.

APPENDIX

We derive here expressions for the Green's functions of the electromagnetic field in a homogeneous absorbing medium with complex dielectric constant $\epsilon(\omega)$.

Equation (9) obtained above is satisfied by the retarded function D^R if a special gauge $\varphi = 0$ is chosen. Inasmuch as in an homogeneous space D^R depends only on the difference of the coordinates $\mathbf{r}-\mathbf{r}'$, we have, by going over to the Fourier components of this equation,

$$[(\omega^2\varepsilon - k^2)\,\delta_{il} + k_ik_l]\,D^R_{lk}(k, \omega) = 4\pi\delta_{ik}. \qquad (A1)$$

Now we determine the function $D^R_{\alpha\beta}$ for an arbitrary gauge of the vector potential. To do this we multiply both halves of (A1) by ω^2 and introduce the function $D^E_{ik} = \omega^2 D^R_{ik}$. (Here D^R_{ik} is the retarded function corresponding to the gauge $\varphi = 0$.) The quantity thus obtained is already gauge-invariant (it differs from the retarded function made up of the components of the electric field intensity by the constant term $4\pi\delta_{ik}$) and satisfies the equation

$$[(\omega^2\varepsilon - k^2)\,\delta_{il} + k_ik_l]\,D^E_{lk}(k, \omega) = 4\pi\omega^2\delta_{ik}. \qquad (A2)$$

D^E_{ik} is related to $D^R_{\alpha\beta}$ by the obvious equation

$$D^E_{ik} = \omega^2 D^R_{ik} - \omega k_i D^R_{0k} - \omega k_k D^R_{i0} + k_ik_k D^R_{00}. \qquad (A3)$$

From considerations of symmetry, D^R_{i0} can be directed only along the vector $\mathbf{k}$:

$$D^R_{0i} = D^R_{i0} = dk_i. \qquad (A4)$$

By the same token, D^R_{ik} can be rewritten as

$$D^R_{ik} = a\delta_{ik} + bk_ik_k. \qquad (A5)$$

Substituting (A3) and (A4) into (A2), we obtain two equations for D^R_{00}, a, b, and d:

$$a(\varepsilon\omega^2 - k^2) = 4\pi,$$
$$a + \varepsilon(\omega^2 b + D^R_{00} - 2\omega d) = 0. \qquad (A6)$$

Thus we see that $D^R_{\alpha\beta}$ is defined to within two arbitrary functions. We shall now derive formulas for certain particular cases. Let d = b = 0. Then

$$D^R_{ik} = 4\pi\delta_{ik}/(\varepsilon\omega^2 - k^2),$$

$$D^R_{00} = -4\pi/\varepsilon(\varepsilon\omega^2 - k^2), \qquad D^R_{i0} = 0. \tag{A7a}$$

The case $\varphi = 0$ corresponds to $D_{00} = d = 0$ and

$$D^R_{ik} = \frac{4\pi}{\varepsilon\omega^2 - k^2}\left(\delta_{ik} - \frac{k_i k_k}{\varepsilon\omega^2}\right). \tag{A7b}$$

Finally, for the so-called transverse gauge, div $\mathbf{A} = 0$, we have

$$D^R_{ik} = \frac{4\pi}{\varepsilon\omega^2 - k^2}\left(\delta_{ik} - \frac{k_i k_k}{k^2}\right),$$
$$D^R_{00} = 4\pi/\varepsilon k^2, \qquad D^R_{0i} = 0. \tag{A7c}$$

The temperature Green's function $\mathfrak{D}_{\alpha\beta}(\mathbf{k}, \omega_n)$ is related to $D^R_{\alpha\beta}(\mathbf{k}, \omega)$ by

$$\mathfrak{D}_{\alpha\beta}(k, \omega_n) = D^R_{\alpha\beta}(k, i\omega_n), \qquad \omega_n > 0,$$
$$\mathfrak{D}_{\alpha\beta}(k, \omega_n) = \mathfrak{D}^*_{\beta\alpha}(k, |\omega_n|), \qquad \omega_n < 0,$$

whence we obtain in the above-cited three cases [we recall that $\epsilon(i\omega_n)$ is a real function for $\omega_n > 0$]:

$$\mathfrak{D}_{ik} = -\frac{4\pi}{\varepsilon(i|\omega_n|)\omega_n^2 + k^2}\delta_{ik}, \qquad \mathfrak{D}_{00} = \frac{4\pi/\varepsilon(i|\omega_n|)}{\varepsilon(i|\omega_n|)\omega_n^2 + k^2},$$

$$\mathfrak{D}_{0i} = 0; \tag{A8a}$$

$$\mathfrak{D}_{ik} = -\frac{4\pi}{\varepsilon(i|\omega_n|)\omega_n^2 + k^2}\left(\delta_{ik} + \frac{k_i k_k}{\varepsilon(i|\omega_n|)\omega_n^2}\right),$$

$$\mathfrak{D}_{00} = \mathfrak{D}_{0i} = 0; \tag{A8b}$$

$$\mathfrak{D}_{ik} = -\frac{4\pi}{\varepsilon(i|\omega_n|)\omega_n^2 + k^2}\left(\delta_{ik} - \frac{k_i k_k}{k^2}\right),$$

$$\mathfrak{D}_{00} = \frac{4\pi}{\varepsilon(i|\omega_n|)k^2}, \qquad \mathfrak{D}_{0i} = 0. \tag{A8c}$$

We now write expressions for the usual "Feynman" Green's function $D_{\alpha\beta}$. Its real and imaginary parts are related to the retarded function $D^R_{\alpha\beta}$ by the equations (see reference 5 and also reference 7):

$$\mathrm{Re}\, D_{\alpha\beta}(\mathbf{r}_1, \mathbf{r}_2, \omega) = \mathrm{Re}\, D^R_{\alpha\beta}(\mathbf{r}_1, \mathbf{r}_2, \omega),$$
$$\mathrm{Im}\, D_{\alpha\beta}(\mathbf{r}_1, \mathbf{r}_2, \omega) = \coth\frac{\omega}{2T}\,\mathrm{Im}\, D^R_{\alpha\beta}(\mathbf{r}_1, \mathbf{r}_2, \omega). \tag{A9}$$

The function D is of particular interest at absolute zero, when the usual techniques of quantum field theory can be used. Going to the limit $T = 0$ in (A9), we obtain (in components of a Fourier expansion in $\mathbf{r} - \mathbf{r}'$)

$$\mathrm{Re}\, D_{\alpha\beta}(k, \omega) = \mathrm{Re}\, D^R_{\alpha\beta}(k, \omega),$$
$$\mathrm{Im}\, D_{\alpha\beta}(k, \omega) = \frac{\omega}{|\omega|}\mathrm{Im}\, D^R_{\alpha\beta}(k, \omega). \tag{A10}$$

Noting that the real part of $\epsilon(\omega)$ is an even function of ω, and that the imaginary part is an odd function, it is easy to verify that to go from D^R to D at $T = 0$ it is necessary to replace ω by $|\omega|$ in (A7). Thus we obtain for the gauge (A8a)

$$D_{ik} = \frac{4\pi}{\varepsilon(|\omega|)\omega^2 - k^2}\delta_{ik}, \qquad D_{00} = -\frac{4\pi/\varepsilon(|\omega|)}{\varepsilon(|\omega|)\omega^2 - k^2},$$

$$D_{0i} = 0. \tag{A11}$$

Equation (A11) may turn out to be useful in the calculation of the energy losses of fast particles in matter.[6]

[1] L. D. Landau and E. M. Lifshitz, Статистическая физика. (Statistical Physics), GITTL, 1951.

[2] E. M. Lifshitz, J. Exptl. Theoret. Phys. (U.S.S.R.) **29**, 94 (1955), Soviet Phys. JETP **2**, 73 (1956).

[3] L. D. Landau and E. M. Lifshitz, Электродинамика сплошных сред (Electrodynamics of Continuous Media), GITTL, 1957.

[4] T. Matsubara, Prog. Theoret. Phys. **14**, 351 (1955).

[5] Abrikosov, Gor'kov, and Dzyaloshinskiĭ, J. Exptl. Theoret. Phys. (U.S.S.R.) **36**, 900 (1959), Soviet Phys. JETP **9**, 636 (1959); E. S. Fradkin, J. Exptl. Theoret. Phys. (U.S.S.R.) **36**, 1286 (1959), Soviet Phys. JETP **9**, 912 (1959).

[6] A. A. Abrikosov and L. P. Gor'kov, J. Exptl. Theoret. Phys. (U.S.S.R.) **36**, 319 (1959), Soviet Phys. JETP **9**, 220 (1959).

[7] L. D. Landau, J. Exptl. Theoret. Phys. (U.S.S.R.) **34**, 262 (1957), Soviet Phys. JETP **7**, 182 (1958).

[8] M. I. Ryazanov, J. Exptl. Theoret. Phys. (U.S.S.R.) **32**, 1244 (1957), Soviet Phys. JETP **5**, 1013 (1957).

Translated by M. A. MacLeod
364

ENERGY LEVELS AND APPROXIMATE WAVE FUNCTIONS OF MESIC ATOMS

G. E. PUSTOVALOV

Moscow State University

Submitted to JETP editor January 20, 1959

J. Exptl. Theoret. Phys. (U.S.S.R.) **36**, 1806-1817 (June, 1959)

A calculation of the energies of the 1S, 2S, 3S, 2P, and 3P levels of mesic atoms is made in nonrelativistic approximation for a constant distribution of the charge density of the nucleus inside a sphere of radius R_0. By numerical solution of the Schrödinger equation formulas are found for the dependence of the quantum defect Δn on the quantity $t = R_0 Z/a_\mu$ (a_μ is the Bohr radius of the meson orbit). Approximate wave functions are given for the corresponding states. It is shown how to use these wave functions in perturbation theory to find relativistic corrections and level shifts arising from a change of the shape of the charge distribution of the nucleus.

1. INTRODUCTION

THERE has recently been great interest in processes associated with the distribution of the positive charge inside the nucleus. One of the means for studying this distribution is μ-mesic atoms.[1-3] For the interpretation of the experimental data one must be able to calculate the positions of the energy levels of the meson in a mesic atom for various distributions of the charge of the nucleus, and also to calculate a number of other effects that affect the positions of the levels.

The problem of mesic atoms differs considerably from that of ordinary electronic atoms. First of all, a mesic atom is hydrogenlike. The probability of capture of two or more mesons by a single atom is very small, and the electrons of the atom, being much farther from the nucleus, have practically no effect on the motion of the meson.* On the other hand the size and shape of the nucleus have important effects on the motion of the meson. The Bohr radius of the meson orbit, $a_\mu = \hbar/me^2$ (m is the reduced mass of the meson) is 200 to 300 times smaller than the electronic Bohr radius, since the mass of the meson is this many times larger than that of the electron. Calculations show that in heavy μ-mesic atoms the meson spends more than half of the time inside the nucleus.[1] In first approximation the nucleus can be regarded as a sphere uniformly charged with positive electricity. Therefore a heavy mesic atom is to a high degree reminiscent of the Thomson model of the atom with an oscillator potential inside the nucleus. It still turns out, however, that though for mesic atoms with $Z < 10$ the Rutherford model with a point nucleus is a good approximation (the correction to the energy levels caused by the finite volume of the nucleus is not more than 1 percent), even for the heaviest mesic atoms the Thomson model (with an oscillator potential of infinite extent),[4,5] though it is a better approximation than the Rutherford model, cannot be taken as a zeroth approximation if one wants to get really good results (cf. Fig. 1).

Thus the basic difficulties in the calculation of the energy levels of mesic atoms (for μ or π mesons with $Z > 10$) lie in the fact that there does not exist an exact solution of the wave equation (even for the simplest types of distribution of the charge of the nucleus) that can be taken as the zeroth approximation. It must be pointed out that all other factors affecting the positions of the levels (small changes of the charge distribution inside the nucleus, magnetic and electric moments of the nucleus, vacuum polarization, polarization of the nucleus by the meson, and so on)[1-4,6,7] give corrections to the levels that are of the order of 1 to 2 percent, and consequently can be calculated by first-order perturbation theory, at least in the present situation as to experimental accuracy. The relativistic corrections are also rather small.[4,8] Because of the smearing out of the charge over the volume of the nucleus these cor-

*This is true, of course, if we are interested in the motion of the meson and its spectrum. On the other hand, the presence of the meson in a mesic atom has considerable effect on the motion of the electrons. Because of the screening of the nucleus by the meson the effective charge producing the field in which the electrons move is reduced practically by unity, and from the point of view of chemical and optical properties the atom must be shifted one place to the left in the periodic table.

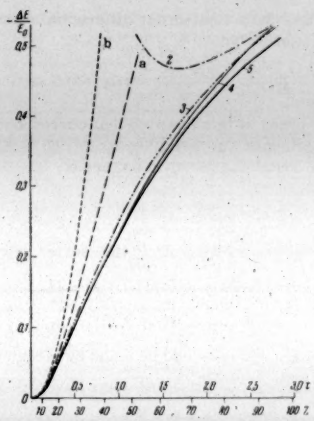

FIG. 1. Dependence on the parameter t of the shift of the 1S level owing to the effect of the volume of the nucleus, as found by various methods: 1) first-order perturbation theory with Kepler wave functions: a) complete result, b) first term of expansion in powers of t ($\Delta E/E_0 \approx 0.8t^2$); 2) first-order perturbation theory with oscillator wave functions;[5] 3) variation method;[12] 4) expansion of the right member of Eq. (4) in powers of Δn (including term in $(\Delta n)^2$); 5) asymptotic representation of the external wave functions and exact (numerical) solution (not distinguishable on this scale). For cases 4 and 5 the left member of Eq. (4) was calculated from Eq. (14). The scale of Z on the axis of abscissas is given for μ-mesic atoms ($R_0 = 1.2A^{1/3} \times 10^{-13}$ cm).

rections for heavy nuclei are somewhat smaller than the corresponding quantities as found from the formulas for point nuclei, i.e., from the usual fine-structure formulas.

With electronic computers available one can of course find to any degree of accuracy the solution of any relativistic equation with the potential given by a prescribed distribution of the charge of the nucleus, as has been done, for example, in the paper of Ford and Hill.[7] But the programming for an electronic computer is in itself rather laborious, and the presence of many parameters does not allow the possibility of foreseeing all the choices for which the need may arise. In many investigations there is often no need to know the result with high precision, but one does need to be able to find rather quickly an approximate value of a quantity and to know how it will change with changes of a number of parameters. Therefore it is desirable to have a sufficiently simple approximate solution that can be taken as a zeroth approximation and gives the possibility of calculating the effects of various factors on the position of the levels of mesic atoms by the universally familiar methods of perturbation theory.

Formulas are obtained in this paper that permit us to find the first five energy levels of mesic atoms in nonrelativistic approximation for a constant distribution of charge density inside the nucleus. Approximate wave functions are given, and also examples of the calculation with these wave functions of several corrections to the levels by means of perturbation theory.

2. DETERMINATION OF THE SOLUTION OF THE WAVE EQUATION

For a uniform distribution of the charge of the nucleus inside a sphere of radius R_0 the charge density

$$\rho(r) = 3eZ/4\pi R_0^3, \qquad 0 \leqslant r \leqslant R_0,$$

$$\rho(r) = 0, \qquad R_0 < r \leqslant \infty \qquad (1)$$

corresponds to a Thomson (oscillator) potential inside the nucleus and a Coulomb potential outside:

$$\varphi(r) = (eZ/R_0)[^3/_2 - {}^1/_2(r/R_0)^2], \qquad 0 \leqslant r \leqslant R_0,$$

$$\varphi(r) = eZ/r, \qquad R_0 < r \leqslant \infty. \quad (2)$$

The basis taken for the determination of the approximate energy eigenvalues and approximate wave functions was the solution of the nonrelativistic Schrödinger equation with the potential (2). After separation of the variables one gets for the radial part R(r) of the wave funtion the equation

$$\frac{d^2R}{dr^2} + \frac{2}{r}\frac{dR}{dr} + \left(\frac{2m}{\hbar^2}E + \frac{2me}{\hbar^2}\varphi(r) - \frac{l(l+1)}{r^2}\right)R = 0. \quad (3)$$

The reasons for the choice of this equation are, firstly, that it is the same for mesons of any spin; the relativistic and spin corrections can be found by perturbation theory, if the nonrelativistic solution is known. Secondly, in this case the solution is a function of only one parameter, $t = R_0Z/a_\mu$. Owing to the linear dependence of t on the mass of the meson, the radius of the nucleus, and the atomic number, it is very easy to find the change of the energy of a level with change of any of these three parameters.

The method of matching was used to find the energy eigenvalues. In this method one requires continuity of the wave function and its first derivative at the edge of the nucleus, or, what is equivalent but more convenient for the unnormalized functions, continuity of the logarithmic derivative:

$$\frac{d}{dr}(\ln R_i)_{r=R_0} = \frac{d}{dr}(\ln R_e)_{r=R_0}. \qquad (4)$$

Here $R_i(r)$ and $R_e(r)$ are solutions of Eq. (3)

respectively inside and outside the nucleus. On R_i we impose the requirement of finiteness at the origin, and R_e must vanish at infinity. The equation (4) is a transcendental equation for the energy E, which occurs as a parameter in R_i and R_e. The energy eigenvalues can be found by numerical solution of this equation.

Let us introduce

$$x = r/R_0, \quad x^{-1}R(x) = y(x), \quad t = R_0 Z/a_\mu,$$

$$E_0 = -me^4Z^2/2\hbar^2, \quad \varepsilon = E/E_0, \quad \gamma = \varepsilon^{-1/2}. \tag{5}$$

Here E_0 is the energy of the ground state of the meson for a point nucleus. The quantity γ has the meaning of an effective quantum number and can be represented in the form

$$\gamma = n + \Delta n, \tag{6}$$

where n is an integer that defines the number of the shell in which the meson is (principal quantum number), and Δn is the addition caused by the finiteness of the nuclear volume (quantum defect).* Using the notation of (5) we get from Eq. (2) an expression for the potential energy of the meson in the field of the nucleus [$U_0 = -e\varphi(r)$]:

$$U_0 = (E_0/t)(3 - x^2), \qquad 0 \leqslant x \leqslant 1,$$

$$U_0 = 2E_0/tx, \qquad 1 \leqslant x \leqslant \infty \tag{7}$$

and from Eq. (3) we get two equations for the regions inside and outside the nucleus, respectively:

$$\frac{d^2y_i}{dx^2} + \frac{2(l+1)}{x}\frac{dy_i}{dx} - [t(\varepsilon t - 3) + tx^2]\,y_i = 0,$$

$$0 \leqslant x \leqslant 1, \tag{8a}$$

$$\frac{d^2y_e}{dx^2} + \frac{2(l+1)}{x}\frac{dy_e}{dx} - \left(\frac{t^2}{\gamma^2} - \frac{2t}{x}\right)y_e = 0,$$

$$1 \leqslant x \leqslant \infty. \tag{8b}$$

a) Solution of the wave equation inside the nucleus. We can represent the solution of Eq. (8a) in the form of a power series

$$y_i(x) = \sum_{k=0}^{\infty} a_k x^k, \tag{9}$$

with its coefficients connected by the recurrence relation

$$a_k = [t(\varepsilon t - 3)a_{k-2} + ta_{k-4}]/(2l + k + 1)k. \tag{10}$$

The series contains only the even powers of x; for simplicity we take the arbitrary coefficient a_0 to be unity.

For the quantity $z = d(\ln y_i)/dx$ we can get from Eq. (8a) a first-order differential equation of the Riccati type

$$\frac{dz}{dx} + z^2 + \frac{2(l+1)}{x}z = t(t\varepsilon - 3) + tx^2. \tag{11}$$

The solution of this equation that corresponds to the solution of Eq. (8a) given by Eq. (9) is a power series containing only odd powers of x:

$$z = \sum_{k=1}^{\infty} b_k x^k. \tag{12}$$

The first two coefficients in this series are

$$b_1 = t(\varepsilon t - 3)/[2(l+1) + 1],$$

$$b_3 = (t - b_1^2)/[2(l+1) + 3],$$

and subsequent ones can be found by means of the recurrence formula

$$b_k = -[2(l+1) + k]^{-1} \sum_{j=1}^{k-2} b_j b_{k-1-j} \qquad (k > 3). \tag{13}$$

If the coefficients b_k have been found, the left member of Eq. (4) can be put in the form

$$\frac{d}{dx}(\ln R_i)_{x=1} = l + \frac{d}{dx}(\ln y_i)_{x=1} = l + \sum_{k=1}^{\infty} b_k. \tag{14}$$

b) Solution of the wave equation outside the nucleus. The solution of Eq. (8b) that vanishes at infinity can be expressed in terms of the Whittaker function (cf. e.g., reference 9):*

$$y_e(x) = c_1 x^{-(l+1)} W_{\gamma, l+1/2}(2tx/\gamma). \tag{15}$$

For large values of x we can also represent the solution (15) by the asymptotic expansion (cf. reference 10, Eq. 7.327):

$$y_e(x) \approx c_2 x^{\gamma-l-1} e^{-tx/\gamma}\left[1 + (l+\gamma)(l+1-\gamma)\frac{1}{1!}\left(\frac{\gamma}{2tx}\right) + (l+\gamma)(l-1+\gamma)\times(l+1-\gamma)(l+2-\gamma)\frac{1}{2!}\left(\frac{\gamma}{2tx}\right)^2 + (l+\gamma)(l-1+\gamma)(l-2+\gamma)(l+1-\gamma) \times (l+2-\gamma)(l+3-\gamma)\frac{1}{3!}\left(\frac{\gamma}{2tx}\right)^3 + \ldots\right]. \tag{16}$$

The coefficients c_1 and c_2 are determined by matching the expressions (9), (15), and (16).

Using the recurrence relation for the derivative of the Whittaker function (cf. reference 10, Eq. 7.334,3), we find the right member of Eq. (4):

$$\frac{d}{dx}(\ln R_e(x))_{x=1} = (\gamma - l - 1)(\gamma + l)$$

$$\frac{W_{\gamma-1,\, l+1/2}(2t/\gamma)}{W_{\gamma,\, l+1/2}(2t/\gamma)} - 1 - \frac{t}{\gamma} + \gamma. \tag{17}$$

*Unlike the quantum defect used to describe the spectral series of the alkali elements, Δn is a positive quantity in the case of mesic atoms.

*The Whittaker function with half-integral second index has a logarithmic singularity at the origin. For its series representation see, for example, reference 10, Eq. 7.338.

TABLE I

	1S	2S	3S	2P	3P
A_0	−0.032885	−0.038028	−0.038028	—	—
A_1	0.165892	0.179527	0.179527	—	—
A_2	0.013883	0.000123	0.000123	−0.0033673	−0.0039119
A_3	−0.008312	−0.004548	−0.005011	0.0087840	0.0104438
A_4	0.001082	0.000635	0.000715	−0.0019263	−0.0024545
A_5	—	—	—	0.0001244	0.0001707
B_1	5.0446	4.7209	4.7209	2.6086	2.6698
B_2	0.9826	0.6281	0.6281	0.7091	0.7723
B_3	−0.5560	−0.4890	−0.4890	0.7000	0.7000
B_4	2.9875	1.9286	1.9286	—	—
C_0	0.032885	0.038028	0.038028	—	—
C_2	—	—	—	0.0033673	0.0039119

The expression (17) can also be written in terms of the asymptotic expansion of the Whittaker function.*

3. RESULTS OF THE NUMERICAL SOLUTION

To get the dependence of the meson energy levels on the parameter t, and the approximate wave functions, Eqs. (4) and (8a), (8b) were solved numerically for the levels† 1S, 2S, 2P, 3S, and 3P for a number of values of t in the interval $0 \leq t \leq 2.75$. This range of values provides for the computation of the energy levels of all μ-mesic and π-mesic atoms for $Z \lesssim 70$ and of K-mesic atoms for $Z \lesssim 20$.

a) Determination of the energy levels. To facilitate the numerical computations preliminary values of ϵ were found by various approximate methods. For the 1S level the results of the calculations by the approximate methods are shown in Fig. 1. The final results were obtained by the use of Eqs. (14) and (17). For the 2S and 3S levels for $t > 1.5$ the series (14) converges slowly, but its convergence can be considerably improved by the choice of a suitable geometrical progression.

It was found convenient to represent not the value of ϵ, but the quantum defect Δn as a function of the parameter t. For the range of t indicated above, the interpolation formula

$$\Delta n = A_0 + A_1 t + A_2 t^2 + A_3 t^3 + A_4 t^4 + A_5 t^5 + (C_0 + C_2 t^2)\exp(-B_1 t - B_2 t^2 - B_3 t^3 - B_4 t^4) \quad (18)$$

was chosen on the basis of the individual values of Δn found by numerical solution (for $t > 1$ the term containing the exponential can be neglected). The coefficients in the formula (18) for the various levels are shown in Table I. According to Eqs. (5) and (6) the quantity ϵ can be calculated by the formula

$$\epsilon = \gamma^{-2} = (n + \Delta n)^{-2}. \quad (19)$$

Use of the formulas (18) and (19) gives the value of ϵ correct to at least four significant figures.

b) The numerical wave functions. To find $y_i(x)$ for $0 \leq x \leq 1$ we used Eqs. (9) and (10). Since computations by Eq. (15) are rather laborious, the determination of $y_\epsilon(x)$ for $x \geq 1$ was made by numerical integration of Eq. (8b) by the Runge-Kutta method with the initial conditions

$$y_\epsilon(1) = \sum_{k=0}^{\infty} a_k, \qquad y_\epsilon'(1) = \sum_{k=2}^{\infty} k a_k.$$

The numerical integration was broken off at values of x for which the asymptotic representation of $y_\epsilon(x)$ was accurate enough. Beyond this the computations were made by Eq. (16). The step for the numerical integration and the value of x at which it was broken off were chosen so that the values were obtained with an accuracy of the order of 0.001 of the value $y(0) = 1$. For the unnormalized wave functions so obtained the normalization constants C were found from the condition

$$C^2 \int_0^\infty x^{2l+2} y^2(x)\, dx = 1 \quad (20)$$

The integral (20) was computed by Simpson's rule. Figure 2 shows the unnormalized wave functions for $t = 2.279$ (μ-mesic lead, $R_0 = 1.2 A^{1/3} \times 10^{-13}$ cm).

c) Approximate wave functions. It turned out to be possible to express the wave functions inside the nucleus ($0 \leq x \leq 1$) approximately in the forms

$$R_{n0}(x) = C(1 - ax^{3/4}), \quad (21a)$$

$$R_{n1}(x) = C(1 - ax^{3/4})x. \quad (21b)$$

*Regarding the use of the asymptotic expansion to solve the Dirac equation with effects of the volume of the nucleus included, see reference 11.

†For the higher levels the calculation of the energy can be made by perturbation theory with the wave functions of the Kepler problem as zeroth approximations (cf., e. g., references 2 and 7).

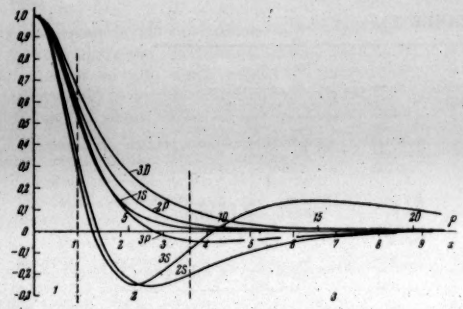

FIG. 2. Unnormalized functions $x^{-l}R(x)$ for μ-mesic lead (t = 2.279): 1) solution in form of power series; 2) numerical integration; 3) asymptotic formulas; $\rho = tx = Zr/a_\mu$.

for S and P states respectively. The parameter a is so chosen that at x = 1 the approximate wave function equals the exact value.

Outside the nucleus (for $x \geq 1$) we have represented the wave functions for the states 1S, 2P, 2S, 3P, and 3S in the respective forms

$$R_{10}(x) = Cu\exp[b(1-x)], \quad (22a)$$

$$R_{21}(x) = Cux\exp[b(1-x)], \quad (22b)$$

$$R_{20}(x) = C(u-vx)\exp[b(1-x)], \quad (22c)$$

$$R_{21}(x) = C(u-vx)x\exp[b(1-x)], \quad (22d)$$

$$R_{30}(x) = C(u-vx+wx^2)\exp[b(1-x)]. \quad (22e)$$

The numerical values of the parameters u, v, w have been chosen so that, first, the approximate wave functions are continuous at the surface of the nucleus (x = 1), and second, the zeroes of the approximate wave functions for the 2S, 3P, and 3S states coincide with those of the corresponding numerically computed functions.

From the parameters found for the individual values of t, formulas were devised for the calculation of the parameters:

$$\left.\begin{array}{ll} \text{for all states} & \begin{cases} tb^{-1} \\ u^{-1} \end{cases} \\ \text{for 2S and 3S states} & a \\ \text{for 3P state} & (1-a)^{-1} \\ \text{for 3S state} & v(a+u-1)^{-1} \end{array}\right\} = D_0 + D_1 t + D_2 t^2 + D_3 t^3. \quad (23)$$

The values of the coefficients in Eq. (23) for the various parameters and states are given in Table II. The remaining parameters are determined by the formulas

$$\begin{array}{ll} a = 1-u & \text{for states 1S and 2P} \\ v = a+u-1 & \text{for states 2S and 3P} \\ w = 1+v-a-u & \text{for state 3S} \end{array} \quad (24)$$

The approximate wave functions thus chosen reproduce the behavior of the numerical wave functions inside the nucleus rather well (the differences of the ordinates do not exceed 2 percent). Outside the nucleus the agreement between the approximate functions and the numerical functions is poorer (especially for the 3S state). This is explained by the fact that the asymptotic behaviors of the approximate functions, $\sim x^{n-1}\exp(-bx)$, and the numerical functions, $\sim x^{\gamma-1}\exp(-tx/\gamma)$,

TABLE II

State	Parameter	D_0	D_1	D_2	D_3
1S	u^{-1}	1	0.4501	—0.0424	0.00580
	tb^{-1}	1	0.3068	0.0212	—0.00977
2P	u^{-1}	1	0.2650	0.0187	—0.00220
	tb^{-1}	2	0.0015	0.0388	—0.00333
2S	a	—	0.4425	—0.0848	0.00846
	u^{-1}	1	—0.0861	0.0382	—0.00314
	tb^{-1}	2	0.4095	0.0180	—0.01177
3P	$(1-a)^{-1}$	1	0.2662	0.0296	0.00483
	u^{-1}	1	0.1009	—0.0183	0.00237
	tb^{-1}	3	—0.0177	0.0496	—0.00289
3S	a	—	0.4469	—0.0718	0.00572
	u^{-1}	1	—0.2523	0.0813	—0.00986
	$v(a+u-1)^{-1}$	1	0.1141	—0.0088	0.00050
	tb^{-1}	3	0.4464	0.0258	—0.01305

are different. One could, of course, choose somewhat more complicated approximate wave functions, which would be much closer to the numerical functions, by taking, for example, for the function outside the nucleus an expression close to the asymptotic expression: $x^{\gamma-1} P_{n-l-1}(x) \exp(-tx/\gamma)$ [$P_k(x)$ is a polynomial of degree k], and for the function inside the nucleus several terms of the series (9). This, however, complicates the computations for a small gain of accuracy, if the calculations are made by first-order perturbation theory.

4. EXAMPLES OF CALCULATIONS WITH THE APPROXIMATE WAVE FUNCTIONS

In first-order perturbation theory for a spherically symmetrical case the shift of an energy level is given by the expression

$$\Delta E = \int_0^\infty x^2 R^2(x)\, \Delta U\, dx, \tag{25}$$

where $\Delta U = U_1 - U_0$; U_1 is the potential energy for which one is calculating the shift of the level, and U_0 is the potential energy used in the zeroth approximation, in our case that given by Eq. (7). For the calculation of the integrals (25) for the various perturbations with the approximate wave functions it is convenient to use the notations

$$F_m = \int_0^1 (1 - ax^{1/4})^2 x^m dx = \frac{1}{m+1} - \frac{4a}{2m+5} + \frac{a^2}{m+4}, \tag{26a}$$

$$G(\xi,\ m;\ x_1, x_2) = e^\xi \int_{x_1}^{x_2} x^m e^{-\xi x} dx$$

$$= \frac{m!}{\xi^{m+1}} \left[e^{\xi(1-x_1)} \sum_{k=0}^{m} \frac{(\xi x_1)^k}{k!} - e^{\xi(1-x_2)} \sum_{k=0}^{m} \frac{(\xi x_2)^k}{k!} \right] \tag{26b}$$

$$H(\xi,\ m) = \int_0^1 x^{m/2} e^{-\xi x} dx$$

$$= \frac{m(m-2)(m-4)\ldots 3\cdot 1}{(2\xi)^{(m+1)/2}} \sqrt{\frac{\pi}{\xi}}\, \Phi(\sqrt{2\xi})$$

$$- 2e^{-\xi} \left[\frac{1}{2\xi} + \frac{m}{(2\xi)^2} + \frac{m(m-2)}{(2\xi)^3} \right.$$

$$\left. + \ldots + \frac{m(m-2)(m-4)\ldots 3}{(2\xi)^{(m+1)/2}} \right], \tag{26c}$$

where $\Phi(x) = (2/\pi)^{1/2} \int_0^x e^{-z^2/2}\, dz$ is the probability integral. Special cases of these notations are

$$G_m = G(2b,\ m;\ 1, \infty) = \frac{m!}{(2b)^{m+1}} \sum_{k=0}^{m} \frac{(2b)^k}{k!}, \quad G_0 = 1 \tag{26d}$$

$$G(\xi,\ m;\ 0,\ 1) = \frac{m!}{\xi^{m+1}} \left(e^\xi - \sum_{k=0}^{m} \frac{\xi^k}{k!} \right). \tag{26e}$$

a) The normalization coefficients. The normalization coefficient C of the approximate wave function (21a), (22a) for the 1S state can be found from the condition

$$\int_0^\infty x^2 R^2(x)\, dx$$

$$= C^2 \left\{ \int_0^1 (1 - ax^{1/4})^2 x^2 dx + u^2 e^{2b} \int_1^\infty x^2 e^{-2bx} dx \right\} = 1. \tag{27}$$

Using Eqs. (26a and d), we get

$$C^{-2} = F_2 + u^2 G_2. \tag{28}$$

In the same way it is easy to get the normalization coefficients for the states 2S and 3S:

$$C^{-2} = F_2 + u^2 G_2 - 2uvG_3 + v^2 G_4 \qquad (2S), \tag{29}$$

$$C^{-2} = F_2 + u^2 G_2 - 2uvG_3$$

$$+ (v^2 + 2uw) G_4 - 2vwG_5 + w^2 G_6 \qquad (3S). \tag{30}$$

The normalization coefficients for the 2P and 3P states are obtained by replacing F_m, G_m by F_{m+2}, G_{m+2} in Eqs. (28) and (29), respectively.

b) The relativistic corrections. For particles of spin $\frac{1}{2}$ (μ mesons) the relativistic corrections include (cf., e.g., reference 13): 1) the correction for the relativistic change of mass, 2) the correction for the spin-orbit interaction, and 3) a correction characteristic of the Dirac theory which has no classical analogue. For particles of spin 0 (π mesons) only the first correction has to be included.

1) In the case of a central field the relativistic change of mass can be taken into account in first approximation by adding to the potential energy the term

$$\Delta U' = -(2mc^2)^{-1} (U_0 - E)^2. \tag{31}$$

Here U_0 and E are the values of the potential and total energies in zeroth approximation ($E = \epsilon E_0$). Using the expression (7) for the potential energy, and also the fact that $E_0/2mc^2 = -(\alpha Z/2)^2$ (where $\alpha = e^2/\hbar c$ is the fine-structure constant), we get

$$\Delta U' = (\alpha Z/2t)^2 E_0 (3 - x^2 - \epsilon t)^2, \quad 0 \leqslant x \leqslant 1,$$

$$\Delta U' = (\alpha Z/2t)^2 E_0 (2x^{-1} - \epsilon t)^2, \quad 1 \leqslant x \leqslant \infty. \tag{32}$$

By means of the approximate wave functions (21a), (22a), the notations (26a, d), and Eq. (25) we find the correction for the relativistic change of mass

TABLE III

Mesic atom	Method of calculation*	$1S_{1/2}$	$2P_{1/2}$	$2P_{3/2}$	$2S_{1/2}$	$3P_{1/2}$	$3P_{3/2}$	$3S_{1/2}$
$t = 1.1829$	I	5.370	1.881	1.832	1.585	—	—	—
$_{51}Sb$	II	5.369	1.880	1.832	1.583	—	—	—
$t = 2.279$	I	10.477	4.787	4.607	3.568	2.131	2.084	1.753
$_{82}Pb$	II	10.477	4.780	4.604	3.561	2.127	2.081	1.747
$t = 2.675$	I	12.112	5.924	5.695	4.303	—	—	—
$_{92}U$	II	12.112	5.917	5.691	4.299	—	—	—

*I is numerical solution of the Dirac equation; II is solution with the approximate wave functions. The energy levels are given in Mev. The radius of the nucleus was computed from the formula $R_0 = 1.2\,A^{1/3} \times 10^{-13}$ cm.

for the 1S level:

$$\Delta\varepsilon_{10}' = (\Delta E_{10}'/E_0) = (\alpha ZC/2t)^2\,[(\varepsilon t - 3)^2 F_2 + 2(\varepsilon t - 3)F_4 + F_6 + u^2(4G_0 - 4\varepsilon t G_1 + \varepsilon^2 t^2 G_2)]. \quad (33)$$

The correction $\Delta\epsilon_{21}'$ for the 2P level is obtained by replacing F_m, G_m by F_{m+2}, G_{m+2} in Eq. (33).

2) The spin-orbit interaction is taken into account by adding to the potential energy the expression

$$\Delta U'' = (2m^2c^2)^{-1}\frac{1}{r}\frac{dU_0}{dr}(\mathbf{LS}) = \frac{\alpha^2 Z^3}{2t^3}\frac{1}{x}\frac{dU_0}{dx}\frac{(\mathbf{LS})}{\hbar^2}. \quad (34)$$

For the S levels the quantity $(\mathbf{L}\cdot\mathbf{S})/\hbar^2$ is zero. In the case of the P levels $(\mathbf{L}\cdot\mathbf{S})/\hbar^2 = -1$ for the $2P_{1/2}$ sublevel, and $(\mathbf{L}\cdot\mathbf{S})/\hbar^2 = \frac{1}{2}$ for the $2P_{3/2}$ sublevel. From Eq. (7) we find

$$\frac{1}{x}\frac{dU_0}{dx} = -\frac{2E_0}{t}, \qquad 0 \leqslant x \leqslant 1,$$
$$\frac{1}{x}\frac{dU_0}{dx} = -\frac{2E_0}{tx^3}, \qquad 1 \leqslant x \leqslant \infty. \quad (35)$$

It is now easy to get the corrections for the spin-orbit interaction for the $2P_{1/2}$ and $2P_{3/2}$ sublevels; using the approximate wave functions (21b), (22b), we have:

$$\Delta\varepsilon_{1/2}'' = -2\Delta\varepsilon_{3/2}'' = (\alpha^2 Z^2 C^2/t^3)(F_4 + u^2 G_1). \quad (36)$$

3) The specific Dirac correction is taken into account by adding to the potential energy the term

$$\Delta U''' = -\left(\frac{\hbar}{2mc}\right)^2\frac{dU}{dr}\frac{d}{dr} = -\left(\frac{\alpha Z}{2t}\right)^2\frac{dU}{dx}\frac{d}{dx}. \quad (37)$$

Using the fact that U satisfies the Poisson equation

$$\frac{1}{r^2}\frac{d}{dr}\left(r^2\frac{dU}{dr}\right) = 4\pi e\rho(r), \quad (38)$$

by integrating the expression

$$\int_0^\infty R(x)\frac{dU}{dx}\frac{dR(x)}{dx}x^2\,dx$$

by parts we can show that the corrections to the energy levels will be given by averaging the nuclear charge density over the wave functions of the states in question*

$$\Delta E''' = -(\pi e R_0^3\alpha^3 Z^2/2t^2)\int_0^\infty \rho(x)R^2(x)x^3dx. \quad (39)$$

Taking the expression (1) for the charge density and the approximate wave functions (21a), we find for the S levels

$$\Delta\varepsilon_{n0}''' = -(3\alpha^2 Z^3 C^2/4t^3)F_2. \quad (40)$$

The expression for the correction to the P levels is obtained by replacing F_2 by F_4 in Eq. (40).

To give an idea of the accuracy of the approximate calculation of the energy levels of mesic atoms for constant density of the nuclear charge, as made by means of Eqs. (18) and (19) with the relativistic corrections given by Eqs. (34), (36), and (40), there are shown in Table III the energy levels of several μ-mesic atoms as found by this method, and also the results of exact (numerical) solution of the Dirac equation.[14] We can also compare the data on the energy levels of μ-mesic lead, as obtained by Hill and Ford[7] for constant charge density with $R_0 = 1.17\,A^{1/3}\ 10^{-13}$ cm ($t = 2.2235$), with the results of a calculation by our method:

$1S_{1/2}$	$2P_{1/2}$	$2P_{3/2}$	
10.620	4.809	4.623	according to Hill and Ford
10.614	4.799	4.618	according to our method

(the energies are given in Mev). Some part of the difference between our data and those of Hill and Ford is evidently due to the somewhat different values of the constants used in the calculations.

c) The exponential density. Hill and Ford have also made calculations of the energy levels of the mesic lead atom using an exponential density distribution of the charge of the nucleus:

$$\rho(x) = (eZ\delta^3/8\pi R_0^3)\exp(-\delta x). \quad (41)$$

*See also the remark on page 131 of reference 13.

Here R_0 is the radius of the nucleus with constant density, taken as the zeroth approximation, and δ is a parameter characterizing the extent of the distribution. R_0 can be chosen, for example, so as to make the mean square radii of the distributions (41) and (1) the same. The potential energy U_1 corresponding to the distribution (41) can be found by integrating the Poisson equation (38):

$$U_1 = (E_0/t)[2x^{-1} - (2x^{-1} + \delta)\exp(-\delta x)]. \quad (42)$$

The difference between U_1 and the potential energy (7) of the zeroth approximation is

$$\Delta U = (E_0/t)[2x^{-1} - (2x^{-1} + \delta)\exp(-\delta x) - 3 + x^2],$$
$$0 \leqslant x \leqslant 1,$$
$$\Delta U = -(E_0/t)(2x^{-1} + \delta)\exp(-\delta x),$$
$$1 \leqslant x \leqslant \infty. \quad (43)$$

In accordance with Eq. (25) we find the correction to the energy ϵ of the zeroth approximation for the 1S level by using the approximate wave functions (21a), (22a); with the notations (26a, b, and c) it is:

$$\Delta\varepsilon = (\zeta^2/t)(2F_1 - 3F_2 + F_4 - e^{-\delta}[2G(\delta, 1; 0, 1) + \delta G(\delta, 2; 0, 1) + 2a^2 G(\delta, 4; 0, 1) + \delta a^2 G(\delta, 5; 0, 1)] + 4aH(\delta, 5) + 2a\delta H(\delta, 7) - u^2 e^{-\delta}[2G(2b + \delta, 1; 1, \infty) + \delta G(2b + \delta, 2; 1, \infty)]). \quad (44)$$

The shift of the 2P level is found by replacing F_m, $G(\xi, m; x_1, x_2)$, and $H(\delta, m)$ in Eq. (44) by F_{m+2}, $G(\xi, m+2; x_1, x_2)$, and $H(\delta, m+4)$, respectively.

The results of the calculation by Eq. (44) with inclusion of the relativistic corrections are: 10.458 Mev ($1S_{1/2}$), 4.683 Mev ($2P_{1/2}$), 4.507 Mev ($2P_{3/2}$); they can be compared with the results of Hill and Ford: 10.504 Mev ($1S_{1/2}$), 4.684 Mev ($2P_{1/2}$), 4.508 Mev ($2P_{3/2}$). The comparatively large discrepancy for the $1S_{1/2}$ level is explained by the fact that the relativistic corrections for this level are especially sensitive to the shape of the charge distribution over the volume of the nucleus. From this point of view the exponential distribution is particularly unfavorable for our calculations, since it differs very strongly from the constant distribution, for which the wave functions we used in calculating the relativistic corrections were obtained.

[1] J. A. Wheeler, Phys. Rev. **92**, 812 (1953).
[2] L. N. Cooper and E. M. Henley, Phys. Rev. **92**, 801 (1953).
[3] E. M. Henley, Revs. Modern Phys. **30**, 438 (1958).
[4] J. A. Wheeler, Revs. Modern Phys. **21**, 133 (1949).
[5] S. W. Flügge and F. T. Adler, Naturwiss. **40**, 601 (1953).
[6] A. D. Galanin and I. Ya. Pomeranchuk, Dokl. Akad. Nauk SSSR **86**, 251 (1952).
[7] D. L. Hill and K. W. Ford, Phys. Rev. **94**, 1617 (1954).
[8] D. West, Repts. Prog. Phys. (Physical Soc., London) **21**, 271 (1958).
[9] V. I. Smirnov, Курс высшей математики (Course of Higher Mathematics), Gostekhizdat, Moscow, 1953, Vol. 3, Part 2.
[10] I. M. Ryzhik and I. S. Gradshtein, Таблицы интегралов, сумм, рядов и произведений. (Tables of Integrals, Sums, Series, and Products), Gostekhizdat, Moscow-Leningrad, 1951.
[11] V. L. Fitch and J. Rainwater, Phys. Rev. **92**, 789 (1952).
[12] G. E. Pustovalov, J. Exptl. Theoret. Phys. (U.S.S.R.) **32**, 1519 (1957), Soviet Phys. JETP **5**, 1234 (1957).
[13] E. U. Condon and G. H. Shortley, The Theory of Atomic Spectra, Cambridge, 1944. Russ. Transl., IIL, 1949.
[14] D. D. Ivanenko and G. E. Pustovalov, Usp. Fiz. Nauk **61**, 27 (1957).

Translated by W. H. Furry
365

THE INFLUENCE OF ANISOTROPY ON THE THERMAL CONDUCTIVITY OF SUPERCONDUCTORS

I. M. KHALATNIKOV

Institute for Physical Problems, Academy of Sciences, U.S.S.R.

Submitted to JETP editor December 18, 1958

J. Exptl. Theoret. Phys. (U.S.S.R.) **36**, 1818-1822 (June, 1959)

We have evaluated the electronic part of the thermal conductivity of a superconductor taking anisotropy into account. We show that the temperature dependence of the thermal conductivity may be different along different crystallographic axes for uniaxial crystals.

THE electronic part of the thermal conductivity of superconductors was evaluated by a number of authors[2,3] on the basis of the theory of Bardeen, Cooper, and Schrieffer.[1] In these papers an isotropic model of a superconductor was considered. In the following we shall give a similar evaluation taking anisotropy into account. It will be shown that in some cases the temperature dependence of the coefficient of thermal conductivity may change with direction.

Bogolyubov, Tolmachev, and Shirkov[4] obtained the energy spectrum of a superconductor taking anisotropy into account by the same method as was used for the isotropic case. One can in that case start either from Fröhlich's Hamiltonian, or from the model Hamiltonian of Bardeen's. In the given case the model Hamiltonian can be written in the form

$$H = \sum (E_k - \mu) a_k^+ a_k + \tfrac{1}{2} \sum g(\mathbf{k}_1', \mathbf{k}_2'; \mathbf{k}_1, \mathbf{k}_2) a_{\mathbf{k}_1' \nu_1}^+ a_{\mathbf{k}_2' - \nu_2}^+ a_{\mathbf{k}_1 \nu_1} a_{\mathbf{k}_2 - \nu_2}, \quad (1)$$

where μ is the chemical potential. The function $g(\mathbf{k}_1', \mathbf{k}_2'; \mathbf{k}_1, \mathbf{k}_2)$ satisfies the conditions

$$g(\mathbf{k}_1', \mathbf{k}_2'; \mathbf{k}_1, \mathbf{k}_2) = g(\mathbf{k}_1, \mathbf{k}_2; \mathbf{k}_1', \mathbf{k}_2') = g(-\mathbf{k}_1, -\mathbf{k}_2; -\mathbf{k}_1', -\mathbf{k}_2'). \quad (2)$$

because of its invariance with respect to a permutation of the particles and to spatial inversion. Performing, furthermore, a transformation from the particle operators $a_{\mathbf{k}}$ to the excitation operators $\alpha_{\mathbf{k}}$ according to

$$a_{\mathbf{k}\nu_2} = u_k \alpha_{\mathbf{k}0} + \nu_k \alpha_{\mathbf{k}1}^+, \qquad a_{\mathbf{k}-\nu_2} = u_k \alpha_{\mathbf{k}1} - \nu_k \alpha_{\mathbf{k}0}^+, \quad u_k^2 + \nu_k^2 = 1 \quad (3)$$

and considering in the Hamiltonian only the pair interactions for particles with equal, but opposite momenta, we find the excitation spectrum in the form

$$\varepsilon_k = \sqrt{\xi_k^2 + \Delta^2(\mathbf{e_k})}, \qquad \xi_k = E_k - \mu \quad (4)$$

($\mathbf{e_k}$ is a unit vector in the $\mathbf{k}$ direction). The anisotropic gap $\Delta(\mathbf{e_k})$ is determined by the condition*

$$\Delta(\mathbf{e}_k) = \sum_{k'} g(\mathbf{k}, -\mathbf{k}; \mathbf{k}', -\mathbf{k}') \Delta(\mathbf{e}_{k'}) / 2\varepsilon_{k'}. \quad (5)$$

The transformation parameters $u_{\mathbf{k}}$ and $v_{\mathbf{k}}$ are in this case equal to

$$u_k^2 = \tfrac{1}{2}(1 + \xi_k/\varepsilon_k), \qquad v_k^2 = \tfrac{1}{2}(1 - \xi_k/\varepsilon_k). \quad (6)$$

We shall assume that the electronic thermal conductivity is caused by the scattering of the excitations by impurities. The Hamiltonian for the interaction of an electron with an impurity is equal to

$$H_{int} = \sum V_{kk'} a_k^+ a_{k'}. \quad (7)$$

Performing the u, v transformation (3) we get the Hamiltonian for the interaction of the excitation with an impurity

$$H_{int} = \sum V_{kk'} (u_k u_{k'} - v_k v_{k'}) \alpha_k^+ \alpha_{k'}. \quad (8)$$

The transport equation for the excitations

$$\frac{\partial n}{\partial t} + \frac{\partial n}{\partial r}\frac{\partial \varepsilon}{\partial k} - \frac{\partial n}{\partial k}\frac{\partial \varepsilon}{\partial r} = I(n) \quad (9)$$

[I(n) is the collision integral] assumes the following form

$$\frac{n}{T^2}\xi_k \left(\frac{\partial E}{\partial k} \nabla T\right) = I(n). \quad (10)$$

under stationary conditions and in the presence of a temperature gradient.

We shall perform the further calculations for the case of sufficiently low temperatures when the inequality

$$T \ll \Delta_{min}. \quad (11)$$

*We have assumed that the function g depends only on the angles characterizing the directions $\mathbf{k}$ and $\mathbf{k}'$.

is satisfied. The magnitude of the gap $\Delta(\mathbf{e_k})$ depends on the direction. It follows that the gap will take on minimum values Δ_{min} for some extremal directions. It is also clear that there will be for each extremal direction a corresponding equivalent extremal direction in the opposite direction. For the case of temperatures near T_c when the values of Δ are small, an analysis of the transport equation in the anisotropic case becomes not very instructive. At low temperatures, however, when the value of Δ practically ceases to depend on the temperature, one can solve the problem completely and one can take as the distribution function for the excitations the classical Boltzmann function.

Since the number of excitations moving in a given direction will basically be determined by the exponent $\exp(-\Delta/T)$, it is natural that the largest contribution to the energy current will be given by excitations moving near to the extremal directions. It is thus sufficient to perform the analysis of the transport equation only in the neighborhood of these directions. The problem consists thus in finding the distribution function for the excitations moving near the extremal directions.

For elastic scattering by an impurity only the energy is conserved in the anisotropic case. As to the momentum of the excitation, its absolute magnitude is clearly not conserved. The collision integral $I(n)$ is in the case under consideration equal to

$$I(n) = -\frac{2\pi}{\hbar}\int |V_{kk'}|^2 (u_k u_{k'} - v_k v_{k'})^2 \times \delta(\varepsilon_k - \varepsilon_{k'})(n_k - n_{k'})\, d\tau_{k'}. \quad (12)$$

We have used here (8) and the fact that the distribution function is classical. We further use Eqs. (6) and integrate the δ-function in (12) over $d\xi_{k'}$. We get as a result

$$I(n) = -\frac{\pi}{2\hbar}\int |V_{kk'}|^2 \frac{(\xi_k + \xi_{k'})^2}{\varepsilon_k |\xi_{k'}|}\left(\frac{\partial^2\tau}{\partial\xi_k \partial o'}\right) do'(n_k - n_{k'}). \quad (13)$$

(do' is an element of solid angle).

We write the required non-equilibrium function n_k in the form

$$n_k = n_k^0(1 + \chi_k), \quad (14)$$

where n_k^0 is the equilibrium distribution function. Substituting (13) into (10) we get then the following integral equation to determine the function χ_k:

$$-\frac{\varepsilon_k}{T^2}\left(\frac{\partial E}{\partial k}\nabla T\right) = \frac{\pi}{2\hbar}\int |V_{kk'}|^2 \frac{(\xi_k + \xi_{k'})^2}{\xi_k |\xi_{k'}|}\left(\frac{\partial^2\tau}{\partial\xi_{k'}\partial o'}\right)(\chi_k - \chi_{k'})\, do'. \quad (15)$$

This equation can easily be solved for the extremal directions. We consider the case when there are only two (opposite) extremal directions.

Let the gradient ∇T be directed along the extremal direction and let us denote by ϑ the angle between ∇T and the vector $\mathbf{k}$. We introduce, moreover, the following notation (for the sake of simplicity we have assumed Δ to be independent of the azimuthal angle φ):

$$\eta_k^2 = \xi_k^2 + \Delta\Delta''\vartheta^2, \qquad y = \xi_k/\gamma_k \qquad (\Delta'' = \partial^2\Delta/\partial\vartheta^2). \quad (16)$$

Taking into account that the temperature is low we can everywhere in (15) neglect the quantity ξ_k compared to Δ. As a result the integral Eq. (15) assumes the following form:

$$\frac{1}{\gamma_k^2} Ay = V_0^2 \int_{-1}^{1} (y + y')^2 (\chi_y - \chi_{y'})\, dy' + V_\pi^2 \int_{-1}^{1} (y + y')^2 (\chi_y + \chi_{y'})\, dy', \quad (17)$$

where

$$A = -\frac{\hbar}{\pi^2}\left(\frac{\partial E}{\partial k}\right)_F^2 \frac{\Delta^2\Delta''}{T^2}\left(\frac{\partial^2\tau}{\partial k \partial o}\right)_F^{-1} |\nabla T|, \quad (18)$$

V_0 and V_π are the matrix elements for scattering over an angle 0 and an angle π, respectively, for excitations moving initially in the extremal direction. The first integral arises from integrating in (15) over the region in the neighborhood of the extremal direction, and the second integral from the region near the opposite direction. In deriving (17) we have used the fact that $\eta_k^2 = \eta_{k'}^2$ because of the conservative law for energy. The quantity Δ'' occurring in the equations is the second derivative of the gap Δ with respect to the angle ϑ near its extrema (it is obvious that $\Delta' = 0$). Derivatives of E and τ with respect to k are taken in the extremal direction on the Fermi surface. Finally we have used the obvious consequence of Eq. (15), namely, that $\chi_{y'}$ for the direction opposite to the extremal direction differs from χ_y only in sign.

From Eq. (17) one sees easily that χ_y is an odd function of y, i.e.

$$\chi_y = -\chi_{-y}. \quad (19)$$

To find χ_y from (17) we get, if we take this fact into account, the following equation

$$\chi_y = A\psi_y/\gamma_k^2,$$

$$y = 2(V_0^2 + V_\pi^2)(y^2 + \tfrac{1}{3})\psi_y + 2y(V_\pi^2 - V_0^2)\int_{-1}^{1} \psi_{y'} y'\, dy'. \quad (20)$$

The solution of Eq. (20) is elementary

$$\psi_y = y/2\left(y^2+\tfrac{1}{3}\right)[(V_\pi^2+V_0^2) + 2(1-\pi/3\sqrt{3})(V_\pi^2-V_0^2)]. \quad (21)$$

There only remains for us to evaluate the energy current

$$\mathbf{q} = \int \varepsilon_{\mathbf{k}} \frac{\partial \varepsilon}{\partial k} n^0 \chi_{\mathbf{k}} d\tau_{\mathbf{k}}. \quad (22)$$

We only need perform the integration in (22) over the regions near the extremal directions. The distribution function near the extremal directions can be written in the form

$$n^0 = \exp\{-\Delta/T - \eta_{\mathbf{k}}^2/2\Delta T\}. \quad (23)$$

Substituting (21) into (22) we get after some simple transformations

$$q = \frac{2\pi A e^{-\Delta/T}}{\Delta\Delta''}\left(\frac{\partial^2\tau}{\partial k \partial o}\right)_F \frac{1}{(V_\pi^2+V_0^2)+2(1-\pi/3\sqrt{3})(V_\pi^2-V_0^2)} \times \int_0^\infty \eta_{\mathbf{k}} d\eta_{\mathbf{k}} \exp\left\{-\frac{\eta_{\mathbf{k}}^2}{2\Delta T}\right\} \int_{-1}^{1} \frac{y^2 dy}{y^3+1/3}. \quad (24)$$

From this we finally get for the coefficient of thermal conductivity along the extremal direction

$$\varkappa_\parallel \approx \frac{8\hbar\Delta^2}{5\pi T}\left(\frac{\partial E}{\partial k}\right)_F^2 \frac{1}{1.8V_\pi^2+0.2V_0^2} e^{-\Delta/T}. \quad (25)$$

To evaluate the coefficient of thermal conductivity along directions perpendicular to the extremal one, it is necessary to solve anew the integral Eq. (15). We now take the temperature gradient along an axis perpendicular to the extremal direction (x axis). We get then easily the following equation for the function χ, if we go over to the variables (16),

$$\cos\varphi \frac{A}{\eta_{\mathbf{k}}\sqrt{\Delta\Delta''}} y\sqrt{1-y^2} = (V_0^2+V_\pi^2)\int_{-1}^{1}(y+y')^2(\chi_y-\chi_{y'})\,dy'. \quad (26)$$

The solution of this equation is also obtained elementarily and we get

$$\chi_y = \psi_y A\cos\varphi/\eta_{\mathbf{k}}\sqrt{\Delta\Delta''}(V_0^2+V_\pi^2), \quad (27)$$

$$\psi_y = \frac{y}{2(y^2+1/3)}\left(\sqrt{1-y^2}+\frac{\pi}{6}\frac{1}{1-2(1-\pi/3\sqrt{3})}\right). \quad (28)$$

The heat current in this case is equal to

$$q_\perp = \int \varepsilon_{\mathbf{k}} \frac{\partial \varepsilon}{\partial k} \vartheta \cos\varphi n^0 \chi_{\mathbf{k}} d\tau_{\mathbf{k}}. \quad (29)$$

Substituting here χ from (27) and going over to the variables $\eta_{\mathbf{k}}$ and y we get

$$q_\perp = \frac{2\pi A e^{-\Delta/T}}{(\Delta\Delta'')^2(V_0^2+V_\pi^2)} \times \int_0^\infty \eta_{\mathbf{k}}^3 d\eta_{\mathbf{k}} \exp\left\{-\frac{\eta_{\mathbf{k}}^2}{2\Delta T}\right\} \int_{-1}^{1} \psi_y \sqrt{1-y^2}\, y dy, \quad (30)$$

or finally

$$\varkappa_\perp \approx \frac{10\hbar\Delta^2}{3\pi\Delta''}\left(\frac{\partial E}{\partial k}\right)_F^2 \frac{1}{V_0^2+V_\pi^2} e^{-\Delta/T}. \quad (31)$$

The ratio $\varkappa_\perp/\varkappa_\parallel$ is equal to

$$\varkappa_\perp/\varkappa_\parallel \approx (2T/\Delta'')(1.8V_\pi^2+0.2V_0^2)/(V_\pi^2+V_0^2). \quad (32)$$

The thermal conductivity in a direction perpendicular to the extremal one is thus less than its extremal value roughly by a factor T/Δ. The main (exponential) part of the temperature dependence of $\varkappa$ is here, of course, the same in all directions. A qualitative picture of the dependence of the coefficient of thermal conductivity on the angle θ, reckoned from the extremal direction, at low temperatures will be in the form of a rosette, shown in the figure and determined by the following obvious relation

$$\varkappa = \varkappa_\parallel \cos^2\theta + \varkappa_\perp \sin^2\theta. \quad (33)$$

Dependence of the thermal conductivity on the angle θ (for the case $\varkappa_\perp/\varkappa_\parallel = 1/5$).

The situation considered here, where there is only one pair of extremal directions, is clearly rare. It could be realized in the case of a uniaxial crystal with the extremal direction along the main axis of symmetry. More typical will be the case where there are several extremal directions which are not lying in one plane. One can see that the temperature dependence of the thermal conductivity will in that case be unique in all directions in the approximation considered here.

The preliminary results of N. V. Zavaritskiĭ on the thermal conductivity of Ga in the superconducting state[5] indicate the presence of a different temperature dependence along the directions of the crystallographic axes. If these results are confirmed this will mean that a situation takes place in Ga where there are two extremal directions for Δ.

In conclusion I express my deep gratitude to L. D. Landau for discussing the results of the present paper.

[1] Bardeen, Cooper, and Schrieffer, Phys. Rev. **108**, 1175 (1957).

[2] B. T. Geĭlikman, J. Exptl. Theoret. Phys. (U.S.S.R.) **34**, 1042 (1958), Soviet Phys. JETP **7**, 721 (1958).

[3] J. Bardeen, Physica **24**, S27 (1958).

[4] Bogolyubov, Tolmachev, and Shirkov, Новый метод в теории сверхпроводимости, (A New Method in the Theory of Superconductivity) U.S.S.R. Acad. Sci. Press, 1958, Fortschr. Phys. **6**, 605 (1958).

[5] N. V. Zavaritskiĭ, Abstract of a Contribution to the Fifth All-Union Congress on the Physics of Low Temperatures, Tbilisi 1958.

Translated by D. ter Haar
366

THE RADIATION REACTION IN THE MOTION OF A CHARGE IN A MEDIUM

V. L. GINZBURG and V. Ya. ÉĬDMAN

Radiophysics Institute, Gorkiĭ State University

Submitted to JETP editor December 20, 1958

J. Exptl. Theoret. Phys. (U.S.S.R.) **36**, 1823-1833 (June, 1959)

The radiation reaction force is computed for a charge that moves in a medium which, for generality, is taken to be anisotropic and gyrotropic. The radiation force in the medium can be important in cases in which the particle moves in a magneto-active plasma, in channels and slits in dielectrics, or in waveguides. At velocities greater than the phase velocity of light in the medium, the radiation force that affects the oscillation because of the anomalous Doppler effect has a different sign than that due to dissipation associated with the normal Doppler effect. The total radiation force which affects the amplitude of the oscillations of the particle in an isotropic medium corresponds to dissipation for motion at velocities greater than the velocity of light. However this dissipation force may be appreciably smaller than the dissipation associated with motion at velocities smaller than the velocity of light. In an isotropic medium the oscillations can be strengthened instead of attenuated. The reduction in the radiative dissipation force may be related to the peculiarities of the anomalous Doppler effect as found in the quantum-mechanical analysis and the instability of particle beams which move at velocities greater than the velocity of light.

SINCE the presence of a medium has a pronounced effect on the nature of the electromagnetic waves produced by a moving particle it is clear that the radiation reaction forces in the medium are affected by the medium. As an example we may note that an oscillator of frequency ω in an isotropic plasma with a refractive index $n^2 = 1 - 4\pi e^2 N/m\omega^2$ will not radiate when $4\pi e^2 N/m > \omega^2$ if $n^2 < 0$; in a magneto-active plasma in the nonrelativistic approximation no radiation is produced by an electron which rotates in a magnetic field H_0 at a frequency $\omega_H = eH_0/mc$ (cf. reference 1). In both of these cases the radiation force is obviously zero; in vacuum this force is $\mathbf{f}_0 = (2e^2/3c^3)\dot{\mathbf{v}}$. On the other hand, in uniform motion in a medium, if $v > c/n(\omega)$, Cerenkov radiation occurs; in the isotropic case the radiation force associated with this radiation is[2]

$$\mathbf{f}_{Cer} = -\frac{e^2\mathbf{v}}{c^2 v}\int\limits_{c/n<v}\left(1-c^2/v^2n^2(\omega)\right)\omega d\omega. \qquad (1)$$

In light of the above alone, it is of interest to compute the radiation reaction forces for arbitrary motion of a charge in an arbitrary medium. To the best of our knowledge, this problem has not yet been investigated.

The apparent reason for this is that the radiation force for motion in a medium is usually much smaller than the braking forces associated with ionization losses. Thus, the Cerenkov radiation losses, which may be considered radiation losses, amount to only a small fraction of the total losses even in a transparent but dense medium. In the case of nonuniform motion of a charge the situation is generally the same.

There are, however, cases of practical interest in which it is important to take account of the radiation forces for motion in a medium. This situation arises in the motion of particles in channels or slits in a medium, motion in a vacuum close to a medium, and motion in waveguides. If the channel is narrow the radiation produced is essentially the same as the radiation in a continuous medium.[3,4] Thus, motion in channels or slits in a medium can in most cases be treated in the same way as motion through a medium (the channel is essentially a mechanism for avoiding the ionization losses). The radiation forces can also be important for motion of a charge in a rarefied plasma (in particular, in a magneto-active plasma).

The problem of radiation forces in a medium acquires a special interest at velocities greater than the velocity of light. For these cases the radiation force which affects the amplitude of the particle oscillations can be very small and even zero [this is due to the nature of the anomalous Doppler effect (cf. references 5 and 6)]. We

shall pay special attention to this point since it is intimately related to the problem of the stability of beams which travel faster than the velocity of light.

Before dealing with these problems, we compute the radiation reaction force in a medium for the general case.

1. To compute the radiation reaction force we first assume that the charge is not a point charge but is characterized by a density distribution $\rho = eg(\mathbf{r}-\mathbf{R})$, where $\mathbf{R}(t)$ is the radius vector to the center of gravity of the charge and $\int g(\mathbf{r}-\mathbf{R})\,d\mathbf{r} = 1$. Under these conditions the field equations and the equations of motion assume the form

$$\operatorname{curl}\mathbf{H} = \frac{4\pi}{c}ev g(\mathbf{r}-\mathbf{R}) + \frac{1}{c}\frac{\partial \mathbf{D}}{\partial t}, \quad \operatorname{div}\mathbf{D} = 4\pi e g(\mathbf{r}-\mathbf{R}),$$

$$\operatorname{curl}\mathbf{E} = -\frac{1}{c}\frac{\partial \mathbf{H}}{\partial t}, \quad \operatorname{div}\mathbf{H} = 0; \tag{2}$$

$$\frac{d}{dt}\left(\frac{m\mathbf{v}}{\sqrt{1-v^2/c^2}}\right) = e\left\{\mathbf{E}^{(0)} + \frac{1}{c}\mathbf{v}\times\mathbf{H}^{(0)}\right\} + e\int\left\{\mathbf{E}(\mathbf{r}) + \frac{1}{c}\mathbf{v}\times\mathbf{H}(\mathbf{r})\right\} g(\mathbf{r}-\mathbf{R})\,d\mathbf{r}, \tag{3}$$

where the charge is assumed to move as a whole with velocity $\mathbf{v} = \dot{\mathbf{R}}$; $\mathbf{H}^{(0)}$ and $\mathbf{E}^{(0)}$ are the external fields, $\mathbf{E}$ and $\mathbf{H}$ are the fields produced by the charge itself and for simplicity the medium is assumed to have a magnetic permeability of unity ($\mu = 1$).

Having in mind applications to a magneto-active plasma we shall assume that the medium is anisotropic and gyrotropic, writing

$$\widetilde{D}_\alpha^{(\omega)} = \varepsilon_{\alpha\beta}(\omega)\widetilde{E}_\beta(\omega), \qquad \alpha, \beta = 1, 2, 3, \tag{4}$$

where the double subscripts indicate summation and the symbol ω indicates that the Fourier components are taken and the real fields are $\mathbf{D} = \widetilde{\mathbf{D}} + \widetilde{\mathbf{D}}^*$ and so on. The tensor $\epsilon_{\alpha\beta}(\omega)$ is assumed to be Hermitian ($\epsilon_{\alpha\beta} = \epsilon^*_{\beta\alpha}$), i.e., absorption is neglected; in principle it is possible to remove this restriction.

For an arbitrary medium the only effective method for solving the problem is expansion of the fields into normal plane waves.[7-9] Thus, we write

$$\mathbf{A} = \widetilde{\mathbf{A}} + \widetilde{\mathbf{A}}^*, \quad \widetilde{\mathbf{A}} = \sqrt{4\pi c}\sum_{\lambda,\,j=1,2}\frac{q_{\lambda j}(t)\,\mathbf{a}_{\lambda j}}{n_{\lambda j}}e^{i\mathbf{k}_\lambda \mathbf{r}},$$

$$\mathbf{E} = \frac{1}{c}\frac{\partial \mathbf{A}}{\partial t} - \nabla\varphi, \quad \mathbf{H} = \operatorname{curl}\mathbf{A}, \tag{5}$$

where $n_{\lambda j}$ is the refractive index and $\mathbf{a}_{\lambda j} = \mathbf{a}_{\lambda j1} + i\mathbf{a}_{\lambda j2}$ ($j = 1, 2$) is the complex polarization vector which corresponds to the normal (extraordinary or ordinary) wave; the summation over $\mathbf{k}_\lambda$ in (5) is taken over the upper hemisphere in $\mathbf{k}$-space.

In order to simplify the relations it is convenient to impose the following condition on $\mathbf{A}$

$$\varepsilon_{\alpha\beta}\partial\widetilde{A}_\alpha/\partial x_\beta + \text{c.c.} = 0.$$

The equations for $\mathbf{A}$ and φ which follow from (2) and (6) are as follows:

$$\Delta\widetilde{\mathbf{A}} - \operatorname{grad}\operatorname{div}\widetilde{\mathbf{A}} - \frac{1}{c^2}\varepsilon_{\alpha\beta}\frac{\partial^2\widetilde{A}_\beta}{\partial t^2}\mathbf{e}_\alpha - \frac{1}{c}\varepsilon_{\alpha\beta}\frac{\partial^2\widetilde{\varphi}}{\partial t\,\partial x_\beta}\mathbf{e}_\alpha + \text{c.c.} = -\frac{4\pi}{c}ev g(\mathbf{r}-\mathbf{R}),$$

$$\varepsilon_{\alpha\beta}\frac{\partial^2\widetilde{\varphi}}{\partial x_\alpha \partial x_\beta} + \text{c.c.} = -4\pi e g(\mathbf{r}-\mathbf{R}), \tag{7}$$

where $\mathbf{e}_\alpha$ is a unit vector along the α axis.

In the normalization of the potentials which has been chosen the part of the field $\mathbf{E}$ which is equal to $-\nabla\varphi$ makes no contribution to the radiation reaction and will not be considered below.

Substituting Eq. (5) in the expansion in (7), after multiplication by $\sqrt{4\pi c}\,(\mathbf{a}^*_{\lambda j}/n_{\lambda j})\,e^{-i\mathbf{k}\lambda\mathbf{r}}$ and integration over the volume we have

$$\ddot{q}_{\lambda j} + \omega^2_{\lambda j}q_{\lambda j} = \sqrt{4\pi}e\int g(\mathbf{r}'-\mathbf{R})\frac{(\mathbf{v}\mathbf{a}^*_{\lambda j})}{n_{\lambda j}}\exp(-i\mathbf{k}_\lambda\mathbf{r}')\,d\mathbf{r}' = f(t), \tag{8}$$

where $\omega^2_{\lambda j} = k^2_\lambda c^2/n^2_{\lambda j}$ (this calculation is considered in greater detail in references 7 and 8). It should be noted that in using the quantity $n_{\lambda j}$ in Eq. (5) and below, because this quantity is a function of ω we are not being consistent since the time dependence of $q_{\lambda j}(t)$ is still not known. Actually, however, in the calculation of the radiated energy for the radiation reaction force the quantity $q_{\lambda j}$ refers to the radiation field and the entire calculation can be carried out assuming at the outset that $n_{\lambda j}$ is constant and by taking account of the dependence of $n_{\lambda j}$ on ω in the final result before integration over frequency (cf. reference 7).

It follows from Eq. (8) that

$$q_{\lambda j}(t) = q_{\lambda j}(0) + \frac{1}{\omega_{\lambda j}}\int_0^t f(t')\sin\omega_{\lambda j}(t-t')\,dt',$$

$$\widetilde{\mathbf{A}} = 4\pi ce\sum_{\lambda j}\frac{\mathbf{a}_{\lambda j}}{n_{\lambda j}\omega_{\lambda j}}e^{i\mathbf{k}_\lambda\mathbf{r}} \times\int_{r'}\int_0^t g(\mathbf{r}'-\mathbf{R}')\,(\dot{\mathbf{R}}'\mathbf{a}^*_{\lambda j})\,e^{-i\mathbf{k}_\lambda\mathbf{r}'}\sin\omega_{\lambda j}(t-t')\,dt'd\mathbf{r}' + \widetilde{\mathbf{A}}(0), \tag{9}$$

where $\mathbf{R}' = \mathbf{R}(t')$ and $\dot{\mathbf{R}}' = \dot{\mathbf{R}}(t') = \mathbf{v}'(t')$. We neglect the free solution $\mathbf{A}(0)$ below. Computing $\mathbf{E}$ and $\mathbf{H}$ from Eq. (9) and substituting in Eq. (3) we have

$$\frac{d}{dt}\frac{m\mathbf{v}}{\sqrt{1-v^2/c^2}} = \mathbf{F}^{(0)} - \frac{e^2}{2\pi^3}\sum_{j=1,2}\int g(\mathbf{r}-\mathbf{R})\,g(\mathbf{r}'-\mathbf{R}')\,e^{i\mathbf{k}(\mathbf{r}-\mathbf{r}')}$$

$$\times\left\{\frac{\mathbf{a}_j(\mathbf{v}'\mathbf{a}_j^*)}{n_j^2}\cos[\omega_j(t-t')] - i\,\mathbf{v}\times(\mathbf{k}\times\mathbf{a}_j)\right.$$

$$\left.\times\frac{\mathbf{v}'\mathbf{a}_j^*}{n_j^2\omega_j}\sin[\omega_j(t-t')]\right\}dt'd\mathbf{k}d\mathbf{r}'d\mathbf{r} + \text{c.c.}, \qquad (10)$$

where

$$\mathbf{F}^{(0)} = e\{\mathbf{E}^{(0)} + c^{-1}\mathbf{v}\times\mathbf{H}^{(0)}\},$$

and as usual we carry out the integration over $\mathbf{k}$ (density of states $d\mathbf{k}_\lambda/8\pi^3$). The second term in the curly brackets in Eq. (10) is to be associated with the magnetic radiation reaction force; in vacuum in the nonrelativistic approximation this term is v/c times smaller than the first and is neglected. In the presence of a medium the magnetic field $H \sim nE$ [for a plane wave $\sim e^{i\omega t - i\mathbf{kr}}$ we have $\mathbf{k}\times\mathbf{E} = \omega\mathbf{H}/c$, $k^2 = (\omega n/c)^2$] and the magnetic reaction force differs from the electric reaction force by a factor of approximately vn/c. For motion at velocities greater than that of light, in which we shall be especially interested, $vn/c > 1$; thus, the magnetic force cannot be neglected even if $v/c \ll 1$. Obviously the magnetic force does no work.

Below we shall compute only that part of the reaction force which does not depend on the dimensions of the particle. Hence, till we drop the term containing the electromagnetic mass it is convenient to take the form factor $g(\mathbf{r}-\mathbf{R})$ as a δ-function, $\delta(\mathbf{r}-\mathbf{R})$, cutting off the integration over $\mathbf{k}$ at $k_{max} = \omega_{max}/c \sim 2\pi/r_0$, where r_0 is the radius of the particle. We write Eq. (10) in the form

$$\frac{d}{dt}\left(\frac{m\mathbf{v}}{\sqrt{1-v^2/c^2}}\right) = \mathbf{F}^{(0)} - \frac{e^2}{2\pi^3}\sum_{j=1,2}\int_0^t\int_0^{k_{max}}\left\{\frac{\mathbf{a}_j(\mathbf{v}'\mathbf{a}_j^*)}{n_j^2}\cos\omega_j(t-t')\right.$$

$$\left. - i\,\mathbf{v}\times(\mathbf{k}\times\mathbf{a}_j)\frac{\mathbf{v}\mathbf{a}_j^*}{n_j^2\omega_j}\sin\omega_j(t-t')\right\}e^{i\mathbf{k}(\mathbf{R}-\mathbf{R}')}\,dt'd\mathbf{k}$$

$$+ \text{c.c.} = \mathbf{F}^{(0)} + \mathbf{f}_r. \qquad (11)$$

The method of computing the radiation reaction forces which is being used here is convenient either in an isotropic medium or in vacuum (cf. references 10 and 11). To verify this statement and to check the results we consider the non-relativistic motion of a particle in a vacuum. In this case, as the $\mathbf{a}_j$ we take the real unit vectors which are perpendicular to $\mathbf{k}$ and to each other; one of these, which lies in the plane defined by the vectors $\mathbf{k}$ and $\mathbf{v}'$, will be denoted simply by $\mathbf{a}$. The second term in the integral in Eq. (11) is neglected since it is of order v/c. Introducing polar coordinates in $\mathbf{k}$-space ($k^2 = \omega^2/c^2$) we have:

$$m\frac{d\mathbf{v}}{dt} = \mathbf{F}^{(0)} - \frac{e^2}{\pi^2c^3}\int_0^t\int_0^{\omega_{max}}\int_\Omega \mathbf{a}(\mathbf{v}(t')\mathbf{a})\cos\omega(t-t')$$

$$\times\cos(\mathbf{kR}(t)-\mathbf{R}(t'))\,\omega^2d\omega d\Omega dt'. \qquad (12)$$

Writing

$$\cos\omega(t-t') \equiv -\frac{1}{\omega}\frac{d}{dt'}[\sin\omega(t-t')]$$

and integrating by parts over t' we transform the integral in Eq. (12) to the form

$$\int\frac{d}{dt'}\{\mathbf{a}(\mathbf{v}'\mathbf{a})\cos\mathbf{k}(\mathbf{R}-\mathbf{R}')\}\sin\omega(t-t')\,\omega d\omega d\Omega dt',$$

where we have dropped the term that depends on the initial conditions and exists only when $t \lesssim 1/\omega_{max}$ (this is considered in greater detail in references 10 and 11). Carrying out another integration by parts and integrating with respect to $d\Omega = \sin\theta\,d\theta\,d\varphi$, we have

$$m\frac{d\mathbf{v}}{dt} = \mathbf{F}^{(0)} - \frac{4e^2}{3\pi}\frac{\omega_{max}}{c^3}\frac{d\mathbf{v}}{dt} + \frac{2e^2}{\pi c^3}\int_0^t\int_0^{\omega_{max}}\frac{d^2\mathbf{a}(\mathbf{va}')\cos\mathbf{k}(\mathbf{R}-\mathbf{R}')}{dt'^2}$$

$$\times\cos\omega(t-t')\,dt'd\omega\sin\theta d\theta. \qquad (12a)$$

The second term on the right side of Eq. (12a) is proportional to the electromagnetic mass $4e^2\omega_{max}/3\pi c^3 \sim e^2/r_0c^2$ and must be discarded since by m we understand the experimental value of the mass (this procedure, which has been used for many years, is identical with mass renormalization, which is sometimes assumed to be of recent origin). The third term on the right side of Eq. (12a), if one neglects quantities which approach zero as $\omega_{max}\to\infty$ (i.e., $r_0\to 0$), is the well-known expression $(2e^2/3c^3)\ddot{\mathbf{R}}$, since in the nonrelativistic case $\cos\mathbf{k}(\mathbf{R}-\mathbf{R}')$ varies much slower with t' than $\cos\omega(t-t')$ while

$$\lim_{\omega_{max}\to\infty}\int_0^t\int_0^{\omega_{max}}\varphi(t')\cos\omega(t-t')\,dt'd\omega = \tfrac{1}{2}\pi\varphi(t).$$

As a second example we consider uniform motion ($\mathbf{R} = \mathbf{vt}$) in an isotropic medium with velocity $v > c/n$. The polarization vector $\mathbf{a}$ may be conveniently chosen as in the preceding case and the magnetic force vanishes identically as follows immediately from symmetry considerations. As a result we obtain the reaction force

$$\mathbf{f}_r = \mathbf{f}_{\text{Cer}} = -\frac{2e^2}{\pi c^3}\int_0^t\int_0^{\omega_{max}}\int_0^{\pi/2}\mathbf{a}(\mathbf{va})\cos\omega(t-t')$$

$$\times\cos\mathbf{kv}(t-t')\,n\omega^2\sin\theta dt'd\omega d\theta.$$

Integration over t′ leads to the appearance of two terms, one of which contains the factor

$$\frac{\sin\omega[1-(nv/c)\cos\theta]t}{1-(nv/c)\cos\theta}\to\pi\delta\left(1-\frac{nv}{c}\cos\theta\right)\quad\text{for } t\to\infty.$$

Since $\cos\theta = c/nv$, we have Eq. (1), since the term which does not contain the δ-function does not make any real contribution in the expression for the force.

In the general case of accelerated motion in an arbitrary medium the reaction force $\mathbf{f_r}$ is determined by Eq. (11). Since $\mathbf{f_r}$ is small, in the calculation the quantities $\mathbf{R}$ and $\mathbf{v} = \dot{\mathbf{R}}$ can be the functions which correspond to the motion of the particle with the radiation reaction neglected.

2. We consider motion of an oscillator at velocities greater than that of light in an isotropic medium, a case which is of interest in connection with microwave radiation.[12]

Choosing the velocity of the reciprocatory motion $\mathbf{v_0}$ along the z axis, we start with an oscillator which oscillates parallel to $\mathbf{v_0}$. In this case the vector quantities in the problem are as follows:

$$\mathbf{R}=\{0,\ 0,\ v_0t+R_0\sin\Omega t\},\qquad \mathbf{v}=\{0,\ 0,\ v_0+v_a\cos\Omega t\},$$
$$v_a=R_0\Omega,\qquad \mathbf{a}_1=\{1,\ 0,\ 0\},\qquad \mathbf{a}_2=\{0,\ \cos\theta,\ -\sin\theta\},$$
$$\mathbf{k}=\{0,\ k\sin\theta,\ k\cos\theta\}. \tag{13}$$

Then, from Eq. (11), for the force f_{rz} we have

$$f_{rz}=-\frac{e^2}{2\pi^2}\int_0^t\int_0^{k_{max}}\frac{\sin^2\theta}{n^2}(v_0+v_a\cos\Omega t')\cos\omega(t-t')$$
$$\times\exp\{ik\cos\theta[v_0(t-t')$$
$$+R_0(\sin\Omega t-\sin\Omega t')]\}\,dt'd\mathbf{k}, \tag{14}$$

where we have neglected the complex conjugate expression which is implied wherever complex quantities are used. At the outset we shall not assume that the oscillation amplitude is small; in Eq. (14) we use the well-known expansion

$$\exp(ik\cos\theta R_0\sin\Omega t)=\sum_{s=-\infty}^{+\infty}J_s(kR_0\cos\theta)\,e^{is\Omega t}. \tag{15}$$

As a result we obtain

$$f_{rz}=-\frac{e^2}{2\pi^2}\sum_{s,\,s'=-\infty}^{\infty}\int_0^t\int_0^{k_{max}}\frac{\sin^2\theta}{n^2}\cos\omega(t-t')\,J_sG_{s'}$$
$$\times\exp\{i[kv_0\cos\theta\cdot(t-t')+\Omega(st-s't')]\}\,d\mathbf{k}dt',$$
$$G_{s'}(x)=J_{s'}(x)(v_0+v_as'/x). \tag{16}$$

Integrating over t′ and keeping only the term which corresponds to the $\delta(y)$-function [$\lim(\sin\alpha y/\pi y)$ for $\alpha\to\infty$] we have

$$f_{rz}=-\frac{e^2}{4\pi}\sum_{ss'}\int\frac{\sin^2\theta}{n^2}J_s(kR_0\cos\theta)\,G_{s'}(kR_0\cos\theta)$$
$$\times e^{i\Omega(s-s')t}\delta(y)\,d\mathbf{k},$$
$$f_{rx}=f_{ry}=0,\quad y=\omega-s'\Omega-kv_0\cos\theta,\quad k=\omega n/c. \tag{17}$$

The work of the radiation reaction force on the particle is

$$A=\int_0^T vf_{rz}\,dt=v_0\int_0^T f_{rz}\,dt+v_a\int_0^T\cos\Omega t f_{rz}\,dt=A_0+A_a, \tag{18}$$

where $T = 2\pi l/\Omega$, $l = 1, 2, 3, 4, \ldots$, i.e., T is equal to a whole number of periods.

For high values of T, only those terms for which $s-s'=0$ and $s-s'=\pm1$ make a contribution to the integrals in Eq. (18). Thus, since

$$J_{s'-1}(x)+J_{s'+1}(x)=(2s'/x)J_{s'}(x),$$

we have

$$A=-\frac{e^2T}{c^2}\sum_{s=-\infty}^{\infty}\int\sin^2\theta G_s^2(kR_0\cos\theta)\,n(\omega)\sin\theta\omega^2\delta(y)\,d\theta d\omega. \tag{19}$$

The term with $s = 0$ yields the Cerenkov radiation and will not be considered below (the usual formula for the intensity of the Cerenkov radiation[2] is obtained from Eq. (19) when $s = 0$ if the quantity $kR_0\cos\theta$, which in this case is $\omega R_0/v_0$, is much smaller than unity). For an oscillator characterized by small amplitudes, where

$$kR_0=(\omega/c)n(\omega)R_0\ll1, \tag{20}$$

we need consider only those terms for which $s_{\pm}=\pm1$.

It is apparent that when (20) is satisfied

$$G_{\pm1}^2(kR_0\cos\theta)=\tfrac{1}{4}(v_0\pm v_a/kR_0\cos\theta)^2(kR_0\cos\theta)^2$$
$$=v_a^2/4(1-\beta_0n\cos\theta)^2,$$

since the vanishing of the argument of the δ-function yields the Doppler condition

$$\omega=\Omega/|1-\beta_0n(\omega)\cos\theta|,\qquad \beta_0=v_0/c. \tag{21}$$

In this case the anomalous Doppler effect, ($\beta n\cos\theta>1$), corresponds to $s=-1$, while the normal effect ($\beta n\cos\theta<1$) corresponds to $s=+1$. Integrating over θ we have ($A=A^++A^-$)

$$A_{s=1}\equiv A^+$$
$$=-\frac{e^2R_0^2T}{4c^2\beta_0}\int_{\beta_0n(\omega)\cos\theta<1}\omega^3\left\{1-\frac{1}{\beta_0^2n^2(\omega)}\left(1-\frac{\Omega}{\omega}\right)^2\right\}d\omega,$$
$$A_{s=-1}\equiv A^-$$
$$=-\frac{e^2R_0^2T}{4c^2\beta_0}\int_{\beta_0n(\omega)\cos\theta>1}\omega^3\left\{1-\frac{1}{\beta_0^2n^2(\omega)}\left(1+\frac{\Omega}{\omega}\right)^2\right\}d\omega, \tag{22}$$

where $\cos\theta$ is expressed in terms of ω by means of Eq. (21). It is apparent that this result can also be obtained directly from Eq. (14) if the condition in (20) is used at the beginning.

From Eq. (22), or, directly from Eq. (19), when (20) applies, with n = const we have

$$A^+ = -\frac{e^2\Omega^4 R_0^2 nT}{4c^3}\int\limits_{\theta>\theta_0}\frac{\sin^3\theta d\theta}{(1-\beta_0 n\cos\theta)^3},$$

$$A^- = -\frac{e^2\Omega^4 R_0^2 nT}{4c^3}\int\limits_{\theta<\theta_0}\frac{\sin^3\theta d\theta}{(\beta_0 n\cos\theta-1)^3}, \qquad (23)$$

where θ_0 is the Cerenkov angle ($\cos\theta_0 = c/nv_0$).

In a number of cases it is convenient to approximate the function $n(\omega)$ by a step function (motion in channels, radiation from bunches, cf. reference 6): $n(\omega) = n$ when $\omega < \omega_c$ and $n(\omega) = 1$ when $\omega > \omega_c$. Under such conditions, as before, the relations in (23) are used but for the radiation frequency $\omega < \omega_c$ in A^+ the limits of integration are $\cos^{-1}[(1-\Omega/\omega_c)/\beta_0 n]$ and π while in A^- the limits of integration are 0 and $\cos^{-1}[(1+\Omega/\omega c)/\beta_0 n]$.

The quantity $W^\pm = -A^\pm$ is the energy radiated inside the Cerenkov cone (A^-) and outside the cone (A^+). In this case Eq. (23) coincides with that given by Frank.[13]

We now divide the work $A^\pm$ into the parts $A_0^\pm$ and $A_a^\pm$, where $A_a^\pm$ corresponds to the work associated with the attenuation or amplification of the particle oscillations [cf. Eq. (18)]. It is apparent that $A_0^\pm$ is always negative whereas

$$A_a^+ = -\frac{e^2\Omega R_0^2 T}{4c^3\beta_0}\int\limits_{\beta_0 n\cos\theta<1}\omega^2\left\{1-\frac{1}{\beta_0^2 n^2}\left(1-\frac{\Omega}{\omega}\right)^2\right\}d\omega, \qquad (24a)$$

$$A_a^- = \frac{e^2\Omega R_0^2 T}{4c^3\beta_0}\int\limits_{\beta_0 n\cos\theta>1}\omega^2\left\{1-\frac{1}{\beta_0^2 n^2}\left(1+\frac{\Omega}{\omega}\right)^2\right\}d\omega \qquad (24b)$$

(we may recall that $A_a = A_a^+ + A_a^-$ and the total work $A = A_0 + A_a$, where $A_0 = A_0^+ + A_0^-$). For n = const or a "step"

$$A_a^\pm = \mp(e^2\Omega^4 R_0^2 nT/4c^3)\int(1-\beta_0 n\cos\theta)^{-4}\sin^3\theta d\theta. \qquad (25)$$

Thus, the radiation which appears in the region outside the Cerenkov cone leads to a decay of oscillations ($A_a^+ < 0$) whereas the radiation inside the cone corresponds to the anomalous Doppler effect and enhancement of the oscillations ($A_a^- > 0$). This result is in complete agreement with that obtained from quantum mechanical considerations.[5,6]

One is easily convinced that the limits of integration over ω in Eq. (24a) are further apart than in Eq. (24b); for example, with n = const, the limits in Eq. (24a) are ∞, $\Omega/(1+\beta_0 n)$ while in Eq. (24b) these limits are ∞, $\Omega/(\beta_0 n - 1)$. The integrand in Eq. (24a) is also larger than that in Eq. (24b). For this reason it is always true that $|A_a^+| \geq A_a^-$ where $|A_a^+| = A_a^-$, if in the actual region of integration $\beta_0 n(\omega) \to \infty$. Thus, at greater-than-light velocities the damping of the oscillations of the oscillator is weakened and can even almost vanish although amplification can never occur.

We now consider an oscillator that vibrates perpendicularly to the velocity $\mathbf{v}_0$; in this case

$$\mathbf{R} = \{R_0\sin\Omega t,\ 0,\ v_0 t\},\quad \mathbf{v} = \{v_a\cos\Omega t,\ 0,\ v_0\},$$
$$\mathbf{a}_1 = \{\sin\varphi,\ -\cos\varphi,\ 0\},$$
$$\mathbf{a}_2 = \{\cos\theta\cos\varphi,\ \cos\theta\sin\varphi,\ -\sin\theta\};$$
$$\mathbf{k} = \{k\sin\theta\cos\varphi,\ k\sin\theta\sin\varphi,\ k\cos\theta\}, \qquad (26)$$

where the polar axis (z) has again been chosen in the direction of the velocity $\mathbf{v}_0$. Proceeding as above we obtain

$$f_{rz} = -\frac{e^2}{4\pi}\sum_{s,\,s'=-\infty}^{\infty}\int J_s(\zeta)\,G'_{s'}(\zeta)$$
$$\times\left\{\sin\theta - \frac{v_a n}{c}[\cos\Omega t(\cos\theta\sin\varphi + \cos\varphi)]\right\}$$
$$\times e^{i\Omega(s-s')t}\delta(y)\frac{dk}{n^2};$$
$$G'_{s'}(\zeta) = \left[v_0\sin\theta - \frac{v_a(\sin\varphi+\cos\theta\cos\varphi)s'}{kR_0\sin\theta\cos\varphi}\right]J_{s'}(\zeta);$$
$$\zeta = kR_0\sin\theta\cos\varphi;\quad y = \omega - s'\Omega - kv_0\cos\theta. \qquad (27)$$

If the condition in (20) is satisfied

$$A_z^+ = \int\limits_0^T v_0 f_{rz}\,dt$$
$$= -\frac{e^2R_0^2T}{8c^3\beta_0}\int\omega^3\left(1-\frac{\Omega}{\omega}\right)\left[\frac{\Omega^2}{\omega^2}+\frac{1}{\beta_0^2 n^2(\omega)}\left(\varkappa+\frac{\Omega}{\omega}\right)^2\right]d\omega,$$
$$A_z^- = -\frac{e^2R_0^2T}{8c^3\beta_0}\int\omega^3\left(1+\frac{\Omega}{\omega}\right)\left[\frac{\Omega^2}{\omega^2}+\frac{1}{\beta_0^2 n^2(\omega)}\left(\varkappa-\frac{\Omega}{\omega}\right)^2\right]d\omega, \qquad (28)$$

where

$$\varkappa = \beta_0^2 n^2(\omega) - 1.$$

Furthermore,

$$f_{rx} = -\frac{e^2}{4\pi}\sum_{ss'}\int J_s G'_{s'}\left[(\sin\varphi+\cos\theta\cos\varphi)\right.$$
$$\left.-\frac{v_0 n}{c}(\cos\varphi+\sin\varphi\cos\theta)\right]e^{i\Omega(s-s')t}\frac{dk}{n^2}; \qquad (29)$$

$$A_x \equiv A_a = \int\limits_0^T v_a f_{rx}\,dt = A_a^+ + A_a^-,$$

$$A_a^+ = -\frac{e^2R_0^2\Omega T}{8c^3\beta_0}\int\omega^2\left[\frac{\Omega^2}{\omega^2}+\frac{1}{\beta_0^2 n^2(\omega)}\left(\varkappa+\frac{\Omega}{\omega}\right)^2\right]d\omega,$$

$$A_a^- = \frac{e^2R_0^2\Omega T}{8c^3\beta_0}\int\omega^2\left[\frac{\Omega^2}{\omega^2}+\frac{1}{\beta_0^2 n^2(\omega)}\left(\varkappa-\frac{\Omega}{\omega}\right)^2\right]d\omega. \qquad (30)$$

In this case it is also true that $|A_{\tilde{a}}^{+}| \geq A_{\tilde{a}}^{-}$. For helical motion, for example along a magnetic field, when $\Omega = \omega_H = (eH_0/mc)\sqrt{1-v^2/c^2}$, it is necessary to set $\mathbf{R} = \{R_0 \cos \Omega t,\ R_0 \sin \Omega t,\ v_0 t\}$; it is easy to compute the radiation force $\mathbf{f_r}$:

$$f_{rx} = -\frac{e^2}{c^3} \sum_{s=-\infty}^{\infty} \int n\omega^2 \delta(y)\, \Phi_s \sin\theta\, d\theta\, d\omega,$$

$$\Phi_s = J_s^2(kR_0 \sin\theta)\left[-\sin\theta + \frac{\Omega s}{\omega \sin\theta}\right]\left[\frac{sv_a \cos\theta}{kR_0 \sin\theta} - v_0 \sin\theta\right]$$

$$+ \frac{v_a^2 n}{c} \cos\theta J_s'^2(kR_0 \sin\theta);$$

$$f_{ry} = -\frac{e^2 \sin \Omega t}{c^3} \sum_{s=-\infty}^{\infty} \int n\omega^2 \delta(y)\, \Phi_s^a \sin\theta\, d\theta\, d\omega,$$

$$\Phi_s^a = (n\beta_0 \cos\theta - 1)\, v_a J_s'^2(kR_0 \sin\theta)$$

$$+ \frac{(n\beta_0 - \cos\theta)\, s}{kR_0 \sin\theta}\left(\frac{sv_a \cos\theta}{kR_0 \sin\theta} - v_0 \sin\theta\right) J_s^2(kR_0 \sin\theta) \quad (31)$$

where f_{ry} differs from f_{rx} by the substitution of $-\sin \Omega t$ for $\cos \Omega t$. The work performed by this force and its components $A_{\tilde{a}}^{\pm}$ is equal to the expressions in (28) and (30) multiplied by 2 if the condition in (20) is satisfied.

If the charge moves in a very narrow channel or slit in the case of oscillations along $\mathbf{v}_0$ [cf. Eq. (13)] there is no change in the radiation intensity (the work $A^{\pm}$) and the reaction force. For an oscillator which oscillates along the x axis [cf. Eq. (26)] the radiation intensity remains unchanged for motion in a narrow slit in the plane $y = 0$. Finally, in the case of helical motion which takes place in a narrow cylindrical channel of circular cross section the radiation intensity is multiplied by the factor $4\epsilon^2/(\epsilon+1)^2$. The remarks concerning channels follow from the results obtained in reference 4.

3. In the case of an anisotropic medium we may consider motion along the axis of a uniaxial nongyrotropic crystal, with the electron assumed to be oscillating in the same direction. Under these conditions

$$\mathbf{R} = \{0, 0, v_0 + R_0 \sin \Omega t\}, \qquad \mathbf{k} = \{0, k \sin\theta, k\cos\theta\};$$

$$\mathbf{a}_1 = \{0, \cos\theta + K_1 \sin\theta, -\sin\theta + K_1 \cos\theta\};$$

$$\mathbf{a}_2 = \{1, 0, 0\}, \qquad K_1 = (n_1^2 - \varepsilon_\perp)\cos\theta / \varepsilon_\perp \sin\theta,$$

$$n_1^{-2} = \sin^2\theta / \varepsilon_\parallel + \cos^2\theta / \varepsilon_\perp, \quad (32)$$

where n_1 is the index of refraction for the extraordinary wave which, in the present case, is the only one radiated: K_1 is the ratio of the electric field components parallel and perpendicular to the vector $\mathbf{k}$ in the extraordinary wave; this electric vector is parallel to the polarization vector $\mathbf{a}_1$, the length of which satisfies the condition $n_1^{-2}\{\epsilon_\parallel a_z^2 + \epsilon_\perp a_y^2\} = 1$ (cf. reference 7).

Substituting Eq. (32) in Eq. (11), we obtain results similar to those obtained for the isotropic medium, where we have in Eq. (21) $n_{1,2}(\theta, \omega)$ in place of $n(\omega)$. Here we present only the expressions that correspond to Eqs. (22) and (24):

$$A_{s=\pm 1} \equiv A^{\pm}$$

$$= -\frac{e^2 R_0^2 T}{4c^3 \beta_0} \int \frac{\omega^3 \varepsilon_\perp^2(\omega) \sin^2\theta\, d\omega}{(\varepsilon_\perp \sin^2\theta + \varepsilon_\parallel \cos^2\theta)^2\, |1 - (\mathrm{ctg}\,\theta / n_1)\, \partial n_1 / \partial\theta|}, \quad (33)$$

$$A_{\tilde{a}}^{\pm} = \mp \frac{e^2 \Omega R_0^2 T}{4c^3 \beta_0} \int \frac{\omega^2 \varepsilon_\perp^2(\omega) \sin^2\theta\, d\omega}{(\varepsilon_\perp \sin^2\theta + \varepsilon_\parallel \cos^2\theta)^2\, |1 - (\mathrm{ctg}\,\theta / n_1)\, \partial n_1 / \partial\theta|}$$

$$= \mp \frac{e^2 \Omega^4 R_0^2 T}{4c^3} \int \frac{n_1^5 \sin^3\theta\, d\theta}{\varepsilon_\parallel^2\, |1 - \beta_0 n_1 \cos\theta|^3\, |1 - \beta_0 \cos\theta\, \partial(\omega n_1)/\partial\omega|}, \quad (34)$$

where $A = A^+ + A^- = A_0 + A_a = A_0^+ + A_0^- + A_a^+ + A_a^-$ [cf. Eqs. (18) and (22)] while $\cos\theta$, $\sin\theta$ and $n_1(\omega, \theta)$ must be expressed in terms of ω through the Doppler expression (21).

Thus, for the normal effect in Eqs. (33) and (34)

$$s = 1, \qquad \cos\theta = (1 - \Omega/\omega)/\beta_0 n_1[\omega, \theta(\omega)]$$

and the integration is taken over the region for which $\beta_0 n_1 \cos\theta < 1$; for the anomalous effect

$$s = -1, \qquad \cos\theta = (1 + \Omega/\omega)/\beta_0 n_1$$

and the integration is taken over the region for which $\beta_0 n_1 \cos\theta > 1$. We may note that the factor

$$\varepsilon_\perp^2 \sin^2\theta / (\varepsilon_\perp \sin^2\theta + \varepsilon_\parallel \cos^2\theta)^2 = n_1^4 \sin^2\theta / \varepsilon_\parallel^2,$$

which appears in Eqs. (33) and (34) is also equal to a_{1z}^2, when $\epsilon_\perp = \epsilon_\parallel$ equals $\sin^2\theta$ and this corresponds to the transition from Eqs. (22) to (24).

In an anisotropic medium it is possible for amplification as well as attenuation to occur (in this case $|A_{\tilde{a}}^{+}| > A_{\tilde{a}}^{-}$). As an example we consider the following idealized case: $\epsilon_\perp$ and $\epsilon_\parallel$ are independent of frequency and $\epsilon_\perp > 0$ and $\epsilon_\parallel < 0$. In this case $n_1^2(\theta_\infty) = \infty$ at the angle θ_∞ determined from the condition $\epsilon_\perp \sin^2\theta_\infty + \epsilon_\parallel \cos^2\theta_\infty = 0$. Furthermore n_1^2 is a minimum and equal to $\epsilon_\perp$ when $\theta = 0$ while $\pi/2 > \theta > \theta_\infty$ for $n_1^2 < 0$ and propagation is impossible. If now $\beta_0 \epsilon_\perp > 1$, it is always possible to choose $\epsilon_\parallel$ in such a way that the Cerenkov angle $\theta_0 = \cos^{-1}(1/\beta_0 n_1)$ is larger than θ_∞. Under these conditions there is no Cerenkov radiation and in the forward direction (for $\theta < \pi/2$) only anomalous Doppler waves are radiated. In the backward direction ($\pi - \theta < \theta_\infty$) normal Doppler waves are radiated but here $(1 - \beta_0 n \cos\theta) = (1 + \beta_0 n |\cos\theta|)$ and, as follows from Eq. (34), the work $|A_{\tilde{a}}^{+}|$ is always smaller than the work $A_{\tilde{a}}^{-}$.

It should be noted that at large values of n both in anisotropic and in isotropic media it may turn

out that Eq. (20) is not satisfied; a number of the formulas given here are then inapplicable. This situation is especially important for anisotropic media in cases in which the signs of $\epsilon_{\parallel}$ and $\epsilon_{\perp}$ are different and n_2 becomes infinite over a wide range of frequencies.

The case of helical motion of a charge in a magneto-active plasma* has been considered in detail in another paper.[14] Here we limit ourselves to the remark that if there is an anomalous Doppler region we know that there will be a weakening of the radiation dampening which leads to a reduction of the particle velocity perpendicular to the external magnetic field. At certain values of the parameters the damping becomes negative, i.e., oscillations are excited.

4. As noted above, the difference in the signs of the forces which affect the oscillatory motion of a particle for the normal and anomalous Doppler effects are in complete agreement with the results which follow from simple quantum mechanical considerations.[5,6] In particular, in the anomalous Doppler effect the system makes a transition from a lower level to a higher level; this corresponds to excitation rather than dissipation. Hence, from the quantum-mechanical point of view the system (for example a moving oscillator) must have some probability of making transitions to higher and higher oscillatory levels so long as these transitions are consistent with the condition $\beta_0 n(\omega)\cos\theta > 1$. At the same time, in the classical approximation, in an isotropic medium the oscillations are always attenuated, i.e., the system makes transitions to lower levels although the rate of "fall" may be slowed down considerably at velocities greater than that of light. There is actually no inconsistency. Consider a wave packet, composed of wave functions with approximately the same energies (energies of oscillatory motion). At velocities below the velocity of light there are only transitions to lower levels and, aside from the reduction in the mean energy of the packet, the width of the energy spectrum is increased. At velocities greater than the velocity of light it is also possible to have transitions to upper levels and the variation of the energy spectrum of the packet is different; in particular, in the total ensemble of states there will be a state with energy greater than the initial energy. In this sense we have excitation of transverse oscillations. However, in the classical approximation, i.e., if one neglects the spread of the packet, only the change in the mean energy of the packet is important. This change, as has been shown, always corresponds to a reduction in mean energy in an isotropic medium. It can be shown that at velocities greater than the velocity of light the system becomes unstable to some extent. In the first place we have the excitation of oscillations in the quantum approximation, as already noted; secondly, in an anisotropic medium it is possible to have excitation of oscillations even in the classical approximation; in the third place (and in practice this is the most important) there is an instability and excitation of oscillations when we consider a particle bunch moving at velocities greater than light rather than a single particle.[15] This excitation is associated with the fact that the beam exhibits negative absorption (reabsorption) in the region of the anomalous Doppler frequencies (in this region, in absorbing a photon the system makes a transition in the downward direction whereas a transition in the upward direction corresponds to induced emission). It is completely obvious that this instability of "superlight" bunches, which occurs in an isotropic medium even in the classical approximation, is closely associated with the problem of radiation reaction which has been considered above in connection with a single particle.

*This case is automatically realized for motion of an electron in a plasma in a magnetic field.

[1] V. L. Ginzburg and V. V. Zheleznyakov, Изв. ВУЗов, Радиофизика, (Bulletin of Instit. of Higher Learning, Radiophysics) **1**, 2, 59 (1958).

[2] I. E. Tamm and I. M. Frank, Dokl. Akad. Nauk SSSR, **14**, 107 (1937).

[3] V. L. Ginzburg and I. M. Frank, Dokl. Akad. Nauk SSSR, **56**, 699 (1947).

[4] V. L. Ginzburg and V. Ya. Éĭdman, J. Exptl. Theoret. Phys. (U.S.S.R.) **35**, 1508 (1958), Soviet Phys. JETP **8**, 1055 (1959).

[5] V. L. Ginzburg and I. M. Frank, Dokl. Akad. Nauk SSSR, **56**, 583 (1947).

[6] V. L. Ginzburg and V. M. Faĭn, J. Exptl. Theoret. Phys. (U.S.S.R.) **35**, 817 (1958), Soviet Phys. JETP **8**, 567 (1959).

[7] V. L. Ginzburg, J. Exptl. Theoret. Phys. (U.S.S.R.) **10**, 601 (1940); J. Phys. (U.S.S.R.) **3**, 95 (1940).

[8] A. A. Kolomenskiĭ, J. Exptl. Theoret. Phys. (U.S.S.R.) **24**, 167 (1953).

[9] V. Ya. Éĭdman, J. Exptl. Theoret. Phys. (U.S.S.R.) **34**, 131 (1958), Soviet Phys. JETP **7**, 91 (1958).

[10] A. P. Belousov, J. Exptl. Theoret. Phys. (U.S.S.R.) **9**, 658 (1939).

[11] V. L. Ginzburg, Труды ФИАН СССР (Trans. Phys. Inst. U.S.S.R. Acad. Sci.) **3**, 2, 195 (1946); J. Exptl. Theoret. Phys. (U.S.S.R.) **13**, 33 (1943); J. Phys. (U.S.S.R.) **8**, 33 (1944).

[12] V. L. Ginzburg, Dokl. Akad. Nauk SSSR, **56**, 145 (1947); Izv. Akad. Nauk SSSR, Ser. Fiz. **11**, 165 (1947).

[13] I. M. Frank, Izv. Akad. Nauk SSSR, Ser. Fiz. **6**, 3 (1942).

[14] V. Ya. Éĭdman, Изв. ВУЗов, Радиофизика, (Bulletin of Inst. of Higher Learning, Radiophysics) **2** (1959).

[15] V. V. Zheleznyakov, Изв. ВУЗов, Радиофизика, (Bulletin of Inst. of Higher Learning, Radiophysics) **1**, 4 (1958).

Translated by H. Lashinsky
367

MOTION OF A PLASMA LOOP IN AN AXIALLY SYMMETRIC MAGNETIC FIELD

L. M. KOVRIZHNYKH

P. N. Lebedev Physics Institute, Academy of Sciences, U.S.S.R.

Submitted to JETP editor December 25, 1958

J. Exptl. Theoret. Phys. (U.S.S.R.) **36**, 1834-1838 (June, 1959)

Problems related to the dynamics of a plasma loop in an inhomogeneous axially symmetric magnetic field are considered.

OSOVETS[1] and Shafranov[2] have considered the conditions of equilibrium of a plasma loop carrying a current in a magnetic field. In the present work, assuming stability over a small radius b, we consider the motion of such a loop as a whole in an axially symmetric magnetic field and find the relation which describes the variation of its large radius as a function of time.

1. BASIC EQUATIONS

We consider an axially symmetric magnetic field $\mathbf{H}(r, z, t)$ which is specified by the vector potential $\mathbf{A} = \{0, A_\varphi, 0\}$. It will be assumed that the axis of the loop coincides with the symmetry axis of the field so that the configuration of the loop is given completely by the z coordinate of its center and the quantity r, its large radius. The equations of motion can then be written in the form*

$$\frac{d^2\xi}{dt^2} = \omega_H^2 i \frac{\partial a}{\partial \xi}, \tag{1}$$

$$\frac{d^2x}{dt^2} = \omega_H^2 \frac{i}{x^2}\left[x\frac{\partial}{\partial x}(ax) + i\left(ax + \frac{1}{l} + \frac{1}{2}\right)\right], \tag{2}$$

$$i = -\tau \frac{d}{dt}[ax + (1 + \alpha x) i], \tag{3}$$

where

$$\omega_H^2 = 2\pi R_0 H_0^2 / Ml, \quad \alpha = 2\pi R_0 / Nlr_0, \quad i = Jlx / R_0 cH_0,$$

$$\tau = \sigma sl / c^2, \quad a = A_\varphi / R_0 H_0,$$

$$l = L / 2\pi r = 2[\ln(8r/b) - 2], \quad \xi = z / R_0, \quad x = r / R_0,$$

M is the total mass of the loop, N is the number of electrons, $r_0 = e^2/mc^2$ is the classical electron radius, L is the inductance of the loop, σ is the conductivity of the loop, $s = \pi b^2$ is the cross section, and R_0 and H_0 are constants which have the dimensions of length and field respectively.*

As follows from Eq. (3), the effective real loss is characterized by the quantity $\gamma \approx T/2\pi\tau(1+\alpha)$, where T is some characteristic time during which the current changes. For reasons which will be made clear below we shall be interested in the case $\gamma \ll 1$, i.e., the case in which the reactive component is much larger than the real component.

At the outset we consider the case characterized by $\gamma = 0$; we then introduce corrections for the real losses.

As can be easily shown, Eqs. (1) – (3) can be written in the form

$$d^2\xi/dt^2 = -\partial U/\partial\xi, \qquad d^2x/dt^2 = -\partial U/\partial x, \tag{4}$$

where

$$U(x, \xi, t) = \omega_H^2 (ax - \varphi_0)^2 / 2x(1 + \alpha x), \tag{5}$$

and $\varphi_0 = [ax + (1+\alpha x) i]_{t=t_0}$ is a constant which is determined from the initial conditions (for $t = t_0$ we have $x = x_0$, $\xi = \xi_0$, $i = i_0$ and so on).

If it is assumed that $\partial U/\partial t \ll dU/dt$, the system of equations in (4) yields the approximate energy integral (exact when $\partial U/\partial t = 0$)

$$\left(\frac{dx}{dt}\right)^2 + \left(\frac{d\xi}{dt}\right)^2 = \left(\frac{dx}{dt}\right)_0^2 + \left(\frac{d\xi}{dt}\right)_0^2 + 2[U_0 - U(x, \xi, t)]. \tag{6}$$

Whence it follows that if $U(x, \xi, t) < U_0 = U(x_0, \xi_0, t_0)$, then if the loop leaves such a field it acquires an energy increment $\Delta E = MR_0^2[U_0 - U]$. This effect lies at the basis of acceleration of a plasma in inhomogeneous magnetic fields.[3,4]

Without making a detailed analysis of Eq. (4), we may note certain features of the behavior of the large radius, assuming for simplicity that $(dx/dt)_0 = (d\xi/dt)_0 = 0$.

*Generally speaking, the right side of Eq. (2) should contain an additional term which describes the force due to the material pressure inside the loop. However, when $b/r \ll 1$ the introduction of this term in Eqs. (1) and (2) would only lead to a small correction and for this reason is neglected.

*Since the quantities which appear in Eqs. (1), (2), and (3) depend on b logarithmically, the dependence of the small radius of the ring on time can be neglected in the first approximation.

1) In the case in which

$$\partial U/\partial x|_{x_0,\xi_0} < 0, \quad U(x_0,\xi) > U(x,\xi) \tag{7}$$

for all $x > x_0$ and $\xi > \xi_0$, the radius of the loop increases without limit in the acceleration process.

2) If, however,

$$\partial U/\partial x|_{x_0,\xi_0} > 0, \quad U(x_0,\xi) > U(x,\xi) \tag{8}$$

for all $x < x_0$ and $\xi > \xi_0$, the radius of the loop approaches zero (this can happen only when $\varphi_0 = 0$).

3) In the remaining cases the radius of the loop can oscillate about one of the stationary radius values x_{st} determined from the conditions

$$\partial U/\partial x = 0, \quad \partial^2 U/\partial x^2 > 0, \tag{9}$$

where the oscillation amplitude generally increases monotonically during the acceleration process. We note, however, that for a strong dependence of x_{st} on ξ [and also when $(dx/dt)_0 \neq 0$, $(d\xi/dt)_0 \neq 0$] it may turn out that the loop moves from a stability region into a region of instability during the acceleration process [as determined by Eq. (7) or (8)]; conversely, if there are also values of ξ for which the second of the conditions of (7) or (8) is violated, a loop which is in a region of instability may be "captured" in a stability region. In conclusion we may note that if ax and φ_0 are of the same sign, acceleration will be effective only when $x_0 > x_m$, where x_m is the first root of Eq. (9) for which $(\partial^2 U/\partial x^2)\, x_m < 0$.

2. MAGNETIC MIRRORS*

We consider the problem of reflection of a loop from an inhomogeneous magnetic field which remains constant in time.

First of all we may note that when $\gamma \gg 1$ it is impossible to achieve effective reflection. Actually, since the current in this case is approximately $d(ax)/dt$, when the ring comes to rest the restoring forces vanish; the kinetic energy of the ring is converted entirely into heat. Thus, the efficiency of reflection increases as γ is reduced. At the outset we consider the case in which $\gamma = 0$. It follows immediately from simple physical considerations that in order for reflection to take place it is necessary that the energy of the reciprocatory motion of the loop be converted into magnetic energy and not into energy associated with radial motion. Furthermore, in most cases it is desirable that the loop receive no radial velocity as a result of the reflection. Obviously, these requirements will be satisfied if the initial radius of the loop x_0 is made equal to $x_{st}(\xi_0)$ under the condition that x_{st} depends weakly on ξ. Carrying out the operations indicated in Eq. (9) we have

$$h_z \equiv \frac{1}{x}\frac{\partial ax}{\partial x} = \left(\bar{h} - \frac{2\varphi_0}{x^2}\right)\frac{\beta}{2}, \quad \beta = \frac{l + 2(1+\alpha x l)}{2l(1+\alpha x)}, \tag{10}$$

where $\bar{h} = 2a/x$ is the mean field at the radius x. For the case $\alpha = 0$ this condition has already been obtained by Osovets.[1]

We consider the case in which the fields are such that the stationary radius does not depend on ξ. This will be the case, obviously, if the vector potential is of the form $a(x, \xi) = R(x)\, z(\xi)$ and φ_0 is set equal to zero.

Assuming at the outset that the orbit is stable, assuming that departures from the orbit $\rho = x - 1$, are small,* and limiting ourselves to the first nonvanishing terms, we have

$$d^2\xi/dt^2 + \frac{\partial}{\partial\xi} U(1,\xi) = 0, \tag{11}$$

$$d^2\rho/dt^2 + 2\beta\mu U(1,\xi)\,\rho = 0, \tag{12}$$

where

$$\mu = [2 - \beta + \partial \ln h_z/\partial \ln x - \partial \ln \beta/\partial \ln x]|_{x=1}. \tag{13}$$

If we now require that $z^2(\xi)$ be an even function of ξ, we obtain "oscillatory" (generally speaking, nonlinear) motion for the ξ-motion; consequently the ρ-motion is described by the Hill equation which, with an appropriate choice of parameters, allows of stable solutions.

Thus we see that a loop which receives an initial velocity $(d\xi/dt)_0$ and is elastically scattered from regions occupied by the field will execute oscillations about the plane $\xi = 0$ with a period

$$T = 2\sqrt{2}\int_0^{\xi_1} [U(1,\xi_1) - U(1,\xi)]^{-1/2} d\xi, \tag{14}$$

where ξ_1 is the maximum excursion from the plane $\xi = 0$, determined from the relation

$$U(1,\xi_1) = U(1,\xi_0) + {}^1/_2 (d\xi/dt)_0^2. \tag{15}$$

If we denote the boundary of the magnetic mirror by ξ_b, the maximum energy of the loop E_m for which reflection takes place is

$$E_m = MR_0^2 U(1,\xi_b). \tag{16}$$

If one now takes account of the real losses, certain correction terms appear in Eqs. (11) and (12) (these terms are of order γ); these terms cause a weak damping of the amplitude of the ξ-motion and an increase in the radial oscillations.

*This problem has been considered in connection with a proposal by Veksler for using inhomogeneous magnetic fields for coherent cyclic acceleration.[5]

*The constant R_0 is chosen to make $x_{st} = 1$.

As an example we consider the motion of a loop in a field described by

$$a(x,\xi)=\begin{cases}\xi x/2 & \text{for } x\leqslant x_1,\\ {}^1/_2 a_1\xi\,[x+(\Delta a/a_1)\,x_1^2/x] & \text{for } x\geqslant x_1,\end{cases} \tag{17}$$

where $\Delta a = 1 - a_1$. In this case

$$T = 2\pi(1+\alpha)^{1/2}\beta/a_1\omega_H, \tag{18}$$

$$E_m = a_1^2\omega_H^2 M R_0^2\xi_b^2/2\beta^2(1+\alpha), \tag{19}$$

where the equilibrium radius R_0 is found from the relations

$$R_0^2 = r_1^2\,\frac{\Delta a}{a_1}\,\frac{\beta}{2-\beta}\Big|_{x=1}, \qquad r_1 = R_0 x_1.$$

We now introduce the effect of the real losses, assuming that $\gamma \ll 1$. Taking account of Eq. (17), we substitute the expression for the current i from Eq. (3) in Eqs. (1) and (2) and expand the right sides of the equations in a series in ρ. Assuming now that when $t = 0$, $\xi = 0$, $i = 0$, and $d\xi/dt = \xi_0$, and limiting ourselves to the first non-vanishing terms in the expansion in ρ and first-order terms in γ, we obtain

$$\frac{d^2\xi}{dt^2}+\Omega^2\xi=\frac{\Omega^2}{\tau'}\,e^{-t/\tau'}\int_0^t e^{t'/\tau'}\xi(t')\,dt', \tag{20}$$

$$\frac{d^2\rho}{dt^2}+\mu\beta\Omega^2\xi^2(t)\,\rho=-\frac{\Omega^2}{\tau'}\,\beta\xi(t)\,e^{-t/\tau'}\int_0^t e^{t'/\tau'}\xi(t')\,dt', \tag{21}$$

where

$$\Omega^2=\omega_H^2 a_1^2/\beta^2(1+\alpha), \qquad \tau'=\tau(1+\alpha).$$

Whence, to first-order in $\gamma = 1/\Omega\tau'$,

$$\xi(t)=\frac{\dot\xi_0}{\Omega}\,[e^{-t/2\tau'}\sin\Omega t+\gamma(1-e^{-t/2\tau'}\cos\Omega t)]. \tag{22}$$

Now, substituting Eq. (22) in Eq. (21) we have, to the same accuracy,

$$d^2\rho/dt^2+\mu\beta\dot\xi_0^2 e^{-t/\tau'}\sin^2\Omega t\cdot\rho = -\gamma\beta\dot\xi_0^2\,[1-e^{-t/2\tau'}\cos\Omega t]\,e^{-t/2\tau'}\sin\Omega t. \tag{23}$$

With an appropriate choice of parameters this equation can have oscillatory solutions, the amplitudes of which increase slowly in time. Thus, if the loop does not receive additional energy the amplitude of its oscillations along the z axis decay approximately as $\exp(-t/2\tau')$, whereas the radial oscillations grow. If, however, the loop receives energy in such a way that its oscillation amplitude along the z axis remains constant the equation for the ρ-motion assumes the form

$$d^2\rho/dt^2+\mu\beta\dot\xi_0^2\sin^2\Omega t\cdot\rho = \gamma\dot\xi_0^2\beta\,[\cos\Omega t-e^{-t/\tau'}]\sin\Omega t, \tag{24}$$

i.e., the amplitude of the radial oscillations remains bounded. In the case in which the energy of the loop increases the radial oscillations first decay,* and then, when $E \gtrsim MR_0^2\Omega^2/2\beta\mu$, increase sharply, i.e., the loop becomes unstable. In the present case this is what actually determines the maximum energy and thus there is no reason for making $\xi_b > (\beta\mu)^{-1/2}$.

3. STABILITY OF A LOOP IN A HIGH-FREQUENCY FIELD

We consider the case in which the field is a harmonic function of time, i.e.,

$$a(x,\xi,t)=\tilde a(x,\xi)\sin\omega t.$$

We shall be interested in a stationary loop which executes small oscillations about the plane $z = 0$ and some equilibrium orbit R_0. Assuming that the field is "barrel-shaped" i.e., $a(-\xi) = a(\xi)$, it is easy to see that the stationary radius, determined from Eq. (10), will be independent of ξ (to first-order terms in ξ). Assuming that $i = 0$ when $t = 0$, we find that in the absence of real losses ($\gamma = 0$) x_{st} is independent of the time. When the real resistance is taken into account the equilibrium radius no longer remains constant but becomes a function of time. It can be shown that for sufficiently large values of γ the presence of real losses leads either to breakup of the beam in the inward direction in the first quarter cycle (cf. reference 6) or to breakup in the outward direction in the first few cycles.

To achieve stable operation it is necessary to make the relative magnitude of the real resistance small.

As before, assuming a stable radius, we expand the right sides of Eqs. (2) and (3) in a series about $x = x_{st} = 1$, $\xi = 0$. Then, limiting ourselves to first-order terms in $\rho = x - 1$, ξ, and γ we have

$$d^2\xi/d\theta^2+n\rho\,(1-\cos 2\theta)=0, \tag{25}$$

$$d^2\rho/d\theta^2+\mu\rho\,(1-\cos 2\theta)=2\gamma' p\,[\cos\theta-e^{-\gamma\theta}]\sin\theta, \tag{26}$$

where

$$\theta=\omega t, \qquad \gamma'=[\omega\tau(1+\alpha)]^{-1}, \qquad n=-\frac{\partial\ln h_z}{\partial\ln x}\Big|_{x=1},$$

$$p=\frac{\pi R_0 H^2(R_0)}{M\omega^2\beta(1+\alpha)}.$$

It follows from Eqs. (25) and (26) that taking account of the real resistance has no effect on the ξ-motion in the first approximation. In the equation for ρ, however, the real losses lead to the

*We bear in mind the fact that the parameters are chosen for operation in the first stability region, i.e. $\dot\xi_0^2\mu\beta < \Omega^2$.

appearance of a small external force (of order γ), which does not represent any danger as far as stability is concerned. Although Eqs. (25) and (26) allow a whole series of stability regions, because of their relative narrowness, only the first region is of practical interest. For this region the parameters n, μ, and p must be chosen in such a way that the quantities np and μp lie in the interval $(0, \sim 0.5)$. Assuming that $n \sim \mu \sim \frac{1}{2}$, we find that the loop will be stable if its parameters, and the amplitude and frequency of the magnetic field are chosen in such a way as to satisfy the condition $p < 1$. From the expression for p it follows that for a given total number of particles in the loop and a given magnetic field this condition can be satisfied by making the field frequency sufficiently high.

[1] S. M. Osovets, Физика плазмы и пробдема управляемых термоядерных реакций (Plasma Physics and the Problem of a Controlled Thermonuclear Reaction), Vol II, p 283, U.S.S.R. Acad. Sci. Press, 1958.

[2] V. D. Shafranov, J. Exptl. Theoret. Phys. (U.S.S.R.) **33**, 710 (1957); Soviet Phys. JETP **6**, 545 (1958).

[3] I. S. Shpigel', J. Exptl. Theoret. Phys. (U.S.S.R.) **36**, 411 (1959), Soviet Phys. JETP **9**, 285 (1959).

[4] A. I. Morozov, J. Exptl. Theoret. Phys. (U.S.S.R.) **32**, 305 (1957), Soviet Phys. JETP **5**, 215 (1957).

[5] V. I. Veksler, Proceedings of CERN Symposium on High Energy Accelerators and Pion Physics, Vol. 1, Geneva, 1956.

[6] S. M. Osovets and N. I. Shchedrin, Физика плазмы и проблема управляемых термоядерных реакций (Plasma Physics and the Problem of a Controlled Thermonuclear Reaction), Vol III, p 196, U.S.S.R. Acad. Sci. Press, 1958.

Translated by H. Lashinsky
368

THREE-PHOTON ANNIHILATION OF POSITRONIUM IN THE P STATE

A. I. ALEKSEEV

Moscow Engineering Physics Institute

Submitted to JETP editor December 27, 1958

J. Exptl. Theoret. Phys. (U.S.S.R.) **36**, 1839-1844 (June, 1959)

A relativistically invariant expression for the probability amplitude for three-photon annihilation of positronium is obtained by the summation of an infinite number of diagrams of a definite class. The probability of three-photon annihilation of positronium in the P state is calculated in the nonrelativistic limit, and the selection rules for this process are found.

DEPENDING on the charge parity of a state of positronium, it can decay into two or three photons (a larger number of photons is less probable). Two-photon annihilation of positronium in the S state has been dealt with in a calculation by Pomeranchuk,[1] and three-photon annihilation of positronium in the S state has been considered in a paper by Ore and Powell.[2] The methods given in these papers, however, cannot be applied to the calculation of the probability of annihilation of positronium in excited states. It has been suggested by the writer[3] that the amplitude for annihilation of positronium be found by summation of an infinite number of Feynman diagrams; this makes it possible to calculate the probability for annihilation of positronium in any excited state. In the paper referred to the probability for two-photon annihilation of positronium in the P state was calculated. In the present communication the technique of summation of diagrams is applied to the problem of the three-photon annihilation of positronium.

1. THE PROBABILITY AMPLITUDE FOR THREE-PHOTON ANNIHILATION OF POSITRONIUM

The diagram that describes three-photon annihilation of free particles is shown in Fig. 1.* To get the probability amplitude for three-photon annihilation of bound particles, we adjoin to the irreducible diagram (Fig. 1) all the reducible diagrams of the "ladder type" (Fig. 2), which describe the interaction of the particles before the annihilation. We get as the result the amplitude for three-photon annihilation of an interacting electron and positron (which can also be in a bound state) in the following form (cf. reference 3):

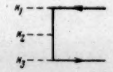

FIG. 1

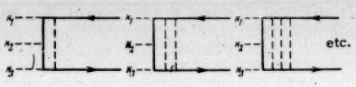

FIG. 2

$$A = -ie^3 \int \Phi_{\nu_1\nu_2\nu_3}(x_2x x_1)\,(C\gamma_{\nu_1}K(x_2-x)\gamma_{\nu_2}K(x-x_1)\gamma_{\nu_3})_{\rho_1\rho_2} \times \Psi_{\rho_1\rho_2}(x_1x_2)\,d^4x d^4x_1 d^4x_2. \quad (1)$$

Here $\Psi(x_1x_2)$ is the wave function of the interacting electron and positron, which satisfies the Bethe-Salpeter equation,[4] and

$$\Phi_{\nu_1\nu_2\nu_3}(x_2xx_1) = 2\pi\sqrt{2\pi/\omega_1\omega_2\omega_3} \times [l_{1\nu_1}l_{2\nu_2}l_{3\nu_3}\exp i(k_1x_2 + k_2x + k_3x_1) + \ldots] \quad (2)$$

is the symmetrized function of the photons with frequencies ω_1, ω_2, ω_3, momenta $\mathbf{k}_1$, $\mathbf{k}_2$, $\mathbf{k}_3$ and polarizations $\mathbf{l}_1$, $\mathbf{l}_2$, $\mathbf{l}_3$. In the expression (2), and also in the subsequent calculations, the series of dots corresponds to the similar terms with all possible permutations of the photons. Furthermore $C = \alpha_2$, $\gamma_0 = \beta$, $\gamma_{1,2,3} = \beta\alpha_{1,2,3}$, and $K(x)$ is the electron Green's function.[5] Throughout we have set $\hbar = c = 1$, and have adopted the following rule of summation over vector indices:

$$ab = a_\nu b_\nu = a_0b_0 - a_1b_1 - a_2b_2 - a_3b_3.$$

The expression (1) gives the first nonvanishing contribution for the process in question. If we take into account radiative corrections, then every matrix γ in Eq. (1) is replaced by a vertex operator Γ, and every Green's function K is replaced by

*In Figs. 1 and 2 the similar diagrams that differ from each other and that shown by permutations of the three photons k_1, k_2, k_3 are omitted.

G, where Γ and G include the radiative corrections.[6] In dealing with the radiative corrections to the amplitude (1) we must add in on an equal basis with diagrams like Fig. 2 diagrams that describe the interaction of the electron and positron associated with their virtual annihilation.[3] Then the wave function $\Psi(x_1, x_2)$ involved in Eq. (1) will be the solution of a Bethe-Salpeter type equation in which along with the ordinary interaction there is also the specific exchange interaction associated with the virtual annihilation of the electron and positron.[7,6]

2. THE NONRELATIVISTIC APPROXIMATION FOR THE AMPLITUDE

In relative-momentum variables p the amplitude (1) can be rewritten in the form

$$A=\frac{ie^3(2\pi)^{3/2}}{\sqrt{\omega_1\omega_2\omega_3}}\int\left(C\hat{1}_3\frac{[\hat{p}+{}^1/_3(\hat{k}_3-\hat{k}_2-\hat{k}_1)+m]\hat{1}_2[\hat{p}+{}^1/_3(\hat{k}_3+\hat{k}_2-\hat{k}_1)+m]\hat{1}_1}{[(p+{}^1/_2(k_3-k_2-k_1))^2-m^2][(p+{}^1/_3(k_3+k_2-k_1))^2-m^2]}+\dots\right)_{\rho_2\rho_1}\psi_{\rho_2\rho_1}(p)\,d^4p\,\delta(K-k_1-k_2-k_3),\qquad(3)$$

where $\psi(p)$ is the positronium wave function in the relative-momentum space, K is the total momentum of the positronium atom, m is the mass of the electron, and for any vector a we write $\hat{a}=a_\mu\gamma_\nu$.

In the calculation of the amplitude (3) we make use of the smallness of the velocity v of the relative motion of the particles in the positronium atom (v is of the order e^2) and shall hereafter neglect all terms of order v^2 and higher. For convenience we go over in Eq. (3) from the matrices γ to the two-rowed (2×2) Pauli matrices σ, and regard as nonvanishing only those of the small components of the wave function $\psi(p)$ that are of the order of magnitude v. Then in the coordinate system of the center of mass of the positronium atom ($K_0=2m-E$, $\mathbf{K}=0$) we get

$$\begin{aligned}A=\frac{ie^3(2\pi)^{3/2}}{\sqrt{\omega_1\omega_2\omega_3}}\{\sum\Big[\Big(p_0+\omega_3+\frac{1}{2}E-m\Big)^2-(\mathbf{p}+\mathbf{k}_3)^2-m^2\Big]^{-1}\\ \times\Big[\Big(p_0-\omega_1-\frac{1}{2}E+m\Big)^2-(\mathbf{p}-\mathbf{k}_1)^2-m^2\Big]^{-1}\\ \times\{\mathrm{Sp}\,\sigma_2[(p_0^2+p_0(\omega_3-\omega_1)-\omega_3\omega_1)\,\hat{1}_3\hat{1}_2\hat{1}_1\\ +\hat{1}_3(\hat{\mathbf{p}}+\hat{\mathbf{k}}_3)\hat{1}_2(\hat{\mathbf{p}}-\hat{\mathbf{k}}_1)\hat{1}_1]\psi^{\mathrm{L}}(p)+m\,\mathrm{Sp}\,\sigma_2[\hat{1}_3(\hat{\mathbf{p}}+\hat{\mathbf{k}}_3)\hat{1}_2\hat{1}_1\\ +\hat{1}_3\hat{1}_2(\hat{\mathbf{p}}-\hat{\mathbf{k}}_1)\hat{1}_1](\psi^{\mathrm{M}_1}(p)+\psi^{\mathrm{M}_2}(p))\\ +\mathrm{Sp}\,\sigma_2[(p_0-\omega_1+m)\,\hat{1}_3(\hat{\mathbf{p}}+\hat{\mathbf{k}}_3)\hat{1}_2\hat{1}_1\\ +(p_0+\omega_3-m)\,\hat{1}_3\hat{1}_2(\hat{\mathbf{p}}-\hat{\mathbf{k}}_1)\hat{1}_1]\\ \times(\psi^{\mathrm{M}_1}(p)-\psi^{\mathrm{M}_2}(p))\}\,d^4p+\dots\Big\}\,\delta(K-k_1-k_2-k_3).\qquad(4)\end{aligned}$$

Here $\psi^{\mathrm{L}}(p)$ is the large two-rowed component of the wave function $\psi(p)$, and $\psi^{\mathrm{M}_1}(p)$ and $\psi^{\mathrm{M}_2}(p)$ are the small (order of magnitude v) two-rowed components of the wave function $\psi(p)$, which in the mixed representation for $t>0$ has the following form:[8]

$$\psi(\mathbf{p},t)=\begin{pmatrix}\psi^{\mathrm{L}}(\mathbf{p},t) & \psi^{\mathrm{M}_1}(\mathbf{p},t)\\ \psi^{\mathrm{M}_1}(\mathbf{p},t) & 0\end{pmatrix}=\begin{pmatrix}\varphi(\mathbf{p}) & -\varphi(\mathbf{p})\,\hat{\mathbf{p}}^T/2m\\ \hat{\mathbf{p}}\varphi(\mathbf{p})/2m & 0\end{pmatrix}\exp\Big[-i\Big(\frac{E}{2}+\frac{\mathbf{p}^2}{2m}\Big)t\Big],\qquad(5)$$

where the index T means transposition. For $t<0$ the sign of the exponent in Eq. (5) is reversed. E is the binding energy of the particles in the positronium atom, and for any three-dimensional vector $\mathbf{q}$ we have used throughout the notation $\hat{\mathbf{q}}=(\mathbf{q}\cdot\boldsymbol{\sigma})=q_m\sigma_m$. The nonrelativistic two-rowed function $\varphi(\mathbf{p})$ in Eq. (5) satisfies the Schrödinger equation written for the electron and positron, and also is an eigenfunction of the operators for the total angular momentum of the system and for an angular-momentum component.

It is easy to see that in the case of the P state of positronium the functions $\psi^{\mathrm{L}}(p)$, $\psi^{\mathrm{M}_1}(p)$, and $\psi^{\mathrm{M}_2}(p)$ make contributions of the same order of magnitude to the amplitude (4), whereas in the case of the S state the functions $\psi^{\mathrm{M}_1}(p)$ and $\psi^{\mathrm{M}_2}(p)$ can be neglected. If in calculating the annihilation of positronium in the S and P states we confine ourselves to the first nonvanishing contributions, then in integrating over the variable p_0 we can set $p_0=0$ in all the coefficients of $\psi^{\mathrm{L}}(p)$, $\psi^{\mathrm{M}_1}(p)$, and $\psi^{\mathrm{M}_2}(p)$ in the integral (4) (cf., e.g., reference 8). Then the remaining integral over the relative momentum $\mathbf{p}$ will contain the nonrelativistic two-rowed positronium wave function $\varphi(\mathbf{p})$. Since $\varphi(\mathbf{p})$ has appreciable nonvanishing values in the region of small momenta, $|\mathbf{p}/m|=v\ll1$, the terms in Eq. (4) that contain $\mathbf{p}^2\psi^{\mathrm{L}}$, $\hat{\mathbf{p}}\psi^{\mathrm{M}_1}$, and $\hat{\mathbf{p}}\psi^{\mathrm{M}_2}$ are beyond the limits chosen for the accuracy of the calculation. Thus we get for the amplitude (4)

$$\begin{aligned}A\quad&\frac{ie^3(2\pi)^{3/2}}{\sqrt{\omega_1\omega_2\omega_3}}\frac{1}{2m}\Big\{\sum|2m\omega_3-2(\mathbf{pk}_3)+\mathbf{p}^2-mE|^{-1}\\ &|2m\omega_1-2(\mathbf{pk}_1)+\mathbf{p}^2-mE|^{-1}|2m\,\mathrm{Sp}\,\sigma_2(\omega_3\omega_1\hat{1}_3\hat{1}_2\hat{1}_1\\ &\hat{1}_3\hat{\mathbf{k}}_3\hat{1}_2\hat{\mathbf{k}}_1\hat{1}_1)\varphi(\mathbf{p})+2m\,\mathrm{Sp}\,\sigma_2(\hat{1}_3\hat{\mathbf{p}}\hat{1}_2\hat{\mathbf{k}}_1\hat{1}_1-\hat{1}_3\hat{\mathbf{k}}_2\hat{1}_2\hat{\mathbf{p}}\hat{1}_1)\varphi(\mathbf{p})\\ &+m\,\mathrm{Sp}\,\sigma_2(\hat{1}_3\hat{1}_2\hat{\mathbf{k}}_1\hat{1}_1-\hat{1}_3\hat{\mathbf{k}}_3\hat{1}_2\hat{1}_1)(\hat{\mathbf{p}}\varphi(\mathbf{p})\quad\varphi(\mathbf{p})\hat{\mathbf{p}}^T)\\ &\mathrm{Sp}\,\sigma_2(\hat{1}_3\hat{\mathbf{k}}_3\hat{1}_2\hat{1}_1(\omega_1-m)\quad(\omega_3-m)\hat{1}_3\hat{1}_2\hat{\mathbf{k}}_1\hat{1}_1)(\hat{\mathbf{p}}\varphi(\mathbf{p})\\ &+\varphi(\mathbf{p})\hat{\mathbf{p}}^T)|d^3p\quad\dots\Big\}\delta(K\quad k_1\quad k_2-k_3).\qquad(6)\end{aligned}$$

In the integral (6) we have kept the small quan-

tity E in the denominator to avoid later divergences in the integration over the photon energies. The further calculations are considerably simplified if we take the photons to be circularly polarized. Then for the polarization vector $\boldsymbol{l}$ of each photon $\mathbf{k} = n\hat{\omega}$ we have

$$\mathbf{l} = (\boldsymbol{\tau} + i\lambda[\mathbf{n}\times\boldsymbol{\tau}])\sqrt{2}, \quad \lambda = \pm 1,$$

$$\boldsymbol{\tau}\times[\mathbf{n}\times\boldsymbol{\tau}] = \mathbf{n}, \quad \hat{\mathbf{n}}\hat{\mathbf{l}} = \lambda\hat{\mathbf{l}}. \tag{7}$$

Setting $\varphi(\mathbf{x}) = \Phi_{s_z}\psi_{\text{nonrel}}(\mathbf{x})$, where Φ_{s_z} is the spin function and $\psi_{\text{nonrel}}(\mathbf{x})$ is the coordinate-space nonrelativistic wave function of the positronium atom, we get for the amplitude for annihilation of positronium, for example in the S state:

$$A = -\frac{ie^3(2\pi)^{1/2}}{2m^2\sqrt{V\omega_1\omega_2\omega_3}}\{(1-\lambda_3\lambda_1)[(\mathbf{l}_3\mathbf{l}_2)\,l_{1m} + (\mathbf{l}_2\mathbf{l}_1)\,l_{3m} - (\mathbf{l}_3\mathbf{l}_1)\,l_{2m}] + \text{c.p.}\}$$
$$\times (\mathrm{Sp}\,\sigma_2\sigma_m\Phi_{s_z})\,\psi_{\text{nonrel}}(0)\,\delta(K-k_1-k_2-k_3), \tag{8}$$

where the notation c.p. in the curly brackets means the similar terms obtained by cyclic permutations of the indices 1, 2, 3. The expression (8) leads to the well known value for the probability W of three-photon annihilation of orthopositronium in the S state:[2]

$$W = \frac{2(\pi^2-9)}{9\pi n^3}(e^2)^6 m = \frac{0.72}{n^3}\cdot 10^7\ \text{sec}^{-1}, \tag{9}$$

where n is the principal quantum number fixing the energy state of the positronium atom. For parapositronium in the S state the probability of three-photon annihilation is zero according to Eq. (8), in agreement with the law of conservation of charge parity. In the writing of formulas (9) and (13) for the probability of three-photon annihilation of positronium an additional factor of $1/6$ is introduced to allow for the identity of states of the system that differ only by permutation of the momenta of the photons.

3. ANNIHILATION IN THE P STATE

In the case of the P state the wave function of the positronium atom is odd, $\varphi(-\mathbf{p}) = -\varphi(\mathbf{p})$, and by Eqs. (6) and (7) the amplitude for three-photon annihilation takes the form

$$A = -\frac{ie^3(2\pi)^{1/2}}{V\sqrt{\omega_1\omega_2\omega_3}}\frac{1}{2m}\left\{\int\frac{(1-\lambda_3\lambda_1)\,[(\mathbf{n}_1-\mathbf{n}_2)\,\mathbf{p}]\,\mathrm{Sp}\,\sigma_2\hat{\mathbf{l}}_3\hat{\mathbf{l}}_2\hat{\mathbf{l}}_1\varphi(\mathbf{p})}{2m^2}d^3p + \int(2m\omega_3 + mE + \mathbf{p}^2)^{-1}(2m\omega_1\right.$$
$$+ mE + \mathbf{p}^2)^{-1}[2m\,\mathrm{Sp}\,\sigma_2\,(\omega_1\lambda_1\hat{\mathbf{l}}_3\hat{\mathbf{p}}\hat{\mathbf{l}}_2\hat{\mathbf{l}}_1 + \omega_3\lambda_3\hat{\mathbf{l}}_3\hat{\mathbf{l}}_2\hat{\mathbf{p}}\hat{\mathbf{l}}_1)\varphi(\mathbf{p}) + m(\omega_1\lambda_1 + \omega_3\lambda_3)\,\mathrm{Sp}\,\sigma_2\hat{\mathbf{l}}_3\hat{\mathbf{l}}_2\hat{\mathbf{l}}_1(\hat{\mathbf{p}}\varphi(\mathbf{p}) - \varphi(\mathbf{p})\,\hat{\mathbf{p}}^T)$$
$$\left. + (\omega_1\omega_3(\lambda_1-\lambda_3) - m(\omega_1\lambda_1 - \omega_3\lambda_3))\,\mathrm{Sp}\,\sigma_2\hat{\mathbf{l}}_3\hat{\mathbf{l}}_2\hat{\mathbf{l}}_1(\hat{\mathbf{p}}\varphi(\mathbf{p}) + \varphi(\mathbf{p})\,\hat{\mathbf{p}}^T)]\,d^3p + \ldots\right\}\delta(K-k_1-k_2-k_3). \tag{10}$$

The terms in the amplitude (10) can be divided into three groups, each of which involves two photons symmetrically and differs from the other two groups by cyclic permutation of the three photons (cf. Figs. 1 and 2). If we examine all the terms of one such group it is easily seen that the function $\varphi(\mathbf{p})$ occurring in the amplitude (10) must be antisymmetric in the spin indices. Consequently, the functions $\hat{\mathbf{p}}\varphi(\mathbf{p})$ and $-\varphi(\mathbf{p})\hat{\mathbf{p}}^T$ (the small components of the wave function (5)) make the same contribution to the amplitude (10); for example,

$$\mathrm{Sp}\,\sigma_2(\hat{\mathbf{l}}_3\hat{\mathbf{l}}_2\hat{\mathbf{l}}_1 + \hat{\mathbf{l}}_1\hat{\mathbf{l}}_2\hat{\mathbf{l}}_3)(-\varphi\hat{\mathbf{p}}^T) = \mathrm{Sp}\,\sigma_2(\hat{\mathbf{l}}_3\hat{\mathbf{l}}_2\hat{\mathbf{l}}_1 + \hat{\mathbf{l}}_1\hat{\mathbf{l}}_2\hat{\mathbf{l}}_3)\hat{\mathbf{p}}\varphi. \tag{11}$$

This means that in calculating the value of the expression (10) we can replace the expression $\hat{\mathbf{p}}\varphi(\mathbf{p}) - \varphi(\mathbf{p})\mathbf{p}^T$ by the factor $2\hat{\mathbf{p}}\varphi(\mathbf{p})$ or the factor $-2\varphi(\mathbf{p})\hat{\mathbf{p}}^T$, and the expression $\hat{\mathbf{p}}\varphi(\mathbf{p}) + \varphi(\mathbf{p})\hat{\mathbf{p}}^T$ is to be set equal to zero. We get

$$A = -\frac{ie^3(2\pi)^{3/2}}{V\sqrt{\omega_1\omega_2\omega_3}}\frac{\mathrm{Sp}\,\sigma_2\Phi}{m}\int\left\{\frac{(\lambda_1+\lambda_2)\,[1-(\mathbf{n}_1\mathbf{n}_2)]\,(\mathbf{l}_3\mathbf{p})}{2m\omega_3 + mE + \mathbf{p}^2} + \text{c.p.}\right\}$$
$$\times\psi_{\text{nonrel}}(\mathbf{p})\,d^3p\,\delta(K-k_1-k_2-k_3). \tag{12}$$

Here $\varphi(\mathbf{p}) = \Phi\psi_{\text{nonrel}}(\mathbf{p})$, where Φ is the spin function and $\psi_{\text{nonrel}}(\mathbf{p})$ is the nonrelativistic coordinate wave function for positronium in the P state. In Eq. (12) terms not containing ω in the denominator have been dropped, since they make only a small contribution (see below). In Eq. (12) account has also been taken of the fact that if the energy of one of the photons goes to zero, $\omega \to 0$, then for each of the other two photons $\omega \to m$.

The spin function Φ appearing in Eqs. (12) and (10) is antisymmetric. Therefore the amplitude for three-photon annihilation of positronium in the P state is different from zero only for states with total spin $s = 0$ (parapositronium). On the other hand, for total spin $s = 1$ (orthopositronium) the probability of three-photon annihilation in the P state is zero. This selection rule is an expression of the law of conservation of charge parity.

According to Eq. (12) the probability W of three-photon annihilation of parapositronium in the P state can be written in the form

$$W = \frac{e^6}{3m^2(2\pi)^5}\int \sum_{\lambda_1\lambda_2\lambda_3}\sum_{M}\left|\int \frac{(\lambda_1+\lambda_2)\,[1-(\mathbf{n}_1\mathbf{n}_2)]\,(\mathbf{l}_0\mathbf{p})}{2m\omega_3+mE+\mathbf{p}^2}\,\psi_{n_0 0 1 M}(\mathbf{p})\,d^3p\right|^2$$

$$\times\,\delta(K-k_1-k_2-k_3)\,\frac{d^3k_1d^3k_2d^3k_3}{\omega_1\omega_2\omega_3} = \frac{me^{16}\,(n^2-1)}{72\pi^9n^5}$$

$$\times\int \frac{m^2\,[1-(\mathbf{n}_1\mathbf{n}_2)]^2\omega_1\omega_2\,\delta\,(2m-E-\omega_1-\omega_2-\omega_3)}{(\sqrt{2m\omega_3+mE}+\sqrt{mE})^4\omega_3}\,d\Omega_1d\Omega_2d\omega_1d\omega_2, \tag{13}$$

where the summation over the index M comes from the averaging over the three states of parapositronium with the orbital angular momentum $l = 1$. In the expression (13) we have kept only terms in which the large factor $\ln(2m/E) \gg 1$ appears on integration over the energies of the photons. For the terms dropped in Eq. (13) the integral over the photon energies is not of an order larger than unity.

In Eq. (13) it is convenient to integrate first over the angles, using the fact that

$$d\Omega_1d\Omega_2 = -8\pi^2d(\cos(\mathbf{n}_1\mathbf{n}_2)). \tag{14}$$

The integration over the angles removes the δ function, and the expression (13) takes the form

$$W = \frac{4m^{-16}\,(n^2-1)}{9\pi n^5}\int_0^{m-E/2}d\omega_1$$

$$\times\int_{m-\omega_1-E/2}^{m-E/2}d\omega_2\,\frac{n^4\,(\omega_1+\omega_2-m+E/2)^2}{\omega_1^2\omega_2^2\,(\sqrt{2m\,(2m-\omega_1-\omega_2-E)}+mE}+\sqrt{mE})^4} \tag{15}$$

The region of variation of the independent variables of integration ω_1 and ω_2 in Eq. (15) is limited by the laws of conservation of energy and momentum. Since two quanta can simultaneously have the energy $m - E/2$, the upper limit of the integration over ω_1 and ω_2 is $m - E/2$. If $\omega_1 < m - E/2$, the smallest value for ω_2 is given by the condition $\omega_3 = m - E/2$, i.e., it is $\omega_2 = m - \omega_1 - E/2$. The integral over ω_1 and ω_2 in Eq. (15) is equal to $\ln(2m/E) \gg 1$, if we drop a term of value about unity.

Thus the probability W of three-photon annihilation of parapositronium in the P state is

$$W = \frac{n^2-1}{9\pi n^5}\left[\ln\left(\frac{8n^2}{e^4}\right)\right](e^2)^6m. \tag{16}$$

In particular, if the principal quantum number n for parapositronium in the P state takes its smallest value n = 2, we have

$$W = \frac{1}{3\cdot 2^5}\left[\ln\left(\frac{2^5}{e^4}\right)\right](e^2)^6m = 0.3\cdot 10^9\ \text{sec}^{-1}$$

It follows from Eqs. (12) and (15) that in three-photon annihilation of parapositronium in the P state there is a preference for the production of two large quanta with combined energy almost equal to m, while the energy of the third quantum is of the order of E.

For parapositronium in the P state the most favored process is optical transition to the S state with probability of the order of 10^8 sec^{-1}, and subsequent two-photon annihilation.

The writer is grateful to V. A. Mashinin for checking some of the calculations involved in the present work.

[1] I. Ya. Pomeranchuk, Dokl. Akad. Nauk SSSR **60**, 213 (1948).

[2] A. Ore and J. L. Powell, Phys. Rev. **75**, 1696 (1949).

[3] A. I. Alekseev, J. Exptl. Theoret. Phys. (U.S.S.R.) **34**, 1195 (1958), Soviet Phys. JETP **7**, 826 (1958).

[4] E. E. Salpeter and H. A. Bethe, Phys. Rev. **84**, 1232 (1951).

[5] R. P. Feynman, Phys. Rev. **76**, 749 (1949).

[6] A. I. Alekseev, J. Exptl. Theoret. Phys. (U.S.S.R.) **32**, 852 (1957), Soviet Phys. JETP **5**, 696 (1957).

[7] R. Karplus and A. Klein, Phys. Rev. **87**, 848 (1952).

[8] A. I. Alekseev, J. Exptl. Theoret. Phys. (U.S.S.R.) **36**, 1435 (1959), Soviet Phys. JETP **9**, 1020 (1959).

Translated by W. H. Furry
369

THEORY OF RELATIVISTIC MAGNETOHYDRODYNAMIC WAVES

I. A. AKHIEZER and R. V. POLOVIN

Physico-Technical Institute, Academy of Sciences, Ukrainian S.S.R.

Submitted to JETP editor December 27, 1958

J. Exptl. Theoret. Phys. (U.S.S.R.) **36**, 1845-1852 (June, 1959)

One-dimensional simple waves in relativistic magnetohydrodynamics and relativistic hydrodynamic discontinuities (contact, tangential, Alfvén, and fast and slow shock waves) are considered. The Zemplen theorem is proved for shock waves of arbitrary intensity.

THE general formulation of the problem of discontinuous solutions in relativistic magnetohydrodynamics has been given by de Hoffman and Teller,[1] who obtained an equation for the nonrelativistic shock adiabat and showed that the shock wave is always plane. These authors proved a theorem which is the inverse of the Zemplen theorem for an ideal gas in the particular case in which a magnetic field is parallel to the surface of the discontinuity. However, neither this work or other work published in this field has, to the best of our knowledge, been concerned with the stability of a relativistic magnetohydrodynamic shock wave. The Zemplen theorem has not been proved and the behavior of the magnetic field in the shock wave has been investigated only in particular cases. Relativistic magnetohydrodynamic discontinuities (contact, tangential, Alfvén, fast and slow shock waves) have not been classified. All of these problems are treated in the present paper.

As in ordinary hydrodynamics, in relativistic magnetohydrodynamics a shock wave results from a simple wave as a consequence of the fact that the points of the liquid which have the highest density are displaced with the highest velocity.

Simple waves are related to the low-amplitude waves which have been investigated in relativistic magnetohydrodynamics by Khalatnikov,[2] Zumino,[3] and Harris.[4] We start with an investigation of simple plane waves in relativistic magnetohydrodynamics in which all quantities are given in the form of functions of one of the quantities which, in turn, is a function of the coordinate x and the time t.

1. SIMPLE WAVES*

The complete system of relativistic magnetohydrodynamic equations for zero viscosity and infinite electrical conductivity is as follows:

$$\partial T_{ik}/\partial x_k = 0, \tag{1.1}$$

$$\operatorname{curl}\mathbf{E} = -\partial\mathbf{H}/\partial t, \quad \operatorname{div}\mathbf{H} = 0, \tag{1.2}$$

$$\mathbf{E} = -[\mathbf{v}\times\mathbf{H}], \tag{1.3}$$

$$\partial(nu_k)/\partial x_k = 0, \tag{1.4}$$

where $T_{ik} = T^{h}_{ik} + T^{em}_{ik}$, and

$$T^{h}_{ik} = nwu_iu_k + p\delta_{ik}, \tag{1.5}$$

$$T^{em}_{\alpha\beta} = \frac{1}{4\pi}\left\{-H_\alpha H_\beta - E_\alpha E_\beta + \frac{1}{2}\delta_{\alpha\beta}(H^2+E^2)\right\},$$

$$T^{em}_{\alpha 4} = \frac{i}{4\pi}[\mathbf{E}\times\mathbf{H}]_\alpha, \quad T^{em}_{44} = -\frac{1}{8\pi}(E^2+H^2), \tag{1.6}$$

and the u_i are the components of the four-dimensional velocity, w and n are the internal energy per particle and the density in the reference system that moves with the wave, p is the pressure (the velocity of light is taken as unity).

Since the magnetohydrodynamic equations (1.1) — (1.6) constitute a hyperbolic system of first-order linear and homogeneous partial differential equations, we can apply the results obtained in reference 7; in particular, the differential equations which relate the magnetohydrodynamic variables in a simple wave can be obtained from the relations between the amplitudes of these quantities in waves of infinitesimally small amplitude. These relations are as follows:

Alfvén wave

$$d\mathbf{v}_t = -\varepsilon(V_{Ax}/H_x)\,d\mathbf{H}_{0t}, \quad H_{0y}dH_{0y} + H_{0z}dH_{0z} = 0,$$
$$dv_x = dW = dp = dH_{0x} = 0; \tag{1.7}$$

magnetoacoustic waves

$$dv_x = \varepsilon\frac{V_\pm dW}{W(1+c^2)}, \quad d\mathbf{v}_t = -\varepsilon\frac{V_\pm}{W(1+c^2)}\frac{U_{Ax}\mathbf{U}_{At}}{U_\pm^2 - U_{Ax}^2}\,dW,$$

$$dH_{0x} = 0, \quad d\mathbf{H}_{0t} = \frac{4\pi\mathbf{H}_{0t}(V_\pm^2 - c^2)}{(1+c^2)\,\mathbf{H}_{0t}^2(1-V_\pm^2)}\,dW, \tag{1.8}$$

where the quantities $\mathbf{V}_A$, $\mathbf{U}_A$, $V_\pm$, and $U_\pm$ are defined by the relations

*Simple waves have been considered by Stanyukovich[5,6] for the particular case in relativistic magnetohydrodynamics in which $H_x = 0$. A number of papers[7-13] have been devoted to studies of simple waves in non-relativistic magnetohydrodynamics.

$$\mathbf{V}_A = \mathbf{U}_A / \sqrt{1+\mathbf{U}_A^2}, \quad V_\pm = U_\pm / \sqrt{1+U_\pm^2}, \quad (1.9)$$

$$\mathbf{U}_A = \mathbf{H}_0 / \sqrt{4\pi W}, \quad (1.10)$$

$$V_\pm = \left\{ \frac{[c^2(1+U_{Ax}^2)+\mathbf{U}_A^2] \pm \sqrt{[c^2(1+U_{Ax}^2)-\mathbf{U}_A^2]^2 + 4c^2\mathbf{U}_{At}^2}}{2(1+\mathbf{U}_A^2)} \right\}^{1/2}, \quad (1.11)$$

$\mathbf{H}_0$ is the magnetic field in the reference system which moves with the wave; W = nw; c is the velocity of sound; $\mathbf{U}_{At}$ is the component of the vector $\mathbf{U}_A$ perpendicular to the direction of propagation of the wave (i.e., perpendicular to the x axis); the quantity ϵ is (+1) if the wave propagates in the positive x direction and (−1) if the wave propagates in the opposite direction; the plus sign in Eq. (1.11) corresponds to the fast magnetoacoustic wave and the minus sign refers to the slow magnetoacoustic wave.

Equations (1.7) and (1.8) are not to be considered as relations between the amplitudes dW, and $d\mathbf{H}, \ldots$ for constant W, $\mathbf{H}, \ldots$, but as differential equations from which all the quantities may be expressed as functions of one of these quantities, for example W.

The equations in (1.8) apply only in the moving reference system. Hence they can be used only in the case in which the velocity of the liquid $\mathbf{v}$ is small compared with the velocity of light.

The quantity W satisfies the equation

$$\partial W/\partial t + V\partial W/\partial x = 0, \quad (1.12)$$

where V is the phase velocity of propagation of a wave of infinitely small amplitude which corresponds to the given simple wave. The phase velocity is a function of the magnetohydrodynamic quantities (W, $\mathbf{H}, \ldots$ etc.). For this reason points corresponding to different values of W are displaced with different velocities and in general there is a distortion of the wave shape.

In the simple Alfvén wave the phase velocity remains constant since the quantities v_X, H_X, $\mathbf{H}_t$, and W do not change. Hence the Alfvén wave propagates without distortion.

In order to determine the manner in which the shape of the magnetoacoustic wave changes it is necessary to compute the derivative dV_p/dW, where V_p is the phase velocity, given by

$$V_p = v_x + V_\pm \quad (1.13)$$

(we may recall that the velocity $\mathbf{v}$ is nonrelativistic).

Differentiating the equation

$$V_\pm^4(1+\mathbf{U}_A^2) - V_\pm^2[\mathbf{U}_A^2 + c^2(1+U_{Ax}^2)] + U_{Ax}^2c^2 = 0$$

and making use of Eq. (1.8) we have

$$\frac{dV_p}{dW} = \frac{1}{4V_\pm W(1+c^2)A}\Big[(V_\pm^2-c^2)V_\pm^2(1-c^2) + 2(V_\pm^2\mathbf{U}_A^2 - c^2U_{Ax}^2) + 2Bc^4 + BWn^2c^6\left(\frac{\partial^2(w/n)}{\partial p^2}\right)_s\Big], \quad (1.14)$$

where

$$A = V_\pm^2(1+\mathbf{U}_A^2) - {}^1/_2[\mathbf{U}_A^2 + c^2(1+U_{Ax}^2)],$$
$$B = V_\pm^2(1+U_{Ax}^2) - U_{Ax}^2. \quad (1.15)$$

For fast magnetoacoustic waves the following inequalities hold:

$$V_+ > c, \quad A > 0, \quad B > 0, \quad V_+ > cU_{Ax}/U_A,$$

whereas for slow waves the following hold:

$$V_- < c, \quad A < 0, \quad B < 0, \quad V_- < cU_{Ax}/U_A.$$

It follows from Eq. (1.14) that both for fast and slow waves, when the following condition holds:

$$(\partial^2(w/n)/\partial p^2)_s > 0 \quad (1.16)$$

(s is the entropy per particle), we have

$$dV_p/dW > 0. \quad (1.17)$$

Under these conditions points characterized by higher densities are displaced more rapidly than points of low density.* This means that at compression points the density gradient is increased whereas at rarefaction points the density gradient is reduced.

The further analysis of simple waves is essentially the same as that for nonrelativistic magnetohydrodynamics.[8] At the compression points discontinuities arise; the self similar waves are always rarefaction waves.

It follows from Eq. (1.8) that in a fast self-similar magnetoacoustic simple wave the magnetic field falls off; in a slow wave it increases.

2. DISCONTINUITIES

The following boundary conditions[1] hold at the surface of a discontinuity:

$$\{nwv_x^2/(1-v^2) + p + (\mathbf{H}_t^2 - E_x^2)/8\pi\} = 0, \quad (2.1)$$

$$\{nwv_xv_y/(1-v^2) - H_xH_y/4\pi\} = 0, \quad (2.2)$$

$$\{nwv_xv_z/(1-v^2) - H_xH_z/4\pi\} = E_x\{E_x\}/4\pi, \quad (2.3)$$

$$\{nwv_x/(1-v^2)\} = \{H_x(\mathbf{v}_t\mathbf{H}_t) - v_x\mathbf{H}_t^2\}/4\pi, \quad (2.4)$$

$$j = n_1v_{1x}/\sqrt{1-v_1^2} = n_2v_{2x}/\sqrt{1-v_2^2}, \quad (2.5)$$

*Because of the thermodynamic relation $(\partial W/\partial n)_s > 0$, an increase in W corresponds to an increase in density.

$$E_{1y} = E_{2y} = v_{2x}H_{2z} - v_{2z}H_x = 0, \quad (2.6)$$

$$E_{1z} = E_{2z} = -v_{1x}H_{1y} = -v_{2x}H_{2y} + v_{2y}H_x, \quad (2.7)$$

$$\{H_x\} = 0. \quad (2.8)$$

The subscript "1" refers to the region in front of the discontinuity while the subscript "2" refers to the region behind the discontinuity. The x axis is taken normal to the discontinuity and points from region 1 to region 2.

We shall use a reference system which moves with the discontinuity which is such that the following relation holds in region 1:

$$v_{1y} = v_{1z} = H_{1z} = 0. \quad (2.9)$$

The boundary conditions can be simplified considerably if we go over to a reference system in which the vectors $\mathbf{v}$ and $\mathbf{H}$ at both sides of the discontinuity surface are parallel. In this case the electric fields $\mathbf{E}_1$ and $\mathbf{E}_2$ and the right sides of Eqs. (2.3) and (2.4) all vanish.

It should be noted that a reference system in which the velocity of the liquid is parallel to the magnetic field does not necessarily exist for all discontinuities. The quantity v_{1x} is fixed (this is the velocity of the discontinuity with respect to the liquid in region 1). The quantity $\mathbf{v}_{1t}$ is determined from the condition that the vectors $\mathbf{v}_1$ and $\mathbf{H}_1$ be parallel:

$$\mathbf{v}_{1t} = v_{1x}\mathbf{H}_{1t}/H_x.$$

In order that the total velocity $\sqrt{v_{1x}^2 + \mathbf{v}_{1t}^2}$ be smaller than the velocity of light the following relation must hold

$$v_{1x}^2\mathbf{H}_1^2/H_x^2 < 1. \quad (2.10)$$

As we shall see below, in general this relation is not satisfied for fast shock waves* (for $H_x \neq 0$).

The classification of discontinuities in relativistic magnetohydrodynamics is similar to the classification in nonrelativistic magnetohydrodynamics.[14] The following types of discontinuities exist:

1) Discontinuities that are at rest with respect to the liquid, $j = 0$.

a) Contact discontinuities: $H_x \neq 0$.

From the boundary conditions it follows that:

$$\mathbf{v} = 0, \quad \mathbf{E} = 0, \quad \{\mathbf{H}\} = 0, \quad \{p\} = 0.$$

b) Tangential discontinuities: $H_x = 0$.

From the boundary conditions it follows that

$$v_x = 0, \quad \mathbf{E}_t = 0, \quad \{p + (\mathbf{H}_t^2 - E_x^2)/8\pi\} = 0;$$

the discontinuities in the remaining thermodynamic quantities are arbitrary.

2) Discontinuities that move with respect to the liquid, $j \neq 0$.

From the boundary conditions (2.1) — (2.9) it follows that:

$$[n_2w_2v_{2x}^2/(1 - v_2^2) - H_x^2/4\pi + E_{2z}^2/4\pi]H_{2z} = 0. \quad (2.11)$$

If the first factor vanishes the discontinuity is called an Alfvén discontinuity; if the second factor vanishes the discontinuity is called a shock wave. We consider these in greater detail.

a) Alfvén discontinuities: $H_{2Z} \neq 0$.

$$n_2w_2v_{2x}^2/(1 - v_2^2) - H_x^2/4\pi + E_{2z}^2/4\pi = 0. \quad (2.12)$$

The following similar relation holds for region 1:

$$\frac{n_1w_1v_{1x}^2}{1 - v_1^2} - \frac{H_x^2}{4\pi} + \frac{v_{1x}^2H_{1y}^2}{4\pi} = 0. \quad (2.13)$$

Converting to the moving reference system we find that the Alfvén discontinuity is displaced with respect to the liquid in region 1 with a velocity V_{Ax}, which is defined by Eq. (1.9).

For the Alfvén discontinuity the relation in (2.10) is satisfied; hence we can convert to a reference system in which the velocity of the liquid is parallel to the magnetic field. In this reference system, it follows from the boundary conditions that

$$\{w/n\} = 0, \quad \{p + H_x^2n^2/8\pi j^2\} = 0. \quad (2.14)$$

In view of the continuity of H_X and j at the discontinuity, the independent thermodynamic quantities can be taken as w/n and $p + H_x^2n^2/8\pi j^2$. It follows from Eq. (2.14) that at the Alfvén discontinuity all the thermodynamic quantities are continuous

$$\{n\} = \{w\} = \{p\} = 0. \quad (2.15)$$

The vectors associated with the magnetic field and the velocity of the liquid do not change in absolute magnitude but rotate through the same angle about the x axis. We emphasize that this rotation of the vectors $\mathbf{v}$ and $\mathbf{H}$ takes place only in the reference system in which the velocity of the liquid is parallel to the magnetic field.

b) Shock waves: $H_{2Z} = 0$.

In this case, in accordance with Eq. (2.6) we find that $v_{2Z} = 0$, i.e., the shock wave is a plane discontinuity and the vectors $\mathbf{v}$ and $\mathbf{H}$ lie in the xy plane.

We now consider the stability of shock waves.

To have a stable shock wave it is necessary that the number of waves of infinitely small intensity which diverge from the surface of the discontinuity be equal to the number of independent boundary

*The assertion of de Hoffman and Teller that for any shock wave there is a reference system in which the velocity of the liquid is parallel to the magnetic field is not true in general.

conditions which relate the magnetohydrodynamic quantities at both sides of the discontinuity surface. On the basis of the considerations given in reference 15 we find that there are two kinds of stable magnetohydrodynamic shock waves: slow shock waves, for which

$$V_{1-} < v_{1x} < V_{1Ax}, \qquad v_{2x} < V_{2-} \tag{2.16}$$

and fast shock waves, for which

$$V_{1+} < v_{1x}, \qquad V_{2Ax} < v_{2x} < V_{2-}. \tag{2.17}$$

In accordance with Eq. (2.16), for slow shock waves there is a reference system in which the velocity of the liquid is parallel to the magnetic field.

In the case of fast shock waves the inequality in (2.10) need not necessarily hold and in this case such a reference system does not exist.

3. ZEMPLEN THEOREM*

We now show that in relativistic magnetohydrodynamics, just as in ordinary relativistic hydrodynamics,[19] there is a Zemplen theorem, according to which the pressure and density in a shock wave increase if the conditions in (1.16) hold† and if

$$(\partial s / \partial p)_{w/n} > 0. \tag{3.1}$$

The proof goes as follows.

In the absence of a magnetic field $\mathbf{H} = 0$, along the thermodynamically stable portion of the shock adiabat ($s_2 > s_1$) the following relations hold:[19] $p_2 > p_1$, $w_2/n_2 < w_1/n_1$.

There is no portion of the shock adiabat for which $w_2/n_2 > w_1/n_1$, $p_2 < p_1$ since this corresponds to a shock wave for which the entropy is reduced ($s_2 < s_1$). By virtue of the inequality in (3.1) this section of the shock adiabat lies in the (w/n, p) plane below the Poisson adiabat (s = const). We show that in the presence of a magnetic field the portion of the shock adiabat which corresponds to a rarefaction shock wave $w_2/n_2 > w_1/n_1$ lies still lower. From this it will follow that on this section the entropy is reduced ($s_2 < s_1$), and this is impossible.

For the proof we write the equation of the shock adiabat in the presence of a magnetic field

$$w_2^2 - w_1^2 - (p_2 - p_1)(w_1/n_1 + w_2/n_2) = Q, \tag{3.2}$$

$$Q = \frac{H_{1y}^2 (w_2/n_2)^2 (v_{1x}/v_{2x} - 1)^2 (w_1/n_1 - w_2/n_2)}{8\pi (w_2/n_2 - H_x^2/4\pi j^2)^2}. \tag{3.3}$$

Equations (3.2) and (3.3) are obtained from the boundary conditions (2.1) – (2.9) by eliminating the variables. When $w_1/n_1 < w_2/n_2$ the quantity Q is negative if $H_{1y} \neq 0$, whereas when $H_{1y} = 0$ the quantity Q vanishes.

We shall now investigate the behavior of the curve (3.2), (3.3) (in the w_2/n_2, p_2 plane) if Q, which we take as a parameter, vanishes. Differentiating Eq. (3.3) with respect to p_2 at constant w_2/n_2, we have

$$\left(\frac{\partial Q}{\partial p_2}\right)_{w_2/n_2} = 2w_2 \left(\frac{\partial w_2}{\partial p_2}\right)_{w_2/n_2} - \left(\frac{w_1}{n_1} + \frac{w_2}{n_2}\right).$$

On the other hand we have the thermodynamic relation

$$\left(\frac{\partial w}{\partial p}\right)_{w/n} = \frac{1}{n} + T\left(\frac{\partial s}{\partial p}\right)_{w/n},$$

whence

$$\left(\frac{\partial Q}{\partial p_2}\right)_{w_2/n_2} = \left(\frac{w_2}{n_2} - \frac{w_1}{n_1}\right) + 2w_2 T_2 \left(\frac{\partial s_2}{\partial p_2}\right)_{w_2/n_2}.$$

By virtue of (3.1), when $w_2/n_2 > w_1/n_1$, this quantity is positive. The fact that the derivative $(\partial Q/\partial p_2)_{w_2/n_2}$ is positive indicates that with fixed w_2/n_2 a reduction of Q means a reduction in p_2. In other words, a curve of the shock adiabat (3.2) and (3.3) for $H_{1y} \neq 0$ actually lies lower than the shock adiabat in the absence of the magnetic field.

Thus, in the shock wave the pressure and the quantity n/w increase

$$p_2 > p_1, \quad w_2/n_2 < w_1/n_1. \tag{3.4}$$

Using the Zemplen theorem we can draw certain conclusions concerning the behavior of the magnetic field in shock waves.* In a slow shock wave it is possible to go over to a reference system in which the velocity of the liquid is parallel to the magnetic field. In this case, from the boundary conditions we have

*The Zemplen Theorem was proved by Iordanskiĭ[16] and Polovin and Lyubarskiĭ[17,18] in nonrelativistic magnetohydrodynamics for shock waves of arbitrary intensity.

†For a relativistic ideal gas

$$\left(\frac{\partial^2 (w/n)}{\partial p^2}\right)_s = \frac{2(2-\gamma)}{\gamma(\gamma-1)} \frac{1}{pn^2}, \quad \left(\frac{\partial s}{\partial p}\right)_{w/n} = \frac{2-\gamma}{\gamma-1} \frac{1}{2nT}.$$

These expressions are positive since the quantity γ lies in the interval[20] $1 < \gamma \leq 5/3$. In addition to the inequalities in (1.16) and (3.1), just as in references 19 and 21 we show that the pressure increases monotonically along a shock adiabat.

*Landau and Lifshitz[21] have investigated the change of magnetic field in nonrelativistic magnetohydrodynamic shock waves of low intensity and in nonrelativistic waves of arbitrary intensity for the case in which $H^2 \ll p$. An increase in the magnetic field in fast nonrelativistic magnetohydrodynamic shock waves for $H^2 \ll p$ has been noted by Helfer.[22]

The change in the magnetic field in nonrelativistic magnetohydrodynamic shock waves has been considered by Lyubarskiĭ and Polovin.[18] The relativistic case for which $H_x = 0$ has been treated by Stanyukovich.[23]

$$H_{2y} = H_{1y} \frac{w_1/n_1 - H_x^2/4\pi j^2}{w_2/n_2 - H_x^2/4\pi j^2}. \qquad (3.5)$$

From the Zemplen theorem (3.4), the condition of stability for a slow shock wave (2.16), and the relation in (3.5) it follows that in a slow shock wave the tangential magnetic field does not change direction and is reduced. This statement is valid also for the moving reference system since the magnetic field is the same in this system as in the reference system in which the velocity of the liquid is parallel to the magnetic field.

For a fast shock wave, as has already been indicated, there may not be a reference system in which **v** is parallel to **H**. Hence the relation in (3.5) must be replaced by the more complicated relations

$$H_{2y} = H_{1y} \frac{w_2 v_{1x}/n_2 v_{2x} - H_x^2/4\pi j^2}{w_2/n_2 - H_x^2/4\pi j^2}, \qquad (3.6)$$

$$v_{1x}^2 H_{1y}^2 = \frac{4\pi j^2 (w_1/n_1 - w_2 v_{1x}/n_2 v_{2x})(w_2/n_2 - H_x^2/4\pi j^2)}{(w_2/n_2)(v_{1x}/v_{2x} - 1)}, \qquad (3.7)$$

which follow from the boundary conditions in (2.2), (2.4), (2.7), and (2.9). Since the shock wave is a compression wave ($w_2 > w_1$, $n_2 > n_1$) from (2.5), (2.9), and (3.7) it follows that

$$v_1 > v_2, \quad v_{1x} > v_{2x}. \qquad (3.8)$$

Equation (3.6) together with the stability conditions (2.17) indicate that in a fast shock wave the tangential magnetic field does not change direction and is increased. The last statement applies in a reference system in which the equality in (2.9) is satisfied. Carrying out a Lorentz transformation to the moving reference system and using (3.8) we find that the magnetic field also increases in this system.

The author is indebted to A. I. Akhiezer and G. Ya. Lyubarskiĭ for valuable discussions.

[1] F. de Hoffmann and E. Teller, Phys. Rev. **80**, 692 (1950); Russ. transl. in Пробл. совр. физ. (Prob. Modern Physics), **2**, 47 (1954).

[2] I. M. Khalatnikov, J. Exptl. Theoret. Phys. (U.S.S.R.) **32**, 1102 (1957), Soviet Phys. JETP **5**, 901 (1957).

[3] B. Zumino, Phys. Rev. **108**, 1116 (1957).

[4] E. G. Harris, Phys. Rev. **108**, 1357 (1957).

[5] K. P. Stanyukovich, Dokl. Akad. Nauk SSSR **103**, 73 (1955).

[6] K. P. Stanyukovich, Izv. Akad. Nauk SSSR, Ser. Fiz. **19**, 639 (1955), Columbia Tech. Transl. p. 578.

[7] Akhiezer, Lyubarskiĭ, and Polovin, Укр. физ. журн. (Ukr. Phys. J.) **3**, 433 (1958).

[8] G. Ya. Lyubarskiĭ and R. V. Polovin, Укр. физ. журн. (Ukr. Phys. J.) **3**, 7 (1958).

[9] S. A. Kaplan and K. P. Stanyukovich, Dokl. Akad. Nauk SSSR **95**, 769 (1954).

[10] R. Z. Sagdeev, Физика плазмы и проблемы управляемых термоядерных реакций, (Plasma Physics and the Problem of a Controlled Thermonuclear Reaction), Vol IV, p 384, U.S.S.R. Acad. Sci. Press, 1958.

[11] A. G. Kulikovskiĭ, Dokl. Akad. Nauk SSSR, **121**, 987 (1958), Soviet Phys. "Doklady" **3**, 743 (1959).

[12] G. Ya. Lyubarskiĭ and R. V. Polovin, J. Exptl. Theoret. Phys. (U.S.S.R.) **35**, 509 (1958), Soviet Phys. JETP **8**, 35 (1959).

[13] S. Segre, Nuovo cimento, **9**, 1054 (1958).

[14] S. I. Syrovat-skiĭ, J. Exptl. Theoret. Phys. (U.S.S.R.) **24**, 622 (1953).

[15] Akhiezer, Lyubarskiĭ, and Polovin, J. Exptl. Theoret. Phys. (U.S.S.R.) **35**, 731 (1958), Soviet Phys. JETP **8**, 507 (1959).

[16] S. V. Iordanskiĭ, Dokl. Akad. Nauk SSSR **121**, 610 (1958), Soviet Phys. "Doklady" **3**, 736 (1959).

[17] R. V. Polovin and G. Ya. Lyubarskiĭ, J. Exptl. Theoret. Phys. (U.S.S.R.) **35**, 510 (1958), Soviet Phys. JETP **8**, 35 (1959).

[18] R. V. Polovin and G. Ya. Lyubarskiĭ, Укр. физ. журн. (Ukr. Phys. J.) **3**, 11 (1958).

[19] R. V. Polovin, J. Exptl. Theoret. Phys. (U.S.S.R.) **36**, 956 (1959), Soviet Phys. JETP **9**, 675 (1959).

[20] A. H. Taub, Phys. Rev. **74**, 328 (1948).

[21] L. D. Landau and E. M. Lifshitz, Электродинамика сплошных сред. (Electrodynamics of Continuous Media). Moscow, GITTL, (1957).

[22] H. L. Helfer, Astrophys. J. **117**, 177 (1953); Russ. trans. Пробл. совр. физ. (Prob. Modern Phys.) **2**, 68 (1954).

[23] K. P. Stanyukovich, J. Exptl. Theoret. Phys. (U.S.S.R.) **35**, 520 (1958), Soviet Phys. JETP **8**, 358 (1959).

Translated by H. Lashinsky
370

TRANSITION RADIATION AND CERENKOV RADIATION

V. E. PAFOMOV

P. N. Lebedev Physics Institute, Academy of Sciences, U.S.S.R.

Submitted to JETP editor December 30, 1958

J. Exptl. Theoret. Phys. (U.S.S.R.) **36**, 1853-1858 (June, 1959)

The angular distribution of the radiation produced by a charged particle which passes through the interface between a vacuum and an isotropic ferrite is considered; the case of a vacuum and a crystalline dielectric is also considered. It is shown that the radiation depends on the sign of the group velocity. The transition radiation is considered in connection with the characteristics of Cerenkov radiation in crystals and in isotropic media in the frequency region characterized by negative group velocities. The "inverse" Doppler effect is considered.

1. INTRODUCTION

TRANSITION radiation of a charged particle which moves perpendicularly to the boundary between two media with different dielectric constants was first considered by Ginzburg and Frank.[1] The problem has also been treated by other methods in later work.[2-5]

In the present paper we consider transition radiation, taking account of the magnetic permeability. It is shown that this radiation is affected significantly by the sign of the group velocity. We also consider transition radiation in connection with the characteristics of Cerenkov radiation in frequency regions associated with negative group velocities. In these regions the solutions of Maxwell's equations appear as advanced potentials which carry energy from the radiator; it is found that the Cerenkov ray forms an obtuse angle with the direction of motion of the particle. In this case a sharp intensity peak (in the transition radiation) due to the generation of Cerenkov radiation in the medium should be observed in the vacuum if the particle moves from vacuum into the medium.

We also consider the radiation of a charged particle which moves perpendicularly to the boundary between a vacuum and a uniaxial crystalline dielectric. This problem is of interest in connection with Cerenkov radiation in crystals because in certain frequency regions the radiation is described by an advanced potential characterized by a phase which moves along the particle trajectory. There is also a frequency region in which the Cerenkov ray forms an obtuse angle with the direction of motion of the charged particle (cf. reference 6).

In an isotropic medium these characteristics of the Cerenkov radiation are found in a single frequency region — the region in which the group velocity is negative.

In conclusion we consider the so-called "inverse" Doppler effect — low-frequency radiation in the forward direction. From the inverse Doppler effect it follows that in the case of a source of zero frequency which moves with a velocity greater than the phase velocity of light the Cerenkov radiation which is produced should form an obtuse angle with respect to the direction of motion.

2. RADIATION OF A CHARGED PARTICLE THAT PASSES THROUGH THE BOUNDARY BETWEEN A VACUUM AND AN ISOTROPIC FERRITE

The problem is solved conveniently in cylindrical coordinates. Taking the z axis in the direction of the particle velocity **v** we write the current density, as in reference 3, in the following form:

$$j = \frac{e}{(2\pi)^2} \int_{-\infty}^{+\infty} e^{i\omega(t - z/v)}\, d\omega \int_0^\infty \alpha J_0(\alpha r)\, d\alpha. \qquad (1)$$

Introducing the Hertz vector in accordance with the expression

$$\mathbf{E}_\omega = \frac{1}{\varepsilon\mu} \operatorname{grad} \operatorname{div} \Pi_\omega + \frac{\omega^2}{c^2} \Pi_\omega, \qquad \mathbf{H}_\omega = \frac{i\omega}{\mu c} \operatorname{curl} \Pi_\omega, \qquad (2)$$

we obtain the following solution for Maxwell's equations:

$$\Pi = -\frac{ie}{\pi} \int_{-\infty}^{+\infty} \frac{\mu e^{i\omega t}}{\omega}\, d\omega \int_0^\infty \alpha J_0(\alpha r) \left[\frac{e^{-i\omega z/v}}{\alpha^2 + (\omega/v)^2 (1 - \varepsilon\mu\beta^2)} + A \exp\left(z \sqrt{\alpha^2 - \varepsilon\mu\omega^2 c^{-2}}\right) + B \exp\left(-z \sqrt{\alpha^2 - \varepsilon\mu\omega^2 c^{-2}}\right) \right] d\alpha, \qquad (3)$$

where the last two terms satisfy the source free equation and are determined from the boundary conditions. The Hertz vector has only one non-vanishing component; this is along the z axis (in Eq. (3) we have dropped the z subscript).

We shall assume that the boundary coincides with the plane $z = 0$ and that the ferrite occupies the semi-space $z < 0$. In the vacuum region ($z > 0$) the solution is expressed by Eq. (3) if we take $\epsilon = 1$ and $\mu = 1$. If

$$\operatorname{Re}\sqrt{\alpha^2 - \varepsilon_f \mu_f \omega^2/c^2} > 0$$

to satisfy the requirement that the solution be finite at infinity we take $B_f = 0$ and $A_v = 0$.

Using the boundary conditions*

$$\frac{1}{\varepsilon_f}\frac{\partial \Pi_f}{\partial z} = \frac{\partial \Pi_v}{\partial z}, \quad \frac{1}{\mu_f}\Pi_f = \Pi_v, \tag{4}$$

we find the components A_f and B_v which differ from zero.

In what follows we shall be interested in the radiation energy in the vacuum region. The radiation field in the vacuum is completely described by the term which contains B_v, which does not become infinite if the ferrite has losses. In this case the integration over α can be carried out by the method of stationary phase. The important contribution in the integral is due to a small region of order $\sqrt{\omega/cR}$ close to $\alpha = (\omega/c)\sin\vartheta$, where R is the distance from the origin of coordinates to the point of observation. Hence, at large distances from the origin integration over α means approximately that we replace α by $(\omega/c)\sin\vartheta$. Carrying out this integration and computing the Poynting vector flux through an isolated hemisphere we obtain the vacuum radiation energy for a charged particle which moves from the ferrite into the vacuum:

$$W = \frac{2e^2\beta^2}{\pi c^3}\int_0^\infty d\omega \int_0^{\pi/2} \frac{\sin^3\vartheta\cos^2\vartheta}{(1-\beta^2\cos^2\vartheta)^2} \times \left| \frac{(\varepsilon-1)(1-\beta\sqrt{\varepsilon\mu-\sin^2\vartheta}) - \beta^2(\varepsilon\mu-1)}{(1-\beta\sqrt{\varepsilon\mu-\sin^2\vartheta})(\varepsilon\cos\vartheta + \sqrt{\varepsilon\mu-\sin^2\vartheta})} \right|^2 d\vartheta, \tag{5}$$

where $\beta = v/c$ is the ratio of the particle velocity to the velocity of light in vacuum and ϑ is the angle between the z axis and the direction of observation.

In the case in which the particle moves from vacuum into the ferrite, the vacuum radiation energy is obtained from Eq. (5) by replacing β by $-\beta$. When $\mu = 1$, Eq. (5) becomes the equation which has been obtained earlier (cf. references 1 – 5). Equation (5) describes the entire energy which appears in the vacuum region, including the Cerenkov radiation generated in the medium.*

The integration over α (to within a numerical factor) leads to the replacement of α by $(\omega/c)\sin\vartheta$. Whence it follows that the inequality which we have taken above ($\operatorname{Re}\sqrt{\alpha^2 - \epsilon\mu\omega^2/c^2} > 0$) corresponds to the following inequality:

$$\operatorname{Im}\sqrt{\varepsilon\mu - \sin^2\vartheta} < 0. \tag{6}$$

Equation (5), which is written under the assumption that (6) holds, is valid over the entire frequency range, including the range in which the group velocity is negative.

We may note that in principle the group velocity in a ferrite ($\epsilon \neq 1$, $\mu \neq 1$) can be negative.† In order to show this, we substitute a plane wave in Maxwell's equations ($\mathbf{E}, \mathbf{H} \sim \exp[i(\omega t - \mathbf{kr})]$) in which case the following vector relation holds:

$$k\mathbf{E}^2 = (\omega\mu_a/c)[\mathbf{E}\times\mathbf{H}] = (\omega\mu_a/4\pi)\mathbf{S}, \qquad k = \omega\sqrt{\varepsilon\mu}/c,$$

where $\mathbf{S}$ is the Poynting vector. Undamped electromagnetic waves can exist both for $\epsilon > 0$, $\mu > 0$ as well as for $\epsilon < 0$, $\mu < 0$ since the index of refraction $n = \sqrt{\epsilon\mu}$ is a real quantity in both of these cases. It is apparent from the last relation that in the first case the Poynting vector coincides in direction with the wave vector $\mathbf{k}$; in the second case $\mathbf{S}$ and $\mathbf{k}$ point in opposite directions, i.e., the group velocity is negative. In the frequency region in which the following relation is not satisfied: $\operatorname{Re}(\partial\omega/\partial\mathbf{k}) \gg \operatorname{Im}(\partial\omega/\partial\mathbf{k})$ the concept of group velocity has no meaning. In this case the term "positive (negative) group velocity" is no longer meaningful in the above sense.

In the frequency region in which the group ve-

*The subscript "f" corresponds to quantities taken in the region $z < 0$, occupied by the ferrite, while the subscript "v" corresponds to vacuum quantities ($z > 0$).

*In this connection we wish to point out an error in the interpretation of the corresponding result in reference 4, where an analysis is made of the radiation of a charged particle which moves through a vacuum-dielectric boundary and it is asserted that the Cerenkov waves do not make a contribution in the first integral in Eq. (27). At the large distances for which the first integral in Eq. (27) is computed in reference 4 the cylindrical Cerenkov wave is transformed into a spherical wave and the second integral can be neglected. To convince ourselves of this it is only necessary to take account of the fact that the residue at the pole in the integration over $\varkappa$ in Eq. (23) is to be taken only when the pole in the complex plane lies between the real axis and the line of steepest descent (if there is damping, in Eq. (27) of reference 4 the quantity ε should be used instead of ε'.

†The group velocity can also be negative in a medium with spatial dispersion (cf. reference 7). The features associated with a negative group velocity which are being considered in the present paper are quite general.

locity is negative the solution is given by advanced potentials, with phases which do not move away from the radiator but approach it. In this case one expects peculiar features for the radiation in moving systems. In the figure is shown a diagram of the propagation of waves which are excited by a uniformly moving particle which interacts with the electromagnetic field. If the velocity of the particle exceeds the phase velocity of light ($n\beta > 1$) then in the direction given by ϑ, which satisfies the relation $n\beta \cos\vartheta = 1$, all the elementary waves are propagated in the same phase. The Cerenkov waves formed in this way exhibit a surface of uniform phase in the form of a cone with the vertex in the forward direction. The phase velocity forms an acute angle ϑ with the direction of motion of the particle. However, the energy flow is in the opposite direction. As a result a narrow peak in the transition radiation intensity, due to the Cerenkov radiation, should be observed in vacuum when the particle moves from vacuum into the medium. One is easily convinced of this if one introduces damping $\epsilon = \epsilon' - i\epsilon''$, $\mu = \mu' - i\mu''$, where $\epsilon'' > 0$ and $\mu'' > 0$. In this case, in the region of negative group velocity (6) corresponds to the inequality $\mathrm{Re}\sqrt{\epsilon\mu - \sin^2\vartheta} < 0$. Taking account of this situation and replacing β by $-\beta$ we see that Eq. (5) yields a narrow maximum ($\beta^2(\epsilon\mu - \sin^2\vartheta_C) = 1$) in the direction of the refracted Cerenkov angle. Under these conditions, in the vacuum at small distances from the medium there will be a converging cylindrical Cerenkov wave which, after intersecting the normal to the boundary, diverges and fills the inner part of the Cerenkov cone. One is easily convinced of this result from an analysis of the diffraction of the plane waves at the boundary.

In actual ferrites there is no frequency region in which $\epsilon < 0$ and $\mu < 0$; however these materials do not represent the only possibility. As we have noted above, the group velocity can be negative in a medium characterized by spatial dispersion.*

3. RADIATION OF A CHARGED PARTICLE WHICH MOVES THROUGH A VACUUM-CRYSTAL BOUNDARY

As has been indicated in reference 6, the Cerenkov ray generated in a crystalline dielectric may form an obtuse angle with the direction of motion of the charged particle. It is of interest to consider the radiation of a point charge which passes through a vacuum-crystal boundary in connection with this feature of Cerenkov radiation.

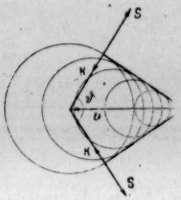

We take the velocity to be along the z axis and introduce the Hertz vector:

$$\Pi_\omega = \frac{1}{\varepsilon_0}\operatorname{grad}\frac{\partial\Pi_\omega}{\partial z} + \frac{\omega^2}{c^2}\Pi_\omega, \qquad \mathbf{H}_\omega = i\frac{\omega}{c}\operatorname{curl}\Pi_\omega, \tag{7}$$

for a uniaxial crystal with axis in the z direction we obtain the following solution for Maxwell's equations:

$$\Pi = -\frac{ie}{\pi}\int_{-\infty}^{+\infty}\frac{e^{i\omega t}}{\omega}d\omega\int_0^\infty \alpha J_0(\alpha r)\left\{\frac{e^{-i\omega z/v}}{\alpha^2 + (\varepsilon_e\omega^2/c_0v^2)(1-\varepsilon_0\gamma^2)}\right.$$
$$+ A\exp\left[z\sqrt{(\alpha^2 - \varepsilon_e\omega^2/c^2)\varepsilon_0\varepsilon_e}\right]$$
$$\left. + B\exp\left[-z\sqrt{(\alpha^2 - \varepsilon_e\omega^2/c^2)\varepsilon_0\varepsilon_e}\right]\right\}d\alpha, \tag{8}$$

where ϵ_0 and ϵ_e are the transverse (to the crystal axis) and longitudinal components of the dielectric primitivity tensor. The Hertz vector has one non-vanishing component (along the z-axis) so that we drop the index (also the vector nature of Π).

We assume that the crystal fills the half-space $z < 0$ and that the region for which $z > 0$ is a vacuum. Assuming that

$$\mathrm{Re}\sqrt{(\alpha^2 - \varepsilon_e\omega^2/c^2)\varepsilon_0\varepsilon_e} > 0, \tag{9}$$

we determine the solution completely by requiring that the solution be finite at infinity (the vacuum wave diverges from the origin), using the continuity conditions on the tangential components of the electric and magnetic fields; these are equivalent to the relations

$$\frac{1}{\varepsilon_0}\frac{\partial\Pi_v}{\partial z} = \frac{\partial\Pi_c}{\partial z}, \qquad \Pi_c = \Pi_v$$

where the subscript "c" denotes quantities taken in the crystal.

Carrying out the calculations as in the preceding section we obtain the vacuum radiation energy for a charged particle which moves from the crystal into the vacuum:

*In reference 8 the Cerenkov radiation has been considered for isotropic gyrotropic media in which spatial dispersion is taken into account. The energy in reference 8 which corresponds to the Cerenkov radiation in the region of negative group velocity moves at an obtuse angle with respect to the direction of motion of the particle.

$$W = \frac{2e^2\beta^2}{\pi c^2}\int_0^\infty d\omega \int_0^{\pi/2} \frac{\sin^3\vartheta\cos^2\vartheta}{(1-\beta^2\cos^2\vartheta)^2}\left|B(\omega,\vartheta)\right|^2 d\vartheta,$$

$$B(\omega,\vartheta) = \frac{\varepsilon_0}{\varepsilon_e}\left[\beta(1-\beta^2-\frac{\varepsilon_e}{\varepsilon_0}+\beta^2\varepsilon_e)\sqrt{\varepsilon_0-\frac{\varepsilon_0}{\varepsilon_e}\sin^2\vartheta}\right.$$
$$\left.+(\beta^2\sin^2\vartheta+1-\beta^2-\beta^2\varepsilon_0\sin^2\vartheta-\varepsilon_e+\beta^2\varepsilon_0\varepsilon_e)\right]\left[\varepsilon_0\cos\vartheta\right.$$
$$\left.+\sqrt{\varepsilon_0-\frac{\varepsilon_0}{\varepsilon_e}\sin^2\vartheta}\right]^{-1}\left[1-\beta^2\left(\varepsilon_0-\frac{\varepsilon_0}{\varepsilon_e}\sin^2\vartheta\right)\right]^{-1}. \quad (10)$$

The vacuum radiation energy for the case of motion of a particle from vacuum into a crystal is obtained from Eq. (10) by replacing β by $-\beta$. When $\epsilon_0 = \epsilon_e = 1$ the quantity W vanishes as is to be expected and when $\epsilon_0 = \epsilon_e = \epsilon$ Eq. (10) gives the familiar result (cf. references 1 – 5).

In the integration over α, as in the preceding section, the important region is the small region in the vicinity of the point of stationary phase and in integrating over α we replace α by $\frac{\omega}{c}\sin\vartheta$. Hence the relation in (9) becomes:

$$\operatorname{Im}\sqrt{\varepsilon_0-(\varepsilon_0/\varepsilon_e)\sin^2\vartheta} < 0. \quad (11)$$

In Eq. (10) it is assumed that this inequality is satisfied.

As has already been shown in reference 6, the Cerenkov ray forms an obtuse angle in the frequency region in which $\epsilon_0 < 0$ and $\epsilon_e > 0$. By introducing a small damping factor ($\epsilon_{0,e} = \epsilon'_{0,e} - i\epsilon''_{0,e}$, $\epsilon''_{0,e} > 0$) we can show that when $\epsilon_0 < 0$ and $\epsilon_e > 0$ the following inequality is satisfied

$$\operatorname{Re}\sqrt{\varepsilon_0-(\varepsilon_0/\varepsilon_e)\sin^2\vartheta} < 0, \quad (12)$$

where ϑ is the refracted Cerenkov angle which, as has been shown, satisfies the equation

$$\beta^2\left(\varepsilon_0-\frac{\varepsilon_0}{\varepsilon_e}\sin^2\vartheta\right) = 1. \quad (13)$$

Making use of Eq. (12) and replacing β by $-\beta$, from Eq. (10) we can show that in the direction of the refracted Cerenkov ray there should be a sharp radiation maximum because in this frequency region the Cerenkov ray forms an obtuse angle with the direction of motion.

4. "INVERSE" DOPPLER EFFECT

In the frequency region in which the Cerenkov ray forms an obtuse angle with the direction of motion one also expects peculiar properties for the radiation of a moving oscillator. This is apparent from the Doppler formula

$$|\omega_\vartheta - \mathbf{kv}| = \omega_0, \quad (14)$$

where ω_0 is the source frequency in the rest system, $\mathbf{v}$ is the velocity, $\mathbf{k}$ is the wave vector: $k = \omega_\vartheta n(\omega_\vartheta, \vartheta)/c$ (ϑ is the angle between the vectors $\mathbf{k}$ and $\mathbf{v}$). It is apparent from Eq. (14) that in the frequency region in which the projections of the wave vector and the group velocity on the direction of motion have different signs lower frequencies are radiated in the forward direction ("inverse" Doppler effect).* From the "inverse" Doppler effect it follows that for zero frequency of a source which moves with a velocity exceeding the phase velocity of light the Cerenkov radiation forms an obtuse angle with the direction of motion.†

In conclusion the author wishes to thank V. L. Ginzburg for a number of valuable comments and a discussion of these results.

[1] V. L. Ginzburg and I. M. Frank, J. Exptl. Theoret. Phys. (U.S.S.R.) **16**, 15 (1946).

[2] G. Beck, Phys. Rev. **74**, 795 (1948).

[3] P. Klepikov, Вестник МГУ (Bull. Moscow State Univ.) **8**, 5, 61 (1951).

[4] G. M. Garibyan, J. Exptl. Theoret. Phys. (U.S.S.R.) **33**, 1403 (1957), Soviet Phys. JETP **6**, 1079 (1958).

[5] N. A. Korkhmazyan, Izv. Akad. Nauk ArmSSR **10**, 4, 29 (1957).

[6] V. E. Pafomov, J. Exptl. Theoret. Phys. (U.S.S.R.) **32**, 366 (1957), Soviet Phys. JETP **5**, 307 (1957).

[7] V. L. Ginzburg, J. Exptl. Theoret. Phys. (U.S.S.R.) **34**, 1593 (1958), Soviet Phys. JETP **7**, 1096 (1958).

[8] Agranovich, Pafomov and Rukhadze, J. Exptl. Theoret. Phys. (U.S.S.R.) **36**, 238 (1959), Soviet Phys. JETP **9**, 160 (1959).

[9] K. A. Barsukov, J. Exptl. Theoret. Phys. (U.S.S.R.) **36**, 1485 (1959), Soviet Phys. JETP **9**, 1052 (1959).

[10] I. M. Frank, J. Exptl. Theoret. Phys. (U.S.S.R.) **36**, 823 (1959), Soviet Phys. JETP **9**, 580 (1959).

Translated by H. Lashinsky
371

*The "inverse" Doppler effect in anisotropic gyrotropic media has been considered in reference 9.

†The role of the group velocity in the radiation of a moving oscillator has been discussed by Frank.[10]

SOVIET PHYSICS JETP VOLUME 36(9), NUMBER 6 DECEMBER, 1959

THE MEAN FREE PATH OF AN EXCITON IN A POLAR CRYSTAL

A. V. TULUB

Leningrad State University

Submitted to JETP editor December 31, 1958

J. Exptl. Theoret. Phys. (U.S.S.R.) **36**, 1859-1868 (June, 1959)

We have used Low's method to evaluate in the intermediate coupling approximation the scattering amplitude for the scattering of a phonon by an exciton by expressing it in the form of a matrix element between exact eigenfunctions of the energy operator corresponding to the initial and final states of the exciton. Our basic approximation consists in the use of Haken's functions for the exciton wave functions. We have carried out detailed calculations for the case of large quantum numbers and for the ground state of the exciton. It is shown that the mean free path remains finite also for the case where the effective masses of the electron and of the hole are the same.

THE Wannier-Mott approximation, according to which the exciton is a system of an electron and a positively charged hole with a Coulomb interaction between the two, is valid for excitons of large radii. The periodic field of the lattice is, as usual, taken into account by introducing effective masses which may be assumed to be isotropic if we consider a crystal of cuprous oxide.

Both particles, the electron and the hole, interact with the crystalline lattice, and in polar crystals and the main interaction is the one, known from polaron theory, of the particles with the longitudinal optical phonons.[1] The existence of a phonon interaction leads according to Haken[2] to the fact that the potential is of the form $-e^2/\epsilon r$, at large distances and $-e^2/n^2 r$ at small ones. Describing the relative motion of the electron and hole in classical terms one can say that at small distances the motion is fast and the ions do not have time to shift from their equilibrium positions. The potential is thus equal to $-e^2/n^2 r$ where the index of refraction n takes the polarization of the electron shells of the atoms into account. At large distances, however, the motion is slow and the interaction is characterized by the static dielectric constant ϵ.

This difference in the character of the interaction is automatically obtained if one takes into account the recoil connected with the emission of phonons.[4]

It is essential to note that if the effective masses of the electron and of the hole are equal, as will be the case in cuprous oxide,[3] the phonon interaction does not vanish, and the exciton still causes a polarization of the lattice. The statements to the opposite which are in the literature[7] are based upon the approximation which writes the wave function of the system in the form

$$\Psi(r, a) = \psi_n(r)\,\Omega(a), \qquad (1)$$

where $\psi_n(r)$ is a function of the spatial coordinates r, $\Omega(a)$ a functional depending only on the phonon field variables a.

Approximation (1) leads to the fact that when the effective masses are equal the probability for a collision of a phonon with the exciton turns out to be equal to zero and the mean free path tends to infinity.[5,6] Taking the interaction of the exciton with the acoustic lattice vibrations into account cannot change this result as in the approximation of a continuous medium the constants for the interaction of an electron and a hole with the phonons turn out to be equal, and under those conditions the mean free path is also equal to infinity.[6]

To obtain a finite collision probability one must use more exact functionals for the exciton state which take into account not the polarization in the medium, but the polarization produced by each of the particles separately.

The most convenient mathematical apparatus to consider this problem is Low's method,[8] which makes it possible to evaluate the phonon scattering cross section without using the usual perturbation theory set-up. This fact is of the greatest importance for polar crystals as in that case the coupling is either strong or intermediate. The evaluation of the matrix elements is performed with respect to the phonon field in the same approximation as in the paper by Low and Pines[10] where the scattering of a phonon by a polaron was considered. The results obtained are valid in the intermediate coupling region.

The energy operator for an exciton in the Wannier-Mott model is of the form

$$H = -\frac{1}{2M}\nabla_R^2 - \frac{1}{2M'}\nabla_r^2 - \frac{e^2}{\varepsilon r} + \sum_k \omega a_k^+ a_k + \sum_k (V_k(r)\, e^{i\mathbf{kR}} a_k + V_k^*(r)\, e^{-i\mathbf{kR}} a_k^+). \quad (2)$$

Our notation is the following ($\hbar = 1$): $M = m_1 + m_2$ is the total mass, M' the reduced mass, ω the limiting frequency for the longitudinal optical vibrations, a_k^+ and a_k the creation and annihilation operators for the phonons, $\mathbf{R} = \mu_1\mathbf{r}_1 + \mu_2\mathbf{r}_2$ the center of mass coordinate, $\mu_i = m_i/M$, $\mathbf{r} = \mathbf{r}_1 - \mathbf{r}_2$, the coefficient V_k is equal to

$$V_k = \gamma_k (e^{i\mathbf{kr}\mu_2} - e^{-i\mathbf{kr}\mu_1}), \quad (3)$$

$$\gamma_k = -i\frac{\omega}{k}(2m\omega)^{-1/4}(4\pi\alpha/V)^{1/2}, \quad (4)$$

α plays the role of the coupling constant:

$$\alpha = \tfrac{1}{2} e^2 (2m/\omega)^{1/2} (1/\varepsilon^2 - 1/\varepsilon). \quad (5)$$

One can easily show that the matrix element of the scattering matrix S corresponding to a transition from a state with phonon momentum $\mathbf{k}_0$ and total exciton momentum $\mathbf{P}_0$ to a state k,P is equal to (see references 8 and 9)

$$S_{nn} = 1 - 2\pi i\delta(E_i^{(n)} - E_f^{(n)})\, T, \quad (6)$$

where T is the following matrix:

$$T = \int d^3R \int d^3r \left(\Psi_f e^{-i\mathbf{kR}} V_k^* \frac{1}{H - E - \omega - i\varepsilon} e^{i\mathbf{k}_0\mathbf{R}} V_{k_0} \Psi_i\right) + \int d^3R \int d^3r \left(\Psi_f e^{i\mathbf{k}_0\mathbf{R}} V_{k_0} \frac{1}{H - E + \omega - i\varepsilon} e^{-i\mathbf{kR}} V_k^* \Psi_i\right) \quad (7)$$

In Eq. (7) Ψ_i and Ψ_f are the exact eigenfunctions of the initial and final states, ϵ is an infinitesimal quantity which leads to an outgoing wave in coordinate representation, $E_i^{(n)}$ and $E_f^{(n)}$ are the energies of the initial and final states*

$$E_i^{(n)} = P_0^2/2M^* + E_n = E, \quad (8)$$

E_n is the exciton energy in the n-th state. We shall use for the functionals Ψ_i and Ψ_f those obtained by Haken[2]†

$$\Psi_i = \exp\left\{ i\left(\mathbf{P}_0 - \sum_k \mathbf{k} a_k^+ a_k\right)\mathbf{R}\right\} U \psi_n(r)\, \Phi_0, \quad (9)$$

where

$$U = \exp\left(\sum_k a_k^+ f_k - a_k f_k^*\right), \quad a_k \Phi_0 = 0,$$

$$f_k(P) = -\gamma_k' \{\nu_2^{-1} e^{-i\mathbf{kr}\mu_2} - \nu_1^{-1} e^{i\mathbf{kr}\mu_1}\},$$

$$\nu_i = \left\{\omega + k^2\left(\frac{1}{2M} + \frac{\mu_i^2}{2M'}\right) - \frac{\mathbf{Pk}(1-\eta_i)}{M}\right\}. \quad (10)$$

*We have omitted from the expression for the energy an additive constant which is inessential for our problem.

†Haken considered the case $P = 0$ in the paper quoted.

The functions f_k and $\psi_n(r)$ satisfy the following equations

$$-\frac{1}{2M'}\nabla_r^2 f_k + \left(\omega + \frac{k^2}{2M} - \frac{\mathbf{Pk}}{M}(1-\eta_i)\right) f_k + V_k^* = 0,$$

$$\left\{-\frac{1}{2M'}\nabla_r^2 - \frac{e^2}{\varepsilon r} + \sum_k |f_k(0)|^2\left(\omega + \frac{k^2}{2M}\right) + \sum_k f_k(0) V_k + f_k^*(0) V_k^* + \frac{1}{2M'}\sum_k |\nabla f_k(0)|^2\right\}\psi_n = E_n\psi_n. \quad (11)$$

The functional (9) is obtained by assuming that $\psi_n(r)$ is a spherically symmetric function. If we evaluate the expectation value of the energy using the functional (9) and after that using the functional (1), it turns out that the value will be less in the latter case. The choice of the solution in the form (9) is thus the more correct one. The value of the renormalization constant η will be found below.

For small momenta P_0 which are different from zero there will only be the first term in (7). To evaluate this expression we take the terms depending on P_0 through the operator $(H - E - \omega)^{-1}$ and integrate over d^3R. We get as a result

$$S - 1 = -i(2\pi)^4 \delta(E_i - E_f)\, \delta(\mathbf{P}_0 + \mathbf{k}_0 - \mathbf{P} - \mathbf{k})\, Q, \quad (12)$$

where

$$Q = \int d^3r \langle \Phi_0\psi_n, \quad V_k^* U^{-1}(P) \frac{1}{\overline{H} - E - \omega - i\varepsilon} U(P_0) V_{k_0} \psi_n \Phi_0 \rangle,$$

$$\overline{H}(\mathbf{P}_0) = H(\mathbf{P}_0 + \mathbf{k}_0 - \sum_k \mathbf{k} a_k^+ a_k). \quad (13)$$

It is convenient to write the quantity Q as a sum of two terms $Q = Q_1 + Q_2$, corresponding to the two terms in (3):

$$Q_2 = \gamma_{k_0} \int d^3r \langle \Phi_0\psi_n, V_k^* U^{-1}(P) \times \frac{1}{\overline{H} - E - \omega - i\varepsilon} U(P_0)\, e^{i\mathbf{k}_0\mathbf{r}\mu_2}\psi_n \Phi_0 \rangle. \quad (14)$$

Q_1 is obtained from Q_2 by the substitution $\exp\{i\mathbf{k}_0\mathbf{r}\mu_2\} \to \exp\{-i\mathbf{k}_0\mathbf{r}\mu_1\}$. We shall consider the evaluation of Q_2.

We shall transfer the operator U from the right to the left. We must, of course, be careful when differentiating U, since ∇U does not commute with U. We shall use the general formula

$$\frac{d}{dx} e^{\varphi(x)} = e^{\varphi(x)} \left\{\varphi' + \frac{1}{2!}[\varphi', \varphi] + \frac{1}{3!}[[\varphi', \varphi], \varphi] + \ldots\right\}. \quad (15)$$

From (15) it follows that

$$\nabla U = U\left\{\sum_k \nabla f_k a_k^+ - \nabla f_k^* a_k + \tfrac{1}{2}\mathbf{j}_k\right\},$$

$$\mathbf{j}_k = f_k^* \nabla f_k - f_k \nabla f_k^*.$$

The expression div $\mathbf{j}_k$ can be rewritten in the form

$$-(1/2M')\,\mathrm{div}\,\mathbf{j}_k = \tfrac{1}{2}(f_k V_k - f_k^* V_k^*),$$

because of (11). The average value of div $\mathbf{j}_k$ eval-

uated over a spherically symmetric function tends to zero. We shall now transfer the factor $\exp\{i\mathbf{k}_0\mathbf{r}\mu_2\}$ in (14) from the right to the left. As a result of this we can write Q_2 in the form

$$Q_2 = \gamma_{k_0} \int d^3r \langle \Phi_0 \psi_n; V_k^* e^{i\mathbf{k}_0\mathbf{r}\mu_2} \frac{1}{H_0 + H_1 - E - \omega - i\varepsilon} \psi_n \Phi_0 \rangle. \quad (16)$$

Considering in the following the case of small momenta we have replaced $U^{-1}(P_f)U(P_0)$ by unity. This is permissible since the only expression where it is important that P be finite is the denominator in the integrand of (14), which can be studied separately. $H_0 = H_0^{(1)} + H_0^{(2)}$ is the following operator

$$H_0 = -\frac{1}{2M'}\nabla_r^2 - \frac{e^2}{n^2 r} + \sum_k V_k f_k + V_k^* f_k^* + \sum_k |f_k|^2 \left(\omega - \frac{\mathbf{kP}_0}{M} + \frac{k^2}{2M}\right) + \frac{1}{2M'}\sum_k |\nabla f_k|^2 + \sum_k \omega a_k^+ a_k + \frac{1}{2M}\left(\mathbf{P}_0 - \sum_k \mathbf{k} a_k^+ a_k\right)^2 + \frac{k_0^2}{2M} + \frac{k_0^2}{2M'}\mu_2^2 + \frac{1}{M}\left(\mathbf{P}_0\mathbf{k}_0 - \sum_k (\mathbf{kk}_0) a_k^+ a_k\right) + \frac{1}{M}\sum_k \mathbf{k} a_k^+ a_k \sum_k \mathbf{k} |f_k|^2 - \frac{1}{M}\sum_k (\mathbf{kk}_0) |f_k|^2 + \frac{1}{2M}\left(\sum_k \mathbf{k} |f_k|^2\right)^2. \quad (17)$$

The splitting up of the operator H_0 into $H_0^{(1)}$ and $H_0^{(2)}$ is done as follows. Each of the last three terms in (17) can be written as a sum of two terms: the first which is independent of r must be assigned to $H_0^{(1)}$, and the second one to $H_0^{(2)}$. In the other terms $f_k = f_k(P)$ and $|f_k(P)|^2$ must be expanded in power series in P, while $f_k(O)$, and $|f_k(O)|^2$ must be assigned to $H_0^{(1)}$. Terms quadratic in P can in turn be split into two parts; terms which do not contain an r-dependence are assigned to $H_0^{(1)}$, and the rest to $H_0^{(2)}$; it turns out that the latter are unimportant in the following. Let us, for instance consider the expression

$$\sum_k \mathbf{k} |f_k|^2 = \sum_k \mathbf{k} |\gamma_k|^2 \{\nu_1^{-2} + \nu_2^{-2} - \nu_1^{-1}\nu_2^{-1}(e^{ikr} + e^{-ikr})\}. \quad (18)$$

If we make the transition from a summation to an integration between infinite limits, the first two terms in (18) give

$$(2\pi)^{-3}\int \mathbf{k} |\gamma_k|^2 (\nu_1^{-2} + \nu_2^{-2})\, d^3k = \frac{\alpha(m)}{6}(1-\eta)\left\{\left(\frac{m_1}{m}\right)^{1/2}\frac{m_1}{M} + \left(\frac{m_2}{m}\right)^{1/2}\frac{m_2}{M}\right\} \quad (19)$$

Similarly, up to terms of $O(P^4)$

$$\sum_k |f_k(P)|^2 (\omega - \mathbf{kP}/M + k^2/2M) = \sum_k f_k(0)|^2 (\omega + k^2/2M) + 3(1-\eta)^2 M^{-2} \sum_k |\gamma_k|^2 (\mathbf{kP})^2 (\omega + k^2/2M)(\nu_1^{-4}(0) + \nu_2^{-4}(0)) - 2(1-\eta) M^{-2} \sum_k |\gamma_k|^2 (\mathbf{kP})^2 (\nu_1^{-3}(0) + \nu_2^{-3}(0)) + \text{terms depending upon the spatial coordinates.}$$

Taking away the terms quadratic in the momentum we get, apart from an additive constant,

$$H_0^{(1)} = -\frac{1}{2M'}\nabla_r^2 + W(r) + \frac{P_0^2}{2M_1^*} + \sum_k a_k^+ a_k \left(\omega - \frac{\mathbf{kP}_0}{M^*} - \frac{\mathbf{kk}_0}{M}\right) + \frac{k_0^2}{2M} + \frac{k_0^2}{2M'}\mu_2^2 + \frac{\mathbf{k}_0\mathbf{P}_0}{M^*} + \frac{1}{2M}\left(\sum_k \mathbf{k} a_k^+ a_k\right)^2, \quad (20)$$

where

$$W(r) = -\frac{e^2}{n^2 r} + \frac{1}{2M'}\sum_k |\nabla f_k|^2 + \sum_k |f_k|^2 \left(\omega + \frac{k^2}{2M}\right) + \sum_k f_k V_k + f_k^* V_k^*.$$

If $m_1 = m_2$, the potential W(r) is of the form[3,4]

$W(r) = -e^2/\varepsilon r - (1/n^2 - 1/\varepsilon) r^{-1} \exp(-r\sqrt{2m\alpha})$.

From (19) we have

$$M^{*-1} = M^{-1}\{1 - 1/6\,\alpha(m)(1-\eta)[(m_1/m)^{1/2} m_1/M + (m_2/m)^{1/2} m_2/M]\}. \quad (21)$$

The mass M_1^* is somewhat different from M^*.

Let us consider the operator $H_I = H_I^{(1)} + H_I^{(2)}$.

$$H_I^{(1)} = -\frac{1}{2M'}\sum_{k,k'} \{\nabla f_k \nabla f_{k'} a_k^+ a_{k'} - 2\nabla f_k \nabla f_{k'}^* a_k^+ a_{k'} + \nabla f_k^* \nabla f_{k'}^* a_k a_{k'}\} + \frac{1}{2M}\sum_{k,k'} (\mathbf{kk}')\{f_k f_{k'} a_k^+ a_{k'}^+ + 2 f_k f_{k'}^* a_k^+ a_{k'} + f_k^* f_{k'} a_k a_{k'}^+ + f_k^* a_k^+ a_{k'} a_{k'} + f_{k'} a_k^+ a_{k'}^+ a_k\} - \frac{1}{M}\sum_k (\mathbf{kk}_0)(a_k f_k^* + a_k^+ f_k) - \frac{1}{M'}\sum_k (\nabla f_k a_k^+ - \nabla f_k^* a_k)\nabla - \frac{i\mu_2}{M'}\mathbf{k}_0 \sum_k \nabla f_k a_k^+ - \nabla f_k^* a_k - \frac{1}{M'}\sum_k (\nabla f_k a_k^+ - \nabla f_k^* a_k) \times \sum_{k'} \mathbf{j}_{k'} - \frac{1}{2M'}\sum_k \nabla^2 f_k a_k^+ - \nabla^2 f_k^* a_k + \sum_k a_k^+ \left\{V_k^* + f_k\left(\omega - \frac{\mathbf{P}_0\mathbf{k}}{M} + \frac{k^2}{2M}\right) + \frac{\mathbf{k}}{M}\sum_{k'} \mathbf{k}' |f_{k'}|^2\right\} + \sum_k a_k \left\{V_k + f_k^*\left(\omega - \frac{\mathbf{P}_0\mathbf{k}}{M} + \frac{k^2}{2M}\right) + \frac{\mathbf{k}}{M}\sum_{k'} \mathbf{k}' |f_{k'}|^2\right\},$$

$$H_I^{(2)} = -\frac{1}{2M'}\sum_k \operatorname{div} \mathbf{j}_k - \frac{1}{2M'}\left(\sum_k \mathbf{j}_k\right)^2 - \frac{1}{M'}\sum_k \mathbf{j}_k \nabla - \frac{i\mu_2}{M'}\mathbf{k}_0 \sum_k \mathbf{j}_k - \frac{i\mu_2}{M'}(\mathbf{k}_0\nabla). \quad (22)$$

Using the equation for the function f_k we can write the last three sums in the expression for $H_I^{(1)}$ in

the following form:

$$\frac{1}{M}\sum_k \gamma_k k^2 a_k \{e^{i\mathbf{k}r_1}\nu_2^{-1}\mu_2^2 + e^{-i\mathbf{k}r_2}\nu_1^{-1}\mu_1^2\} = \sum_k \delta_k a_k. \quad (23)$$

We shall show in the following that one can neglect the term $\Sigma\mathbf{k}|\gamma_k|^2\nu_1^{-1}\nu_2^{-1}e^{\pm i\mathbf{k}\mathbf{r}}a_k$ in (22). Let us now turn to Eq. (16). For the evaluation of the matrix element we shall follow Low and Pines[10] and introduce a functional Ψ by

$$c\Psi = (H_0^{(1)} + H_0^{(2)} + H_I - E - \omega - i\varepsilon)^{-1}\psi_n\Phi_0, \quad (24)$$

which satisfies the following integral equation

$$\Psi = \psi_n\Phi_0 - (H_0^{(1)} - E - \omega - i\varepsilon)^{-1}(H_0^{(2)} + H_I)\Psi,$$

$$c^{-1} = k_0^2/2M + k_{0'}^2\mu_2^2/2M' + \mathbf{k}_0\mathbf{P}_0/M^* - \omega. \quad (25)$$

Putting $\Psi = u(\mathbf{r})\Phi_0 + \Sigma_{\mathbf{k}} v_{\mathbf{k}}(\mathbf{r})\, a_{\mathbf{k}}^+\Phi_0$ we can obtain the following set of integro-differential equations for the functions u(r) and v(r):

$$\mathcal{H}_0 u + \frac{1}{c}u = \frac{1}{c}\psi_n + \frac{1}{M}\sum_k (\mathbf{k}\mathbf{k}_0) f_k^* v_k - i\frac{\nu_2}{M'}\sum_k \mathbf{k}_0 \nabla f_k^* v_k$$
$$- \frac{1}{M'}\sum_k \nabla f_k^* \nabla v_k - \frac{1}{M'}\sum_k \mathbf{j}_k \nabla f_k^* v_k - H_I^{(2)} u$$
$$- \langle\Phi_0, H_0^{(2)}\Phi_0\rangle u - \sum_k \delta_k v_k, \quad (26)$$

$$\mathcal{H}_0 v_k + \Delta E v_k = \frac{1}{M}u(\mathbf{k}\mathbf{k}_0) f_k + \frac{1}{M'}\nabla f_k \nabla u + \frac{1}{M'}u\nabla f_k \sum_{k'}\mathbf{j}_{k'}$$
$$+ i\frac{\nu_2}{M'}u\mathbf{k}_0\nabla f_k - H_1^{(2)} v_k - \langle a_k^*\Phi_0,\ H_0^{(2)} a_k^+\Phi_0\rangle v_k$$
$$- \frac{1}{M} f_k \mathbf{k}\sum_{k'}\mathbf{k}' f_{k'}^* v_{k'} - \frac{1}{M'}\nabla f_k \sum_{k'}\nabla f_{k'}^* v_{k'}, \quad (27)$$

where

$$\mathcal{H}_0 = -\nabla_r^2/2M' + W(r) - E_n;$$

$$\Delta E = k_0^2/2M + k_{0'}^2\mu_2^2/2M' + k^2/2M$$
$$- \mathbf{k}\mathbf{k}_0/M + \mathbf{P}_0(\mathbf{k}_0 - \mathbf{k})/M^* - i\varepsilon. \quad (28)$$

Let us consider the case of most interest, when the effective masses of the electron and of the hole are the same. From (18) and (17),

$$\langle a_k^+\Phi_0,\ H_0^{(2)} a_k^+\Phi_0\rangle = -\frac{1}{M}(\mathbf{k} - \mathbf{k}_0)\sum_{k'}\mathbf{k}' v_{k'}^{-2}(P_0)\, 2\cos\mathbf{k}'\mathbf{r}.$$

If we write the function $v_{\mathbf{k}}$ as $v_{\mathbf{k}} = \exp(-i\mathbf{k}\mathbf{r}/2)\, v_{\mathbf{k}}^{(1)}$, we get for u and $v_{\mathbf{k}}^{(1)}$ the following equations

$$\mathcal{H}_0 u + \frac{1}{c}u = \frac{1}{c}\psi_n - \frac{1}{m}\sum_k (\mathbf{k}\mathbf{k}_0)\varphi_k v_k^{(1)}$$
$$- \frac{1}{M'}\sum_k (\nabla f_k^*)(\nabla e^{-i\mathbf{k}r/2} v_k^{(1)}) + \frac{i}{2M'}(\mathbf{k}_0\nabla)u - \sum_k \delta_k v_k, \quad (26a)$$

$$\mathcal{H}_0 v_k^{(1)} + \frac{i}{m}(\mathbf{k} - \mathbf{k}_0)\nabla v_k^{(1)} + \Delta E^{(1)}(\mathbf{P}_0) v_k^{(1)}$$
$$- \frac{1}{M}(\mathbf{k} - \mathbf{k}_0)\sum_{k'}\mathbf{k}' v_{k'}^{-2}(P_0)\, 2\cos\mathbf{k}'\mathbf{r}\, v_k^{(1)} = -\frac{u}{m}(\mathbf{k}\mathbf{k}_0)\varphi_k^*$$
$$- \frac{1}{M'}(1 - e^{-i\mathbf{k}\mathbf{r}})\varphi_k^*(i\mathbf{k}\nabla u)$$
$$- \frac{1}{m}\varphi_k^*\mathbf{k}\sum_{k'}\mathbf{k}'\varphi_{k'}(1 + \exp(i\mathbf{r}(\mathbf{k} - \mathbf{k}'))) v_{k'}^{(1)}, \quad (27a)$$

where

$$\varphi_k = \gamma_k(\omega + k^2/2m)^{-1},$$

$$\Delta E^{(1)}(\mathbf{P}_0) = (\mathbf{k}_0 - \mathbf{k})^2/2m + (\mathbf{P}_0/M^*)(\mathbf{k}_0 - \mathbf{k}) - i\varepsilon. \quad (28a)$$

One can neglect the P_0 dependence of the functions φ_k for small P_0.

We shall expand the functions u and $v_{\mathbf{k}}^{(1)}$ in terms of a complete set of functions of the operator $\mathcal{H}_0$:

$$u = \sum_n a_n\psi_n, \qquad v_{\mathbf{k}}^{(1)} = \sum_n b_{nk}\psi_n. \quad (29)$$

Since at large distances the potential W(r) behaves like $-e^2/\epsilon r$ we can take for the exciton wave functions ψ_n for the states with n = 2,3,4,... hydrogen functions, taking the radius of the Bohr orbit to be equal to ϵ/me^2. If we substitute, for the zeroth approximation, $u = a_n\psi_n$ into the right hand side of (27a), it is clear that the coefficient b_n will be the main one. Multiplying the left and right hand side of (27a) by ψ_n and integrating over the coordinates we obtain an equation for the coefficient b_{nk}. The magnitude of the renormalized exciton mass will then be determined by the expression

$$\mathbf{P}_0/M_n^* = \mathbf{P}_0/M - \frac{1}{M}\sum_k \mathbf{k}\,|\gamma_k|^2(2\nu_k^{-2}(\mathbf{P}_0)$$
$$- 2\nu_k^{-2}(\mathbf{P}_0)\langle n|\cos\mathbf{k}\mathbf{r}\,|n\rangle).$$

One can show (see Appendix) that $\langle n|\exp(\pm i\mathbf{k}\mathbf{r})|n\rangle$ tends to zero as $n \to \infty$. The limiting value of M_n^* will thus be equal to M^*. It is, on the other hand, obvious that for large quantum numbers the electron and the hole move so slowly that they have time to polarize not only the atomic shells, but also to shift the ions. For large n the exciton mass must therefore be equal to twice the polaron mass. The latter is, for instance, in the Lee, Low, and Pines approximation[11] connected with the coupling constant α by the relation $m^* = m(1 + \alpha/6)$ so that the parameter η in (9) and (19) will be equal to $\eta = (\alpha/6)(1 + \alpha/6)^{-1}$. We shall consider the solution of Eqs. (26a) and (27a) in the limiting cases of large and small quantum numbers n.

In the case of large n the quantity $\langle n|\exp(\pm i\mathbf{k}\mathbf{r})|n\rangle$ can be considered to be small compared to unity. The equations for the coefficients a_n and b_{nk} take the form

$$a_n = 1 - \frac{c}{m}\sum_k (\mathbf{k}\mathbf{k}_0)\varphi_k b_{kn}, \quad (26b)'$$

$$\Delta E_n^{(1)} b_{nk} = -\frac{a_n}{m}(\mathbf{k}\mathbf{k}_0)\varphi_k^* - \frac{1}{m}\varphi_k^*\mathbf{k}\sum_{k'}\mathbf{k}'\varphi_{k'} b_{nk'}. \quad (27b)$$

The solution of this set of equations is of the form*

$$cu_n = \left(\frac{k_0^2}{2m}\frac{1 - I}{1 + I} - \omega\right)^{-1}\psi_n,$$

$$I = \sum_k (\mathbf{k}\mathbf{k}_0)^2 |\varphi_k|^2 m\Delta E^{(1)}(P_0) = I_1 + iI_2, \quad (31)$$

*The P_0 dependence is only contained in $\Delta E^{(1)}(P_0)$.

where I_2 is proportional to P_0,

$$I_2 = \frac{2\alpha\omega^2}{(2m\omega)^{1/2}(\omega + k^2/2m)^2}\frac{m}{M_n^*}P_0.$$

The required matrix element Q is thus equal to

$$Q = Q_1 + Q_2 = |\gamma_{k_s}|^2\left(\frac{k_0^2}{2m}\frac{1-l}{1+l} - \omega\right)^{-1}\rho_n(k_0), \quad (32)$$

where

$$\rho_n(k_0) = |\gamma_{k_s}|^{-2}\int |\psi_n(r)|^2 |V_{k_s}(r)|^2 d^3r. \quad (33)$$

The first factor in (32) has the same form as the amplitude for the scattering of a phonon by a polaron[10] while the factor $\rho_n(k_0)$ plays the role of a form factor.

Integrating (13) over the final state and over the initial phonon momentum k_0 we get the following expression for the scattering probability $1/\tau$ per unit time

$$\frac{1}{\tau} = \frac{M_n^*}{8\pi^4}P_0\int |\gamma_{k_s}|^4\rho_n^2(k_0)e^{-\omega/kT}\left|\frac{k_0^2}{2m}\frac{1-l}{1+l} - \omega\right|^{-2} d^3k_0. \quad (34)$$

The factor $\exp(-\omega/kT)$ gives the volume dependence of the number of phonons on the temperature T. For small P_0 we get by using the well known limit $\lim \epsilon/(x^2+\epsilon^2) = \pi\delta(x)$

$$\frac{1}{\tau} = \left(\frac{M_n^*}{M}\right)^2 2\alpha\omega\, f(\alpha)\, e^{-\omega/kT}(2\rho_n(k_0))^2, \quad (35)$$

where $f(\alpha)$ is a slowly changing function of α, the value of which was given in reference 10. The mean free path l is connected with $1/\tau$ through the relation $l = v\tau$ where v is the exciton velocity.

We shall now consider the exciton ground state. The exciton dimensions in the ground state are several times less than the characteristic length $\bar{k}^{-1} = (2m\omega)^{-1/2}$; if we take the wave function in the form $\psi_0(r) = (\pi r_0^3)^{-1/2}\exp(-r/r_0)$ the constant r_0 must then satisfy the inequality $\bar{k}r_0 < 1$. Taking this inequality into account one can put

$$\langle\psi_0|\exp(\pm ir(\mathbf{k}-\mathbf{k}'))|\psi_0\rangle = 1 + O(\bar{k}^2 r_0^2),$$

and the equations for the coefficients a_0 and b_{0k} take the form

$$a_0 = 1 - \frac{c}{m}\sum_k (\mathbf{k}\mathbf{k}_0)\varphi_k b_{0k},$$

$$\Delta E_0 b_{0k} = -\frac{a_0}{m}(\mathbf{k}\mathbf{k}_0)\varphi_k^* - \frac{2}{m}\varphi_k^*\mathbf{k}\sum \mathbf{k}'\varphi_{k'}b_{0k'}. \quad (36)$$

From (36) we get

$$cu_0 = (k_0^2/2m(1+2l) - \omega)^{-1}\psi_0. \quad (37)$$

The renormalized exciton mass is in the case of the ground state up to terms of $O(r_0^2\bar{k}^2)$ equal to the unrenormalized one according to (30). This result corresponds to the intuitive feeling that in the ground state both particles move "fast" and they do not have time to shift the average positions of the neighboring ions. The function $\rho(k_0)$ can for the ground state be approximately replaced by $r_0^2k_0^2$. Calculations analogous to the foregoing ones lead to the following value of $1/\tau$:

$$1/\tau = 2\alpha\omega e^{-\omega/kT}4(k_r r_0)^4/\varphi(\alpha), \quad (38)$$

where

$$\varphi(\alpha) = (1+x_r^2)\{1/x_r - x_r^{-2}\partial I_1/\partial x_r\}, \quad (39)$$

x_r is the root of the equation

$$x_r^2 = 1 + 2I_1(x_r), \qquad x = k_0/\sqrt{2m\omega}. \quad (40)$$

The root of Eq. (40) is close to unity so that when we estimate the order of smallness of different terms we can—as we did in the foregoing—substitute instead of k_r the value $\bar{k}$. The function $\varphi(\alpha)$ is close to unity and changes slowly with α.

Representing the crystal as a continuous medium and assuming the mass to be isotropic is, of course, crude for a consideration of the exciton ground state.[12]

Nevertheless, for a qualitative description of the character of the interaction of an exciton in the ground state with the crystalline lattice, the Wannier-Mott model can be useful. According to Zhilich's calculations[13] the wave function of an electron forming an exciton state has its main maximum at a distance of approximately 4.3 atomic units from the central oxygen ion O^{--} in a Cu_2O crystal. This means that the electron moves essentially at the boundaries of the four copper ions which are the nearest neighbors of O^{--}. If we use an approximate representation for the electron and the hole the main part of their interaction will be described by a potential $-e^2/n^2r$, where the refractive index n takes into account the polarization of the copper atoms. The potential W(r) considered above behaved for small r just like $-e^2/n^2r$. When r_0 is decreased the exciton is by and large more and more a neutral system, and the probability for collision with a phonon will according to (38) decrease fast.

For excitons with large radii the mean free path is of the same order of magnitude as the polaron mean free path.

This result is explained by the fact that the electron and the hole polarize the crystal individually [the function U in (9) depends on the spatial coordinates]. Even though the exciton is an electrically neutral system, it deforms the lattice none the less, even if $m_1 = m_2$, and the phonons are scattered by the deformed lattice. The usual per-

turbation theory is not able to take this effect correctly into account which for $m_1 = m_2$ also leads to an infinitely large mean free path.

In conclusion I express my sincere gratitude to Academician V. A. Fock for a discussion of the present paper.

APPENDIX

We shall consider the evaluation of the integral $J_n(k) = \langle n|\exp i\mathbf{kr}|n\rangle$, where $|n\rangle$ is a spherically symmetric function of the discrete hydrogen atom spectrum

$$|n\rangle = NL_n^{(1)}(\rho)e^{-\rho/2}, \quad \rho = 2r/na, \quad a = \hbar/me^2.$$

Using the integral representation of the Laguerre polynomials

$$L_n(\rho) = \frac{1}{2\pi i}\oint_C u^{-n-1}(1+u)^n e^{-\rho u}\,du,$$

where the contour C encloses the coordinate origin, we can perform first of all the integration over the spatial coordinates

$$J_n(k) = N^2\pi a^3 \frac{1}{2\pi i}\oint u^{-n}(1+u)^n\,du$$

$$\times \frac{1}{2\pi i}\oint v^{-n}(1+v)^n \frac{u+v+1}{[(u+v+1)^2+k_n^2]^2}\,dv,$$

$k_n = kan/2$.

The integration over dv is easily performed if the integration contour is pulled towards the poles of the function $[(u+v+1)^2 + k_n^2]^{-2}$. A change of variables $u = ik_n t/(t-1-ik_n)$ reduces the integral over du to a hypergeometric function

$$J_n(k) = \frac{(-1)^{n+1}}{4ik_n}(1+k_n^2)^{-n-1}\{(1+ik_n)^{2n} - (1-ik_n)^{2n}\}$$

$$\times F(1-n, 1+n, 2; (1+k_n^2)^{-1}).$$

As $n\to\infty$ the function $J_n(k)$ tends to zero. If we expand $J_n(k)$ in a power series in k we can obtain from the expression given here the well known equations for $\overline{r^2}$, $\overline{r^4}$, and so on.

[1] S. I. Pekar, Исследования по электронной теории кристаллов (Investigations on the Electron Theory of Crystals) M., Gostekhizdat, 1951 [Untersuchungen über die Elektronentheorie der Kristalle, Akademieverlag, Berlin, 1954].

[2] H. Haken, Z. Physik **146**, 527 (1956); Fortschr. Physik **6**, 271 (1958).

[3] E. F. Gross, Vestn. Akad. Nauk SSSR **10**, 11 (1958); Usp. Fiz. Nauk **63**, 575 (1957).

[4] A. V. Tulub, J. Exptl. Theoret. Phys. (U.S.S.R.) **34**, 1641 (1958), Soviet Phys. JETP **7**, 1127 (1958).

[5] H. Haken, Z. Naturf. **11a**, 875 (1956).

[6] A. I. Ansel'm and Yu. A. Firsov, J. Exptl. Theoret. Phys. (U.S.S.R.) **28**, 151 (1955), Soviet Phys. JETP **1**, 139 (1955); J. Exptl. Theoret. Phys. (U.S.S.R.) **30**, 719 (1956), Soviet Phys. JETP **3**, 564 (1956).

[7] H. J. G. Meyer, Physica **22**, 109 (1956); A. V. Tulub, Вестник ЛГУ (Bull. Leningr. State Univ.) **4**, 53 (1957); I. P. Ipatova, J. Tech. Phys. (U.S.S.R.) **26**, 2787 (1956), Soviet Phys. Tech. Phys. **1**, 2692 (1957).

[8] F. E. Low, Phys. Rev. **97**, 1392 (1955).

[9] G. F. Chew and F. E. Low, Phys. Rev. **101**, 1570 (1956).

[10] F. E. Low and D. Pines, Phys. Rev. **98**, 414 (1955).

[11] Lee, Low, and Pines, Phys. Rev. **90**, 297 (1953).

[12] W. R. Heller and A. Marcus, Phys. Rev. **84**, 809 (1951).

[13] A. G. Zhilich, Вестник ЛГУ (Bull. Leningr. State Univ.) **4**, 31 (1957).

Translated by D. ter Haar
372

AN INVESTIGATION OF THE SUPERFLUID STATE OF AN ATOMIC NUCLEUS

V. G. SOLOV'EV

Joint Institute for Nuclear Research

Submitted to JETP editor January 3, 1959

J. Exptl. Theoret. Phys. (U.S.S.R.) 36, 1869-1874 (June, 1959)

The variational principle proposed by N. N. Bogolyubov and the physical ideas and mathematical methods developed in the theory of superconductivity are applied to a study of the properties of a heavy nucleus. Using the nuclear shell model we consider the residual interactions of nucleons in an outer shell; this leads to the appearance of a superfluid state of the nucleus. We have evaluated the energy of the superfluid ground state and those of a number of excited states both in the case of an even and in the case of an odd number of nucleons in the shell. We found some regularities in the level spectrum of even-even nuclei and of odd A nuclei.

Changes in the nuclear ground state energy were evaluated for the case where the number of outer shell nucleons was changed by one; this made it possible to conclude that even-even nuclei are more stable than odd-odd nuclei as regards β decay, which agrees numerically with von Weizsäcker's semi-empirical formula. The results obtained depend little on the nuclear model chosen, and they are also valid for highly deformed nuclei.

A certain similarity between the properties of the Fermi-systems in a nucleus and in a metal makes it possible to apply the physical ideas and mathematical methods developed in the theory of superconductivity[1] to a study of nuclear matter and of a finite nucleus.[2-7] Belyaev[6] and the author[5,7] have used the nuclear shell model to show that the interactions between the outer shell nucleons lead to a superfluid nuclear state (a state energetically lower than the one with a completely degenerate Fermi-gas).

In the present paper we continue the study of the superfluid nuclear state and, in particular, the energies of the excited states of shells both with an even and with an odd number of nucleons will be evaluated and the problem of the stability of nuclear isobars as regards β decay will be considered.

1. THE SUPERFLUID GROUND STATE

We shall investigate the superfluid state of an atomic nucleus using a new variational principle proposed by Bogolyubov[8] which is a generalization of Fock's well-known method.[9]

We take the following model of a heavy nucleus: the nucleons which form the inner shells produce a central-symmetrical field which is somewhat distorted by the outer shell nucleons. Let us consider the residual interactions between the nucleons (protons or neutrons) which are in the outer nuclear shells. We shall characterize the nucleon state by a set of quantum numbers s and by the quantum number m of the total angular momentum component along the symmetry axis of the nucleus.

Let us consider the residual interactions of nucleons which are in the immediate vicinity of the energy of the Fermi surface with a Hamiltonian

$$H = \sum' (E(s,m) - \lambda)\, a_{m\rho}(s)^+ a_{m\rho}(s) + \frac{1}{4}\sum' J(s_1, s_2 s_1', s_2' | \rho_1 m_1, \rho_2 m_2; \rho_1' m_1', \rho_2' m_2')\, a_{m_1\rho_1}(s_1)^+ \times a_{m_2\rho_2}(s_2)^+ a_{m_2'\rho_2'}(s_2') a_{m_1'\rho_1'}(s_1'). \quad (1)$$

The summation is here carried out over all values of all numbers s, s_1, s_2, ..., over positive values of the numbers m, m_1, m_2, ... and over the values ± 1 of the numbers ρ which characterize the sign of m, where

$$\rho_1 m_1 + \rho_2 m_2 = \rho_1' m_1' + \rho_2' m_2', \qquad \rho_1 m_1 \neq \rho_1' m_1';$$

$a_{m\rho}(s)^+$, $a_{m\rho}(s)$ are the creation and annihilation operators for the nucleons; E(s, m) is the energy of a nucleon in the outer shell in an s, m state; λ is a parameter which plays the role of the chemical potential and which is determined from the condition

$$n = \sum_{s,m,\rho}' \overline{a_{m\rho}(s)^+ a_{m\rho}(s)}. \quad (2)$$

We shall, morevoer, perform a linear canonical transformation of the Fermi amplitudes, as in references 5 and 7

$$a_{m\rho}(s) = u_m(s)\, \alpha_{m,-\rho}(s) + \rho v_m(s)\, \alpha_{m\rho}(s)^+, \quad (3)$$

we shall define a new vacuum state $\alpha_{m\rho}(s)\,\Psi = 0$, and

find the average value of the energy operator $\overline{H}$ over this state. We shall determine $u_m(s)$, $v_m(s)$ from requiring $\overline{H}$ to be a minimum, and as a result we get the following equation

$$C_m(s) = -\frac{1}{2}\sum_{s',m'} J(s,s'\,|\,m,-m;m',-m') \times C_{m'}(s')/\sqrt{C_{m'}(s')^2+\xi_{m'}(s')^2} \tag{4}$$

where

$$C_m(s) = \sum_{s'm'} J(s,s'\,|\,m,-m;m',-m')u_{m'}(s')v_{m'}(s'), \tag{5}$$

$$\xi_m(s) = E(s,m) - \lambda - {}^1\!/_2 \sum_{s'm'}\{J(s,s';\,s',s\,|\,m,m';m',m) + J(s,s';s',s\,|\,m,-m',-m',m)\}v_{m'}(s')^2, \tag{6}$$

$$\varepsilon(s,m) = \sqrt{C_m(s)^2+\xi_m(s)^2},$$

$$J(s,s;s',s'\,|\,\ldots) \equiv J(s,s'\ldots).$$

We note that if the total angular momentum j is a good quantum number we only need sum over m′ in (4). The trivial solution of (4) $C_m(s) = 0$ corresponds to the state of the completely degenerate Fermi gas. It was shown in references 4 and 7 that it is necessary that $J < 0$ for energies near the Fermi surface in order that there be a non-trivial solution of (4).

In reference 5 we obtained the asymptotic solution of (4) (as $J \to 0$) and showed that the interactions of nucleons with equal and opposite angular momentum components along the symmetry axis of the nucleus play the leading part. In references 6 and 7 solutions of (4) were found assuming that $J(s,s'|m,-m;m',-m')$ did not depend on s, s′, m; m′, and it was shown that in this crude approximation the main properties of the asymptotic solution were retained.

Let us consider the approximation

$$J = \text{const}, \quad \rho = \text{const}, \tag{7}$$

i.e., J and the level density $\rho(E)$ do not depend on E.

We can neglect the interactions of nucleons with different m, s since it was shown in reference 5 that they will give a small correction which can be evaluated by perturbation theory. We have then

$$\xi_m(s) = E(s,m) - \lambda.$$

The energy of nucleons in the outer shell is in the neighborhood of the Fermi surface, i.e.,

$$E_F - \delta \leqslant E(s,m) \leqslant E_F + \Delta.$$

We go over in (4) from a sum to an integral and get

$$C_m(s) = -\frac{1}{2}\int_{E_F-\delta}^{E_F+\Delta} dE'\rho(E')J(s\,s'\,|\,m,-m;m',-m') \times C_{m'}(s')/\sqrt{C_{m'}(s')^2+(E-\lambda)^2}, \tag{4'}$$

where λ is determined from the equation

$$n = \int_{E_F-\delta}^{E_F+\Delta} dE\,\rho(E)\{1-(E-\lambda)/\sqrt{C_m(s)^2+(E-\lambda)^2}\}. \tag{8}$$

In the approximation (7) the solutions of (4′) and (8) will be found in the following form

$$C = \frac{\sqrt{(2\Omega-n)n}}{\rho(e^{2/G}-1)}e^{1/G}, \tag{9}$$

$$E_F - \lambda = \frac{\Omega-n}{\rho(e^{2/G}-1)} + \delta - \frac{n}{2\rho}, \tag{10}$$

where $G = -\overline{\rho}\,\overline{J}$, n is the number of nucleons, and Ω the number of levels in the outer nuclear shell. In the approximation

$$G \gg 1, \quad |E_{max} - E_{min}| \ll \Omega G/2\rho \tag{11}$$

we have

$$\varepsilon \approx \Omega G/2\rho. \tag{12}$$

We note that if j is a good quantum number the form of Eqs. (9)—(12) remains the same, but ρ, n, and Ω refer to levels with a given value of j.

2. EXCITED STATES

We shall calculate the energy of the excited nuclear states, taking into account the interaction of the nucleons in the outer shell. It is well known that the wave function Ψ of the new vacuum state is a superposition of states with an even number of nucleons; in this connection the wave function of the ground state of a system with an odd number of particles is $\alpha_{m\rho}(s)^+\Psi$.

We shall evaluate the energy of the excited states of a shell with an even number of nucleons in it. The difference ΔE^1 between the energy of the first excited state $\alpha_{m+}(s)^+\alpha_{m-}(s)^+\Psi$ and that of the superfluid ground state Ψ is of the form

$$\Delta E^1 = 2\varepsilon(s,m). \tag{13}$$

The addition to (13) is small in the case of different values of s and m. The first excited state is thus in shells with an even number of nucleons separated by a gap from the ground state, and then there follows a number of levels with successively increasing spin values which are lying close to one another. We shall investigate the problem of the further sequence

of excited states of the form*

$$\alpha_{m_1\rho_1}(s_1)^+ \alpha_{m_2\rho_2}(s_2)^+ \alpha_{m_3\rho_3}(s_3)^+ \alpha_{m_4\rho_4}(s_4)^+ \Psi.$$

We shall therefore evaluate the difference ΔE^{II} between excited states of such a kind and excited states $\alpha_{m-}(s)^+ \alpha_{m+}(s)^+ \Psi$, namely

$$\Delta E^{II} = \varepsilon(s, m) + \varepsilon(s', m') + 2\frac{C_{m'}(s')\, C_m(s)}{\varepsilon(s', m')\, \varepsilon(s, m)} J(s, s' \mid m, -m; m', -m'). \quad (14)$$

In the approximations of (7) and (11), Eq. (14) is appreciably simplified

$$\Delta E^{II} \approx \frac{G}{\rho}\left(\Omega - 2\frac{(2\Omega - n)\, n}{\Omega^2}\right). \quad (14')$$

Terms which lead to a decrease of ΔE^{II} in the approximation (7), (11) are relatively small, the greatest decrease of ΔE^{II} arising when the levels of the shell are half filled.

We have thus the following picture of the excited states of even-even nuclei: the first excited state is separated from the ground state by a distinctly expressed gap, there follow then a number of excited states with successively increasing spin values, after which there occur levels with small spin values corresponding to the break-up of a second pair, and the lowest of these is separated by ΔE^{II} from the first excited state. Levels with high spin values may not show up experimentally and it may thus look as if there is a second gap. For energies larger than the ground state energy by $\Delta E^{I} + \Delta E^{II}$ the level density must at least increase appreciably.

We shall now calculate the energies of the excited states of a shell with an odd number of nucleons. The ground state wave function is $\alpha_{m_0\rho_0}(s)^+ \Psi$ if $E(s_0, m_0) < E(s, m)$. When the system is excited it must go over from the state $\alpha_{m_0\rho_0}(s_0)^+ \Psi$ to a state $\alpha_{m_1\rho_1}\Psi$ where $E(s_1, m_1) > E(s_0, m_0)$, and so on, while the spins of the states will also increase. The more strongly excited states will be states of the form

$$\alpha_{m_1\rho_1}(s_2)^+ \alpha_{m_2\rho_2}(s_2)^+ \alpha_{m_1\rho_1}(s_1)^+ \Psi.$$

The difference ΔE between the energy of an excited state of this kind and the ground state energy will be obtained in the following form

$$\Delta E = \varepsilon(s, m) + \varepsilon(s', m') + \frac{C_{m'}(s')\, C_m(s)}{\varepsilon(s', m')\, \varepsilon(s, m)} J(s, s' \mid m, -m; m', -m'), \quad (15)$$

and in the approximations (7) and (11)

$$\Delta E \approx \frac{G}{\rho}\left\{\Omega - \frac{(2\Omega - n)\, n}{\Omega^2}\right\}. \quad (15')$$

We are thus led to the following picture in the case of odd nuclei: in the immediate neighborhood of the ground state there is a number of excited states with successively increasing spin values. If states with high spin values do not appear experimentally there will not be levels somewhat below the energy of the excited states of an even shell. Moreover, the level density must increase strongly.

It should be noted that in Bogolyubov's new variational principle[8] the form of the canonical transformation picks out the important part of the interaction in the Hamiltonian. In the case considered, the canonical transformation picks out the interactions of nucleons with equal and opposite values of the angular momentum component along the symmetry axis of the nucleus while the other quantum numbers are equal, if j is a good quantum number, and with arbitrary values of the other quantum numbers in the opposite case while the results depend very little on the actual values of the other quantum numbers and thus also on the details of the nuclear model. It is therefore essential both for the results obtained earlier and for the results of the next section to distinguish the quantum number m from all other quantum numbers of the nucleons near the energy of the Fermi surface. The details of the nuclear model are thus inessential and the results obtained can therefore also be applied to the case of highly deformed nuclei.

3. THE STABILITY OF NUCLEAR ISOBARS AS REGARDS BETA DECAY

The fact that even-even nuclei are more stable against β decay than odd-odd nuclei is reflected in von Weizsäcker's semi-empirical formula for nuclear masses by the introduction of a term $\pm\delta/2A$, where the positive sign refers to the odd-odd isobar, and the negative one to the even-even one. We shall investigate the problem of how the stability of isobars, with regard to β decay, is influenced by taking the interaction of the nucleons in the outer nuclear shell into account. Let us calculate for this purpose the change in the ground state energy if the number of nucleons in the outer shell is changed by one. The difference in the energies of shells containing $2n_0 \pm 1$ and $2n_0$ nucleons is expressed as follows

$$\mathcal{E}(2n_0 \pm 1) - \mathcal{E}(2n_0) = \bar{H}(2n_0 \pm 1) - \bar{H}(2n_0) + \varepsilon(s, m). \quad (16)$$

In the approximations (7) and (11) this expression takes on a very simple form, namely,

*I express my sincere gratitude to Prof. B. S. Dzhelepov who drew my attention to the possibility of the appearance of a "second gap."

$$\mathcal{E}(2n_0+1)-\mathcal{E}(2n_0)=(\Omega-2n_0-{}^1/_2)/\rho\,(e^{2/G}-1), \quad (17)$$

$$\mathcal{E}(2n_0-1)-\mathcal{E}(2n_0)=(\Omega+2n_0-{}^1/_2)/\rho\,(e^{2/G}-1). \quad (17')$$

From (17) and (17') it is clear that the addition of one nucleon to an even shell does not change the energy of the shell appreciably, while, on the other hand, one needs to spend a considerable energy to take one nucleon away from an even shell. Moreover, the addition of one nucleon to an odd shell causes a considerable release of energy, while one needs spend only a small amount of energy to remove one nucleon from an odd shell.

If we determine G roughly from the magnitude of the gap in even-even nuclei and evaluate by using (17) and (17') the difference in mass of the even-even and odd-odd isobars, we obtain a rough numerical agreement with the experimental data as reflected in Weizsäcker's formula.

One can easily show that one can not reach any clear-cut conclusions from (17) and (17') about the relative stability of odd nuclei.

We have considered a rather idealized nuclear model and obtained a number of regularities which follow automatically from the properties of nuclear superfluidity. These regularities should be made more precise and concrete by using a more complicated nuclear model, by improving the approximation, and by comparison with the experimental data.

The investigations carried out in this paper and in references 3–7 confirm the fruitfulness of applying the physical ideas and mathematical methods developed in the theory of superconductivity to a study of the properties of the atomic nucleus.

In conclusion I express my sincere thanks to N. N. Bogolyubov and D. F. Zaretskiĭ for very interesting discussions.

[1] Bogolyubov, Tolmachev, and Shirkov, Новый метод в теории сверхпроводимости (A New Method in the Theory of Superconductivity) U.S.S.R. Acad. Sci. Press, 1958, Fortschr. Physik **6**, 605 (1958); Bardeen, Cooper, and Schrieffer, Phys. Rev. **108**, 1175 (1957).

[2] N. N. Bogolyubov, Dokl. Akad. Nauk SSSR **119**, 52 (1958), Soviet Phys. "Doklady" **3**, 279 (1958).

[3] Bohr, Mottelson, and Pines, Phys. Rev. **110**, 936 (1958).

[4] V. G. Solov'ev, Dokl. Akad. Nauk SSSR **123**, 437 (1958); Nuovo cimento **10**, 1022 (1958).

[5] V. G. Solov'ev, J. Exptl. Theoret. Phys. (U.S.S.R.) **35**, 823 (1958), Soviet Phys. JETP **8**, 572 (1959); Dokl. Akad. Nauk SSSR **123**, 652 (1958), Soviet Phys. "Doklady" **3**, 1197 (1958).

[6] S. T. Belyaev, Kgl. Danske Videnskab. Selskab, Mat.-fys. Medd. **31**, No. 11 (1958).

[7] V. G. Solov'ev, Nucl. Phys. **9**, 655 (1959); J. Exptl. Theoret. Phys. (U.S.S.R.) **36**, 293 (1959), Soviet Phys. JETP **9**, 201 (1959).

[8] N. N. Bogolyubov, Dokl. Akad. Nauk SSSR **119**, 244 (1958), Soviet Phys. "Doklady" **3**, 292 (1958).

[9] V. Fock, Z. Physik **61**, 126 (1930).

[10] J. M. Blatt and V. F. Weisskopf, Theoretical Nuclear Physics, J. Wiley, New York, 1952, Russ. Transl. IIL, 1954.

Translated by D. ter Haar
373

SOVIET PHYSICS JETP VOLUME 36(9), NUMBER 6 DECEMBER, 1959

THE EXCITATION OF COLLECTIVE STATES IN NUCLEI BY SCATTERING OF CHARGED PARTICLES

S. I. DROZDOV

Submitted to JETP editor January 14, 1959

J. Exptl. Theoret. Phys. (U.S.S.R.) **36**, 1875-1881 (June, 1959)

Elastic and inelastic scattering of fast charged particles on black nonspherical nuclei is investigated in the diffraction approximation. The radius of the nucleus and its nonsphericity parameter can be determined by comparing the calculations with experimental data.

1. INTRODUCTION

EXCITATION of collective states in the nucleus takes place during the scattering of nucleons on nonspherical nuclei by the process of direct interaction of the incident particle with the nuclear surface. In this connection we will investigate the scattering of charged particles (protons, alpha particles) with an energy E which considerably exceeds the coulomb barrier $ZZ'e^2/R$ when condition (1) is fulfilled

$$kR \gg \eta, \tag{1}$$

where $\eta = ZZ'e^2/\hbar v$ is the Coulomb parameter, k is the wave number of the incident particle, and R is the radius of the nucleus. Assuming that the nucleus is black, we find the differential cross section for elastic and inelastic scattering with excitation of the first rotational level of an even-odd nucleus. If, in addition to (1), condition (2) is fulfilled

$$kR\Delta E/E \ll 1, \tag{2}$$

where ΔE is the energy of the excited level, then in the process of scattering the nucleus can be considered immovable and the change in the energy of the particles in inelastic scattering can be ignored. In this case the adiabatic approximation is applicable, according to which the solution of the scattering problem reduces to finding the scattering amplitudes $f(\Omega, \omega)$ of particles from a fixed nucleus, where the angles $\Omega = (\theta, \phi)$ determine the direction of scattering and the angles $\omega = (\vartheta, \varphi)$ show the orientation of the axis of symmetry of the nucleus. Formula (3) gives the differential scattering cross section with excitation of the rotational level of the even-odd nucleus with momentum λ.

$$\sigma_\lambda(\theta) = \sum_\mu |\langle Y^*_{\lambda\mu}(\omega) f(\Omega, \omega) Y_{00}\rangle|^2. \tag{3}$$

If condition (1) is fulfilled, it is possible to calculate the scattering amplitude $f(\Omega, \omega)$ from the fixed black nucleus using the diffraction theory method[1-4] in which the energy of interaction is considered as excitation.

2. SCATTERING AMPLITUDE

If the energy of the particles considerably exceeds the coulomb barrier (1) then the wave function describing the scattering of charged particles from a black nucleus, in cylindrical coordinates with the polar axis z along the wave vector k of the incident particles, has the form[1]

$$\Psi_k(\rho, z) = \Omega(\rho) \exp i\left[kz - \frac{1}{\hbar v}\int_{-z_0}^{z} U(\rho, z)\, dz\right]. \tag{4}$$

Here, $\Omega(\rho)$ is the function which accounts for the characteristics of a black nucleus: to the right of the nucleus ($z > 0$), $\Omega(\rho) = 1$ on all planes z = const, aside from the shadow of the nucleus within whose limits $\Omega(\rho) = 0$. The function $U(\rho_2 z)$ is the energy of the electric interaction of the particle with the nucleus. If the equation of the nuclear surface, in the coordinate system connected with the axis of symmetry of the nucleus, can be written in the form $r(\mu) = R(1 + \alpha_\lambda P_\lambda(\mu))$, $\lambda = 2$, then for small nonsphericity parameters α_λ we have

$$U(\rho, z) = ZZ'e^2\left(\frac{1}{r} + \frac{3\alpha_\lambda}{2\lambda+1} r^{-\lambda-1} P_\lambda(\mu)\right). \tag{5}$$

in formula (4) z_0 signifies a rather large scattering to the left of the nucleus for which the wave function satisfies the condition

$$\Psi_k(\rho, -z_0) = e^{-ikz_0}. \tag{6}$$

According to Akhiezer and Sitenko[2] the scattering amplitude for particles from a fixed nucleus can be represented in the following form:

$$f(\Omega,\omega)=-\frac{ik}{2\pi}\int d\rho e^{-ik'\rho}\left[\Psi_k(\rho,z_0)e^{-ikz_0}-1\right], \quad (7)$$

where k' is the wave vector of the scattered particle, and the integration is done over the entire plane. The square brackets contain the expression which represents the scattered wave.

For scattering through the angles $\theta \neq 0$, the last term in square brackets can be omitted. In addition, using (4), (5) with $z_0 \to \infty$ we have

$$e^{-ikz_0}\Psi_k(\rho,z_0)=\Omega(\rho)\exp\left\{-i\eta\left[2\ln 2kz_0-2\ln k\rho\right.\right.$$
$$\left.\left.+\sum_\mu\frac{12\pi\alpha_\lambda R^\lambda}{(2\lambda+1)^2}Y^*_{\lambda\mu}(\omega)\int_{-\infty}^{\infty}r^{-\lambda-1}Y_{\lambda\mu}\left(\frac{r}{r}\right)dz\right]\right\}. \quad (8)$$

In discarding the inessential phase factor $\exp(-i2\eta\ln 2kz_0)$ and changing the variable of integration, we obtain with the help of (7) and (8) the following expression for the scattering amplitude:

$$f(\Omega,\omega)=-\frac{ik}{2\pi}\int_0^{2\pi}d\varphi'\int_{\rho(\varphi')}^{\infty}d\rho\,\rho\,(k\rho)^{2i\eta}$$
$$\times\exp\left\{-i\left[k\rho\theta\cos(\varphi'-\phi)+\eta_\lambda\sum_\mu\frac{12\pi\alpha_\lambda R^\lambda\rho^{-\lambda}}{(2\lambda+1)^2}Y^*_{\lambda\mu}(\omega)\right.\right.$$
$$\left.\left.\times\int_{-1}^{1}(1-\mu'^2)^{\lambda/2-1}Y_{\lambda\mu}(\mu',\varphi')\,d\mu'\right]\right\}. \quad (9)$$

In this formula the integration is done over the entire plane except for the nuclear shadow. It is not difficult to show that in the linear approximation for small non-sphericity parameters α_λ the nuclear shadow on the plane perpendicular to the vector k has the following form

$$\rho(\varphi')=R+R\alpha_\lambda\sum_\mu\frac{4\pi}{2\lambda+1}Y^*_{\lambda\mu}(\omega)\,Y_{\lambda\mu}\left(\frac{\pi}{2},\varphi'\right). \quad (10)$$

To find the cross section for elastic or inelastic scattering (3), we expand amplitude (9) into a series for small non-sphericity parameters α_λ, which are limited by the linear approximation. According to reference 5 this can be done if

$$\alpha_\lambda kR\theta \ll 1. \quad (11)$$

As a result of this expansion the integrals appear in the form

$$\frac{1}{2\pi}\int_0^{2\pi}d\varphi\exp i(\mu\varphi-z\cos\varphi)=i^{-\mu}J_\mu(z),$$

which reduce to Bessel functions. Thus we obtain the following expression for the scattering amplitude of charged particles from a fixed nucleus ($\lambda = 2$):

$$f(\Omega,\omega)=\frac{i}{k}(kR)^{2(1+i\eta)}\left\{-(kR\theta)^{-2(1+i\eta)}\int_{kR\theta}^{\infty}x^{1+2i\eta}J_0(x)\,dx\right\}$$
$$+\frac{i}{k}(kR)^{2(1+i\eta)}\sum_\mu\frac{4\pi\alpha_\lambda}{2\lambda+1}Y^*_{\lambda\mu}(\omega)e^{i\mu\phi}\,i^{-\mu}$$
$$\times\left\{Y_{\lambda\mu}\left(\frac{\pi}{2},0\right)J_\mu(kR\theta)+i\eta_\lambda\frac{3}{2\lambda+1}\right.$$
$$\left.\times\int_{-1}^{1}Y_{\lambda\mu}(\mu',0)\,d\mu'(kR\theta)^{-2i\eta}\int_{kR\theta}^{\infty}x^{-1+2i\eta}J_\mu(x)\,dx\right\}. \quad (12)$$

Using the formula in reference 6

$$\int_0^{\infty}x^{-2\nu+\mu-1}J_\mu(x)\,dx=2^{-2\nu+\mu-1}\Gamma(\mu-\nu)/\Gamma(1+\nu), \quad (13)$$

we obtain from (12) the following expression for the elastic scattering amplitude

$$\langle Y_{00}f(\Omega,\omega)Y_{00}\rangle=f_{E0}(\theta)$$
$$+\frac{i}{k}(kR)^{2(1+i\eta)}(kR\theta)^{-2(1+i\eta)}\int_0^{kR\theta}x^{1+2i\eta}J_0(x)\,dx, \quad (14)$$

where $f_{E0}(\theta)$ is the scattering amplitude in the field $ZZ'e^2/r$:

$$f_{E0}(\theta)=-\frac{2\eta_1}{k\theta^2}\exp\left(-2i\eta\ln\frac{\theta}{2}\right)\frac{\Gamma(1+i\eta_1)}{\Gamma(1-i\eta_1)}. \quad (15)$$

Thus the amplitude of elastic scattering consists of the amplitude of elastic scattering in the electric field of the nucleus and the nuclear part of the elastic scattering amplitude.

In the linear approximation for a small non-sphericity parameter α_λ the angular distributions for elastic scattering on spherical[4] and non-spherical nuclei are the same.

The amplitude of inelastic scattering, as a result of which the nucleus transfers from the ground state to the rotational state $Y_{\lambda\mu}(\omega)$ has the following matrix element:

$$\langle Y^*_{\lambda\mu}(\omega)f(\Omega,\omega)Y_{00}\rangle$$
$$=e^{-i\mu\phi}\,i^{\mu+1}\frac{(kR)^{2(1+i\eta)}}{k}\frac{(4\pi)^{1/2}\alpha_\lambda}{2\lambda+1}\left[Y_{\lambda\mu}\left(\frac{\pi}{2},0\right)J_\mu(kR\theta)\right.$$
$$\left.+i\eta\frac{3}{2\lambda+1}\int_{-1}^{1}Y_{\lambda\mu}(\mu',0)\,d\mu'(kR\theta)^{-2i\eta}\int_{kR\theta}^{\infty}x^{-1+2i\eta}J_\mu(x)\,dx\right]. \quad (16)$$

The integral in this formula can be put in the form $\int_0^{\infty}f(x)\,dx-\int_0^{\infty}f(x)dx$ after which the first integral is done with the help of formula (13). We obtain

$$\langle Y^*_{\lambda\mu}f(\Omega,\omega)Y_{00}\rangle$$
$$=\langle Y^*_{\lambda\mu}f_E(\Omega,\omega)Y_{00}\rangle+\langle Y^*_{\lambda\mu}f_n(\Omega,\omega)Y_{00}\rangle. \quad (17)$$

The first term in the right hand part of this formula as shown in the Appendix is the amplitude of electric quadrupole excitation. According to formulas (13) and (16) it looks like

$$\langle Y^*_{\lambda\mu}(\omega)\, f_E(\Omega,\omega)\, Y_{00}\rangle = \delta_{\mu\pm 2} e^{-i\mu\varphi}\left(\frac{3}{2}\right)^{1/2} \frac{\alpha_\lambda kR^2}{(2\lambda+1)^{1/2}} \frac{\eta(1+i\eta)}{1+\eta^2} \times \exp\left(-2i\eta \ln\frac{\theta}{2}\right) \frac{\Gamma(1+i\eta)}{\Gamma(1-i\eta)}. \quad (18)$$

The second term of formula (17), which can be called the nuclear part of the inelastic scattering amplitude, can be described by the expression

$$\langle Y^*_{\lambda\mu}(\omega)\, f_n(\Omega,\omega)\, Y_{00}\rangle = e^{-i\mu\varphi} i^{\mu+1} \frac{(kR)^{2(1+i\eta)}}{\cdot\ k} \frac{\alpha_\lambda}{(2\lambda+1)^{1/2}} \times \left[\left(\frac{4\pi}{2\lambda+1}\right)^{1/2} Y_{\lambda\mu}\left(\frac{\pi}{2}, 0\right) J_\mu(kR\theta) - \delta_{\mu\pm 2} \frac{6^{1/2}}{2\lambda+1} i\eta_1 (kR\theta)^{-2i\eta} \int_0^{kR\theta} x^{-1+2i\eta} J_2(x)\, dx\right]. \quad (19)$$

With $\eta = 0$ formula (19) describes the inelastic scattering of neutrons.†

3. SCATTERING CROSS SECTION

The differential cross section for inelastic scattering of charged particles with excitation of the first rotational level of the even-odd nucleus is determined by the square of the absolute value of the amplitude (17):

$$\sigma_\lambda(\theta) = \sigma_{E\lambda}(\theta) + \sigma_{n\lambda}(\theta) + \sigma_{\mathrm{int}\,\lambda}(\theta); \qquad \lambda = 2;$$

$$\sigma_{E\lambda}(\theta) = \alpha_\lambda^2 \frac{(kR)^4}{k^2(2\lambda+1)^3} \frac{3\eta^2}{1+\eta^2};$$

$$\sigma_{n\lambda}(\theta) = \alpha_\lambda^2 \frac{(kR)^4}{k^2(2\lambda+1)} \left\{\frac{1}{4}\left[J_0^2(kR\theta) + 3J_2^2(kR\theta)\right] + \frac{6\eta_1}{2\lambda+1}\left[\frac{2\eta}{2\lambda+1}\left|F(kR\theta)\right|^2 + J_2(kR\theta)\,\mathrm{Im}\,F(kR\theta)\right]\right\};$$

$$\sigma_{\mathrm{int}\,\lambda}(\theta) = -\alpha_\lambda^2 \frac{(kR)^4}{k^2(2\lambda+1)^2} \frac{6\eta_1}{1+\eta^2}\left\{(\eta_1 \sin\chi + \cos\chi)\frac{2\eta}{2\lambda+1}\,\mathrm{Re}\,F(kR\theta) + (\eta_1\cos\chi - \sin\chi)\left[\frac{2\eta}{2\lambda+1}\,\mathrm{Im}\,F(kR\theta) + \frac{1}{2}J_2(kR\theta)\right]\right\}. \quad (20)$$

Here

$$F(a) = a^{-2i\eta}\int_0^a x^{-1+2i\eta} J_2(x)\, dx;$$

$$\chi = 2\eta_1 \ln\frac{kR\theta}{2} - 2\delta, \qquad \delta = \arg\Gamma(1+i\eta).$$

Thus, the cross section for inelastic scattering $\sigma_\lambda(\theta)$ is the sum of the cross section for coulomb excitation $\sigma_{E\lambda}(\theta)$, the nuclear part of the inelastic scattering cross section $\sigma_{n\lambda}(\theta)$ and the interference term $\sigma_{\mathrm{int}\lambda}(\theta)$. At sufficiently great magnitudes of ZZ′ all these functions are of the first order of magnitude with the exception of the interference term which, as can be seen from formula (20), can be disregarded in the region of very small scattering angles $kR\theta \ll 1$. We should also mention that the form of the angular distribution of inelastically scattered particles (20), is not dependent on the nonsphericity parameter α_λ of the nucleus and is determined by the parameters kR and η. With $\eta = 0$ formula (2) describes the angular distribution of neutrons scattering inelastically with excitation of the first collective level of the even-odd nucleus:†

$$\sigma_{n\lambda}(\theta) = \alpha_\lambda^2 \frac{(kR)^4}{4k^2(2\lambda+1)}\left[J_0^2(kR\theta) + 3J_2^2(kR\theta)\right], \quad (21)$$

assuming that $kR \gg 1$ and $\alpha_\lambda kR\theta \ll 1$.

The angular distribution of particles scattering inelastically with excitation of the first rotational level of the even-odd nucleus as shown in reference 5, under corresponding conditions, coincides with the angular distribution of particles scattering with excitation of the first vibrational level.

4. RESULTS OF CALCULATION AND COMPARISON WITH EXPERIMENTAL DATA

The complex function F(a) in formula (20) for angular distributions, on the basis of the known relationship

$$J_2(x) = \left(\frac{x}{a}\right)^2 \sum_{m=0}^{\infty} \frac{a^m J_{2+m}(a)}{m!\, 2^m}\left(1 - \frac{x^2}{a^2}\right)^m$$

and the characteristics of Γ functions, can be represented in the form

$$F(a) = \sum_{m=0}^{\infty} \frac{a^m J_{2+m}(a)}{2^{m+1}} \prod_{p=0}^{m} \frac{p+1-i\eta}{(p+1)^2+\eta^2}. \quad (22)$$

For instance, with $a \leq 8$, for calculating the real and imaginary part of the function F(a) with good accuracy it is sufficient to use the first eight terms of sum (22).

The angular distributions of charged particles from inelastic scattering on non-spherical nuclei calculated according to formulas (20) and (22) are shown in Figs. 1–3. A comparison of theoretical and experimental[8,9] data for angular distributions of protons and alpha-particles inelastically scattered by the nucleus Mg^{24}_{12} (Figs. 1 and 2) makes it possible to evaluate the non-sphericity parameter of this nucleus: $\alpha_2 = 0.17$ to 0.20.

In conclusion I wish to thank L. D. Landau, B. T. Geĭlikman, K. A. Ter-Martirosyan for their fruitful advice on this work and also T. V. Novikov and A. V. Cherenkov who did the numerical calculations.

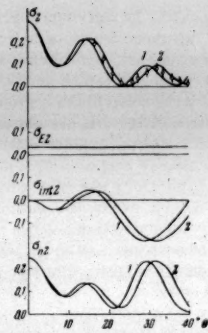

FIG. 1. Functions $\sigma_1(\theta)$, $\sigma_{E2}(\theta)$, $\sigma_{int\,2}(\theta)$, $\sigma_{n2}(\theta)$ in units $\alpha_1^2(kR)^4/5k^2$, describing the angular distribution of 31.5-Mev alpha particles inelastically scattered from M_{12}^{24} with excitation of its first collective level. The calculation was done with $R = 4.9 \times 10^{-13}$ cm (curve 2) and $R = 5.3 \times 10^{-13}$ cm (curve 1). Small circles indicate experimental data.[4] Comparison of theoretical and experimental data gives the value of the parameter of nonsphericity of the nucleus Mg_{12}^{24}: $\alpha_2 = 0.17$ to 0.20

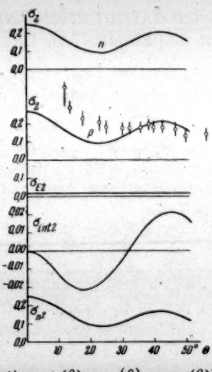

FIG. 2. Functions $\sigma_1(\theta)$, $\sigma_{E2}(\theta)$, $\sigma_{int\,2}(\theta)$, $\sigma_{n2}(\theta)$ in units $\alpha_2^2(kR)^4/5k^2$, describing the angular distribution of 18-Mev protons (p) inelastically scattered from Mg_{12}^{24} with excitation of its first collective level. For comparison the angular distribution of inelastically scattering neutrons $\sigma_2(\theta)$ are presented (n) in the same units. The calculation was done with $R = 4.7 \times 10^{-13}$ cm. The small circles show experimental data.[9] The discrepancy between theoretical and experimental data at $\theta < 20°$ can possibly be explained by the fact that we were unable to separate experimentally the group of elastically scattered protons from the inelastically scattered group. Therefore the comparison of experimental and theoretical data with $\theta = 30$ to 50° gives a value of the parameter of non-sphericity of the nucleus Mg_{12}^{24}, $\alpha_2 = 0.31$, which exceeds α_2 obtained from an analysis of experiments on the scattering of alpha particles (see Fig. 1).

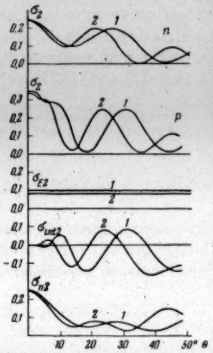

FIG. 3. Graphs of the same quantities as in Fig. 2, for the case of inelastic scattering of protons and neutrons, with energies of 20 Mev (1) and 30 Mev (2), from the nucleus Gd_{64}^{160}: $R = 1.3 \times 10^{-13} A^{1/3}$ cm.

APPENDIX

We shall show that formula (18) determines the amplitude of electric quadrupole excitation for small scattering angles $\theta \ll 1$ in the adiabatic approximation when the corresponding parameter[10] is $\xi = \eta\Delta E/2E \ll 1$. Actually, if the condition $\alpha_2\eta \ll 1$ is fulfilled[5] then the amplitude of scattering in the electrical field of the nucleus (5) in the first approximation of the theory of excitation can be presented in the form ($\lambda = 2$):

$$f_E(\Omega, \omega) = f_{E0}(\theta) - \eta_i k \sum_{\mu} \frac{6\alpha_\lambda R^\lambda}{(2\lambda+1)^2} Y_{\lambda\mu}^*(\omega) \left\langle \mathbf{k}_f \left| r^{-\lambda-1} Y_{\lambda\mu}\left(\frac{\mathbf{r}}{r}\right) \right| \mathbf{k}_i \right\rangle, \quad (1.1)$$

where k_i, k_f are the wave vectors of the incident and scattered particle; $|k>$ is the Coulomb wave function. From (1.1) we obtain the following expression for the amplitude of inelastic scattering in the adiabatic approximation:

$$\langle Y_{\lambda\mu}^*(\omega) f_E(\Omega, \omega) Y_{00} \rangle = -e^{-2i\mu\phi} \frac{6\alpha_\lambda \eta_i k R^\lambda}{(2\lambda+1)^2 (4\pi)^{1/2}} \left\langle \mathbf{k}_f \left| r^{-\lambda-1} Y_{\lambda\mu}\left(\frac{\mathbf{r}}{r}\right) \right| \mathbf{k}_i \right\rangle. \quad (1.2)$$

Selecting k_i as a polar axis and using expansions of Coulomb functions $|k>$ in spherical functions we have (see reference 10, page 449):

$$\left\langle \mathbf{k}_f \left| r^{-\lambda-1} Y_{\lambda\mu}\left(\frac{\mathbf{r}}{r}\right) \right| \mathbf{k}_i \right\rangle = \left(\frac{4\pi}{2\lambda+1}\right)^{1/2} \sum_{l_i\, l_f} i^{l_i - l_f} e^{i(\delta_{l_i} + \delta_{l_f})} (2l_i+1)(2l_f+1) \times C_{l_i 0 l_f 0}^{\lambda 0} C_{l_i 0 l_f \mu}^{\lambda\mu} \left[\frac{(l_f-\mu)!}{(l_f+\mu)!}\right]^{1/2} P_{l_f}^{\mu}(\cos\theta)\, M_{l_i l_f}^{-\lambda-1}, \quad (1.3)$$

where $M_{l_i l_f}^{-\lambda-1}$ is the radial matrix element $C_{l_i m_i l_f m_f}^{\lambda\mu}$ are the Clebsh-Gordan coefficients,

$\delta_i = \arg\Gamma(1 + l_i + i\eta)$.

The large magnitudes of l_i, l_f play a basic role in sum (1.3) when we observe scattering through small angles. Therefore, independently of the magnitude of η (according to reference 10, page 456) the radial matrix elements are

$$M^{\lambda-1}_{l_i l_f} = \frac{k^{\lambda-2}}{4\eta^{\lambda}} I_{\lambda m}(\vartheta, 0), \qquad \tan\frac{\vartheta}{2} = \frac{\eta}{l},$$

$$l = \frac{l_f + l_i}{2}, \; m = l_f - l_i. \tag{1.4}$$

Where $I_{\lambda m}(\vartheta, \xi)$ are the orbital integrals of the theory of coulomb excitation (reference 10, page 482) where in this case the parameter of adiabaticity is $\xi = 0$. In addition we can use the following asymptotic characteristics of the Γ function, spherical functions and Clebsh-Gordan coefficients[10,11]:

$$e^{i(\delta_i + \delta_f)} = l^{2i\eta}; \quad \left[\frac{(l_f - \mu)!}{(l_f + \mu)!}\right]^{1/2} P^{\mu}_{l_f}(\cos\theta) = J_{\mu}(l\theta),$$

$$C^{\lambda 0}_{l_i 0 l_f 0} C^{\lambda\mu}_{l_i 0 l_f \mu} = \frac{2\lambda + 1}{2l + 1} D^{\lambda}_{0m}\left(0, \frac{\pi}{2}, 0\right) D^{\lambda}_{\mu m}\left(0, \frac{\pi}{2}, 0\right), \tag{1.5}$$

Where $D^{\lambda}_{\mu m}(\varphi_1, \vartheta_1, \varphi_2)$ are generalized spherical functions.[11] Substituting (1.4) and (1.5) into (1.3) and changing the double sum over l_i, l_f to the integral over $l = (l_f + l_i)/2$ and changing the sum over $m = l_f - l_i$ we obtain

$$\left\langle \mathbf{k}_f \middle| r^{-\lambda-1} Y_{\lambda\mu}\left(\frac{\mathbf{r}}{r}\right) \middle| \mathbf{k}_i \right\rangle = (-1)^{\mu} e^{i\mu\Phi} \frac{k^{\lambda-2}}{\eta^{\lambda}} [\pi(2\lambda + 1)]^{1/2} \times \sum_m i^{-m} D^{\lambda}_{0m}\left(0, \frac{\pi}{2}, 0\right) D^{\lambda}_{\mu m}\left(0, \frac{\pi}{2}, 0\right) \times \int_0^{\infty} x^{1+2i\eta} J_{\mu}(x\theta) I_{\lambda m}(\vartheta, 0)\, dx, \tag{1.6}$$

where $\tan(\vartheta/2) = \eta/x$. Since in the integral over x, $x \sim 2\eta/\theta$ with $\theta \ll 1$ plays an important role, the function $x^{\lambda} I_{\lambda m}(\vartheta, 0)$ can be expanded in a series for small η/x. According to reference 10 (page 482) with $\lambda = 2$ we have

$$x^2 I_{2\pm 2}(\vartheta, 0) = \frac{\pi}{3}\eta^2, \qquad x^2 I_{20}(\vartheta, 0) = 2\eta^2.$$

By applying the well-known values of the functions[11] $D^{\lambda}_{\mu m}(0, \pi/2, 0)$ we obtain from (1.6) and (13) formula (18) for the amplitude of electric quadrupole excitation with scattering through small angles in adiabatic approximation.

[1] L. D. Landau and E. M. Lifshitz, Квантовая механика (Quantum Mechanics), part I, M. - L. 1948, p. 184.

[2] A. I. Akhiezer and A. G. Sitenko, J. Exptl. Theoret. Phys. (U.S.S.R.) **32**, 794 (1957), Soviet Phys. JETP **5**, 652 (1957).

[3] L. I. Schiff, Phys. Rev. **103**, 443 (1956)

[4] A. I. Akheizer and I. Ya. Pomeranchuk, Некоторые вопросы теории ядра (Certain Problems in Nuclear Theory) Gostekhizdat, M. - L. 1950. No. 22.

[5] S. I. Drozdov, J. Exptl. Theoret. Phys. (U.S.S.R.) **28**, 734 (1955), Soviet Phys. JETP **1**, 591 (1955); J. Exptl. Theoret. Phys. (U.S.S.R.) **30**, 786 (1956), Soviet Phys. JETP **3**, 759 (1956); J. Exptl. Theoret. Phys. (U.S.S.R.) **34**, 1288 (1958), Soviet Phys. JETP **5**, 889 (1958); Атомная энергия (Atomic Energy) **2**, 501 (1957).

[6] G. N. Watson, Theory of Bessel Functions, part I, Cambridge, 1949.

[7] E. V. Inopin, J. Exptl. Theoret. Phys. (U.S.S.R.) **31**, 901 (1956) Soviet Phys. JETP **4**, 764 (1957).

[8] H. J. Watters, Phys. Rev. **103**, 1763 (1956).

[9] P. C. Gugelot and P. R. Phillips, Phys. Rev. **101**, 1614 (1956).

[10] Alder, Bohr, Huus, Mottelson, and Winther, Revs. Modern Phys. **28**, 432 (1956).

[11] P. J. Brussaard and H. A. Tolhoek, Physica **23**, 955 (1957).

Translated by Genevra Gerhart
374

RADIATIVE DEVIATIONS FROM THE COULOMB LAW AT SMALL DISTANCES

V. G. VAKS

Submitted to JETP editor January 14, 1959

J. Exptl. Theoret. Phys. (U.S.S.R.) **36**, 1882-1889 (June, 1959)

The radiative corrections to the Dirac equation in a Coulomb field are examined for distances $r \ll \hbar/mc$. The calculations are carried to the first order in $e^2/\hbar c$ and the second order in $Ze^2/\hbar c$. The resulting change in the Coulomb singularity of the wave functions is small and is hard to distinguish from the effects of the finite size of the nucleus.

1. For an electron moving in an external field the radiative corrections are made up of two qualitatively different effects: the polarization of the electron-positron vacuum by the external field, and the interaction with the fluctuations of the photon vacuum. The first of these effects strengthens the interaction, since the electron penetrates inside the screening cloud, and in the domain of applicability of perturbation theory the vacuum-polarization potential has the form:[1]

$$V_{\text{pol}} = -\frac{Z\alpha^2}{r}\frac{2}{3\pi}\left(\ln\frac{1}{mr} - \frac{5}{6} - \ln\gamma\right),$$

$$\hbar = c = 1, \quad \gamma = 1.781,$$

$$r \ll 1/m, \quad \alpha = e^2 = 1/137. \tag{1}$$

The photon fluctuations, on the other hand, lead to a "trembling" of the electron, weaken the coupling of the electron with the external field, and decrease the interaction. In the region of nonrelativistic motion of the electron, $r > 1/m$, the effect of the trembling on the behavior of the electron can be described[2] by replacing the potential energy by its average value over the fluctuation motion in the photon vacuum

$$V(\mathbf{r}) \to \langle V(\mathbf{r} + \hat{\Delta}\mathbf{r})\rangle_{\text{fl}}$$

$$= -\frac{Z\alpha}{2\pi^2}\int\frac{d\mathbf{q}}{q^2}\exp\{i\mathbf{qr} - q^2\langle\Delta r^2\rangle/6\}, \tag{2}$$

where

$$\Delta\mathbf{r} = \frac{ie}{m}\sum_{\mathbf{k}}\sqrt{2\pi/k^3}\,\mathbf{e}_{\mathbf{k}}(a_{\mathbf{k}} - a_{\mathbf{k}}^+),$$

$$\langle\Delta r^2\rangle = \frac{2\alpha}{\pi m^2}\int_{k_{min}}^{k_{max}}\frac{dk}{k} = \frac{2\alpha}{\pi m^2}\ln\frac{m}{\epsilon_0}.$$

In this way, as is well known, one gets the correct result for the Lamb shift. But if one applies Eq. (2) for $r < 1/m$, then beginning at a distance $r \sim r_c = (\langle\Delta r^2\rangle)^{1/2} \sim \alpha^{1/2}/m$ the Coulomb rise of the potential is arrested, and the $1/r$ law is replaced by a constant, $1/r \to 1/r_c$. This would mean that at distances 10 times nuclear dimensions the effective potential acting on the electron has nothing in common with the Coulomb potential and has no singularity. Such a result comes naturally from the argument in question, since the potential is averaged over the region of the "trembling" of the electron, of the order of r_c, and an electron near the nucleus is constantly carried out of the region of small r by the oscillations in the photon vacuum, so that the "average over the oscillations" $\langle V(\mathbf{r} + \hat{\Delta}\mathbf{r})\rangle$ is finite even for $r = 0$. This approach is that of the "adiabatic" problem, in which the potential for a slow motion is obtained by averaging over a fast motion. Actually the region $r < 1/m$ corresponds to ultrarelativistic motion of the electron, so that the "frequency" of its motion, $\sim 1/r$, exceeds the characteristic frequency of the virtual quanta, $\omega \sim m$, and the oscillations have little effect on the motion. We can say that in this region the strong Coulomb field damps the fluctuation motion of the electron, and reduces the "smearing out." It turns out that the effective fluctuation radius for $r < 1/m$ falls off linearly with the distance: $(\langle\Delta r^2\rangle)^{1/2} \sim r\alpha^{1/2}$. The resultant "correction to the potential" is of the order

$$\langle V(\mathbf{r} + \hat{\Delta}\mathbf{r})\rangle - V(r) \sim \frac{\partial^2 V}{\partial r^2}\langle\Delta r^2\rangle \sim \alpha r^2\frac{V}{r^2} = \alpha V,$$

i.e., unlike the effect of vacuum polarization the correction from the photon fluctuations is small compared with V for all r. Therefore the weakening of the interaction because of the oscillations remains finite at extremely small distances, and is described by perturbation theory for arbitrary r (the asymptotic values of $\Gamma(p_1, p_2)$ and $G(p)$ for $p \to \infty$ are equal to their "null" values to accuracy $e_0^2 < 1$).[3]

It is not only as a matter of principle that the study of the radiative deviations from the Coulomb law at small r is of interest. In electron-nuclear

phenomena (β decay, K capture, the conversion of high-energy quanta) the behavior of the electron wave function for $r \sim r_{nuc} \sim 10^{-13}$ cm is very important. These functions have a Coulomb relativistic singularity at $r = 0$

$$\psi \sim (r/a_0)^{\sqrt{1-Z^2\alpha^2}-1} = \exp\left\{(1-\sqrt{1-Z^2\alpha^2})\ln\frac{a_0}{r}\right\},$$

$$a_0 = 1/mZ\alpha.$$

The quantity $\ln(a_0/r_{nuc})$ is about 5 for intermediate and large Z. Noting that measurable quantities involve squares and fourth powers of the wave functions, we may suppose that a change of the singularity by a quantity of the order α will be observable and comparable with, for example, the effect of the finite size of the nucleus.

In the language of diagrams we want to find the corrected "end" of the electron line in the Coulomb field for the case of processes taking place in the region $r \gg 1/m$, that is, $p \gg m$. The result in the form of a "corrected wave function" can be substituted into the various transition amplitudes. In many-step transitions, for example conversions, additional virtual processes are possible, and then the corresponding radiative corrections must be added to those we have found here.

Calculations of the vacuum-polarization potential have been made previously (see the papers of Schwinger[1] and of Wichmann and Kroll[4]).* Therefore it suffices to find the correction associated with the "trembling." The sign of the effect will of course be opposite to that of the effect of the vacuum; there is after all still a "weakening" of the external field.

2. We start with Schwinger's equation for the motion of an electron in an external field:[5,6]

$$[i(\hat{p} - e\hat{A} - e\hat{A}_p) + m]\psi(x) + \int M(x, y)\psi(y)\,d^4y = 0. \quad (3)$$

Here A_p is the potential of the vacuum polarization, and M(x, y) is the mass operator. In the first radiative approximation

$$M(x, y) = \delta m_0 \delta(x - y) - 4\pi i\alpha\gamma_\mu G(x, y)\gamma_\mu D(x - y). \quad (4)$$

Here G(x, y) is the Green's function of the electron in the external field:

$$[i(\hat{p} - e\hat{A}) + m]G(x, y) = \delta(x - y);$$

D(x − y) is the Green's function of the quanta:

$$D(x - y) = (2\pi)^{-4}\int D(k)\,e^{ik(x-y)}\,d^4k = (2\pi)^{-4}\int\frac{d^4k}{k^2}e^{ik(x-y)};$$

and δm_0 is the renormalization constant—the difference of the "bare" and observed masses. In the renormalization we follow Karplus and Klein[6] and Feynman.[7] Let us consider the mass operator in the first radiative approximation; then in the mass term we take the unperturbed Coulomb wave function, which satisfies the equation

$$[i(\hat{p} - e\hat{A}) + m]\psi_c(x) = 0 \quad (5a)$$

or in the momentum representation

$$\int d^4p_2\,[\delta(p_1 - p_2)(i\hat{p}_2 + m) - ie\hat{A}_{p_1-p_2}]\psi_c(p_2) = 0. \quad (5b)$$

Further let us introduce instead of the function D(k) the cut-off function $D_\Lambda(k) = k^{-2}\Lambda^2/(\Lambda^2 + k^2)$, presuming that at the end of the calculations $\Lambda \to \infty$. Then the constant $\delta m_0(\Lambda)$ is chosen so that in the absence of the external field Eq. (3) would go over into the Dirac equation with the observed mass m:[7]

$$\delta m_0(\Lambda) = m_0 - m = -m\frac{3\alpha}{2\pi}\left(\ln\frac{\Lambda}{m} + \frac{1}{4}\right). \quad (6)$$

Then on using Eqs. (5) and (6) in the mass term and letting Λ go to ∞, we get an unambiguous final result, which describes the interaction of the particle with the vacuum fluctuations. The mass operator acting on the Dirac wave functions absorbs within itself in gauge-invariant form all the divergences of the proper energy and vertex parts, and gives the physical effects directly.

The interpretation of the mass term in Eq. (3) is obvious from a comparison of Eq. (3) with Eq. (2): it is the exact relativistic analogue of the expression $(\langle V(\mathbf{r} + \hat{\Delta}\mathbf{r})\rangle - V(\mathbf{r}))\Psi(\mathbf{r})$, i.e., the smearing out of the external field by the "trembling," which is valid in the relativistic domain.

Going over to the momentum representation, we get

$$M(p_1, p_2) = (2\pi)^{-4}\delta m_0(\Lambda)\delta(p_1 - p_2)$$

$$- 4\pi i\alpha\int d^4k\cdot\gamma_\mu G(p_1 - k, p_2 - k)\gamma_\mu D_\Lambda(k).$$

In what follows we shall be interested in distances $r \ll 1/m$, i.e., $p_1, p_2 \gg m$. Therefore we shall set $m = 0$ everywhere in the mass operator. At the same time the constant δm_0 also vanishes: its divergent part would in any case cancel out, and the finite part is proportional to m. The mass operator takes the form

$$M(p_1, p_2) = -\frac{\alpha}{2^6\pi^7}\int\frac{d^4k}{k^2}\frac{\Lambda^2}{\Lambda^2 + k^2}\gamma_\mu\left(\frac{1}{\hat{p} - e\hat{A}}\right)_{p_1-k,\ p_1-k}\gamma_\mu \quad (7a)$$

or

$$M(p_1, p_2) = -\frac{\alpha}{2^6\pi^7}\int\frac{d^4k}{k^2}\frac{\Lambda^2}{\Lambda^2 + k^2}\gamma_\mu\left[\delta(p_1 - p_2)\frac{1}{\hat{p}_1 - \hat{k}}\right.$$

$$\left. + \frac{1}{\hat{p}_1 - \hat{k}}e\hat{A}_{p_1-p_2}\frac{1}{\hat{p}_2 - \hat{k}} + \cdots\right]. \quad (7b)$$

*The effect of the finiteness of the nuclear radius, which diminishes the interaction for $r < r_{nuc}$, on the motion is opposite to that of the "incomplete screening" associated with the polarization of the vacuum. Therefore the result of reference 4, that these effects have different signs, is obvious without calculation.

For the Coulomb-field case under consideration

$$ie\hat{A}_q = Z\alpha\delta(q_0)\beta / 2\pi^2 q^2.$$

After integration over the time Eq. (3) goes over into the equation

$$\left(\alpha\mathbf{p} - \frac{Z\alpha}{r} - V_{\text{pol}} + \beta m\right)\psi(\mathbf{r}) + \int \mathfrak{M}(\mathbf{r}, \mathbf{r}')\psi(\mathbf{r}')\,d\mathbf{r}' = 0, \quad (8)$$

where $\mathfrak{M}(\mathbf{r}, \mathbf{r}') = \int d\mathbf{p}\,d\mathbf{p}'\,\mathfrak{M}(\mathbf{p}, \mathbf{p}')e^{i\mathbf{p}\mathbf{r} - i\mathbf{p}'\mathbf{r}'}$, with

$$\mathfrak{M}(\mathbf{p}_1, \mathbf{p}_2) = -\frac{\alpha}{2^5\pi^6}\int \frac{d^4k}{k^2}\,\frac{\Lambda^2}{\Lambda^2 + k^2}\,\beta\gamma_\mu \left(\frac{1}{\hat{p} - \hat{k} - e\hat{A}}\right)_{\mathbf{p}_1,\,\mathbf{p}_2} \gamma_\mu$$

$$= -\frac{\alpha}{2^5\pi^6}\int \frac{d^4k}{k^2}\,\frac{\Lambda^2}{\Lambda^2 + k^2}\,\beta\gamma_\mu \Big[\delta(\mathbf{p}_1 - \mathbf{p}_2)\,\frac{1}{\hat{p}_1 - \hat{k}}$$

$$+ \frac{1}{\hat{p}_1 - \hat{k}}\,e\hat{A}_{\mathbf{p}_1 - \mathbf{p}_2}\,\frac{1}{\hat{p}_2 - \hat{k}}$$

$$+ \frac{1}{\hat{p}_1 - \hat{k}}\int d\mathbf{q}\,e\hat{A}_{\mathbf{p}_1 - \mathbf{q}}\,\frac{1}{\hat{q} - \hat{k}}\,e\hat{A}_{\mathbf{q} - \mathbf{p}_2}\,\frac{1}{\hat{p}_2 - \hat{k}} + \dots\Big]$$

$$= \mathfrak{M}^{(0)} + \mathfrak{M}^{(1)} + \mathfrak{M}^{(2)} + \dots;$$

$$ie\hat{A}_{\mathbf{q}} = \beta Z\alpha / 2\pi^2 q^2; \qquad \hat{p}_{1,2} = \gamma\mathbf{p}_{1,2} - i\hat{\varepsilon}_0 \approx \gamma\mathbf{p}_{1,2}; \quad (9)$$

γ, β are the Dirac matrices; ϵ_0 is the energy of the bound state.

3. By introducing Feynman ordering indices[8] it is easy to carry out the integration over the momenta k of the quanta in Eq. (7a), and even to perform the renormalization. [Here one uses $(\hat{\mathbf{p}} - e\hat{\mathbf{A}})\Psi_C = 0$, so that terms of the form const $\times$ $(\hat{\mathbf{p}} - e\hat{\mathbf{A}})$ are dropped.]

It is, however, more difficult to "disentangle" the resulting symbolic expression, even by expansion in powers of $Z\alpha$, that to calculate the terms of the series (7b) directly. Therefore we use the expansion (9). The calculations will be carried to terms in $Z^2\alpha^2$, inclusive; as will be shown, the change of the wave function at the origin begins only with terms $\sim Z^2\alpha^2$, so that it is necessary to go to the second approximation. Since because of the presence of a numerical factor $1/2\pi$ as a common multiplier the effect is a small one, calculation of the terms $\sim Z^3\alpha^3$ and of higher orders can hardly be of interest, although experimental manifestation of the effect could be expected only for large Z.

Let us find $\mathfrak{M}^{(0)}$; to make the method (cf., e.g., reference 9) clear we shall do the calculation in detail, although the result is known.[8]

$$\mathfrak{M}^{(0)}(\mathbf{p}_1, \mathbf{p}_2) = \alpha(2\pi)^{-4}\delta(\mathbf{p}_1 - \mathbf{p}_2)\beta J_0(p_1),$$

$$J_0(p) = -i\gamma_n \frac{\Lambda^2}{\pi^2}\int_0^\infty dx \int_0^\infty dy \int_0^\infty dz \int d^4k \cdot \exp\{-i[k^2(x + y + z)$$

$$- 2kpx + \Lambda^2 y]\}\,(p_n - k_n)$$

$$= -\hat{p}\Lambda^2 \int_0^\infty \frac{dxdydz\,(y + z)}{(x + y + z)^3}\,\exp\left\{-i\left(p^2\,\frac{x(y + z)}{x + y + z} + \Lambda^2 y\right)\right\}.$$

Let us introduce the variable $u = y + z$, $du = dy$, and then integrate with respect to z:

$$J_0(p) = i\hat{p}\int_0^\infty dx\,du\,\frac{u}{(x + u)^3}\,e^{-ip^2xu/(x+u)}\left(1 - e^{-i\Lambda^2 u}\right).$$

Setting now $x = ut$, $dx = udt$ and integrating with respect to u, we find

$$J_0(p) = i\hat{p}\int_0^\infty \frac{dt}{(t + 1)^3}\ln\frac{\Lambda^2 + p^2t/(t + 1)}{p^2t/(t + 1)} \underset{\Lambda\to\infty}{\to} i\hat{p}\left(\ln\frac{\Lambda}{p} + \frac{3}{4}\right).$$

Thus we have

$$\mathfrak{M}^{(0)}(\mathbf{p}_1, \mathbf{p}_2) = \frac{\alpha}{(2\pi)^4}\,\delta(\mathbf{p}_1 - \mathbf{p}_2)\left(\ln\frac{\Lambda}{p_1} + \frac{3}{4}\right)\beta i\hat{p}_2. \quad (10)$$

According to Eq. (5b), in our case the operator $f(\mathbf{p}_1)\,\delta(\mathbf{p}_1 - \mathbf{p}_2)\,i\hat{\mathbf{p}}_2$ is equivalent to $f(\mathbf{p}_1)\,ie\hat{A}_{\mathbf{p}_1 - \mathbf{p}_2}$, and therefore $\mathfrak{M}^{(0)}$ can also be represented in the form

$$\mathfrak{M}^{(0)}(\mathbf{p}_1, \mathbf{p}_2) = \frac{\alpha}{(2\pi)^4}\,\beta\,ie\hat{A}_{\mathbf{p}_1 - \mathbf{p}_2}\left(\ln\frac{\Lambda}{p_1} + \frac{3}{4}\right). \quad (11)$$

Applying the method described above, we find

$$\mathfrak{M}^{(1)}(\mathbf{p}_1, \mathbf{p}_2) = -\frac{\alpha}{2^5\pi^6}\,\beta\int \frac{d^4k}{k^2}\,\frac{\Lambda^2}{\Lambda^2 + k^2}$$

$$\times \gamma_\mu \frac{\hat{p}_1 - \hat{k}}{(p_1 - k)^2}\,e\hat{A}_{\mathbf{p}_1 - \mathbf{p}_2}\,\frac{\hat{p}_2 - \hat{k}}{(p_2 - k)^2}\,\gamma_\mu$$

$$= \frac{\alpha}{(2\pi)^4}\,i\,ie\hat{A}_{\mathbf{p}_1 - \mathbf{p}_2}\left[-\ln\frac{\Lambda}{|\mathbf{p}_1 - \mathbf{p}_2|} - \frac{1}{4} + J_1(\mathbf{p}_1, \mathbf{p}_2)\right], \quad (12)$$

where

$$J_1(\mathbf{p}_1, \mathbf{p}_2) = \int_0^\infty \frac{d\xi dt}{(\xi - t + 1)^2}\,\frac{\frac{1}{2}\xi(p_1^2 + p_2^2t) - \hat{p}_2\hat{p}_1\xi}{(p_1^2 + p_2^2t)\xi + (\mathbf{p}_1 - \mathbf{p}_2)^2 t}. \quad (13)$$

Combining Eqs. (11) and (12), we now get the following expression for the mass operator in first approximation in α and $Z\alpha$ for $\mathbf{p}_1, \mathbf{p}_2 \gg m$, $|\mathbf{p}_1|$, $|\mathbf{p}_2| \gg p_0 = \epsilon_0$:

$$\mathfrak{M}_1(\mathbf{p}_1, \mathbf{p}_2) = \mathfrak{M}^{(0)} + \mathfrak{M}^{(1)}$$

$$eV_{\mathbf{p}_1 - \mathbf{p}_2}\frac{\alpha}{(2\pi)^4}\left(\ln\frac{|\mathbf{p}_1 - \mathbf{p}_2|}{p_1} + \frac{1}{2} + J_1(\mathbf{p}_1, \mathbf{p}_2)\right). \quad (14)$$

For the Coulomb field $eV_{\mathbf{p}_1 - \mathbf{p}_2} = Z\alpha/2\pi^2|\mathbf{p}_1 - \mathbf{p}_2|^2$. The gauge invariance of Eq. (14) can be checked easily: for $V_{\mathbf{p}_1 - \mathbf{p}_2} \to \delta(\mathbf{p}_1 - \mathbf{p}_2)$ the expression (14) goes to zero.

We shall not give here the cumbersome form of the operator $\mathfrak{M}_1(\mathbf{r}_1, \mathbf{r}_2)$ in the coordinate representation. We remark only that it can be seen from Eq. (9) that for the Coulomb field $\mathfrak{M}(\mathbf{r}_1, \mathbf{r}_2)$ is a homogeneous function of $\mathbf{r}_1, \mathbf{r}_2$ of degree -4. From Eqs. (14) and (13) it follows further that for $r_1 \to 0$, $\mathfrak{M}_1$ diverges not more strongly than as $1/r_1$. Therefore it is clear that for the values of r_1 and r_2 in question the mass operator contains $\delta(\mathbf{r}_1 - \mathbf{r}_2)/r_1$ and analogous expressions. For example, the last term in $J_1(\mathbf{p}_1, \mathbf{p}_2)$ gives in the coordinate representation

$$-\frac{Z\alpha^2}{(2\pi)^6}\int d\mathbf{p}_1 d\mathbf{p}_2 \exp\left(i\mathbf{p}_1\mathbf{r}_1 - i\mathbf{p}_2\mathbf{r}_2\right)$$

$$\times \int_0^\infty \frac{\xi d\xi dt}{\left(\xi - t - 1\right)^2} \frac{\hat{p}_2 \hat{p}_1}{\left(p_1^2 - p_2^2 t\right)\xi + \left(\mathbf{p}_1 - \mathbf{p}_2\right)^2 t},$$

$$-\frac{Z\alpha^2}{(2\pi)^2}\left(\alpha, \alpha\Gamma_2\right)\left(\Gamma_1\right)\frac{1}{r_{12}\left(r_1 - r_2 - r_{12}\right)};$$

$$r_{12} = |\mathbf{r}_1 - \mathbf{r}_2|, \qquad \nabla_{1,2} = \partial/\partial\mathbf{r}_{1,2}.$$

Consequently the important region in the integration of the expression $\int \mathfrak{M}(\mathbf{r}_1, \mathbf{r}_2)\psi_C(\mathbf{r}_2)d\mathbf{r}_2$ over $\mathbf{r}_2$ is that in which $|\mathbf{r}_1 - \mathbf{r}_2| \lesssim r_1$. In the nonrelativistic case $r_1 > 1/m$ the important region is that in which $|\mathbf{r}_1 - \mathbf{r}_2| \lesssim 1/m$.[6] The difference is due to the difference we have mentioned between the natures of the fluctuation motion for $r > 1/m$ and $r < 1/m$: for $r < 1/m$ the "radius of fluctuation" is proportional to r.

4. In order to find the change of the Coulomb singularity of the S and $P_{1/2}$ states, in what follows we shall seek to obtain directly the quantity $\int \mathfrak{M}(\mathbf{r}_1, \mathbf{r}_2)\psi_C(\mathbf{r}_2)d\mathbf{r}_2$ in Eq. (8); here $\psi_C(\mathbf{r})$ is the Coulomb function. If we consider elements other than the very lightest, so that $rm \sim r_{nuc}m \ll Z\alpha$, the wave function in which we are interested has the form (for definiteness we shall speak of the S state):

$$\psi_r(\mathbf{r}) = \text{const}\cdot r^{-\gamma}\begin{pmatrix} u_0 \\ (i\gamma - Z\alpha)(\boldsymbol{\sigma}\mathbf{r})u_0 \cdot r \end{pmatrix},$$

$$u_0 = \begin{pmatrix} 1 \\ 0 \end{pmatrix} \text{ or } \begin{pmatrix} 0 \\ 1 \end{pmatrix} \qquad (15a)$$

or in the momentum representation

$$\psi_r(\mathbf{p}) = p^{-3}\begin{pmatrix} c_1(Z\alpha)u_0 \\ c_2(Z\alpha)(\boldsymbol{\sigma}\mathbf{p})u_0 \cdot p \end{pmatrix}, \qquad (15b)$$

where $\gamma = 1 - (1 - Z^2\alpha^2)^{1/2}$, and c_1 and c_2 are certain functions of $Z\alpha$.

Since $\psi_C(\mathbf{p})$ and $\mathfrak{M}$ are homogeneous functions of $\mathbf{p}_1$, $\mathbf{p}_2$, the quantity $\int \mathfrak{M}(\mathbf{p}_1, \mathbf{p}_2)\psi_C(\mathbf{p}_2)d\mathbf{p}_2$ is obviously proportional to $p_1^{\gamma-2}$; that is, in the coordinate representation

$$\int \mathfrak{M}(\mathbf{r}_1, \mathbf{r}_2)\psi_r(\mathbf{r}_2)d\mathbf{r}_2 = \frac{\alpha}{2\pi}\hat{B}\left(Z\alpha, \frac{\mathbf{r}_1}{r_1}\right)\frac{\psi_r(\mathbf{r}_1)}{r_1}, \qquad (16)$$

where $\hat{B}$ is a certain spinor operator; the factor $\alpha/2\pi$ is separated out for convenience. From what has been said there follows the assertion used earlier, that for $p_1 \gg m$ values $p_2 \sim p_1 \gg m$ are also important in $\mathfrak{M}(\mathbf{p}_1, \mathbf{p}_2)$: the integral $\int \mathfrak{M}(\mathbf{p}_1, \mathbf{p}_2)\psi_C(\mathbf{p}_2)d\mathbf{p}_2$ converges in the region $p_2 \sim p_1$.

From the invariance of the complete equation (3), (8) under rotational and space-time reflections it follows that the operator $\hat{B}$ in Eq. (16) has the form

$$\hat{B}\left(Z\alpha, \frac{\mathbf{r}}{r}\right) = Z\alpha f_1(Z^2\alpha^2) + i\frac{\boldsymbol{\alpha}\mathbf{r}}{r}Z^2\alpha^2 f_2(Z^2\alpha^2), \qquad (17)$$

where f_1, f_2 are real even functions of $Z\alpha$.

We shall calculate the operator $\hat{B}$ to accuracy $Z^2\alpha^2$. Using the fact that the difference between each component of the wave function and the first term of its expansion in powers of $Z\alpha$ is a quantity $\sim\gamma \sim Z^2\alpha^2$, and that the operator $\mathfrak{M}$ already contains $Z\alpha$, in finding B we can replace the wave function (15) in the mass integral by the first terms of the expansion:

$$\psi_r(\mathbf{r}) - \psi_0(\mathbf{r}) = \begin{pmatrix} \varphi_0(\mathbf{r}) \\ \chi_0(\mathbf{r}) \end{pmatrix} = \text{const}\cdot\begin{pmatrix} u_0 \\ (i\gamma/Z\alpha)(\boldsymbol{\sigma}\mathbf{r}\,u_0) \cdot r \end{pmatrix},$$

$$\psi_r(\mathbf{p}) - \psi_0(\mathbf{p}) = \text{const}\cdot\begin{pmatrix} \delta(\mathbf{p})u_0 \\ (\gamma/Z\alpha)(\boldsymbol{\sigma}\mathbf{p}\,u_0) \cdot \pi^2 p^4 \end{pmatrix}. \qquad (18)$$

Having so obtained the answer in the form of Eq. (16) with ψ as given in Eq. (18), we shall determine the first terms of the expansion of B, i.e., of the functions f_1 and f_2 in Eq. (17). Having found B, we can again use Eq. (16) with the exact Coulomb function $\psi_C(\mathbf{r})$. This decidedly simplifies the calculations; to use the formulas (15) in finding B would be to get useless further accuracy, since B is subject to expansion in powers of $Z\alpha$.

Thus Eq. (8) with $\mathfrak{M}$ from Eq. (14) is now written

$$\boldsymbol{\sigma}\mathbf{p}\chi - (Z\alpha/r + V_{\text{pol}})\varphi + m\varphi = \int \mathfrak{M}_1(\mathbf{r}, \mathbf{r}')\varphi_0(\mathbf{r}')d\mathbf{r}' = 0, \qquad (19a)$$

$$\boldsymbol{\sigma}\mathbf{p}\varphi - (Z\alpha/r - V_{\text{pol}})\chi - m\chi = \int \mathfrak{M}_1(\mathbf{r}, \mathbf{r}')\chi_0(\mathbf{r}')d\mathbf{r}' = 0. \qquad (19b)$$

The mass term in Eq. (19a) is found immediately:

$$\text{const}\cdot\frac{Z\alpha^2}{2\pi}\frac{1}{2\pi^2}\int \frac{d\mathbf{p}_1 d\mathbf{p}_2 \exp\left(i\mathbf{p}_1\mathbf{r}\right)}{\left(\mathbf{p}_1 - \mathbf{p}_2\right)^2}\left(\ln\frac{|\mathbf{p}_1 - \mathbf{p}_2|}{p_1} - \frac{1}{2}\right)$$

$$\times\int_0^\infty \frac{d\xi dt}{\left(\xi - t - 1\right)^2}\frac{1 + \xi\left(p_1^2 - p_2^2 t\right) - \hat{p}_2\hat{p}_1\xi}{\left(p_1^2 - p_2^2 t\right)\xi + \left(\mathbf{p}_1 - \mathbf{p}_2\right)^2 t}$$

$$\times\hat{\alpha}(\mathbf{p}_2)\frac{Z\alpha^2}{2\pi r}\varphi_0(\mathbf{r}). \qquad (20)$$

The direct calculation of the mass term in Eq. (19b) is rather cumbersome. Using Eqs. (17) and (20), however, we at once conclude that this term is $(Z\alpha^2/2\pi r)\chi_0(\mathbf{r})$.

Thus, combining the results of the first approximation, we have for the equation (8), with accuracy $Z\alpha^2$

$$(\boldsymbol{\sigma}\mathbf{p} + m - Z\alpha/r - V_{\text{pol}} - Z\alpha^2/2\pi r)\psi(\mathbf{r}) = 0.$$

5. In finding the next approximation we again

use Eq. (17); we shall carry through the calculation only for the integral $\int \mathfrak{M}^{(2)}(\mathbf{p}, \mathbf{p}')(2\pi)^3\delta(\mathbf{p}')d\mathbf{p}'$.

According to Eq. (9) we have

$$(2\pi)^3\mathfrak{M}^{(2)}(\mathbf{p}, 0) = \frac{Z^3\alpha^3}{2^4\pi^7}\beta \times\int\frac{d^4k}{k^2}\gamma_\mu\frac{\hat{p}-\hat{k}}{(p-k)^2}\beta\frac{\hat{q}-\hat{k}}{(q-k)^2}\beta\frac{-\hat{k}}{k^2}\gamma_\mu\frac{dq}{q^2(p-q)^2} \quad (21)$$

(throughout, the two-dimensional part of the product of the four-rowed matrices is to be understood). It is convenient to separate the factor $-\hat{k} = -\boldsymbol{\gamma}\mathbf{k} - \beta k_4$ into its space and time parts and calculate the corresponding integrals J_A and J_B separately:

$$(2\pi)^3\mathfrak{M}^{(2)}(\mathbf{p}, 0) = \frac{Z^3\alpha^3}{2\pi}\beta(J_A + J_B),$$

$$J_{A,B} = \frac{1}{2^3\pi^6}\int\frac{dq}{q^2(p-q)^2}\gamma_\mu\gamma_n\beta\gamma_m\beta \times\int\frac{d^4k}{k^2}(-\boldsymbol{\gamma}\mathbf{k}, -\beta k_4)\gamma_\mu\frac{(p-k)_n(q-k)_m}{(p-k)^2(q-k)^2}. \quad (22)$$

Applying the method that has been described for the integration over k, using the equation $\partial f/\partial\mathbf{k} \times (\mathbf{p}-\mathbf{k}) = -\partial f(\mathbf{p}-\mathbf{k})/\partial\mathbf{p}$ in the calculation of J_A, and noting in the calculation of J_B that the fourth components of $\mathbf{p}$ and $\mathbf{q}$ are absent, i.e., the terms linear in k_4 are to be set equal to zero, we get

$$J_A = -\frac{i\gamma}{(2\pi)^4}\int\frac{dq}{q^3}\left(\frac{\partial}{\partial q}+\frac{\partial}{\partial p}\right)\frac{1}{(p-q)^2} \times\int_0^\infty\frac{d\xi dt}{(\xi+t+1)^2}\cdot\frac{1/_2(p^2+q^2t)-\xi\hat{q}\hat{p}}{(p^2+q^2t)\xi+(\mathbf{p}-\mathbf{q})^2t},$$

$$J_B = \frac{i}{2^3\pi^4}\int\frac{dq}{q^3(p-q)^2}\int_0^\infty\frac{\xi d\xi dt}{(\xi+t+1)^2}\left(2\frac{\hat{p}+\hat{q}t}{\xi+t+1} - \hat{p}-\hat{q}\right)\frac{1}{(p^2+q^2t)\xi+(\mathbf{p}-\mathbf{q})^2t}. \quad (23)$$

The calculation of the integrals J_A, J_B is accomplished by integration by parts, change of variables, and integration in the complex plane; because of the special nature of the expressions we omit the calculations. The results are:

$$\beta J_A = \frac{\alpha\rho}{4\pi\rho^3}\left(\frac{\pi^2}{12}-\frac{1}{4}\right), \quad \beta J_B = \frac{\alpha\rho}{4\pi\rho^3}\left(\frac{\pi^2}{12}-\frac{5}{4}\right). \quad (24)$$

Equating the Fourier transform of Eq. (17) to Eqs. (24), (22), we find

$$f_2(Z^2\alpha^2) = \frac{1}{6}\pi^2 - \frac{3}{2} + O(Z^2\alpha^2). \quad (24')$$

The expansion of the vacuum-polarization potential contains only odd powers of $Z\alpha$,[4] so that to our present accuracy Eq. (8) for small distances can be written

$$\left[\boldsymbol{\alpha}\mathbf{p} + \beta m - \frac{Z\alpha}{r} - V_{\text{pol}} + \frac{Z\alpha^3}{2\pi r} + \frac{i\alpha r}{r^2}\frac{Z^2\alpha^3}{2\pi}\left(\frac{\pi^2}{6}-\frac{3}{2}\right)\right]\psi(\mathbf{r}) = 0. \quad (25)$$

For the main component $\varphi(\mathbf{r})$ of the wave function we get in the region in question

$$\varphi(\mathbf{r})/\varphi_c(\mathbf{r}) = 1 + \delta\varphi_{\text{pol}}/\varphi_c - \delta\varphi_{f1}/\varphi_c = 1 + \frac{Z^3\alpha^3}{2\pi}\left\{\frac{2}{3}\left[\ln^2\frac{1}{rm} + \ln\frac{1}{rm} + \frac{1}{2} - \left(\frac{5}{6}+\ln\gamma\right)\ln\frac{1}{mZ\alpha r}\right] - \left(\frac{\pi^2}{6}-\frac{1}{2}\right)\ln\frac{1}{mZ\alpha r}\right\}. \quad (26)$$

For $Z = 92$, $r \sim r_{\text{nuc}} = 6\times10^{-13}$ cm the right member of Eq. (26) differs from unity by

$$\delta\varphi(r_{\text{nuc}})/\varphi_c(r_{\text{nuc}}) = 2.7\cdot10^{-3}. \quad (27)$$

At present such a small change of the wave function cannot be distinguished from the effects of the finite dimensions of the nucleus, the distribution of charge in the nucleus, etc., and is obviously unobservable.

[1] J. Schwinger, Phys. Rev. **75**, 651 (1949); Russ. Transl. in collection: Новейшее развитие квантовой электродинамики (Latest Developments in Quantum Electrodynamics), IIL, 1954.

[2] T. Welton, Phys. Rev. **74**, 1157 (1948); Russ. Transl. in collection: Вопросы причинности в квантовой механике (Problems of Causality in Quantum Mechanics), IIL, 1955.

[3] Landau, Abrikosov, and Khalatnikov, Doklady Akad. Nauk SSSR **95**, 497, 773, 1177; **98**, 261 (1954).

[4] E. Wichmann and N. Kroll, Phys. Rev. **101**, 843 (1956).

[5] J. Schwinger, Proc. Nat Acad, **37**, 455 (1955); Russ. Transl.: Пробл. совр. физ. (Probl. Mod. Phys.) **3** (1955).

[6] R. Karplus and A. Klein, Phys. Rev. **85**, 972 (1952); Russ. Transl. in collection: Новейшее развитие квантовой электродинамики (Latest Developments in Quantum Electrodynamics), IIL, 1954.

[7] R. P. Feynman, **76**, 769 (1949); Russ. Transl. in collection: Новейшее развитие квантовой электродинамики (Latest Developments in Quantum Electrodynamics), IIL, 1954.

[8] R. P. Feynman, Phys. Rev. **84**, 108 (1951); Russ. Transl.: Пробл. совр. физ. (Probl. Mod. Phys.) **3** (1955).

[9] W. Heitler, The Quantum Theory of Radiation Oxford, 1953 (Russ. Transl., IIL, 1956), Chapter 6.

Translated by W. H. Furry
375

ON THE POSSIBILITY OF DETERMINING THE π-π SCATTERING AMPLITUDES FROM THE ANALYSIS OF THE $\gamma + p \to N + \pi + \pi$ REACTIONS NEAR THRESHOLD

A. A. ANSEL'M and V. N. GRIBOV

Submitted to JETP editor January 19, 1959

J. Exptl. Theoret. Phys. (U.S.S.R.) **36**, 1890-1893 (June, 1959)

It is shown that a study of the reactions $\gamma + p \to p + \pi^+ + \pi^-$, $p + \pi^0 + \pi^0$, $n + \pi^+ + \pi^0$ near threshold should allow the determination of the $\pi-\pi$ zero energy scattering amplitudes if the $\pi-\pi$ interaction has resonance character, and the determination of a certain combination of these amplitudes if the interaction does not have resonance character.

At present there does not exist any conclusive evidence on the interaction between π mesons. It is therefore of importance to find any parameters which are connected with this interaction. In the present paper it is shown that an experimental investigation of the photoproduction of two mesons near the threshold can yield information on the zero energy $\pi-\pi$ scattering amplitude.

In the following we shall consider two cases:

1) The interaction between π mesons does not have resonance character at small energies. In this case the energy and angular distribution of the reaction can be obtained by the method developed in references 1-3.

However, the case of photoproduction of two π mesons differs considerably from the decay of the τ meson which was treated in references 1-3. It allows generally an easier way to determine the $\pi-\pi$ scattering amplitudes.

2) The $\pi-\pi$ scattering at small energies is of resonance character. The characteristic energy dependence associated with this case has been already investigated for other reactions.[4] Since at resonance the final state interaction of the π mesons produces an effect of the order of magnitude unity this case would be particularly favorable from the experimental point of view.

1. THE CASE OF A NONRESONATING INTERACTION

In references 1-3 it has been shown that in reactions involving the creation of three particles a final state interaction leads to considerable changes in the angular and energy distributions. In particular, at energies close to threshold when terms up to the first power in kr_0 have been retained (k – momentum corresponding in order of magnitude to the energy excess above the threshold; r_0 – range of the interaction) the matrix element of the S matrix has the form

$$\langle f|S|i\rangle = (1 + ik_{12}a_{12} + ik_{13}a_{13} + ik_{23}a_{23})\langle f_0|S|i\rangle, \quad (1)$$

where k_{12}, k_{13}, k_{23} and a_{12}, a_{13}, a_{23} are the relative momenta and the scattering amplitudes between two particles respectively and the wave function of the final state in the matrix element of the right hand side f_0, is to be taken at zero energy of the three particles. The quantity $\langle f_0|S|i\rangle$ nevertheless still depends on the energy through the initial state wavefunction $|i\rangle$. However, close to threshold the matrix element $\langle f_0|S|i\rangle$ is an analytic function of the energy E and thus differs from the matrix element at threshold $\langle f_0|S|i_0\rangle$ by a term of the order $\sim \Delta E \sim k^2$. Therefore for an accuracy linear in k one can set $\langle f_0|S|i\rangle = \langle f_0|S|i_0\rangle$. The fact that $\langle f_0|S|i\rangle$ is analytical can be understood if one recalls that the branch points in matrix elements of the type $\langle f|S|i\rangle$ at the thresholds usually are due to the final state. This can be demonstrated using a method analogous to the method which was used by Lehmann[5] to show the analyticity of the scattering amplitude as a function of the momentum transfer.

It has been shown[2,3] for the case of τ-meson decay that, owing to the reality of the matrix elements of the type $\langle f_0|S|i\rangle$, the terms linear in k vanish in the expressions for the probability of the process. This circumstance not only considerably decreases the magnitude of the effect but also leads to the necessity of a much more detailed investigation of the final three-particle state. For this situation in the expressions for the probability there are two types of terms which are quadratic in k. They are, first, terms which determine the correlations between the outgoing particles, and which can be expressed in terms of the scattering amplitudes between pairs of particles, and second, terms which cannot be evaluated but which do not influence the angular distributions. Thus one cannot obtain the energy distributions near the threshold. It is therefore of value only to study the angular correlations.

It will be shown below that in the case of photoproduction of two π mesons the terms linear in k are present in the expression for the probability of the process when the reaction has a real intermediate state which differs from the initial and the final state (viz., in the present case, a nucleon plus a π meson) and when the reaction can go via channels which differ in the charge of the created particles. The relations given below allow in principle to determine a certain combination of the $\pi-\pi$ scattering amplitudes without a detailed investigation of the angular correlations of the reaction.

There are three possible reactions of production of two π mesons by γ quanta:

$$\gamma + p \to p + \pi^+ + \pi^-, \tag{2.1}$$
$$\gamma + p \to p + \pi^0 + \pi^0, \tag{2.2}$$
$$\gamma + p \to n + \pi^+ + \pi^0. \tag{2.3}$$

We shall denote the respective matrix elements at zero energy by

$$\lambda_1 = \rho_1 \exp(i\varphi_1), \qquad \lambda_2 = \rho_2 \exp(i\varphi_2), \qquad \lambda_3 = \rho_3 \exp(i\varphi_3).$$

Utilizing the method which was applied in reference (2) to the decay of the τ meson one can easily obtain expressions for the squares of the matrix elements of the reactions (2) with an accuracy of terms linear in k:

$$|\langle p\pi^+\pi^- | S | p\gamma\rangle|^2 = \rho_1^2\Big[1 + \rho_{12}\sin\varphi_{12}\cdot\tfrac{2}{3}k_{12}(a_2-a_0) - \rho_{13}\sin\varphi_{13}\cdot\tfrac{2}{3}\sqrt{2}\,k_{23}(b_{3/2}-b_{1/2})\Big],$$

$$|\langle p\pi^0\pi^0 | S | p\gamma\rangle|^2 = \rho_2^2\Big[1 + \rho_{21}\sin\varphi_{21}\cdot\tfrac{4}{3}k_{12}(a_2-a_0) + \rho_{23}\sin\varphi_{23}\cdot\tfrac{2}{3}\sqrt{2}\,(k_{13}+k_{23})(b_{3/2}-b_{1/2})\Big],$$

$$|\langle n\pi^+\pi^0 | S | p\gamma\rangle|^2 = \rho_3^2\Big[1 + \rho_{31}\sin\varphi_{31}\cdot\tfrac{2}{3}\sqrt{2}\,k_{23}(b_{3/2}-b_{1/2}) + \rho_{32}\sin\varphi_{32}\cdot\tfrac{2}{3}\sqrt{2}\,k_{13}(b_{3/2}-b_{1/2})\Big],$$

$$\rho_{ik} = \rho_k/\rho_i, \qquad \varphi_{ik} = \varphi_i - \varphi_k. \tag{3}$$

Here a_0 and a_2 are the $\pi-\pi$ mesons scattering amplitudes at zero energy for states with isotopic spin 0 and 2 (since the π mesons close to threshold are created in a relative S-state an isotopic spin 1 is impossible), while $b_{1/2}$ and $b_{3/2}$ are $\pi-\pi$ meson scattering amplitudes at zero energy for states with isotopic spin 1/2 and 3/2. In k_{12}, k_{13}, and k_{23} the indices 1 and 2 refer to mesons, the index 3 to the nucleon. Comparing with the case of the τ-meson decay, one sees that the quantities λ_1, λ_2, and λ_3 are not real and have relative phases differing from zero. They can be expressed in terms of measurable quantities. By studying all three reactions (2) we can determine the charge exchange amplitudes $(a_2-a_0)/3$ and $(\sqrt{2}/3)\times(b_{3/2}-b_{1/2})$. However, since the amplitudes $b_{3/2}$ and $b_{1/2}$ are well known it is possible to simplify the analysis considerably by utilizing the isotopic invariance. So one can determine $(a_2-a_0)/3$ by studying only one reaction (e.g. $\gamma + p \to p + \pi^+ + \pi^-$).

The electromagnetic interaction is the sum of an isotopic scalar and a vector. Therefore the final state isotopic spin can be 1/2 or 3/2 (but not 5/2). Each of the final states (2) can be expanded as the sum of two states. In one of them the isotopic spin of the two π mesons $T_{12} = 0$ and the total isotopic spin $T = 1/2$; in the other $T_{12} = 2$, $T = 3/2$. We can easily verify that the following relation between λ_1, λ_2 and λ_3 arises:

$$\lambda_3 = -(\lambda_1+\lambda_2)/\sqrt{2}, \tag{4}$$

from which follows, for example

$$\rho_{12}\sin\varphi_{12} = -\sqrt{2}\,\rho_{13}\sin\varphi_{13}. \tag{5}$$

This relation allows us to determine a_2-a_0 from only the first reaction if the coefficients of k_{12} and k_{23} have been found experimentally.

2. THE CASE OF A RESONATING INTERACTION

The formulae given above concern the case where the $\pi-\pi$ interaction at small energies does not have a resonance character, i.e., if the $\pi-\pi$ scattering amplitude is of the order of the range of the forces (Compton wavelength of the π meson): $a \approx r_0 \approx 1/\mu$. We now assume the opposite case, i.e., we take $a \gg r_0$ and, as before, $kr_0 \ll 1$ while we assume $ka \approx 1$. In this case the π-nucleon interaction evidently does not play such an important role as the $\pi-\pi$ interaction since the former as is well known does not have a resonance character at zero energy. Effects of this type have been already treated repeatedly.[4] We therefore give only the final results. For the three processes (2) we have in this case [instead of (3)]:

$$|\langle p\pi^+\pi^- | S | \gamma p\rangle|^2 = \rho_1^2(1+k_{12}^2a_0^2)^{-1}(1+k_{12}^2a_2^2)^{-1}\times\Big\{\Big[1+\tfrac{1}{3}\rho_{12}\sin\varphi_{12}k_{12}(a_2-a_0)\Big]^2 + k_{12}^2\Big[\tfrac{1}{3}(2a_2+a_0) - \tfrac{1}{3}\rho_{12}\cos\varphi_{12}(a_2-a_0)\Big]^2\Big\},$$

$$|\langle p\pi^0\pi^0 | S | \gamma p\rangle|^2 = \rho_2^2(1+k_{12}^2a_0^2)^{-1}(1+k_{12}^2a_2^2)^{-1}\times\Big\{\Big[1+\tfrac{2}{3}\rho_{21}\sin\varphi_{21}k_{12}(a_2-a_0)\Big]^2 + k_{12}^2\Big[\tfrac{1}{3}(a_2+2a_0) - \tfrac{2}{3}\rho_{21}\cos\varphi_{21}(a_2-a_0)\Big]^2\Big\},$$

$$|\langle n\pi^+\pi^0 | S | \gamma p\rangle|^2 = \rho_3^2(1+k_{12}^2a_2^2)^{-1}. \tag{6}$$

As can be seen from (6) in this case one can determine both amplitudes a_0 and a_2 separately.

In conclusion the authors express their thanks to S. V. Dresvin who performed some computations.

[1] V. N. Gribov, J. Exptl. Theoret. Phys. (U.S.S.R.) **33**, 1431 (1957), Soviet Phys. JETP **6**, 1102 (1958).

[2] V. N. Gribov, Nuclear Phys. **5**, 653 (1958).

[3] V. N. Gribov, J. Exptl. Theoret. Phys. (U.S.S.R.) **34**, 749 (1958), Soviet Phys. JETP **7**, 514 (1958).

[4] K. M. Watson, Phys. Rev. **88**, 1163 (1952); A. B. Migdal, J. Exptl. Theoret. Phys. (U.S.S.R.) **28**, 10 (1955), Soviet Phys. JETP **1**, 7 (1955).

[5] H. Lehmann, Nuovo cimento **10**, 579 (1958).

Translated by M. Danos
376

ACTION AS A SPACE COORDINATE. X.

YU. B. RUMER

Institute of Radiophysics and Electronics, Siberian Branch, Academy of Sciences, U.S.S.R.

Submitted to JETP editor January 20, 1959

J. Exptl. Theoret. Phys. (U.S.S.R.) **36**, 1894—1902 (June, 1959)

The difficulties encountered in five-optics in formulation of the spinor equations are surmounted in the present paper. It is shown that the requirement of invariance with respect to physically permissible transformations leads to correct spinor equations.

The requirement of physical admissibility separates subgroups of general transformations of the four-dimensional space-time and gauge transformations from the general transformation group of five-dimensional space. Restriction of the group of permissible transformations does in no means signify that the five-dimensional conception is not valid in principle. The most important feature of the five-dimensional theory is the periodic dependence (with period h) of the fields on the action coordinate. This fact and its consequences cannot be reduced to a simple unification of the four-coordinate point-transformation group with the gauge-transformation group. Another essentially five-dimensional effect is the existence of the scalar χ-field whose appearance in the theory of the field of a charged material particle yields formulas that differ from those of present-day gravitation theory.

1. INTRODUCTION

FIVE-dimensional optics,[1] the subject of this series of communications (1949—1953), begins with the observed deep symmetry of the laws of nature in three spatial coordinates, time, and action. This symmetry permits the relativistic problem (classical and quantum) of the motion of a charged material point in a specified gravitational and electromagnetic field to be formulated as a problem in five-dimensional optics (geometrical and wave), concerning the propagation of wave fields in the Riemann configuration space of coordinates, time, and action. The metric tensor of this space is

$$G_{\mu\nu} = \begin{pmatrix} g_{ik} + (1+\chi) g_i g_k & (1+\chi) g_k \\ (1+\chi) g_i & (1+\chi) \end{pmatrix}, \qquad (1.1)$$

where g_{ik} are gravitational potentials, $g_i = (e/mc^2)A_i$ are electromagnetic potentials, and χ is a new scalar field that appears in five-dimensional optics.

The five-dimensional space of five-optics is topologically closed in the fifth action coordinate, and the period of the fifth coordinate is equal to Planck's constant h. This means that all the components of the metric tensor $G_{\mu\nu}$ are periodic functions of the fifth coordinate, with a period equal to h.

In the classical approximation $h \to 0$ the periodicity condition imposed on the field $G_{\mu\nu}$, degenerates into a condition that all $G_{\mu\nu}$ be independent of the fifth action coordinate, i.e., into the so-called cylindricity condition of the earlier five-dimensional theories (Kalutza-Klein-Fock).

It has been shown in the papers of this series that in the case of tensor particles (particles with integral spin) an account of the external gravitational and electromagnetic fields is made possible by a general covariant formulation of the equations of motion for a free particle. A connection was established between five-dimensional tensor analysis and the so-called D-formalism (replacement of the operators ∂_k by the operators $\partial_k - i(e/\hbar c)A_k$).

In the previous papers "general covariance of five-dimensional equations" meant covariance under general transformations of all five coordinates (x^i, $x^5 = S$)

$$x^{i'} = x^i + f^i(x^1, x^2, x^3, x^4, S),$$
$$S' = S + f(x^1, x^2, x^3, x^4, S) \qquad (1.2)$$

with that substantial limitation, that only those functions f^i, f are admitted, which are periodic with respect to the coordinate S (with period h),

$$f^i(\ldots, S+h) = f^i(\ldots, S),$$
$$f(\ldots, S+h) = f(\ldots, S), \qquad (1.3)$$

since only such transformations are admitted by the topological structure of five-dimensional space.

In the case of spinor particles (particles with half-integer spin), five-optics encountered a con-

siderable difficulty, which was emphasized in the papers of this series and remained unsurmountable. Specifically, the general-covariant formulation of the equation for the free electron has led to an incorrect expression for the current-density vector

$$\bar{\psi}\gamma_k\psi + \frac{i}{8}\partial_l[\bar{\psi}(\gamma_k\gamma_l - \gamma_l\gamma_k)\psi], \qquad (1.4)$$

in which the second term differs from that in the correct expression. Further, in the presence of an external electromagnetic field, the following incorrect expression was obtained

$$\{\gamma_k(\partial_k - ieA_k) + m.\text{—}(ie/8\ m)\gamma_k\gamma_l F_{kl}\}\psi = 0. \qquad (1.5)$$

This differs from the correct one by a term proportional to F_{kl}.

We shall show in the present communication where the error lies in the general-covariant formulation of the field equations, and shall derive correct equations for spinor particles.

2. PHYSICALLY-ADMISSIBLE TRANSFORMATIONS OF FIVE-DIMENSIONAL SPACE

Let us investigate whether all the transformations of group (1.2) are physically admissible. We start with the premise that if the metric potentials $G_{\mu\nu}$ do not depend on the fifth action coordinate, and consequently transitions of particles from one charged state into another with emission of charged quanta are forbidden, then this forbiddenness should be retained in any other physically admissible coordinate system.

This requirement is incompatible with the requirement of covariance with respect to the general transformations (1.2), and leads to a narrowing of this group to two subgroups: groups of point transformations of space-time, and groups of gauge transformations

$$x^{i'} = x^i + f^i(x^1, x^2, x^3, x^4), \quad S' = S + f(x^1, x^2, x^3, x^4). \qquad (2.1)$$

The narrowing of the group of admissible transformation does not mean giving up five-dimensionality. The most important feature of the five-dimensional theory is the periodic dependence of the fields on the action coordinate, with period h. This fact and its consequences cannot be reduced to a simple unification of a group of point transformations of four coordinates with a group of gauge transformations.

An important five-dimensional effect is also the scalar χ-field, the appearance of which in the problem of the field of a charged material point leads to formulas that differ from the formulas of modern theory of gravitation.

Thus, the geometry of five-dimensional space of five-optics is Riemannian only in a limited sense. A two-dimensional model of such a space is a cylinder with a constant radius $h/2\pi$. The admissible transformations represent all possible extensions along the axis of the cylinder and "rotation of wheels". These lead to changes in the coordinate lines on the surface. Here, however, cross sections perpendicular to the axis cylinder transform into themselves, while the radius of the cylinder remains unchanged. Thus, Planck's constant h has an invariant geometrical meaning only for the subgroup of physically admissible transformations.

Many authors have noted that spinor fields can be introduced into Riemann space only with the aid of local systems of orthogonal references, which admit local rotations. A systematic reference-system analysis, which permits unique formulation of the equations for tensor and spinor fields, was proposed by the author.[2] The principal premises and formulas of the reference-system analysis are given in the appendix.

Let us now consider the physical limitations that are superimposed on the choice of local coordinate systems, i.e., on the rotation of four-dimensional references.

In the four-dimensional case the choice of one of the vectors of the reference is limited to the physical condition that the fourth vector of the reference must be time-like, thus restricting the permissible rotations of the reference. A transition from one reference to another one, connected with the initial orthogonal transformation, denotes physically the transition from one Einsteinian lift into another one, moving uniformly and in a straight line relative to the first one. The group of local rotations is none other than the local Lorentz group.

In special relativity theory the equations of the field are invariant under two groups of transformations: a) translation group, $x^{i'} = x^i + a^i$, with which the laws of energy and momentum conservation are related, b) Lorentz group $x^{i'} = \Sigma_k l_{ik} x^k$, with which are connected the laws of conservation of angular momentum and the symmetry of the energy-momentum tensor.

In general relativity theory, the roles of these two groups are assumed by the following: a) group of general transformations of coordinates, $x^{i'} = x^i + f^i(x^1, x^2, x^3, x^4)$ and b) local Lorentz group $\Omega^{i'}(k) = L(k,l)\,\Omega^i(l)$. Were the world to contain only tensor fields and no spinor ones, it would not be necessary to introduce the Lorentz local group, and only transformations of group a) need be considered.

The existence of spinor fields, the components of which transform in accordance with the repre-

sentations of the local Lorentz groups, indicates the fundamental significance of this group also in general relativity theory.

In the case of five-dimensional space, one of the directions—the "direction" of action—is physically separate. While the space-time coordinates can be measured by physical instruments, the action coordinate cannot be measured by an instrument. The restriction to the group of admissible transformations (2.1) shows that the "direction" of action is conserved under all admissible point transformations. We can therefore choose for the fifth vector $\Omega^{\sigma}(5)$ a vector tangent to the coordinate line x^5, and admit only orthogonal transformations that leave the vector $\Omega^{\sigma}(5)$ invariant. Obviously, the group of these transformations is indeed the Lorentz group of local transformations, i.e., the transition from one Einstein lift to another.

We have formulated above a principle, by which the metric or the components of the reference are independent of the fifth coordinate in physically admissible coordinate system regardless of the choice of the system. It follows therefore that the coefficients of orthogonal transformations $L(n, m)$ cannot depend on the fifth coordinate x^5 if this transformation is physically admissible.

In our earlier papers, the physical limitations on the group of point transformations and the group of reference relations were not considered. It was assumed that the equation should be covariant with respect to extensive groups of all point transformations (1.2) and five-dimensional rotations of the reference. This has led to an incorrect equation for spinor particles. We shall show that the restriction to groups of permissible transformations makes it possible to obtain a correct equation for the electron.

Let us construct, in accordance with the above, a reference field.

Let x^1, x^2, x^3, x^4 be space-time coordinates, which determine the localization of an event in space-time, and x^5 the action coordinate. Then the components of the metric five-tensor $G_{\mu\nu}$ are periodic functions of the coordinate x^5. To separate in the five-dimensional space the four-dimensional subspace (space + time) and the orthogonal linear action subspace, which is orthogonal to the other subspace, we begin to orthogonalize the metric tensor

$$G_{\mu\nu} = \begin{pmatrix} g_{ik} + (1+\chi) g_i g_k & (1+\chi) g_k \\ (1+\chi) g_i & 1+\chi \end{pmatrix}. \qquad (2.2)$$

For this purpose we chose a unit vector $\Omega^{\sigma}(5)$ tangent to the action lines

$$\Omega^{\sigma}(5) = (0, 0, 0, 0, 1/\sqrt{1+\chi}),$$
$$\Omega_{\sigma}(5) = (\sqrt{1+\chi}\, g_1, \sqrt{1+\chi}\, g_2, \sqrt{1+\chi}\, g_3, \sqrt{1+\chi}\, g_4, \sqrt{1+\chi}). \qquad (2.3)$$

We choose four unit vectors $\Omega_{\sigma}(n)$, $(n = 1, 2, 3, 4)$, orthogonal to each other and orthogonal to the vector $\Omega^{\sigma}(5)$. In virtue of $\Omega^{\sigma}(5)\,\Omega_{\sigma}(n) = \delta(5, n)$, all the components of $\Omega_5(n)$ should vanish. Denoting

$$\Omega_{\sigma}(n) = \{\omega_i(n), 0\}, \qquad (2.4)$$

we have

$$\Omega_{\sigma}(\alpha) = \begin{pmatrix} \omega_1(1) & \omega_1(2) & \omega_1(3) & \omega_1(4) & \sqrt{1+\chi}\, g_1 \\ \omega_2(1) & \omega_2(2) & \omega_2(3) & \omega_2(4) & \sqrt{1+\chi}\, g_2 \\ \omega_3(1) & \omega^3(2) & \omega_3(3) & \omega_3(4) & \sqrt{1+\chi}\, g_3 \\ \omega_4(1) & \omega_4(2) & \omega_4(3) & \omega_4(4) & \sqrt{1+\chi}\, g_4 \\ 0 & 0 & 0 & 0 & \sqrt{1+\chi} \end{pmatrix}. \qquad (2.5)$$

Calculation of the covariant components of the reference field yields

$$\Omega^{\sigma}(\alpha) = \begin{pmatrix} \omega^1(1) & \omega^1(2) & \omega^1(3) & \omega^1(4) & 0 \\ \omega^2(1) & \omega^2(2) & \omega^2(3) & \omega^2(4) & 0 \\ \omega^3(1) & \omega^3(2) & \omega^3(3) & \omega^3(4) & 0 \\ \omega^4(1) & \omega^4(2) & \omega^4(3) & \omega^4(4) & 0 \\ -\omega^i(1) g_i & -\omega^i(2) g_i & -\omega^i(3) g_i & -\omega^i(4) g_i & 1/\sqrt{1+\chi} \end{pmatrix} \qquad (2.6)$$

Reference tensor analysis (see Appendix) introduces, along with ordinary derivatives ∂_{σ}, the reference derivatives $D(\alpha) = \Omega^{\sigma}(\alpha)\partial_{\sigma}$. We note that reference derivatives $D(\alpha)$, for the foregoing choice of the five-dimensional reference, have the form

$$D(k) = \omega^i(k)(\partial_i - g_i\partial_5), \qquad D(5) = (1+\chi)^{-1/2}\partial_5 \qquad (2.7)$$

If we neglect the χ-field, confine ourselves to a harmonic dependence of the functions on the coordinate x^5, and replace the operators ∂_5 by im, then D(k) goes into the operator of generalized momentum of a particle in an electromagnetic field.

We shall henceforth consider only reference-component quantities since spinors have only reference components.

If we restrict ourselves to physically admissible transformations, the quantities that are invariants of point transformations and tensors of local rotations are

$$T(\alpha), \qquad D(5)\,T(\alpha), \qquad \nabla^{(5)}T(\alpha), \qquad (2.8)$$

where $T(\alpha)$ are the invariant components of the tensors, $D(\alpha)$ is the reference derivative, and $\nabla(\alpha)$ is the invariant derivative. Definitions of these quantities and their properties are given in the Appendix.

3. FIVE-DIMENSIONAL FIELD EQUATIONS

According to five-optics, allowance is made in particle wave equations for the external electromagnetic field by a general-covariant formulation (with the limitations indicated in Sec. 2) of the equations for the free particles in the Riemannian five-dimensional space. We agree from now on to distinguish between "five-dimensional" quantities or operators, which will be denoted by capital letters, and "four-dimensional" quantities or operators, denoted by lower-case letters (see Appendix for symbols).

Five-dimensional quantities:

$$G_{\mu\nu},\ \Omega_\mu(\alpha),\ G^{\mu}_{\alpha\beta},\ \Delta(\alpha,\beta,\gamma),\ \Lambda=\det|\Omega_\alpha(\varkappa)|=\lambda\sqrt{1+\chi}.$$

Four-dimensional quantities:

$$g_{ik},\omega_i(k),\ \Gamma^l_{ik},\ \delta(i,k,l),\ \lambda=\det|\omega_i(k)|.$$

Five-dimensional operators:

$$D(\alpha),\quad \nabla(\alpha),\quad B(\alpha).$$

Four-dimensional operators:

$$d(k),\quad \delta(k),\quad b(k).$$

Let us consider the five-dimensional Lagrange integral

$$J=\frac{1}{2i}\int d^5x\Lambda\{\overline{W}\mu(\alpha)(D(\alpha)W)-(D(\alpha)\overline{W})\mu(\alpha)W\},\quad (3.1)$$

where, according to (2.7)

$$D(k)W=(d(k)W-g(k)\partial_5 W),$$
$$D(k)\overline{W}=(d(k)\overline{W}-g(k)\partial_5\overline{W}),$$
$$D(5)W=(1+\chi)^{-1/2}\partial_5 W,\ D(5)\overline{W}=(1+\chi)^{-1/2}\partial_5\overline{W}.$$

The integral (3.1) can be written in the form

$$J=\frac{1}{2i}\int d^5x\cdot\lambda\sqrt{1+\chi}\{\overline{W}(d(k)-g(k)\partial_5)\mu(k)W$$
$$-[(d(k)-g(k)\partial_5)\overline{W}]\mu(k)W$$
$$+\frac{1}{\sqrt{1+\chi}}(\overline{W}\mu(5)\partial_5 W-(\partial_5\overline{W})\mu(5)W)\}.\quad (3.2)$$

The integral (3.2) is invariant under general admissible point coordinate transformations (2.1), but still does not admit of a free four-dimensional rotatability of the reference field in space-time. This free rotatability, however, appears immediately if we replace the reference derivatives in (3.2) by invariant derivatives:

$$d(k)W\to\delta(k)W=d(k)W-b(k)W,$$
$$d(k)\overline{W}\to\delta(k)\overline{W}=d(k)W+\overline{W}b(k).\quad (3.3)$$

We obtain a new Lagrange integral $\tilde{J}$, which differs from the integral J by the additional term

$$\tilde{J}-J=-\frac{1}{2i}\int d^5x\cdot\lambda\sqrt{1+\chi}[\overline{W}(\mu(k)b(k)+b(k)\mu(k))W].\quad (3.4)$$

The Lagrangian $\tilde{J}$ satisfies all the requirements of five-optic covariance, i.e., it remains invariant under transformations of the (local) Lorentz group and under transformations of groups (2.1).

If the metric fields are independent of the coordinate x^5, then the transitions from one charged state into another are forbidden, and the spinors W, $\overline{W}$ depend harmonically on the coordinate x^5.

$$W=U(x^1,x^2,x^3,x^4)\exp(imx^5),$$
$$\overline{W}=\overline{U}(x^1,x^2,x^3,x^4)\exp(-imx^5).\quad (3.5)$$

Inserting (3.5) into (3.4) and integrating over x^5 we get

$$\tilde{J}=\frac{1}{2i}\int d^4x\cdot\lambda\sqrt{1+\chi}\{\omega^l(k)\overline{U}\mu(k)(\delta_l U-img_l U)$$
$$+\frac{2im}{\sqrt{1+\chi}}\overline{U}\mu(5)U-\omega^l(k)(\partial_l\overline{U}+img_l\overline{U})\mu(k)U$$
$$-\overline{U}(\mu(k)b(k)+b(k)\mu(k))U\}.\quad (3.6)$$

We now introduce the notation

$$U=\psi,\quad i\overline{U}\mu(5)=\overline{\psi},\quad i\mu(k)\mu(5)=\gamma(k),$$
$$\sqrt{1+\chi}\omega^l(k)=\tilde{\omega}^l(k)$$

and rewrite (3.6) in the form

$$\tilde{J}=\frac{1}{2i}\int d^4x\cdot\lambda\{\tilde{\omega}^l(k)[\overline{\psi}\gamma(k)(\partial_l\psi-img_l\psi)$$
$$-(\partial_l\overline{\psi}+img_l\overline{\psi})\gamma(k)\psi]$$
$$+2m^2\overline{\psi}\psi-\overline{\psi}(\gamma(k)b(k)+b(k)\gamma(k))\psi\}.\quad (3.7)$$

We see that the external electromagnetic field is computed by formulating equations for the free electron, covariant with respect to groups of admissible transformations. The scalar χ-field, which is specific for five-optics, is calculated by replacing the true gravitational references $\omega^l(k)$ by the effective gravitational references $\tilde{\omega}^l(k)$.

It was shown in the earlier communications that in five-optics the energy-momentum four-tensor and the current vector are combined into a common energy-momentum-charge five-tensor:

$$\theta^\gamma(\alpha)=\Lambda^{-1}\delta\tilde{J}/\delta\Omega_\alpha(\varkappa),\quad (3.8)$$

where $\tilde{J}$ is an invariant Lagrange integral

$$\tilde{J}=\int d^5x\cdot\Lambda\mathcal{L}.\quad (3.9)$$

It was also shown that the invariance of the Lagrangian $\mathcal{L}$ with respect to the group of local five-dimensional rotations leads to the symmetry of the five-tensor $\theta(\alpha,\beta)=\theta(\beta,\alpha)$.

We restrict ourselves to requiring invariance with respect to physically admissible rotations, i.e., the four-dimensional Lorentz group. Therefore the five-tensor of the energy-momentum-charge, generally speaking, will not be symmetrical. Only the energy-momentum four-tensor will be symmetrical, $\theta(m, n) = \theta(n, m)$ $(m, n = 1, 2, 3, 4)$, but in general $\theta(5, n) \neq \theta(n, 5)$. Thus in accordance with the general theory of relativity, we obtain a symmetrical energy-momentum tensor. In our previous papers we obtained an incorrect expression for the electron current vector, since the Lagrange integral was assumed invariant with respect to the five-dimensional rotation group. We obtain a correct expression by calculating the functional derivative of $\overline{J}$ with respect to $\Omega_i(5) = g_i\sqrt{1+\chi}$. From (3.6) we get

$$\Lambda\theta^i(5) = \delta\overline{J}/\delta\Omega_i(5)$$
$$= -\lambda m\overline{\psi}_\mu(k)\omega^i(k)U = \lambda m(\overline{\psi}\gamma(k)\psi). \quad (3.10)$$

Taking (2.5) into account, we obtain

$$\theta^i_5 = \Omega_5(\alpha)\theta^i(\alpha) = \Omega_5(5)\theta^i(5) = m\widetilde{\omega}^i(k)(\overline{\psi}\gamma(k)\psi), \quad (3.11)$$

i.e., a correct expression for the current vector.

We see that by giving up the extensive group of transformations (1.2) and restricting ourselves to the narrower transformation group (2.1), together with foregoing the free rotatability of the five-reference, we obtain correct equations for the spinor field in the presence of an external field. The absence of invariance relative to five-dimensional (local) Lorentz group and the general group of point transformations of all five coordinates is a manifestation of the absence of a principle of equivalence for the electromagnetic field. The absoluteness of the "direction" of the lines of action and "the relativity" of the directions of all the remaining coordinates lines indeed shows the impossibility of producing a coordinate system in which the electromagnetic field (in the small) would be "transformed."

Proceeding to tensor fields, we note that a particular case is possible when the requirement of covariance of the field equations with respect to the narrow group of transformations (2.1) involves automatically the covariance with respect to the total group (1.2). This case occurs for the meson field considered in the earlier communications.

For example, the equations for scalar and vector meson fields in five-dimensional covariant notation have the form

$$\partial_\lambda\sqrt{|G|}W^\lambda = \sqrt{|G|}Q, \quad \partial_\mu W_\lambda - \partial_\lambda W_\mu = 0, \quad (3.12)$$
$$\partial_\mu\sqrt{|G|}W^{\lambda\mu} = \sqrt{|G|}Q^\lambda,$$
$$\partial_\nu W_{\lambda\mu} + \partial_\lambda W_{\mu\nu} + \partial_\mu W_{\nu\lambda} = 0. \quad (3.13)$$

In these cases it makes no difference whether we use "five-dimensional" or "four-dimensional" covariant differentiation, inasmuch as the Christoffel symbols cancel each other out. The situation is analogous for equations for pseudo-vector and pseudo-scalar meson fields.

Consequently, everything said in the preceding communications with respect to meson fields remains fully in force, the energy-momentum-charge five-tensor remains symmetrical, and the equations for the fields are correct.

APPENDIX

At each point of space we introduce a field of covariant reference $\Omega_i(n)$. We denote by $\Omega^i(n)$ the reciprocal reference, satisfying the condition

$$\Omega_i(n)\Omega^i(m) = \delta(n, m). \quad (A1)$$

If we express $\Omega^i(n)$ in terms of the contravariant components of the vector $\Omega_i(n)$, we introduce into the space a Riemannian matrix, whose metric tensor g_{ik} is determined by

$$g_{ik} = \Omega_i(n)\Omega_k(n) \quad (A2)$$

(we agree to drop the summation sign over the reference indices). The metric is invariant with respect to local orthogonal transformation of references:

$$\Omega^{i'}(n) = L(n, m)\Omega^i(m). \quad (A3)$$

Along with the covariant and contravariant tensor components we introduce invariant components, in accordance with the formula

$$T(k) = \Omega_i(k)T^i = \Omega^i(k)T_i. \quad (A4)$$

The quantities $T(n)$ are invariants of the group of point transformations and tensors of the local Lorentz group.

Along with the ordinary derivative ∂_k we introduce the reference derivative

$$D(n) = \Omega^k(n)\partial_k. \quad (A5)$$

Quantities of the type $D(n)T(m)$ are invariants of the group of point transformations, but are not the tensors of the local Lorentz group if the coefficients $L(n,m)$ depend on the coordinates. It is possible to introduce an invariant vector derivative defined by

$$\nabla(n)T(m) = \Omega^i(n)\Omega^k(m)\nabla_i T_k, \quad (A6)$$

where ∇_i is a symbol of covariant vector differentiation of a vector. This quantity is an invariant of point transformations and a tensor of second rank of the rotation group. Calculation yields

$$\nabla(n)\,T(m) = D(n)\,T(m) - \Delta(n, m, l)\,T(l), \qquad \text{(A7)}$$

where Δ (n, m, l) $= -\Delta$ (n, l, m) are called Ricci symbols and are expressed in terms of components of the reference Ω^{i}(n) in the following manner:

$$\Delta(n, m, l) = {}^{1}/_{2}\{(\Omega^{s}(m)\,\Omega^{r}(l) - \Omega^{s}(l)\,\Omega^{r}(m))\,\partial_{s}\Omega_{r}(n) + (\Omega^{s}(l)\,\Omega^{r}(n) - \Omega^{s}(n)\,\Omega^{r}(l))\,\partial_{s}\Omega_{r}(m) - (\Omega^{s}(n)\,\Omega^{r}(m) - \Omega^{s}(m)\,\Omega^{r}(n))\,\partial_{s}\Omega_{r}(l)\}. \qquad \text{(A8)}$$

In reference analysis, the Δ(n, m, l) play a role analogous to the Christoffel symbols in tensor analysis.

The spinors ψ and $\bar{\psi}$ are defined as quantities having the following transformation properties:

a) They are invariant under general point coordinate transformations

$$\psi'(x') = \psi(x), \quad \bar{\psi}'(x') = \bar{\psi}(x). \qquad \text{(A9)}$$

b) Under free rotations of the reference $\Omega^{i\prime}$(n) = L (m, n) Ω^{i}(m) they transform in accordance with

$$\psi' = S\psi, \quad \bar{\psi}' = \bar{\psi}S^{-1}, \qquad \text{(A10)}$$

where the matrices S are connected with the matrix $||$ L (m, n)$||$ by the ordinary relation

$$S^{-1}\gamma(n)\,S = L(n, m)\,\gamma(m), \qquad \text{(A11)}$$

where γ(k) are four matrices that satisfy the conditions

$$\gamma(n)\,\gamma(m) + \gamma(m)\,\gamma(n) = 2\delta(n, m).$$

From the laws of spinor transformations it follows that the quantities $\bar{\psi}\gamma(k)\,\psi$ form a four-vector with reference components. The components of the spinor are analogues of the reference components of the tensors with that substantial difference, that for spinors there exist no contravariant or covariant components, and that it is therefore impossible to introduce spinors in Riemann spaces, retaining the introduction of the metric with the aid of the tensor field g_{ik}.

The reference derivative of a spinor is determined by the formula

$$D(k)\,\psi = \Omega^{i}(k)\,\partial_{i}\psi, \qquad \text{(A12)}$$

which remains invariant under point transformation of the coordinates.

The invariant derivative of a spinor is introduced by the formula

$$\nabla(k)\,\psi = D(k)\,\psi - B(k)\,\psi, \quad \nabla(k)\,\bar{\psi} = D(k)\,\bar{\psi} + \bar{\psi}B(k), \qquad \text{(A13)}$$

and the matrices B (k) are defined such as to obtain the correct expression for the invariant derivative of the vector.

We have

$$\nabla(k)\,(\bar{\psi}\gamma(n)\,\psi) = D(k)\,(\bar{\psi}\gamma(n)\,\psi) - \Delta(k, n, m)\,(\bar{\psi}\gamma(m)\,\psi), \qquad \text{(A14)}$$

from which it follows that

$$B(k) = {}^{1}/_{4}\,\Delta(k, n, m)\,\gamma(n)\,\gamma(m). \qquad \text{(A15)}$$

[1] Yu. B. Rumer Исследования по 5-оптике, (Investigations in 5-Optics), GTTI, 1956. This monograph contains all the previous articles of this series, which have been revised and supplemented.

[2] Yu. B. Rumer, J. Exptl. Theoret. Phys. (U.S.S.R.) **25**, 271 (1953).

Translated by J. G. Adashko
377

ON THE THEORY OF SCATTERING VIA QUASI-STATIONARY STATES

V. I. SERDOBOL'SKIĬ

P. N. Lebedev Physics Institute, Academy of Sciences, U.S.S.R.

Submitted to JETP editor January 23, 1959

J. Exptl. Theoret. Phys. (U.S.S.R.) 36, 1903-1908 (June, 1959)

The continuous-spectrum wave function that describes S scattering is expanded in series in terms of a system of wave functions of quasi-stationary states with complex energies. The validity of the expansion is established by a study of the analytic properties of the solution. The resulting dispersion formulas express the energy dependence of the cross section in a more convenient way than that provided by previous theories.

THE theory generally used at present to explain the existence of resonances in the cross sections for scattering and nuclear reactions is that of Wigner and Eisenbud.[1,2] Only a formal significance, however, attaches to the energy levels of the compound system and the widths of the resonance curves as obtained in this theory, since the system of basis functions used for the expansion is chosen arbitrarily, without any correspondence to the physical meaning of the problem. It would be natural to try to expand the solution in terms of the actual wave functions of the quasi-stationary states that satisfy the Schrödinger equation with complex energies.[3] There are difficulties here, however, owing to the fact that the system of such functions (nonorthogonal and linearly dependent) may be incomplete. In the present paper these difficulties are overcome by means of a study of the asymptotic properties of the solution in the complex-energy region.

THE PROPERTIES OF THE ANALYTIC CONTINUATION $\psi(x, k)$

We write down the Schrödinger equation for our case:

$$(d^2/dx^2 + k^2)\psi = V\psi. \tag{1}$$

Here $\psi(x, k)$ is the solution of the scattering problem for complex k, and V is the interaction operator. Since the nuclear forces fall off sharply at a certain boundary, we assume that V vanishes at the distance x_0; the kernel $V(x, x') = 0$ for x or $x' > x_0$.

We prescribe the boundary conditions in the form

$$\psi(0, k) = 0, \quad \psi(x, k) - \sin kx \sim e^{ikx} \quad \text{for } x > x_0. \tag{2}$$

Equation (1) and the boundary conditions lead to two symmetry relations:

$$\psi(x, k) = -S(k)\psi(x, -k), \quad \psi(x, k) = -\psi^*(x, -k^*). \tag{3}$$

Here $S(k) = e^{2i\delta}$ is the one-dimensional scattering matrix. At a point k_λ of the complex k plane where S(k) has a pole, $\psi(x, k)$ also has a pole, and the function $[\operatorname{Res}\ \psi(x, k)]_{k_\lambda}$ contains only an outgoing wave and describes the quasi-stationary state λ. For convenience in what follows we choose the wave functions of the quasi-stationary states in the following way:

$$c_\lambda\psi_\lambda(x) = [\operatorname{Res}\psi(x, k)\, e^{ikx_0}]_{k_\lambda}, \quad \psi_\lambda(x_0) = 1. \tag{4}$$

We retain this definition of the function $\psi_\lambda(x)$ and coefficients c_λ also for the nondecaying stationary states, which are characterized by poles in the upper half of the complex k plane. From Eq. (3) it follows that the poles occur in pairs, so that to every pole k_λ there corresponds a pole $-k_\lambda^*$. Corresponding to the function $c_\lambda\psi_\lambda(x)$ is the function $c_\lambda^*\psi_\lambda^*(x)$.

The coefficients c_λ are determined by the relations

$$2k_\lambda\int_0^{x_0}\psi_\lambda^2(x)\,dx + i = -k_\lambda/c_\lambda. \tag{5}$$

If a pole in the lower half-plane comes close to the real axis, $\operatorname{Im} k_\lambda = 0$, resonances occur in the cross section. From Eq. (1) we can derive the relation for the functions $\psi_\lambda(x)$ and $\psi_\lambda^*(x)$:

$$2\operatorname{Im} k_\lambda\int_0^x |\psi_\lambda(x)|^2\,dx - 1 = 0. \tag{6}$$

It can be seen that for $\operatorname{Im}(k_\lambda x_0) \ll 1$ the wave function is relatively large in the inner region $x < x_0$. Let us separate the function $\psi_\lambda(x)$ into its real and imaginary parts:

$$\psi_\lambda(x) = \psi_R(x) + i\psi_I(x).$$

Applying Green's formula, we get

$$\psi_R(x)\frac{d\psi_I(x)}{dx}-\psi_I(x)\frac{d\psi_R(x)}{dx}=2\,\mathrm{Re}\,k_\lambda\,\mathrm{Im}\,k_\lambda\int_0^x|\psi_\lambda(x)|^2\,dx. \quad (7)$$

In the approximation of small width of the resonance level,

$$|\mathrm{Re}\,(k_\lambda x_0)\,\mathrm{Im}\,(k_\lambda x_0)|\ll 1 \quad (\Gamma_\lambda\ll\hbar^2/mx_0^2),$$

it follows from Eq. (7) and the stipulation (4) that $\psi_\lambda(x)$ is real. This corresponds physically to the formation of a standing wave inside the nucleus. For the case in which $\psi_\lambda(x)$ is real right up to the very edge, we can find from Eqs. (5) and (6) the approximate value of c_λ:

$$c_\lambda\approx k_\lambda\,\mathrm{Im}\,k_\lambda/\mathrm{Re}\,k_\lambda. \quad (8)$$

For stationary states the c_λ are easily calculated by means of the integral equation of Gell-Mann and Goldberger (cf., e.g., reference 4).

In what follows we shall assume that $\psi(x, k)$ for $|k|<\infty$ has only simple poles. The correctness of this proposition has been proved only for potentials with infinitely small radius of action.[5] The condition for the presence of a pole of higher order is

$$2k_\lambda\int_0^{x_0}\psi_\lambda^2(x)\,dx+i=0.$$

Comparing Eqs. (5) and (6) we can see that poles near the real axis are not of order higher than the first. As for distant poles of nth order, they can be split up into sets of n closely spaced poles of first order by a small change of the potential.

THE ASYMPTOTIC PROPERTIES

The behavior of $\psi(x, k)$ for $k\to\infty$ in the complex plane depends on the differential properties of the kernel $V(x, x')$, or of the function $V(x)$, if $V = V(x)$. The integral equations for the scattering hold in the upper half-plane, and the asymptotic properties of $\psi(x, k)$ for $k\to\infty$ are determined by the Born approximation

$$\psi(x, k)\approx\sin kx+\iint G(x, x')V(x', x')\sin kx''dx'dx'', \quad (9)$$

where

$$G(x, x')=\frac{i}{2k}\,[e^{ik(x+x')}-e^{ik|x-x'|}].$$

The passage to the lower half of the complex plane is made by means of Eq. (3). By using Eq. (9) we can also find out the asymptotic properties of the S matrix. For $k\to\infty$ along upward rays ($\mathrm{Im}\,k/\mathrm{Re}\,k=\mathrm{const}$, $\mathrm{Im}\,k>0$) the main term of the function S(k) has the form

$$S(k)\approx-\frac{1}{2}\,\frac{e^{-2ikx_0}}{(ik)^{m+n+3}}\left[\frac{\partial^{m+n}V(x, x')}{\partial x^m\partial x'^n}\right]_{x=x'=x_0}; \quad (10)$$

if $V = V(x)$, then

$$S(k)\approx\frac{e^{-2ikx_0}}{(2ik)^{n+2}}\left[\frac{\partial^n V(x)}{\partial x^n}\right]_{x_0}. \quad (11)$$

The right members of Eqs. (10) and (11) contain the first nonvanishing derivatives, m, $n\geqslant 0$. For the passage to the lower half-plane we have only to use the formula $S(k)S(-k)=1$. Equation (9) enables us to find the asymptotic distribution of the zeroes of S(k) in the upper half-plane, and at the same time the poles for $\mathrm{Im}\,k_\lambda<0$:

$$\mathrm{Re}\,k_\lambda\approx\pm\pi\lambda/x_0,\qquad \mathrm{Im}\,k_\lambda\approx-s\ln(\pi|\lambda|)/2x_0,\qquad \lambda\to\infty, \quad (12)$$

where λ is an integer, and $s = m + n + 3$ or $n + 2$. Since

$$\psi_\lambda(x)=-2i\exp\{-ik_\lambda x_0\}\,\psi(x,-k_\lambda),$$

we have for $\lambda\to\infty$

$$\psi_\lambda(x)\approx\exp\{ik_\lambda(x-x_0)\}-\exp\{-ik_\lambda(x+x_0)\}. \quad (13)$$

Furthermore, using Eq. (5), we can calculate the index of increase of the coefficients c_λ: $c_\lambda\approx k_\lambda^s$, $\lambda\to\infty$.

In what follows we shall find it advantageous for the coefficients c_λ not to increase too rapidly. On the other hand, physical considerations suggest that the behavior at infinity must not depend in any essential way on the interaction in the region of finite energy. Let us add to the potential-energy operator a small quantity $\delta V=\epsilon\delta(x-x_0)$. The change of the S matrix will then be

$$\delta S=(2\epsilon/ik)\,[\psi(x_0, k)]^2.$$

The nature of the increase of the coefficients c_λ, however, is decidedly changed. Using Eqs. (5) and (13), we find

$$c_\lambda\approx-ik_\lambda/2x_0\epsilon. \quad (14)$$

The asymptotic relations that hold for $k_\lambda\to\infty$ along upward rays are:

$$S(k)\,e^{2ikx_0}\sim\mathrm{const}/k;\qquad \psi(x, k)\,e^{ikx_0}\sim\mathrm{const}/k,$$

$$x<x_0;\qquad \psi(x_0, k)\approx-1/2i.$$

Along downward rays:

$$S(k)\,e^{2ikx_0}\sim k;\qquad \psi(x, k)\,e^{ikx_0}\sim\mathrm{const},$$

$$x<x_0;\qquad \psi(x_0, k)\,e^{ikx_0}\sim k.$$

Let us now expand $S(k)\,e^{2ikx_0}$ in a Mittag-Leffler series:

$$S(k)\,e^{2ikx_0}=2i\sum_\lambda kc_\lambda/k_\lambda(k-k_\lambda)+F(k). \quad (15)$$

According to Eqs. (2) and (4) the sum over all λ is the principal part of $S(k)e^{2ikx_0}$ near the poles. Using Eqs. (12) and (14) we can show that this sum increases as $-ik/\epsilon$ for $k\to\infty$ along rays not co-

inciding with the real axis. F(k) is an integral analytic function of k. For $k \to \infty$ along a ray, F(k) does not increase faster than k, and therefore F(k) = ik/ϵ + C. Setting k = 0, we find that C = 1. The Mittag-Leffler series for $\psi(x, k)e^{ikx_0}$ has the form

$$\psi(x, k)\, e^{ikx_0} = \sum_\lambda \frac{k}{k_\lambda} \frac{c_\lambda \psi_\lambda(x)}{k - k_\lambda}. \tag{16}$$

According to Eqs. (12), (13), and (14) the sum on the right is bounded for $x < x_0$ and $k \to \infty$ along a ray; the corresponding integral function goes to zero. Equations (15) and (16) are the desired expansion of $\psi(x, k)$ in terms of the system of wave functions $\psi_\lambda(x)$ for $x \leqslant x_0$, and it follows from Eq. (16) that the system $\psi_\lambda(x)$ is complete. The equation

$$\sum_\lambda c_\lambda \psi_\lambda(x) \psi_\lambda(x') = -\delta(x' - x'), \quad x < x_0.$$

can be established by direct verification.

It is interesting to check directly that the wave function (16) that has been constructed satisfies the Schrödinger equation and the boundary conditions. For this purpose we consider the series $\Sigma c_\lambda \psi_\lambda(x)/k_\lambda$. By applying Eqs. (12) — (14) we can show that this series converges for all $x < x_0$, and forms a δ functions for $x = x_0$. The coefficient of $\delta(x - x_0)$ is $-i/\epsilon$. By manipulating the expression

$$\int_0^{x_0} \Big(\sum_\mu c_\mu \psi_\mu(x)/k_\mu + \frac{i}{\varepsilon} \delta(x - x_0) \Big) \psi_\lambda(x)\, dx, \tag{17}$$

we verify that

$$\sum_\mu \frac{c_\mu \psi_\mu(x)}{ik_\mu} = -\frac{i}{\varepsilon} \delta(x - x_0). \tag{18}$$

It can be seen from Eqs. (15) and (16) that the wave function that describes scattering at zero energy is given by

$$\psi_0(x) = \lim_{k \to \infty} \frac{\psi(x, k)}{k} = -\sum_\lambda \frac{c_\lambda \psi_\lambda(x)}{k_\lambda^2}, \quad x < x_0, \tag{19}$$

$$\psi_0(x_0) = -\sum_\lambda \frac{c_\lambda}{k_\lambda^2} + \frac{1}{2\varepsilon}. \tag{20}$$

The series (19) converges nonuniformly at $x = x_0$ and may have a discontinuity at this point. Determining the discontinuity from Eq. (18), we find the limit for $x \to x_0 - 0$:

$$\lim \psi_0(x) = -\lim c_\lambda k_\lambda^{-2} \psi_\lambda(x) = \psi_0(x_0).$$

Let us calculate the derivative of Eq. (19) at the point x_0:

$$\lim_{x \to x_0 - 0} \frac{d\psi_0(x)}{dx} = -\lim \sum_\lambda \frac{c_\lambda}{k_\lambda^2} \Big(\frac{d\psi_\lambda(x)}{dx} - ik_\lambda \psi_\lambda(x) \Big) = 1 - \varepsilon \psi_0(x_0).$$

Thus it can be seen that Eq. (19) is continuous at the point x_0 and satisfies the boundary condition (2) to accuracy ϵ.

The function $\psi_0(x)$ must satisfy the Schrödinger equation for zero energy. As the result of formal application of Eq. (1) to Eq. (18) we get

$$\Big(\frac{d^2}{dx^2} - V \Big) \psi_0(x) = \sum_\lambda c_\lambda \psi_\lambda(x).$$

The series on the right diverges; we can, however, introduce the generalized sum (for example, by Abel's method):

$$\sum_\lambda c_\lambda \psi_\lambda(x) = \lim_{\theta \to 1} \sum_\lambda \theta^\lambda c_\lambda \psi_\lambda(x), \quad \theta < 1,$$

Calculation shows that this sum is equal to zero everywhere for $x < x_0$. This completes the proof that $\psi_0(x)$ is the solution of the scattering problem for zero energy. In the case $k \neq 0$ we rewrite Eq. (16) in the form

$$\psi(x, k) = k\psi_0(x) + \sum_\lambda \frac{k^2}{k_\lambda^2} \frac{c_\lambda \psi_\lambda(x)}{k - k_\lambda}. \tag{21}$$

The series converges well enough, and direct verification shows that $\psi(x, k)$ defined by Eq. (20) satisfies the equation (1) and the conditions (2).

THE DISPERSION FORMULAS

According to Eqs. (15) and (20) the scattering amplitude $(2ik)^{-1}$. (S(k) − 1) is given by

$$f(k) = \frac{e^{-2ikx_0} - 1}{2ik} + e^{-2ikx_0} \Big(\psi_0(x_0) + \sum_\lambda \frac{kc_\lambda}{k_\lambda^2 (k - k_\lambda)} \Big). \tag{22}$$

In the case of small widths the coefficients c_λ are determined from Eq. (8). The resulting formula is

$$f(k) = f_0(k) + \frac{e^{-2ikx_0}}{k} \sum_\lambda^{(1/2)} \frac{\Gamma_\lambda/2}{E - |E_\lambda| - i\Gamma_\lambda/2}. \tag{23}$$

Here $E = k^2$, $\Gamma_\lambda = 4k \operatorname{Im} k_\lambda < 0$, and the sum includes the poles located in the half-plane $\operatorname{Re} k_\lambda > 0$; $f_0(k)$ is the remaining slowly varying part of f(k). The cross section for S scattering has the form

$$\sigma(k) = \sigma_0(k) + \frac{4\pi}{E} \sum_\lambda^{(1/2)} \frac{\Gamma_\lambda/2}{(E - |E_\lambda|)^2 + \Gamma_\lambda^2/4} \Big[\frac{\Gamma_\lambda}{2} \cos 2kx_0 - (E - |E_\lambda|) \sin 2kx_0 \Big]. \tag{24}$$

The dispersion formula shows that in the case in which the standing wave inside the nucleus occupies the entire region $x < x_0$ the potential part of the scattering corresponds exactly to the scattering by an impentrable sphere of radius x_0. Integrating Eq. (23), we get the dispersion relations

$$\frac{1}{i\pi}\int_{-\infty}^{+\infty} f(k')\,e^{2ik'x_0}\frac{dk'}{k'-k} + f(k)\,e^{2ikx_0} = 2\sum_{\mathrm{Im}\,k_\lambda>0}\frac{c_\lambda}{k_\lambda(k-k_\lambda)},$$

$$f(0) = -\frac{1}{i\pi}\int_{-\infty}^{+\infty} f(k)\,e^{2ikx_0}\frac{dk}{k} - 2\sum_{\mathrm{Im}\,k_\lambda>0}\frac{c_\lambda}{k_\lambda^2}.$$

In these relations the oscillating exponential plays an essential part; this makes them useless in practice for calculations in nuclear physics. In special cases, however, one can write dispersion relations without the exponential factor.[6] From Eqs. (15) and (20) there follows the sum rule

$$k_\lambda\sum_\mu c_\mu/k_\mu^2(k_\lambda+k_\mu) = 1/2ik_\lambda + x_0 + f(0),$$

and for the poles located near the origin

$$f(0) + x_0 \approx -\sum_\mu c_\mu k_\mu^{-2}.$$

The present expansions (22) and (24) differ from the corresponding formulas of Wigner and Eisenbud[1] by their simplicity and intuitive physical meaning. The positions and widths of the resonance levels are directly connected with the energies and lifetimes of the decaying states. The specific difficulties of the expansion in terms of nonorthogonal functions reduce mainly to the study of the asymptotic behavior of the solution for large energies, which is not dealt with at all in references 1 and 2. The development of an analogous formalism for the general case of an arbitrary nuclear reaction involving charged particles and higher spins and angular momenta would evidently make it possible to construct a version of the formal theory of resonance nuclear reactions without using the concept of the R matrix.

[1] E. P. Wigner and L. Eisenbud, Phys. Rev. **72**, 29 (1947).

[2] A. M. Lane and R. G. Thomas, Rev. Mod. Phys. **30**, 257 (1958).

[3] A. J. F. Siegert, Phys. Rev. **56**, 750 (1939).

[4] L. D. Faddeev, J. Exptl. Theoret. Phys. (U.S.S.R.) **35**, 433 (1958). Soviet Phys. JETP **8**, 299 (1959).

[5] Ning Hu, Phys. Rev. **74**, 131 (1948).

[6] V. I. Serdobol'skiĭ, J. Exptl. Theoret. Phys. (U.S.S.R.) **33**, 1268 (1957). Soviet Phys. JETP **6**, 975 (1958).

Translated by W. H. Furry
378

ACCELERATION OF PLASMOIDS BY HIGH-FREQUENCY ELECTRIC FIELDS

M. A. MILLER

Radio-Physics Institute, Gor'kiĭ State University

Submitted to JETP editor, January 23, 1959

J. Exptl. Theoret. Phys. (U.S.S.R.) **36**, 1909-1917 (June, 1959)

The possibility of accelerating completely ionized quasi-neutral plasmoids in moving high-frequency potential wells is indicated. If such wells are formed by two fields of different frequency the plasmoids can be accelerated by changing the frequency of one of the fields or by using a waveguide of variable cross section. Certain features of linear and cyclical plasma accelerators are analyzed.

1. INTRODUCTION

IN accelerating quasi-neutral plasmoids or charged particles of one sign it is necessary to set up strong fields which provide acceleration as well as spatial stability. The latter requirement is predominant since any system which localizes a fixed plasmoid can, in principle, be used for acceleration if the appropriate displacement of the localizing fields in space can be achieved.

There has been a great deal of recent work in plasma confinement in connection with the well known problem of a controlled thermonuclear reaction. One method is to use a weakly inhomogeneous high-frequency electromagnetic field. The forces (averaged over an oscillation period) which act on a particle in such a field do not depend on the sign of the charge; this feature lies at the basis of all methods of using high-frequency fields for plasma localization.* The inhomogeneous field of the required configuration is produced by an appropriate distribution of sources as well as the perturbations introduced by the plasma itself. In certain cases it has been possible to obtain a self-consistent electrodynamic solution: a plasma sphere in a spherical resonator,[2] a plasma cylinder in a circular waveguide,[3] a two-dimensional plasma layer between ideal planes,† a plane plasma boundary maintained by a plane wave which is normally incident on it.[4] In general form the problem can be solved only for a highly rarefied plasma (density small enough so that distortions introduced by the plasma can be neglected); in this case we actually deal with the localization of single charged particles.[5,6]

Below we consider certain principles for the acceleration of quasi-neutral plasmoids in high-frequency electromagnetic fields. The properties of the plasma are assumed to be as follows: a) the plasma is completely ionized; b) during the time in which the bunch is accelerated a Maxwellian distribution over average particle velocity is maintained; c) all the particles have non-relativistic velocities in the reference system fixed to the bunch; d) the dielectric permittivity of the plasma is approximately unity, i.e., the density of particles N satisfies the requirement $N \ll m_e\omega^2/4\pi e^2 = 3.1\times10^{-8}\omega^2$, where m_e is the mass of the electron, e is the charge of the electron and ω is the angular frequency of the external field. Although the last condition is not a fundamental limitation it does allow us to make a complete analysis of the kinematic part of the problem, i.e., the displacement of the localizing fields in space.

2. LOCALIZATION OF INDIVIDUAL CHARGED PARTICLES

It has been shown by Gaponov and the author[5,6] that charged particles can be localized close to absolute minima* of a high-frequency potential Φ defined by the relation

$$\Phi = (\eta^2/4\omega^2)|\mathbf{E}|^2, \qquad (1)$$

where η is the charge-to-mass ratio and $\mathbf{E}$ is the amplitude of the electric field. If the profile of Φ is a potential well, it will trap particles that have velocities $|v_0| \leq \sqrt{2\Delta\Phi}$ at the center (minimum

*This feature was first pointed out by V. I. Veksler, who proposed the electromagnetic radiation pressure for acceleration of plasma objects.[1]

†Diplomate paper by E. I. Yakubovich, Gor'kiĭ State University, 1958.

*In the presence of a fixed magnetic field localization is possible in regions of maximum E under the condition that $\omega < |\omega_H|$, where ω_H is the cyclotron frequency.[6]

value of Φ) where $\Delta\Phi$ is the minimum potential difference between the edge and center of the well.

We assume that this potential well is formed in a reference system K′ which moves in the +z direction with respect to the laboratory system K with a velocity v ($\beta = v/c$) and an acceleration w where

$$w(1-\beta^2)^{-1/2} = \tilde{w} = \text{const.} \tag{2}$$

Introducing in place of (1) some effective potential* Φ'_{eff}, which includes the potential of the inertia forces $\Phi'_{\text{eff}} = \Phi' + \tilde{w}z'$, we find that if particles are to be trapped the following inequality must be observed

$$\left|\frac{\partial\Phi'}{\partial z'}\right| > \tilde{w}. \tag{3}$$

The condition in (3) imposes an additional limitation on the potential Φ'; one cannot use a Φ with very steep slopes†: in the first place the time-of-flight of the particle through the region of inhomogeneous field ($L \sim \Phi/|\nabla\Phi|$) must be long enough to correspond to a large number of high-frequency periods ($L \gg v_0/\omega$); secondly, the amplitude of the high-frequency oscillations of the particle must be much smaller than L, $L \gg |\eta E/\omega^2|$.

3. LOCALIZATION OF A PLASMOID

If a potential well is filled by a rarified plasma characterized by a kinetic temperature $T(V_T = kT/e)$ the particle density is given by the expression[3]

$$N(\mathbf{r}) = N(0)\exp(-m_e\Delta\Phi_e/2kT),$$

where k is the Boltzmann constant, $\Delta\Phi_e$ is the difference in the high-frequency potentials between the points‡ $\mathbf{r}$ and $\mathbf{r}=0$. If this difference is considerably greater than $2kT/m_e$ in all directions the bunch is essentially localized at the center of the well.

Suppose that the localizing field and the plasmoid move with accelerated motion and that the condition in (2) is satisfied; then, in place of the potential Φ'_e it is necessary to introduce the effective potential Φ'_{eff} (analogous to the potential for the electron) which takes account of the increase in the force of inertia due to the factor m_i/m_e (m_i is the mass of the ion, $m_i \gg m_e$).

$$\Phi'_{\text{eff}} = \Phi'_e + (m_i/m_e)\tilde{w}z'. \tag{4}$$

As an example we consider a sinusoidal (in the z direction) potential profile

$$\Phi'(z') = \Phi'_0 + \Phi'_1\cos 2h'z'. \tag{5}$$

Substituting (5) and (4) and seeking the position of the extrema in Φ'_{eff}

$$\sin 2h'z'_{\text{extr}} = \frac{m_i}{m_e}\frac{\tilde{w}}{2h'\Phi'_1} = \alpha, \tag{6}$$

for a potential difference $\Delta\Phi'_{\text{eff}}$ corresponding to a minimum potential differential between the edge and the center of the well, we have*

$$\Delta\Phi'_{\text{eff}} = 2\Phi_1\Psi(\alpha), \quad \Psi(\alpha) = \sqrt{1-\alpha^2} - \alpha\arccos\alpha. \tag{7}$$

Using these formulas it is an easy matter to find the maximum possible acceleration of the bunch since the potential difference $\Delta\Phi'_{\text{eff}}$ which appears in (7) is determined by the condition of partial or total localization of a plasma at temperature T.

4. MOVING POTENTIAL PROFILES

As has been noted earlier,[7] a simple method of displacing a potential profile consists of using two traveling waves of different frequencies. Suppose that in a reference system K′ moving with uniform motion in the z direction the field is a superposition of two plane non-uniform waves of the same frequency ω':

$$\mathbf{E} = \mathbf{E}'_+(x, y)\exp(i\omega't' - ih'z') + \mathbf{E}'_-(x, y)\exp(i\omega't' + ih'z'), \tag{8}$$

then in the fixed system K this field corresponds to two traveling waves of different frequencies ω_+ and ω_-:

$$\mathbf{E} = \mathbf{E}_+(x, y)\exp(i\omega_+t - ih_+z) + \mathbf{E}_-(x, y)\exp(i\omega_-t + ih_-z). \tag{9}$$

The frequencies $\omega_\pm$ and the wave numbers $h_\pm$ are related to the corresponding quantities in the K′ system by the relations

$$k_\pm = (k' \pm h'\beta)/\sqrt{1-\beta^2}, \quad h_\pm = (h' \pm k'\beta)/\sqrt{1-\beta^2}, \tag{10}$$

where $k_\pm = \omega_\pm/c$, $\beta = v/c$ while v is the velocity of the K′ system with respect to the K system.

Using the fields in Eq. (8) it is possible to produce various profiles for the high-frequency potential Φ'.[6] In particular, in a regular cylindrical

*The primed quantities refer to the moving coordinate system.

†It is precisely as a result of this situation that it is impossible to trap a plasmoid with a sharply defined boundary.

‡For simplicity, the charges of the electrons and ions are assumed to be the same in all cases; in the general case $e_i = Ze$, in place of $\Delta\Phi_e/2$ we write $Z\Delta\Phi_e/(Z+1)$. We may note, moreover, that for dense plasmoids the potential difference $\Delta\Phi_e$ must be determined from a self-consistent solution of the problem.

*Here we are considering only the potential difference in the z direction.

lossless line two propagating waves of the same type form a profile of the form in (5) in which

$$\Phi'_0 = (\eta_1/2\omega')^2\,[|\mathbf{E}'_+|^2 + |\mathbf{E}'_-|^2],$$
$$2\Phi'_1 = (\eta_1/\omega')^2\,|\mathbf{E}'_+\mathbf{E}'_-|. \qquad (11)$$

Particles can be trapped in a finite region with cross section z = const either by virtue of the existence of an absolute minimum in $\Phi'(x, y, z')$ or, if there is no such minimum, by means of a supplementary fixed magnetic field $\mathbf{H}_0 = \mathbf{H}_{0z0}$. The trapping in the z direction occurs as a result of the sinusoidal shape of the profile (5), i.e., trapping is possible when $h' \neq 0$.

The waves in (9) in the K system can propagate in the same direction ($h_+h_- < 0$) or in opposite directions ($h_+h_- > 0$). Quantities referring to waves moving in opposite directions (anti-parallel) will be denoted by the subscript "a" while waves moving in the same direction (parallel) will be denoted by the subscript "p". In the general case it is also necessary to distinguish between the so-called fast waves ($h \leq k$) which exist in waveguides and multi-conductor lines with ideal smooth conducting surfaces and the slow waves ($h \geq k$) which exist in systems with corrugated boundaries or with inhomogeneous (cross section z = const) dielectrics. Although in both cases the dispersion equation is of the form $h_\pm^2 = k_\pm^2 - \kappa_\pm^2$, in the fast-wave case, if one considers waves in a lossless isotropic system the transverse wave number κ is pure real and cannot depend on frequency $\kappa_+ = \kappa_- = \kappa$ (regular waveguides); in the slow wave case κ is an imaginary quantity and, in principle, does depend on frequency ($\kappa_+ \neq \kappa_-$ if $k_+ \neq k_-$). In what follows, for simplicity we shall limit ourselves to regular waveguides and fast waves; the analysis may be carried out in general form without any specification of the waveguide cross section or the field configuration.*

Two important parameters determine the usefulness of the profile (5) from the point of view of acceleration of charged particles: the constant, h', which characterizes the slope of the walls of the potential well, and the quantity $\beta = v/c$, which determines the displacement velocity of the potential wells. Using the dispersion equation $h_\pm^2 = k_\pm^2 - \kappa^2$ and introducing the dimensionless quantities $\gamma = k_+/k_-$, $p^2 = \kappa^2/k_-^2$, $s = h'/k_-$, from (10) we have

$$\beta = (k_+ - k_-)/(|h_+| \pm |h_-|)$$
$$= (\gamma - 1)/(\sqrt{\gamma^2 - p^2} \pm \sqrt{1 - p^2}), \qquad (12)$$

*It should be kept in mind, however, that slow-wave systems (helices, waveguides with ribbed walls, etc.) are preferable in certain respects. Aside from the lower values of the velocity of displacement of the profiles, in the slow-wave case larger values of h' are achieved.

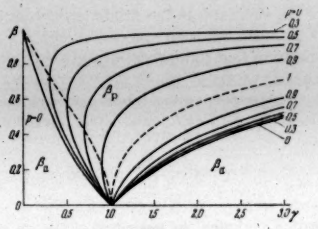

FIG. 1

$$s = [\gamma - p^2 \pm \sqrt{(\gamma^2 - p^2)(1 - p^2)}]^{1/2}/\sqrt{2}. \qquad (13)$$

The upper sign in Eqs. (12) and (13) refers to the anti-parallel waves; the lower sign refers to the parallel waves. In Figs. 1 and 2 are shown the relations between β_a, β_p, s_a, and s_p and γ for various values of p (the number on the curves). Inasmuch as exponentially decaying waves are not being considered,* γ can vary within the limits $p \leq \gamma < \infty$ where $0 \leq p \leq 1$. When $\gamma = p$ or $p = 1$ we have a situation in which the waveguide is excited at one of its critical frequencies, i.e., one of the fields in (9) becomes independent of the z coordinate. The regions of β_a and β_p, and correspondingly, s_a and s_p, are separated in Figs. 1 and 2 by dashed lines.

It is apparent that $\beta_a(\gamma, p) \leq \beta_p(\gamma, p)$ and $s_a(\gamma, p) \geq s_p(\gamma, p)$, i.e., by using waves in the same direction it is always possible to achieve higher displacement velocities for the localizing fields; on the other hand, the anti-parallel fields always form potential wells with steeper sides. The profile with the steepest sides is formed by anti-parallel TEM waves which propagate with the velocity of light ($p = \kappa/k_- = 0$, $h = k$) for which, in accordance with Eq. (13), we have† $\beta_a = \sqrt{\gamma}$. For waves traveling in the same direction the most suitable mode of operation is the one with the maximum values of p: $p_{max} = 1$, $s_p = \sqrt{(\gamma - 1)/2}$.

If the frequencies ω_+ and ω_- are the same ($\gamma = 1$) the profile Φ'_a remains fixed ($\beta_a = 0$). The profile Φ'_p formally must be displaced with the

*We assume that the quantity h' in Eq. (8) is pure real; an exponentially decaying or increasing field in the z-direction (9) (Im h ≠ 0) must correspond, in the K' system, to a field with complex h', as given by Eq. (10).

†The application of slow waves makes it possible to increase the value of s_a, which, as has already been noted, occurs at the expense of a reduction in the velocity β; if the dispersion equation is of the form $h^2 = k^2 + \tilde{\kappa}^2$, for s, in place of Eq. (13), we have

$$2s = [2\tilde{\gamma} + \tilde{p}_-^2 + \tilde{p}_+^2 \pm \sqrt{(\tilde{\gamma}^2 + \tilde{p}_+^2)(1 + \tilde{p}_+^2)}]^{1/2},$$

where $\tilde{p}_\pm^2 = \tilde{\kappa}_\pm^2/k_-^2$, whence it follows that $s_a > \sqrt{\gamma}$.

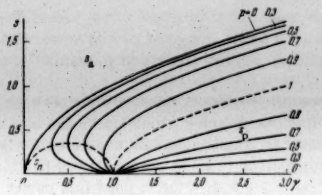

FIG. 2

group velocity of the wave $\beta_p = \sqrt{1-p^2}$; however the potential wells vanish since $s_p(1, p) = 0$.

As the value of γ increases the velocity of displacement of both profiles, Φ'_a and Φ'_p, increases, approaching the velocity of light; as far as purely technical considerations are concerned the velocity which can be achieved is determined by the conditions of localization of the plasma within the potential well. When $\gamma \gg p$, s is given approximately by

$$s \approx [\gamma(1 \pm \sqrt{1-p^2})/2]^{1/2}.$$

Thus s increases asymptotically in proportion to $\sqrt{\gamma}$; starting at some value of the velocity the conditions for applicability of the average description of the motion of the particles in the moving system $L \sim 1/h' \gg v_0/\omega'$ (v_0 is the mean velocity of the electrons in a bunch) is violated: a peculiar "tunneling" of the particles through the potential barriers takes place and it becomes impossible to trap particles, even at very large values of Φ'_1.

5. ACCELERATED POTENTIAL PROFILES

There are two possible methods for accelerating the potential profiles formed by the fields (8). The first method is to vary the frequency of the waves (9) as a function of time; the second method is to vary the propagation constants h_+ and h_- as functions of the z coordinate. In order to maintain the stationarity of the profile Φ' (unless this is done the potential description loses its significance) these changes must be slow as compared with the period $(2\pi/\omega)$ or the wavelength $(2\pi/h)$: $|dk/dt| \ll k^2c$, $|dh/dz| \ll h^2$.

We consider the features of each of these methods. Suppose that the frequency ω_- is fixed while $\omega_+ = \omega_+(t)$; this is equivalent to a variation of γ in Eq. (12) with p = const (cf. Fig. 1). In β_a systems it is possible to start the acceleration from zero velocity ($\gamma = 1$, $\beta_a = 0$); in β_p systems it is necessary to inject a bunch which has first been accelerated. The magnitude of the initial velocity is determined by the conditions under which the potential well is formed at the input of the accelerator ($s_p > 0$). The appropriate values of the acceleration are found by differentiating Eq. (12). The infinite increase in acceleration for $\gamma \to p$ (cf. Fig. 1) excludes the possibility of choosing the variable frequency close to one of the critical frequencies of the waveguide; however, generally speaking the fixed frequency can be set equal to one of the critical frequencies (p = 1). If the frequencies coincide at the starting time $t = 0$ ($\gamma = 1$) and the condition $td\gamma/dt \ll 1$ holds over the extent of the entire cycle, the acceleration, according to (12), is given by the relation

$$d\beta_a/dt = {}^1/_2(1-p^2)^{-1/2}\,d\gamma/dt,$$
$$d\beta_p/dt = {}^1/_2 p^2(1-p^2)^{-1/2}\,d\gamma/dt.$$

Whence it follows, in particular, that a linear variation of frequency corresponds in the first period of acceleration to uniform acceleration of the profile.

An important feature of the second method of acceleration is the fact that fixed frequencies are used; thus it is possible to use resonance excitation of the electrodynamic system and no special nonlinear frequency tuning elements are required. A smooth variation of the propagation constant h(z) can be obtained in quasi-cylindrical waveguides or resonators in which the cross section and, consequently, the transverse wave number κ, vary slowly in the z direction. The appropriate values of the velocities in acceleration are easily determined by Eq. (15) where $d\beta/dt = \beta c(d\beta/dp) \times dp/dz$. Since the parameter p must lie within the limits $0 \le p \le 1$ for fast propagation, the maximum velocity differential, i.e., the difference between the velocities at the input and the output of the accelerator, must be [from Eq. (12)]:

$$\Delta(\beta_a)_{max} = \sqrt{(\gamma-1)/(\gamma+1)} - (\gamma-1)/(\gamma+1),$$
$$(\Delta\beta_p)_{max} = 1 - \sqrt{(\gamma-1)/(\gamma+1)}$$

In this case the initial velocities are different from zero, i.e., preliminary acceleration is required.

It should be kept in mind that in this method the displaced profile necessarily becomes distorted since the acceleration is based on a variation of $h_\pm$ and consequently h'; hence the maximum possible velocity found from Eq. (12) may be unusable because the conditions required for trapping the bunch may no longer hold.

6. CHOICE OF ACCELERATOR PARAMETERS

We now analyze some of the factors that enter into a choice of the parameters of a high-frequency plasma accelerator.

The point of departure is the fact that the conditions required for localizing the bunch must be

observed. Taking account of Eqs. (7) and (8) and the requirement[6] for smooth variation of the field amplitude E, we have

$$L\omega^2/\eta_{i_e} \gg |E_\pm| \gg \sqrt{2}\omega (V_T/\eta_{i_e}\Psi(\alpha))^{1/4}, \qquad (14)$$

where $V_T = kT/e$. Taking $L = \lambda/4 = \pi c/2\omega$ and substituting $\eta_e = 5.3 \times 10^{17}$, we write Eq. (14) in the form

$$5.1 \cdot 10^8 (\Psi/V_T)^{1/4} |E_\pm| \gg \omega \gg 1.1 \cdot 10^7 |E_\pm|. \qquad (15)$$

Whence it follows that the trapping conditions impose a rather stringent limitation on the possible frequency range which can be used; it is convenient to choose ω close to the left-hand limit in Eq. (15) since the limitation on frequency from above is weaker. Secondly, the dimensions of the localization region ($L \sim \lambda/4$) are actually the factors which determine the allowable values of the electric field intensity E: for example with L = 5 cm, ($\omega = 10^{10}$), $V_T = 3.3$ cgs (10^3v), $\Psi = 0.5$, the field strength must be $\sim 10^2$ cgs (3×10^4v/cm); with E = 0.1 cgs (30v/cm), $\omega \approx 10^7$, i.e. $L \approx 50$ m. Thus, to contain a bunch in a relatively small region of space it is necessary to use high-frequency fields of rather high amplitude.

The allowable values of $\tilde{w}$ can be determined from Eq. (6) if it is assumed that the quantity Φ_1', in accordance with Eq. (11), is approximately $\Phi_1' \approx \frac{1}{2}(\eta_e/\omega)^2 E_{av}^2$ where E_{av} is the average value of the electric field in the traveling wave:

$$\tilde{w}_{av} = \alpha_{av}(m_e/m_i)(\gamma_{i_e}/\omega_{av})^2 ksE_{av}^2.$$

For example, with $\omega = 10^{10}$, $\alpha = 0.4$, $\Psi = 0.5$, $m_i/m_e = 1.8 \times 10^3$, s = 0.6, and $E_{av} \approx 10^2$ it is possible to obtain an acceleration $\tilde{w}_{av} \approx 10^{15}$ cm/sec^2.

The acceleration and maximum velocity which can be realized in practice depend on the method of displacing the localizing field and on the electrodynamic nature of the system; in particular, if we require that there be a propagating mode of only one kind in the waveguide* it is necessary to vary the generator frequency in such a way that it remains between the first and second critical frequencies of the waveguide:† $c\kappa_2 \geq \omega \geq c\kappa_1$; this requirement and that given in (18) set additional limitations on the range of ω and determine the maximum possible velocity at the output of the accelerator β_{max}.

From the technical point of view perhaps the most important factor which limits the applicability of high-frequency plasma accelerators is the power required to form the localizing field. If non-resonance excitation is used this power is approximately equal to the mean Poynting vector flux in the traveling wave and can be estimated from the relation

$$P_{TM} = \frac{c}{8\pi}\frac{k}{h}E_{av}^2 S, \quad P_{TE} = \frac{c}{8\pi}\frac{h}{k}E_{av}^2 S, \qquad (16)$$

where S is the effective cross section of the waveguide.

In resonance excitation of an appropriate cylindrical configuration of length l the power P is estimated taking account of the Q of the system:

$$P_Q = \frac{\omega}{8\pi Q}\int |E|^2 dV \approx \frac{c}{16\pi Q}(kl)E_{av}^2 S. \qquad (17)$$

For example with $\lambda = 20$ cm, $S \approx \lambda^2/4 = 10^2$cm^2, $h/k = 0.6$ and $E_{av} \approx 10^2$cgs, $P_{TE} \approx 7 \times 10^{14}$ joules (7×10^7 watts); similarly, for excitation of an appropriate resonator $kl = 10^3$, $Q = 10^4$, $P_Q \approx 6 \times 10^{13}$ joules (6×10^6 watts). A further increase in the amplitude of the field would require the use of sources of enormous power, such as are generally used in pulsed rather than continuous operation.

In conclusion we present typical data for a linear accelerator for hydrogen plasma at a temperature $V_T = 10^3$ ev, which uses anti-parallel TE_{01} waves in a waveguide of rectangular cross section:

a) $\omega_- = 6.3 \times 10^{10}$sec^{-1} ($\lambda_- = 3$ cm), p = 0.9, $\Delta\omega/\omega = 0.27$, $\beta_{max} = 0.2$, $s_{av} = 0.6$, $E_{av} = 10^3$ cgs, $w_{av} = 2 \times 10^{16}$cm/sec^2, $P_{TE} \approx 3 \times 10^8$ watts; for operation with pulses of duration $\Delta t = 3 \times 10^{-7}$ sec the length of the accelerator is $l = 9$ m.

b) $\omega = 10^{10}$sec^{-1} ($\lambda = 20$ cm), p = 0.9, $\Delta\omega/\omega_- = 0.27$, $\beta_{max} = 0.2$, $s_{av} = 0.6$, $E_{av} = 10^2$cgs, $w_{av} = 10^{15}$ cm/sec^2, $P_{TE} = 7 \times 10^7$ watts, $\Delta t = 6 \times 10^{-6}$ sec, $l = 2 \times 10^2$ m.

7. POSSIBILITY OF CYCLIC ACCELERATION OF A PLASMA

The basic difficulty in cyclic acceleration of a plasma lies in the containment of a quasi-neutral plasmoid over a stable closed trajectory. Although the use of weakly inhomogeneous high-frequency fields for this purpose is possible in principle, as will be shown below, these can only be used for small velocities. For example, suppose that it is necessary to achieve stable motion of a plasmoid about a circle of radius $r_\perp = r_0$, which is considerably greater than the dimensions of the plasmoid

*The appearance of higher propagating modes may not only reduce the efficiency of the accelerator but can also cause delocalization of the bunch. Even if the system is excited by an external source which produces only the required mode the latter can be transformed into higher modes directly at the plasma bunches if the dielectric constant of these bunches varies greatly from unity.

†From the point of view of the most favorable conditions it turns out best to use the TEM mode in multiconductor lines for which $\varkappa_1 = 0$ and ω is limited from below only by the condition in (15).

itself. We set up a toroidal channel for the high-frequency potential $\Phi(r_\perp)$ in such a way that the circle $r_\perp = r_0$ lies within the toroidal potential well.* In order to compensate for the centrifugal forces it is necessary that the sides of the potential well be rather steep. In the non-relativistic approximation this limitation, similar in meaning to (3), is written in the form

$$|\partial\Phi/\partial r_\perp|_{r_\perp=r_0} > m_i v_0^2/m_e r_0. \qquad (18)$$

Here $v_\theta = \beta_\theta c$ is the mean linear velocity of the plasmoid. Assuming that $\partial\Phi/\partial r_\perp \sim \Phi/L$ and substituting the value of Φ in Eq. (18) from Eq. (1), we find the condition which limits the field intensity E from below for the field which forms the potential barrier with respect to $r_\perp = r_{\theta}$,

$$|E|/\beta_0 > (L/r_0)^{1/2}(m_i/m_e)^{1/2} 2\omega c/\tau_{i\theta}. \qquad (19)$$

As an example we take the values $\omega = 2 \times 10^{10}$ $\sec^{-1}$, $m_i/m_e = 1.8 \times 10^3$, $L/r_0 \sim 10^{-2}$. Substitution of these values in Eq. (19) yields $|E|/\beta_\theta > 10^4$. Consequently even with velocities $\beta_\theta \sim 10^{-1}$ one requires fields with intensities of $E \sim 10^3$cgs $\times$ (3×10^5v/cm) and, by virtue of Eqs. (16) and (17), sources with powers of the order of $10^7 - 10^9$ watts. Whence it follows that in cyclical plasma accelerators with radial high-frequency focusing the velocities which can be achieved are smaller than those that can be obtained in corresponding linear accelerators; most of the power required from the high-frequency sources goes into the fields which constrain the plasmoids in the radial direction.

Acceleration of plasmoids can be realized by displacement of supplementary potential wells produced by waves which rotate in azimuth. In this connection it is interesting to note that if inside a waveguide system which closes on itself we excite two standing waves of different frequencies it is possible to distinguish four potential profiles, which rotate in pairs in opposite directions with velocities

$$\beta_a = \pm(k_+ - k_-)/(h_+ + h_-), \qquad \beta_p = \pm(k_+ - k_-)/(h_+ - h_-),$$

which offers the possibility of obtaining simultaneous displacement and even acceleration of plasmoids in opposite directions.

*A toroidal channel of this kind can be produced, for example, by means of a TM_{01} mode in a corrugated metal torus of circular cross section, a TE_{01} (usual profile) or a TE_{11} mode (inverted profile) in a smooth-walled torus of circular cross section; symmetric waves in a helical conducting torus, and so on. One of the examples of the production of a two-dimensional circular potential well in a cylindrical resonator has been given for example by Veksler and Kovrizhnykh.[8]

8. CONCLUSION

Thus, high-frequency weakly inhomogeneous fields can be used for accelerating quasi-neutral plasmoids. This possibility has been demonstrated with plasmoids of low density; however, in principle, many of the points relating to the acceleration mechanism, in particular the method of displacing the localizing fields, remain valid for acceleration of dense plasmoids. The high-frequency field is distorted significantly only in the immediate vicinity of the plasmoid; the field is unchanged (in the absence of higher modes) at far distances. Obviously, however, for a complete description of the characteristics of such accelerators it will be necessary to find a self-consistent solution of the problem of the localization of dense plasma inside an accelerated high frequency potential well.

The author is indebted to A. V. Gaponov, V. B. Gil'denburg, and S. B. Mochenev for useful discussion of the results.

[1] V. I. Veksler, Атомная энергия (Atomic Energy) **2**, 427 (1957).

[2] F. B. Knox, Austr. J. Phys., **10**, 565 (1957).

[3] Boot, Self, and Harvie, J. Electron. and Control, **4**, 434 (1958).

[4] R. Z. Sagdeev, Физика плазмы и проблема управляемых термоядерных реакций (Plasma Physics and the Problem of a Controlled Thermonuclear Reaction), U.S.S.R. Acad. Sci. Press, Vol 3, p. 346 (1958).

[5] A. V. Gaponov and M. A. Miller, J. Exptl. Theoret. Phys. (U.S.S.R.) **34**, 242 (1958), Soviet Phys. JETP **7**, 168 (1958).

[6] M. A. Miller, Изв. высших учебн. зав., Радиофизика (Bulletin of Instit. of Higher Learning, Radiophysics), **1**, No. 3, 110 (1958).

[7] A. V. Gaponov and M. A. Miller, J. Exptl. Theoret. Phys. (U.S.S.R.) **34**, 751 (1958), Soviet Phys. JETP **7**, 515 (1958).

[8] V. I. Veksler and L. M. Kovrizhnykh, J. Exptl. Theoret. Phys. (U.S.S.R.) **35**, 1116 (1958), Soviet Phys. JETP **8**, 781 (1959).

Translated by H. Lashinsky
379

MICROSCOPIC DERIVATION OF THE GINZBURG-LANDAU EQUATIONS IN THE THEORY OF SUPERCONDUCTIVITY

L. P. GOR'KOV

Institute for Physical Problems, Academy of Sciences, U.S.S.R.

Submitted to JETP editor February 3, 1959

J. Exptl. Theoret. Phys. (U.S.S.R.) 36, 1918-1923 (June, 1959)

It is shown that the phenomenological Ginzburg-Landau equations follow from the theory of superconductivity in the London temperature region in the neighborhood of T_c. In these equations there occurs, however, twice the electronic charge; this is related to the physical meaning of $\Psi(x)$ as the wave function for Cooper pairs. The constant κ turns out to be small. The problem of the surface energy for the boundary between the normal and superconducting phases in the neighborhood of T_c is discussed.

It is well known that the behavior of superconductors in a magnetic field in the neighborhood of the critical temperature is qualitatively well described by Ginzburg and Landau's phenomenological theory.[1] We shall show in the present paper that equations of the same type as those in Ginzburg and Landau's theory follow indeed from the theory of superconductivity.

We shall start from the equations for the thermodynamic Green functions[3,4] which we obtained earlier.[2] These equations are in a magnetic field of the form

$$\left\{-\frac{\partial}{\partial\tau}+\frac{1}{2m}\left(\frac{\partial}{\partial\mathbf{r}}-ie\mathbf{A}(\mathbf{r})\right)^2+\mu\right\}G(x,x')+\Delta(\mathbf{r})F^+(x,x')=\delta(x-x'),$$

$$\left\{\frac{\partial}{\partial\tau}+\frac{1}{2m}\left(\frac{\partial}{\partial\mathbf{r}}+ie\mathbf{A}(\mathbf{r})\right)^2+\mu\right\}F^+(x,x')-\Delta^*(\mathbf{r})G(x,x')=0; \quad (1)$$

where

$$\Delta^*(\mathbf{r})=gF^+(\tau,\mathbf{r};\tau,\mathbf{r}). \quad (1')$$

The last relation expresses $\Delta(\mathbf{r})$ in terms of the coupling constant and the value of the function $F^+(x, x')$ for equal arguments. If there is no field, Δ = const. The quantity 2Δ is in that case the energy gap in the spectrum. $F^+(x, x')$ tends, in fact, logarithmically to infinity as $x = x'$; this corresponds to the well known logarithmic divergence in the equation determining the gap when one integrates in momentum space. In the papers by Bardeen, Cooper, and Schrieffer[5] and Bogolyubov[6] this divergence was removed by cutting-off the energy of the interacting electrons at distances of the order of the Debye frequency $\tilde{\omega}$ from the Fermi surface; we shall do the same in the following. One verifies easily that such a cut-off corresponds in the coordinate representation to a "spread out" in Eq. (1') over a distance of the order $\hbar v/\tilde{\omega}$.

Let us go over to the Fourier components of the Green functions $G(x, x')$ and $F^+(x, x')$ with respect to the difference of the variables[4] $u = \tau - \tau'$, for instance,

$$G(\mathbf{r},\mathbf{r}';u)=T\sum_n e^{-i\omega_n u}\mathfrak{G}_\omega(\mathbf{r},\mathbf{r}'),$$

$$\mathfrak{G}_\omega(\mathbf{r},\mathbf{r}')=\frac{1}{2}\int_{-1/T}^{+1/T}e^{i\omega_n u}G(\mathbf{r},\mathbf{r}';u)\,du,$$

where $\omega_n = \pi(2n + 1)T$ ($n = \ldots -1, 0, 1, \ldots$). Equations (1) go over into the following equations for the Fourier components $\mathfrak{G}_\omega(\mathbf{r}, \mathbf{r}')$ and $\tilde{\mathfrak{F}}^+_\omega(\mathbf{r}, \mathbf{r}')$:

$$\left\{i\omega_n+\frac{1}{2m}\left(\frac{\partial}{\partial\mathbf{r}}-ie\mathbf{A}(\mathbf{r})\right)^2+\mu\right\}\mathfrak{G}_\omega(\mathbf{r},\mathbf{r}')+\Delta(\mathbf{r})\tilde{\mathfrak{F}}^+_\omega(\mathbf{r},\mathbf{r}')=\delta(\mathbf{r}-\mathbf{r}'),$$

$$\left\{-i\omega_n+\frac{1}{2m}\left(\frac{\partial}{\partial\mathbf{r}}+ie\mathbf{A}(\mathbf{r})\right)^2+\mu\right\}\tilde{\mathfrak{F}}^+_\omega(\mathbf{r},\mathbf{r}')-\Delta^*(\mathbf{r})\mathfrak{G}_\omega(\mathbf{r},\mathbf{r}')=0, \quad (2)$$

and condition (1') can be written in the form

$$\Delta^*(\mathbf{r})=T\sum_n\tilde{\mathfrak{F}}^+_\omega(\mathbf{r},\mathbf{r}). \quad (2')$$

We introduce, finally, $\tilde{\mathfrak{G}}_\omega(\mathbf{r}, \mathbf{r}')$, the Fourier component of the Green function for an electron in the normal metal in a magnetic field. The equation satisfied by $\tilde{\mathfrak{G}}_\omega(\mathbf{r}, \mathbf{r}')$ can be written in two ways:

$$\left\{i\omega_n+\frac{1}{2m}\left(\frac{\partial}{\partial\mathbf{r}}-ie\mathbf{A}(\mathbf{r})\right)^2+\mu\right\}\tilde{\mathfrak{G}}_\omega(\mathbf{r},\mathbf{r}')=\delta(\mathbf{r}-\mathbf{r}') \quad (3)$$

or

$$\left\{i\omega_n + \frac{1}{2m}\left(\frac{\partial}{\partial \mathbf{r}'} + ie\mathbf{A}(\mathbf{r}')\right)^2 + \mu\right\}\mathfrak{G}_\omega(\mathbf{r}, \mathbf{r}') = \delta(\mathbf{r} - \mathbf{r}').$$

It is convenient to use the function $\mathfrak{G}_\omega(\mathbf{r}, \mathbf{r}')$ to write Eqs. (2) in integral form, using the second of Eqs. (3):

$$\mathfrak{G}_\omega(\mathbf{r}, \mathbf{r}') = \mathfrak{G}^0_\omega(\mathbf{r}, \mathbf{r}') - \int \mathfrak{G}_\omega(\mathbf{r}, \mathbf{s})\,\Delta(\mathbf{s})\,\mathfrak{F}^+_\omega(\mathbf{s}, \mathbf{r})\,d^3\mathbf{s},$$

$$\mathfrak{F}^+_\omega(\mathbf{r}, \mathbf{r}') = \int \mathfrak{G}_\omega(\mathbf{s}, \mathbf{r}')\,\Delta^*(\mathbf{s})\,\mathfrak{G}_{-\omega}(\mathbf{s}, \mathbf{r})\,d^3\mathbf{s}. \qquad (4)$$

Before we proceed, we find out what the function $\mathfrak{G}_\omega(\mathbf{r}, \mathbf{r}')$ is equal to. If there is no magnetic field, one sees from (3) that

$$\mathfrak{G}^0_\omega(\mathbf{r} - \mathbf{r}') = -\frac{m}{2\pi R}\exp\left\{\left[i\,\mathrm{sign}\,\omega p_0 - \frac{|\omega_n|}{v}\right]R\right\}. \qquad (5)$$

Here

$$\mathrm{sign}\,\omega = \omega/|\omega|, \quad R = |\mathbf{r} - \mathbf{r}'|, \quad \mu = p_0^2/2m \gg |\omega|.$$

$\mathfrak{G}_\omega(\mathbf{r}, \mathbf{r}')$ in a magnetic field differs from (5) by a phase factor. Indeed,* because p_0 is a large quantity we can use the quasi-classical approximation to determine $\mathfrak{G}_\omega(\mathbf{r}, \mathbf{r}')$, i.e., write it in the following form:

$$\mathfrak{G}_\omega(\mathbf{r}, \mathbf{r}') = e^{i\varphi(\mathbf{r}, \mathbf{r}')}\mathfrak{G}^0_\omega(\mathbf{r} - \mathbf{r}'), \quad \varphi(\mathbf{r}, \mathbf{r}')|_{\mathbf{r}=\mathbf{r}'} = 0. \qquad (6)$$

Substituting (6) into (3) we find for the addition to the action of $\varphi(\mathbf{r}, \mathbf{r}')$

$$\left(\mathbf{n}, \nabla_r\varphi(\mathbf{r}, \mathbf{r}')\right) = \frac{e}{c}(\mathbf{n}, \mathbf{A}(\mathbf{r})), \qquad \mathbf{n} = (\mathbf{r} - \mathbf{r}')/|\mathbf{r} - \mathbf{r}'|. \qquad (7)$$

Near the transition temperature $\Delta(\mathbf{r})$ (and at the same time $\mathfrak{F}^+_\omega(\mathbf{r}, \mathbf{r}')$) is small. We shall therefore expand Eq. (4) in powers of Δ and Δ^* and express $\mathfrak{F}^+_\omega(\mathbf{r}, \mathbf{r}')$ up to terms of the fourth order, and $\mathfrak{G}_\omega(\mathbf{r}, \mathbf{r}')$ up to terms of second order in Δ, inclusive. The substitution of the expression obtained for $\mathfrak{F}^+_\omega(\mathbf{r}, \mathbf{r}')$ into (2′) gives one equation connecting $\Delta(\mathbf{r})$ and $\mathbf{A}(\mathbf{r})$:

$$\Delta^*(\mathbf{r}) = gT\sum_n \int \mathfrak{G}_\omega(\mathbf{r}, \mathbf{r}')\mathfrak{G}_{-\omega}(\mathbf{r}, \mathbf{r}')\,\Delta^*(\mathbf{r}')\,d^3\mathbf{r}'$$

$$- gT\sum_n \int\int\int \mathfrak{G}_\omega(\mathbf{s}, \mathbf{r})\mathfrak{G}_{-\omega}(\mathbf{s}, \mathbf{l})\mathfrak{G}_\omega(\mathbf{m}, \mathbf{l})\mathfrak{G}_{-\omega}(\mathbf{m}, \mathbf{r})$$

$$\times \Delta(\mathbf{s})\,\Delta^*(\mathbf{l})\,\Delta^*(\mathbf{m})\,d^3\mathbf{s}\,d^3\mathbf{l}\,d^3\mathbf{m}. \qquad (8)$$

The important distances in Eq. (8) are of the order $\xi = \hbar v/T_c$, since it can be seen from (5) and (6) that the Green function $\mathfrak{G}_\omega(\mathbf{r}, \mathbf{r}')$ decreases exponentially for $R \gg \xi_0$. At the same time, the changes in the gap $\Delta(\mathbf{r})$ and the field $\mathbf{A}(\mathbf{r})$ take place at distances of the order of the penetration depth which is much larger than ξ_0 near the critical temperature. For the same reason the phase $\varphi(\mathbf{r}, \mathbf{r}')$ in (6) is small near T_c and equal to

$$\varphi(\mathbf{r}, \mathbf{r}') \approx \frac{e}{c}(\mathbf{A}(\mathbf{r}'), \mathbf{r} - \mathbf{r}'). \qquad (9)$$

*This was pointed out by L. D. Landau.

Using these facts we can perform the integration in Eq. (8).

The first term on the right hand side is of the form

$$g\int K(\mathbf{r}, \mathbf{r}')\,\Delta^*(\mathbf{r}')\,d^3\mathbf{r}',$$

where the kernel

$$K(\mathbf{r}, \mathbf{r}') = K_0(\mathbf{r} - \mathbf{r}')\exp\left\{\frac{2ie}{c}(\mathbf{A}(\mathbf{r}'), \mathbf{r} - \mathbf{r}')\right\}$$

has a singularity for $R = |\mathbf{r} - \mathbf{r}'| = 0$:

$$K_0(R) = m^2T/(2\pi R)^2\sinh(2\pi TR/v).$$

This singularity is connected, as was pointed out already in the foregoing, with the cut-off of the interaction at the Debye frequencies $\tilde{\omega}$.

Introducing this cut-off we get

$$\int K_0(R)\,d^3R = \frac{mp_0}{2\pi^2}\int_0^{\tilde{\omega}} \frac{\tanh(\xi/2T)}{\xi}\,d\xi$$

$$= \frac{mp_0}{2\pi^2}\ln\left(\frac{2\gamma}{\pi}\frac{\tilde{\omega}}{T}\right) = \frac{mp_0}{2\pi^2}\left(\frac{1}{g} + \ln\frac{T_c}{T}\right), \qquad (10)$$

where the transition temperature T_c is connected to the gap in the energy spectrum at absolute zero in the well-known way[5]:

$$\frac{\Delta_0\gamma}{\pi} = T_c \qquad \left(\frac{1}{g} = \frac{mp_0}{2\pi^2}\ln\frac{2\tilde{\omega}}{\Delta_0}\right).$$

Expanding the exponents in the Green functions in terms of $\varphi(\mathbf{r}, \mathbf{r}')$ using the fact that $\Delta(\mathbf{r})$ and $\mathbf{A}(\mathbf{r})$ vary slowly near T_c, and eliminating $\tilde{\omega}$ and g by using (10) we get the following equation

$$\left\{\frac{1}{2m}\left(\frac{\partial}{\partial \mathbf{r}} + 2ie\,\mathbf{A}(\mathbf{r})\right)^2 + \frac{1}{\lambda}\left[\frac{T_c - T}{T_c} - \frac{7\zeta(3)}{8(\pi T_c)^2}|\Delta(\mathbf{r})|^2\right]\right\}\Delta^*(\mathbf{r}) = 0, \qquad (11)$$

where $\lambda = 7\,\zeta(3)\,\epsilon_F/12(\pi T_c)^2$ ($\zeta(x)$ is here Riemann's zeta function).

To get a second equation connecting Δ and $\mathbf{A}$ we shall now calculate what the current density $\mathbf{j}(\mathbf{r})$ is equal to. To do this we use the relation expressing $\mathbf{j}(\mathbf{r})$ in terms of a Green function:

$$\mathbf{j}(\mathbf{r}) = \left\{\frac{ie}{m}(\nabla_{r'} - \nabla_r)G(x, x') - \frac{2e^2}{mc}\mathbf{A}(\mathbf{r})\,G(x, x')\right\}_{t'=t+0;\ \mathbf{r}=\mathbf{r}'}$$

(the additional factor of 2 is due to a summation over spin). We note that if we substitute everywhere the Green function for the normal metal in the form (6) and then sum over frequencies we get no contribution to the expression for the current, as should be the case. The total current is thus equal to

$$\mathbf{j}(\mathbf{r}) = \frac{ie}{m}(\nabla_{r'} - \nabla_r)\delta G(x, x')|_{x=x'}, \qquad (12)$$

where

$$\hat{\alpha} G(x, x')|_{x=x'} = -T\sum_n \int\int \mathfrak{G}_\omega(\mathbf{r}, \mathbf{s})\,\mathfrak{G}_\omega(\mathbf{l}, \mathbf{r})\,\mathfrak{G}_{-\omega}(\mathbf{l}, \mathbf{s})\,\Delta^*(\mathbf{l})\,\Delta(\mathbf{s})\,d^3\mathbf{s}\,d^3\mathbf{l}. \tag{13}$$

Restricting ourselves in the expression for the current to terms linear in $\mathbf{A}$ and assuming $\mathbf{A}(\mathbf{r})$ to vary slowly with $\mathbf{r}$ in the London temperature range near T_c we get

$$\mathbf{j}(\mathbf{r}) = \left\{\frac{ic}{m}\left(\Delta\frac{\partial\Delta^*}{\partial\mathbf{r}} - \Delta^*\frac{\partial\Delta}{\partial\mathbf{r}}\right) - \frac{4e^2|\Delta|^2}{mc}\mathbf{A}\right\}\frac{7\zeta(3)N}{16(\pi T)^2} \tag{14}$$

We shall introduce a "wave function" $\Psi(\mathbf{r})$, proportional to $\Delta(\mathbf{r})$:

$$\Psi(\mathbf{r}) = \Delta(\mathbf{r})\sqrt{7\zeta(3)N}/4\pi T_c. \tag{15}$$

The set of Eqs. (11) and (14) takes then a form completely analogous to the equations of the phenomenological Ginzburg-Landau theory:

$$\left\{\frac{1}{2m}\left(\frac{\partial}{\partial\mathbf{r}} - ie^*A(\mathbf{r})\right)^2 + \frac{1}{\lambda}\left[\frac{T_c - T}{T_c} - \frac{2}{N}|\Psi(\mathbf{r})|^2\right]\right\}\Psi(\mathbf{r}) = 0,$$

$$\mathbf{j}(\mathbf{r}) = -\frac{ie^*}{2m}\left(\Psi^*\frac{\partial\Psi}{\partial\mathbf{r}} - \Psi\frac{\partial\Psi^*}{\partial\mathbf{r}}\right) - \frac{e^{*2}}{mc}\mathbf{A}|\Psi|^2, \tag{16}$$

where $e^* = 2e$, N is the number density of the electrons in the normal metal and λ was defined after Eq. (11). There is a difference, however, in that (16) contains the electronic charge e twice, clearly owing to the physical meaning of $\Psi(\mathbf{r})$ as the wave function of a Cooper pair.

These equations arise thus in a natural way in the theory of superconductivity in the London region* near T_c. The phenomenological constant defined in the same way as in the old theory, but with $e^* = 2e$, can now be evaluated and turns out to be equal to

$$\varkappa = 3T_c(\pi/v)^{1/2}(c/ep_0)\sqrt{2/7\zeta(3)}. \tag{17}$$

The region of applicability of Eqs. (16) is small for sharply expressed Pippard metals and occurs very near T_c; at large distances from T_c the local relation (14) ceases to be valid.

For metals of the London type the region of applicability of (16) is determined solely by the smallness of the ratio $(T - T_c)/T_c$.

The possibility to apply (16) to describe the properties of thin films in a magnetic field with the microscopic value (17) of the constant κ is limited by the fact that usually films are polycrystalline specimens with grain sizes of the order of the film thickness. The presence of boundaries between different crystals will act like the presence of foreign impurities. One must therefore possibly describe real films in the microscopic theory from the same point of view as superconducting alloys.

We note now that to evaluate the difference in the free energy of the metal in the normal state and in the superconducting state in a magnetic field we can use the following formula:

$$F_{sH} - F_n = -(1/\lambda N)\int|\Psi(\mathbf{r})|^4\,d^3\mathbf{r}. \tag{18}$$

Indeed, we shall use the thermodynamic relation

$$\delta\Omega/\delta g(\mathbf{r}) = -\langle H_{int}(\mathbf{r})\rangle/g(\mathbf{r}),$$

where according to (5)

$$H_{int}(\mathbf{r}) = {}^1/_2 g(\mathbf{r})(\hat{\Psi}^+(\mathbf{r})(\hat{\Psi}^+(\mathbf{r})\hat{\Psi}(\mathbf{r}))\hat{\Psi}(\mathbf{r})),$$

Ω is the thermodynamic potential [we introduce here for the sake of convenience a variable "interaction constant" $g(\mathbf{r})$]. Taking averages we get

$$\Omega_s - \Omega_n = -\int d^3\mathbf{r}\int_0^g \frac{\delta g(\mathbf{r})}{g^3(\mathbf{r})}|\Delta(\mathbf{r})|^2. \tag{19}$$

Equation (8) determines $1/g(\mathbf{r})$ as a functional of $\Delta(\mathbf{r})$ [for the sake of simplicity we shall consider the real solution for $\Delta(\mathbf{r})$ as is usually done in one-dimensional problems]. Using (8) to integrate (19), and using the fact that small additions to all thermodynamic potentials in the corresponding variables are equal, we get Eq. (18).

The constant κ of (17) is connected with the magnitude of the critical field H_{cm} of a bulk specimen and the penetration depth δ_0 by the relation (which contains the charge e^*):

$$\varkappa = \frac{\sqrt{2}e^*}{\hbar c}H_{cm}\delta_0^2. \tag{20}$$

For metals of the London type or such intermediate metals as tin the region of applicability of Eqs. (16) is fairly large and in that case we should consistently use the experimental data* for H_{cm} and δ_0^2 to compare the theory with experiments. For Pippard metals δ_0 is the penetration depth only in a very narrow range of temperatures near T_c. It is thus convenient in this case to turn to the theoretical formulae for a definition of κ. It can easily be verified that (17) can be written in the form

$$\varkappa \approx 0.96\,\delta_L/\xi_0, \tag{21}$$

where $\delta_L^{-1} = (4\pi Ne^2/mc^2)^{1/2}$ is the London penetration depth and $\xi_0 = 0.18\,\hbar v/kT_c$ is the non-localization parameter introduced in Bardeen, Cooper, and Schrieffer's paper. Using the data given in reference 5 we get from (21) for tin $\kappa \approx 0.14$, and for aluminum $\kappa \approx 0.01$.

We note an interesting consequence of (21). The

*In reference 5 the assumption was stated that some quantity related to the gap should play the role of the expansion parameter Ψ in the theory of reference 1.

*A detailed study of experimental data is given in a paper by Ginzburg.[7]

condition that a superconductor be a London one requires $\kappa \approx \delta_L/\xi_0 \gg 1$. At the same time if $\kappa \gg 1/\sqrt{2}$ a metal displays in a strong field the same behavior as for alloys. A metal which in weak fields at $T = 0$ must be assigned to the London class will thus behave in strong fields near T_c as an "alloy." At the same time the case of small κ corresponds to a Pippard metal.

Let us now stop a moment at the problem of the surface energy at the boundary between the normal and the superconducting phase. For strongly expressed Pippard superconductors we can, because κ is small, use the limiting solution[1]

$$\sigma_{ns}(8\pi/H_{cm}^2) = 1.89\,\delta_0/\varkappa, \qquad (22)$$

where

$$\delta_0 = \delta_L(T=0)/\sqrt{2(1-T/T_c)}.$$

We note that for these metals the applicability of Eq. (22) in an appreciable temperature interval near T_c is just connected with the fact that κ is small, since, as was shown in reference 1, in that case the quantity σ_{ns} does not depend on the distribution of the field in the transition region.

For tin the accuracy of this equation is insufficient and one must use the results of numerical calculations. Estimating σ_{ns} from Ginzburg's calculations[8] we get for $\kappa \approx 0.14$

$$\sigma_{ns}(8\pi/H_n^2) \approx (2 \div 3)\cdot 10^{-5}/\sqrt{1-T/T_c}.$$

According to Sharvin's data[9]

$$\sigma_{ns}(8\pi/H_c^2) = 2.5\cdot 10^{-5}/\sqrt{1-T/T_c},$$

and according to Faber's data[10]

$$\sigma_{ns}(8\pi/H_c^2) = 1.88\cdot 10^{-5}/\sqrt{1-T/T_c}.$$

These results do, apparently, not contradict the theory (See reference 7).

In conclusion the author expresses his gratitude to Academician L. D. Landau for valuable advice and to V. L. Ginzburg for discussing the results of this paper and for helpful comments.

[1] V. L. Ginzburg and L. D. Landau, J. Exptl. Theoret. Phys. (U.S.S.R.) **20**, 1064 (1950).

[2] L. P. Gor'kov, J. Exptl. Theoret. Phys. (U.S.S.R.) **34**, 735 (1958), Soviet Phys. JETP **7**, 505 (1958).

[3] T. Matsubara, Progr. Theoret. Phys. **14**, 352 (1954).

[4] Abrikosov, Gor'kov, and Dzyaloshinskiĭ, J. Exptl. Theoret. Phys. (U.S.S.R.) **36**, 900 (1959), Soviet Phys. JETP **9**, 636 (1959).

[5] Bardeen, Cooper, and Schrieffer, Phys. Rev. **108**, 1175 (1957).

[6] N. N. Bogolyubov, J. Exptl. Theoret. Phys. (U.S.S.R.) **34**, 58 (1958), Soviet Phys. JETP **7**, 41 (1958).

[7] V. L. Ginzburg, J. Exptl. Theoret. Phys. (U.S.S.R.) **36**, 1930 (1959), Soviet Phys. JETP this issue, p 1372.

[8] V. L. Ginzburg, J. Exptl. Theoret. Phys. (U.S.S.R.) **30**, 593 (1956), Soviet Phys. JETP **3**, 621 (1956).

[9] Yu. V. Sharvin, J. Exptl. Theoret. Phys. (U.S.S.R.) **33**, 1341 (1957), Soviet Phys. JETP **6**, 1031 (1958).

[10] T. E. Faber, Proc. Roy. Soc. (London) **A248**, 460 (1958).

Translated by D. ter Haar
380

Letters to the Editor

THE PROBLEM OF DETERMINING THE DIELECTRIC PERMITTIVITY AND MAGNETIC PERMEABILITY TENSORS OF A MEDIUM

G. S. KRINCHIK and M. V. CHETKIN

Moscow State University

Submitted to JETP editor December 29, 1958

J. Exptl. Theoret. Phys. (U.S.S.R.) **36**, 1924-1925 (June, 1959)

In the study of gyrotropic media, both in optical and in radiofrequency investigations,[1,2] it is important to know whether the gyrotropy of the medium is connected with its dielectric permittivity or with its magnetic permeability.

By solving Maxwell's equations in a medium described by tensors ϵ and μ with the following nonvanishing components:

$$\varepsilon_{xx} = \varepsilon_{yy} = \varepsilon, \quad \varepsilon_{xy} = -\varepsilon_{yx} = -i\varepsilon M, \quad \varepsilon_{zz} = \varepsilon_0,$$
$$\mu_{xx} = \mu_{yy} = \mu, \quad \mu_{xy} = -\mu_{xy} = -i\mu M', \quad \mu_{zz} = \mu_0,$$

it is not difficult to obtain the equation that determines the index of refraction n^* of such a medium:

$$[\mu_0\gamma^{*2} + \mu(\alpha^{*2} + \beta^{*2})][\varepsilon_0\gamma^{*2} + \varepsilon(\alpha^{*2} + \beta^{*2})]n^{*4}$$
$$- [\varepsilon^2\mu\mu_0(1 - M^2)(\alpha^{*2} + \beta^{*2})$$
$$+ \varepsilon_0\varepsilon\mu^2(1 - M'^2)(\alpha^{*2} + \beta^{*2}) + 2\varepsilon_0\mu_0\varepsilon\mu(1 + MM')\gamma^{*2}]n^{*2}$$
$$+ \varepsilon_0\mu_0\varepsilon^2\mu^2(1 - M^2)(1 - M'^2) = 0, \qquad (1)$$

where α^*, β^*, and γ^* are the direction cosines of the wave normal. The Faraday effect and the polar and meridional Kerr effects (in all three cases the magnetization vector lies in the plane of incidence of the light) do not permit a separation of the effects of the parameters M and M′; for to the first order in M and M′, (1) gives the following equation for the index of refraction of circularly polarized waves:

$$n^{*2} = n^2[1 \pm \gamma^*(M + M')],$$

where $n = \sqrt{\epsilon_0\mu_0}$ is the index of refraction of the unmagnetized medium.

A different result is obtained for the case of transverse magnetization (magnetization vector perpendicular to the plane of incidence of the light). In this case $\gamma^* = 0$, and we get from (1)

$$n_1^{*2} = \varepsilon\mu_0(1 - M^2), \qquad (2a)$$

$$n_2^{*2} = \varepsilon_0\mu(1 - M'^2). \qquad (2b)$$

It can be shown that n_1^* relates to a wave whose electric vector is parallel to the plane of incidence (p-wave), n_2^* to a wave whose electric vector is perpendicular to the plane of incidence (s-wave). Thus we have obtained generalized formulas for the Cotton-Mouton effect.*

A similar separation of M and M′ is obtained also in the case of reflection of light with transverse magnetization. The condition of continuity of the tangential components of the electric and magnetic field intensities, together with the condition div **B** = 0, leads in the approximation of small M and M′ to the following reflection coefficients:

$$\frac{R_p}{A_p} = \frac{\alpha n - \alpha^*\mu_0}{\alpha n + \alpha^*\mu_0} - 2iM\frac{\alpha\beta\mu_0}{(\alpha n + \alpha^*\mu_0)^2}, \qquad (3a)$$

$$\frac{R_s}{A_s} = \frac{\alpha n - \alpha^*\varepsilon_0}{\alpha n + \alpha^*\varepsilon_0} - 2iM'\frac{\alpha\beta\varepsilon_0}{(\alpha n + \alpha^*\varepsilon_0)^2}, \qquad (3b)$$

where $\alpha = \cos\varphi$, $\beta = \sin\varphi$; φ is the angle of incidence of the light. From (3b) we obtain a formula for the relative change of intensity of the reflected light for a gyromagnetic medium:

$$\delta = \frac{I - I_0}{I_0} = \frac{2\sin 2\varphi}{(1 - \varepsilon_1)^2 + \varepsilon_2^2}[M_1'\varepsilon_2 - M_2'(1 - \varepsilon_1)],$$

where $\epsilon = \epsilon_0 = \epsilon_1 - i\epsilon_2$, $\mu = \mu_0 = 1$; $M' = M_1' - iM_2'$. The analogous formula for the p-wave was obtained in reference 4; there, however, it was incorrectly supposed that the formula held also for a gyromagnetic medium. Thus in the case of a gyroelectric medium, the transverse effects are determined by formulas (2a) and (3a); in the case of a gyromagnetic, by formulas (2b) and (3b). If the medium is bi-gyrotropic, i.e., described simultaneously by the tensors ϵ and μ, then (2) and (3) can be used to separate the effects of the gyroelectric and gyromagnetic parts.

The existing experimental material on measurement of the transverse effects allows the following conclusions to be drawn. Metallic ferromagnetics at optical frequencies possess gyroelectric properties, since the effect determined by formula (3a) differs from zero.[2] Ferrites at superhigh frequencies possess gyromagnetic properties, since the effect determined by formula (2b) differs from zero.[5] It is clear that the Hall effect should lead to gyroelectricity of the medium; this is apparently the origin of the gyrotropic properties of germanium in the same frequency range.[6] In this connection one should look for bi-gyrotropy in ferrites and metallic ferromagnetics that have a large Hall effect.

*We observe that formulas similar to (1) and (2) obtained by Sokolov[3] are erroneous, in consequence of the fact that the components of the expression curl $\mu \mathbf{H} - \mu$ curl $\mathbf{H}$ are quantities of the first order in $\mathbf{M}'$.

[1] P. Epstein, Usp. Fiz. Nauk **65**, 283 (1958) [translated from Revs. Modern Phys. **28**, 3 (1956)]. M. A. Gintsburg, Dokl. Akad. Nauk SSSR **95**, 489 (1954).

[2] G. S. Krinchik, Izv. Akad. Nauk SSSR, Ser. Fiz. **21**, 1293 (1957), Columbia Tech. Transl. p. 1279. G. S. Krinchik and R. D. Nuralieva, J. Exptl. Theoret. Phys. (U.S.S.R.) **36**, 1022 (1959), Soviet Phys. JETP **9**, 724 (1959).

[3] A. V. Sokolov, Физика металлов и металловедение (Physics of Metals and Metal Research) **3**, 210 (1956).

[4] G. S. Krinchik, Физика металлов и металловедение (Physics of Metals and Metal Research) **7**, 181 (1959).

[5] M. T. Weiss and A. G. Fox, Phys. Rev. **88**, 146 (1952).

[6] N. N. Neprimerov, Izv. Akad. Nauk SSSR, Ser. Fiz., **21**, 1288 (1957), Columbia Tech. Transl. p. 1275.

Translated by W. F. Brown, Jr.
381

ON THE OVERHAUSER EFFECT IN SATURATION OF FORBIDDEN RESONANCE

L. L. BUISHVILI

Tbilisi State University

Submitted to JETP editor December 30, 1958

J. Exptl. Theoret. Phys. (U.S.S.R.) **36**, 1926-1927 (June, 1959)

KHUTSISHVILI[1] has considered the stationary Overhauser effect in saturation of an allowed transition in paramagnetic-resonance spectrum.

In the present paper we consider the stationary Overhauser effect, but in saturation of a forbidden transition in the paramagnetic-resonance spectrum (we note that Jeffries[2] has considered dynamic polarization of the nuclei, obtained in saturation of a forbidden transition, but for the case when the relaxation time of the nuclei is considerably longer than the relaxation time of the electrons).

Let us consider a system consisting of an electron shell with an effective spin S of one-half and a nucleus with spin I placed in an external magnetic field H. Considering the external field to be sufficiently strong, we neglect (in the calculation of the level population) the energies of the spin-spin interaction and the Zeeman energy of the nucleus. In such an approximation, we obtain $2I + 1$ pairs of levels, the difference in the energies of the components of each pair being $g\beta H$. The level scheme is shown in the diagram (M and m are the projections of the spins of the electron and nucleus on the external field).

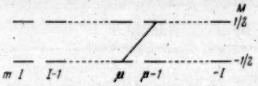

In the case of axial symmetry of the intra-crystalline electric field and in the case of an external field H parallel to the symmetry axis (the z axis), we obtain transitions that satisfy the selection rules $\Delta M = -\Delta m = \pm 1$ if the alternating field is parallel to H. For other directions of H relative to z we obtain also other forbidden transitions, in particular, transitions that satisfy the selection rule $\Delta M = \Delta m = \pm 1$.

We assume henceforth that only vertical relaxation (transitions $\Delta M = \pm 1$, $\Delta m = 0$) and relaxation due to the hyperfine interaction (transitions $\Delta M = -\Delta M = \pm 1$) are present.

For brevity we denote by μ the state corresponding to $M = -\frac{1}{2}$, $m = \mu$, and by μ' the state with $M = \frac{1}{2}$, $m = \mu$. We can write for relaxation transitions

$$W(\mu, \mu') = We^{-\delta}, \quad W(\mu', \mu) = We^{\delta},$$

$$W(\mu, \mu - 1') = \lambda We^{-\delta}, \quad W(\mu - 1', \mu) = \lambda We^{\delta},$$

where $2\delta = g\beta H/kT$, W is a certain function of the temperature and of the external field, and λ is a function of T, H, and μ.

Let the forbidden resonance $\mu \rightleftarrows \mu - 1'$ be saturated. We denote by $W(\mu)$ the probability of this transition, caused by an alternating field, per unit time. We introduce a resonance saturation parameter $s(\mu)$ in accordance with the formula

$$N(\mu) - N(\mu - 1') = \frac{N}{2I+1} \tanh\delta\,[1 - s(\mu)].$$

We can obtain the following expression for $s(\mu)$ and the parameters that characterize the degree of orientation of the nuclei:

$$s(\mu) = \frac{W(\mu)\,[(I+1-\mu)\,e^{-\delta} + (I+\mu)\,e^{\delta}]}{W(\mu)\,[(I+1-\mu)\,e^{-\delta} + (I+\mu)\,e^{\delta}] + \lambda W(2I+1)},$$

$$f_1(\mu) = -s(\mu)\,\frac{[I + (I+1) - \mu(\mu-1)]\sinh\delta}{I\,[(I+1-\mu)\,e^{-\delta} + (I+\mu)\,e^{\delta}]},$$

$$f_2(\mu) = -s(\mu)\,\frac{(2\mu-1)\,[I(I+1) - \mu(\mu-1)]\sinh\delta}{I(2I-1)\,[(I+1-\mu)\,e^{-\delta} + (I+\mu)\,e^{\delta}]}.$$

We also calculated the parameters f_1 and f_2 in saturation of one of the transitions, satisfying the selection rules $\Delta M = \Delta m = \pm 1$. However, these expressions are too unwieldy to repeat here.

In conclusion, the author thanks G. R. Khutsishvili for help in this work.

[1] G. R. Khutsishvili, J. Exptl. Theoret. Phys. (U.S.S.R.) **35**, 1031 (1958), Soviet Phys. JETP **8**, 720 (1959); Nuovo cimento, in press.

[2] C. D. Jeffries, Phys. Rev. **106**, 164 (1957).

Translated by J. G. Adashko
382

ON THE "LARMORON" PLASMA THEORY

S. A. KAPLAN

L'vov State University

Submitted to JETP editor January 30, 1959

J. Exptl. Theoret. Phys. (U.S.S.R.) **36**, 1927-1928 (June, 1959)

IN present-day quantum theory widespread use is made of the method introducing quasi-particles; it usually leads to a more effective and visualizable theory. It seems probable that a similar introduction of effective particles would also appreciably simplify plasma theory (albeit classical).

We shall use the term "larmoron" to define an effective particle situated at the guiding center of the Larmor motion of the real particle with a magnetic moment $\mu = mv_\perp^2/2H$ (where m is the particle mass, $v_\perp$ the component of the velocity perpendicular to magnetic field H) and an energy equal to the total energy of the real particle (we think this nomenclature more felicitous than the expression "Larmor circle" used elsewhere). The idea of larmorons has already been used often (but not always consistently) in many papers (see, for instance, references 1, 2, and others).

For a more consistent definition of a larmoron one must introduce its mean lifetime τ and the average translational velocities of its motion (u and v are the components perpendicular to the field H, and w the one along H). If we assume that the magnetic field is uniform, the velocity of the motion of the real particle under the action of an external acceleration a (along the x axis) in a field H (along the z axis) is of the form

$$v_x = v_x^{(0)}\cos\omega t - (v_y^{(0)} - a/\omega)\sin\omega t, \quad v_z = v_z^{(0)},$$
$$v_y = v_x^{(0)}\sin\omega t + (v_y^{(0)} - a/\omega)\cos\omega t + a/\omega, \qquad (1)$$

where $\mathbf{v}^0$ is the velocity of the real particle at time $t = 0$; ω is the Larmor frequency. Since the probability that a larmoron will live through the interval of time t to t + dt is equal to $e^{-t/\tau}\,dt/\tau$, we have

$$u = \int_0^\infty v_x e^{-t/\tau}\frac{dt}{\tau} = \frac{v_x^{(0)} - v_y^{(0)}\omega\tau + a\tau}{1+(\omega\tau)^2},$$
$$v = \frac{v_y^{(0)} + v_x^{(0)}\omega\tau + a\omega\tau^2}{1+(\omega\tau)^2}, \quad w = v_z^{(0)}. \qquad (2)$$

The total larmoron energy ϵ can be expressed in terms of its velocity as follows:

$$\varepsilon = \frac{m}{2}(v_x^{(0)2} + v_y^{(0)2} + v_z^{(0)2}) = \frac{m}{2}\{[1+(\omega\tau)^2](u^2+v^2) - 2a\tau[u+(\omega\tau)v] + (a\tau)^2 + w^2\}. \qquad (3)$$

If we assume that the distribution function for the velocities $\mathbf{v}^0$ had a Maxwellian form the distribution function for the velocities u, v, w is of the form

$$f_0(u,v,w) = n(m/2\pi kT)^{3/2}[1+(\omega\tau)^2] \times \exp\left\{-\frac{m}{2kT}\left[\left(u\sqrt{1+(\omega\tau)^2} - \frac{a\tau}{\sqrt{1+(\omega\tau)^2}}\right)^2 + \left(v\sqrt{1+(\omega\tau)^2} - \frac{a\omega\tau^2}{\sqrt{1+(\omega\tau)^2}}\right)^2 + w^2\right]\right\}, \qquad (4)$$

where n is the number of larmorons per unit volume. The transport equation for the larmorons of one kind under the conditions where there is a density and a temperature gradient along the x axis can be written in the form $u\,\partial f/\partial x = (\partial f/\partial t)_{coll}$, since the larmoron acceleration is equal to zero (if $\mathbf{a} \perp \mathbf{H}$). If we use the usual method of Lorentz's electron theory, i.e., put $f = f_0 + u\chi$ we get for the transport equation and its solution

$$\partial f_0/\partial x = -\chi/\tau, \quad f = f_0 - \tau u\,\partial f_0/\partial x. \qquad (5)$$

Substituting (4) into (5) and then evaluating, by the usual equations, the fluxes of electric charge, number of particles, and energy, we easily obtain the well known formulae for the coefficients of electrical conductivity, diffusion, and thermal conductivity of a plasma. We must note that the coefficient of electrical conductivity is evaluated with the first term of (5), i.e., with f_0 and with $a = eE/m$.

All calculations in terms of the "larmoron" theory of a plasma are very simple and suffer not at all from the unwieldiness which is so characteristic for the transport theory of a plasma. The weak point of the larmoron theory, in the formu-

lation given here, is the definition of the mean life time τ of a larmoron. One can as a first approximation use for τ the average time of free flight of the real particle, evaluated without taking the magnetic field into account, but changing the values of the parameters in the logarithmic term (the Larmor radius or the Coulomb screening distance, depending on their relative magnitude). In this way we indeed get from (4) and (5) the well known formulae for transport phenomena in a dilute plasma. It is, however, possible in the "larmoron" theory to give also a more rigorous determination of the quantity τ, in particular, by using to this purpose the method of interpreting the collision terms for larmorons in a way similar to the one used in quantum theories of transfer.

If the magnetic field or the acceleration a are non-uniform and depend on the time, we must change (1) and (2) will as a consequence become more complicated. But the "larmoron" theory will even in that case be appreciably simpler than the usual transport theory of a plasma.

I express my gratitude to A. E. Glauberman for discussing this paper.

[1] L. Spitzer Jr., Physics of Fully Ionized Gases, Interscience, New York, 1956, Russ. Transl. IIL, M., 1957.

[2] S. T. Belyaev, Физика плазмы и проблема управляемых термоядерных реакций (Plasma Physics and the Problem of Controlled Thermonuclear Reactions) U.S.S.R. Acad. Sci. Press, M., 1958, pp. 50-66.

Translated by D. ter Haar
383

A DYNAMICAL PRINCIPLE FOR SECOND-ORDER EQUATIONS

A. A. BORGARDT

Dnepropetrovsk State University

Submitted to JETP editor February 9, 1959

J. Exptl. Theoret. Phys. (U.S.S.R.) **36**, 1928-1929 (June, 1959)

A new method to construct a quantum theory of spinor fields based upon second order equations has recently been suggested.* The results of quantum electrodynamics are not changed in such an approach, but a number of interesting possibilities arise for a more correct description of other processes involving spinor particles. The unusual commutation relations for spinor wave functions are due to a number of peculiarities of the theory.

In this note we show that the application of Schwinger's dynamical principle to systems with a Lagrangian of the second order gives unique commutation rules for fermion and boson fields. It is clear from the derivation that the same result is also valid for fields with higher derivatives: Lagrangians of odd order lead to anticommutativity of spinors and Lagrangians of even order require that they commute.

Taking the Lagrangian in the form (m is the eigen mass, the rest of the notation is the same as in reference 1):

$$\mathcal{L}(x) = (1/2m)\,\partial_\mu\chi(x)\,\alpha_\mu\alpha_\nu\partial_\nu\chi(x) - \mathcal{H}(\chi(x)), \qquad (1)$$

we get, after taking the variation, the equation of motion

$$\alpha_\mu\alpha_\nu\partial^2_{\mu\nu}\chi + m\delta_1\mathcal{H}/\delta\chi = \partial^2_{\mu\nu}\chi\alpha_\mu\alpha_\nu + m\delta_r\mathcal{H}/\delta\chi = 0. \qquad (2)$$

We first of all determine the commutation rule for χ on the hypersurface σ with $d\sigma_\mu \to d\sigma_0 = d\sigma$, using the shift operator G_χ

$$G_\chi = \frac{1}{2m}\int_\sigma d\sigma_\mu\,(\delta\chi\alpha_\mu\alpha_\nu\partial_\nu\chi + \partial_\nu\chi\alpha_\nu\alpha_\mu\delta\chi)$$

$$= \frac{1}{m}\int_\sigma d\sigma_\mu\delta\chi\alpha_\mu\alpha_\nu\partial_\nu\chi = \frac{1}{m}\int_\sigma d\sigma_\mu\partial_\nu\chi\alpha_\nu\alpha_\mu\delta\chi. \qquad (3)$$

As $d\sigma_\mu \to d\sigma_0$ we get

$$G_\chi = \frac{1}{m}\int_\sigma d\sigma\partial_\nu\chi\alpha_\nu\alpha_0\delta\chi = \frac{1}{m}\int_\sigma d\sigma\,(\alpha_0\alpha_\nu)^T\delta\chi\partial_\nu\chi,$$

$$[\alpha_0\chi, G_\chi] = i\alpha_0\delta\chi.$$

The matrices α_μ can be of two kinds: a) $\alpha_\mu^T = -\alpha_\mu$, Dirac algebra; b) $\alpha_\mu^T = +\alpha_\mu$, Kemmer algebra. In both cases $\alpha_\mu\alpha_\nu = (\alpha_\nu\alpha_\mu)^T$ so that always

$$[\delta\chi,\ \partial_\nu\chi] = 0. \qquad (4)$$

The commutation relations are the same in both cases:

$$(1/m)\,[\alpha_0\chi(x), \partial_\nu\chi(x')\,\alpha_\nu\alpha_0] = i\alpha_0\delta_\sigma(x - x'), \qquad (5)$$

Using Green's theorem

$$\chi_\alpha(x) = \frac{1}{m}\int_\sigma d\sigma_\mu\,(\Delta(x - x')\ (\alpha_\mu\alpha_\nu\partial_\nu\chi\ (x'))_\alpha$$

$$- \partial_\nu\Delta(x - x')\,(\alpha_\nu\alpha_\mu\chi(x'))_\alpha) \qquad (6)$$

we get for arbitrary points x and x':

$$[\chi_\alpha(x),\ \chi_\beta(x')] = i\delta_{\alpha\beta}\Delta(x - x'). \qquad (7)$$

It is easy to generalize this result to charged

fields. In the case of integer spin the right hand side of (7) must be slightly more complicated to take the auxiliary conditions into account.

*V. Vanyashin's paper "Second-Order Wave Equations for Spinor Wave Functions" at the Conference on the Theory of Elementary Particles, Uzhgorod, October 1958.

[1] J. Schwinger, Phys. Rev. **91**, 713 (1953).

Translated by D. ter Haar
384

COMPARISON OF THE MACROSCOPIC THEORY OF SUPERCONDUCTIVITY WITH EXPERIMENTAL DATA

V. L. GINZBURG

P. N. Lebedev Physics Institute, Academy of Sciences, U.S.S.R.

Submitted to JETP editor February 19, 1959

J. Exptl. Theoret. Phys. (U.S.S.R.) **36**, 1930-1932 (June, 1959)

GOR'KOV[1] has recently shown that the macroscopic equations for superconductors, established earlier by Landau and the author[2] (see also references 3 and 4) follow from the current microscopic theory of superconductivity. He obtained then an essentially new result, namely a confirmation that the charge e_{eff} which occurs in these equations is equal to twice the electronic charge, 2e. This result has an obvious physical meaning since the charge of a Cooper pair is just equal to 2e. Meanwhile, the charge e_{eff} was previously usually put equal to e. It is in that connection advisable to consider a comparison of the macroscopic theory with experiments, putting $e_{eff} = 2e$. The parameter κ entering into the theory is then equal to

$$\varkappa = \frac{\sqrt{2}\,|e_{eff}|}{\hbar c} H_{cM}\delta_L^2 = 4.32\cdot 10^7 H_{cM}\delta_L^2, \qquad (1)$$

where H_{cM} is the critical magnetic field and δ_L the depth of the penetration of the field in a bulk metal at the given temperature T. It is now essential that the theory of reference 2 in a weak field goes over into the theory of F. and H. London and that δ_L in (1) is thus the London penetration depth. Near the critical temperature (this will be the only region with which we shall be concerned) the measured penetration depth δ is for all metals equal to δ_L. If, however, for tin $\delta \approx \delta_L$ for $\Delta T = T_c - T \lesssim 0.1°$ with an accuracy of 10 to 15%, then for aluminum, for instance, $\delta \approx \delta_L$ only when $\Delta T \lesssim 10^{-3}°$. As a result one can for tin, lead, and some other superconductors (in contradistinction to aluminum) determine the value of κ near T_c directly from the experimental data for H_{cM} and δ. Such a method is very suitable since Eq. (1) is practically independent of any assumption when $\delta = \delta_L$ and $T \to T_c$ (the result $e_{eff} = 2e$ was obtained for an isotropic model[5] but is most probably much more generally true).

If we use the empirical law

$$\delta = \delta_{00}[1 - (T/T_c)^4]^{-1/2},$$

we have near T_c

$$\delta = \frac{1}{2}\delta_{00}\sqrt{\frac{T_c}{\Delta T}} \qquad H_{cM} = \left|\frac{dH_{cM}}{dT}\right|_c \Delta T,$$

$$\varkappa = 1.08\cdot 10^7 \left|\frac{dH_{cM}}{dT}\right|_c T_c \delta_{00}^2.$$

For tin

$$\left(T_c = 3.73°,\ \left|\frac{dH_{cM}}{dT}\right|_c = 151,\quad \delta_{00} = 5.1\cdot 10^{-6}\,\text{cm}\right)$$

we have thus $\kappa = 0.158$. The limiting field for supercooling H_{ci} is for such a value of κ equal to $H_{c1}/H_{cM} = \sqrt{2\kappa} = 0.224$. Experimentally[6] $H_{c1}/H_{cM} = 0.232$. For the surface energy $\sigma_{ns} = H_{cM}^2\Delta/8\pi$ we have[7] for $\kappa = 0.158$

$$\Delta = 6.5\delta_L \approx 1.66\cdot 10^{-6}\sqrt{T_c/(T_c - T)}$$

while we have experimentally, instead of 1.66, according to Sharvin's data[8] 2.5 and according to Faber's data[9] 1.88. Since in both cases $T_c - T > 0.1°$ and we are dealing with a limiting law as $T \to T_c$ we can as yet scarcely consider the discrepancy obtained here to be real (if we determine κ from Faber's data for Δ we get $\kappa = 0.15$ and $H_{c1}/H_{cM} = 0.212$). In the isotropic model[5] near T_c

$$\delta_L(T) = \delta_L(0)\sqrt{T_c/2\Delta T}, \quad \delta_L^2(0) = mc^2/4\pi e^2 n \qquad (2)$$

(n is the concentration of "free electrons"). If we use this expression, Eq. (1) takes the form

$$\varkappa = 2.16\cdot 10^7 |dH_{cM}/dT|_c T_c \delta_L^2(0). \qquad (3)$$

For tin $\delta_L(0) = 3.5 \times 10^{-6}$, according to references 10 and 6, whence $\kappa = 0.149$. The value $\kappa = 0.15$ to 0.16 for tin agrees thus with sufficient accuracy both with experiments and with the requirements of the macroscopic as well as of the microscopic theory.

A further check must, in particular, consist in the measurement of a third effect: the change of δ with field.[2,7] The increase of δ in tin near T_c

for an external constant field equal to $H_0 = H_{cM}$ must be $3\kappa/4\sqrt{2} = 8.5\%$ (when we measure in a weak variable field parallel to H_0) and $\kappa/4\sqrt{2} = 2.8\%$ (when we measure in a weak field perpendicular to H_0). We note also that a sharp change in the behavior of Sn + In alloys takes place for 2.3% In (see references 11 and 12) when $\kappa \approx 0.6$ since, according to Chambers,[13] the penetration depth approximately doubles then. Theoretically, however, the change in the properties must occur[2,14] for $\kappa = 1/\sqrt{2} = 0.707$. The well known vagueness particular to experiments on alloys makes it hardly possible to speak here about a discrepancy between theory and experiments. In any case, the agreement is appreciably better for $e_{eff} = 2e$ than for $e_{eff} = e$.

If for Al we use in (1) the experimental value $\delta = \frac{1}{2}\delta_{00}\sqrt{T_c/\Delta T}$ with $\delta_{00} = 4.93 \times 10^{-6}$ (and also $T_c = 1.17$, $|dH_{cM}/dT|_c = 164$) we get $\kappa = 0.05$. In that case, however, $\delta \neq \delta_L$ unless we deal with values $\Delta T \lesssim 10^{-3}$°. We must therefore proceed by two other ways. First we can determine κ through the equation[14] $H_{c1}/H_{cM} = \sqrt{2}\,\kappa$ from the experimental value[6] $H_{c1}/H_{cM} = 0.0363$. Hence $\kappa = 0.0256$ and, according to reference 7 and Eq. (2)

$$\Delta \approx 62\delta_L = 44\delta_L(0)\sqrt{T_c/\Delta T} = 10.9\cdot 10^{-5}\sqrt{T_c/\Delta T},$$

since we have $\delta_L(0) = 2.48 \times 10^{-6}$ if we use (3). Experimentally[9] $\Delta = 9.0 \times 10^{-5}\sqrt{T_c/\Delta T}$ for aluminum, i.e., we get excellent agreement with theory.* Second, we should determine $\delta_L(0)$ by a less consistent method of comparison from independent data; we make then additional assumptions and, according to references 10 and 5, we have for aluminum $\delta_L(0) = 1.6 \times 10^{-6}$ and from Eq. (3) $\kappa = 1.06 \times 10^{-3}$. Hence $H_{c1}/H_{cM} = 0.015$ and $\Delta = 18 \times 10^{-5}\sqrt{T_c/\Delta T}$ which disagrees with experiments by approximately a factor two. Since for aluminum and for other "Pippard" superconductors a comparison of the theory of reference 2 with experiments is difficult it is desirable for this purpose to use in the first instance "London" superconductors (at least for $\Delta T \lesssim 0.1$°) and first of all lead.

We note in conclusion that it leads to difficulties to use data on specimens of small dimensions (films and so on) for a direct comparison of the theory with experiments. This is connected with the polycrystalline structure of such specimens which leads to the impossibility to consider them to be equivalent, thin specimens of the same metal in bulk, but in single crystal form. One should therefore in accordance with the well known considerations of Pippard and others consider thin polycrystalline films rather like alloys.

*We must note that the region of applicability of the theory of reference 2 is considerably wider[4] if we evaluate the values of Δ and H_{c1} than if we evaluate δ. We shall therefore for Al use the necessary formulae of the theory of reference 2 also for $\Delta T \sim 0.1$° when

$$\delta_L/\varkappa \sim 6 \times 10^{-4}/0.0256 = 2.3\cdot 10^{-4} > \xi_0 \sim 10^{-4}$$ (see references 5 and 10).

[1] L. P. Gor'kov, J. Exptl. Theoret. Phys. (U.S.S.R.) **36**, 1918 (1959), Soviet Phys. JETP, this issue, p. 1364.

[2] V. L. Ginzburg and L. D. Landau, J. Exptl. Theoret. Phys. (U.S.S.R.) **20**, 1064 (1950).

[3] V. L. Ginzburg, J. Exptl. Theoret. Phys. (U.S.S.R.) **29**, 748 (1955), Soviet Phys. JETP **2**, 589 (1956).

[4] V. L. Ginzburg, Physica **24**, S42 (1958).

[5] Bardeen, Cooper, and Schrieffer, Phys. Rev. **108**, 1175 (1957).

[6] T. E. Faber, Proc. Roy. Soc. (London) **A241**, 531 (1957).

[7] V. L. Ginzburg, J. Exptl. Theoret. Phys. (U.S.S.R.) **30**, 593 (1956), Soviet Phys. JETP **3**, 621 (1956).

[8] Yu. V. Sharvin, J. Exptl. Theoret. Phys. (U.S.S.R.) **33**, 1341 (1957), Soviet Phys. JETP **6**, 1031 (1958).

[9] T. E. Faber, Proc. Roy. Soc. (London) **A248**, 460 (1958).

[10] T. E. Faber and A. B. Pippard, Proc. Roy. Soc. (London) **A231**, 336 (1955).

[11] A. B. Pippard, Trans. Roy. Soc. (London) **A248**, 97 (1955).

[12] P. R. Doidge, Trans. Roy. Soc. (London) **A248**, 553 (1956).

[13] R. G. Chambers, Proc. Cambridge Phil. Soc. **52**, 363 (1956).

[14] V. L. Ginzburg, J. Exptl. Theoret. Phys. (U.S.S.R.) **31**, 541 (1956), Soviet Phys. JETP **4**, 594 (1957).

Translated by D. ter Haar
385

INFLUENCE OF NUCLEAR SHELLS ON THE DISTRIBUTION OF THE KINETIC ENERGY OF FRAGMENTS IN FISSION BY FAST NEUTRONS

A. N. PROTOPOPOV, I. A. BARANOV, Yu. A. SELITSKIĬ, and V. P. ÉĬSMONT

Submitted to JETP editor February 21, 1959

J. Exptl. Theoret. Phys. (U.S.S.R.) **36**, 1932-1933 (June, 1959)

A double ionization chamber was used to obtain data on the distribution of the total kinetic energy of the fragments in fission of U^{238} by 14.9-Mev neutrons. The measured values of the energy were corrected for the ionization defect. From the experimental half-widths of the distribution of the kinetic energy we subtracted the broadening due to the distribution of the charge, to the effect of recoil from the neutrons, to fluctuations of the number of evaporated neutrons, to the instrumental error, and to the averaging over the final interval of the mass ratio. The dependences thus obtained for the mean kinetic energy E and for the half-width ΔE of its distribution on the fragment mass ratio are shown in Fig. 1. For comparison, the same figure shows the distribution of the kinetic energy of the fragments in fission of U^{235} by 14.1-Mev neutrons[1] and the distribution of the dispersion calculated for this case.

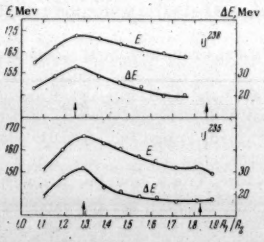

FIG. 1. Dependence of the total kinetic energy and its distribution half-width on the ratio of the fragment masses. The positions of the "magic" fragments are noted on the graph by vertical arrows.

It is seen that both E and ΔE have maximum values at a fragment mass ratio of $1.25 - 1.3$. The presence of a maximum on the curve for the dependence of the total kinetic energy on the mass ratio was noted earlier by Brunton and Hanna[2] in an investigation of the fission of U^{233} and U^{235} by thermal neutrons. Similar maxima in the kinetic-energy distribution are observed at different mass

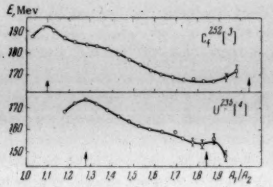

FIG. 2. Change in the total kinetic energy as a function of the ratio of the fragment masses. The curves were plotted from the experimental data of Fraser and Milton[3] and Stein.[4] The positions of the "magic" fragments are indicated by arrows.

ratios for all known cases of fission of heavy nuclei. Figure 2 shows the distributions of the kinetic energies in fission of U^{235} by thermal neutrons and in the spontaneous fission of Cf^{252}, obtained by measuring the time of flight. It is interesting to note that in all cases the kinetic energy has a maximum when the heavy fragment has a mass number close to 132, and probably, represents a nucleus with filled shells of 50 protons and 82 neutrons. In addition, there is a certain kink at a fragment mass ratio corresponding to a light fragment with mass number $82 - 84$, probably with a closed shell of 50 neutrons. A similar influence of closed shells is observed also in the variation of the energy dispersion (ΔE) with the fragment mass ratio, which we determined for U^{233} and U^{235} by processing the results of Brunton and Hanna.

It can be assumed that the foregoing features are connected with the influence of the degree of filling of the nuclear shells on the shape of the fragment during the instant of separation. Starting with this assumption, qualitative conclusions can be drawn concerning the character of the dependence of the neutron emission on the fragment mass. Indeed, one might think that a "magic" undeformed fragment should emit fewer neutrons than its mate, the "non-magic"* one, i.e., most neutrons should be emitted from the lighter fragment at small mass ratios and from the heavier one at large mass ratios. Such conclusions are in agreement with the data of Fraser and Milton for the fission of U^{233} by thermal neutrons[5] and the data of Whetstone[6] on spontaneous fission of Cf^{252}.

***It is assumed here that the degree of deformation of the fragments during the instant of separation determines, essentially, the excitation after separation.**

[1] J. S. Wahl, Phys. Rev. **95**, 226 (1954).

[2] D. C. Brunton and G. H. Hanna, Phys. Rev. **75**, 990 (1949).

[3] J. S. Fraser and J. D. C. Milton, Second UN Intern. Conference on the Peaceful Uses of Atomic Energy, Canada, April 1958 (A/conf. 15/P/199).
[4] W. R. Stein, Phys. Rev. **108**, 94 (1957).
[5] J. S. Fraser and J. D. C. Milton, Phys. Rev. **93**, 818 (1954).
[6] S. L. Whetstone, Bull. Am. Phys. Soc. **2**, 3 (1958).

Translated by J. G. Adashko
386

INTERACTION OF ACCELERATED NITROGEN NUCLEI WITH BISMUTH

V. A. KARNAUKHOV

Institute of Atomic Energy, Academy of Sciences, U.S.S.R.

Submitted to JETP editor February 23, 1959

J. Exptl. Theoret. Phys. (U.S.S.R.) **36**, 1933-1935 (June, 1959)

We have investigated reactions that lead to the production of α-active isotopes upon interaction of accelerated N^{14} nuclei with bismuth. A stack of ten layers of bismuth (~ 0.8 mg/cm^2 each), deposited on thin nickel foils ($\sim 1.5\,\mu$) was exposed in the internal beam of the cyclotron to nitrogen ions with energies of ~ 102 Mev. The foils were attached to a special sampler in front of the current collector, to control the ion current to the target during the irradiation process. The nitrogen ions lost approximately 3 Mev upon passing from one layer of bismuth to another. The results of Oganesyan[1] were used to calculate the deceleration of the ions. To avoid overheating the target, the current did not exceed $0.01\,\mu$a.

Using a luminescent α-particle counter insensitive to the β and γ background, we investigated in detail the decay of the activity induced in the bismuth layers. The α-particle energy was measured with an ionization chamber (emitters 1 and 2) and a photoemulsion (emitter 3). We were thus able to establish the production of the α emitters, the characteristics of which are indicated in the table (emitters 4 and 5 were not investigated in detail).

α-emitter	1	2	3	4	5
T	15±2 hr	25±2 min	150 days	2—3 min	5—7 hr
E_α, Mev	5.7±0.2 7.3±0.2	6.1±0.2	5.2±0.3		

The first α activity must be quite unambiguously ascribed to Rn^{211} ($T = 16$ hours, $E_\alpha = 5.82$ Mev) and to the At^{211} ($T = 7.5$ hours, $E_\alpha = 5.89$ Mev) and Po^{211} ($T = 0.5$ sec, $E_\alpha = 7.43$ Mev) which are in equilibrium with it. Emitter 2 is obviously also a radon isotope — Rn^{212} ($T = 23$ min, $E_\alpha = 6.23$ Mev). It must noted that Rn^{209}, Rn^{208}, and Fr^{212} do not differ greatly from Rn^{212} in the half-lives and energies of the α particles. However, estimates show that the contribution of these isotopes into the observed activities is small. The Rn^{209} may be the result of α-decay of Ra^{213} ($T = 2.7$ min), which is the product of the reactions (N, 6n) and (N, α6n). From the yield of the α emitter with half-life of 2 — 3 minutes we can surmise that, for nitrogen ions with energy 100-Mev (which, obviously, corresponds to the maximum probability of the reaction with emission of six neutrons), Rn^{209} can cause not more than 5 or 10% of the observed activity with a half-life of 25 minutes. The contribution of Rn^{208} and Fr^{212} should be even less, since reactions with emission of not less than seven nucleons would be necessary for their appearance.

The dependence of the cross sections for the production of Rn^{212} and Rn^{211} on the energy of the nitrogen ions is shown in the diagram. The

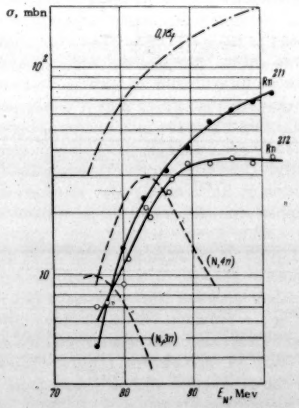

relative course of the curves is determined, essentially, by statistical errors, which do not exceed 10%. The inaccuracy in determining the absolute value of the cross sections is on the order of 50%. It is connected with the errors that arise

in the measurement of the thickness of the bismuth layer, of the intensity of the beam, and of the efficiency of the α-particle counter. The diagram indicates also the cross section σ_f for the fission of the compound nucleus Th^{223}, which is almost identical with the cross section for its production.[2]

The isotopes Rn^{212} and Rn^{211} may result from α-decay of the reaction products, with emission of neutrons only, (N, 3n) and (N, 4n), and may also be due to reactions with emission of α particles, (N, xα3n) and (N, xα4n), where x = 1 or 2. The dependence of the cross sections for the production of Rn^{212} and Rn^{211} on the energy of the nitrogen nuclei makes it possible to ascertain which one of these reactions is the more probable. The diagram shows (dotted) the calculated curves for the cross sections of the reactions (N, 3n) and (N, 4n). The cross sections are given in arbitrary units. It has been assumed in the calculations that $\sigma_{xn}(E) \sim \sigma_c(E) w_{xn}$, where $\sigma_c(E)$ is the cross section for the production of a compound nucleus by nitrogen ions with energy E, while w_{xn} is the probability of evaporation of x neutrons at a corresponding excitation energy of the compound nucleus.[3] Comparison of the experimental and calculated curves leads to the conclusion that the reactions (N, 3n) and (N, 4n) can give a decisive contribution (> 50%) to the yield of Rn^{212} and Rn^{211} only at nitrogen-ion energies less than 78 and 86 Mev, respectively. At large energies the yield of this isotope is obviously determined by the reactions of type (N, xα3n) and (N, xα4n). The possible shift of the position of the maxima for reactions with emission of only neutrons by 2 — 3 Mev towards the side of higher energies, which is due to the angular momentum of the compound nucleus,[4] does not change the conclusions substantially. Considering the cross section for the production of Rn^{211} for 83-Mev nitrogen ions to be the upper limit for the cross section of the reaction (N, 4n), we can estimate the value of the ratio Γ_n/Γ_f for the isotopes $Th^{223-219}$, namely $\Gamma_n/\Gamma_f < 0.8$.

The isotopes with half life ~ 150 days is obviously Po^{210} (T = 140 days, E = 3.53 Mev), which is produced by various reactions such as (N, xαn), (N, p4n), (N, N^{13}), and several others. The cross section for the production of Po^{210} increases with increasing energy, and reaches $\sim 10^{-25}$ cm^2 at E = 100 Mev.

The author expresses deep gratitude to Professor G. N. Flerov for useful discussions.

[1] Yu. Ts. Oganesyan, J. Exptl. Theoret. Phys. (U.S.S.R.) **36**, 936 (1959), Soviet Phys. JETP **9**, 661 (1959).

[2] S. M. Polikanov and V. A. Druin, J. Exptl. Theoret. Phys. (U.S.S.R.) **36**, 744 (1959), Soviet Phys. JETP **9**, 522 (1959).

[3] T. D. Jacksón, Canad. J. Phys. **34**, 767 (1956).

[4] Karamyan, Gerlit, and Myasoedov, J. Exptl. Theoret. Phys. (U.S.S.R.) **36**, 621 (1959), Soviet Phys. JETP **9**, 431 (1959).

Translated by J. G. Adashko
387

MAGNETIC MOMENTS AND CURIE POINTS OF FERRITES OF THE Cu-Cd *SYSTEM*

N. Z. MIRYASOV and L. G. KOLOMIN

Moscow State University

Submitted to JETP editor February 27, 1959

J. Exptl. Theoret. Phys. (U.S.S.R.) **36**, 1935-1936 (June, 1959)

We have studied the temperature dependence of the specific saturation magnetization σ_S and have determined the magnetic moments of solid-solution ferrites of the system $Cd_xCu_{1-x}Fe_2O_4$, in which the Cd^{+2} concentration was increased beyond 10% of the total number of bivalent ions. As far as we know, no one has previously carried out such studies of this system.

The specific magnetization σ was measured in the field interval 6000 to 13,000 oe, at six different values of temperature in the interval 78 to 293° K. The saturation magnetization at each temperature was determined by extrapolation to $H = \infty$ of the relation $\sigma = \sigma_S(1 - a/H)$. It was established that for the specimens rich in copper ions, and possessing the higher Curie points, the results of the measurements are best summarized by the formula $\sigma_S = \sigma_0(1 - \alpha T^{3/2})$. For the specimens rich in cadmium ions, with the lower Curie points, the relation $\sigma_S = \sigma_0(1 - \alpha T^2)$ holds. The absolute saturation magnetization σ_0 at each composition was determined by linear extrapolation to 0° K of the appropriate relation between σ_S and $T^{3/2}$ or T^2.

The curve in Fig. 1 shows the dependence of the magnetic moment, expressed in Bohr magnetons per "molecule" of the solid solution, on its composition. The dashed line shows the values of the magnetic moment calculated theoretically by assuming complete antiparallelism of the spins of the A and B sublattices. The deviations of the experimental data on the magnetic moment from the theo-

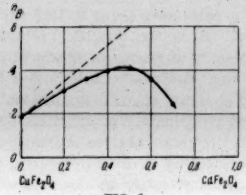

FIG. 1

retical values find an explanation in modern theory. In particular, Gorter[1] obtained similar moment curves for a number of other systems of mixed ferrites $MeFe_2O_4$-$ZnFe_2O_4$ and provided an explanation of them from the standpoint of Néel's theory; his explanation is also completely applicable to our system of ferrites.

It is known that the magnetic moment of copper ferrite, $CuFe_2O_4$, depends on the rate of cooling of the specimen. Néel explained this on the basis that the concentration of copper ions on A sites is a function of the temperature of the specimen. Rapid cooling to room temperature leads to retention of the ion distribution that existed at the quench temperature. This produces a higher percent noninversion of the ferrite and increases its magnetic moment. The cooling conditions for our $CuFe_2O_4$ specimen apparently were not conducive to attainment of a stable equilibrium in the arrangement of ions in the lattice, since the magnetic moment of the specimen was abnormally large, being equal to 1.92 Bohr magnetons. To confirm this, we subjected our specimen to an annealing for 100 hours at t = 370°C. As a result of this annealing its magnetic moment decreased to 1.28 ± 0.02 Bohr magnetons which agrees well with Gorter's data.[1]

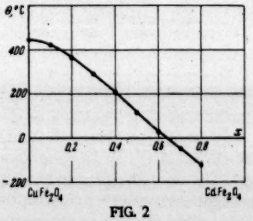

FIG. 2

The curve in Fig. 2 shows the Curie temperature Θ as a function of composition. A similar behavior of the Curie-temperature curve of this ferrite system was obtained earlier by Smolenskiĭ.[2,3] However, for our specimen of composition $CuFe_2O_4$, Θ = 450 ± 3°C, in agreement with the standard value of Θ for this composition, whereas according to Smolenskiĭ $\Theta \sim 425$°C. Accordingly our curve is higher in the neighborhood of the origin.

[1] E. W. Gorter, Usp. Fiz. Nauk **57**, 279 (1955) [translated from Phil. Res. Rep. **9**, 295, 321, 403 (1954)].

[2] G. A. Smolenskiĭ, Dokl. Akad. Nauk SSSR **78**, 921 (1951).

[3] G. A. Smolenskiĭ, Izv. Akad. Nauk SSSR, Ser. Fiz. **16**, 728 (1952).

Translated by W. F. Brown, Jr.
388

POLARIZATION OF PROTONS IN SCATTERING BY C^{12}

S. A. BALDIN and V. I. MAN' KO

Submitted to JETP editor February 27, 1959

J. Exptl. Theoret. Phys. (U.S.S.R.) **36**, 1937 (June, 1959)

ANALYSIS of data on the elastic scattering of protons makes it possible to obtain sometimes sufficiently complete information on the position and characteristics of the levels of atomic nuclei. One such case is the scattering by C^{12}, at which the lower levels of N^{13} are excited.

Reich et al.[1] investigated elastic scattering of protons by C^{12} in the interval from 1.5 – 5.5 Mev and carried out a sufficiently complete phase analysis, whereby the following levels of N^{13} were identified: 1.698 ($\frac{1}{2}^-$); 1.748 ($\frac{5}{2}^+$); 4.808 ($\frac{5}{2}^+$), and 5.37 ($\frac{3}{2}^+$).

Measurement of the proton polarization due to scattering can supplement considerably our information on the levels of a given nucleus. Using the phase analysis given in reference 1, we have calculated the dependence of the polarization and of the cross section on the energy in p-C^{12} scattering in the energy interval 2.5 – 4.5 Mev at scattering angles 0 – 180° c.m.s. The principal results are shown in a diagram: The curves represent the energy dependence of the polarization at several scattering angles. The values of the polarization (particularly in the interval from 30 – 90°) are quite sensitive to the values of the D phases: for example, a 5° change in the $D_{3/2}$ phase at 4.5 Mev changes the value of the polarization in the forward angles by a factor of 2 or 3, while the cross

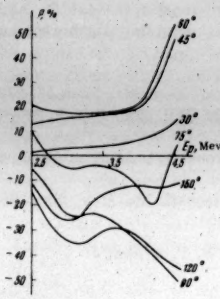

sections change by merely 5 or 10%. Thus, a study of the polarization makes possible a much more accurate phase analysis and thereby establishes more definitely the parameters of the levels of N^{13}. From the foregoing data it is evident that the polarization becomes considerable in this energy interval. Carbon can therefore be used to obtain and to analyze polarized proton beams with energies 2 – 5 Mev, which in many cases is more convenient than the use of He^4.

[1] Reich, Phillips, and Russell, Phys. Rev. **104**, 193 (1956).

Translated by J. G. Adashko
389

SCATTERING OF PROTONS ON TRITONS AT SMALL ENERGIES

Yu. G. BALASHKO, I. Ya. BARIT, and Yu. A. GONCHAROV*

P. N. Lebedev Physics Institute, Academy of Sciences, U.S.S.R.

Submitted to JETP editor February 27, 1959

J. Exptl. Theoret. Phys. (U.S.S.R.) **36**, 1937-1939 (June, 1959)

THE existence of a level in He^4 with excitation energy about 20 Mev is indicated by a series of experiments. Thus, a phase-shift analysis[1] of p-T scattering at $E_p = 1$ to 3.5 Mev indicates a resonance behavior of the phase in the $^1S_0$ state. The large magnitude of the cross section for the $He^3(n, p)T$ reaction, and its deviation[2] from the 1/v law in the domain $E_n < 25$ kev can also be explained by a resonance level in He^4 with characteristics 0^+. However, this level is not revealed in the study of reactions in which He^4 appears as the final nucleus.[3] On the other hand, a phase-shift analysis of p-T scattering[1] cannot be considered as undoubted proof of the existence of the level in He^4, in so far as the analysis is carried out neglecting the reaction $T(p, n)He^3$ and making use of simplifying assumptions on the phase. In this situation, considerable interest attaches to the measurement of the cross-section for p-T scattering at energies below the threshold for the reaction $T(p, n)He^3$, where p-scattering plays a smaller role also. Since measurements in this domain are not sufficiently reliable or extensive, we have started to measure the p-T scattering cross section at low energies.

The features of the method employed have been noted previously.[4] The target chamber was filled with a mixture of hydrogen and deuterium, to measure the incident beam with respect to the outgoing α-particles from the reaction $T(d, n)\alpha$. The cross section for the elastic scattering of tritons by hydrogen was measured at bombarding energies below 530 kev for three angles.

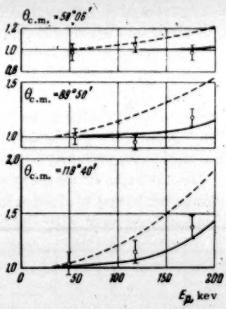

The results are shown in the figure (ordinate: ratio of the measured cross section to the cross section for scattering by a Coulomb field). Within experimental error, they can be described by pure s-scattering. The contributions to the scattering from higher angular momenta are seen to be insignificant from a calculation of potential scattering for p-waves. For an interaction radius $a = 3 \times 10^{-13}$, calculations indicate that the contributions of the p-phase to the scattering cross section in the energy interval under consideration does not exceed 1% (for $E_p = 200$ kev and $\theta = 120°$). Analogous results can also be obtained if we extrapolate the p-phases, obtained by Frank and

Gammel,[1] to the energy domain below 1 Mev, using the theoretical energy dependence of the p-phases for potential scattering. In this case the maximum contribution of the p-phase to the scattering cross section does not exceed 3%.

A phase-shift analysis of the measured results was carried out, assuming pure s-scattering, for 176.7 and 118 kev protons. The following values of the phases were obtained (two solutions):

$$E_p = 176.7 \text{ kev}$$

$$\text{I}\begin{cases}\delta_0^1 = 6^\circ \pm 5^\circ \\ \delta_0^0 = -15^\circ \pm 7^\circ\end{cases} \qquad \text{II}\begin{cases}\delta_0^1 = -5^\circ \pm 1^\circ \\ \delta_0^0 = 17^\circ \pm 12^\circ\end{cases}$$

$$E_p = 118 \text{ kev}$$

$$\text{I}\begin{cases}\delta_0^1 = 3^\circ \pm 3^\circ \\ \delta_0^0 = -8^\circ \pm 8^\circ\end{cases} \qquad \text{II}\begin{cases}\delta_0^1 = -2^\circ \pm 2^\circ \\ \delta_0^0 = 7^\circ \pm 8^\circ\end{cases}$$

A characteristic feature of these solutions is that the singlet and triplet phases are opposite in sign. The second of these agrees with the values of the phases obtained by extrapolating the data of Frank and Gammel to the domain of small energies and with the deductions of reference 2 on the existence, in this energy domain, of a resonance level with the momentum I = 0.

Curves for the scattering cross section calculated according to reference 1 are also drawn in the figures (continuous curve). The triplet S-phase, extrapolated to the domain of small energies, was taken to be the potential scattering phase, while the singlet S-phase was calculated using the level parameters deduced in reference 1. The p-phase was neglected. The same figure shows also curves (dotted) calculated on the assumption of pure potential scattering in both spin states. The interaction radius was taken to be $a = 3 \times 10^{-13}$ cm. Experimental values for the scattering cross section, as seen from the figure, are in good agreement with the assumption of resonance scattering in the $^1S_0$ state and not in agreement with the assumption of pure potential scattering in both spin states.

Thus, the results of the present work indicate that the scattering in the domain of low energies is described by the phases of reference 1. The scattering cannot be considered as pure potential, one of the s-phases must be positive. According to references 1 and 2 the singlet phase must be positive.

The authors express their thanks to Professors I. M. Frank and F. L. Shapiro for suggesting the problem and discussing the results of the work.

*Deceased.

[1] R. M. Frank and J. L. Gammel, Phys. Rev. **99**, 1406 (1955).

[2] Bergman, Isakov, Popov, and Shapiro, J. Exptl. Theoret. Phys. (U.S.S.R.) **33**, 9 (1957), Soviet Phys. JETP **6**, 6 (1958). тр. Московской конференции по ядерным реакциям, 1957 (Trans. Moscow Conference on Nuclear Reactions, 1957), in press.

[3] J. Benveniste and B. Cork, Phys. Rev. **89**, 422 (1953); R. M. Eisberg, Phys. Rev. **102**, 1104 (1956); J. C. Allred, Phys. Rev. **84**, 694 (1951).

[4] Yu. G. Balashko and I. Ya. Barit, J. Exptl. Theoret. Phys. (U.S.S.R.) **34**, 1034 (1958); Soviet Phys. JETP **7**, 715 (1958).

Translated by Kenneth Smith
390

CERENKOV RADIATION OF A MAGNETIC DIPOLE IN AN ANISOTROPIC MEDIUM

G. A. BEGIASHVILI and É. V. GEDALIN

Tbilisi State University, Institute of Physics, Academy of Sciences, Georgian S.S.R.

Submitted to JETP editor February 27, 1959

J. Exptl. Theoret. Phys. (U.S.S.R.) **36**, 1939-1940 (June, 1959)

THE Cerenkov radiation of a point magnetic dipole in an isotropic medium has been considered by a number of authors.[1-5] In the present note we consider the Cerenkov radiation of a point magnetic dipole in anisotropic and gyrotropic media.

Let a transparent medium be characterized by the dielectric permativity tensor and the magnetic susceptibility tensor

$$\varepsilon_{ik} = \begin{pmatrix} \varepsilon_1, & -i\varepsilon_2, & 0 \\ i\varepsilon_2, & \varepsilon_1, & 0 \\ 0, & 0, & \varepsilon_3 \end{pmatrix} \qquad \mu_{ik} = \begin{pmatrix} \mu_1, & -i\mu_2, & 0 \\ i\mu_2, & \mu_1, & 0 \\ 0, & 0, & \mu_3 \end{pmatrix}.$$

If the dipole moves along the optical axis (with velocity v) and the magnetic moment μ_0 points in the direction of motion the energy losses due to Cerenkov radiation are given by the expression

$$-\frac{d\mathcal{E}}{dz} = \frac{\mu_0^2}{v^4}\int_\Gamma \frac{\omega^3 d\omega}{\varepsilon_1^2 a^2 \varepsilon_3^2 \beta^4} \{[a\varepsilon_1 n_1^2\beta^2 - \varepsilon_1\varepsilon_3\beta^2 - a(\varepsilon_1 - \varepsilon_3)]^2 g$$
$$- [\varepsilon_2 a - \varepsilon_1 b][2\beta^2\varepsilon_1 abn_1^2 - \beta^2\varepsilon_2(\varepsilon_1 b + \varepsilon_3 a) - 2\varepsilon_1 ab$$
$$+ 2\varepsilon_3 ab]\}(\beta^2 n_1^2 - 1)[n_1^2 - n_2^2]^{-2}$$
$$+ \frac{\mu_0^2}{v^4}\int_\Pi \frac{\omega^3 d\omega}{\varepsilon_1^2 a^2 b^2 \beta^4} \{[a\varepsilon_1 n_2^2\beta^2 - \varepsilon_1\varepsilon_3\beta^2 - a(\varepsilon_1 - \varepsilon_3)]^2 g$$
$$- [\varepsilon_2 a - \varepsilon_1 b][2\beta^2\varepsilon_1 abn_2^2 - \beta^2\varepsilon_2(\varepsilon_1 b + \varepsilon_3 a) - 2\varepsilon_1 ab$$
$$+ 2\varepsilon_3 ab]\}(\beta^2 n_2^2 - 1)[n_2^2 - n_1^2]^{-2},$$

where

$$n_{1,2}^2 = \{(ag - a^2)\varepsilon_1 + ag(\varepsilon_1 - \varepsilon_3) + b^2\varepsilon_1 + (\varepsilon_1^2 a - \varepsilon_2^2 a + \varepsilon_1\varepsilon_3 g)\beta^2 \pm [(\varepsilon_1^2 a - \varepsilon_2^2 a - \varepsilon_1\varepsilon_3 g)^2\beta^4 - 2a\varepsilon_1(\varepsilon_3 g - \varepsilon_1 a)^2\beta^2 + 2a^2\varepsilon_2^2(\varepsilon_1 a + \varepsilon_3 g)\beta^2 + 2b^2\varepsilon_1(a\varepsilon_1^2 - a\varepsilon_2^2 + g\varepsilon_1\varepsilon_3)\beta^2 - 8abg\varepsilon_1\varepsilon_2\varepsilon_3\beta^2 + (g\varepsilon_3 - \varepsilon_1 a)^2 a^2 + b^2\varepsilon_1(b^2\varepsilon_1 - 2a^2\varepsilon_1 + 2ag\varepsilon_3)]^{1/2}\} / 2\varepsilon_1 ag\beta^2,$$

$a = \mu_1 / (\mu_1^2 - \mu_2^2)$, $b = \mu_2 / (\mu_2^2 - \mu_1^2)$, $g = 1 / \mu_3$.

The regions of integration are determined by the following inequalities (cf. reference 3):

$$\text{I: } \beta^2 n_m^2 > \beta^2 n_1^2 > 1, \quad \text{II: } \beta^2 n_m^2 > \beta^2 n_2^2 > 1.$$

In the case of a non-gyrotropic uniaxial crystal ($\epsilon_2 = b = 0$) we have

$$-d\mathcal{E}/dz = \mu_0^2 v^{-4} \int_{\mu_3(\varepsilon_1\mu_1\beta^2 - 1)/\mu_1 > 1} \omega^3 d\omega \cdot \mu_3^2 (\varepsilon_1\mu_1\beta^2 - 1) \cdot \mu_1.$$

From the above it is apparent that the radiation intensity for an anisotropic dielectric ($\mu_1 = \mu_3 = 1$) differs from an isotropic dielectric only in that $\epsilon \to \epsilon_1$. In this case, in general ϵ_3 does not appear in the final expression. The formula for the isotropic case coincides with the well known expression obtained by Frank[1] (cf. also reference 4). It should be noted that the results which have been obtained apply for Cerenkov radiation of a small closed current loop. In this case by μ_0 we are to understand the magnetic moment associated with the current loop.

The author is indebted to N. M. Polievktov-Nikoladze for his interest in this work.

[1] I. M. Frank, Сб. Памяти С. И. Вавилова (Vavilov Memorial) U.S.S.R. Acad. Sci. Press, p. 172 1952.

[2] V. L. Ginzburg, ibid., p. 193.

[3] B. M. Bolotovskii, Usp. Fiz. Nauk, **62**, 201 (1957).

[4] Yu. M. Loskutov and A. B. Kukanov, J. Exptl. Theoret. Phys. (U.S.S.R.) **34**, 477 (1958), Soviet Phys. JETP **7**, 328 (1958).

[5] N. L. Balasz, Phys. Rev. **104**, 1220 (1956).

Translated by H. Lashinsky
391

RELATION BETWEEN THE GRAVITATIONAL CONSTANT, THE CHARGE TO MASS RATIO OF THE ELECTRON, AND THE FINE STRUCTURE CONSTANT

I. G. IVANTER

Institute of Scientific Information, Academy of Sciences, U.S.S.R.

Submitted to JETP editor March 2, 1959

J. Exptl. Theoret. Phys. (U.S.S.R.) **36**, 1940 (June, 1959)

THE following numerical relation exists between the gravitational constant $G = 6.673 \times 10^{-8}\ g^{-1}\ cm^3\ sec^{-2}$, the electron mass m, the electron charge e, and the fine structure constant $\alpha = e^2/\hbar c = (137.0377 \pm 0.0016)^{-1}$

$$\frac{1}{G}\left(\frac{e}{m}\right)^2 = \left(\frac{4\pi}{3}\right)^{\frac{1}{2}} e^{2/2\alpha^2}.$$

This relation is extremely sensitive to the value of the fine structure constant; nevertheless, the numerical relation holds to an accuracy of 1%.

It may be assumed that this simple relation is no accident.

Translated by A. M. Bincer
392

SATURATION IN A HYPERON SYSTEM

V. A. FILIMONOV

Institute for Nuclear Physics, Electronics, and Automation, Tomsk Polytechnic Institute

Submitted to JETP editor March 5, 1959

J. Exptl. Theoret. Phys. (U.S.S.R.) **36**, 1941-1942 (June, 1959).

THE phenomenon of saturation is a characteristic property of a system of nucleons. At the present time it is believed that saturation is due to certain attributes of two-body nucleon forces — namely the repulsion at short distances and the exchange character of some of the forces. The main features of contemporary phenomenological nucleon-nucleon potential are deduced from meson theory. Thus repulsion at short distances is related to the existence of the function $\delta(\mathbf{r})$ in the second-order interaction potential of pseudoscalar meson theory. The energy of a system of nucleons depends strongly on the radius of the repulsive core and on the admixture of exchange forces. A decrease in the radius of the repulsive core and in the amount of exchange forces leads to a considerable increase in the binding energy of a system of nucleons.[1]

According to present-day ideas about hyperons

the forces between them are of the same order of magnitude as nucleon-nucleon forces. However the details of the mechanism responsible for hyperon-hyperon forces may be different from those involved in nucleon-nucleon interactions. Thus, for example, second order forces arising from the exchange of a single π or K meson between two Λ^0 particles are forbidden by isotopic invariance of strong interactions. In these cases the forces may arise in fourth order as a result of the exchange of two π or K mesons:

$$\Lambda + \Lambda \to \Sigma + \pi + \pi + \Sigma \to \Lambda + \Lambda,$$
$$\Lambda + \Lambda \to N + K + K + N \to \Lambda + \Lambda,$$
$$\Lambda + \Lambda \to \Xi + K + K + \Xi \to \Lambda + \Lambda$$

The main part of these forces has a non-exchange character. The absence of forces due to the exchange of a single particle eliminates the theoretical basis for the introduction of repulsion at short distances as is done in the nucleon-nucleon case.

This different character of hyperon-hyperon forces should affect the behavior of a system of many hyperons. In particular it is possible that conditions may exist favorable to the formation of a hyperon system with a large mass defect which would be stable against transformation into the proton-neutron state. For a system of Λ particles and nucleons the stability condition against transition to the nucleon state has the form

$$L(m_\Lambda - m_N) + B(A + L) + T_N + T_\Lambda + U < 0, \quad (1)$$

where A and L are the number of nucleons and Λ partieles; m_N, T_N, m_Λ, T_Λ are the masses and kinetic energies of the nucleons and Λ particles respectively; B is the absolute value of the binding energy per nucleon in nuclear matter; and U is the potential energy due to the interaction between the particles.

To estimate the conditions necessary for the fulfillment of the inequality (1), a calculation of binding energy of a system of nucleons and Λ particles was carried out under certain assumptions about the forces. It was assumed that a Wigner-type short range force acts between two Λ hyperons and between a Λ hyperon and a nucleon which gives rise to zero binding energy for the $\Lambda\Lambda$ and ΛN systems. In the interaction of nucleons with each other only a repulsion at $r_c = 0.4$ f was taken into account. The nucleons and hyperons were treated as a degenerate Fermi gas. Under these assumptions it was found that when the Λ particles are distributed with constant density inside a sphere of radius $R = r_0 L^{1/3}$, condition (1) is satisfied for $r_0 \approx 0.9$ f. Here the minimum energy is obtained if the nucleons are distributed inside a sphere of the same radius and the ratio of nucleons to Λ particles is $A/L \approx 1.6$ f.

When condition (1) is satisfied the proton-neutron state will be metastable against a transition to the hyperon-nucleon state.

At present only incomplete information exists about the hyperon-nucleon interaction and none about the hyperon-hyperon forces. Neither can meson theory given an unambiguous answer to this question. Therefore it is not possible to draw any definite conclusions about the behavior of a system of many heavy particles or about the saturation properties of such a system; however neither should one discount the possibility that a stable baryon system other than the proton-neutron state might exist.

[1] K. A. Brueckner, Revs. Modern Phys. **30**, 561 (1958).

Translated by A. M. Bincer
393

DYNAMICAL MODEL IN THE THEORY OF THE BROWNIAN MOTION

V. B. MAGALINSKIĬ

Moscow State University

Submitted to JETP editor March 7, 1959

J. Exptl. Theoret. Phys. (U.S.S.R.) **36**, 1942-1944 (June, 1959)

LET us consider a dynamical model that has been discussed repeatedly[1-3] in connection with the problem of the reciprocal relations of dynamical processes and statistical laws: an oscillator with mass m and frequency ω_0 linearly coupled with a set of a large number of independent harmonic oscillators with frequencies ω_k ($k = 1, 2, \ldots, N$; $N \gg 1$). In the present note we give a simple derivation of some general relations in the theory of the Brownian motion on the basis of this model.

The Hamiltonian of the system in question is written in the form

$$H = \frac{p^2}{2m} + \frac{1}{2} m\omega_0^2 q^2 + \frac{1}{2} \sum_k (p_k^2 + \omega_k^2 q_k^2) + gq \sum_k \alpha_k q_k, \quad (1)$$

where q and p are the coordinate and momentum of the oscillator with frequency ω_0, q_k and p_k

are those of the k-th oscillator of the medium, and $g\alpha_k$ is the coefficient of the coupling with the k-th oscillator.

Solving the system of Hamilton's equations corresponding to Eq. (1), we get the equation of motion for q:

$$m\ddot{q} + m\omega_0^2 q + \int_0^t K(t-\tau)\, q(\tau)\, d\tau - qK(0) + q_0 K(t) = f(t), \tag{2}$$

where

$$K(t) = g^2 \sum_k \alpha_k^2 \omega_k^{-2} \cos \omega_k t, \tag{3}$$

$$f(t) = -g \sum_k \alpha_k \left(q_{k0} \cos \omega_k t + \frac{p_{k0}}{\omega_k} \sin \omega_k t \right), \tag{4}$$

and q_{k_0} and p_{k_0} are the initial values of the canonical variables.

It can be seen from Eq. (2) that the force caused by the interaction of the particle with the medium falls in a natural way into two parts: the random force (4) (the "impulses"), which does not depend on the state of the particle, and the dissipative force, which is connected with the position of the particle by a functional relation of the type of a persistent action.

Let us consider the correlation of the "impulses," $\varkappa(t-\tau) = \overline{f(t) f(\tau)}$, where the averaging is over all the microscopic states of the oscillators of the medium. If the medium is a thermostat, i.e., if these states are canonically distributed, we have

$$\overline{p_{i0}\, p_{k0}} = \delta_{ik} E(\omega_k, \Theta),$$
$$q_{i0}\, q_{k0} = \delta_{ik} E(\omega_k, \Theta)\, \omega_k^{-2}, \quad \overline{q_{i0}\, p_{k0}} = 0,$$

where

$$E(\omega_k, \Theta) = {}^1/_2 \hbar\omega_k \coth(\hbar\omega_k / 2\Theta)$$

is the average energy of the k-th oscillator at temperature Θ. In this case it is obvious that

$$\varkappa(t-\tau) = g^2 \sum_k \alpha_k^2 \omega_k^{-2} E(\omega_k, \Theta) \cos \omega_k (t-\tau). \tag{5}$$

Assuming the frequency spectrum of the oscillators of the medium sufficiently dense and replacing the sums by integrals by the rule

$$\sum_k F_k = A \int_0^\infty F(\omega)\, \omega^2 d\omega,$$

we get

$$K(t) = Ag^2 \int_0^\infty \alpha^2(\omega) \cos \omega t\, d\omega, \tag{3'}$$

$$\varkappa(t) = Ag^2 \int_0^\infty \alpha^2(\omega)\, E(\omega, \Theta) \cos \omega t\, d\omega. \tag{5'}$$

Let us find the macroscopic physical meaning of the coefficients $\alpha(\omega)$. We introduce the impedance $Z(\omega)$ of the system by the relation

$$\Phi(\omega) = Z(\omega)\, \dot{q}_\omega, \tag{6}$$

where $\Phi(\omega)$ and $\dot{q}(\omega)$ are the Fourier components of the dissipative force

$$\Phi(t) = \int_0^t K(t-\tau)\, \dot{q}(\tau)\, d\tau$$

and the velocity $\dot{q}(t)$, respectively. From the definition (6) and Eq. (3') it at once follows that

$$K(t) = \frac{2}{\pi} \int_0^\infty R(\omega) \cos \omega t\, d\omega, \quad \alpha^2(\omega) = 2R(\omega)/\pi A g^2, \tag{7}$$

where $R(\omega) = \mathrm{Re}\, Z(\omega)$.

Substituting Eq. (7) in Eq. (3') we get, finally, the general formula that connects the correlation of the fluctuation force with the dissipative properties of the system:

$$\varkappa(t) = \frac{2}{\pi} \int_0^\infty R(\omega)\, E(\omega, \Theta) \cos \omega t\, d\omega. \tag{8}$$

The relation (8) known as the quantum Nyquist formula, was first obtained by Callen and Welton[4] by an application of quantum-mechanical perturbation theory to calculate the energy exchange between a linear system with prescribed dissapative properties ($Z(\omega)$) and a thermostatic oven.

In conclusion I regard it as my duty to express my gratitude to Professor Ya. P. Terletskiĭ for his interest in this work.

[1] N. N. Bogolyubov, О некоторых статистических методах в математической физике (On Some Statistical Methods in Mathematical Physics), Ukr. S.S.R. Acad. Sci. Press, 1945

[2] Ya. P. Terletskiĭ, Динамические и статистические законы физики (Dynamical and Statistical Laws of Physics), Moscow State University Press, 1949.

[3] M. Toda, J. Phys. Soc. Japan **13**, 1266 (1958).

[4] H. B. Callen and T. A. Welton, Phys. Rev. **83**, 34 (1951).

Translated by W. H. Furry
394

NUCLEAR POLARIZATION OF WEAKLY-MAGNETIC ELEMENTS INTRODUCED INTO A FERROMAGNET

B. N. SAMOĬLOV, V. V. SKLYAREVSKIĬ and E. P. STEPANOV

Submitted to JETP editor March 10, 1959

J. Exptl. Theoret. Phys. (U.S.S.R.) **36**, 1944-1946 (June, 1959)

WE have already described[1] the polarization of Au^{198} nuclei in an Au-Fe alloy. In the present communication data are presented on the nuclear polarization of Sb^{122} and In^{114m} in weak solutions of antimony and indium in iron.

The apparatus for cooling the magnetized specimens differed from the previous one in that an electromagnet was used instead of a constant magnetic field. This magnet was placed inside the helium Dewar and enabled us to obtain in the specimen position a field of up to 2,000 oersteds which was 2 – 2.5 times larger than the field used in the experiments with Au^{198}. The error due to incomplete magnetization of the ferromagnetic specimen was thus reduced. Otherwise the method of cooling the specimen and measuring the γ-ray anisotropy were the same as in the experiments with Au^{198}.

A specimen of an Sb-Fe alloy (0.6% Sb by weight) was irradiated by thermal neutrons in a reactor. The activity of the Sb^{122} nuclei formed in the specimen amounted, at the time of the experiment, to about 4 μc. In the figure results are presented of one of the experiments to measure the anisotropy of the 566-kev γ rays ($2^+ \to 0^+$ transition) emitted after the β decay of Sb^{122} ($2^- \to 2^+$ transition). The experimental points show the variation with time after salt demagnetization, of the γ-ray counting rates at detectors disposed along ($\theta = 0°$) and across ($\theta = 90°$) the direction of the specimen magnetizing field. These

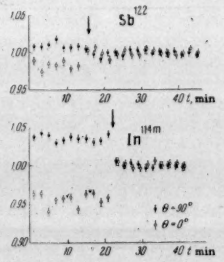

rates were normalized to the counting rates after the specimen was heated up. In the interval from five minutes to fifteen minutes the temperature changed from 0.025 to 0.035° K. The specimen was heated by increasing the amplitude of the alternating magnetic field used to measure the magnetic temperature. The moment at which heat was applied is shown in the figure by an arrow. Assuming that ten minutes after demagnetization the specimen had taken up the temperature of the salt (0.03° K), we obtained for the value of γ-ray anisotropy at this temperature $\epsilon = 2.5\%$ ($\epsilon = 1 - N(0°)/N(90°)$), where $N(\theta)$ is the number of counts for the detector at angle θ. From this value of ϵ, using the formulae of Tolhoek and Cox,[2] we calculated the polarization f_1 of Sb^{122} nuclei and the effective magnetic field H_n at the antimony nucleus in the lattice of the alloy. It appeared that $f_1 \approx 25\%$ and $H_n \approx 1.9 \times 10^5$ oersted. For the calculations we took the magnetic moment of the Sb^{122} nucleus as equal to 1.9 nuclear magnetons.[3]

A specimen of In-Fe alloy (0.5% In by weight) was produced by alloying metallic indium – previously irradiated in a reactor – with iron. Shown in the figure are the results of one of the experiments to measure the anisotropy of the 192-kev γ rays from In^{114m} ($5^+ \to 1^+$ transition). Five minutes after demagnetization the temperature of the salt was $\sim 0.035°$ K; heat was applied at a temperature of $\sim 0.045°$ K. From the value of the anisotropy $\epsilon \approx 8\%$ at T = 0.04° K, it follows that the nuclear polarization f_1 at this temperature is $\sim 30\%$ and the effective magnetic field at the indium nuclei $H_n \approx 1.5 \times 10^5$ oersteds. For the calculations the magnetic moment of the In^{114m} nucleus was taken to be equal to 4.7 nuclear magnetons.[3]

We made an attempt to find the polarization of Cr^{51} nuclei in a Cr-Fe alloy. Measurements in the temperature range 0.03 – 1° K of the anisotropy of the 320-kev γ rays ($5/2^- \to 7/2^-$ transition) emitted by Cr^{51} after K capture ($7/2^- \to 5/2^-$ transition) gave a negative result with an accuracy of not less than 0.5%. This result could be simply due to the magnetic moment of the Cr^{51} nucleus – which, unfortunately, is unknown – being too small.

The error in the values obtained for the magnetic field at the Sb and In nuclei in alloys of these elements with iron amounts to $^{+50}_{-20}$ %.

These errors were determined by the statistics of quanta-counting, and by the inaccuracy of determining the specimen temperature* – also, for Sb^{122}, by the absence of data on the characteristics of β decay and, for In^{114m}, by incomplete separation of the 192-kev γ rays from harder scattered

γ rays. The latter strongly interfered with the counts at the detector disposed in the direction of the field, since in this case part of the detector was screened by the pole of the magnet. Apparently, one can thus explain the fact that the ratio of the change in counts along the field to the change in counts across the field was not equal to two (see figure). The accuracy of the results presented will be increased in further experiments.

In our previous communication[1] we thought that the presence of an intrinsic magnetic moment at the gold atoms was needed to form the strong magnetic field at the Au^{198} nuclei in the Au-Fe alloy. However, it now appears highly probable that a large (or basic) contribution to this field arises in the conduction electrons. This possibility was first pointed out to us by E. K. Zavoĭskiĭ. Recently Marshall[4] proposed a mechanism for the creation of a "contact" field at the nucleus of a ferromagnetic atom. Apparently this mechanism also applies in our case, with the difference that the conduction electrons are polarized close to the neighboring atoms of iron and pass to the impurity atoms without change of orientation. Unfortunately, existing calculations of the magnetic field created by the conduction electrons in a ferromagnet are still only estimates. We hope to obtain more definite data on the origin of this field in further experiments (in particular by the study of the magnetic field at In and Au nuclei in In-Ni and Au-Ni alloys).

From the results we have obtained it would seem that the method of polarizing nuclei of weakly-magnetic atoms by introducing them into ferromagnets is of general applicability and allows a relatively high degree of polarization to be obtained.

The authors express their deep gratitude to E. K. Zavoĭskiĭ for much valuable advice, to L. D. Puzikov for assistance in calculating the γ-ray angular distributions and to L. V. Groshev, V. M. Galitskiĭ, and D. P. Grechukhin for discussion of results.

*The errors in temperature determination are associated both with the inaccuracy of measuring the thermodynamic temperature of the salt itself and with the difference in the temperatures of salt and specimen (due to the short time elapsing after the demagnetization of the salt).

[1] Samoĭlov, Sklyarevskiĭ, and Stepanov, J. Exptl. Theoret. Phys. (U.S.S.R.) **36**, 644 (1959), Soviet Phys. JETP **9**, 448 (1959).

[2] H. A. Tolhoek and J. A. M. Cox, Physica **19**, 101, 673 (1953).

[3] Strominger, Hollander, and Seaborg, Revs. Modern Phys. **30**, 585 (1958).

[4] W. Marshall, Phys. Rev. **110**, 1280 (1958).

Translated by K. F. Hulme
395

LIFETIMES OF THE FIRST EXCITED STATES OF Rb^{85} *AND* Pr^{141}

N. A. BURGOV, A. V. DAVYDOV, and G. R. KARTASHOV

Institute for Theoretical and Experimental Physics, Academy of Sciences, U.S.S.R.

Submitted to JETP editor March 13, 1959

J. Exptl. Theoret. Phys. (U.S.S.R.) **36**, 1946-1947 (June, 1959)

We have measured the lifetimes of the 150-kev level of Rb^{85} and of the 142-kev level of Pr^{141} by the method of delayed β-γ coincidences. The apparatus consisted of two scintillation counters with diphenyl acetylene crystals and FEU-33 photomultipliers and of a coincidence circuit with a resolving time of $2\tau_0 = 4.5 \times 10^{-9}$ sec. It was possible to insert calibrated sections of 200-ohm coaxial cable as delay lines into either channel.

As sources we used Kr^{85} and Ce^{141}, produced by exposure of natural krypton and cerium in a reactor. The gaseous radioactive krypton was contained at an absolute pressure of 3 atmos in a brass cylinder, 15 mm in length and diameter. The faces of the cylinder, through which the electrons and γ rays escaped, were covered with a 1 mg/cm^2 nylon film. The cerium source was a thin layer of cerium oxide powder mounted on aluminum foil.

The number $N_{\beta\gamma}$ of β-γ coincidences is related to the delay t in the channel of the β

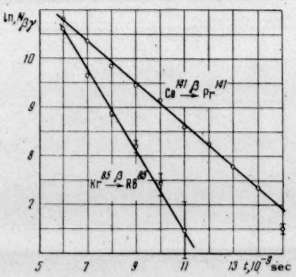

counter by the formula $N_{\beta\gamma} = N_0 \exp(-t/\tau_\gamma)$ if $t \gg \tau_0$. Here τ_γ is the mean life of the excited nuclear state with respect to γ emission. The data obtained are shown in the figure. Treatment of the data by the method of least squares yields

$$\tau_\gamma(Rb^{85}) = (1.14 \pm 0.12)\cdot 10^{-9} \text{ sec},$$
$$\tau_\gamma(Pr^{141}) = (2.32 \pm 0.17)\cdot 10^{-9} \text{ sec}.$$

The value of τ_γ for Pr^{141} agrees with the result of de Waard and Gerholm.[1]

The ratios of the experimentally determined lifetime to that calculated for single-particle transitions from the formulas of Moszkowski[2] are 210 and 230 for Rb^{85} and Pr^{141}, respectively.

[1] H. de Waard and T. R. Gerholm, Nuclear Physics **1**, 281 (1956).

[2] S. A. Moszkowski, Beta- and Gamma-Ray Spectroscopy, p. 391, ed. Kai Siegbahn, North-Holland Publ. Co., Amsterdam 1955.

Translated by J. Heberle
396

ON THE PROBLEM OF THERMAL CONDUCTIVITY AND ABSORPTION OF SOUND IN SUPERCONDUCTORS

V. Z. KRESIN

Moscow State Pedagogical Institute

Submitted to JETP editor March 19, 1959

J. Exptl. Theoret. Phys. (U.S.S.R.) **36**, 1947-1948 (June, 1959)

IN the present note we consider the absorption of sound in superconductors for the case where $\omega\tau \ll 1$ (ω is the sound frequency and τ the relaxation time). If such a sound field is present, the electron finds itself in a lattice with a slightly altered lattice constant. The absorption of sound energy occurs when we take into account the irreversibility of the process of deforming the lattice.

The solution of the transport equation for the distribution function of the electronic excitations of the superconductor which interact with the phonons, and the subsequent evaluation of the dissipative function which determines the absorption of the sound energy, leads to the following result for the coefficient for the absorption of sound:

$$\gamma_s = 4\gamma_n (e^b + 1)^{-2} F(T_k)/F(T). \qquad (1)$$

Here $\gamma_n = \text{const}\cdot T^{-5}$ is the coefficient for the absorption of sound in the normal metal, evaluated by Akhiezer in reference 1; $b = \Delta/kT$; Δ is the gap in the energy spectrum;

$$F(T) = 96\zeta(4)\ln(1+e^{-b}) + \sum_{s=1}^{\infty} s^{-5}e^{-2bs}(80b^4s^4 + 160b^3s^3 + 240b^2s^2 + 240bs + 120) - \ln(e^b+1)\sum_{s=1}^{\infty} s^{-4}e^{-2bs}(64b^3s^3 + 96b^2s^2 + 96bs + 48)$$

($\zeta(s)$ is the zeta-function). We have given a graph of $F(T)/F(T_k)$ in the figure.

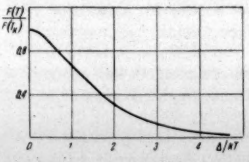

We can consider the problem of the influence of the electron-phonon interaction on the electronic thermal conductivity of superconductors in a similar way. This interaction, as was already noted by Geĭlikman[2] must be taken into account at temperatures close to T_k. We get in this case for the coefficient of thermal conductivity

$$\varkappa_s = \varkappa_n \frac{12F(T_k)}{\pi^2 F(T)}\left[\sum_{s=1}^{\infty}\frac{(-1)^{s+1}}{s^2}e^{-bs} + b\ln(1+e^{-b}) - \frac{b^2}{2(e^b+1)}\right]^2. \qquad (2)$$

$\varkappa_n = \text{const}\cdot T^{-2}$ is the thermal conductivity in the normal state considered by Landau and Pomeranchuk in reference 3.

We give here some values of $\varkappa_s/\varkappa_n$:

Δ/kT	0	0.25	0.5	0.75	1
$\varkappa_s/\varkappa_n$	1	0.81	0.72	0.58	0.46

In conclusion I express my sincere thanks to B. T. Geĭlikman for suggesting this subject and for valuable advice.

[1] A. I. Akhiezer, J. Exptl. Theoret. Phys. (U.S.S.R.) **8**, 1331 (1938).

[2] B. T. Geĭlikman, J. Exptl. Theoret. Phys. (U.S.S.R.) **34**, 1042 (1958), Soviet Phys. JETP **7**, 721 (1958).

[3] L. D. Landau and I. Ya. Pomeranchuk, J. Exptl. Theoret. Phys. (U.S.S.R.) **7**, 379 (1937).

Translated by D. ter Haar
397

POSSIBLE METHOD OF SEARCH FOR THE ρ^0 MESON

V. G. ZINOV, A. D. KONIN, S. M. KORENCHENKO and B. PONTECORVO

Joint Institute for Nuclear Research

Submitted to JETP editor March 23, 1959

J. Exptl. Theoret. Phys. (U.S.S.R.) **36**, 1948-1950 (June, 1959)

IT has been shown by Wigner, Baz', and Okun'[1,2,3] that the cross section for a reaction proceeding through a given channel has singularities near the threshold for an inelastic process proceeding through a new channel. In this connection Baz', Okun', and Smorodinskiĭ suggested to us that a study of the energy dependence of the cross section for pion-nucleon scattering near the threshold for meson production ($\pi + N \rightarrow 2\pi + N$) would be of interest for the purpose of obtaining information on the π-π interaction. We saw no singularities* in the total π^-p cross section in experiments covering the energy range from 150 to 180 Mev; but became aware of the fact that a study of the energy dependence of the cross section for π-meson interaction with hydrogen, with high energy resolution, is of great interest not only near the meson production threshold but also at other energies where it may give information about the existence of the ρ^0 meson.

The aim of this note is to present the principle and outline the possibilities of a method† of search for ρ^0 mesons which in our opinion is more realistic than other methods proposed to date.[4]

We propose to look for a rather narrow singularity in the energy dependence of the π^-p interaction cross section, because such a singularity would in principle testify to the existence of the ρ^0 meson. Indeed, it is to be expected that near the threshold for the reaction $\pi^- + p \rightarrow \rho^0 + n$ an anomaly should appear in the energy dependence of the reactions $\pi^- + p \rightarrow \pi^- + p$ and $\pi^- + p \rightarrow \pi^0 + n$. From the experimental point of view the first step should be a search for singularities in the energy dependence of the total π^-p-interaction cross section. Subsequent studies of angular distributions in the singularity region would be of great interest and could yield information on the relative parity of the ρ^0 and π mesons.

The width of the singularity depends on the interaction radius R and may be obtained from the condition $kR \ll 1$ where k is the wave vector of the produced ρ^0 meson[2] in the barycentric system. Assuming that $R \sim \hbar/m_\pi c$ then the maximum width of the singularity in the energy dependence of the π^-p-interaction cross section is $\Delta E \sim 40$ Mev for ρ^0 mesons with mass ~ 400 Mev/c^2. Here ΔE is the energy interval of the incident π mesons in the laboratory frame of reference outside of which the singularity disappears. The width of the singularity may be considerably less than ΔE which underscores the necessity for high energy resolution in the experiment.

It was assumed in the above that the lifetime of the ρ^0 meson is long compared to the nuclear time $\hbar/m_\pi c^2$, i.e., that the threshold for ρ^0 production is sharp. The relative amplitude of the singularity $\Delta\sigma/\sigma$ is of the order of magnitude of $\sigma(\pi^-p \rightarrow \rho^0 n)_{k=1/R}/\sigma_{\text{total}}(\pi^-p)$, and may therefore be as much as a few percent.

The method outlined above can be used to detect any neutral meson with sufficiently small natural width. We discuss here only ρ^0 mesons, assuming that they differ from π^0 mesons only in isotopic spin ($T = 0$). In that case the ρ^0 meson cannot decay fast into either two π mesons (owing to parity conservation) or three π mesons (owing to conservation of the G quantum number[4,5]), but will decay through the channel $\rho^0 \rightarrow \gamma + \gamma$ or, if its mass is sufficiently large, $\rho^0 \rightarrow \pi + \pi + \gamma$. If the mass of the ρ^0 meson is substantially larger than 560 Mev/c^2 then a decay into four π mesons will proceed with a nuclear lifetime and our method would not be useful.‡

Independent of the nature of the ρ^0 meson one may ask whether the maximum observed in the energy dependence of the cross section of π-meson photoproduction on protons[6] and the peaks recently observed** in the energy dependence of the π^-p-interaction cross section at 700 and 1000 Mev are due to threshold effects. It seems to us that the answer to this question is negative: the widths of these peaks are apparently too great to be due to threshold effects. If one or both peaks are connected with the ρ^0 meson then it must be through a resonance interaction and the mass of the ρ^0 meson must be much less than 600 or 800 Mev/c^2.

Generally speaking the most outstanding difference between a resonance maximum and a threshold singularity (in the case when the latter is a peak and not a valley or step) is in their widths.

As regards the mass difference of the ρ^0 and π^0 mesons we observe that the experimental data accumulated in high energy physics indicates that interactions in different isotopic spin states have quite different intensities. It is just this circum-

stance that leads to the mutual transformations of different particles of an isotopic multiplet (the phenomenon of charge exchange scattering). In particular, as was pointed out to us by Ya. B. Zel'dovich, the very existence of antiproton exchange scattering ($\tilde{p} + p \to \tilde{n} + n$) implies a ρ^0-π^0 mass difference.

In a subsequent communication we shall describe the main features of an experimental setup which is being used in the search for ρ^0 mesons and report preliminary results of completed measurements.

We are extremely grateful to L. I. Baz', V. B. Belyaev, B. N. Zakharev, L. B. Okun', and Ya. A. Smorodinskiĭ for numerous discussions.

*It is easy to see that for a three-particle final state the threshold singularity practically disappears.[2]

†We have recently been informed that V. I. Gol'danskiĭ and Ya. I. Smorodinskiĭ proposed and analogous method.

‡Barrier effects, having to do with high orbital angular momentum, may appreciably slow down[4] the decay of the ρ^0 meson into four π mesons if its mass is only slightly larger than the sum of the four π-meson masses.

**Private communication from D. Frish to V. I. Gol'danskiĭ.

[1] E. P. Wigner, Phys. Rev. **73**, 1002 (1948).

[2] A. I. Baz', J. Exptl. Theoret. Phys. (U.S.S.R.) **33**, 923 (1957), Soviet Phys. JETP **6**, 709 (1958).

[3] A. I. Baz' and L. B. Okun', J. Exptl. Theoret. Phys. (U.S.S.R.) **35**, 757 (1958), Soviet Phys. JETP **8**, 526 (1959).

[4] Ya. B. Zel'dovich, J. Exptl. Theoret. Phys. (U.S.S.R.) **34**, 1644 (1958), Soviet Phys. JETP **7**, 1130 (1958).

[5] T. D. Lee and C. N. Yang, Nuovo cimento **3**, 749 (1956).

[6] R. R. Wilson et al., R. L. Walker et al., Proc. Annual Intern. Conf. High Energy Physics, Geneva, 1958, p. 87.

Translated by A. M. Bincer
398

SINGULARITIES OF THE S MATRIX AND THE ρ^0 MESON

V. I. GOL'DANSKIĬ and Ya. A. SMORODINSKIĬ

P. N. Lebedev Physics Institute, Academy of Sciences, U.S.S.R.; Joint Institute for Nuclear Research

Submitted to JETP editor April 4, 1959

J. Exptl. Theoret. Phys. (U.S.S.R.) **36**, 1950-1951 (June, 1959)

THE hypothesis that another neutral meson (ρ^0 meson) exists with zero spin and strangeness has been discussed in several papers. All the methods proposed for verifying this hypothesis were based on the observation of some reaction producing the ρ^0 meson or on the detection of its decay products.

We wish to point out here that still another method exists, based on an essentially different idea, which may turn out to be considerably more convenient for actual experiments. It has to do with the study of singularities in the energy dependence of a reaction near the threshold for the production of a new particle. This method was first studied in a general form by Wigner.[1] Later Baz'[2] indicated the interesting consequences resulting from an application of this method to nuclear reactions (see also the work by Breit and others,[3] which was published simultaneously).

The same idea was used in a study of photodisintegration near threshold for the γn reaction[4] and in a study of K-meson properties.[5] This same method was used[6] to detect the dineutron in a study of the energy dependence of elastic neutron scattering by nuclei near the threshold for the (n, 2n) reaction.

It is natural to apply the consideration of Baz' et al.[6] to a study of the analogous problem concerning the existence of the ρ^0 meson. Specifically let us consider elastic scattering on protons of π mesons with energy in excess of 270 Mev.* The scattering cross section for the process may exhibit two types of singularities.

a) Singularities connected with the "isobaric" state, e.g., $\pi^+ + p \to$ "isobar" ($T = 3/2$, $I = 3/2$). A pole in the S matrix in the complex energy plane corresponds to this type of singularity; and near this pole, for real values of the energy, the cross section curve has the well known resonance shape.

b) The threshold for the production of a new particle, e.g., $\pi^- + p \to \rho^0 + n$. A branch point on the real axis corresponds to the threshold of such a reaction.† At such a point the derivative (in our case, the first derivative) of the cross section is discontinuous. It is this type of singularity that we are interested in. Its existence leads to the appearance of breaks in the cross section curve in the form of a "step" or "valley" or "peak" type

cusps (cf. reference 2), and these should be found experimentally. In the first two cases the singularity can be interpreted unambiguously. If, however, the singularity is of the "peak" type then it may easily be mistaken for a resonance. In that case the fact that the peak should, generally speaking, be rather narrow (of the order of 10 – 20 Mev) may help to identify it. This last circumstance makes the possibility unlikely that the observed maxima for $T = \frac{1}{2}$ for π mesons of energies 680 and 940 Mev (private communication from D. Frish) could be due to the production of the ρ^0 meson ("ρ^0-mass" – 1200 and 1520 electron masses). Another method for distinguishing resonance and threshold singularities may be based on a comparison of interactions in systems with the same energy but different isotopic spin. Thus, for example, if the singularities in π^-p scattering at 680 and 940 Mev are threshold singularities then corresponding singularities should appear in K^-p scattering at K-meson energies of 520 and 810 Mev (in the $T = 0$ state).

A study of the magnitude of the singularity would permit an estimate of the upper limit for the possible production cross section of the ρ^0 meson. To this end it is convenient to make use of the quantity

$$2\left(\frac{\delta\sigma(\varepsilon)}{\sigma(\varepsilon)}\right)^2 = \left(\frac{\sigma(E_0+\varepsilon)-\sigma_{thr}}{\sigma_{thr}}\right)^2 + \left(\frac{\sigma(E_0-z)-\sigma_{thr}}{\sigma_{thr}}\right)^2,$$

where E is the threshold energy and is the elastic cross section. It is easy to show that

$$\delta\sigma(\varepsilon)/\sigma(\varepsilon) = (k/4\pi)\,\sigma_\rho(\varepsilon)/\sqrt{\sigma(\varepsilon)}.$$

Here k is the π-meson wave vector and σ_ρ is the ρ^0 production cross section at a π-meson energy $E + \epsilon$.

In conclusion we note that the same idea was proposed independently by Pontecorvo et al.[7] to whom we are grateful for useful discussions.

*If the threshold for ρ^0 production were to correspond to a π-meson energy of less than 270 Mev then the relatively fast decay $K^+ \to \pi^+ + \rho^0$ ($\Delta T = \frac{1}{2}$) would be possible, which however, has not been observed.

†This is connected with the fact that the scattering phase shift δ_0 becomes complex above threshold (near threshold): $\delta_0 = \delta_{01} + i\delta_{02}$, with δ_{01} an even function of k (the ρ^0 wave vector) and δ_{02} an odd function. Hence below threshold δ_{02} is imaginary and therefore δ_0 is real.

[1] E. Wigner, Phys. Rev. **73**, 1002 (1948)

[2] A. I. Baz', J. Exptl. Theoret. Phys. (U.S.S.R.) **33**, 923 (1957), Soviet Phys. JETP **6**, 709 (1958).

[3] G. Breit, Phys. Rev. **107**, 1612 (1957).

[4] Baz', Smorodinskiĭ, Lazareva et al., Report at the Geneva Conference on Peaceful Uses of Atomic Energy, 1958.

[5] A. I. Baz' and L. B. Okun', J. Exptl. Theoret. Phys. (U.S.S.R.) **35**, 757 (1958), Soviet Phys. JETP **8**, 526 (1959).

[6] A. I. Baz' and Ya. A. Smorodinskiĭ, Report at the Nuclear Conference, Paris, 1958.

[7] Zinov, Konin, Korenchenko, and Pontecorvo, J. Exptl. Theoret. Phys. (U.S.S.R.) **36**, 1948 (1959), Soviet Phys. JETP this issue, p. 1386.

Translated by A. M. Bincer
399

ANISOTROPY OF THE ABSORPTION COEFFICIENTS OF ULTRASONICS IN SUPERCONDUCTORS

P. A. BEZUGLYĬ, A. A. GALKIN, and A. P. KOROLYUK

Physico-Technical Institute, Academy of Sciences, Ukrainian S.S.R.

Submitted to JETP editor April 7, 1959

J. Exptl. Theoret. Phys. (U.S.S.R.) **36**, 1951-1952 (June, 1959)

IT is known that both the energy gap at $T = 0$ and the temperature dependence of the gap width (ϵ_0) can be determined from measurements of ultrasonic attenuation in superconductors.[1] The agreement between experiment and theory is satisfactory.

There have also been determinations of the effect of isotopic constitution[2] and of unidirectional lattice deformation[3] on T_k, and consequently on the gap width too. One might expect anisotropy of the lattice to have a greater influence than isotopic constitution.

In this note we report the results of an experimental determination of the attenuation of 70-Mcs ultrasound in the superconducting and normal states. The arrangement was such that at each temperature the absorption coefficient could be measured along the twofold (C_2) and the fourfold (C_4) axes for a spherical tin specimen.

The results are shown in the table, and also the values of ϵ_0 calculated from them according to the Bardeen, Cooper, and Schrieffer theory.[4] It can be seen that the temperature dependence of the ratio of absorption coefficients, α_s/α_n, is different in the two directions. Better agreement

Temperature	α_s/α_n	ε_s/kT_k	α_s/α_n	ε_s/kT_k	Temperature	α_s/α_n	ε_s/kT_k	α_s/α_n	ε_s/kT_k
	Along C_4		Along C_2			Along C_4		Along C_2	
3.73	1.00	0.00	1.00	0.00	3.30	0.51	0.96	0.42	1.18
3.72	0.97	0.06	0.94	0.12	3.20	0.46	1.03	0.37	1.26
3.70	0.91	0.17	0.83	0.33	3.10	0.41	1.12	0.34	1.32
3.66	0.82	0.35	0.74	0.52	3.00	0.37	1.19	0.30	1.39
3.60	0.74	0.51	0.65	0.71	2.80	0.29	1.34	0.25	1.46
3.55	0.68	0.62	0.59	0.82	2.50	0.20	1.48	0.18	1.54
3.50	0.64	0.70	0.55	0.91	2.10	0.12	1.54	0.11	1.60
3.40	0.57	0.84	0.48	1.06					

with the isotropic theory of superconductivity is obtained for the case of sound propagation along the fourfold axis.

[1] R. W. Morse and H. V. Bohm, Phys. Rev. **108**, 1094 (1957).

[2] Lock, Pippard, and Shoenberg, Proc. Camb. Phil. Soc. **47**, 811 (1951), Reynolds, Serin, Wright and Nesbitt, Phys. Rev. **78**, 487 (1950).

[3] B. G. Lazarev and L. S. Kan, J. Exptl. Theoret. Phys. (U.S.S.R.) **14**, 463 (1944).

[4] Bardeen, Cooper and Schrieffer, Phys. Rev. **108**, 1175 (1957).

Translated by R. Berman
401

STORAGE OF COLD NEUTRONS

Ya. B. ZEL' DOVICH

Submitted to JETP editor April 3, 1959

J. Exptl. Theoret. Phys. (U.S.S.R.) **36**, 1952-1953 (June, 1959)

THE idea of retaining slow neutrons has been mentioned many times, but the corresponding experiments have not yet been performed, and the literature does not contain even rough estimates pertaining to this problem.

It is known that slow neutrons experience total internal reflection in glancing incidence on the surface of most substances. At sufficiently low velocities, the neutrons cannot penetrate in such a substance even under normal incidence. Thus, for carbon with a density $\sim 2 g/cm^3$ the critical neutron velocity is close to 5 m/sec, for beryllium it is approximately 7 m/sec. Let us place neutrons in a cavity surrounded on all sides by graphite. The neutrons of speed higher than critical will rapidly leave the cavity, but neutrons of less than critical speed are blocked in the cavity and vanish only as they decay, with a half-life of approximately 12 minutes. Such slow neutrons will penetrate into the wall only a depth on the order of their wavelength; taking into account dimensionless factors, the depth is $\sim 10^{-6}$ cm. Therefore if the cavity has a considerable volume, the fraction of the time that the neutrons stay in the material of the shell is quite small; for a one-cubic-meter cavity this fraction is $\sim 10^{-7}$.

The capture cross section of carbon (4.5×10^{-27} cm^2 at $v = 2.2 \times 10^5$ cm/sec) obeys the 1/v law and corresponds to a neutron lifetime in carbon of ~ 0.01 sec regardless of its velocity. For neutrons in a cavity we obtain an absorption time of $0.01/10^{-7} = 10^5$ sec 1 day. Slow neutrons will also be lost, as they acquire energy by collision; obviously, however, this process is greatly suppressed, because the neutrons are for the most time in the cavity and not in the material of the shell.

The most difficult feat is to obtain a sufficient number of such neutrons. For a Maxwellian distribution at room temperature, the fraction of such neutrons is on the order of 10^{-8}.

It is advisable first to cool the neutrons in a volume filled with liquid helium, and then the fraction of the necessary neutrons increases to 10^{-5}. As a result of the long life of the slow neutrons in the cavity, their concentration after a few seconds becomes equal to the Maxwellian equilibrium concentration. The principal difficulty is connected with the need for having a large volume of liquid helium, because of the long range of the neutrons in helium (50 cm).

With a fully moderated neutron flux of 10^{12} cm^{-2} sec^{-1} from a reactor, the flux of neutrons emitted with a temperature of 3°K can amount to 10^{11} cm^{-2} sec^{-1}, which corresponds at an average velocity on the order of 2×10^4 cm/sec to a density of 5×10^6 cm^{-3} of thermal neutrons, in-

cluding 50 cm^{-3} slow ones (with velocity less than 500 cm/sec). Thus, under the most favorable assumptions, it is possible to accumulate up to 5×10^7 slow neutrons in a cavity 1 m^3 in volume.

By placing a graphite partition over the opening that joins the cavity with the liquid helium it is possible to remove the cavity with slow neutrons from the reactor and make the measurements at a small background.

It may prove advantageous to use a palliative variant without helium, by cooling the neutron say to 70°K and accumulating up to 10^5 neutrons. We note that the index of refraction of the moderator should be less than the index of refraction of the cavity material, or else the moderator will not admit necessary neutrons in from the vacuum, and consequently will not let any out. An experiof this type is quite difficult, but it seems that it can give the experimentators a valuable method of investigating the interaction of slow neutrons with substances introduced into the cavity. By introducing an (n, γ) absorber of neutrons into the cavity, it is easy to measure the number of neutrons left intact at the instant of observation.

We note that the neutrons in the cavity can be effectively heated to a speed above critical by mechanical displacement of the graphite surfaces at a speed of several meters per second.

The theory of the coefficient of refraction and the total internal reflection of neutrons is well known; we note only that it remains valid also at those small energies, at which the absorption cross section, following the 1/v law, becomes equal to or greater than the scattering cross section. It is easy to verify that the imaginary part of the pseudo-potential, the part describing the absorption, is small compared with the real part, which describes the scattering. Their ratio is equal to $\sqrt{\pi\sigma_s}/\lambda_1$, where λ_1 is the wavelength of the neutron for which $\sigma_s = \sigma_a$. Consequently, in the case of total internal reflection, absorption does not change the exponential law of damping of the wave function of the neutron in the medium.

[1] D. J. Hughes, Pile Neutron Research, Addison-Wesley, Cambridge, Mass., 1953. Russ. Transl. IIL, M., 1954.

[2] N. V. Vlasov, Нейтроны, (Neutrons), GTTI, 1955.

Translated by J. G. Adashko
401

PIEZOMAGNETISM IN THE ANTIFERROMAGNETIC FLUORIDES OF COBALT AND MANGANESE

A. S. BOROVIK-ROMANOV

Institute of Physical Problems, Academy of Sciences, U.S.S.R.

Submitted to JETP editor April 1, 1959

J. Exptl. Theoret. Phys. (U.S.S.R.) **36**, 1954-1955 (June, 1959)

THE magnetic symmetry of some antiferromagnetic crystals permits the existence of a piezomagnetic effect,[1,2] i.e., the appearance of a spontaneous moment on applying pressure. For a group of transition element fluorides in which the antiferromagnetic vector is directed along the four-fold axis (z) of the tetragonal cell,[4] Dzyaloshinskiĭ[3] has shown that, on applying a shear stress σ_{xz}, a ferromagnetic moment $m_y = \lambda\sigma_{xz}$ should be observed. No piezomagnetic effect has been experimentally observed to date.

To detect piezomagnetism we used a specially constructed magnetic torsion balance, in which a press containing the specimen was suspended on vertical wires. Following a proposal made by P. L. Kapitza, the press was controlled with the aid of evacuated sealed bellows. When the pressure of helium gas in the space surrounding the press was reduced, the compressed bellows tried to expand and by way of a lever applied a magnified pressure to the specimen. For a specimen of 1 mm^2 cross section, the maximum pressure was ~ 500 kg/cm^2.

Single crystals of CoF_2 and MnF_2 were studied, out of which parallelipipeds were sawed—the crystallographic axes being disposed as shown in the figure. On applying a pressure, p, to such a specimen, shear stresses $\sigma_{xz} = p/2$ arise in it. The specimen was situated in an inhomogeneous magnetic field directed along the y axis, and the magnetic moment m_y was measured for several values of the field. The measurements were made at liquid hydrogen temperature (20.4°K), where the antiferromagnetic ordering of the fluorides considered is almost at saturation. The relative accuracy of the measurements was ±0.3%; the error in the absolute values of the moment could amount to 10%.

The results of the measurements obtained on the CoF_2 specimen are given in the figure, where the dependence of molar magnetic moment on field is shown. With no pressure (line 1) we have m =

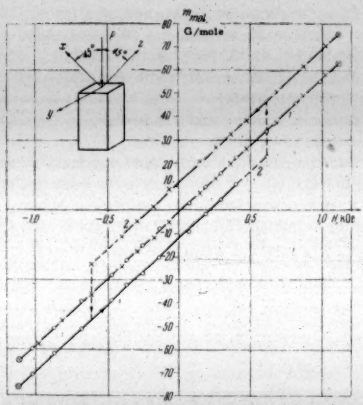

The dependence of molar magnetic moment on the size of the applied field: 1 – without pressure, 2 – pressure on specimen ~ 500 kg/cm²; ○ – values obtained while changing the field from – 1100 oersteds to + 1100 oersteds × – while changing the field in the opposite direction.

$\chi_\perp$; thus, in agreement with the data of previous studies,[5,6] the crystal does not possess a spontaneous moment* and is in a purely antiferromagnetic state. On applying a pressure of ~ 500 kg/cm² (curve 2), the paramagnetic moment remains unchanged, but a spontaneous piezomagnetic moment is added to it, the magnitude of which, $m_0 \sim 10$ G/mole, does not depend on field. In weak fields (up to 500 oersteds) the direction of the piezomagnetic moment remains unchanged. In large fields of opposite direction to the spontaneous moment, the magnetization of the specimen reverses. The process of magnetization reversal is comparatively slow – in a field of 1100 oersteds the equilibrium values are attained in 15 – 20 minutes.

A piezomagnetic effect was also observed in the MnF_2 specimen. However, its magnitude in MnF_2 is approximately 100 times smaller than in CoF_2.

A fuller description of the experimental details, the results, and their analysis, will be published after completing a study of specimens with other orientations.

In conclusion the author expresses his deep gratitude to Acad. P. L. Kapitza for constant interest in the work. The author is very grateful to N. N. Mikhaĭlov and O. S. Zaĭtsev for preparing the single crystals of CoF_2 and MnF_2. He also cordially thanks I. E. Dzyaloshinskiĭ for useful discussion.

*The small downward displacement of the line (approximately 1 G/mole) is in all probability associated with plastic deformations of the crystal.

[1] B. A. Tavger and V. M. Zaĭtsev, J. Exptl. Theoret. Phys. (U.S.S.R.) **30**, 564 (1956), Soviet Phys. JETP **3**, 430 (1956).

[2] L. D. Landau and E. M. Lifshitz, Электродинамика сплошных сред (Electrodynamics of Continuous Media), Gostekhizdat, 1957.

[3] I. E. Dzyaloshinskiĭ, J. Exptl. Theoret. Phys. (U.S.S.R.) **33**, 807 (1957), Soviet Phys. JETP **6**, 621 (1958).

[4] R. A. Erickson, Phys. Rev. **90**, 779 (1953).

[5] I. W. Stout and L. M. Matarrese, Revs. Modern Phys. **25**, 338 (1953).

[6] Astrov, Borovik-Romanov, and Orlova, J. Exptl. Theoret. Phys. (U.S.S.R.) **33**, 812 (1957), Soviet Phys. JETP **6**, 626 (1958).

Translated by K. F. Hulme
402

DETERMINATION OF THE CAPTURE FREQUENCY OF SLOW MESONS BY LIGHT AND HEAVY NUCLEI IN PHOTOEMULSIONS

D. K. KOPYLOVA, Yu. B. KOROLEVICH, N. I. PETUKHOVA, and M. I. PODGORETSKIĬ

Joint Institute for Nuclear Research

Submitted to JETP editor February 28, 1959

J. Exptl. Theoret. Phys. (U.S.S.R.) **36**, 1955-1956 (June, 1959)

In many uses of photoemulsions it is necessary to determine how much of the interaction is with the light nuclei (C, N, O) and how much is with the heavy ones (Ag, Br). The presently known separation methods (see, for example, references 1 and 2) are based on the use of special emulsions, and can therefore not always be used. We describe below a simple separation method, free of this shortcoming.

In order to be specific, we discuss only nuclear capture of stopped negative pions. If an Auger electron was produced when the negative pion was stopped, the capture was by the heavy nucleus of the emulsion.[1,3-5] If the σ_π star produced after stopping contains a particle with a range $\leq 50\mu$ (so-called sub-barrier particle) the corresponding capture must be attributed to a light nucleus.[1,4,6*]

Let N_H be the number of σ_π stars of the first step, N_L that of the second, and N_N the number of σ_π stars that remain unseparated. We now choose some additional identification, which may be common to σ_π stars of all types, and denote by n_H, n_L, and n_N the number of σ_π stars in each of the three groups having this identification.† We can then write

$$N_N = M_H + M_L, \quad n_N = (n_H / N_H) M_H + (n_L / N_L) M_L,$$

where M_H and M_L is the number of captures by heavy and light nuclei among the stars of group N. Consequently, the total number of captures by heavy nuclei will be

$$N_H + M_H = N_H + \frac{n_N - (n_L / N_L) N_N}{n_H / N_H - n_L / N_L} = N_H + N_N \frac{\alpha_N - \alpha_L}{\alpha_H - \alpha_L},$$

where α_H, α_L, and α_N is the frequency of appearance of the additional selected identification in groups H, L, and N. Analogously, the total number of captures by light nuclei will be

$$N_L + M_L = N_L + N_N (\alpha_N - \alpha_H) / (\alpha_L - \alpha_H).$$

The foregoing method was tested with 349 σ_π stars, taken from reference 3.‡ The σ_π stars were considered to have an additional identification, if they contained more than one black prong ($N_H \geq 2$). The frequency of capture of pions by heavy nuclei was found to be $(63 \pm 2.8)\%$, which is in good agreement with the results obtained by other methods.[1,2,7,8] It was assumed here that prongless stars are formed in 27% of all cases of capture of π^- mesons[9] and that 13.7% of all the σ_π stars produced in the capture of π^- mesons by light nuclei are prongless.[10] By way of one possible application, it would be interesting to estimate by the same method the frequency of capture of slow K mesons by light and heavy emulsion nuclei.

*Both statements are not true, naturally, in all cases. However, the exceptions are very rare and can be disregarded in practice.

†It is assumed that the indicated third identification is statistically independent of the first two.

‡The authors are grateful to S. A. Azimov and U. G. Gulyamov for furnishing the material.

[1] Menon, Muirhead, and Rochat, Phil. Mag. **41**, 583 (1950).

[2] G. Brown and J. S. Hughes, Phil. Mag. **2**, 777, 1957.

[3] Azimov, Gulyamov, Zamchalova, Inzametdinova, Podgoretskiĭ, and Yuldashev, J. Exptl. Theoret. Phys. (U.S.S.R.) **31**, 756 (1956), Soviet Phys. JETP **4**, 632 (1957).

[4] D. H. Perkins, Phil. Mag. **40**, 601 (1949).

[5] W. F. Ery, Nuovo cimento **10**, 490 (1953).

[6] K. Lanius, Nucl. Phys. **3**, 391 (1957).

[7] de Sabbata, Manaresi, and Puppi, Nuovo cimento **10**, 1704 (1953).

[8] Demeur, Huleux, and Vanderhaeghe, Nuovo cimento **4**, 509 (1956).

[9] Gardner, Barkas, Smith, and Bradner, Science **111**, 191 (1950).

[10] P. Ammiraju and L. M. Lederman, Nuovo cimento **4**, 283 (1956).

Translated by J. G. Adashko
403

A CORRECTION TO V. M. STRUTINSKIĬ'S PAPER "EXCITATION OF ROTATIONAL STATES IN ALPHA DECAY OF EVEN-EVEN NUCLEI"

V. M. STRUTINSKIĬ

Submitted to JETP editor May 6, 1959

J. Exptl. Theoret. Phys. (U.S.S.R.) **36**, 1957 (June, 1959)

IN the calculation of deformation parameters α of even-even nuclei from the relative intensity of α decay into the state 2^+ (ξ_2), inexact experimental data, quoted by the author from Gol'din's survey,[2] were employed in reference 1 in a number of cases. Cited below are the parameters α for these nuclei, obtained on repeated calculation, using experimental data on the fine structure of α decay as cited in references 3 and 4. The values of α were also determined as in reference 1 and with the aid of the same curves (similar to those shown in Fig. 2) as were previously plotted for all even-even nuclei considered in reference 1. The daughter nuclei, $\xi_{2(\exp)}$, and the values of α for $r_0 = 1.4 \times 10^{-13}$ cm. are successively indicated. Negative values of α are given in those instances when they too can be reconciled with the intensity distribution.

Rn^{218} : 0.04 [4], + 0.06, —0.10; Th^{230} : 0.39 [3, 4], + 0.15;
U^{230} : ~ 0.33 [4], + 0.12;
U^{232} : 0.45 [3], + 0.15; 0.39 [4], + 0.13;
U^{236} : 0.32 [2, 3, 4], + 0.12; Pu^{240} : 0.30 [3, 4], + 0.11;
Cm^{246} : 0.20 [3, 4], + 0.09, —0.16;
Cm^{248} : 0.18 [3, 4], + 0.09, —0.16;
Cf^{250} : 0.20 [3, 4], + 0.08, —0.19.

Values of the deformation parameters for 11 even-even nuclei were also cited in the paper by Gol'din and Ter-Martirosyan[5] (Table IX) where they were obtained as a result of the numerical solution of an initial exact equation describing α decay. A comparison of our results with the values of α obtained by these authors[5] shows that they practically coincide with each other — the deviation does not exceed 10%.

[1] V. M. Strutinskiĭ, J. Exptl. Theoret. Phys. (U.S.S.R.) **32**, 1412 (1957), Soviet Phys. JETP **5**, 1150 (1957).

[2] Gol'din, Novikova, and Peker, Usp. Fiz. Nauk **59**, 459 (1956).

[3] Strominger, Hollander, and Seaborg, Revs. Modern Phys. **30**, 2, part II (1958).

[4] I. Perlman and J. O. Rasmussen, Alpha Radioactivity, Handbuch der Phys., **17** (1957).

[5] L. L. Gol'din, K. A. Ter-Martirosyan et al., J. Exptl. Theoret. Phys. (U.S.S.R.) **35**, 184 (1958), Soviet Phys. JETP **8**, 127 (1959).

Translated by Z. Barnea
404

RESONANCE TRANSITIONS IN PARALLEL FIELDS IN CERTAIN Mn^{++} AND Fe^{+++} SALTS

N. S. GARIF' YANOV

Physico-Technical Institute, Kazan' Branch, Academy of Sciences, U.S.S.R.

Submitted to JETP editor April 9, 1959

J. Exptl. Theoret. Phys. (U.S.S.R.) **36**, 1957-1958 (June, 1959)

KURUSHIN[1] and Kutuzov[2] have communicated that at $\nu \sim 10^{10}$ Cps at room temperature the $\chi''(H)$ absorption curves in certain Mn^{++} and Fe^{+++} salts possess a maximum when investigated in parallel fields (an oscillating magnetic field H_ν directed parallel to a constant magnetic field H). This absorption in parallel fields was explained by a spin-spin relaxation and identified with the phenomenon discovered experimentally by Gorter et al.[3] In addition it was also noted in references 1 and 2 that the experimental $\chi''(H)$ curves do not fit Shaposhnikov's theory.[4]

As is known, for certain Mn^{++} and Fe^{+++} salts[5] in perpendicular fields, at $\nu \sim 10^{10}$ cps and room temperature, a peak due to the forbidden transition from $\Delta m = \pm 2$ is observed in addition to the main resonance peak corresponding to the allowed transition from $\Delta m = \pm 1$. The intensity of this peak is approximately a hundred times smaller than the intensity of the main peak.

Our measurements of $\chi''(H)$ at 9500 Mcs and $T = 295°K$ in $FeNH_4(SO_4)_2 \cdot 12H_2O$ have shown that in the course of a smooth change from perpendicular to parallel fields (the angle between H_ν and H changes from 90° to 0°) the intensity of the peak for the transition from $\Delta m = \pm 2$ increases by approximately one order of magnitude, while the intensity for $\Delta m = \pm 1$ decreases practically to zero. At the same time, the resonance value of the intensity of the constant magnetic field H = 1680 oersteds remains unchanged for the transition from $\Delta m = \pm 2$.

On the basis of this experiment, we can draw the conclusion that the maximum absorption $\chi''(H)$ in parallel fields observed by Kurushin and Kutuzov is not caused by spin-spin relaxation, but by resonance. There are grounds to believe that the phenomena discovered by Gorter in parallel fields at lower frequencies of H_ν are also, in a number of instances, due to resonance transitions.

[1] A. I. Kurushin, J. Exptl. Theoret. Phys. (U.S.S.R.) **32**, 938 (1957), Soviet Phys. JETP **5**, 766 (1957).

[2] A. N. Kutuzov, J. Exptl. Theoret. Phys. (U.S.S.R.) **35**, 1304 (1958), Soviet Phys. JETP **8**, 910 (1959).

[3] Smits, Derkson, Verstelle, and Gorter, Physica **22**, 773 (1956).

[4] I. G. Shaposhnikov, J. Exptl. Theoret. Phys. (U.S.S.R.) **18**, 533 (1948).

[5] E. K. Zavoĭskiĭ, Dokl. Akad. Nauk SSSR **47**, 887 (1947).

Translated by Z. Barnea
405

ERRATA TO VOLUME 9

Page	Reads	Should read
115, Col. 2, line 18 from top	R. Gatto and M. A. Ruderman, [Nuovo cimento 8, 775, (1958)]	T. Goto, Nuovo cimento 8, 625 (1958)
294, Col. 2, line 4 from bottom	$N = N_{exp}(p, \theta)\, F(p, \theta)$	$N = N_{exp}(p, \theta)\, 1 + F(p, \theta)$
462, Col. 1, line 8 from top	which are approximately 13Z ev	and approximately equal to 13Z ev
646, Col. 1, line 3 from top	$\langle j_1' t_1' \alpha \vert R^{J_2} \vert j_1 t_1 \alpha_1 \rangle$	$\langle j_1' t_1' \alpha \vert R^{J_1} \vert j_1 t_1 \alpha_1 \rangle$
661, Col. 1, line 6 from top	$\chi = 2.14 \times 10^{-13}$	$\chi = 1.04 \times 10^{-13}$

Author Index to Volume 36 (9)

References with L are Letters to the Editor

Abaulina-Zavaritskaya, E. I. The Electrical Conductivity of Germanium in High Electric Fields at Low Temperatures — 953.

Abrikosov, A. A. and L. P. Gor'kov. Superconducting Alloys at Finite Temperatures — 220L.

— L. P. Gor'kov, and I. E. Dzyaloshinskiĭ. On the Application of Quantum-Field-Theory Methods to Problems of Quantum Statistics at Finite Temperatures — 636.

Abrosimov, A. T., V. A. Dmitriev, G. V. Kulikov, E. I. Massal'skiĭ, K. P. Solov'ev, and G. B. Khristiansen. High-Energy Nuclear-Active Component of Extensive Air Showers at Sea Level — 528.

Adamovich, M. I. (see Kharlamov, S. P.) — 668L.

Afrosimov, V. V. (see Fedorenko, N. V.) — 267.

— (see Il'in, R. N.) — 29.

Agranovich, V. N., V. E. Pafomov, and A. A. Rukhadze. Cerenkov Radiation of an Electron Moving in a Medium with Spatial Dispersion — 160.

Akhiezer, A. I. and I. Ya. Pomeranchuk. Interaction between Conduction Electrons in Ferromagnets — 605.

— B. G. Bar'yakhtar, and S. V. Peletminskiĭ. On the Theory of Relaxation Processes in Ferrodielectrics at Low Temperatures — 146.

Akhiezer, I. A. and R. V. Polovin. Theory of Relativistic Magnetohydrodynamic Waves — 1316.

Akulov, N. S. Contribution to the Theory of Ferroelectric Polarization Curves — 772.

Alekseev, A. I. Non-Relativistic Solution of the Bethe-Salpeter Equation — 1020.

— Three-Photon Annihilation of Positronium in the P State — 1312.

Alekseevskiĭ, N. E. and Yu. P. Gaĭdukov. Measurement of the Electrical Resistance of Metals in a Magnetic Field as a Method of Investigating the Fermi Surface — 311.

Ali-Zade, S. A., I. I. Gurevich, Yu. P. Dobretsov, B. A. Nikol'skiĭ, and L. V. Surkova. Asymmetry of Angular Distribution $\mu^+ - e^+$ Decay Electrons in a 27,000 Gauss Magnetic Field — 940L.

Alikhanov, A. I. and V. A. Lyubimov. Possibility of Determining the Chirality of the Muon by Means of δ-Electron Cascades from Magnetized Iron — 946L.

— G. P. Eliseev, V. Sh. Kamalyan, V. A. Lyubimov, B. N. Moiseev, and A. A. Khrimyan. Investigation of the Nature and Spectra Produced by High-Energy Nucleons — 280.

Alikhanov, R. A. Neutron Diffraction Investigation of the Antiferromagnetism of the Carbonates of Manganese and Iron — 1204.

Alikhanyan, A. I. and F. R. Arutyunyan. The Scattering of Muons in Lead — 23.

Alimov, Yu. I. (see Skrotskiĭ, G. V.) — 899.

Alkhazov, D. K., A. P. Grinberg, I. Kh. Lemberg, and V. V. Rozhdestvenskiĭ. Coulomb Excitation of Neon — 222L.

Ansel'm, A. A. A Model of a Field Theory with Nonvanishing Renormalized Charge — 608.

— and V. N. Gribov. On the Possibility of Determining the Scattering Amplitudes from the Analysis of the $\gamma + p - N + \pi + \pi$ Reactions Near Threshold — 1345.

Anton'eva, N. M., A. A. Bashilov, B. S. Dzhelepov, and B. K. Preobrazhenskiĭ. Gd^{146} and Eu^{146} Conversion-Electron Spectra — 20.

Artyushkov, E. V. (see Karchevskiĭ, A. I.) — 442L.

Arutyunyan, F. R. Determination of Charged Particle Mass from Scattering and Residual Range in Multiplate Cloud Chambers — 697.

— (see Alikhanyan, A. I.) — 23.

Arutyunyan, V. M. and R. M. Muradyan. Scattering of Dirac Particles in the Second Born Approximation — 1094.

— (see Sokolov, A. A.) — 412.

Askar'yan, G. A. Acceleration of Charged Particles in Running or Standing Electromagnetic Waves — 430L.

Astaf'ev, V. A. Dual Scattering of Relativistic Pions by Nucleons — 70.

Azhgireĭ, L. S., I. K. Vzorov, V. P. Zrelov, M. G. Meshcheryakov, B. S. Neganov, R. M. Ryndin, and A. F. Shabudin. Interaction between 660-Mev Protons and Atomic Nuclei and the Nuclear Internal Momentum Distribution of Nucleons — 1163.

Babetskiĭ, Ya. S. (see Vernov, S. N.) — 691.

Bakulina, I. N. and N. I. Ionov. Determination of the Ionization Potential of Uranium by a Surface Ionization Method — 709.

Balandin, M. P., V. A. Moiseenko, A. I. Mukhin, and S. Z. Otvinovskiĭ. An Investigation of $\pi^+ + \mu^+ - e^+$ Decay with the Aid of a Propane Bubble Chamber and Scintillation Counters — 296.

Balashko, Yu. G., I. Ya. Barit, and Yu. A. Goncharov. Scattering of Protons on Tritons at Small Energies — 1378L.

Balashov, V. V. Nuclear Forces and Levels of the Lithium Isotopes — 798.

— On the Phase Factors for Transition from "Particle" to "Hole" States in the Nuclear Shell Theory — 988.

— and A. F. Tulinov. On the Question of Collective Effects in Light Nuclei — 426L.

Baldin, S. A. and V. I. Man'ko. Polarization of Protons Scattered by C^{12} — 1377L.

Baradzeĭ, L. T., M. V. Solov'ev, Z. I. Tulinova, and L. I. Filatova. Momentum Spectrum of Particles of the Hard Component of Cosmic Rays at an Altitude of 9 km — 1151.

Baranov, I. A. (see Protopopov, A. N.) — 650L.

— (see Protopopov, A. N.) — 1143L.

— (see Protopopov, A. N.) — 1374L.

Barashenkov, V. S. and Huang Nen-Ning. Non-Uniqueness of the Phase Shift Analysis of Proton-Proton Collisions — 587.

— and Huang Nen-Ning. Nucleon Interaction Cross Sections at 9 Bev Energy — 935L.

— and V. M. Mal'tsev. Production of Strange Particles

in 3-Bev p-p Collisions — 659L.
— (see Blokhintsev, D. I.) — 1145L.
Barbashov, B. M. (see Blokhintsev, D. I.) — 1145L.
Barit, I. Ya. (see Balashko, Yu. G.) — 1378L.
Barsukov, K. A. On the Doppler Effect in an Anistropic and Gyrotropic Medium — 1052.
Bar'yakhtar, B. G. (see Akhiezer, A. I.) — 146.
Bashilov, A. A. (see Anton'eva, N. M.) — 20.
Bayatyan, G. L., I. M. Gramenitskiĭ, A. A. Nomofilov, M. I. Podgoretskii, and E. S. Skrzypczak. Generation of Neutral Pions in the Interaction between 9 Bev Protons and Photographic Emulsion Nuclei — 483.
Baz', A. I. Resonance Effects in the Scattering of Particles Near a Reaction Threshold — 1256.
Bedenov, A. A. Thermodynamic Properties of a Degenerate Plasma — 446L.
Bedritskiĭ, A. I. Radiation from a Spin-2 Particle Moving Uniformly in a Medium — 234L.
Begiashvili, G. A. and É. V. Gedalin. Cerenkov Radiation of a Magnetic Dipole in an Anisotropic Medium — 1379L.
Belokon', B. A. Disappearance of the Isothermal Jump at Large Radiation Density — 235L.
— Belokon', V. A. The Permanent Structure of Shock Waves with Joule Dissipation — 932L.
Belousov, A. S., B. B. Govorkov, and V. I. Gol'danskiĭ. Generalized Form of the Dependence of the Pion Cross Section in Complex Nuclei on the Number of Nucleons — 164.
Belov, K. P. and Z. D. Sirota. Effect of Atomic Ordering on Exchange Interaction in the Fe_3Pt Alloy — 752.
— M. A. Zaĭtseva, and L. A. Malevskaya. Magnetic and Resonance Properties of Yttrium Ferrite-Garnets with Replacement of Fe^{3+} and Al^{3+} Ions — 138L.
— M. A. Zaĭtseva, and A.V. Ped'ko. Magnetic Properties of Gadolinium Oxides — 1191.
Berdyshev, A. A. and B. V. Karpenko. Indirect Coupling of d Electrons in Transition Metals. I. Ferromagnetism — 577.
Berestetskiĭ, V. B. and I. Ya. Pomeranchuk. Beta-Interaction and Nucleon Formfactor — 936L.
Berlovich, É. Z., V. G. Fleĭsher, V. I. Breslav, and B. K. Preobrazhenskiĭ. Quadrupole Moment of Er^{168} — 1128L.
Beshidze, V. L. Thermodynamic Theory of Ferromagnetic Absorption — 654L.
Bezuglyĭ, P. A., A. A. Galkin, and A. P. Korolyuk. Anisotropy of the Absorption Coefficients of Ultrasonics in Superconductors — 1388.
Bilen'kiĭ, S. M. A Possible Method for the Determination of the Parity of Strange Particles — 199.
— and R. M. Ryndin. On the Relativistic Relation Between Polarization and Asymmetry — 1144L.
Birbrair, B. L., L. K. Peker, and L. A. Sliv. Quadrupole Oscillations of Deformed Nuclei — 566.
Birger, N. G. and Yu. A. Smorodin. The Kinematics of Elementary Interactions — 823.
Bizina, G. E. (see Burgov, N. A.) — 1146L.
Blokhintsev, D. I., V. S. Barashenkov, and B. M. Barbashov. Electromagnetic Structure of the Proton and Neutron — 1145L.
Blokhintsev, L. D. Adsorption of Polarized Negative Muons by Nuclei and Neutron Polarization — 175.
Bochvar, D. A., N. P. Gambaryan, I. V. Stankevich, and A. L. Chistyakov. On Some Symmetry Properties of the Eigenfunctions of the Schrödinger Equation — 435L.
Bogdanovich, L. S. Radiation from a Current-Carrying Ring Moving Uniformly in a Plasma Situated in a Magnetic Field — 589.
Bogdanov, G. F., N. A. Vlasov, C. P. Kalinin, B. V. Rybakov, L. N. Samoĭlov, and V. A. Sidorov. The Reaction $T(p, n)He^3$ at 7 — 12 Mev Proton Energy — 440L.
Bonch-Bruevich, V. L. A Method of Evaluating Electrical Conductivity — 653L.
Borgardt, A. A. A Dynamical Principle for Second-Order Equations — 1371L.
Borovik, E. S. and V. G. Volotskaya. Investigation of Galvanomagnetic Phenomena in Chromium at Low Temperatures — 1175.
Borovik-Romanov, A. S. Investigation of Weak Ferromagnetism in the $MnCO_3$ Single Crystal — 539.
— Piezomagnetism in the Antiferromagnetic Fluorides of Cobalt and Manganese — 1390L.
Borovskiĭ, I. B. and K. P. Gurov. Effect of Impurities on the X-Ray Spectra of Transition Metals — 856.
Borzunov, N. A., D. V. Orlinskiĭ, and S. M. Osovets. Investigation of High Current Pulse Discharges in Conical Chambers — 502.
Boyarkina, A. N. and A. F. Tulinov. Lifetime of the First Excited State in Be^{10} — 244.
Breslav, V. I. (see Berlovich, E. E.) — 1128L.
Brodskiĭ, A. M. and D. D. Ivanenko. Anomalous Spinors and Bosons — 907.
Budagov, Yu. A., S. Viktor, V. P. Dzhelepov, P. F. Ermolov, and V. I. Moskalev. Observation of the $-e^- + e^+ + e^- + e^+$ Decay — 767.
Buishvili, L. L. On the Overhauser Effect in Saturation of Forbidden Resonance — 1396L.
Burgov, N. A., A. V. Davydov, and G. R. Kartashov. Lifetime of the First Excited States of Rb^{85} and Pr^{141} — 1384L.
— Yu. V. Terekhov, and G. E. Bizina. Resonant Scattering of Gamma Rays by Ni^{60} — 1146L.
Charakhch'yan, A. N. (see Rymko, N. P.) — 1202.
Chasnikov, I. Ya. (see Grauovskiĭ, Ya. I.) — 795.
Cheishvili, O. D. (see Matinyan, S. G.) — 143.
Chen Chun-Sian and Chou Shih-Hsun. The Basic Compensation Equation in Superconductivity Theory when the Coulomb Interaction is Taken into Account — 885.
Chetkin, M. V. (see Krinchik, G. S.) — 1368L.
Chicherin, A. G. Amplitude to Reconstruct the Potential Near its Boundary — 1368L.
Chistyakov, A. L. (see Bochvar, D. A.) — 435L.
Chizhov, V. P. and L. A. Kul'chitskiĭ. Intermediate-Energy Photodeuterons from C^{12} and Be^9 — 239.
Chou Kuang-Chao. Reactions Involving Polarized Particles of Zero Rest Mass — 642.
— Some Symmetry Properties in Process of Antihyperon Production with Annihilation of Antinucleons — 663L.
— (see Ogievetskiĭ, V. I.) — 179.
Chou Shih-Hsun (see Chen Chun-Sian) — 885.
Chueva, S. A. (see Varfolomeev, A. A.) — 495.
Daĭon, M. I. and L. I. Potapov. Measurement of the Mass of Cosmic-Ray Particles Underground — 650L.

— and L. I. Potapov. Underground Muon Spectrum at ~ 40 Meter Water Equivalent — 488.
Darovskikh, V. F. and N. A. Perfilov. Bi Fission at Very High Excitation Energies — 456.
Davydov, A. S. Rotational States of Odd Nuclei Without Axial Symmetry — 1103.
— and G. F. Filippov. On the Shape of Even-Even Nuclei — 1061.
— and V. S. Rostovskiĭ. Transition Probabilities between the Levels of the Rotational Band of Non-Axial Nuclei — 1275.
— and D. A. Zaikin. Gamma Oscillations of the Surface of an Atomic Nucleus — 157.
Davydov, A. V. (see Burgov, N. A.) — 1384L.
Deĭgen, M. F. and A. B. Roĭtsin. Paramagnetic Resonance of F Centers in Static Magnetic Fields of Arbitrary Strength — 120.
Delyagin, N. N. and M. Preĭsa. M1-Transition in V^{51} and the Seniority Quantum Number — 1127L.
Demirkhanov, R. A., T. I. Gutkin and V. V. Dorokhov. Mass of the Isotope Pu^{239} — 1134L.
Demkov, Yu. N. Symmetry Group of the Isotropic Oscillator — 63.
— and A. M. Ermolaev. Fock Expansion for the Wave Functions of a System of Charged Particles — 633.
Dmitriev, V. A., G. V. Kulikov, E. I. Massalskiĭ, and G. B. Khristiansen. Lateral Distribution of the Energy Flux of the Electron-Photon Component of Extensive Air Showers — 702.
— (see Abrosimov, A. T.) — 528.
Dobretsov, Yu. P. (see Ali-Zade, S. A.) — 940L.
Dobrokhotov, E. I., V. R. Lazarenko, and S. Yu. Luk'yanov. A Search for Double Beta Decay in Ca^{48} — 54.
Dobrynin, Yu. P. (see Sosnovskiĭ, A. N.) — 717.
Dolginov, A. Z. and N. P. Popov. Polarization of Beta Particles and Beta-Gamma Correlation for First-Forbidden Transitions of Oriented Nuclei — 368.
Dolgoshein, B. A. and B. I. Luchkov. Polarization of the Meson Current at Sea Level — 445L.
— (see Kirillov-Ugryumov, V. G.) — 290.
Dolinskiĭ, É. I. Absorption of μ^--mesons by Polarized Nuclei. Angular Distribution of the Neutrons — 838.
Dorokhov, V. V. (see Demirkhanov, R. A.) — 1134L.
Dovzhenko, O. I., S. I. Nikol'skiĭ, and I. V. Rakobol'skaya. Cloud Chamber Investigation in the Cores of Extensive Air Showers — 11.
Drozdov, S. I. The Excitation of Collective States in Nuclei by Scattering of Charged Particles — 1335.
Druin, V. A. (see Polikanov, S. M.) — 522.
Dunaĭtsev, A. F. and Yu. D. Prokoshkin. The Reaction $p + p \rightarrow p + p + \pi^0$ in the Energy Range from Threshold to 665 Mev — 1179.
Dzhelepov, B. S. (see Anton'eva, N. M.) — 20.
Dzhelepov, V. P. (see Bugdanov, Yu. A.) — 767.
— (see Golovin, B. M.) — 302.
— (see Golovin, B. M.) — 516.
Dzhrbashyan, V. A. A Possible Method for the Determination of the Direction of Polarization of μ^- Mesons — 1115L.
— Angular Distribution and Angular Correlation of the Radiations from Nuclei with Oriented Electron Shells — 881.
— Depolarization of the Negative Muon in Mesic-Atom Transitions — 188.
Dzyaloshinskiĭ, I. E. and L. P. Pitaevskiĭ. Van der Waals Forces in an Inhomogeneous Dielectric — 1282.
— (see Abrikosov, A. A.) — 636.
Dyatlov, I. T. Dispersion Relations for the Electromagnetic Form Factor of the Pion — 351.
Éĭdman, V. Ya. Correction to the Paper by V. Ya. Éĭdman "Radiation of an Electron Moving in a Magneto-Active Plasma" — 947L.
— (see Ginzburg, V. L.) — 1300.
Éĭsmont, V. P. (see Protopopov, A. N.) — 1116L.
— (see Protopopov, A. N.) — 1143L.
— (see Protopopov, A. N.) — 650L.
— (see Protopopov, A. N.) — 386L.
Eliseev, G. P. (see Alikhanov, A. I.) — 280.
Emel'yanov, A. A. Viscosity in the Hydrodynamic Theory of Multiple Particle Production — 1100.
Ergakov, V. A. (see Trebukhovskiĭ, Yu. V.) — 931L.
Ermolaev, A. M. (see Demkov, Yu. N.) — 633.
Ermolov, P. F. (see Budagov, Yu. A.) — 767.
Esel'son, B. N., M. I. Kaganov, and I. M. Lifshitz. Reply to the Letter by M. P. Mokhnatkin — 681L.
Éstulin, I. V. (see Kalinkin, L. F.) — 1146L.
Faĭn, V. M. On the Theory of the Coherent Spontaneous Emission — 562.
Faĭnberg, V. Ya. On Analytic Properties of Casual Commutators — 1066.
Fakidov, I. G. and V. P. Krasovskiĭ. The Magnetization and Magnetocaloric Effect of Manganese Phosphide — 755.
Fedorenko, N. V., V. V. Afrosimov, R. N. Il'in, and D. M. Kaminker. Dissociation of the Molecular H_2^+ in Collisions with Gases — 267.
— (see Il'in, R. N.) — 29.
Fetisov, I. K. Wall Probe in a Magnetic Field — 789.
Fikhtengol'ts, I. G. Geodesics in Friedman-Lobachevsky Space — 937L.
Filatova, L. I. (see Baradzeĭ, L. T.) — 1151.
Filimonov, A. I. (see Peshkov, V. P.) — 734.
Filimonov, V. A. Saturation in a Hyperon System — 1380L.
— On the Depth of the Potential Well Λ Particles in Heavy Hypernuclei — 1113L.
Filippov, G. F. (see Davydov, A. S.) — 1061.
Filippova, K. V. (see Volkov, V. V.) — 536.
Filov, R. A. (see Ostroumov, V. I.) — 254
Firsov, O. B. A Qualitative Interpretation of the Mean Electron Excitation Energy in Atomic Collisions — 1076.
Fisher, I. Z. (see Prokhorenko, V. K.) — 928L.
Fleĭsher, V. G. (see Berlovich, E. E.) — 1128L.
Flerov, G. N., V. I. Kalashnikova, A. V. Podgurskaya, E. D. Vorob'ev, and G. A. Stolyarov. High-Energy Neutrons in Cosmic Rays — 511.
Fogel', Ya. M., V. F. Kozlov, and A. A. Kalmykov. On the Existence of the Negative Nitrogen Ion — 963.
— V. F. Kozlov, A. A. Kalmykov, and V. I. Muratov. Direct Proof of the Applicability of the Massey Adiabatic Criterion to Processes of Double Charge Exchange — 929L.
Fomichev, V. A. (see Karamyan, A. S.) — 979.

Fong Soy-Cen (see Kolomenskiĭ, A. A.) — 184.
Forafontov, N. F., and A. A. Sorokin. Concerning the Ce^{141} Decay Scheme — 227L.
Fradkin, E. S. A Refinement of the Thomas-Fermi Model at Small Distances — 1087.
— On a Relation in Quantum Statistics — 872L.
— The Green's Function Method in Quantum Statistics — 912.
Frank, I. M. The Role of Group Velocity of Light Emitted in a Refractive Medium — 580.
Freĭdman, G. I. (see Gaponov, A. V.) — 675L.
Gabovich, M. D. and L. L. Pasechnik. Anomalous Electron Scattering and the Excitation of Plasma Oscillations — 727.
Gachechiladze, T. G. (see Mdivani, O. M.) — 1131L.
Gaĭdukov, Yu. P. (see Alekseevskiĭ, N. E.) — 311.
Galkin, A. A. and A. P. Korolyuk. Anisotropy of the Absorption Ultrasound in Metals in a Magnetic Field — 925L.
— (see Bezuglyĭ, P. A.) — 1388L.
Gal'perin, F. M. (Connection between Structural and Magnetic Parameters of the Transition Metals — 862.
Gambaryan, N. P. (see Bochvar, D. A.) — 435L.
Gandel'man, G. M. Correlation between the Direction of an Internal Bremsstrahlung Quantum and Circular Polarization of a Gamma Quantum Emitted by an Excited Nucleus after K Capture — 406.
— and V. N. Mokhov. Radiative Capture of Polarized Mesons by Nuclei — 296.
Gaponov, A. V. and G. I. Freĭdman. On Electromagnetic Shock Waves in Ferrites — 675L.
Gaponov, Yu. V. Beta-Gamma Correlation in First-Forbidden Beta Transitions — 131.
Garber, R. I. and L. M. Polyakov. Investigation of the Initial Stages of Plastic Deformation of Rock-Salt — 1158.
— I. A. Gindin, and Yu. V. Shubin. Slipping of Beryllium Single Crystals at Low Temperatures. III. — 260.
Garif'yanov, N. S. Resonance Transitions in Parallel Fields in Certain Mn^{++} and Fe^{+++} Crystals — 1393L.
Gedalin, E. V. (see Begiashvili, G. A.) — 1379L.
Geĭlikman, B. T. Breakup of a Charged Liquid Drop and Nuclear Fission — 168.
— and V. Z. Kresin. On the Heat Conductivity and Attenuation of Sound in Superconductors — 677L.
Gerasimova, R. I. (see Varfolomeev, A. A.) — 495.
Gerlit, Yu. B. (see Karamyan, A. S.) — 431L.
Gershteĭn, S. S. Ranges of Mu-Mesic Atoms in Hydrogen Chambers — 927L.
Geshkenbeĭn, B. V., S. A. Nemirovskaya, and A. P. Rudik. Polarization of Beta-Electrons from RaE — 360.
Gindin, I. A. (see Garber, R. I.) — 260.
Ginzburg, V. L. Comparison of the Macroscopic Theory of Superconductivity with Experimental Data — 1372L.
— and V. Ya. Éĭdman. The Radiation Reaction in the Motion of a Charge in a Medium — 367.
Glagolev, V. L., O. M. Kovrizhnykh, Yu. V. Makarov, and P. A. Yampol'skiĭ. Millisecond Half-Life Isomers Produced in Reactions Involving 14-Mev Neutrons — 742.
Gnedich, A. V., L. N. Kryukova, and V. V. Murav'eva. Concerning a 100-kev Transition in the Spectrum of Ce^{144} — 226L.
Gol'danskiĭ, V. I. Direct Neutron-Exchange Interaction of Complex Nuclei — 366.
— and Ya. A. Smorodinskiĭ. Singularities of the S Matrix and the ρ^0 Meson. — 1387L.
— (see Belousov, A. S.) — 164.
Gol'din, L. L., G. I. Novikova, and K. A. Ter-Martirosyan. On the Shape of Alpha-Active Nuclei — 356.
— (see Tret'yakov, E. F.) — 250.
Golovin, B. M., V. P. Dzhelepov, Yu. V. Katyshev, A. D. Konin, and S. V. Medved'. Scattering of 590-Mev Neutrons by Protons in the Small Angle Region — 516.
—, V. P. Dzhelepov, V. S. Nadezhdin, and V. I. Satarov. On Possible Sets of Experiments for Simultaneous Analysis of Data on Nucleon-Nucleon Scattering and Polarization in p-n Collisions at 635 Mev — 302.
Goncharov, Yu. A. (see Balashko, Yu. G.) — 1378L.
Gorchakov, E. V. (see Vernov, S. N.) — 877.
Gor'kov, L. P. Microscopic Derivation of the Ginzburg-Landau Equation in the Theory of Superconductivity — 1364.
— (see Abrikosov, A. A.) — 220L.
— (see Abrikosov, A. A.) — 636.
Goryunov, N. N. (see Vernov, S. N.) — 468.
— (see Vernov, S. N.) — 691.
Govorkov, B. B. (see Belousov, A. S.) — 164.
Gramenitskiĭ, I. M. (see Bayatyan, G. L.) — 483.
Granovskiĭ, Ya. I. Concerning the ρ^0 Meson — 433L.
— Simplification of the Formulas for Statistical Weight Calculations — 923L.
— The Mass Spectrum of Mesons in Heisenberg's Theory — 819.
— and I. Ya. Chasnikov. On the Analysis of High-Energy Showers — 795.
Grashin, A. F. Angular Correlations Near Multiple-Production Thresholds — 290.
— Nucleon-Nucleon Scattering in High Angular Momentum States — 1223.
Grechishkin, V. S. Line Width of the Chlorine Quadrupole Resonance in Chlorates of Barium, Sodium, and Potassium — 438L.
Gribov, V. N. Renormalization of the Vertex Part in Pseudoscalar Meson Theory — 384.
— (see Ansel'm, A. A.) — 376.
Grigor'ev, E. P. and A. V. Zolotavin. Relative Probabilities for the Photoeffect in Shells and Subshells of the Atom — 272.
Grigor'ev, V. K. (see Trebukhovskiĭ, Yu. V.) — 931L.
Grigorov, N. L., V. S. Murzin, and I. D. Rapoport. Interaction between 10^{11} – 10^{12} ev Particles and Iron Nuclei — 759.
Grinberg, A. P. (see Alkhazov, D. G.) — 222L.
Grishin, V. G. and M. I. Podgoretskiĭ. Remarks on the Optical Model of the Nucleus — 1132L.
Gurevich, A. V. Hysteresis and Non-Stationary Effects in the Electron Temperature in Plasma in Inert Gases — 434L.
Gurevich, I. I. (see Ali-Zade, S. A.) — 940L.
Gurov, K. P. (see Borovskiĭ, I. B.) — 856.
Guseĭnov, I. I. The Elastic Scattering of Polarized Dirac Particles by a Short Range Center of Force in the Damping Theory — 228L.

Guseva, L. I. (see Volkov, V. V.) — 536.
Guseva, M. I., E. V. Inopin, and S. P. Tsytko. Depth of Penetration and Character of Distribution of Atoms Injected into Si^{30} Isotope Targets — 1.
Gutkin, T. I. (see Demirkhanov, R. A.) — 1134L.
Guzhavin, V. V. and I. P. Ivanenko. On the Dependence of the Angle between the Direction of Motion of Shower Particles and the Axis of the Shower on the Distance from the Axis — 1070.
Gvozdev, V. S. and Yu. L. Khazov. Cross Section of Te^{125m} Production via the (n, γ) Reaction — 439L.
Huang Nen-Ning (see Barashenkov, V. S.) — 587.
— (see Barashenkov, V. S.) — 935L.
Il'in, R. N., V. V. Afrosimov, and N. V. Fedorenko. Ionization of Air by H^+ and H_2^+ Ions — 29.
— (see Fedorenko, N. V.) — 267.
Inopin, E. V. (see Guseva, M. I.) — 1.
— (see Vysotskiĭ, G. L.) — 398.
Iogansen, L. V. Quantum Corrections to Radiation from a Rigid Rotator — 216L.
Ionov, N. I. (see Bakulina, I. N.) — 709.
Ishmukhametov, B. Kh. (see Vlasov, K. B.) — 921L.
Ivanchik, I. I. Diffraction Stripping of Relativistic Particles — 427L.
— and V. S. Popov. Energy and Angular Distribution in Diffraction Processes — 347.
Ivanenko, D. D. (see Brodskiĭ, A. M.) — 907.
Ivanenko, I. P. (see Guzhavin, V. V.) — 1070.
— (see Vernov, S. N.) — 877.
Ivanter, I. G. Polarization Correlation in Coulomb Scattering of Electrons and Muons by Light Nuclei Including Radiation Corrections — 224L.
— Polarization in Pair Production by Circularly Polarized Quanta — 777.
— Relation between the Gravitational Constant, the Charge-to-Mass Ratio of the Electron and the Fine-Structure Constant — 1380L.
Kaganov, M. I. and V. M. Tsukernik. Phenomenological Theory of Kinetic Processes in Ferromagnetic Dielectrics. II. Interaction of Spin Waves with Phonons — 151.
— (see Esel'son, B. N.) — 681L.
Kaĭtmazov, S. D. and A. M. Prokhorov. Electronic Paramagnetic Resonance Spectra of Frozen OH Radicals — 944L.
Kalashnikova, V. I. (see Flerov, G. N.) — 511.
Kalinin, S. P. (see Bogdanov, G. F.) — 440L.
Kalinkin, B. N. Resonance Scattering of Low-Energy Gamma Rays on Nuclei — 1022.
Kalinkin, L. F., A. S. Melioranskiĭ, and I. V. Éstulin. Certain Gamma Transitions in I^{128} and in Neodymium Isotopes — 1146L.
Kalitsin, N. S. Concerning Ryabushko's Work, "On the Equations of Motion of Rotating Masses in the General Theory of Relativity" — 1112L.
Kalmykov, A. A. (see Fogel', Ya. M.) — 929L.
— (see Fogel', Ya. M.) — 963.
Kamalyan, V. Sh. (see Alikhanov, A. I.) — 280.
Kaminker, D. M. (see Fedorenko, N. V.) — 267.
Kaminskiĭ, A. K. and Yu. M. Shirokov. On the Electromagnetic Radii of the Lightest Nuclei in the Ground and Lowest Excited States — 616.
Kaplan, S. A. On the "Larmoron" Plasma Theory — 1370L.
Karamyan, A. S., Yu. B. Gerlit, and B. F. Myasoedov. Concerning the Production of Compound Nuclei in the Interaction between Atomic Nuclei — 431L.
—, L. I. Rusinov, and V. A. Fomichev. Production of Mo^{93m} in the Reaction $Se^{80}(O^{16}, 3n)$.
Karchevskiĭ, A. I. Magnetocaloric Effect in Uranium Hydride and Deuteride — 443L.
—, E. V. Artyushkov, and L. I. Kikoin. Isotopic Shift of the Curie Point in Uranium Hydride and Deuteride — 442L.
Karnaukhov, V. A. Interaction between Accelerated Nitrogen Nuclei and Bismuth — 1375L.
—, G. M. Ter-Akop'yan, and V. I. Khalizev. Two-Neutron Capture Reaction in the Interaction between N^{14} and Nuclei of Some Elements — 525.
Karpenko, B. V. (see Berdyshev, A. A.) — 577.
Kartashov, G. R. (see Burgov, N. A.) — 1384L.
Katyshev, Yu. V. (see Golovin, B. M.) — 516.
Kazarov, R. E. Hodoscope Investigation of the Penetrating Component of Extensive Air Showers — 35.
Kel'man, V. M. and R. Ya. Metskhvarishvili. Exact Measurement of the Ratios of Internal-Conversion Coefficients of 411.7-kev Gamma Quanta in Hg^{198} — 486.
Kerimov, B. K. (see Sadykhov, F. S.) — 938L.
Kessel', A. R. Resonance Absorption of Ultrasound on Nuclei — 1031.
Khalatnikov, I. M. The Influence of Anisotropy on the Thermal Conductivity of Superconductors — 1296.
Khalfin, L. A. New Dispersion Relations in Quantum Field Theory — 774.
Khalizev, V. I. (see Karnaukhov, V. A.) — 525.
Kharadze, G. A. On the Influence of the Isobaric State of a Nucleon on the Electron-Neutron Interaction — 1119L.
Kharlamov, S. P., M. I. Adamovich, and V. G. Larionova. On the Magnitude of the Radio σ^-/σ^+ Near the Threshold of Meson Production — 668L.
Khazov, Yu. L. (see Gvozdev, V. S.) — 439L.
Kheifets, S. A. On a Possible Determination of the Sign of Muon Polarization — 1128L.
Khlebnikov, G. I. (see Tretyakov, E. F.) — 250.
Khokhlov, Yu. K. On the Moment of Inertia of a Many-Particle System; I. — 203.
Khrimyan, A. V. (see Alikhanov, A. I.) — 280.
Khristiansen, G. B. (see Abrosimov, A. T.) — 528.
— (see Dmitriev, V. A.) — 702.
— (see Vernov, S. N.) — 691.
— (see Vernov, S. N.) — 468.
— (see Vernov, S. N.) — 877.
Kikoin, L. I. (see Karchevskiĭ, A. I.) — 442L.
Kirillov-Ugryumov, V. G., B. A. Dolgosheĭn, A. M. Moskvichev, and L. P. Morozov. Scattering of Muons with Momenta Near 100 Mev/c by Copper and Iron — 290.
Klimentovskaya, M. V. and P. I. Shavrin. An Investigation of the Excited States of Re^{187} — 269.
Klimontovich, Yu. L. Charged Particle Energy Losses Due to Excitation of Plasma Oscillations — 999.
Kocharov, G. E., A. P. Komar, and G. A. Korolev. Energy Spectra of Alpha Particles from the Long-Lived Isotopes Th^{232} and U^{238} — 48.
Kokin, A. A. On the Theory of Electron Paramagnetic

Resonance in Electrolyte Solutions — 353.
— (see Skrotskiĭ, G. V.) — 116.
— (see Skrotskiĭ, G. V.) — 335.
— (see Skrotskiĭ, G. V.) — 658L.
Kolachevskiĭ, N. N. Measurement of the Noise of Cyclic Remagnetization of Ferromagnetic Substances at Low Temperatures — 278.
Kolomeets, E. V. Small Effects of Solar Flares and the Energy Spectrum of Primary Variation of Cosmic Rays — 960.
Kolomenskiĭ, A. A. and Fong Soy-Cen. Cyclic Motion of Charged Particles in an Electric Field — 184.
Kolomin, L. G. (see Miryasov, N. Z.) — 1376L.
Komar, A. A. and M. A. Markov. On a Certain Version of Nonlocal Electromagnetic Field Theory — 602.
Komar, A. P. (see Kocharov, G. E.) — 48.
Komarov, V. V. and A. M. Popova. Direct Interaction in Reactions with Emission of Two Nucleons — 1118L.
Kondrat'ev, L. N. (see Tret'yakov, E. F.) — 250.
Kondrat'ko, M. Ya. (see Kovrigin, B. S.) — 217L.
Konin, A. D. (see Golovin, B. M.) — 516.
— (see Zinov, V. G.) — 1386L.
Kopylov, G. I. Results of a Model of the p-p Interaction at 10 Bev — 1136L.
Kopylova, D. K., Yu. B. Korolevich, N. I. Petukhova, and M. I. Podgoretskiĭ. Determination of the Frequency of Capture of Slow Mesons by Light and Heavy Nuclei in Photoemulsions — 1391L.
Korenchenko, S. M. (see Zinov, V. G.) — 429L.
— (see Zinov, V. G.) — 1386L
Kornienko, L. S. and A. M. Prokhorov. A Paramagnetic Amplifier and Generator, Using Fe^{3+} Ions in Corundum — 649L.
Korolev, G. A. (see Kocharov, G. E.) — 48.
Korolevich, Yu. B. (see Kopylova, D. K.) — 1391L.
Korolyuk, A. P. (see Bezuglyi, P. A.) — 1388L.
— (see Galkin, A. A.) — 925L.
Kostanashvili, N. I. and O. A. Shakhulashvili. Production of Strange Particles in the Interaction between 9-Bev Protons and Emulsion Nuclei — 713.
Kotkin, G. L. Ultrasonic Attenuation in Metals — 664L.
Kovrigin, B. S., M. Ya. Kondrat'ko, and K. A. Petrzhak. Energy Spectrum of Fragments from the Photofission of U^{238} — 217L.
Kovrizhnykh, L. M. Motion of a Plasma Loop in an Axially Symmetric Magnetic Field — 1308.
— Oscillations of a Completely Ionized Plasma in a Cylindrical Cavity — 592.
Kovrizhnykh, O. M (see Glagolev, V. L.) — 742.
Kozak, M. I. (see Zhuravlev, V. A.) — 236L.
Kozlov, V. F. (see Fogel', Ya. M.) — 967.
— (see Fogel', Ya. M.) — 929L.
Koz'minykh, M. D. (see Mitsuk, V. E.) — 1139L.
Krasovskiĭ, V. P. (see Fakidov, I. G.) — 755.
Kravtsov, V. A. Empirical Regularities in the Nucleon Pair Production Energies in Nuclei — 871.
Kresin, V. Z. On the Problem of Thermal Conductivity and Absorption of Sound in Superconductors — 1385L.
— (see Geilikman, B. T.) — 677L.
Kresnin, A. A. (see Visotskiĭ, G. L.) — 398.
Krinchik, G. S. and M. V. Chetkin. The Problem of Determining the Dielectric-Permittivity and Magnetic-Permeability Tensors of a Medium — 1368L.
— and R. D. Nuralieva. Magneto-Optical Resonance in Nickel at Infrared Frequencies — 724.
Kryukova, L. N. (see Gnedich, A. V.) — 226L.
Kucherov, R. Ya. and L. É. Rikenglaz. Slipping and Temperature Discontinuity at the Boundary of a Gas Mixture — 1253.
Kul'chitskiĭ, L. A. (see Chizhov, V. P.) — 239.
Kulikov, G. V. (see Abrosimov, A. T.) — 528.
— (see Dmitriev, V. A.) — 702.
— (see Vernov, S. N.) — 691.
— (see Vernov, S. N.) — 468.
Kurdgelaidze, D. F. Theory of the Nonlinear Field $(\Box - \lambda\varphi^2)\varphi = 0$ — 594.
Kurepin, A. B. and V. G. Neudachin. Comparison of the Differential Cross Sections for the (dp) and (dt) — 1229.
Kutikov, I. E. (see Sosnovskiĭ, A. N.) — 717.
Lapidus, L. I. Estimate of the Contribution of Nucleon-Antinucleon Interaction in the Dispersion Relation for Nucleon-Nucleon Scattering — 193.
Larionova, V. G. (see Kharlamov, S. P.) — 668L.
Larkin, A. I. (see Vedenov, A. A.) — 806.
Lazarenko, V. R. (see Dobrokhotov, E. I.) — 54.
Lazarev, B. G. and O. N. Ovcharenko. The Energy of Formation and Migration of Vacancies in Gold and Platinum — 42.
Lazukin, V. N. Oscillations of a Plasma in a Magnetic Field at Frequencies Close to the Cyclotron Frequency — 685.
— Some Features of Multiplet Ferromagnetic Resonance in Ferrites — 477.
Lemberg, I. Kh. (see Alkhazov, D. G.) — 222L.
Leonov, G. S. (see Zaĭtsev, A. A.) — 944L.
Levanyuk, A. P. Contribution to the Theory of Light Scattering near the Second-Order Phase-Transition Points — 571.
Lifshitz, I. M. (see Esel'son, B. N.) — 681L.
Loginov, Yu. E. and K. I. Yakovlev. The Gamma Rays of As^{74} — 664L.
Loktionov, A. A. and Zh. S. Takibaev. Production of Pions by High-Energy Cosmic-Ray Alpha Particles — 1209.
Loskutov, Yu. M. (see Sokolov, A. A.) — 657L.
Luchkov, B. I. (see Dolgosheĭn, B. A.) — 445L.
Luk'yanov, S. Yu. and V. I. Sinitsin. Spectroscopic Investigation of an Intense Pulsed Discharge in Hydrogen. III. Determination of the Parameters of a High-Temperature Plasma — 1155.
— (see Dobrokhotov, E. I.) — 54.
Lysov, B. A. Particle Energy Losses Due to the Excitation of Longitudinal Waves — 221L.
Lyubarskiĭ, G. Ya. and R. V. Polovin. The Disintegration of Unstable Shock Waves in Magnetohydrodynamics — 902.
Lyubimov, V. A. (see Alikhanov, A. I.) — 946L.
— (see Alikhanov, A. I.) — 280.
Magalinskiĭ, V. B. Angular Momentum and Parity Conservation Laws in the Statistical Theory of Multiple Production — 67.
— Dynamical Model in the Theory of Brownian Motion — 1381L.

— On the Evaluation of Coordinate Probabilities for Non-Linear Systems by Gibbs' Method — 1011.
— and Ya. P. Terletskiĭ. An Equation for the Diffusion in Phase Space for Nonlinear Systems — 1234.
Makarina, L. A. (see Varfolomeev, A. A.) — 495.
Makarov, Yu. V. (see Glagolev, V. L.) — 742.
Makaryunas, K. V. (see Starodubtsev, S. V.) — 1133L.
Makhnovskiĭ, E. D. Ratio of the Deuteron and Proton Yields in the Photodisintegration of Au^{197} — 519.
Maksimov, L. A. On the Scattering Matrix in an Indefinite Metric — 324.
— Remarks Regarding Heisenberg's Paper on the Lee Model — 97.
Maksimov, M. Z. Breakup of Charged Particles by a Nuclear Coulomb Field — 315L.
— Nuclear Excitation by High Energy Particles — 652L.
Malevskaya, L. A. and G. M. Nurmukhamedov. Temperature Dependence of Ferromagnetic Resonance in Yttrium Ferrite-Garnets — 1137L.
— (see Belov, K. P.) — 1138L.
Mal'tsev, V. M. (see Barashenkov, V. S.) — 659L.
Mandel'shtam, S. L. (see Mazing, M. A.) — 941L.
Man'ko, V. I. (see Baldin, S. A.) — 1377L.
Markov, M. A. (see Komar, A. A.) — 602.
Mashkevich, V. S. Electrical, Optical, and Elastic Properties of Crystals of the Diamond Type. III. Dispersion and Absorption of Light — 76.
— Electrical, Optical, and Elastic Properties of Crystals of the Diamond Type. IV. Interaction between Conduction Electrons and Lattice Vibrations — 1237.
Massal'skiĭ, E. I. (see Abrosimov, A. T.) — 528.
— (see Dmitriev, V. A.) — 702.
Matinyan, S. G. and O. D. Cheishvili. Polarization Effects in Σ^--Hyperon Capture by Deuterons — 143.
— and L. B. Okun'. The K_{e3} and $K_{\mu 3}$ Decays — 933L.
Mazing, M. A. and S. L. Mandel'shtam. Broadening of Spectral Lines in Strongly Ionized Plasma — 941L.
Mdivani, O. M. and T. G. Gachechiladze. The Angular Distribution of Neutrons from the Reaction $C^{13}(d, n)O^{16}$ — 1131L.
Medved', S. V. (see Golovin, B. M.) — 516.
Medvedev, B. A. (see Sklyarevskiĭ, V. V.) — 225L.
Melioranskiĭ, A. S. (see Kalinkin, L. F.) — 1146L.
Mel'nikov, M. A. Statistical Delay of Discharge in NaCl and KBr — 425L.
Meshcheryakov, M. G. (see Azhgireĭ, L. S.) — 1163.
Metskhvarishvili, R. Ya. (see Kel'man, V. M.) — 486.
Mikhaĭlov, G. V. The Influence of Temperature and Pressure on the Raman Spectrum of Nitrogen — 974.
Miller, M. A. Acceleration of Plasmoids by High-Frequency Electric Fields — 1358.
Minervina, Z. V. and E. A. Pesotskaya. Certain Cases of Elastic Scattering of Positrons from π^+-μ^+-e^+ Decay by Emulsion Electrons — 309.
Miryasov, N. Z. and L. G. Kolomin. Magnetic Moments and Curie Points of Ferrites of the Cu-Cd System — 1376L.
Mitskevich, N. V. A Nonlinear Vacuum Effect in Gravitation Theory — 859.
Mitsuk, V. E. and M. D. Koz'minykh. Electric Field in a Microwave Plasma as a Function of Time — 1139L.
Mnev, V. N. (see Zaĭtsev, A. A.) — 1130L.
Moiseenko, V. A. (see Balandin, M. P.) — 296.
Moiseev, B. N. (see Alikhanov, A. I.) — 280.
Mokhnatkin, M. P. On the Thermodynamics of Helium 680L.
Mokhov, V. N. (see Gandel'man, G. M.) — 1073.
Morozov, A. M. and P. A. Yampol'skiĭ. New Short-Lived Isomers As^{75m} and Ga^{70m} Excited by Fast Protons — 671L.
Morozov, L. P. (see Kirillov-Ugryumov, V. G.) — 290.
Moskalenko, S. A. and K. B. Tolpygo. On the Energy Spectrum of a Mott Exciton in Ionic Crystals — 103.
Moskalev, V. I. (see Budagov, Yu. A.) — 767.
Moskvichev, A. M. (see Kirillov-Ugryumov, V. G.) — 290.
Mukhin, A. I. (see Balandin, M. P.) — 296.
Muradyan, R. M. (see Arutyunyan, V. M.) — 301.
— (see Sokolov, A. A.) — 412.
Muratov, V. I. (see Fogel', Ya. M.) — 929L.
Murav'eva, V. V. (see Gnedich, A. V.) — 226L.
Murzin, V. S. (see Grigorov, N. L.) — 759.
Myasoedov, B. F. (see Karamyan, A. S.) — 431L.
Nadezhdin, V. S. (see Golovin, B. M.) — 302.
Nadzhafov, I. M. Pair Production by a Circularly Polarized Photon — 232L.
Nechin, Yu. A. (see Vernov, S. N.) — 468.
— (see Vernov, S. N.) — 691.
Neganov, B. S. (see Azhgirei, L. S.) — 1163.
Nemirovskaya, S. A. (see Geshkenbein, B. V.) — 360.
Nemirovskiĭ, P. É. Calculation of Polarization of Medium-Energy Neutrons — 408.
— On the Stability of Nuclei — 627.
Neudachin, V. G. and Yu. F. Smirnov. Parentage Coefficients in the Generalized Nuclear Model — 127.
—, I. B. Teplov, and O. P. Shevchenko. On the Role Played by Exchange Effects in Stripping Reactions — 599.
— (see Kurepin, A. B.) — 1229.
Nikishov, A. I. A General Formula for the Electromagnetic Scattering of Two Different Particles of Spin $\frac{1}{2}$ — 1140L.
— On the Production of Pion and Muon Pairs by the Annihilation of High-Energy Positrons — 937L.
Nikol'skiĭ, B. A. (see Ali-Zade, S. A.) — 940L.
Nikol'skiĭ, S. I. (see Dovzhenko, O. I.) — 11.
Nomofilov, A. A. (see Bayatyan, G. L.) — 483.
Nosov, V. G. Alpha Decay Constants of Non-Spherical Nuclei — 1122L.
Novikova, G. I. (see Gol'din, L. L.) — 356.
Novozhilov, Yu. V. and I. A. Terent'ev. The Two-Nucleon LS Potential in Nonrelativistic Meson Theory — 89.
Nuralieva, R. D. (see Krinchik, G. S.) — 724.
Nurmukhamedov, G. M. (see Malevskaya, L. A.) — 1137L.
Oganesyan, Yu. Ts. Range-Energy Dependence of C_{12}, C_{14} and O_{16} Ions in Aluminum, Copper, and Gold in the Energy Interval from 50 to 110 Mev — 661L.
Ogievetskiĭ, V. I. Interaction between K and π Mesons — 447L.
— and Chou Kuang-Chao. Charge-Symmetry Properties and Representations of the Extended Lorentz Group in the Theory of Elementary Particles — 179.
Okonov, É. O. Some Characteristics of the Annihilation of an Antiproton in the Deuteron — 1134L.

Okun', L. B. and I. Ya. Pomeranchuk. Peripheral Interactions between Elementary Particles.
— (see Matinyan, S. G.) — 933L.
Orlinskiĭ, D. V. (see Borzunov, N. A.) — 502.
Osovets, S. M. (see Borzunov, N. A.) — 502.
Ostroumov, V. I., N. A. Perfilov, and R. A. Filov. Cascade Alpha Particles in Stars Produced by 360 and 660 Mev Protons — 254.
Otvinovskiĭ, S. Z. (see Balandin, M. P.) — 296.
Ovcharenko, O. N. (see Lazarev, B. G.) — 42.
Pafomov, V. E. Transition Radiation and Cerenkov Radiation — 1321.
— (see Agranovich, V. N.) — 160.
Pasechnik, L. L. (see Gabovich, M. D.) — 727.
Pasyuk, A. S. (see Volkov, V. V.) — 536.
Ped'ko, A. V. (see Belov, K. P.) — 1191.
Pekar, S. I. On the Theory of Absorption and Dispersion of Light in Crystals — 314.
Peker, L. K. (see Birbrair, B. L.) — 566.
Peletminskiĭ, S. V. (see Akhiezer, A. I.) — 146.
Perelomov, A. M. (see Zhivopistsev, F. A.) — 333.
Perfilov, N. A. (see Darovskikh, V. F.) — 456.
— (see Ostroumov, V. I.) — 254.
Peshkov, V. P., K. N. Zinov'eva, and A. I. Filimonov. He^3 Cryostats — 734.
Pesotskaya, E. A. (see Minervina, Z. V.) — 309.
Petrzhak, K. A. (see Kovrigin, B. S.) — 217L.
Petukhova, N. I. (see Kopylova, D. K.) — 1391L.
Pik-Pichak, G. A. Anisotropic Fission of Rotating Nuclei — 679L.
Pikel'ner, S. B. Structure of a Magnetohydrodynamic Shock Wave in a Partially Ionized Gas — 1089.
Piliya, A. D. Excitation of Rotational Nuclear Levels by Charged Particles — 843.
— The Nuclear Interaction in the Scattering of Charged Particles from Nonspherical Nuclei — 992.
Pitaevskiĭ, L. P. Properties of the Spectrum of Elementary Excitations near the Disintegration Threshold of the Excitations — 830.
— (see Dzyaloshinskiĭ, I. E.) — 1282.
Podgoretskiĭ, M. I. (see Bayatyan, G. L.) — 483.
— (see Grishin, V. G.) — 1132L.
— (see Kopylova, D. K.) — 1391L.
Podgurskaya, A. V. (see Flerov, G. N.) — 511.
Pokatilov, E. P. The Resonance of Charge Carriers Produced by an Ultrasonic Wave — 1037.
Polikanov, S. M. and V. A. Druin. Fission Induced in Heavy Elements by Carbon, Nitrogen, and Oxygen Nuclei — 522.
Polovin, R. V. Zemplen's Theorem in Relativistic Hydrodynamics — 675L.
— (see Akhiezer, I. A.) — 1316.
— (see Lyubarskiĭ, G. Ya.) — 902.
Polyakov, L. M. (see Garber, R. I.) — 1158.
Pomeranchuk, I. Ya. (see Akhiezer, A. I.) — 605.
— (see Beresteskiĭ, V. B.) — 936L.
— (see Okun', L. B.) — 207.
Pontecorvo, B. The Universal Fermi Interaction and Astrophysics — 1148.
— (see Zinov, V. G.) — 1386L.
Popov, N. P. (see Dolginov, A. Z.) — 368.
Popov, V. S. (see Ivanchik, I. I.) — 347.
Popova, A. M. (see Komarov, V. V.) — 311L.
Popova, V. M., N. G. Semashko, and F. R. Yagudina. Photoproduction of Low Energy Charged Pions from Complex Nuclei — 965.
Potapov, L. I. (see Daĭon, M. I.) — 650L.
— (see Daĭon, M. I.) — 488.
Preĭsa, M. (see Delyagin, N. N.) — 1127L.
Preobrazhenskiĭ, B. K. (see Anton'eva, N. M.) — 20.
— (see Berlovich, É. E.) — 1128L.
Prokhorenko, V. K. and I. Z. Fisher. Fluctuations of Atomic Structures in Liquid Helium — 928L.
Prokhorov, A. M. (see Kaitmazov, S. D.) — 944L.
— (see Kornienko, L. S.) — 649L.
— (see Zverev, G. M.) — 451L.
Prokof'ev, Yu. A. (see Sosnovskiĭ, A. N.) — 717.
Prokoshkin, Yu. D. and T'ang Hsiao-Wei. Showers Produced by Positrons in 100 to 400 Mev Range — 6.
— (see Dunaĭtsev, A. F.) — 1179.
Protopopov, A. N. and V. P. Éĭsmont. Dependence of the Angular Anisotropy of Fission on the Nuclear Structure — 1116L.
— and B. M. Shiryaev. Gamma Rays Accompanying the Fission of U^{238} by 2.8 and 14.7 Mev Neutrons — 674L.
—, I. A. Baranov, and V. P. Éĭsmont. Angular Anisotropy of Scattering of Fragments in Fission of Am^{241} by 14.7 Mev Neutrons — 650L.
— I. A. Baranov, and V. P. Éĭsmont. Angular Anisotropy and Energy Characteristics of the Fission Process — 334.
—, I. A. Baranov, Yu. A. Selitskiĭ, and V. P. Éĭsmont. Effect of Nuclear Shells on the Distribution of the Kinetic Energy of Fragments in Fission by Fast Neutrons — 1374L.
Pustovalov, G. E. Energy Levels and Approximate Wave Functions of Mesic Atoms — 1288.
Puzikov, L. D. and Ya. A. Smorodinskiĭ. Polarization Tensors in the Born Approximation — 1126L.
Rabin, N. V. (see Vaĭsenberg, A. O.) — 1197.
Raĭzer, Yu. P. A Simple Method of Calculating the Degree of Ionization and Thermodynamic Functions of a Multiply Ionized Ideal Gas — 1124L.
Rakobol'skaya, I. V. (see Dovzhenko, O. I.) — 11.
Rapoport, I. D. (see Grigorov, N. L.) — 759.
Rashba, É. I. Effect of Resonance Excitation Transfer in the Theory of a Large-Radius Exciton — 1213.
Rikenglaz, L. É. (see Kucherov, R. Ya.) — 359.
Roĭtsin, L. B. (see Deĭgen, M. F.) — 120.
Romantseva, A. S. (see Varfolomeev, A. A.) — 495.
Rostovskiĭ, V. S. (see Davydov, A. S.) — 1275.
Rozental', I. L. On the Possible Multiple Production of Muons — 666L.
Rozhdestvenskiĭ, V. V. (see Alkhazov, D. G.) — 222L.
Rudakov, V. P. (see Vlasov, N. A.) — 17.
Rudik, A. P. (see Geshkenbeĭn, B. V.) — 360.
Rukhadze, A. A. (see Agranovich, V. N.) — 160.
Rumer, Yu. B. Action as a Space Coordinate, X. — 1348
Rusinov, L. I. (see Karamyan, A. S.) — 979.
Rus'kin, V. I. Effects of a Resonant Pion-Pion Interaction in Fermi's Statistical Theory of Multiple Particle Production — 113.
— Interpretation of the Maximum in the Total Cross Section for Proton-Proton Scattering in the 1 Bev Region — 660L

Rybakov, B. V. (see Bogdanov, G. F.) — 440L.
Rymko, N. P., V. F. Tulinov, and A. N. Charakhch'yan. A Case of a Sharp Increase in Cosmic-Ray Intensity in the Stratosphere — 1202.
Ryndin, R. M. (see Azhgirei, L. S.) — 1163.
— (see Bilen'kiĭ, S. M.) — 1144.
Ryzhanov, S. G. Alpha Decay of Th^{227} in the Collective Model and the Spin of Ra^{223} in Its Lowest State — 656L.
Sadykhov, F. S. and B. K. Kerimov. On Pair Production by the Collision of Two Circularly Polarized Gamma-Ray Quanta — 938L.
Samoĭlov, B. N., V. V. Sklyarevskiĭ, and E. P. Stepanov. Nuclear Polarization of Weakly-Magnetic Elements Introduced into a Ferromagnet — 1383.
—, V. V. Sklyarevskiĭ, and E. P. Stepanov. Polarization of Au^{198} Nuclei in a Solution of Gold in Iron — 448L.
—, V. V. Sklyarevskiĭ, and E. P. Stepanov. Polarization of Cobalt and Iron Nuclei in Ferromagnets — 972.
Samoĭlov, L. N. (see Bogdanov, G. F.) — 440L.
Satarov, V. I. (see Golovin, B. M.) — 302.
Savchenko, I. A. (see Zaĭtsev, A. A.) — 944L.
Seidl, M. Statistical Electron Capture Mechanism in Betatrons — 924L.
Selitskiĭ, Yu. A. (see Protopopov, A. N.) — 1374L.
Semashko, N. G. (see Popova, V. M.) — 965.
Serdobol'skiĭ, V. I. On the Theory of Scattering Via Quasi-Stationary States — 1354.
Shabudin, A. F. (see Azhgireĭ, L. S.) — 343.
Shakhulashvili, O. A. (see Kostanashvili, N. I.) — 713.
Sharvin, Yu. V. (see Zernov, V. B.) — 737.
Shavrin, P. I. (see Klimentovskaya, M. V.) — 967.
Shavtvalov, L. Ya. (see Vasil'ev, S. S.) — 218L.
Shchelkin, K. I. Two Cases of Unstable Combustion — 416.
Shekhter, V. M. Beta Decay of Strange Particles — 920L.
— On the Weak-Interaction Types Possible in the Scheme of Feynman and Gell-Mann — 403.
Shevchenko, O. P. On the Role Played by Exchange Effects in Stripping Reactions — 599.
Shirkov, D. V. On the Compensation Equation in Superconductivity Theory — 421.
Shirokov, M. I. Azimuthal Symmetries in Cascade Reactions and Parity Conservation — 1081.
Shirokov, Yu. M. A Group-Theoretical Consideration of the Basis of Relativistic Quantum Mechanics. V. — 620.
— Relativistic Corrections to Phenomenological Hamiltonians — 330.
— (see Kaminskiĭ, A. K.) — 616.
— (see Zhivopistsev, F. A.) — 333.
Shiryaev, B. M. (see Protopopov, A. N.) — 674L.
Shklyarevskiĭ, G. M. One-Particle Mechanism in Photonuclear Reactions — 1057.
Shmushkevich, I. M. Depolarization of Mu-Mesons in the Formation of Mu-Mesic Atoms — 449L.
— Polarization of the Nucleus by Capture of Polarized Negative Muons into the Mesonic K Shell — 673L.
Shpigel', I. S. Plasma Acceleration — 285.
Shubin, Yu. V. (see Garber, R. I.) — 260.
Shul'man, L. A. On the Theory of the Electron Spin Resonance of F Centers in Crystals with NaCl Structure — 1217.
Sidorov, V. A. (see Gogdanov, G. F.) — 440L.
Silin, V. P. The Problem of the Optical Constants of Conductors — 1025.
Sinitsin, V. I. (see Luk'yanov, S. Yu.) — 1155.
Sirota, Z. D. (see Belov, K. P.) — 752.
Sitenko, A. G. Fission of Nonspherical Nuclei — 555.
— Scattering of Fast Pi-Mesons by Deuterons — 1008.
— (see Vysotskii, G. L.) — 812.
Sklyarevskiĭ, V. V., E. P. Stepanov, and B. A. Medvedev. K-Level X-Rays from Fission Fragments and Distribution of Fragments by Charges — 225L.
— (see Samoĭlov, B. N.) — 1383L.
— (see Samoĭlov, B. N.) — 448L.
— (see Samoĭlov, B. N.) — 972.
Skrotskiĭ, G. V. and Yu. I. Alimov. Effect of Specimen Shape on Ferromagnetic Resonance in a Strong Radio-Frequency Field — 899.
— and A. A. Kokin. A System of Magnetic Moments in a Weak Variable Magnetic Field — 116.
— and A. A. Kokin. On the Theory of Nuclear Paramagnetic Resonance in Liquids — 335.
— and A. A. Kokin. Random Free Precession of Magnetic Moments of Atomic Nuclei — 658L.
Skrzypczak, E. S. (see Bayatyan, G. L.) — 483.
Slavnov, D. A. and A. D. Sukhanov. On Causality in a Theory with an Indefinite Metric — 1044.
Sliv, L. A. and B. A. Volchok. Investigation of the Average Nuclear Potential Parameters — 374.
— (see Birbrair, B. L.) — 566.
Smirnit-skiĭ, V. A. (see Vaĭsenberg, A. O.) — 230L.
— (see Vaĭsenberg, A. O.) — 1197.
Smirnov, Yu. F. (see Neudachin, V. G.) — 127.
Smorodin, Yu. A. (see Birger, N. G.) — 823.
Smorodinskiĭ, Ya. A. The "Complete Experiment" in Beta-Decay — 1142L.
— (see Gol'danskiĭ, V. I.) — 1387L.
— (see Puzikov, L. D.) — 1126L.
Sokolik, G. A. A New Class of Representations of the Full Lorentz Group — 781.
Sokolov, A. A., V. M. Arutyunyan, and R. M. Muradyan. Calculation of Scattering Phase Shifts with Inclusion of the Second Approximation — 412.
—, I. M. Ternov, and Yu. M. Loskutov. On the Problem of the Covariant Definition of the Spin Pseudovector — 657L.
Sokolov, I. B. (see Vagradov, G. M.) — 669L.
Solov'ev, K. I. (see Abrosimov, A. T.) — 528.
Solov'ev, M. V. (see Baradzei, L. T.) — 1151.
Solov'ev, V. G. An Investigation of the Superfluid State of an Atomic Nucleus — 1231.
— Conditions for Superfluidity of the Atomic Nucleus and the Temperature of the Phase Transition — 201.
— On the Problem of Testing Parity Conservation in the Strong Interactions — 436L.
Sorokin, A. A. (see Forafontov, N. F.) — 227L.
Sosnovskiĭ, A. N., P. E. Spivak, Yu. A. Prokof'ev, I. E. Kutikov, and Yu. P. Dobrynin — 717.
Spivak, P. E. (see Sosnovskiĭ, A. N.) — 717.
Stankevich, I. V. (see Bochvar, D. A.) — 435L.
Stanyukovich, K. P. Concerning the Impact of Solids at High Velocities — 1141L.
— Cylindrical and Plane Magnetohydrodynamic Waves — 1271.

Starodubtsev, S. V. and K. V. Makaryunas. Angular Distribution of Tritons from the Reaction $Li^7(\alpha, t)Be^5$ — 1133.
Stavinskiĭ, V. S. On the Emission Mechanism of Prompt Fission Neutrons — 437L.
Stepanov, E. P. (see Samoĭlov, B. N.) — 1383L.
— (see Samoĭlov, B. N.) — 448L.
— (see Samoĭlov, B. N.) — 972.
— (see Sklyarevskiĭ, V. V.) — 225L.
Stepanov, K. N. Penetration of an Electromagnetic Field into a Plasma — 1035.
Stoletov, G. D. (see Zrelov, V. P.) — 461.
Stolyarov, G. A. (see Flerov, G. N.) — 511.
Strugalskiĭ, Z. S. (see Vernov, S. N.) — 468.
— (see Vernov, S. N.) — 691.
Strutinskiĭ, V. M. A Correction to V. M. Strutinskiĭ's Paper "Excitation of Rotational States During the Alpha Decay of Even-Even Nuclei" — 404L.
Sukhanov, A. D. (see Slavnov, D. A.) — 1044.
Sukharevskiĭ, V. G. Angular Distributions in the Reactions $Ne^{22}(d, p)Ne^{23}$ and $A^{36}(d, p)A^{37}$ — 981.
— (d, p) Stripping Reactions in the Silicon Isotopes — 37.
Surkova, L. V. (see Ali-Zade, S. A.) — 940L.
Svetlolobov, I. A. (see Varfolomeev, A. A.) — 1263.
Svirskiĭ, M. S. (see Vonsovskiĭ, S. V.) — 894.
T'ang Hsiao-Wei (see Prokoshkin, Yu. D.) — 6.
Takibaev, Zh. S. (see Loktionov, A. A.) — 1209.
Taluts, G. G. (see Zyryanov, P. S.) — 100.
Tarantin, N. I. (see Volkov, V. V.) — 536.
Teplov, I. B. (see Neudachin, V. G.) — 599.
Ter-Akop'yan, G. M. (see Karnaukhov, V. A.) — 525.
Ter-Martirosyan, K. A. (see Gol'din, L. L.) — 356.
Ter-Mikaelyan, M. L. Contribution to the Theory of Multiple Scattering — 171.
Terekhov, Yu. V. (see Burgov, N. A.) — 1146L.
Terent'ev, I. A. (see Novozhilov, Yu. V.) — 89.
Terletskiĭ, Ya. P. (see Magalinskiĭ, V. B.) — 1234.
Ternov, I. M. (see Sokolov, A. A.) — 657L.
Tishkov, P. G. Measurement of Spin-Lattice Relaxation in Mn^{++} Salt Solutions — 949.
Tolpygo, K. B. (see Moskalenko, S. A.) — 103.
Toptygin, I. N. Multiple Scattering of Polarized Electrons — 340.
Trebukhovskiĭ, Yu. V., V. V. Vladimirskiĭ, V. K. Grigor'ev, and V. A. Ergakov. Electron-Neutrino Angular Correlation in the Beta Decay of the Free Neutron — 931L.
Tretyakov, E. V., L. N. Kondrat'ev, G. I. Khlebnikov, and L. I. Gol'din. Spectrum of the Internal Conversion Electrons Accompanying the Alpha Decay of Pu^{238} and Pu^{240} — 250.
Tsekhmistrenko, Yu. V. Some Applications in the Theory of Metals of the Method of Summation of the Main Feynman Diagrams — 1097.
Tsirul'nikova, L. M. The Phenomenological Theory of the Voigt Effect in Paramagnetics — 1015.
Tsukernik, V. M. (see Kaganov, M. I.) — 151.
Tsytko, S. T. (see Guseva, M. I.) — 1.
Tulinov, A. F. (see Balashov, V. V.) — 426L.
Tulinov, V. F. (see Boyarkina, A. N.) — 244.
— (see Rymko, N. P.) — 1202.
Tulinova, Z. I. (see Baradzeĭ, L. T.) — 1151.
Tulub, A. V. The Influence of the Electron-Phonon Interaction on the Cyclotron Resonance Frequency — 392.
— The Mean Free Path of an Exciton in Polar Crystals — 1326.
Turov, E. A. On the Theory of Weak Ferromagnetism — 890.
Turovtsev, V. V. On the Mechanism of the Leptonic Decay of Hyperons — 939L.
Vagradov, G. M. and I. B. Sokolov. On the Scattering of Pions by Deuterons — 669L.
Vaĭsenberg, A. O. Low Energy Positrons from the μ^+-e^+ Decay — 722.
— and V. A. Smirnit-skiĭ. Decay of a Beryllium Hyperfragment — 230L.
—, N. V. Rabin, and V. A. Smirnit-skiĭ. Depolarization of μ^+ Mesons in Nuclear Emulsion — 1197.
Vaks, V. G. Radiative Deviations from the Coulomb Law at Small Distances — 375.
Valiev, K. A. On the Theory of Lattice Spin Relaxation — 1242.
Valuev, B. N. Comments on the Covariants in the Beta-Decay Interaction — 1121L.
Varfolomeev, A. A. and I. A. Svetlolobov. Monte-Carlo Calculations of Electromagnetic Cascades with Account of the Influence of the Medium on Bremsstrahlung — 1263.
—, R. I. Gerasimova, L. A. Makarina, A. S. Romantseva, and S. A. Chueva. Ionization along the Tracks of High-Energy Electron-Positron Pairs — 495.
Vasil'ev, S. S. and L. Ya. Shavtvalov. The Beta Spectra of F^{20} and F^{17} — 218L.
Vasil'eva, M. Ya. (see Zaĭtsev, A. A.) — 1130.
Vedenov, A. A. Free Energy of Strong Electrolytes — 665L.
— Thermodynamic Properties of a Degenerate Plasma — 446.
— and A. I. Larkin. Equation of State of a Plasma — 806.
Veklenko, B. A. Green's Function for the Resonance Radiation Diffusion Equation — 138.
Velikhov, E. P. Stability of a Plane Poiseuille Flow of and Ideally Conducting Fluid in a Longitudinal — 848.
— Stability of an Ideally Conducting Liquid Flowing between Cylinders Rotating in a Magnetic Field — 995.
Vernov, S. N., E. V. Gorchakov, I. P. Ivanenko, and G. B. Khristiansen. Development of the Nuclear-Active Component of Extensive Atmospheric Showers — 877.
—, N. N. Goryunov, G. T. Zatsepin, G. V. Kulikov, Yu. A. Nechin, Z. S. Strugalskiĭ, and G. B. Khristiansen. Investigation of the Core of Extensive Air Showers — 468.
—, Ya. S. Babetskiĭ, N. N. Goryunov, G. V. Kulikov, Yu. A. Nechin, Z. S. Strugal'skiĭ, and G. B. Khristiansen. Structure of the Core and of the Central Region of an Extensive Air Shower at Sea Level — 691.
Viktor, S. (see Budagov, Yu. A.) — 767.
Vladimirskiĭ, V. V. (see Trebukhovskiĭ, Yu. V.) — 931L.
Vlasov, K. B. and B. Kh. Ishmukhametov. On the Rotation of the Plane of Polarization of Elastic Waves in a Magnetically Polarized Medium — 921L.
Vlasov, N. A. and V. P. Rudakov. Beta-Gamma Angular Correlation in Ba^{139} Decay and the Relative Sign of the Beta-Interaction Coupling Constants — 17.
— (see Bogdanov, G. F.) — 440L.
Volchok, B. A. (see Sliv, L. A.) — 374.

Volkov, D. V. On the Quantization of Half-Integer Spin Fields — 305.
Volkov, V. V., L. I. Guseva, A. S. Pasyuk, N. I. Tarantin, and K. V. Filippova. Cross-Sections for the Production of Californium Isotopes by the Bombardment of U^{238} by Accelerated Carbon Ions — 536.
Volotskaya, V. G. (see Borovik, E. S.) — 1175.
Vonsovskiĭ, S. V. and M. S. Svirskiĭ. On the Superfluidity of a System of Polar Bose Excitations — 894.
Vorob'ev, E. D. (see Flerov, G. N.) — 511.
Vysotskiĭ, G. L. and A. G. Sitenko. On the Theory of Direct Nuclear Reactions Involving Polarized Particles — 812.
—, E. V. Inopin, and A. A. Kresnin. Scattering of Neutrons by Oriented Nonspherical Nuclei — 398.
Vzorov, I. K. (see Azhgirei, L. S.) — 1163.
Yagudina, F. R. (see Popova, V. M.) — 965.
Yakovlev, K. I. (see Loginov, Yu. E.) — 664L.
Yampol'skiĭ, P. A. (see Glagolev, V. L.) — 742.
— (see Morozov, A. M.) — 671L.
Yankov, V. V. Behavior of a Conducting Gaseous Sphere in a Quasi-Stationary Electromagnetic Field — 388.
Yanoukh, F. On the Probability of Double Beta Decay — 231L.
Zaikin, D. A. On the Axial Asymmetry of Atomic Nuclei — 1114L.
— (see Davydov, A. S.) — 157.
Zaĭtsev, A. A., G. S. Leonov, and I. A. Savchenko. On Electron Oscillations in a Plasma — 944L.
—, M. Ya. Vasil'eva, and V. N. Mnev. Possibility of Determining the Potential Distribution of a Plasma from the Characteristics of the Noise Generated in a Gaseous discharge — 391L.
Zaĭtseva, M. A. (see Belov, K. P.) — 1138L.
— (see Belov, K. P.) — 1191.
Zaretskiĭ, D. F. On Radiative Transitions between Rotational Levels in Spin $\frac{1}{2}$ Nuclei — 803.
— On the Theory of Nuclear Magnetic Moments — 612.
Zatsepin, G. T. (see Vernov, S. N.) — 468.
Zel'dovich, Ya. B. Converging Cylindrical Detonation Wave — 550.
— On $\mu^+\mu^-$ Annihilation and the Decay of Neutral Mesons — 450L.
— Parity Nonconservation in the First Order in the Weak-Interaction Constant in Electron Scattering and other Effects — 682L.
— Storage of Cold Neutrons — 1389L.
— The Transformation $K_2^0 - K_1^0$ by Electrons — 274.
Zernov, V. B. and Yu. V. Sharvin. Measurement of the Resistance of High Purity Tin at Helium Temperatures — 737.
Zevin, V. Ya. Frequency Spectrum of Electron Spin Double Resonance at Color Centers in Alkali Halide Crystals — 81.
Zhivopistsev, F. A., A. M. Perelomov, and Yu. M. Shirokov. Relativistic Corrections to the Phenomenological Theory of Levels of Light Nuclei — 333.
Zhuravlev, V. A. and M. I. Kozak. The Conductivity of Semi-Conductors in an Ultrasonic Field — 236L.
Zil'berman, G. E. The Motion of an Electron in a Crystal Located in an External Field — 1040.
Zinov, V. G. and S. M. Korenchenko. Scattering of 240-Mev and 270-Mev Negative Pions on Hydrogen — 429L.
—, A. D. Konin, S. M. Korenchenko, and B. Pontecorvo — 1386L.
Zinov'eva, K. N. (see Peshkov, V. P.) — 734.
Zoellner, W. Dispersion Relations and Chew-Low Type Equations for Inelastic Meson Processes in the Fixed Source Case — 784.
Zolotavin, A. V. (see Grigor'ev, E. P.) — 272.
Zrelov, V. P. and G. D. Stoletov. Range-Energy Relation for 660-Mev Protons — 461.
— (see Azhgireĭ, L. S.) — 343.
Zverev, G. M. and A. M. Prokhorov. Electron Paramagnetic Resonance of Co^{++} in Corundum — 451L.
Zyryanov, P. S. and G. G. Taluts. Electroacoustic Phenomena in a Degenerate Electron-Ion Plasma — 100.

ANALYTIC SUBJECT INDEX TO VOLUME 36(9)

References with L are Letters to the Editor. Items are listed under the following categories:

Acoustics
Astrophysics
Atomic and Molecular Beams
Atomic Mass and Abundance
Atomic Structure and Spectra
Biographical Material
Chemical Effects and Properties
Cosmic Radiation
Crystalline State
Dielectrics and Dielectric Properties
Diffraction
Diffusion
Elasticity and Plasticity
Electrical Conductivity and Resistance
Electrical Discharges
Electrical Properties
Electromagnetic Theory and Electrodynamics
Electrons and Positrons
Elementary Particle Interactions
Errata
Field Theory
Films, Properties
Fluid Dynamics
Gamma Rays
Gases
Helium, Liquid
Imperfections in Solids
Ionization
Ions
Ions and Electrons, Mobility
Liquids
Magnetic Properties
Magnetic Resonance
Mathematical Methods
Mechanics
Mesons and Hyperons
Methods and Instruments
Microwaves
Miscellaneous
Molecular Structure and Spectra
Neutrino
Noise
Nuclear Fission
Nuclear Moments and Spin
Nuclear Photoeffects
Nuclear Reactions, General
Nuclear Reactions Induced by α Particles and He^3
Nuclear Reactions Induced by Deuterons and Tritons
Nuclear Reactions Induced by Mesons
Nuclear Reactions Induced by Neutrons
Nuclear Reactions Induced by Protons
Nuclear Spectra
Nuclear Structure Theory
Optical Properties
Quantum Electrodynamics
Quantum Mechanics
Radiation
Radioactivity
Range and Energy Loss of Particles
Relativity and Gravitation
Scattering, General
Scattering of α Particles
Scattering of Deuterons
Scattering of Electrons and Positrons
Scattering of Mesons
Scattering of Neutrons
Scattering of Protons
Semiconductors
Spectra, General
Statistical Mechanics and Thermodynamics
Superconductivity
Thermal Properties
X-rays

Absorption of Radiation (see Radiation)
Acoustics
Anisotropy of the Absorption Coefficients of Ultrasonics in Superconductors. P. A. Bezuglyĭ, A. A. Galkin, and A. P. Korolyuk — 1388L.
Anisotropy of the Absorption of Ultrasound in Metals in a Magnetic Field. A. A. Galkin and A. P. Korolyuk — 925L.
Cylindrical and Plane Magnetohydrodynamic Waves — 1271.
Electroacoustic Phenomena in a Degenerate Electron-Ion Plasma. P. S. Zyryanov and G. G. Taluts — 100.
On the Heat Conductivity and Attenuation of Sound in Superconductors. B. T. Geĭlikman and V. Z. Kresin — 677L.
On the Rotation of the Plane of Polarization of Elastic Waves in a Magnetically Polarized Medium. K. B. Vlasov and B. Kh. Ishmukhametov — 921L.
Phenomenological Theory of Kinetic Processes in Ferromagnetic Dielectrics. II. Interaction of Spin Waves with Phonons. M. I. Kaganov and V. M. Tsukernik — 151.
Resonance Absorption of Ultrasound on Nuclei. A. R. Kessel' — 1031.
The Conductivity of Semi-Conductors in an Ultrasonic Field. V. A. Zhuravlev and M. I. Kozak — 236L.
The Disintegration of Unstable Shock Waves in Magnetohydrodynamics. G. Ya. Lyubarskiĭ and R. V. Polovin — 902.
The Permanent Structure of Shock Waves with Joule Dissipation. V. A. Belokon' — 932L.

The Resonance of Charge Carriers Produced by Ultrasonic Wave. E. P. Pokatilov — 1037.
Ultrasonic Attenuation in Metals. G. L. Kotkin — 664L.
Afterglow (see Electrical Discharges)
Alloys (see Crystalline State)
Annihilation (see Electrons and Positrons)
Antiferroelectric Phenomena (see Dielectrics and Dielectric Properties)
Antiferromagnetism (see Magnetic Properties)
Arcs (see Electric Discharges)
Astrophysics
Stability of an Ideally Conducting Liquid Flowing between Cylinders Rotating in a Magnetic Field. E. P. Velikhov — 995.
The Universal Fermi Interaction and Astrophysics. B. Pontecorvo — 1148L.
Atomic and Molecular Beams
On the Existence of the Negative Nitrogen Ion. Ya. M. Fogel', V. F. Kozlov, and A. A. Kalmykov — 963.
On the Stability of Nuclei. P. É. Nemirovskiĭ — 627.
Atomic Mass and Abundance
Mass of the Isotope Pu^{239}. R. A. Demirkhanov, T. I. Gutkin, and V. V. Dorokhov — 1134L.
Atomic Structure and Spectra
A Qualitative Interpretation of the Mean Electron Excitation Energy in Atomic Collisions. O. B. Firsov — 1076.
A Refinement of the Thomas-Fermi Model at Small Distances. E. S. Fradkin — 1087.
Broadening of Spectral Lines in Strongly Ionized Plasma. M. A. Mazing and S. L. Mandel'shtam — 941L.
Depolarization of Mu-Mesons in the Formation of Mu-Mesic Atoms. I. M. Shmushkevich — 449L.
Energy Levels and Approximate Wave Functions of Mesic Atoms. G. E. Pustovalov — 1288.
Fluctuations of Atomic Structures in Liquid Helium. V. K. Prokhorenko and I. Z. Fisher — 928L.
Fock Expansion for the Wave Functions of a System of Charged Particles. Yu. N. Demkov and A. M. Ermolaev — 633.
Green's Function for the Resonance Radiation Diffusion Equation. B. A. Veklenko — 138.
Relative Probabilities for the Photoeffect and Subshells of an Atom. E. P. Grigor'ev and A. V. Zolotavin — 272.
Scattering of Neutrons by Oriented Nonspherical Nuclei. G. L. Vysotskiĭ, E. V. Inopin, and A. A. Kresnin — 398.
The Influence of Temperature and Pressure on the Raman Spectrum of Nitrogen. G. V. Mikhaĭlov — 974.
Auger Effect (see Atomic Structure and Spectra)
Barkhausen Effect (see Magnetic Properties)
Biographical Material
Academician Lev Andreyevich Artsimovich — 453.
Boson Theory (see Radiation)
Broadening of Spectral Lines (see Atomic Structure and Spectra; Spectra, General)
Capture Cross Sections (see Electrons and Positrons; Nuclear Reactions, General; Radiation)
Cerenkov Effect (see Radiation)
Chemical Effects and Properties
Electronic Paramagnetic Resonance Spectra of Frozen OH Radicals. S. D. Kaĭtmazov and A. M. Prokhorov — 944L.
Line Width of the Chlorine Quadrupole Resonance in Chlorates of Barium, Sodium and Potassium. V. S. Grechishkin — 438L.
On the Theory of Electron Paramagnetic Resonance in Electrolyte Solutions. A. A. Kokin — 353.
Chemiluminescence (see Luminescence)
Cold Emission (see Electrical Properties)
Compton Effect (see Radiation)
Conductivity, Electrical (see Electrical Conductivity and Resistance)
Cosmic Radiation
A Case of a Sharp Increase in Cosmic-Ray Intensity in the Stratosphere. N. P. Rymko, V. F. Tulinov, and A. N. Charakhch'yan — 1202.
Cloud Chamber Investigations in the Cores of Extensive Air Showers. O. I. Dovzhenko, S. I. Nikol'skiĭ, and I. V. Rakobol'skaya — 11.
Determination of Charged Particle Mass from Scattering and Residual Range in Multiplate Cloud Chambers. F. R. Arutyunyan — 697.
Development of the Nuclear-Active Component of Extensive Atmospheric Showers. S. N. Vernov, E. V. Gorchakov, I. P. Ivanenko, and G. B. Khristiansen — 877.
High-Energy Nuclear-Active Component of Extensive Air Showers at Sea Level. A. T. Abrosimov, V. A. Dmitriev, G. V. Kulikov, E. I. Massal'skiĭ, K. I. Solov'ev, and G. B. Khristiansen — 528.
High-Energy Neutrons in Cosmic Rays. G. N. Flerov, V. I. Kalashnikova, A. V. Podgurskaya, E. D. Vorob'ev, and G. A. Stolyarov — 511.
Hodoscope Investigation of the Penetrating Component of Extensive Air Showers. R. E. Kazarov — 35.
Interaction between $10^{11} - 10^{12}$ ev Particles and Iron Nuclei. N. L. Grigorov, V. S. Murzin, and I. D. Rapoport — 759.
Investigation of the Core of Extensive Air Showers. S. N. Vernov, N. N. Goryunov, G. T. Zatsepin, G. V. Kulikov, Yu. A. Nechin, Z. S. Strugal'skiĭ, and G. B. Khristiansen — 468.
Investigation of the Nature and Spectra of Particles Produced by High-Energy Nucleons. A. I. Alikhanov, G. P. Eliseev, V. Sh. Kamalyan, V. A. Lyubimov, B. N. Moiseev, and A. V. Khrimyan — 280.
Lateral Distribution of the Energy Flux of the Electron-Photon Component of Extensive Air Showers. V. A. Dmitriev, G. V. Kulikov, E. I. Massal'skiĭ, and G. B. Khristiansen — 702.
Measurement of the Mass of Cosmic-Ray Particles Underground. M. I. Daĭon and L. I. Potapov — 650L.
Momentum Spectrum of Particles of the Hard Component of Cosmic Rays at an Altitude of 9 km. L. T. Baradzeĭ, M. V. Solov'ev, Z. I. Tulinova, and L. I. Filatova — 1151.
Monte-Carlo Calculations of Electromagnetic Cascades with Account of the Influence of the Medium on Bremsstrahlung. A. A. Varfolomeev and I. A. Svetlolobov — 361.
On the Analysis of High-Energy Showers. Ya. I. Granovskiĭ and I. Ya. Chasnikov — 795.

On the Dependence of the Angle between the Direction of Motion of Shower Particles and the Axis of the Shower on the Distance from the Axis. V. V. Guzhavin and I. P. Ivanenko — 1070.
On the Possible Multiple Production of Muons. I. L. Rozental' — 666L.
Polarization of the μ^+ Meson Current at Sea Level. B. A. Dolgoshein and B. I. Luchkov — 445L.
Production of Pions by High-Energy Cosmic-Ray Alpha Particles. A. A. Loktionov and Zh. S. Takibaev — 1209.
Scattering of Muons with Momenta Near 100 Mev/c by Copper and Iron. V. G. Kirillov-Ugryumov, B. A. Dolgoshein, A. M. Moskvichev, and L. P. Morozov — 290.
Showers Produced by Positrons in 100 to 400 Mev Range. Yu. D. Prokoshkin and T'ang Hsiao-Wei — 6.
Small Effects of Solar Flares and the Energy Spectrum of Primary Variation of Cosmic Rays. E. V. Kolomeets — 960.
Structure of the Core and of the Central Region of an Extensive Air Shower at Sea Level. S. N. Vernov, Ya. S. Babetskiĭ, N. N. Goryunov, G. V. Kulikov, Yu. A. Nechin, Z. S. Strugal'skiĭ, and G. B. Khristiansen — 691.
Underground Muon Spectrum at ~ 40 Meter Water Equivalent. M. I. Daĭon and L. I. Potapov — 488.
Cosmology (see Relativity and Gravitation)
Critical Potentials (see Atomic Structure and Spectra)
Cross Section (see Electrons and Positrons; Nuclear Reactions, General; Scattering, General)
Crystal Counters (see Methods and Instruments)
Crystalline State (see also Electrical Properties; Magnetic Properties; Semiconductors; etc.)
A Paramagnetic Amplifier and Generator, Using Fe^{3+} Ions in Corundum. L. S. Kornienko and A. M. Prokhorov — 649L.
Connection between Structural and Magnetic Parameters of the Transition Metals. F. M. Gal'perin — 862.
Effect of Resonance Excitation Transfer in the Theory of a Large-Radius Exciton. É. I. Rashba — 1213.
Electrical, Optical, and Elastic Properties of Crystals of the Diamond Type. III. Dispersion and Absorption of Light. V. S. Mashkevich — 76. IV. Interaction between Conduction Electrons and Lattice Vibrations. V. S. Mashkevich — 1237.
Electric Paramagnetic Resonance of Co^{2+} in Corundum. G. M. Zverev and A. M. Prokhorov — 451L.
Frequency Spectrum of Electron Spin Double Resonance at Color Centers in Alkali Halide Crystals. V. Ya. Zevin — 81.
Indirect Coupling of d Electrons in Transition Metals. I. Ferromagnetism. A. A. Berdyshev and B. V. Karpenko — 577.
Investigation of the Initial Stages of Plastic Deformation of Rock-Salt Crystals. R. I. Garber and L. M. Polyakov — 1158.
Investigation of Weak Ferromagnetism in the $MnCO_3$ Single Crystal. A. S. Borovik-Romanov — 539.
Isotopic Shift of the Curie Point in Uranium Hydride and Deuteride. A. I. Karchevskiĭ, E. V. Artyushkov, and L. I. Kikoin — 442L.
Line Width of the Chlorine Quadrupole Resonance in Chlorates of Barium, Sodium and Potassium. V. S. Grechishkin — 438L.
Magnetic Properties of Gadolinium Oxides. K. P. Belov, M. A. Zaĭtseva, and A. V. Ped'ko — 1191.
Magnocaloric Effect in Uranium Hydride and Deuteride. A. I. Karchevskiĭ — 443L.
Measurement of the Electrical Resistance of Metals in a Magnetic Field as a Method of Investigating the Fermi Surface. N. E. Alekseevskiĭ and Yu. P. Gaĭdukov — 311.
On Some Symmetry Properties of the Eigenfunctions of the Schrödinger Equation. D. A. Bochvar, N. P. Gambaryan, I. V. Stankevich, and A. L. Chistyakov — 435L.
On the Energy Spectrum of a Mott Exciton in Ionic Crystals. S. A. Moskalenko and K. B. Tolpygo — 103.
On the Theory of Absorption and Dispersion of Light in Crystals. S. I. Pekar — 314.
On the Theory of Relaxation Processes in Ferrodielectrics at Low Temperatures. A. I. Akhiezer, B. G. Bar'yakhtar, and S. V. Peletminskiĭ — 146.
On the Theory of the Electron Spin Resonance of F Centers in Crystals with NaCl Structure. L. A. Shul'man — 1217.
Paramagnetic Resonance of F Centers in Static Magnetic Fields of Arbitrary Strength. M. F. Deĭgen and A. B. Roĭtsin — 120.
Phenomenological Theory of Kinetic Processes in Ferromagnetic Dielectrics. II. Interaction of Spin Waves with Phonons. M. I. Kaganov and V. M. Tsukernik — 151.
Piezomagnetism in the Antiferromagnetic Fluorides of Cobalt and Manganese. A. S. Borovik-Romanov — 1390.
Slipping of Beryllium Single Crystals at Low Temperatures. III. R. I. Garber, I. A. Gindin, and Yu. V. Shubin — 260.
Statistical Delay of Discharge in NaCl and KBr. M. A. Mel'nikov — 425L.
The Magnetization and Magnetocaloric Effect of Manganese Phosphide. I. G. Fakidov and V. P. Krasovskiĭ — 755.
The Mean Free Path of an Exciton in Polar Crystals. A. V. Tulub — 1325.
The Motion of an Electron in a Crystal Located in an External Field. G. E. Zil'berman — 1040.
Van der Vaal's Forces in an Inhomogeneous Dielectric. I. E. Dzyaloshinskiĭ and L. P. Pitaevskiĭ — 1282.
Diamagnetism (see Magnetic Properties)
Dielectrics and Dielectric Properties
Contribution to the Theory of Ferroelectric Polarization Curves. N. S. Akulov — 772.
On the Doppler Effect in an Anisotropic and Gyrotropic Medium. K. A. Barsukov — 1052.
Phenomenological Theory of Kinetic Processes in Ferromagnetic Dielectrics. II. Interaction of Spin Waves with Phonons. M. I. Kaganov and V. M. Tsukernik — 151.
The Influence of the Electron-Phonon Interaction on the Cyclotron Resonance Frequency. A. V. Tulub — 392.
The Mean Free Path of an Exciton in Polar Crystals. A. V. Tulub — 1325.

The Problem of Determining the Dielectric-Permittivity- and Magnetic-Permeability Tensors of a Medium. G. S. Krinchik and M. V. Chetkin — 1368.
Van der Waal's Forces in an Inhomogeneous Dielectric. I. E. Dzyaloshinskiĭ and L. P. Pitaevskiĭ — 1282.
Diffraction
Energy and Angular Distribution in Diffraction Disintegration Processes. I. I. Ivanchik and V. S. Popov — 347.
Neutron Diffraction Investigation of the Antiferromagnetism of the Carbonates of Manganese and Iron. R. A. Alikhanov — 1204.
Diffusion
The Energy of Formation and Migration of Vacancies in Gold and Platinum. B. G. Lazarev and O. N. Ovcharenko — 42.
Elasticity and Plasticity
On the Rotation of the Plane of Polarization of Elastic Waves in a Magnetically Polarized Medium. K. B. Vlasov and B. Kh. Ishmukhametov — 921L.
Phenomenological Theory of Kinetic Processes in Ferromagnetic Dielectrics. II. Interaction of Spin Waves with Phonons. M. I. Kaganov and V. M. Tsukernik — 151.
Electrical Breakdown (see Dielectrics and Dielectric Properties; Electrical Discharges)
Electrical Conductivity and Resistance
A Method of Evaluating Electrical Conductivity. V. L. Bonch-Bruevich — 653L.
Electrical, Optical, and Elastic Properties of Diamond-Type Crystals. IV. Interaction between Conduction Electrons and Lattice Vibrations. V. S. Mashkevich — 1237.
Interaction between Conduction Electrons in Ferromagnets. A. I. Akhiezer and I. Ya. Pomeranchuk — 605.
Investigation of Galvanometric Phenomena in Chromium at Low Temperatures. E. S. Borovik and V. G. Volotskaya — 1175.
Measurement of the Electrical Resistance of Metals in a Magnetic Field as a Method of Investigating the Fermi Surface. N. E. Alekseevskiĭ and Yu. P. Gaĭdukov — 311.
Measurement of the Resistance of High Purity Tin at Helium Temperatures. V. B. Zernov and Yu. V. Sharvin — 737.
Stability of an Ideally Conducting Liquid Flowing between Cylinders Rotating in a Magnetic Field. E. P. Velikhov — 995.
The Conductivity of Semi-Conductors in an Ultrasonic Field. V. A. Zhuravlev and M. I. Kozak — 236L.
The Electrical Conductivity of Germanium in High Electric Fields at Low Temperatures. É. I. Abaulina-Zavaritskaya — 953.
The Energy of Formation and Migration of Vacancies in Gold and Platinum. B. G. Lazarev and O. N. Ovcharenko — 42.
Electrical Discharges
Acceleration of Plasmoids by High-Frequency Electric Fields. M. A. Miller — 1358.
Anomalous Electron Scattering and the Excitation of Plasma Oscillations. M. D. Gabovich and L. L. Pasechnik — 727.
Behavior of a Conducting Gaseous Sphere in a Quasi-Stationary Electromagnetic Field. V. V. Yankov — 388.
Charged Particle Energy Losses Due to Excitation of Plasma Oscillations. Yu. L. Klimontovich — 999.
Electric Field in a Microwave Plasma as a Function of Time. V. E. Mitsuk and M. D. Koz'minykh — 1139L.
Hysteresis and Non-Stationary Fields in the Electron Temperature in Plasma in Inert Gases. A. V. Gurevich — 434L.
Investigation of High Current Pulse Discharges in Conical Chambers. N. A. Borzunov, D. V. Orlinskiĭ, and S. M. Osovets — 502.
Motion of a Plasma Loop in an Axially Symmetric Magnetic Field. L. M. Kovrizhnykh — 1308.
On Electron Oscillations in a Plasma. A. A. Zaĭtsev, G. S. Leonov, and I. A. Savchenko — 944L.
On the "Larmoron" Plasma Theory. S. A. Kaplan — 1370L.
Oscillations of a Plasma in a Magnetic Field at Frequencies Close to the Cyclotron Frequency. V. N. Lazukin — 685.
Penetration of an Electromagnetic Field into a Plasma. K. N. Stepanov — 1035.
Plasma Acceleration. I. S. Shpigel' — 285.
Possibility of Determining the Potential Distribution of a Plasma from the Characteristics of the Noise Generated in a Gaseous Discharge. A. A. Zaĭtsev, M. Ya. Vasil'eva, and V. N. Mnev — 1130L.
Spectroscopic Investigation of an Intense Pulsed Discharge in Hydrogen. III. Determination of the Parameters of a High-Temperature Plasma. S. Yu. Luk'yanov and V. I. Sinitsyn — 1155.
Thermodynamic Properties of a Degenerate Plasma. A. A. Bedenov — 446L.
Electrical Properties (see also Dielectrics and Dielectric Properties; Electrical Conductivity and Resistance; Semiconductors; Superconductivity)
Electrical, Optical, and Elastic Properties of Diamond-Type Crystals. IV. Interaction between Conduction Electrons and Lattice Vibrations. V. S. Mashkevich — 1237.
Electroacoustic Phenomena in a Degenerate Electron-Ion Plasma. P. S. Zyryanov and G. G. Taluts — 100.
Interaction between Conduction Electrons in Ferromagnets. A. I. Akhiezer and I. Ya. Pomeranchuk — 605.
Measurement of the Electrical Resistance of Metals in a Magnetic Field as a Method of Investigating the Fermi Surface. N. E. Alekseevskiĭ and Yu. P. Gaĭdukov — 311.
On the Doppler Effect in an Anisotropic and Gyrotropic Medium. K. A. Barsukov — 1052.
Statistical Delay of Discharge in NaCl and KBr. M. A. Mel'nikov — 425L.
The Problem of the Optical Constants of Conductors. V. P. Silin — 1025.
Ultrasonic Attenuation in Metals. G. L. Kotkin — 664L.
Electrodynamics (see Electromagnetic Theory and Electrodynamics)
Electromagnetic Theory and Electrodynamics
Acceleration of Charged Particles in Running or Standing Electromagnetic Waves. G. A. Askar'yan — 430L.
Acceleration of Plasmoids by High-Frequency Electric Fields. M. A. Miller — 1358.

Behavior of a Conducting Gaseous Sphere in a Quasi-Stationary Electromagnetic Field. V. V. Yankov — 388.

Cerenkov Radiation of a Magnetic Dipole in an Anisotropic Medium. G. A. Begiashvili and É. V. Gedalin — 391.

Cerenkov Radiation of an Electron Moving in a Medium with Spatial Dispersion. V. N. Agranovich, V. E. Pafomov, and A. A. Rukhadze — 160.

Cyclic Motion of Charged Particles in an Electric Field. A. A. Kolomenskiĭ and Fong Soy-Cen — 184.

Depolarization of the Negative Muon in Mesic-Atom Transitions. V. A. Dzhrbashyan — 188.

Effect of Specimen Shape on Ferromagnetic Resonance in a Strong Radio-Frequency Field. G. V. Skrotskiĭ and Yu. I. Alimov — 899.

Electric Field in a Microwave Plasma as a Function of Time. V. E. Mitsuk and M. D. Koz'minykh — 1139L.

Hysteresis and Non-Stationary Effects in the Electron Temperature in Plasma in Inert Gases. A. V. Gurevich — 434L.

Motion of a Plasma Loop in an Axially Symmetric Magnetic Field. L. M. Kovrizhnykh — 1308.

On a Certain Version of Nonlocal Electromagnetic Field Theory. A. A. Komar and M. A. Markov — 602.

On Electromagnetic Shock Waves in Ferrites. A. V. Gaponov and G. I. Freĭdman — 675L.

On the Theory of the Coherent Spontaneous Emission. V. M. Faĭn — 562.

Oscillations of a Completely Ionized Plasma in a Cylindrical Cavity. L. M. Kovrizhnykh — 592.

Oscillations of a Plasma in a Magnetic Field at Frequencies Close to the Cyclotron Frequency. V. N. Lazukin — 685.

Particle Energy Losses Due to the Excitation of Longitudinal Waves. B. A. Lysov — 221L.

Penetration of an Electromagnetic Field into a Plasma. K. N. Stepanov — 1035.

Plasma Acceleration. I. S. Shpigel' — 285.

Possibility of Determining the Potential Distribution of a Plasma from the Characteristics of the Noise Generated in a Gaseous Discharge. A. A. Zaĭtsev, M. Ya. Vasil'eva, and V. N. Mnev — 1130L.

Radiation from a Current-Carrying Ring Moving Uniformly in a Plasma Situated in a Magnetic Field. L. S. Bogdankevich — 589.

Stability of a Plane Poiseuille Flow of an Ideally Conducting Fluid in a Longitudinal Magnetic Field. E. P. Velikhov — 848.

Stability of an Ideally Conducting Liquid Flowing between Cylinders Rotating in a Magnetic Field. E. P. Velikhov — 995.

The Problem of Determining the Dielectric-Permittivity and Magnetic-Permeability Tensors of a Medium. G. S. Krinchik and M. V. Chetkin — 1368L.

The Radiation Reaction in the Motion of a Charge in a Medium. V. L. Ginzburg and V. Ya. Éĭdman — 1300.

Theory of Relativistic Magnetohydrodynamic Waves. A. I. Akhiezer and R. V. Polovin — 1316.

Thermodynamic Properties of a Degenerate Plasma. A. A. Bedenev — 446L.

Transition Radiation and Cerenkov Radiation. V. E. Pafomov — 1321.

Van der Waal's Forces in an Inhomogeneous Dielectric. I. E. Dzyaloshinskiĭ and L. P. Pitaevskiĭ — 1282.

Electron Diffraction (see Scattering of Electrons and Positrons)

Electron-Optical Effects (see Optical Properties)

Electron Optics (see Methods and Instruments)

Electrons and Positrons (see also Electromagnetic Theory and Electrodynamics; Elementary Particle Interactions, Scattering of Electrons and Positrons)

An Investigation of π^+-μ^+-e^+ Decay with the Aid of a Propane Bubble Chamber and Scintillation Counters. M. P. Balandin, V. A. Moiseenko, A. I. Mukhin, and S. Z. Otvinovskiĭ — 296.

Asymmetry of Angular Distribution of μ^+-e^+ Decay Electrons in a 27,000 Gauss Magnetic Field. S. A. Ali-Zade, I. I. Gurevich, Yu. P. Dobretsov, B. A. Nikol'skiĭ, and L. V. Surkova — 940L.

Beta-Gamma Angular Correlation in Ba^{139} Decay and the Relative Sign of the Beta-Interaction Coupling Constants. N. A. Vlasov and V. P. Rudakov — 17.

Beta-Gamma Correlation in First-Forbidden Beta Transitions. Yu. V. Gaponov — 131.

Electron-Neutrino Angular Correlation in the Beta Decay of the Free Neutron. Yu. V. Trebukhovskiĭ, V. V. Vladimirskiĭ, V. K. Grigor'ev, and V. A. Ergakov — 931L.

Generation of Neutral Pions in the Interaction between 9 Bev Protons and Photographic Emulsion Nuclei. G. L. Bayatyan, I. M. Gramenitskiĭ, A. A. Nomofilov, M. I. Podgoretskiĭ, and E. S. Skrzypczak — 483.

Ionization along the Tracks of High-Energy Electron-Positron Pairs. A. A. Varfolomeev, R. I. Gerasimova, L. A. Makar'ina, A. S. Romantseva, and S. A. Chueva — 495.

Low Energy Positrons in μ^+-e^+ Decay. A. O. Vaĭsenberg — 722.

Monte-Carlo Calculations of Electromagnetic Cascades with Account of the Influence of the Medium on Bremsstrahlung. A. A. Varfolomeev and I. A. Svetlobov — 1263.

Non-Relativistic Solution of the Bethe-Salpeter Equation. A. I. Alekseev — 1020.

Observation of the $\pi \to e^- + e^+ + e^- + e^+$ Decay. Yu. A. Budagov, S. Viktor, V. P. Dzhelepov, P. F. Ermolov, and V. I. Moskalev — 767.

On Pair Production by the Collision of Two Circularly Polarized Gamma-Ray Quanta. F. S. Sadykhov and B. K. Kerimov — 938L.

On the Production of Pion and Muon Pairs by the Annihilation of High-Energy Positrons. A. I. Nikishov — 937L.

Pair Production by a Circularly Polarized Photon. I. M. Nadzhafov — 232L.

Polarization in Pair Production by Circularly Polarized Quanta. I. G. Ivanter — 777.

Polarization of Beta-Electrons from RaE. B. V. Geshkenbeĭn, S. A. Nemirovskaya, and A. P. Rudik — 360.

Quantum Corrections to Radiation from a Rigid Rotator. L. V. Iogansen — 216L.

Relative Probabilities for the Photoeffect in Shells and Subshells of an Atom. E. P. Grigor'ev and A. V. Zolotavin — 272.

Showers Produced by Positrons in 100 to 400 Mev Range. Yu. D. Prokoshkin and T'ang Hsiao-Wei — 6.
The Motion of an Electron in a Crystal Located in an External Field. G. E. Zil'berman — 1040.
Three-Photon Annihilation of Positronium in the P State. A. I. Alekseev — 1312.
Electrons, Scattering (see Scattering of Electrons and Positrons)
Electrons, Secondary (see Electrical Properties)
Electrostriction (see Dielectrics and Dielectric Properties)
Elementary Particle Interactions
A Possible Method for the Determination of the Direction of Polarization of Mu-Mesons. V. A. Dzhrbashyan — 1115L.
A Possible Method for the Determination of the Parity of Strange Particles. S. M. Bilen'kiĭ — 199.
Absorption of μ^--Mesons by Polarized Nuclei. Angular Distribution of the Neutrons. É. I. Dolinskiĭ — 838.
Adsorption of Polarized Negative Muons by Nuclei and Neutron Polarization. L. D. Blokhintsev — 175.
An Investigation of π^+-μ^+-e^+ Decay with the Aid of a Propane Bubble Chamber and Scintillation Counters. M. P. Balandin, V. A. Moiseenko, A. I. Mukhin, and S. Z. Otvinovskiĭ — 296.
Angular Momentum and Parity Conservation Laws in the Statistical Theory of Multiple Production. V. B. Magalinskiĭ — 67.
Anomalous Spinors and Bosons. A. M. Brodskiĭ and D. D. Ivanenko — 907.
Asymmetry of Angular Distribution of $\mu^+ \rightarrow e^+$ Decay Electrons in a 27,000 Gauss Magnetic Field. S. A. Ali-Zade, I. I. Gurevich, Yu. P. Dobretsov, B. A. Nikol'skiĭ, and L. V. Surkova — 940L.
Azimuthal Symmetries in Cascade Reactions and Parity Conservation. M. I. Shirokov — 1081.
Beta Decay of Strange Particles. V. M. Shekhter — 920L.
Beta-Gamma Angular Correlation in Ba^{139} Decay and the Relative Sign of the Beta-Interaction Coupling Constants. N. A. Vlasov and V. P. Rudakov — 17.
Beta-Gamma Correlation in First-Forbidden Beta Transitions. Yu. V. Gaponov — 131.
Beta-Interaction and Nucleon Formfactor. V. B. Berestetskiĭ and I. Ya. Pomeranchuk — 936L.
Calculation of Polarization of Medium-Energy Neutrons. P. É. Nemirovskiĭ — 408.
Certain Cases of Elastic Scattering of Positrons from π^+-μ^+-e^+ Decay by Emulsion Electrons. Z. V. Minervina and E. A. Pesotskaya — 309.
Charge Symmetry Properties and Representations of the Extended Lorentz Group in the Theory of Elementary Particles. V. I. Ogievetskiĭ and Chou Kuang-Chao — 179.
Comments on the Covariants in the Beta-Decay Interaction. B. N. Valuev — 1121L.
Concerning the ρ^0 Meson. Ya. I. Granovskiĭ — 433L.
Decay of a Beryllium Hyperfragment. A. O. Vaĭsenberg and V. A. Smirnit-skiĭ — 230L.
Depolarization of Mu-Mesons in the Formation of Mu-Mesic Atoms. I. M. Shmushkevich — 449L.
Depth of Penetration and Character of Distribution of Atoms Injected into Si^{30} Isotope Targets. M. I. Guseva, E. V. Inopin, and S. P. Tsytko — 1.
Development of the Nuclear-Active Component of Extensive Atmospheric Showers. S. N. Vernov, E. V. Gorchakov, I. P. Ivanenko, and G. B. Khristiansen — 877.
Direct Proof of the Applicability of the Massey Adiabatic Criterion to Processes of Double Charge Exchange. Ya. M. Fogel', V. F. Kozlov, A. A. Kalmykov, and V. I. Muratov — 929L.
Dispersion Relations and Chew-Low Type Equations for Inelastic Meson Processes in the Fixed Source Case. W. Zoellner — 784.
Effects of a Resonant Pion-Pion Interaction in Fermi's Statistical Theory of Multiple Particle Production. V. I. Rus'kin — 113.
Electromagnetic Structure of the Proton and Neutron. D. I. Blokhintsev, V. S. Barshenkov, and B. M. Barbashov — 1145L.
Electron-Neutrino Angular Correlation in the Beta Decay of the Free Neutron. Yu. V. Trebukhovskiĭ, V. V. Vladimirskiĭ, V. K. Grigor'ev, and V. A. Ergakov — 931L.
Empirical Regularities in the Nucleon Pair Production Energies in Nuclei. V. A. Kravtsov — 871.
Hodoscope Investigation of the Penetrating Component of Extensive Air Showers. R. E. Kazarov — 35.
Interaction between K and π Mesons. V. I. Ogievetskiĭ — 447L.
Interpretation of the Maximum in the Total Cross Section for Proton-Proton Scattering in the 1 Bev Region. V. I. Rus'kin — 660L.
Investigation of the Nature and Spectra of Particles Produced by High-Energy Nucleons. A. I. Alikhanov, G. P. Eliseev, V. Sh. Kamalyan, V. A. Lyubimov, V. N. Moiseev, and A. A. Khrimyan — 280.
Low-Energy Positrons from the μ^+-e^+ Decay. A. O. Vaĭsenberg — 722.
Measurement of the Neutron Half-Life. A. N. Sosnovskiĭ, P. E. Spivak, Yu. A. Prokof'ev, I. E. Kutikov, and Yu. P. Dobrynin — 717.
New Dispersion Relations in Quantum Field Theory. L. A. Khalfin — 774.
Non-Relativistic Solution of the Bethe-Salpeter Equation. A. I. Alekseev — 1020.
Nucleon Interaction Cross Sections at 9 Bev Energy. V. S. Barashenkov and Huang Nen-Ning — 935L.
Observation of the $\pi \rightarrow e^- + e^+ + e^- + e^+$ Decay. Yu. A. Budagov, S. Viktor, V. P. Dzhelepov, P. F. Ermolov, and V. I. Moskalev — 767.
On a Possible Determination of the Sign of Muon Polarization. S. A. Kheĭfets — 1128.
On Analytic Properties of Causal Commutators. V. Ya. Faĭnberg — 1066.
On $\mu^+\mu^-$ Annihilation and the Decay of Neutral Mesons. Ya. B. Zel'dovich — 450L.
On the Analysis of High-Energy Showers. Ya. I. Granovskiĭ and I. Ya. Chasnikov — 795.
On the Depth of the Potential Well for Λ Particles in Heavy Hypernuclei. V. A. Filimonov — 1113L.
On the Influence of the Isobaric State of a Nucleon on the Electron-Neutron Interaction. G. A. Kharadze — 1119L.
On the Mechanism of the Leptonic Decay of Hyperons. V. V. Turovtsev — 939L.

On the Possibility of Determining the π-π Scattering Amplitudes from the Analysis of the $\gamma + p \rightarrow N + \pi + \pi$ Reactions Near Threshold. A. A. Ansel'm and V. N. Gribov — 1346.
On the Probability of Double Beta Decay. F. Yanoukh — 231L.
On the Problem of Testing Parity Conservation in the Strong Interactions. V. G. Solov'ev — 436L.
On the Production of Pion and Muon Pairs by the Annihilation of High-Energy Positrons. A. I. Nikishov — 937L.
On the Quantization of Half-Integer Spin Fields. D. V. Volkov — 1107.
On the Shape of Alpha-Active Nuclei. L. L. Gol'din, G. I. Novikova, and K. A. Ter-Martirosyan — 356.
On the Weak-Interaction Types Possible in the Scheme of Feynman and Gell-Mann. V. M. Shekhter — 403.
Pair Production by a Circularly Polarized Photon. I. M. Nadzhafov — 232L.
Parity Nonconservation in the First Order in the Weak-Interaction Constant in Electron Scattering and Other Effects. Ya. B. Zel'dovich — 682L.
Peripheral Interactions between Elementary Particles. L. B. Okun' and I. Ya. Pomeranchuk — 207.
Polarization Correlation in Coulomb Scattering of Electrons and Muons by Light Nuclei Including Radiation Corrections. I. G. Ivanter — 224L.
Polarization Effects in Σ^--Hyperon Capture by Deuterons. S. G. Matinyan and O. D. Cheishvili — 143.
Polarization of Beta-Electrons from RaE. B. V. Geshenbein, S. A. Nemirovskaya, and A. P. Rudik — 360.
Polarization of Beta Particles and Beta-Gamma Correlation for First-Forbidden Transitions of Oriented Nuclei. A. Z. Dolginov and N. P. Popov — 368.
Possibility of Determining the Chirality of the Muon by Means of δ-Electron Cascades from Magnetized Iron. A. I. Alikhanov and V. A. Lyubimov — 946L.
Possible Method of Search for the ρ^0 Meson. V. G. Zinov, A. D. Konin, S. M. Korenchenko, and B. Pontecorvo — 1386L.
Production of Pions by High-Energy Cosmic-Ray Alpha Particles. A. A. Loktionov and Zh. S. Takibaev — 1209.
Production of Strange Particles in the Interaction between 9-Bev Protons and Emulsion Nuclei. N. I. Kostanashvili and O. A. Shakhulashvili — 713.
Production of Strange Particles in 3-Bev p-p Collisions. V. S. Barashenkov and V. M. Mal'tsev — 659L.
Range-Energy Dependence of C_{12}, C_{14}, and O_{16} Ions in Aluminum, Copper, and Gold in the Energy Interval from 50 to 100 Mev. Yu. Ts. Oganesyan — 661L.
Ranges of Mu-Mesic Atoms in Hydrogen Chambers. S. S. Gershtein — 927L.
Relation between the Gravitational Constant, the Charge-to-Mass Ratio of the Electron, and the Fine-Structure Constant. I. G. Ivanter — 1380L.
Results of a Model of the p-p Interaction at 10 Bev. G. I. Kopylov — 327L.
Saturation in a Hyperon System. V. A. Filimonov — 1380L.
Scattering of Muons with Momenta Near 100 Mev/c by Copper and Iron. V. G. Kirillov-Ugryumov, B. A. Dolgoshein, A. M. Moskvichev, and L. P. Morozov — 290.
Showers Produced by Positrons in 100 to 400 Mev Range Yu. D. Prokoshkin and T'ang Hsiao-Wei — 6.
Simplification of the Formulas for Statistical Weight Calculations. Ya. I. Granovskiĭ — 923L.
Singularities of the S Matrix and the ρ^0 Meson. V. I. Gol'danskiĭ and Ya. A. Smorodinskiĭ — 1387L.
Some Characteristics of the Annihilation of an Antiproton in the Deuteron. É. O. Okonov — 1134L.
Stability of a Plane Poiseuille Flow of an Ideally Conducting Fluid in a Longitudinal Magnetic Field. E. P. Velikhov — 848.
Storage of Cold Neutrons. Ya. B. Zel'dovich — 401L.
The Ke_3 and $K_{\mu 3}$ Decays. S. G. Matinyan and L. B. Okun' — 933L.
The Kinematics of Elementary Interactions. N. G. Birger and Yu. A. Smorodin — 823.
The Mass Spectrum of Mesons in Heisenberg's Theory. Ya. I. Granovskiĭ — 819.
The Role of Group Velocity of Light Emitted in a Refractive Medium. I. M. Frank — 580.
The Transformation K_2^0-K_1^0 by Electrons. Ya. B. Zel'dovich — 984.
The Two-Nucleon LS Potential in Nonrelativistic Meson Theory. Yu. V. Novozhilov and I. A. Terent'ev — 89.
The Universal Fermi Interaction and Astrophysics. B. Pontecorvo — 1148L.
Elements (see Atomic Mass and Abundance)
Energy Loss of Particles (see Range and Energy Loss)
Energy States of Atoms (see Atomic Structure and Spectra)
Energy States of Nucleus (see Nuclear Reactions; Nuclear Spectra; Nuclear Structures)
Errata
A Correction to V. M. Strutinskiĭ's Paper "Excitation of Rotational States During the Alpha Decay of Even-Even Nuclei" — 1392L.
Correction to the Paper by V. Ya. Éĭdman "Radiation of an Electron Moving in a Magneto-Active Plasma" — 947L.
Evaporation (see Liquids)
Excitation of Atoms (see Atomic Structure and Spectra)
Excitation of Nucleus (see Nuclear Reactions; Nuclear Spectra; Nuclear Structure)
Faraday Effect (see Optical Properties)
Ferroelectric Phenomena (see Dielectrics and Dielectric Properties)
Field Emission (see Electrical Properties)
Field Theory
A Dynamical Principle for Second-Order Equations. A. A. Borgardt — 1371L.
A Model of a Field Theory with Nonvanishing Renormalized Charge. A. A. Ansel'm — 608.
Absorption of μ^--Mesons by Polarized Nuclei. Angular Distribution of the Neutrons. É. I. Dolinskiĭ — 838.
Anomalous Spinors and Bosons. A. M. Brodskiĭ and D. D. Ivanenko — 907.
Beta-Gamma Correlation in First-Forbidden Beta Transitions. Yu. V. Gaponov — 131.
Charge Symmetry Properties and Representations of the Extended Lorentz Group in the Theory of Elementary Particles. V. I. Ogievetskiĭ and Chou Kuang-Chao — 179.
Comments on the Covariants in the Beta-Decay Interaction. B. N. Valuev — 1121.

Dispersion Relations and Chew-Low Type Equations for Inelastic Meson Process in the Fixed Source Case. W. Zoellner — 784.
Interaction between K and π Mesons. V. I. Ogievetskiĭ — 447L.
New Dispersion Relations in Quantum Field Theory. L. A. Khalfin — 774.
On a Certain Version of Nonlocal Electromagnetic Field Theory. A. A. Komar and M. A. Markov — 602.
On Analytic Properties of Causal Commutators. V. Ya. Faĭnberg — 1066.
On Causality in a Theory with an Indefinite Metric. D. A. Slavnov and A. D. Sukhanov — 1044.
On $\mu^+\mu^+$ Annihilation and the Decay of Neutral Mesons. Ya. B. Zel'dovich — 450L.
On the Depth of the Potential Well for Λ Particles in Heavy Hypernuclei. V. A. Filimonov — 307.
On the Quantization of Half-Integer Spin Fields. D. V. Volkov — 1107.
On the Scattering Matrix in an Indefinite Metric. L. A. Maksimov — 324.
Pair Production by a Circularly Polarized Photon. I. M. Nadzhafov — 232L.
Polarization Correlation in Coulomb Scattering of Electrons and Muons by Light Nuclei Including Radiation Corrections. I. G. Ivanter — 224L.
Radiation from a Spin-2 Particle Moving Uniformly in a Medium. A. I. Bedritskiĭ — 234L.
Radiative Deviations from the Coulomb Law at Small Distances. V. G. Vaks — 1340.
Remarks Regarding Heisenberg's Paper on the Lee Model. L. A. Maksimov — 97.
Renormalization of the Vertex Part in Pseudoscalar Meson Theory. V. N. Gribov — 384.
Saturation in a Hyperon System. V. A. Filimonov — 1380L.
Simplification of the Formulas for Statistical Weight Calculations. Ya. I. Granovskiĭ — 923L.
The Mass Spectrum of Mesons in Heisenberg's Theory. Ya. I. Granovskiĭ — 819.
The Two-Nucleon LS Potential in Nonrelativistic Meson Theory. Yu. V. Novozhilov and I. A. Terent'ev — 89.
Theory of the Nonlinear Field $(\Box - \lambda\varphi^2)\varphi = 0$. D. F. Kurdgelaidze — 594.
Films, Properties
Depolarization of μ^+ Mesons in Nuclear Emulsions. A. O. Vaĭsenberg, N. V. Rabin, and V. A. Smirnitskiĭ — 1197.
He^3 Cryostats. V. P. Peshkov, K. N. Zinov'eva, and A. I. Filimonov — 734.
Fine Structure (see Atomic Structure and Spectra)
Fission of Nucleus (see Nuclear Fission)
Fluid Dynamics
Charged Particle Energy Losses Due to Excitation of Plasma Oscillations. Yu. L. Klimontovich — 999.
Converging Cylindrical Detonation Wave. Ya. B. Zel'dovich — 550.
Disappearance of the Isothermal Jump at Large Radiation Density. V. A. Belokon' — 235L.
Oscillations of a Completely Ionized Plasma in a Cylindrical Cavity. L. M. Kovrizhnykh — 592.
Stability of an Ideally Conducting Liquid Flowing between Cylinders Rotating in a Magnetic Field. E. P. Velikhov — 995.
Structure of a Magnetohydrodynamic Shock Wave in a Partially Ionized Gas. S. B. Pikel'ner — 1089.
The Disintegration of Unstable Shock Waves in Magnetohydrodynamics. G. Ya. Lyubarskiĭ and R. V. Polovin — 902.
The Permanent Structure of Shock Waves with Joule Dissipation. V. A. Belokon' — 932L.
Theory of Relativistic Magnetodydrodynamic Waves. I. A. Akhiezer and R. V. Polovin — 1316.
Two Cases of Unstable Combustion. K. I. Shchelkin — 416.
Galvanomagnetic Effect (see Magnetic Properties)
Gamma Rays
An Investigation of the Excited States of Re^{187}. M. V. Klimentovskaya and P. I. Shavrin — 967.
Beta-Gamma Angular Correlation in Ba^{139} Decay and the Relative Sign of the Beta-Interaction Coupling Constants. N. A. Vlasov and V. P. Rudakov — 17.
Concerning the Ce^{141} Decay Scheme. N. V. Forafontov and A. A. Sorokin — 227L.
Correlation between the Direction of an Internal Bremsstrahlung Quantum and Circular Polarization of a Gamma Quantum Emitted by an Excited Nucleus after K Capture. G. M. Gandel'man — 406.
Coulomb Excitation of Neon. D. K. Alkhazov, A. P. Grinberg, I. Kh. Lemberg, and V. V. Rozhdestvenskiĭ — 222L.
Energy Spectrum of Fragments from the Photofission of U^{238}. B. S. Kovrigin, M. Ya. Kondrat'ko, and K. A. Petrzhak — 217L.
Gd^{146} and Eu^{146} Conversion-Electron Spectra. N. M. Anton'eva, A. A. Bashilov, B. S. Dzhelepov, and B. K. Preobrazhenskiĭ — 20.
Generation of Neutral Pions in the Interaction between 9 Bev Protons and Photographic Emulsion Nuclei. G. L. Bayatyan, I. M. Gramenitskiĭ, A. A. Nomofilov, M. I. Podgoretskiĭ, and E. S. Skrzypczak — 483.
Lifetimes of the First Excited States of Rb^{85} and Pr^{141}. N. A. Burgov, A. V. Davydov, and G. R. Kartashov — 1384L.
On Pair Production by the Collision of Two Circularly Polarized Gamma-Ray Quanta. F. S. Sadykhov and B. K. Kerimov — 938L.
Relative Probabilities for the Photoeffect in Shells and Subshells of an Atom. E. P. Grigor'ev and A. V. Zolotavin — 272.
Resonance Scattering of Low-Energy Gamma Rays on Nuclei. B. N. Kalinkin — 1022.
Resonant Scattering of Gamma Rays by Ni^{60}. N. A. Burgov, Yu. V. Terekhov, and G. E. Bizina — 1146L.
The Gamma Rays of As^{74}. Yu. E. Loginov and K. I. Yakovlev — 664L.
Gases
Cylindrical and Plane Magnetodydrodynamic Waves. K. P. Stanyukovich — 1271.
Disappearance of the Isothermal Jump at Large Radiation Density. V. A. Belokon' — 235L.
Investigation of High Current Pulse Discharges in Conical Chambers. N. A. Borzunov, D. V. Orlinskiĭ, and S. M. Osovets — 502.
Oscillations of a Completely Ionized Plasma in a Cylindrical Cavity. L. M. Kovrizhnykh — 592.

Slipping and Temperature Discontinuity at the Boundary of a Gas Mixture. R. Ya. Kucherov and L. É. Rikenglaz — 1253.
The Influence of Temperature and Pressure on the Raman Spectrum of Nitrogen. G. V. Mikhailov — 971.
Two Cases of Unstable Combustion. K. I. Shchelkin — 416.
Zemplen's Theorem in Relativistic Hydrodynamics. R. V. Polovin — 675L.
Gravitation (see Relativity and Gravitation)
Gyromagnetization (see Magnetic Properties)
Hall Effect (see Electrical Conductivity and Resistance; Semiconductors)
Helium, Liquid
Fluctuations of Atomic Structures in Liquid Helium. V. K. Prokhorenko and I. Z. Fisher — 928L.
He^3 Cryostats. V. P. Peshkov, K. N. Zinov'eva, and A. I. Filimonov — 734.
On the Thermodynamics of Helium. M. P. Mokhnatkin — 680L.
Properties of the Spectrum of Elementary Excitations near the Disintegration Threshold of the Excitations. L. P. Pitaevskiĭ — 830.
Reply to the Letter by M. P. Mokhnatkin. B. N. Esel'son, M. I. Kaganov, and I. M. Lifshitz — 681L.
High Voltage Tubes and Machines (see Methods and Instruments)
Hyperfine Structure (see Atomic Structure and Spectra; Nuclear Moments and Spin)
Hyperons (see Mesons and Hyperons)
Imperfections in Solids
Effect of Resonance Excitation Transfer in the Theory of a Large-Radius Exciton. É. I. Rashba — 1213.
Investigation of the Initial Stages of Plastic Deformation of Rock-Salt Crystals. R. I. Garber and L. M. Polyakov — 1158.
Measurement of the Resistance of High Purity Tin at Helium Temperatures. V. B. Zernov and Yu. V. Sharvin — 737.
On the Heat Conductivity and Attenuation of Sound in Superconductors. B. T. Geĭlikman and V. Z. Kresin — 677L.
On the Theory of the Electron Spin Resonance of F Centers in Crystals with NaCl Structure. L. A. Shul'man — 1217.
The Energy of Formation and Migration of Vacancies in Gold and Platinum. B. G. Lazarev and O. N. Ovcharenko — 42.
Inelastic Scattering (see Nuclear Reactions; Scattering)
Instruments (see Methods and Instruments)
Internal Conversion (see Nuclear Spectra)
Ionization (see also Electrical Discharges; Range and Energy Loss of Particles)
A Simple Method of Calculating the Degree of Ionization and Thermodynamic Functions of a Multiply Ionized Ideal Gas. Yu. P. Raĭzer — 1124L.
Determination of the Ionization Potential of Uranium by a Surface Ionization Method. I. N. Bakulina and N. I. Ionov — 709.
Energy Spectra of Alpha Particles from the Long-Lived Isotopes Th^{232} and U^{238}. G. E. Kocharov, A. P. Komar, and G. A. Korolev — 48.
Ionization of Air by H^+ and H_2^+ Ions. R. N. Il'in, V. V. Afrosimov, and N. V. Fedorenko — 29.
Ionization Potentials of Atoms (see Atomic Structure and Spectra)
Ions (see also Electrical Discharges)
A Qualitative Interpretation of the Mean Electron Excitation Energy in Atomic Collisions. O. B. Firsov — 1076.
Broadening of Spectral Lines in Strongly Ionized Plasma. M. A. Mazing and S. L. Mandel'shtam — 941L.
Concerning the Production of Compound Nuclei in the Interaction between Atomic Nuclei. A. S. Karamyan, Yu. B. Gerlit, and B. F. Myasoedov — 431L.
Cross-Sections for the Production of Californium Isotopes by the Bombardment of U^{238} by Accelerated Carbon Ions. V. V. Volkov, L. I. Guseva, A. S. Pasyuk, N. I. Tarantin, and K. V. Filippova — 536.
Direct Neutron-Exchange Interaction of Complex Nuclei. V. I. Gol'danskiĭ — 366.
Dissociation of the Molecular Ion H_2^+ in Collisions with Gases. N. V. Fedorenko, V. V. Afrosimov, R. N. Il'in, and D. M. Kaminker — 267.
Electroacoustic Phenomena in a Degenerate Electron-Ion Plasma. P. S. Zyryanov and G. G. Taluts — 100.
On the Existence of the Negative Nitrogen Ion. Ya. M. Fogel', V. F. Kozlov, and A. A. Kalmykov — 963.
Ions and Electrons, Mobility
Direct Proof of the Applicability of the Massey Adiabatic Criterion to Processes of Double Charge Exchange. Ya. M. Fogel', V. F. Kozlov, A. A. Kalmykov, and V. I. Muratov — 929L.
Electrical, Optical, and Elastic Properties of Diamond-Type Crystals. IV. Interaction between Conduction Electrons and Lattice Vibrations. V. S. Mashkevich — 1237.
Investigation of Galvanomagnetic Phenomena in Chromium at Low Temperatures. E. S. Borovik and V. G. Volotskaya — 1175.
The Motion of an Electron in a Crystal Located in an External Field. G. E. Zil'berman — 1040.
Isobars (see Atomic Mass and Abundance)
Isomers, Nuclear (see Nuclear Spectra)
Isotopes (see Atomic Mass and Abundance; Radioactivity)
Kerr Effect (see Optical Properties)
Liquid Helium (see Helium, Liquid)
Liquids
He^3 Cryostats. V. P. Peshkov, K. N. Zinov'eva, and A. I. Filimonov — 734.
On the Theory of Nuclear Paramagnetic Resonance in Liquids. G. V. Skrotskiĭ and A. A. Kokin — 335.
Stability of a Plane Poiseuille Flow of an Ideally Conducting Fluid in a Longitudinal Magnetic Field. E. P. Velikhov — 848.
Stability of an Ideally Conducting Liquid Flowing between Cylinders Rotating in a Magnetic Field. E. P. Velikhov — 995.
Magnetic Fields (see Electromagnetic Theory and Electrodynamics)
Magnetic Properties
A System of Magnetic Moments in a Weak Variable Magnetic Field. G. V. Skrotskiĭ and A. A. Kokin — 116.
Connection between Structural and Magnetic Parameters of the Transition Metals. F. M. Gal'perin — 862.

Depolarization of μ^+ Mesons in Nuclear Emulsion. A. O. Vaisenberg, N. V. Rabin, and V. A. Smirnitskiĭ — 1197.

Effect of Atomic Ordering on Exchange Interaction in the Fe_3Pt Alloy. K. P. Belov and Z. D. Sirota — 752.

Indirect Coupling of d Electrons in Transition Metals. I. Ferromagnetism. A. A. Berdyshev and B. V. Karpenko — 577.

Interaction between Conduction Electrons in Ferromagnets. A. I. Akhiezer and I. Ya. Pomeranchuk — 605.

Isotopic Shift of the Curie Point in Uranium Hydride and Deuteride. A. I. Karchevskiĭ, E. V. Artyushkov, and L. I. Kikoin — 442L.

Investigation of Galvanomagnetic Phenomena in Chromium at Low Temperatures. E. S. Borovik and V. G. Volotskaya — 344.

Investigation of Weak Ferromagnetism in the $MnCO_3$ Single Crystal. A. S. Borovik-Romanov — 539.

Magnetic and Resonance Properties of Yttrium Ferrite-Garnets with Replacement of Fe^{3+} Ions by Cr^{3+} and Al^{3+} Ions. K. P. Belov, M. A. Zaĭtseva, and L. A. Malevskaya — 1138.

Magnetic Moments and Curie Points of Ferrites of the Cu-Cd System. N. Z. Miryasov and L. G. Kolomin — 1376L.

Magnetic Properties of Gadolinium Oxides. K. P. Belov, M. A. Zaĭtseva, and A. V. Ped'ko — 1191.

Magnetocaloric Effect in Uranium Hydride and Deuteride. A. I. Karchevskiĭ — 443L.

Measurement of the Electrical Resistance of Metals in a Magnetic Field as a Method of Investigating the Fermi Surface. N. E. Alekseevskiĭ and Yu. P. Gaĭdukov — 311.

Measurement of the Noise of Cyclic Remagnetization of Ferromagnetic Substances at Low Temperatures. N. N. Kolachevskiĭ — 278.

Nuclear Polarization of Weakly-Magnetic Elements Introduced into a Ferromagnet. B. N. Samoĭlov, V. V. Sklyarevskiĭ, and E. P. Stepanov — 1383L.

Neutron Diffraction Investigation of the Antiferromagnetism of the Carbonates of Manganese and Iron. R. A. Alikhanov — 1204.

On the Rotation of the Plane of Polarization of Elastic Waves in a Magnetically Polarized Medium. K. B. Vlasov and B. Kh. Ishmukhametov — 921L.

On the Theory of Weak Ferromagnetism. E. A. Turov — 890.

Phenomenological Theory of Kinetic Processes in Ferromagnetic Dielectrics. II. Interaction of Spin Waves with Phonons. M. I. Kaganov and V. M. Tsukernik — 151

Piezomagnetism in the Antiferromagnetic Fluorides of Cobalt and Manganese. A. S. Borovik-Romanov — 1390L.

Polarization of Au^{198} Nuclei in a Solution of Gold in Iron. B. N. Samoĭlov, V. V. Sklyarevskiĭ, and E. P. Stepanov — 448L.

Polarization of Cobalt and Iron Nuclei in Ferromagnets. B. N. Samoĭlov, V. V. Sklyarevskiĭ, and E. P. Stepanov — 972.

Stability of an Ideally Conducting Liquid Flowing between Cylinders Rotating in a Magnetic Field. E. P. Velikhov — 995.

Temperature Dependence of Ferromagnetic Resonance in Yttrium Ferrite-Garnets. L. A. Malevskaya and G. M. Nurmukhamedov — 1137L.

The Disintegration of Unstable Shock Waves in Magnetohydrodynamics. G. Ya. Lyubarskiĭ and R. V. Polovin — 902.

The Influence of the Electron-Phonon Interaction on the Cyclotron Resonance Frequency. A. V. Tulub — 392.

The Magnetization and Magnetocaloric Effect of Manganese Phosphide. I. G. Fakidov and V. P. Krasovskiĭ — 755.

The Motion of an Electron in a Crystal Located in an External Field. G. E. Zil'berman — 1040.

The Phenomenological Theory of the Voigt Effect in Paramagnetics. L. M. Tsirul'nikova — 1015.

The Problem of Determining the Dielectric-Permittivity and Magnetic-Permeability Tensors of a Medium. G. S. Krinchik and M. V. Chetkin — 1368.

Ultrasonic Attenuation in Metals. G. L. Kotkin — 664L.

Wall Probe in a Magnetic Field. I. K. Fetisov — 789.

Magnetic Resonance

A Paramagnetic Amplifier and Generator, Using Fe^{3+} Ions in Corundum. L. S. Kornienko, and A. M. Prokhorov — 649L.

Effect of Specimen Shape on Ferromagnetic Resonance in a Strong Radio-Frequency Field. G. V. Skrotskiĭ and Yu. I. Alimov — 899.

Electron Paramagnetic Resonance of Co^{2+} in Corundum. G. M. Zverev and A. M. Prokhorov — 451L.

Electronic Paramagnetic Resonance Spectra of Frozen OH Radicals. S. D. Kaitmazov and A. M. Prokhorov — 944L.

Frequency Spectrum of Electron Spin Double Resonance at Color Centers in Alkali Halide Crystals. V. Ya. Zevin — 81.

Line Width of the Chlorine Quadrupole Resonance in Chlorates of Barium, Sodium, and Potassium. V. S. Grechishkin — 438L.

Magnetic and Resonance Properties of Yttrium Ferrite-Garnets with Replacement of Fe^{3+} Ions by Cr^{3+} and Al^{3+} Ions. K. P. Belov, M. A. Zaĭtseva, and L. A. Malevskaya — 1138.

Magneto-Optical Resonance in Nickel at Infrared Frequencies. G. S. Krinchik and R. D. Nuralieva — 724.

Measurement of Spin-Lattice Relaxation Time in Mn^{++} Salt Solutions. P. G. Tishkov — 949.

On Electromagnetic Shock Waves in Ferrites. A. V. Gaponov and G. I. Freĭdman — 675L.

On the Overhauser Effect in Saturation of Forbidden Resoance. L. L. Buishvili — 1369L.

On the Theory of Electron Paramagnetic Resonance in Electrolyte Solutions. A. A. Kokin — 353.

On the Theory of Lattice Spin Relaxation. K. A. Valiev — 1242.

On the Theory of Nuclear Paramagnetic Resonance in Liquids. G. V. Skrotskiĭ and A. A. Kokin — 335.

On the Theory of the Electron Spin Resonance of F Centers in Crystals with NaCl Structure. L. A. Shul'man — 1217.

Paramagnetic Resonance of F Centers in Static Magnetic Fields of Arbitrary Strength. M. F. Deĭgen and A. B. Roĭtsin — 120.
Random Free Precession of Magnetic Moments of Atomic Nuclei. G. V. Skrotskiĭ and A. A. Kokin — 658L.
Resonance Absorption of Ultrasound on Nuclei. A. R. Kessel' — 285.
Resonance Transitions in Parallel Fields in Certain Mn^{++} and Fe^{+++} Crystals. N. S. Garif'yanov — 1393L.
Some Features of Multiplet Ferromagnetic Resonance in Ferrites. V. N. Lazukin — 477.
Temperature Dependence of Ferromagnetic Resonance in Yttrium Ferrite-Garnets. L. A. Malevskaya and G. M. Nurmukhamedov — 1137L.
The Influence of the Electron-Phonon Interaction on the Cyclotron Resonance Frequency. A. V. Tulub — 392.
The Resonance of Charge Carriers Produced by an Ultrasonic Wave. E. P. Pikatilov — 1037.
Thermodynamic Theory of Ferromagnetic Absorption. V. L. Beshidze — 654L.
Magneto-Optical Effects (see Optical Properties)
Magnetoresistance (see Electrical Conductivity and Resistance; Semiconductors)
Magnetostriction (see Magnetic Properties)
Mathematical Methods
A New Class of Representations of the Full Lorentz Group. G. A. Sokolik — 781.
Action as a Space Coordinate, X. Yu. B. Rumer — 1348.
Anomalous Spinors and Bosons. A. M. Brodskiĭ and D. D. Ivanenko — 907.
Behavior of a Conducting Gaseous Sphere in a Quasi-Stationary Electromagnetic Field. V. V. Yankov — 388.
Calculation of Scattering Phase Shifts with Inclusion of the Second Approximation. A. A. Sokolov, V. M. Arutyunyan, and R. M. Muradyan — 412.
Equation of State of a Plasma. A. A. Vedenov and A. I. Larkin — 806.
Fock Expansion for the Wave Functions of a System of Charged Particles. Yu. N. Demkov and A. M. Ermolaev — 633.
On a Relation in Quantum Statistics. E. S. Fradkin — 672L.
On Analytic Properties of Causal Commutators. V. Ya. Fainberg — 1066.
On Causality in a Theory with an Indefinite Metric. D. A. Slavnov and A. D. Sukhanov — 1044.
On the Application of Quantum-Field-Theory Methods to Problems of Quantum Statistics at Finite Temperatures. A. A. Abrikosov, L. P. Gor'kov, and I. E. Dzyaloshinskiĭ — 636.
On the Problem of the Covariant Definition of the Spin Pseudovector. A. A. Sokolov, I. M. Ternov, and Yu. M. Loskutov — 657L.
On the Scattering Matrix in an Indefinite Metric. L. A. Maksimov — 324.
On the Theory of Scattering Via Quasi-Stationary States. V. I. Serdobol'skiĭ — 1354.
Reactions Involving Polarized Particles of Zero Rest Mass. Chou Kuang-Chao — 642.
Scattering of Dirac Particles in the Second Born Approximation. V. M. Arutyunyan and R. M. Muradyan — 1094.
Simplification of the Formulas for Statistical Weight Calculations. Ya. I. Granovskiĭ — 923L.
Symmetry Group of the Isotropic Oscillator. Yu. N. Demkov — 63.
The Green's Function Method in Quantum Statistics. E. S. Fradkin — 912.
Theory of Relativistic Magnetohydrodynamic Waves. I. A. Akhiezer and R. V. Polovin — 1316.
Three-Photo Annihilation of Positronium in the P State. A. I. Alekseev — 1312.
Measurements (see Methods and Measurements)
Mechanics
Concerning the Impact of Solids at High Velocities. K. P. Stanyukovich — 1141L.
Zemplen's Theorem in Relativistic Hydrodynamics. R. V. Polovin — 657L.
Mechanics, Quantum (see Quantum Mechanics)
Mechanics, Quantum — Atomic Structure and Spectra (see Atomic Structure and Spectra)
Mechanics, Quantum — of Solid Bodies (see Crystalline State)
Mechanics, Statistical (see Statistical Mechanics and Thermodynamics)
Meson Field Theory (see Field Theory)
Mesons and Hyperons (see also Cosmic Radiation; Elementary Particle Interactions; Nuclear Reactions Induced by Mesons; Scattering of Mesons)
A Possible Method for the Determination of the Direction of Polarization of μ^- Mesons. V. A. Dzhrbashyan — 1115L.
A Possible Method for the Determination of the Parity of Strange Particles. S. M. Bilen'kiĭ — 199.
Absorption of μ^- Mesons by Polarized Nuclei. Angular Distribution of the Neutrons. É. I. Dolinskiĭ — 838.
Adsorption of Polarized Negative Muons by Nuclei and Neutron Polarization. L. D. Blokhintsev — 175.
An Investigation of π^+-μ^+-e^+ Decay with the Aid of a Propane Bubble Chamber and Scintillation Counters. M. P. Balandin, V. A. Moĭseenko, A. I. Mukhin, and S. Z. Otvinovskiĭ — 296.
Asymmetry of Angular Distribution of $\mu^+ \rightarrow e^+$ Decay Electrons in a 27,000 Gauss Magnetic Field. S. A. Ali-Zade, I. I. Gurevich, Yu. P. Dobretsov, B. A. Nikol'skiĭ, and L. V. Surkova — 940L.
Azimuthal Symmetries in Cascade Reactions and Parity Conservation. M. I. Shirokov — 1081.
Beta Decay of Strange Particles. V. M. Shekhter — 920L.
Concerning the ρ^0 Meson. Ya. I. Granovskiĭ — 433L.
Depolarization of Mu-Mesons in the Formation of Mu-Mesic Atoms. I. M. Shmushkevich — 449L.
Depolarization of μ^+ Mesons in Nuclear Emulsion. A. O. Vaĭsenberg, N. V. Rabin, and V. A. Smirnitskiĭ — 347.
Depolarization of the Negative Muon in Mesic-Atom Transitions. V. A. Dzhrbashyan — 188.
Determination of Charged Particle Mass from Scattering and Residual Range in Multiplate Cloud Chambers. F. R. Arutyunyan — 697.
Dispersion Relations and Chew-Low Type Equations

for Inelastic Meson Processes in the Fixed Source Case. W. Zoellner — 784.
Dispersion Relations for the Electromagnetic Form Factor of the Pion. I. T. Dyatlov — 351.
Dual Scattering of Relativistic Pions by Nucleons. V. A. Astaf'ev — 70.
Effects of a Resonant Pion-Pion Interaction in Fermi's Statistical Theory of Multiple Particle Production. V. I. Rus'kin — 113.
Generalized Form of the Dependence of the Pion Cross Section in Complex Nuclei on the Number of Nucleons. A. S. Belousov, B. B. Govorkov, and V. I. Gol'danskiĭ — 164.
Generation of Neutral Pions in the Interaction between 9 Bev Protons and Photographic Emulsion Nuclei. G. L. Bayatyan, I. M. Gramenitskiĭ, A. A. Nomofilov, M. I. Podgoretskiĭ, and E. S. Skrzypczak — 483.
Interaction between K and Pi Mesons. V. I. Ogievetskiĭ — 447L.
Interaction between 660-Mev Protons and Atomic Nuclei and the Nuclear Internal Momentum Distribution of Nucleons. L. S. Azhgirei, I. K. Vzorov, V. P. Zrelov, M. G. Meshcheryakov, B. S. Neganov, R. M. Ryndin, and A. F. Shabudin — 1163.
Interpretation of the Maximum in the Total Cross Section for Proton-Proton Scattering in the 1 Bev Region. V. I. Rus'kin — 660L.
Investigation of the Nature and Spectra of Particles Produced by High-Energy Nucleons. A. I. Alikhanov, G. P. Eliseev, V. Sh. Kamalyan, V. A. Lyubimov, B. N. Moiseev, and A. V. Khrimyan — 280.
Observation of the $\pi^0 \to e^- + e^+ + e^- + e^+$ Decay. Yu. A. Budagov, S. Viktor, V. P. Dzhelepov, P. F. Ermolov, and V. I. Moskalev — 767.
On the Possible Determination of the Sign of Muon Polarization. S. A. Kheĭfets — 1128L.
On $\mu^+\mu^-$ Annihilation and the Decay of Neutral Mesons. Ya. B. Zel'dovich — 450L.
On the Magnitude of the Ratio σ^-/σ^+ Near the Threshold of Meson Production. S. P. Kharlamov, M. I. Adamovich, and V. G. Larionova — 668L.
On the Mechanism of the Leptonic Decay of Hyperons. V. V. Turovtsev — 939L.
On the Possibility of Determining the π-π Scattering Amplitudes from the Analysis of the $\gamma + p \to N + \pi + \pi$ Reactions Near Threshold. A. A. Ansel'm and V. N. Gribov — 1345.
On the Possible Multiple Production of Muons. I. L. Rozental' — 666L.
On the Problem of Testing Parity Conservation in the Strong Interactions. V. G. Solov'ev — 436L.
On the Scattering of Pions by Deuterons. G. M. Vagradov and I. B. Sokolov — 669L.
On the Weak-Interaction Types Possible in the Scheme of Feynman and Gell-Mann. V. M. Shekhter — 403.
Peripheral Interactions between Elementary Particles. L. B. Okun' and I. Ya. Pomeranchuk — 207.
Photoproduction of Low Energy Charged Pions from Complex Nuclei. V. M. Popova, N. G. Semashko, and F. R. Yagudina — 965.
Polarization Effects in Σ^--Hyperon Capture by Deuterons. S. G. Matinyan and O. D. Cheishvili — 143.
Polarization of the μ^+ Meson Current at Sea Level. B. A. Dolgoshein and B. I. Luchkov — 445L.
Polarization of the Nucleus by Capture of Polarized Negative Muons in the Mesonic K Shell. I. M. Shmushkevich — 673L.
Possibility of Determining the Chirality of the Muon by Means of δ-Electron Cascades from Magnetized Iron. A. I. Alikhanov and V. A. Lyubimov — 946L.
Possible Method of Search for the ρ^0 Meson. V. G. Zinov, A. D. Konin, S. M. Korenchenko, and B. Pontecorvo — 1386L.
Production of Pions by High-Energy Cosmic-Ray Alpha Particles. A. A. Loktionov and Zh. S. Takibaev — 1209.
Production of Strange Particles in the Interaction between 9-Bev Protons and Emulsion Nuclei. N. I. Kostanashvili and O. A. Shakhulashvili — 713.
Production of Strange Particles in 3-Bev p-p Collisions. V. S. Barashenkov and V. M. Mal'tsev — 659L.
Ranges of Mu-Mesic Atoms in Hydrogen Chambers. S. S. Gershteĭn — 927L.
Results of a Model of the p-$\bar{p}$ Interaction at 10 Bev. G. I. Kopylov — 1136.
Saturation in a Hyperon System. V. A. Filimonov —1380L.
Scattering of Fast Pi Mesons by Deuterons. A. G. Sitenko — 1008.
Scattering of Muons with Momenta Near 100 Mev/c by Copper and Iron. V. G. Kirillov-Ugryumov, B. A. Dolgoshein, A. M. Moskvichev, and L. P. Morozov — 290.
Singularities of the S Matrix and the ρ^0 Meson. V. I. Goldan'skiĭ and Ya. A. Smorodinskiĭ — 1387.
Some Characteristics of the Annihilation of an Antiproton in the Deuteron. É. O. Okonov — 1134.
Some Symmetry Properties in Process of Antihyperon Production with Annihilation of Antinucleons. Chou Kuang-Chao — 663L.
The Reaction $p + p \to p + p + \pi^0$ in the Energy Range from Threshold to 665 Mev. A. F. Dunaĭtsev and Yu. D. Prokoshkin — 1179.
The K_{e3} and $K_{\mu 3}$ Decays. S. G. Matinyan and L. B. Okun' — 933L.
The Scattering of Muons in Lead. A. I. Alikhanyan and F. R. Arutyunyan — 23.
The Transformation K_2^0-K_1^0 by Electrons. Ya. B. Zel'dovich — 984.
The Two-Nucleon LS Potential in Nonrelativistic Meson Theory. Yu. V. Novozhilov and I. A. Terent'ev — 89.
Underground Muon Spectrum at ~40 Meter Water Equivalent. M. I. Daĭon and L. I. Potapov — 488.
Viscosity in the Hydrodynamic Theory of Multiple Particle Production. A. A. Emel'yanov — 1100.
Metals (see Crystalline State)
Metastable Atoms (see Atomic Structure and Spectra)
Methods and Instruments
Acceleration of Plasmoids by High-Frequency Electric Fields. M. A. Miller — 1358.
Coulomb Excitation of Neon. D. K. Alkhazov, A. P. Grinberg, I. Kh. Lemberg, and V. V. Rozhdestvenskiĭ — 222L.
Cyclic Motion of Charged Particles in an Electric Field. A. A. Kolomenskiĭ and Fong Soy-Cen — 184.

Determination of the Frequency of Capture of Slow Mesons by Light and Heavy Nuclei in Photoemulsions. D. K. Kopylova, Yu. B. Korolevich, N. I. Petukhova, and M. I. Podgoretskiĭ — 1391L.
Determination of the Ionization Potential of Uranium by a Surface Ionization Method. I. N. Bakulina and N. I. Ionov — 709.
Electric Field in a Microwave Plasma as a Function of Time. V. E. Mitsuk and M. D. Koz'minykh — 1139.
Energy Spectra of Alpha Particles from the Long-Lived Isotopes Th^{232} and U^{238}. G. E. Kocharov, A. P. Komar, and G. A. Korolev — 48.
Line Width of the Chlorine Quadrupole Resonance in Chlorates of Barium, Sodium and Potassium. V. S. Grechishkin — 438L.
Magneto-Optical Resonance in Nickel at Infrared Frequencies. G. S. Krinchik and R. D. Nuralieva — 724.
Motion of a Plasma Loop in an Axially Symmetric Magnetic Field. L. M. Kovrizhnykh — 1308.
Neutron Diffraction Investigation of the Antiferromagnetism of the Carbonates of Manganese and Iron. R. A. Alikhanov — 1204.
On the Existence of the Negative Nitrogen Ion. Ya. M. Fogel', V. F. Kozlov, and A. A. Kalmykov — 963.
Plasma Acceleration. I. S. Shpigel' — 285.
Possibility of Determining the Potential Distribution of a Plasma from the Characteristics of the Noise Generated in a Gaseous Discharge. A. A. Zaĭtsev, M. Ya. Vasil'eva, and V. N. Mnev — 1130L.
Oscillations of a Plasma in a Magnetic Field at Frequencies Close to the Cyclotron Frequency. V. N. Lazukin — 685.
Resonance Absorption of Ultrasound on Nuclei. A. R. Kessel' — 1031.
Statistical Electron Capture Mechanism in Betatrons. M. Seidl — 924L.
Wall Probe in a Magnetic Field. I. K. Fetisov — 789.

Microwaves
A Paramagnetic Amplifier and Generator, Using Fe^{3+} Ions in Corundum. L. S. Kornienko and A. M. Prokhorov — 649L.
Effect of Specimen Shape on Ferromagnetic Resonance in a Strong Radio-Frequency Field. G. V. Skrotskiĭ and Yu. I. Alimov — 899.
Electric Field in a Microwave Plasma as a Function of Time. V. E. Mitsuk and M. D. Koz'minykh — 1139.
On the Theory of the Electron Spin Resonance of F Centers in Crystals with NaCl Structure. L. A. Shul'man — 1217.
Plasma Acceleration. I. S. Shpigel' — 285.
Some Features of Multiplet Ferromagnetic Resonance in Ferrites. V. N. Lazukin — 477.
Wall Probe in a Magnetic Field. I. K. Fetisov — 789.

Miscellaneous
Broadening of Spectral Lines in Strongly Ionized Plasma. M. A. Mazing and S. L. Mandel'shtam — 941L.
Oscillations of a Completely Ionized Plasma in a Cylindrical Cavity. L. M. Kovrizhnykh — 592.
Plasma Acceleration. I. S. Shpigel' — 285.
The Permanent Structure of Shock Waves with Joule Dissipation. V. A. Belokon' — 932L.
Two Cases of Unstable Combustion. K. I. Shchelkin — 416.

Molecular Structure and Spectra
Effect of Impurities on the X-ray Spectra of Transition Metals. I. B. Borovskiĭ and K. P. Gurov — 856.
The Influence of Temperature and Pressure on the Raman Spectrum of Nitrogen. G. V. Mikhaĭlov — 974.

Moments, Nuclear (see Nuclear Moments and Spin)

Neutrino
A Search for Double Beta Decay in Ca^{48}. E. I. Dobrokhotov, V. R. Lazarenko, and S. Yu. Luk'yanov — 54.
Adsorption of Polarized Negative Muons by Nuclei and Neutron Polarization. L. D. Blokhintsev — 175.
Anomalous Spinors and Bosons. A. M. Brodskiĭ and D. D. Ivanenko — 907.
Electron-Neutrino Angular Correlation in the Beta Decay of the Free Neutron. Yu. V. Trebukhovskiĭ, V. V. Vladimirskiĭ, V. K. Grigor'ev, and V. A. Ergakov — 931L.
On the Probability of Double Beta Decay. F. Yanoukh — 231L.
On the Problem of the Covariant Definition of the Spin Pseudovector. Á. A. Sokolov, I. M. Ternov, and Yu. M. Loskutov — 657L.

Neutrons (see Elementary Particle Interaction)

Noise
Measurement of the Noise of Cyclic Remagnetization of Ferromagnetic Substances at Low Temperatures. N. N. Kolachevskiĭ — 278.

Nuclear Fission
Angular Anisotropy and Energy Characteristics of the Fission Process. A. N. Protopopov, I. A. Baranov, and V. P. Éĭsmont — 1143.
Angular Anisotropy of Scattering of Fragments in Fission of Am^{241} by 14.7-Mev Neutrons. A. N. Protopopov, I. A. Baranov, and V. P. Éĭsmont — 650L.
Anisotropic Fission of Rotating Nuclei. G. A. Pik-Pichak — 679L.
Breakup of a Charged Liquid Drop and Nuclear Fission. B. T. Geĭlikman — 168.
Dependence of the Angular Anisotropy of Fission on the Nuclear Structure. A. N. Protopopov and V. P. Éĭsmont — 1116.
Effect of Nuclear Shells on the Distribution of the Kinetic Energy of Fragments in Fission by Fast Neutrons. A. N. Protopopov, I. A. Baranov, Yu. A. Selitskiĭ, and V. P. Éĭsmont — 1374L.
Energy Spectrum of Fragments from the Photofission of U^{238}. B. S. Kovrigin, M. Ya. Kondrat'ko, and K. A. Petrzhak — 217L.
Fission at Very High Excitation Energies. V. F. Darovskikh, and N. A. Perfilov — 456.
Fission Induced in Heavy Elements by Carbon, Nitrogen, and Oxygen Nuclei. S. M. Polikanov and V. A. Druin — 522.
Fission of Nonspherical Nuclei. A. G. Sitenko — 555.
Gamma Rays Accompanying the Fission of U^{238} by 2.8 and 14.7 Mev Neutrons. A. N. Protopopov and B. M. Shiryaev — 674L.
K-Level X-rays from Fission Fragments and Distribution of Fragments by Charges. V. V. Sklyarevskiĭ, E. P. Stepanov, and B. A. Medvedev — 225L.
On the Emission Mechanism of Prompt Fission Neutrons. V. S. Stavinskiĭ — 437L.

Nuclear Moments and Spin

A System of Magnetic Moments in a Weak Variable Magnetic Field. G. V. Skrotskiĭ and A. A. Kokin — 116.

An Investigation of the Excited States of Re^{187}. M. V. Klimentovskaya and P. I. Shavrin — 967.

Angular Distribution and Angular Correlation of the Radiations from Nuclei with Oriented Electron Shells. V. A. Dzhrbashyan — 881.

Direct Neutron-Exchange Interaction of Complex Nuclei. V. I. Gol'danskiĭ — 366.

Nuclear Polarization of Weakly-Magnetic Elements Introduced into a Ferromagnet. B. N. Samoĭlov, V. V. Sklyarevskiĭ, and E. P. Stepanov — 1383.

On the Axial Asymmetry of Atomic Nuclei. D. A. Zaikin — 1114L.

On the Influence of the Isobaric State of a Nucleon on the Electron-Neutron Interaction. G. A. Kharadze — 1119L.

On the Theory of Nuclear Magnetic Moments. D. F. Zaretskiĭ — 612.

Polarization of the Nucleus by Capture of Polarized Negative Muons into the Mesonic K Shell. I. M. Shmushkevich — 673L.

Quadrupole Moment of Er^{168}. É. Z. Berlovich, V. G. Fleĭsher, V. I. Breslav, and B. K. Preobrazhenskiĭ — 1138L.

Quadrupole Oscillations of Deformed Nuclei. B. L. Birbrair, L. K. Peker, and L. A. Sliv — 566.

Relativistic Corrections to the Phenomenological Theory of Levels of Light Nuclei. F. A. Zhivopistsev, A. M. Perelomov, and Yu. M. Shirokov — 333.

Nuclear Photoeffects

Concerning the Ce^{141} Decay Scheme. N. V. Forafontov and A. A. Sorokin — 227L.

Energy Spectrum of Fragments from the Photofission of U^{238}. B. S. Kovrigin, M. Ya. Kondrat'ko, and K. A. Petrzhak — 217L.

Generalized Form of the Dependence of the Pion Cross Section in Complex Nuclei on the Number of Nucleons. A. S. Belousov, B. B. Govorkov, and V. I. Gol'danskiĭ — 164.

Intermediate-Energy Photodeuterons from C^{12} and Be^{9}. V. P. Chizhov and L. A. Kul'chistskiĭ — 239.

On Radiative Transitions between Rotational Levels in Spin $\frac{1}{2}$ Nuclei. D. F. Zaretskiĭ — 803.

One-Particle Mechanism in Photonuclear Reactions. G. M. Shklyarevskiĭ — 1057.

Photoproduction of Low Energy Charged Pions from Complex Nuclei. V. M. Popova, N. G. Semashko, and F. R. Yagudina — 965.

Ratio of the Deuteron and Proton Yields in the Photodisintegration of Au^{197}. E. D. Makhnovskiĭ — 519.

Nuclear Reactions, General

An Investigation of π^{+}-μ^{+}-e^{+} Decay with the Aid of a Propane Bubble Chamber and Scintillation Counters. M. P. Balandin, V. A. Moĭseenko, A. I. Mukhin, and S. Z. Otvinovskiĭ — 296.

Angular Correlations Near Multiple-Production Thresholds. A. F. Grashin — 1049.

Angular Momentum and Parity Conservation Laws in the Statistical Theory of Multiple Production. V. B. Magalinskiĭ — 67.

Azimuthal Symmetries in Cascade Reactions and Parity Conservation. M. I. Shirokov — 1081.

Breakup of a Charged Liquid Drop and Nuclear Fission. B. T. Geĭlikman — 168.

Breakup of Charged Particles by a Nuclear Coulomb Field. M. Z. Maksimov — 1123.

Concerning a 100-kev Transition in the Spectrum of Ce^{144}. A. V. Gnedich, L. N. Kryukova, and V. V. Murav'eva — 226L.

Coulomb Excitation of Neon. D. G. Alkhazov, A. P. Grinberg, I. Kh. Lemberg, and V. V. Rozhdestvenskiĭ — 222L.

Cross-Sections for the Production of Californium Isotopes by the Bombardment of U^{238} by Accelerated Carbon Ions. V. V. Volkov, L. I. Guseva, A. S. Pasyuk, N. I. Tarantin, and K. V. Filippova — 536.

Diffraction Stripping of Relativistic Particles. I. I. Ivanchik — 427L.

Energy and Angular Distribution in Diffraction Disintegration Processes. I. I. Ivanchik and V. S. Popov — 347.

Exact Measurement of the Ratios of Internal-Conversion Coefficients of 411.7-kev Gamma Quanta in Hg^{198}. V. M. Kel'man and R. Ya. Metskhvarishvili — 486.

Excitation of Rotational Nuclear Levels by Charged Particles. A. D. Piliya — 843.

Generation of Neutral Pions in the Interaction between 9 Bev Protons and Photographic Emulsion Nuclei. G. L. Bayatyan, I. M. Gramenitskiĭ, A. A. Nomofilov, M. I. Podgoretskiĭ, and E. S. Skrzypczak — 483.

Interaction between Accelerated Nitrogen Nuclei and Bismuth. V. A. Karnaukhov — 1375L.

Non-Uniqueness of the Phase Shift Analysis of Proton-Proton Collisions. V. S. Barashenkov and Huang Nen-Ning — 587.

Nuclear Excitation by High Energy Particles. M. Z. Maksimov — 652L.

Nucleon Interaction Cross Sections at 9 Bev Energy. V. S. Barashenkov and Huang Nen-Ning — 935L.

On the Possible Multiple Production of Muons. I. L. Rozental' — 666L.

On the Role Played by Exchange Effects in Stripping Reactions. V. G. Neudachin, I. B. Teplov, and O. P. Shevchenko — 599.

On the Stability of Nuclei. P. É. Nemirovskiĭ — 627.

On the Theory of Direct Nuclear Reactions Involving Polarized Particles. G. L. Vysotskiĭ and A. G. Sitenko — 812.

Production of Mo^{93m} in the Reaction $Se^{80}(O^{16}, 3n)$. A. S. Karamyan, L. I. Rusinov, and V. A. Fomichev — 979.

Ranges of Mu-Mesic Atoms in Hydrogen Chambers. S. S. Gershteĭn — 927L.

Reactions Involving Polarized Particles of Zero Rest Mass. Chou Kuang-Chao — 642.

Relativistic Corrections to the Phenomenological Theory of Levels of Light Nuclei. F. A. Zhivopistsev A. M. Perelomov, and Yu. M. Shirokov — 333.

Remarks on the Optical Model of the Nucleus. V. G. Grishin and M. I. Podgoretskiĭ — 1132.

Some Symmetry Properties in Process of Antihyperon

Production with Annihilation of Antinucleons. Chou Kuang-Chao — 663L.
The Excitation of Collective States in Nuclei by Scattering of Charged Particles. S. I. Drozdov — 1335.
The Kinematics of Elementary Interactions. N. G. Birger and Yu. A. Smorodin — 823.
Viscosity in the Hydrodynamic Theory of Multiple Particle Production. A. A. Emel'yanov — 1100.
Nuclear Reactions Induced by Alpha Particles and He^3
Angular Distribution of Tritons from the Reaction Li^7 (d, t) Be^8. S. V. Strodubtsev and K. V. Makaryunas — 1133L.
The Angular Distribution of Neutrons from the Reaction C^{13} (d, n) O^{16}. O. M. Mdivani and T. G. Gachechiladze — 1131L.
Nuclear Reactions Induced by Deuterons and Tritons Angular Distributions in the Reactions Ne^{22} (d, p) Ne^{23} and A^{36} (d, p) A^{37}. V. G. Sukharevskiĭ — 981.
Comparison of the Differential Cross Sections for the (dp) and (dt) Reactions. A. B. Kurepin and V. G. Neudachin — 1229.
Lifetime of the First Excited State in Be^{10}. A. N. Boyarkina and A. F. Tulinov — 244.
On the Theory of Direct Nuclear Reactions Involving Polarized Particles. G. L. Vysotskiĭ and A. G. Sitenko — 812.
(d, p) Stripping Reactions in the Silicon Isotopes. V. G. Sukharevskiĭ — 37.
The Beta Spectra of F^{20} and F^{17}. S. S. Vasil'ev and L. Ya. Shavtvalov — 218L.
Nuclear Reactions Induced by Mesons
Adsorption of Polarized Negative Muons by Nuclei and Neutron Polarization. L. D. Blokhintsev — 175.
Dual Scattering of Relativistic Pions by Nucleons. V. A. Astaf'ev — 70.
Radiative Capture of Polarized μ Mesons by Nuclei. G. M. Gandel'man and V. N. Mokhov — 1073.
Ranges of Mu-Mesic Atoms in Hydrogen Chambers. S. S. Gershtein — 927L.
Nuclear Reactions Induced by Neutrons
Angular Anisotropy of Scattering of Fragments in Fission of Am^{241} by 14.7-Mev Neutrons. A. N. Protopopov, I. A. Baranov, and V. P. Éĭsmont — 650L.
Concerning the Production of Compound Nuclei in the Interaction between Atomic Nuclei. A. S. Karamyan, Yu. B. Gerlit, and B. F. Myasoedov — 431L.
Cross Section of Te^{125m} Production via the (n, γ) Reaction. V. S. Gvozdev and Yu. L. Khazov — 439L.
Direct Interaction in Reactions with Emission of Two Nucleons. V. V. Komarov and A. M. Popova — 1118L.
Effect of Nuclear Shells on the Distribution of the Kinetic Energy of Fragments in Fission by Fast Neutrons. A. N. Protopopov, I. A. Baranov, Yu. A. Selitskiĭ, and V. P. Eĭsmont — 1374.
Gamma Rays Accompanying the Fission of U^{238} by 2.8 and 14.7 Mev Neutrons. A. N. Protopopov and B. M. Shiryaev — 674L.
Investigation of the Nature and Spectra of Particles Produced by High-Energy Nucleons. A. I. Alikhanov, G. P. Eliseev, V. Sh. Kamalyan, V. A. Lyubimov, B. N. Moĭseev, and A. V. Khrimyan — 28.
Millisecond Half-Life Isomers Produced in Reactions Involving 14-Mev Neutrons. V. L. Glagolev, O. M. Kovrizhnykh, Yu. V. Makarov, and P. A. Yampol'skiĭ — 742.
On Possible Sets of Experiments for Simultaneous Analysis of Data on Nucleon-Nucleon Scattering and Polarization in p-n Collisions at 635 Mev. B. M. Golovin, V. P. Dzhelepov, V. S. Nadezhdin, and V. I. Satarov — 302.
On the Stability of Nuclei. P. É. Nemirovskiĭ — 627.
Storage of Cold Neutrons. Ya. B. Zel'dovich — 1389L.
The Excitation of Collective States in Nuclei by Scattering of Charged Particles. S. I. Drozdov — 1335.
Two-Neutron Capture Reaction in the Interaction between N^{14} and Nuclei of Some Elements. V. A. Karnaukhov, G. M. Ter-Akop'yan, and V. I. Khalizev — 525.
Nuclear Reactions Induced by Protons
Cascade Alpha-Particles in Stars Produced by 360 and 660 Mev Protons. V. I. Ostroumov, N. A. Perfilov, and R. A. Filov — 254.
Depth of Penetration and Character of Distribution of Atoms Injected into Si^{30} Isotope Targets. M. I. Guseva, E. V. Inopin, and S. P. Tsytko — 1.
Direct Interaction in Reactions with Emission of Two Nucleons. V. V. Komarov and A. M. Popova — 1118L.
Fission at Very High Excitation Energies. V. F. Darovskikh and N. A. Perfilov — 456.
Generation of Neutral Pions in the Interaction between 9 Bev Protons and Photographic Emulsion Nuclei. G. L. Bayatyan, I. M. Gramenitskiĭ, A. A. Nomofilov, M. I. Podgoretskiĭ, and E. S. Skrzypczak — 483.
Interaction between 660-Mev Protons and Atomic Nuclei and the Nuclear Internal Momentum Distribution of Nucleons. L. S. Azhgireĭ, I. K. Vzorov, V. P. Zrelov, M. G. Meshcheryakov, B. S. Neganov, R. M. Ryndin, and A. F. Shabudin — 1163.
Investigation of the Nature and Spectra of Particles Produced by High-Energy Nucleons. A. I. Alikhanov, G. P. Eliseev, V. Sh. Kamalyan, V. A. Lyubimov, B. N. Moĭseev, and A. V. Khrimyan — 280.
New Short-Lived Isomers As^{75m} and Ga^{70m} Excited by Fast Protons. A. M. Morozov and P. A. Yampol'skiĭ — 671L.
Non-Uniqueness of the Phase Shift Analysis of Proton-Proton Collisions. V. S. Barashenkov and Huang Nen-Ning — 587.
On Possible Sets of Experiments for Simultaneous Analysis of Data on Nucleon-Nucleon Scattering and Polarization in p-n Collisions at 635 Mev. B. M. Golovin, V. P. Dzhelepov, V. S. Nadezhdin and V. I. Satarov — 302.
On the Theory of Direct Nuclear Reactions Involving Polarized Particles. G. L. Vysotskiĭ and A. G. Sitenko — 812.
Scattering of Protons on Tritons at Small Energies. Yu. G. Balashko, I. Ya. Barit, and Yu. A. Goncharov —1378.
The Excitation of Collective States in Nuclei by Scattering of Charged Particles. S. I. Drozdov — 1335.
The Reaction $p + p \rightarrow p + p + \pi^0$ in the Energy Range from Threshold to 665 Mev. A. F. Dunaĭtsev and Yu. D. Prokoshkin — 1179.
The Reaction T (p, n) He^3 at 7 — 12 Mev Proton Energy. G. F. Bogdanov, M. A. Vlasov, C. P. Kalinin, B. V.

Rybakov, L. N. Samoĭlov, and V. A. Sidorov — 440L.
Nuclear Scattering (see Scattering)
Nuclear Spectra
Alpha Decay Constants of Non-Spherical Nuclei. V. G. Nosov — 1122L.
An Investigation of the Excited States of Re^{187}, M. V. Klimentovskaya and P. I. Shavrin — 967.
An Investigation of the Superfluid State of an Atomic Nucleus. V. G. Solov'ev — 1331.
Angular Distribution and Angular Correlation of the Radiations from Nuclei with Oriented Electron Shells. V. A. Dzhrbashyan — 881.
Angular Distribution in the Reactions $Ne^{22}(d, p)Ne^{23}$ and $A^{36}(d, p)A^{37}$. V. G. Sukharevskiĭ — 981.
Certain Gamma Transitions in I^{128} and in Neodymium Isotopes. L. F. Kalinkin, A. S. Melioanskiĭ, and I. V. Estulin — 1146.
Concerning a 100-kev Transition in the Spectrum of Ce^{144}. A. V. Gnedich, L. N. Kryukova, and V. V. Murav'eva — 226L.
Concerning the Ce^{141} Decay Scheme. N. F. Forafontov and A. A. Sorokin — 227L.
Coulomb Excitation of Neon. D. G. Alkhazov, A. P. Grinberg, I. Kh. Lemberg, and V. V. Rozhdestvenskiĭ — 222L.
Energy Spectra of Alpha Particles from the Long-Lived Isotopes Th^{232} and U^{238}. G. E. Kocharov, A. P. Komar, and G. A. Korolev — 48.
Exact Measurement of the Ratios of Internal-Conversion Coefficients of 411.7-kev Gamma Quanta in Hg^{198}. V. M. Kel'man and R. Ya. Metskhvarishvili — 486.
Gd^{146} and Eu^{146} Conversion-Electron Spectra. N. M. Anton'eva, A. A. Bashilov, B. S. Dzhelepov, and B. K. Preobrazhenskiĭ — 20.
Lifetime of the First Excited State in Be^{10}. A. N. Boyarkina and A. F. Tulinov — 244.
Lifetimes of the First Excited States of Rb^{85} and Pr^{141}. N. A. Burgov, A. V. Davydov, and G. R. Kartashov — 1384.
M1-Transition in V^{51} and the Seniority Quantum Number. N. N. Delyagin and M. Preĭsa — 1127L.
Nuclear Forces and Levels of the Lithium Isotopes. V. V. Balashov — 798.
On Radiative Transitions between Rotational Levels in Spin 1/2 Nuclei. D. F. Zaretskiĭ — 803.
On the Question of Collective Effects in Light Nuclei. V. V. Balashov and A. F. Tulinov — 426L.
Production of Mo^{93m} in the Reaction $Se^{80}(O^{16}, 3n)$. A. S. Karamyan, L. I. Rusinov, and V. A. Fomichev — 979.
Resonance Scattering of Low-Energy Gamma Rays on Nuclei. B. N. Kalinkin — 1022.
The Beta Spectra of F^{20} and F^{17}. S. S. Vasil'ev and L. Ya. Shavtvalov — 218L.
Transition Probabilities between the Levels of the Rotational Band of Non-Axial Nuclei. A. S. Davydov and V. S. Rostovskiĭ — 1275.
Nuclear Structure Theory
Alpha Decay Constants of Non-Spherical Nuclei. V. G. Nosov — 1122L.
An Investigation of the Superfluid State of an Atomic Nucleus. V. G. Solov'ev — 1331.
Breakup of Charged Particles by a Nuclear Coulomb Field. M. Z. Maksimov — 1123L.
Conditions for Superfluidity of the Atomic Nucleus and the Temperature of the Phase Transition. V. G. Solov'ev — 201.
Dependence of the Angular Anisotropy of Fission on the Nuclear Structure. A. N. Protopopov and V. P. Éĭsmont — 1116.
Empirical Regularities in the Nucleon Pair Production Energies in Nuclei. V. A. Kravtsov — 871.
Gamma Oscillations of the Surface of an Atomic Nucleus. A. S. Davydov and D. A. Zaikin — 157.
Investigation of the Average Nuclear Potential Parameters. L. A. Sliv and B. A. Volchok — 374.
Nuclear Forces and Levels of the Lithium Isotopes. V. V. Balashov — 798.
On Radiative Transitions between Rotational Levels in Spin 1/2 Nuclei. D. F. Zaretskiĭ — 803.
On the Axial Asymmetry of Atomic Nuclei. D. A. Zaikin — 308.
On the Electromagnetic Radii of the Lightest Nuclei in the Ground and Lowest Excited States. A. K. Kaminskiĭ and Yu. M. Shirokov — 616.
On the Moment of Inertia of a Many-Particle System. I. Yu. K. Khokhlov — 203.
On the Phase Factors for Transition from "Particle" to "Hole" States in the Nuclear Shell Theory. V. V. Balashov — 988.
On the Question of Collective Effects in Light Nuclei. V. V. Balashov and A. F. Tulinov — 426L.
On the Shape of Even-Even Nuclei. A. S. Davydov and G. F. Filippov — 1061.
On the Stability of Nuclei. P. É. Nemirovskiĭ — 627.
On the Theory of Nuclear Magnetic Moments. D. F. Zaretskiĭ — 612.
Parentage Coefficients in the Generalized Nuclear Model. V. G. Neudachin and Yu. F. Smirnov — 127.
Polarization of Beta-Electrons from RaE. B. V. Geshkenbein, S. A. Nemirovskaya, and A. P. Rudik — 360.
Polarization of Protons Scattered by C^{12}. S. A. Baldin and V. I. Man'ko — 1377L.
Radiative Capture of Polarized μ Mesons by Nuclei. G. M. Gandel'man and V. N. Mokhov — 1073.
Rotational States of Odd Nuclei without Axial Symmetry. A. S. Davydov — 1103.
Scattering of Protons on Tritons at Small Energies. Yu. G. Balashko, I. Ya. Barit, and Yu. A. Goncharov — 1378L.
Spectrum of the Internal Conversion Electrons Accompanying the Alpha Decay of Pu^{238} and Pu^{240}. E. F. Tretyakov, L. N. Kondrat'ev, G. I. Khlebnikov, and L. L. Gol'din — 250.
Transition Probabilities between the Levels of the Rotational Band of Non-Axial Nuclei. A. S. Davydov and V. S. Rostovskiĭ — 1275.
Optical Instruments (see Methods and Instruments)
Optical Properties
Cerenkov Radiation of an Electron Moving in a Medium with Spatial Dispersion. V. N. Agranovich, V. E. Pafomov, and A. A. Rukhadze — 160.
Contribution to the Theory of Light Scattering near the Second-Order Phase-Transition Points. A. P. Levanyuk — 571.
Electrical, Optical, and Elastic Properties of Crystals

of the Diamond Type. III. Dispersion and Absorption of Light. V. S. Mashkevich — 76.
On the Doppler Effect in an Anisotropic and Gyrotropic Medium. K. A. Barsukov — 1052.
On the Energy Spectrum of a Mott Exciton in Ionic Crystals. S. A. Moskalenko and K. B. Tolpygo — 103.
On the Theory of Absorption and Dispersion of Light in Crystals. S. I. Pekar — 314.
The Phenomenological Theory of the Voigt Effect in Paramagnetics. L. M. Tsirul'nikova — 1015.
The Problem of Determining the Dielectric Permittivity and Magnetic-Permeability Tensors of a Medium. G. S. Krinchik and M. V. Chetkin — 1368.
The Role of Group Velocity of Light Emitted in a Refractive Medium. I. M. Frank — 580.
Pair Production (see Electrons and Positrons)
Phosphors and Phosphorescence (see Luminescence; Semiconductors)
Photoconductivity (see Electrical Conductivity and Resistance)
Photodisintegration (see Nuclear Photoeffects)
Photoelectric Effect (see Electrical Properties)
Photography and Photographic Emulsions (see Methods and Instruments; Optical Properties)
Photometry (see Methods and Instruments; Optical Properties)
Photons (see Radiation)
Photovoltaic Effect (see Electrical Properties; Semiconductors)
Piezoelectric Effect (see Dielectrics and Dielectric Properties)
Polarization, Electrical (see Dielectrics and Dielectric Properties)
Positrons (see Electrons and Positrons)
Probability (see Mathematical Methods)
Protons (see Elementary Particle Interactions)
Quantum Electrodynamics (see also Field Theory)
A Dynamical Principle for Second-Order Equations. A. A. Borgardt — 1371L.
Calculation of Scattering Phase Shifts with Inclusion of the Second Approximation. A. A. Sokolov, V. M. Arutyunan, and R. M. Muradyan — 412.
Equation of State of a Plasma. A. A. Vedenov and A. I. Larkin — 806.
On a Certain Version of Nonlocal Electromagnetic Field Theory. A. A. Komar and M. A. Markov — 602.
On $\mu^+\mu^-$ Annihilation and the Decay of Neutral Mesons. Ya. B. Zel'dovich — 450L.
On the Quantization of Half-Integer Spin Fields. D. V. Volkov — 1107.
On the Theory of Relaxation Processes in Ferrodielectrics at Low Temperatures. A. I. Akhiezer, B. G. Bar'yakhtar, and S. V. Peletminskiĭ — 146.
Pair Production by A Circularly Polarized Photon. I. M. Nadzhafov — 232L.
Particle Energy Losses Due to the Excitation of Longitudinal Waves. B. A. Lysov — 221L.
Polarization in Pair Production by Circularly Polarized Quanta. I. G. Ivanter — 777.
Quadrupole Oscillations of Deformed Nuclei. B. L. Birbrair, L. K. Peker, and L. A. Sliv — 566.
Radiation from a Spin-2 Particle Moving Uniformly in a Medium. A. I. Bedritskiĭ — 234L.
Radiative Deviations from the Coulomb Law at Small Distances. V. G. Vaks — 1340.
Renormalization of the Vertex Part in Pseudoscalar Meson Theory. V. N. Gribov — 384.
Van der Waals Forces in an Inhomogeneous Dielectric. I. E. Dzyaloshinskiĭ and L. P. Pitaevskiĭ — 364.
Quantum Mechanics
A Group-Theoretical Consideration of the Basis of Relativistic Quantum Mechanics. V. Yu. M. Shirokov — 620.
A Refinement of the Thomas-Fermi Model at Small Distances. E. S. Fradkin — 1087.
A System of Magnetic Moments in a Weak Variable Magnetic Field. G. V. Skrotskiĭ and A. A. Kokin — 116.
Angular Momentum and Parity Conservation Laws in the Statistical Theory of Multiple Production. V. B. Magalinskiĭ — 67.
Depolarization of Mu Mesons in the Formation of Mu-Mesic Atoms. I. M. Shmushkevich — 449L.
Depolarization of the Negative Muon in Mesic-Atom Transitions. V. A. Dzhrbashyan — 188.
Diffraction Stripping of Relativistic Particles. I. I. Ivanchik — 427L.
Fock Expansion for the Wave Functions of a System of Charged Particles. Yu. N. Demkov and A. M. Ermolaev — 633.
Investigation of the Average Nuclear Potential Parameters. L. A. Sliv and B. A. Volchok — 374.
Non-Relativistic Solution of the Bethe-Salpeter Equation. A. I. Alekseev — 1020.
On a Relation in Quantum Statistics. E. S. Fradkin — 872L.
On Some Symmetry Properties of the Eigenfunctions of the Schrödinger Equation. D. A. Bochvar, N. P. Gambaryan, I. V. Stankevich, and A. L. Chistyakov — 435L.
On the Moment of Inertia of a Many-Particle System; I. Yu. K. Khokhlov — 203.
On the Overhauser Effect in Saturation of Forbidden Resonance. L. L. Buishvili — 1369.
On the Phase Factors for Transition from "Particle" to "Hole" States in the Nuclear Shell Theory. V. V. Balashov — 988.
On the Problem of the Covariant Definition of the Spin Pseudovector. A. A. Sokolov, I. M. Ternov, and Yu. M. Loskutov — 657L.
On the Theory of Absorption and Dispersion of Light in Crystals. S. I. Pekar — 314.
On the Theory of the Coherent Spontaneous Emission. V. M. Faĭn — 562.
Parentage Coefficients in the Generalized Nuclear Model. V. G. Neudachin and Yu. F. Smirnov — 127.
Properties of the Spectrum of Elementary Excitations near the Disintegration Threshold of the Excitations. L. P. Pitaevskiĭ — 830.
Reactions Involving Polarized Particles of Zero Rest Mass. Chou Kuang-Chao — 642.
Relativistic Corrections to Phenomenological Hamiltonians. Yu. M. Shirokov — 330.
Remarks Regarding Heisenberg's Paper on the Lee Model. L. A. Maksimov — 97.

Symmetry Group of the Isotropic Oscillator. Yu. N. Demkov — 63.
The Green's Function Method in Quantum Statistics. E. S. Fradkin — 912.
Thermodynamic Properties of a Degenerate Plasma. A. A. Bedenov — 446L.
Quenching of Radiation (see Radiation)
Radar (see Methods and Instruments; Radiation)
Radiation (see also Range and Energy Loss of Particles)
Angular Distribution and Angular Correlation of the Radiations from Nuclei with Oriented Electron Shells. V. A. Dzhrbashyan — 881.
Cerenkov Radiation of a Magnetic Dipole in an Anisotropic Medium. G. A. Begiashvili and É. V. Gedalin — 1377L.
Correlation between the Direction of an Internal Bremsstrahlung Quantum and Circular Polarization of a Gamma Quantum Emitted by an Excited Nucleus after K Capture. G. M. Gandel'man — 406.
Green's Function for the Resonance Radiation Diffusion Equation. B. A. Veklenko — 138.
Monte-Carlo Calculations of Electromagnetic Cascades with Account of the Influence of the Medium on Bremsstrahlung. A. A. Varfolomeev and I. A. Svetlolobov — 361.
On Radiative Transitions between Rotational Levels in Spin $\frac{1}{2}$ Nuclei. D. F. Zaretskiĭ — 803.
On the Doppler Effect in an Anisotropic and Gyrotropic Medium. K. A. Barsukov — 1052.
On the Theory of the Coherent Spontaneous Emission. V. M. Faĭn — 562.
Quantum Correction to Radiation from a Rigid Rotator. L. V. Iogansen — 216L.
Radiation from a Spin-2 Particle Moving Uniformly in a Medium. A. I. Bedritskiĭ — 234L.
The Radiation Reaction in the Motion of a Charge in a Medium. V. L. Ginzburg and V. Ya. Eĭdman — 1300.
The Universal Fermi Interaction and Astrophysics. B. Pontecorvo — 1148L.
Transition Radiation and Cerenkov Radiation. V. E. Pafomov — 371.
Radioactivity
A Search for Double Beta Decay in Ca^{48}. E. I. Dobrokhotov, V. R. Lazarenko, and S. Yu. Luk'yanov — 54.
Alpha Decay Constants of Non-Spherical Nuclei. V. G. Nosov — 1122.
Alpha Decay of Th^{227} in the Collective Model and the Spin of Ra^{223} in Its Lowest State. S. G. Ryzhanov — 656L.
Angular Distribution and Angular Correlation of the Radiations from Nuclei with Oriented Electron Shells. V. A. Dzhrbashyan — 881.
Certain Gamma Transitions in I^{128} and in Neodymium Isotopes. L. F. Kalinkin, A. S. Melioranskiĭ, and I. V. Estulin — 1146L.
Concerning the Ce^{141} Decay Scheme. N. V. Forafontov and A. A. Sorokin — 227L.
Energy Spectra of Alpha Particles from the Long-Lived Isotopes Th^{232} and U^{238}. G. E. Kocharov, A. P. Komar, and G. A. Korolev — 48.
Gd^{146} and Eu^{146} Conversion-Electron Spectra. N. M. Anton'eva, A. A. Bashilov, B. S. Dzhelepov, and B. K. Preobrazhenskiĭ — 20.
M1-Transition in V^{51} and the Seniority Quantum Number. N. N. Delyagin and M. Preĭsa — 1127L.
Measurement of the Neutron Half-Life. A. N. Sosnovskiĭ, P. E. Spivak, Yu. A. Prokof'ev, I. E. Kutikov, and Yu. P. Dobrynin — 717.
New Short-Lived Isomers As^{75m} and Ga^{70m} Excited by Fast Protons. A. M. Morozov and P. A. Yampol'skiĭ — 671L.
On the Probability of Double Beta Decay. F. Yanoukh — 231L.
On the Shape of Alpha-Active Nuclei. L. L. Gol'din, G. I. Novikova, and K. A. Ter-Martirosyan — 356.
Polarization of Beta Particles and Beta-Gamma Correlation for First-Forbidden Transitions of Oriented Nuclei. A. Z. Dolginov and N. P. Popov — 368.
Polarization of Cobalt and Iron Nuclei in Ferromagnets. B. N. Samoĭlov, V. V. Sklyarevskiĭ, and E. P. Stepanov — 972.
Quadrupole Moment of Er^{168}. É. Z. Berlovich, V. G. Fleisher, V. I. Breslav, and B. K. Preobrazhenskiĭ — 320.
Spectrum of the Internal Conversion Electrons Accompanying the Alpha Decay of Pu^{238} and Pu^{240}. E. V. Tretyakov, L. N. Kontrat'ev, G. I. Khlebnikov, and L. L. Gol'din — 250.
The Beta Spectra of F^{20} and F^{17}. S. S. Vasil'ev and L. Ya. Shavtvalov — 218L.
The "Complete Experiment" in Beta Decay. Ya. A. Smorodinskiĭ — 333.
Two-Neutron Capture Reaction in the Interaction between N^{14} and Nuclei of Some Elements. V. A. Karnaukhov, G. M. Ter-Akop'yan, and V. I. Khalizev — 525.
Range and Energy Loss of Particles
Cerenkov Radiation of an Electron Moving in a Medium with Spatial Dispersion. V. N. Agranovich, V. E. Pafomov, and A. A. Rukhadze — 160.
Depth of Penetration and Character of Distribution of Atoms Injected into Si^{30} Isotope Targets. M. I. Guseva, E. V. Inopin, and S. P. Tsytko — 1.
Ionization of Air by H^+ and H_2^+ Ions. R. N. Il'in, V. V. Afrosimov, and N. V. Fedorenko — 29.
Monte-Carlo Calculations of Electromagnetic Cascades with Account of the Influence of the Medium on Bremsstrahlung. A. A. Varfolomeev and I. A. Svetlolobov — 1263.
On the Doppler Effect in an Anisotropic and Gyrotropic Medium. K. A. Barsukov — 1052.
Range-Energy Relation for 660-Mev Protons. V. P. Zrelov and G. D. Stoletov — 461.
Rectifiers (see Electrical Conductivity and Resistance; Semiconductors)
Relativity and Gravitation
A New Class of Representations of the Full Lorentz Group. G. A. Sokolik — 781.
A Nonlinear Vacuum Effect in Gravitation Theory. N. V. Mitskevich — 859.
Action as a Space Coordinate, X. Yu. B. Rumer — 1348.
Concerning Ryabushko's Work, "On the Equations of Motion of Rotating Masses in the General Theory of Relativity." N. S. Kalitsin — 1112.
Geodesics in Friedman-Lobachevsky Space. I, G. Fikhtengol'ts — 937L.

Relativistic Corrections to Phenomenological Hamiltonians. Yu. M. Shirokov — 330.
Resistance, Electrical (see Electrical Conductivity and Resistance)
Resonance Radiation (see Radiation)
Scattering, General (see also Elementary Particle Interactions; Nuclear Reactions; Range and Energy Loss of Particles)
A General Formula for the Electromagnetic Scattering of Two Different Particles of Spin ½. A. I. Nikishov — 1140L.
A Nonlinear Vacuum Effect in Gravitation Theory. N. V. Mitskevich — 859.
Angular Anisotropy of Scattering of Fragments in Fission of Am^{241} by 14.7-Mev Neutrons. A. N. Protopopov I. A. Baranov, and V. P. Elsmont — 650L.
Breakup of Charged Particles by a Nuclear Coulomb Field. M. Z. Maksimov — 1123L.
Calculation of Scattering Phase Shifts with Inclusion of the Second Approximation. A. A. Sokolov, V. M. Arutyunyan, and R. M. Muradyan — 412.
Contribution to the Theory of Multiple Scattering. M. L. Ter-Mikaelyan — 171.
Diffraction Stripping of Relativistic Particles. I. I. Ivanchik — 427L.
Estimate of the Contribution of Nucleon-Antinucleon Interaction in the Dispersion Relation for Nucleon-Nucleon Scattering. L. I. Lapidus — 193.
Non-Uniqueness of the Phase Shift Analysis of Proton-Proton Collisions. V. S. Barashenkov and Huang Nen-Ning — 587.
Nucleon-Nucleon Scattering in High Angular Momentum States. A. F. Grashin — 1223.
On the Relativistic Relation between Polarization and Asymmetry. S. M. Bilen'kiĭ and R. M. Ryndin — 1144L.
On the Scattering Matrix in an Indefinite Metric. L. A. Maksimov — 324.
On the Theory of Scattering via Quasi-Stationary States. V. I. Serdobol'skiĭ — 378.
Phenomenological Theory of Kinetic Processes in Ferromagnetic Dielectrics. II. Interaction of Spin Waves with Phonons. M. I. Kaganov and V. M. Tsukernik — 151.
Polarization Tensors in the Born Approximation. L. D. Puzikov and Ya. A. Smorodinskiĭ — 1126L.
Ranges of Mu-Mesic Atoms in Hydrogen Chambers. S. S. Gershteĭn — 927L.
Remarks on the Optical Model of the Nucleus. V. G. Grishin and M. I. Podgoretskiĭ — 1132L.
Resonance Effects in the Scattering of Particles Near a Reaction Threshold. A. I. Baz' — 1256.
Resonant Scattering of Gamma Rays by Ni^{60}. N. A. Burgov, Yu. V. Terekhov, and G. E. Bizina — 1146L.
Scattering of Dirac Particles in the Second Born Approximation. V. M. Arutyunyan and R. M. Muradyan — 1094.
Scattering of Muons with Momenta Near 100 Mev/c by Copper and Iron. V. G. Kirillov-Ugryumov, B. A. Dolgoshein, A. M. Moskvichev, and L. P. Morozov — 290.
The Elastic Scattering of Polarized Dirac Particles by a Short Range Center of Force in the Damping Theory. I. I. Guseĭnov — 228L.
The Excitation of Collective States in Nuclei by Scattering of Charged Particles. S. I. Drozdov — 1335.
The Influence of Temperature and Pressure on the Raman Spectrum of Nitrogen. G. V. Mikhaĭlov — 974.
The Nuclear Interaction in the Scattering of Charged Particles from Nonspherical Nuclei. A. D. Piliya — 992.
Use of the Scattering Amplitude to Reconstruct the Potential Near its Boundary. A. G. Chicherin — 1248.
Scattering of Alpha Particles
The Nuclear Interaction in the Scattering of Charged Particles from Nonspherical Nuclei. A. D. Piliya — 992.
Scattering of Deuterons
Diffraction Stripping of Relativistic Particles. I. I. Ivanchik — 427L.
Scattering of Electrons and Positrons (see also Electrons and Positrons)
Certain Cases of Elastic Scattering of Positrons from π^+-μ^+-e^+ Decay by Emulsion Electrons. Z. V. Minervina and E. A. Pesotskaya — 309.
Contribution to the Theory of Multiple Scattering. M. L. Ter-Mikaelyan — 171.
Multiple Scattering of Polarized Electrons. I. N. Toptygin — 340.
Polarization Correlation in Coulomb Scattering of Electrons and Muons by Light Nuclei Including Radiation Corrections. I. G. Ivanter — 224L.
Remarks on the Optical Model of the Nucleus. V. G. Grishin and M. I. Podgoretskiĭ — 1132L.
Scattering of Mesons (see also Nuclear Reactions Induced by Mesons)
A General Formula for the Electromagnetic Scattering of Two Different Particles of Spin ½. A. I. Nikishov — 1140L.
Dispersion Relations and Chew-Low Type Equations for Inelastic Meson Processes in the Fixed Source Case. W. Zoellner — 784.
Dispersion Relations for the Electromagnetic Form Factor of the Pion. I. T. Dyatlov — 351.
Effects of a Resonant Pion-Pion Interaction in Fermi's Statistical Theory of Multiple Particle Production. V. I. Rus'kin — 113.
On the Possibility of Determining the π-π Scattering Amplitudes from the Analysis of the $\gamma + p \rightarrow N + \pi + \pi$ Reactions Near Threshold. A. A. Ansel'm and V. N. Gribov — 1345.
On the Scattering of Pions by Deuterons. G. M. Vagradov and I. B. Sokolova — 669L.
Polarization Correlation in Coulomb Scattering of Electrons and Muons by Light Nuclei Including Radiation Corrections. I. G. Ivanter — 224L.
Remarks on the Optical Model of the Nucleus. V. G. Grishin and M. I. Podgoretskiĭ — 1132L.
Results of a Model of the p-p Interaction at 10 Bev. G. I. Kopylov — 1136L.
Scattering of Fast Pi Mesons by Deuterons. A. G. Sitenko.
Scattering of Muons with Momenta Near 100 Mev/c by Copper and Iron. V. G. Kirillov-Ugryumov, B. A. Dolgoshein, A. M. Moskvichev, and L. P. Morozov — 290.

Scattering of 240-Mev and 270-Mev Negative Pions on Hydrogen. V. G. Zinov and S. M. Korenchenko — 429L.
The Transformation K_2^0-K_1^0 by Electrons. Ya. B. Zel'dovich — 984.
Scattering of Neutrons (see also Nuclear Reactions Induced by Neutrons)
Calculation of Polarization of Medium-Energy Neutrons. P. É. Nemirovskiĭ — 408.
Estimate of the Contribution of Nucleon-Antinucleon Interaction in the Dispersion Relation for Nucleon-Nucleon Scattering. L. I. Lapidus — 193.
Nucleon-Nucleon Scattering in High Angular Momentum States. A. F. Grashin — 1223.
Scattering of 590-Mev Neutrons by Protons in the Small Angle Region. B. M. Golovin, V. P. Dzhelepov, Yu. V. Katyshev, A. D. Konin, and S. V. Medved' — 516.
Scattering of Neutrons by Oriented Nonspherical Nuclei. G. L. Vysotskiĭ, E. V. Inopin, and A. A. Kresnin — 398.
The Excitation of Collective States in Nuclei by Scattering of Charged Particles. S. I. Drozdov — 1335.
Scattering of Protons (see also Nuclear Reactions Induced by Protons)
Interpretation of the Maximum in the Total Cross Section for Proton-Proton Scattering in the 1 Bev Region. V. I. Rus'kin — 660L.
Nucleon-Nucleon Scattering in High Angular Momentum States. A. F. Grashin — 1223.
Polarization of Protons Scattered by C^{12}. S. A. Baldin and V. I. Man'ko — 1377L.
Production of Strange Particles in 3-Bev p-p Collisions. V. S. Barashenkov and V. M. Mal'tsev — 659L.
Scattering of Protons on Tritons at Small Energies. Yu. G. Balashko, I. Ya. Barit, and Yu. A. Goncharov — 1378L.
The Excitation of Collective States in Nuclei by Scattering of Charged Particles. S. I. Drozdov — 1335.
Scattering of Radiation (see Radiation)
Scintillation Counters (see Methods and Instruments)
Secondary Emission (see Electrical Properties)
Semiconductors
Contribution to the Theory of Ferroelectric Polarization Curves. N. S. Akulov — 772.
The Conductivity of Semi-Conductors in an Ultrasonic Field. V. A. Zhuravlev and M. I. Kozak — 236L.
The Electrical Conductivity of Germanium in High Electric Fields at Low Temperatures. É. I. Abaulina-Zavaritskaya — 953.
The Resonance of Charge Carriers Produced by an Ultrasonic Wave. E. P. Pokatilov — 287.
Solid State (see Crystalline State)
Solutions (see Liquids)
Sound (see Acoustics)
Spallation (see Nuclear Reactions)
Spark Discharge (see Electrical Discharges)
Spectra, Atomic (see Atomic Structure and Spectra)
Spectra, General
Broadening of Spectral Lines in Strongly Ionized Plasma. M. A. Mazing and S. L. Mandel'shtam — 941L.
Concerning the Ce^{141} Decay Scheme. N. F. Forafontov and A. A. Sorokin — 227L.
Gd^{146} and Eu^{146} Conversion-Electron Spectra. N. M. Anton'eva, A. A. Bashilov, B. S. Dzhelepov, and B. K. Preobrazhenskiĭ — 20.
The Influence of Temperature and Pressure on the Raman Spectrum of Nitrogen. G. V. Mikhaĭlov — 974.
Spectra, Nuclear (see Nuclear Spectra)
Spectroscopy Technique (see Methods and Instruments)
Spinor Fields (see Field Theory)
Stark Effect (see Atomic Structure and Spectra)
Statistical Mechanics and Thermodynamics
An Equation for the Diffusion in Phase Space for Nonlinear Systems. V. B. Magalinskiĭ and Ya. P. Terletskiĭ — 355.
Angular Momentum and Parity Conservation Laws in the Statistical Theory of Multiple Production. V. B. Magalinskiĭ — 67.
Anisotropy of the Absorption of Ultrasound in Metals in a Magnetic Field. A. A. Galkin and A. P. Korolyuk — 925L.
Contribution to the Theory of Light Scattering near the Second-Order Phase-Transition Points. A. P. Levanyuk — 571.
Dynamical Model in the Theory of Brownian Motion. V. B. Magalinskiĭ — 1381L.
Equation of State of a Plasma. A. A. Vedenov and A. I. Larkin — 806.
Free Energy of Strong Electrolytes. A. A. Vedenov — 665L.
Hysteresis and Non-Stationary Effects in the Electron Temperature in Plasma in Inert Gases. A. V. Gurevich — 434L.
On a Relation in Quantum Statistics. E. S. Fradkin — 672L.
On the Application of Quantum-Field-Theory Methods to Problems of Quantum Statistics at Finite Temperatures. A. A. Abrikosov, L. P. Gor'kov, and I. E. Dzyaloshinskiĭ — 636.
On the Evaluation of Coordinate Probabilities for Nonlinear Systems by Gibb's Method. V. B. Magalinskiĭ — 1011.
On the Thermodynamics of Helium. M. P. Mokhnatkin — 680L.
Phenomenological Theory of Kinetic Processes in Ferromagnetic Dielectrics. II. Interaction of Spin Waves with Phonons. M. I. Kaganov and V. M. Tsukernik — 151.
Properties of the Spectrum of Elementary Excitations near the Disintegration Threshold of the Excitations. L. P. Pitaevskiĭ — 830.
Reply to the Letter by M. P. Mokhnatkin. B. N. Esel'son, M. I. Kaganov, and I. M. Lifshitz — 681L.
Slipping and Temperature Discontinuity at the Boundary of a Gas Mixture. R. Ya. Kucherov and L. É. Rikenglaz — 1253.
The Green's Function Method in Quantum Statistics. E. S. Fradkin — 912.
The Permanent Structure of Shock Waves with Joule Dissipation. V. A. Belokon' — 932L.
Thermodynamic Properties of a Degenerate Plasma. A. A. Bedenov — 446L.
Statistical Methods (see Mathematical Methods)
Superconductivity
Anisotropy of the Absorption Coefficients of Ultra-

sonics in Superconductors. P. A. Bezuglyĭ, A. A. Galkin, and A. P. Korolyuk — 1388L.
Comparison of the Macroscopic Theory of Superconductivity with Experimental Data. V. L. Ginzburg — 1372L.
He^3 Cryostats. V. P. Peshkov, K. N. Zinov'eva, and A. I. Filimonov — 734.
Interaction between Conduction Electrons in Ferromagnets. A. I. Akhiezer and I. Ya. Pomeranchuk — 605.
Microscopic Derivation of the Ginzburg-Landau Equations in the Theory of Superconductivity. L. P. Gor'kov — 1364.
On the Compensation Equation in Superconductivity Theory. D. V. Shirkov — 421.
On the Heat Conductivity and Attenuation of Sound in Superconductors. B. T. Geĭlikman and V. Z. Kresin — 677L.
On the Problem of Thermal Conductivity and Absorption of Sound in Superconductors. V. Z. Kresin — 1385L.
On the Superfluidity of a System of Polar Bose Excitations. S. V. Vonsovskiĭ and M. S. Svirskiĭ — 894.
Some Applications in the Theory of Metals of the Method of Summation of the Main Feynman Diagrams. Yu. V. Tsekhmistrenko — 1097.
Superconducting Alloys at Finite Temperatures. A. A. Abrikosov and L. P. Gor'kov — 220L.
The Basic Compensation Equation in Superconductivity Theory when the Coulomb Interaction Is Taken into Account. Chen Chun-Sian and Chow Shih-Hsun — 885.
The Influence of Anisotropy on the Thermal Conductivity of Superconductors. I. M. Khalatnikov — 1296.
Thermal Properties
He^3 Cryostats. V. P. Peshkov, K. N. Zinov'eva, and A. I. Filimonov — 734.
Magnetic and Resonance Properties of Yttrium Ferrite-Garnets with Replacement of Fe^{+++} Ions by Cr^{+++} and Al^{+++} Ions. K. P. Belov, M. A. Zaĭtseva, and L. A. Malevskaya — 1138L.
Magnetic Properties of Gadolinium Oxides. K. P. Belov, M. A. Zaĭtseva, and A. V. Ped'ko — 1191.
On the Heat Conductivity and Attenuation of Sound in Superconductors. B. T. Geĭlikman and V. Z. Kresin — 677L.
Phenomenological Theory of Kinetic Processes in Ferromagnetic Dielectrics. II. Interaction of Spin Waves with Phonons. M. I. Kaganov and V. M. Tsukernik — 151.
Temperature Dependence of Ferromagnetic Resonance in Yttrium Ferrite-Garnets. L. A. Malevskaya and G. M. Nurmukhamedov — 1137L.
The Magnetization and Magnetocaloric Effect of Manganese Phosphide. I. G. Fakidov and V. P. Krasovskiĭ — 755.
Thermodynamic Theory of Ferromagnetic Absorption. V. L. Beshidze — 645L.
Two Cases of Unstable Combustion. K. I. Shchelkin — 416.
Thermionic Emissions (see Electrical Properties)
Thermodynamics (see Statistical Mechanics and Thermodynamics)
Thermoelectric Effect (see Electrical Properties; Semiconductors)
Total Cross Sections (see Electrons and Positrons; Nuclear Reactions)
Uncertainty Principle (see Quantum Mechanics)
Vacuum Tubes (see Methods and Instruments)
Viscosity (see Liquids)
Wave Mechanics (see Quantum Mechanics)
Work Function (see Electrical Properties)
X-Rays
K-Level X-Rays from Fission Fragments and Distribution of Fragments by Charges. V. V. Sklyarevskiĭ, E. P. Stepanov, and B. A. Medvedev — 225L.

CONTENTS—continued

	Page	Russian Reference	
Radiative Deviations from the Coulomb Law at Small Distances . . . V. G. Vaks	1340	36,	1882
On the Possibility of Determining the π-π Scattering Amplitudes from the Analysis of the $\gamma+p\to N+\pi+\pi$ Reactions near Threshold . . . A. A. Ansel'm and V. N. Gribov	1345	36,	1890
Action as a Space Coordinate, X . . . Yu. B. Rumer	1348	36,	1894
On the Theory of Scattering Via Quasi-Stationary States . . . V. I. Serdobol'skiĭ	1354	36,	1903
Acceleration of Plasmoids by High-Frequency Electric Fields . . . M. A. Miller	1358	36,	1909
Microscopic Derivation of the Ginzburg-Landau Equations in the Theory of Superconductivity . . . L. P. Gor'kov	1364	36,	1918
LETTERS TO THE EDITOR			
The Problem of Determining the Dielectric Permittivity and Magnetic Permeability Tensors of a Medium . . . G. S. Krinchik and M. V. Chetkin	1368	36,	1924
On the Overhauser Effect in Saturation of Forbidden Resonance . . . L. L. Buishvili	1369	36,	1926
On the "Larmoron" Plasma Theory . . . S. A. Kaplan	1370	36,	1927
A Dynamical Principle for Second-Order Equations . . . A. A. Borgardt	1371	36,	1928
Comparison of the Macroscopic Theory of Superconductivity with Experimental Data . . . V. L. Ginzburg	1372	36,	1930
Effect of Nuclear Shells on the Distribution of the Kinetic Energy of Fragments in Fission by Fast Neutrons . . . A. N. Protopopov, I. A. Baranov, Yu. A. Selitskiĭ, and V. P. Éĭsmont	1374	36,	1932
Interaction of Accelerated Nitrogen Nuclei and Bismuth . . . V. A. Karnaukhov	1375	36,	1933
Magnetic Moments and Curie Points of Ferrites of the Cu-Cd System . . . N. Z. Miryasov and L. G. Kolomin	1376	36,	1935
Polarization of Protons in Scattering by C^{12} . . . S. A. Baldin and V. I. Man'ko	1377	36,	1937
Scattering of Protons on Tritons at Small Energies . . . Yu. G. Balashko, I. Ya. Barit, and Yu. A. Goncharov	1378	36,	1937
Cerenkov Radiation of a Magnetic Dipole in an Anisotropic Medium . . . G. A. Begiashvili and É. V. Gedalin	1379	36,	1939
Relation between the Gravitational Constant, the Charge to Mass Ratio of the Electron, and the Fine-Structure Constant . . . I. G. Ivanter	1380	36,	1940
Saturation in a Hyperon System . . . V. A. Filimonov	1380	36,	1941
Dynamical Model in the Theory of Brownian Motion . . . V. B. Magalinskiĭ	1381	36,	1942
Nuclear Polarization of Weakly-Magnetic Elements Introduced into a Ferromagnet . . . B. N. Samoĭlov, V. V. Sklyarevskiĭ, and E. P. Stepanov	1383	36,	1944
Lifetimes of the First Excited States of Rb^{85} and Pr^{141} . . . N. A. Burgov, A. V. Davydov, and G. R. Kartashov	1384	36,	1946
On the Problem of Thermal Conductivity and Absorption of Sound in Superconductors . . . V. Z. Kresin	1385	36,	1947
Possible Method of Search for the ρ^0 Meson . . . V. G. Zinov, A. D. Konin, S. M. Korenchenko, and B. Pontecorvo	1386	36,	1948
Singularities of the S Matrix and the ρ^0 Meson . . . V. I. Goldanskiĭ and Ya. A. Smorodinskiĭ	1387	36,	1950
Anisotropy of the Absorption Coefficients of Ultrasonics in Superconductors. . . . P. A. Bezugly'i, A. A. Galkin, and A. P. Korolyuk	1388	36,	1951
Storage of Cold Neutrons . . . Ya. B. Zel'dovich	1389	36,	1952
Piezomagnetism in the Antiferromagnetic Fluorides of Cobalt and Manganese . . . A. S. Borovik-Romanov	1390	36,	1954
Determination of the Capture Frequency of Slow Mesons by Light and Heavy Nuclei in Photoemulsions . . . D. K. Kopylova, Yu. B. Korolevich, N. I. Petukhova, and M. I. Podgoretskiĭ	1391	36,	1955
A Correction to V. M. Strutinskiĭ's Paper "Excitation of Rotational States in Alpha Decay of Even-Even Nuclei" . . . V. M. Strutinskiĭ	1392	36,	1957
Resonance Transitions in Parallel Fields in Certain Mn^{++} and Fe^{+++} Crystals . . . N. S. Garif'yanov	1393	36,	1957
Author Index	1395	36,	1959
Subject Index	1406		

CONTENTS

	Page	Russian Reference
Momentum Spectrum of Particles of the Hard Component of Cosmic Rays at an Altitude of 9 km. L. T. Baradzeĭ, M. V. Solov'ev, Z. I. Tulinova, and L. I. Filatova	1151	36, 1617
Spectroscopic Investigation of an Intense Pulsed Discharge in Hydrogen. III. Determination of the Parameters of a High-Temperature Plasma. S. Yu. Luk'yanov and V. I. Sinitsyn	1155	36, 1621
Investigation of the Initial Stages of Plastic Deformation of Rock Salt Crystals. R. I. Garber and L. M. Polyakov	1158	36, 1625
Interaction between 660-Mev Protons and Atomic Nuclei and the Nuclear Internal Momentum Distribution of Nucleons. L. S. Azhgireĭ, I. K. Vzorov, V. P. Zrelov, M. G. Meshcheryakov, B. S. Neganov, R. M. Ryndin, and A. F. Shabudin	1163	36, 1631
Investigation of Galvanomagnetic Phenomena in Chromium at Low Temperatures. E. S. Borovik and V. G. Volotskaya	1175	36, 1650
The Reaction $p + p \rightarrow p + p + \pi^0$ in the Energy Range from Threshold to 665 Mev. A. F. Dunaĭtsev and Yu. D. Prokoshkin	1179	36, 1656
Magnetic Properties of Gadolinium Oxides. K. P. Belov, M. A. Zaĭtseva, and A. V. Ped'ko	1191	36, 1672
Depolarization of μ^+ Mesons in Nuclear Emulsion. A. O. Vaĭsenberg, N. V. Rabin, and V. A. Smirnit-skiĭ	1197	36, 1680
A Case of a Sharp Increase in Cosmic-Ray Intensity in the Stratosphere. N. P. Rymko, V. F. Tulinov, and A. N. Charakhch'yan	1202	36, 1687
Neutron Diffraction Investigation of the Antiferromagnetism of the Carbonates of Manganese and Iron. R. A. Alikhanov	1204	36, 1690
Production of Pions by High-Energy Cosmic-Ray Alpha Particles. A. A. Loktionov and Zh. S. Takibaev	1209	36, 1697
Effect of Resonance Excitation Transfer in the Theory of a Large Radius Exciton. É. I. Rashba	1213	36, 1703
On the Theory of the Electron Spin Resonance of F-Centers in Crystals with NaCl Structure. L. A. Shul'man	1217	36, 1709
Nucleon-Nucleon Scattering in High Angular Momentum States. A. F. Grashin	1223	36, 1717
Comparison of the Differential Cross Sections for the (dp) and (dt) Reactions. A. B. Kurepin and V. G. Neudachin	1229	36, 1725
An Equation for the Diffusion in Phase Space for Nonlinear Systems. V. B. Magalinskiĭ and Ya. P. Terletskiĭ	1234	36, 1731
Electrical, Optical, and Elastic Properties of Diamond Type Crystals. IV. Interaction between Conduction Electrons and Lattice Vibrations. V. S. Mashkevich	1237	36, 1736
On the Theory of Lattice Spin Relaxation. K. A. Valiev	1242	36, 1743
Use of the Scattering Amplitude to Reconstruct the Potential Near its Boundary. A. G. Chicherin	1248	36, 1750
Slipping and Temperature Discontinuity at the Boundary of a Gas Mixture. R. Ya. Kucherov and L. É. Rikenglaz	1253	36, 1758
Resonance Effects in the Scattering of Particles Near a Reaction Threshold. A. I. Baz'	1256	36, 1762
Monte Carlo Calculations of Electromagnetic Cascades with Account of the Influence of the Medium on Bremsstrahlung. A. A. Varfolomeev and I. A. Svetlolobov	1263	36, 1771
Cylindrical and Plane Magnetohydrodynamic Waves. K. P. Stanyukovich	1271	36, 1782
Transition Probabilities between the Levels of the Rotational Band of Non-Axial Nuclei. A. S. Davydov and V. S. Rostovskiĭ	1275	36, 1788
Van der Waals Forces in an Inhomogeneous Dielectric. I. E. Dzyaloshinskiĭ and L. P. Pitaevskiĭ	1282	36, 1797
Energy Levels and Approximate Wave Functions of Mesic Atoms. G. E. Pustovalov	1288	36, 1806
The Influence of Anisotropy on the Thermal Conductivity of Superconductors. I. M. Khalatnikov	1296	36, 1818
The Radiation Reaction in the Motion of a Charge in a Medium. V. L. Ginzburg and V. Ya. Éĭdman	1300	36, 1823
Motion of a Plasma Loop in an Axially Symmetric Magnetic Field. L. M. Kovrizhnykh	1308	36, 1834
Three-Photon Annihilation of Positronium in the P State. A. I. Alekseev	1312	36, 1839
Theory of Relativistic Magnetohydrodynamic Waves. I. A. Akhiezer and R. V. Polovin	1316	36, 1845
Transition Radiation and Cerenkov Radiation. V. E. Pafomov	1321	36, 1853
The Mean Free Path of an Exciton in a Polar Crystal. A. V. Tulub	1325	36, 1859
An Investigation of the Superfluid State of an Atomic Nucleus. V. G. Solov'ev	1331	36, 1869
The Excitation of Collective States in Nuclei by Scattering of Charged Particles. S. I. Drozdov	1335	36, 1875

(Contents continued on inside back cover)